UNCLASSIFIED

AD NUMBER
AD355326
CLASSIFICATION CHANGES
TO: unclassified
FROM: secret
LIMITATION CHANGES
TO: Approved for public release, distribution unlimited
FROM: Distribution: Further dissemination only as directed by Defense Atomic Support Agency, Washington, DC 20301, 27 NOV 1964, or higher DoD authority.
AUTHORITY
dna ltr, 5 nov 1984; dna ltr, 8 mar 1985

THIS PAGE IS UNCLASSIFIED

SECRET
RESTRICTED DATA

AD 355326L

DEFENSE DOCUMENTATION CENTER

FOR

SCIENTIFIC AND TECHNICAL INFORMATION

CAMERON STATION, ALEXANDRIA, VIRGINIA

RESTRICTED DATA
SECRET

NOTICE: When government or other drawings, specifications or other data are used for any purpose other than in connection with a definitely related government procurement operation, the U. S. Government thereby incurs no responsibility, nor any obligation whatsoever; and the fact that the Government may have formulated, furnished, or in any way supplied the said drawings, specifications, or other data is not to be regarded by implication or otherwise as in any manner licensing the holder or any other person or corporation, or conveying any rights or permission to manufacture, use or sell any patented invention that may in any way be related thereto.

NOTICE:

THIS DOCUMENT CONTAINS INFORMATION AFFECTING THE NATIONAL DEFENSE OF THE UNITED STATES WITHIN THE MEANING OF THE ESPIONAGE LAWS, TITLE 18, U.S.C., SECTIONS 793 and 794. THE TRANSMISSION OR THE REVELATION OF ITS CONTENTS IN ANY MANNER TO AN UNAUTHORIZED PERSON IS PROHIBITED BY LAW.

CATALOGED BY DDC AS AD No. 355326

355326L

SECRET

Operation

DOMINIC

FISH BOWL SERIES

POR-2018
(WT-2018)
VOLUME 4

This document consists of 502 pages
No. [redacted] of 276 copies, Series A

PROJECT OFFICERS REPORT—PROJECT 6.3

D-REGION PHYSICAL CHEMISTRY (U)

Warren W. Berning, Project Officer

and Staff Members of:

Ballistic Research Laboratories
Aberdeen Proving Ground, Maryland

GROUP-1
Excluded from automatic downgrading and declassification.

RESTRICTED DATA

This document contains restricted data as defined in the Atomic Energy Act of 1954. Its transmittal or the disclosure of its contents in any manner to an unauthorized person is prohibited.

Issuance Date: November 27, 1964

All distribution of this report is controlled. Qualified DDC users shall request through Director, Defense Atomic Support Agency, Washington, D.C. 20301

05757

SECRET

Inquiries relative to this report may be made to

Chief, Defense Atomic Support Agency
Washington, D. C. 20301

When no longer required, this document may be destroyed in accordance with applicable security regulations.

DO NOT RETURN THIS DOCUMENT

USAEC Division of Technical Information Extension, Oak Ridge, Tennessee

SECRET

POR-2018
(WT-2018)
Volume 4

OPERATION DOMINIC

FISH BOWL SERIES

PROJECT OFFICERS REPORT--PROJECT 6.3

D-REGION PHYSICAL CHEMISTRY (U)

Warren W. Berning, Project Officer
and Staff Members of:

Ballistic Research Laboratories
Aberdeen Proving Ground, Maryland

"This document contains information affecting the National
Defense of the United States within the meaning of the Espionage
Laws, Title 18, U.S.C., Sections 793 and 794. The transmission or
revelation of its contents in any manner to an unauthorized person
is prohibited by law."

All distribution of this report is controlled. Qualified DDC users shall request through Director, Defense Atomic Support Agency, Washington, D.C. 20301

GROUP-1
Excluded from automatic downgrading and declassification.

RESTRICTED DATA

This document contains restricted data as defined in the Atomic Energy Act of 1954. Its transmittal or the disclosure of its contents in any manner to an unauthorized person is prohibited.

This document is the author(s) report to the Director, Defense Atomic Support Agency, of the results of experimentation sponsored by that agency during nuclear weapons effects testing. The results and findings in this report are those of the author(s) and not necessarily those of the DOD. Accordingly, reference to this material must credit the author(s). This report is the property of the Department of Defense and, as such, may be reclassified or withdrawn from circulation as appropriate by the Defense Atomic Support Agency.

DEPARTMENT OF DEFENSE
WASHINGTON, D.C. 20301

SECRET

CONTENTS

APPENDIX B ROCKET VEHICLE PERFORMANCE 29
B.1 Introduction 29
B.2 Trajectory Parameters 30
B.3 Trajectory Solutions 32
B.4 Results 39
B.5 Discussion 42

APPENDIX C PROPAGATION EXPERIMENT: INSTRUMENTATION AND PERFORMANCE 103
C.1 Ground Instrumentation and Performance 103
C.1.1 3-Frequency Experiment Ground Instrumentation 103
C.1.2 Satellite Experiment Ground Instrumentation 113
C.1.3 GMD Telemetry and Tracking Ground Instrumentation 123
C.2 Rocket Instrumentation and Performance 126
C.2.1 3-Frequency Experiment Rocket Instrumentation. 126
C.2.2 GMD Rocket Instrumentation . . . 137

C.3 Rocket Dispersive Doppler 139
C.3.1 Star Fish Event 139
C.3.2 Blue Gill Event 144
C.3.3 King Fish Event 148
C.4 Signal Duration and Strength 152
C.4.1 Signal Duration Graphs. 152
C.4.2 Signal Strength Graphs 152

REFERENCES 485

TABLES

B.1 Source of Input Data for Determining Rocket Trajectories, Projects 6.2, 6.3 and 6.4. 47
B.2 Estimated Nose-Over Altitudes for Selected Rockets of Projects 6.2, 6.3, 6.4. 48
C.1 Characteristics of 3-Frequency Ground Antennas. 155
C.2 Description of Magnetic Tape Data Recorded in BRL Van 2, Star Fish Event. 156
C.3 Description of Magnetic Tape Data Recorded in BRL Van 3, Star Fish Event 158
C.4 Description of Chart Data Recorded in BRL Van 2, Star Fish Event. 159

C.5 Description of Chart Data Recorded in BRL Van 5, Star Fish Event. 160
C.6 Description of Magnetic Tape Data Recorded in BRL Van 2, Blue Gill Event. 161
C.7 Description of Magnetic Tape Data Recorded in BRL Van 3, Blue Gill Event. 162
C.8 Description of Chart Data Recorded in BRL Van 2, Blue Gill Event. 163
C.9 Description of Chart Data Recorded in BRL Van 3, Blue Gill Event. 164
C.10 Description of Magnetic Tape Data Recorded in BRL Van 2, King Fish Event. 165
C.11 Description of Magnetic Tape Data Recorded in BRL Van 3, King Fish Event. 166
C.12 Description of Chart Data Recorded in BRL Van 2, King Fish Event. 167
C.13 Description of Chart Data Recorded in BRL Van 3, King Fish Event. 168
C.14 Summary of GMD Telemetry and Tracking Data, Rocket 1 Star Fish Event. 169
C.15 Summary of GMD Telemetry and Tracking Data, Rocket 2, Star Fish Event 170
C.16 Summary of GMD Telemetry and Tracking Data, Rocket 3, Star Fish Event. 171
C.17 Summary of GMD Telemetry and Tracking Data, Rocket 4, Star Fish Event. . . . 172
C.18 Summary of GMD Telemetry and Tracking Data, Rocket 5, Star Fish Event. 173
C.19 Summary of GMD Telemetry and Tracking Data, Rocket 6, Star Fish Event. 174
C.20 Summary of GMD Telemetry and Tracking Data, Rocket 7, Star Fish Event. 175
C.21 Summary of GMD Telemetry and Tracking Data, Rocket 8, Star Fish Event 176
C.22 Summary of GMD Telemetry and Tracking Data, Rocket 9, Star Fish Event 177
C.23 Summary of GMD Telemetry and Tracking Data, Rocket 10, Blue Gill Event. . . . 178
C.24 Summary of GMD Telemetry and Tracking Data, Rocket 11, Blue Gill Event. . . . 179
C.25 Summary of GMD Telemetry and Tracking Data, Rocket 12, Blue Gill Event. . . . 180
C.26 Summary of GMD Telemetry and Tracking Data, Rocket 13, Blue Gill Event. . . . 181
C.27 Summary of GMD Telemetry and Tracking Data, Rocket 14, Blue Gill Event. . . . 182
C.28 Summary of GMD Telemetry and Tracking Data, Rocket 15, Blue Gill Event. . . . 183
C.29 Summary of GMD Telemetry and Tracking Data, Rocket 17, Blue Gill Event. . . . 184
C.30 Summary of GMD Telemetry and Tracking Data, Rocket 18, Blue Gill Event. . . . 185
C.31 Summary of GMD Telemetry and Tracking Data, Rocket 19, King Fish Event. . . . 186

C.5 Description of Chart Data Recorded in BRL Van 5, Star Fish Event. 160
C.6 Description of Magnetic Tape Data Recorded in BRL Van 2, Blue Gill Event. 161
C.7 Description of Magnetic Tape Data Recorded in BRL Van 3, Blue Gill Event. 162
C.8 Description of Chart Data Recorded in BRL Van 2, Blue Gill Event. 163
C.9 Description of Chart Data Recorded in BRL Van 3, Blue Gill Event. 164
C.10 Description of Magnetic Tape Data Recorded in BRL Van 2, King Fish Event. 165
C.11 Description of Magnetic Tape Data Recorded in BRL Van 3, King Fish Event. 166
C.12 Description of Chart Data Recorded in BRL Van 2, King Fish Event. 167
C.13 Description of Chart Data Recorded in BRL Van 3, King Fish Event. 168
C.14 Summary of GMD Telemetry and Tracking Data, Rocket 1 Star Fish Event. 169
C.15 Summary of GMD Telemetry and Tracking Data, Rocket 2, Star Fish Event 170
C.16 Summary of GMD Telemetry and Tracking Data, Rocket 3, Star Fish Event. 171
C.17 Summary of GMD Telemetry and Tracking Data, Rocket 4, Star Fish Event. . . . 172
C.18 Summary of GMD Telemetry and Tracking Data, Rocket 5, Star Fish Event. 173
C.19 Summary of GMD Telemetry and Tracking Data, Rocket 6, Star Fish Event. 174
C.20 Summary of GMD Telemetry and Tracking Data, Rocket 7, Star Fish Event. 175
C.21 Summary of GMD Telemetry and Tracking Data, Rocket 8, Star Fish Event 176
C.22 Summary of GMD Telemetry and Tracking Data, Rocket 9, Star Fish Event 177
C.23 Summary of GMD Telemetry and Tracking Data, Rocket 10, Blue Gill Event. . . . 178
C.24 Summary of GMD Telemetry and Tracking Data, Rocket 11, Blue Gill Event. . . . 179
C.25 Summary of GMD Telemetry and Tracking Data, Rocket 12, Blue Gill Event. . . . 180
C.26 Summary of GMD Telemetry and Tracking Data, Rocket 13, Blue Gill Event. . . . 181
C.27 Summary of GMD Telemetry and Tracking Data, Rocket 14, Blue Gill Event. . . . 182
C.28 Summary of GMD Telemetry and Tracking Data, Rocket 15, Blue Gill Event. . . . 183
C.29 Summary of GMD Telemetry and Tracking Data, Rocket 17, Blue Gill Event. . . . 184
C.30 Summary of GMD Telemetry and Tracking Data, Rocket 18, Blue Gill Event. . . . 185
C.31 Summary of GMD Telemetry and Tracking Data, Rocket 19, King Fish Event. . . . 186

C.32 Summary of GMD Telemetry and Tracking Data, Rocket 20, King Fish Event. . . . 187
C.33 Summary of GMD Telemetry and Tracking Data, Rocket 21, King Fish Event. . . . 188
C.34 Summary of GMD Telemetry and Tracking Data, Rocket 23, King Fish Event. . . . 189
C.35 Summary of GMD Telemetry and Tracking Data, Rocket 24, King Fish Event. . . . 190
C.36 Summary of GMD Telemetry and Tracking Data, Rocket 25, King Fish Event. . . . 191
C.37 Summary of GMD Telemetry and Tracking Data, Rocket 26, King Fish Event. . . . 192
C.38 Summary of GMD Telemetry and Tracking Data, Rocket 27, King Fish Event. . . . 193
C.39 Summary of GMD Telemetry and Tracking Data, Rocket 28, King Fish Event. . . . 194
C.40 Summary of GMD Telemetry and Tracking Data, Rocket 29, King Fish Event 195
C.41 Summary of 3-Frequency Propagation Data Rocket 1, Star Fish Event. 196
C.42 Summary of 3-Frequency Propagation Data Rocket 4, Star Fish Event. 198
C.43 Summary of 3-Frequency Propagation Data Rocket 5, Star Fish Event. 200
C.44 Summary of 3-Frequency Propagation Data Rocket 7, Star Fish Event. 202
C.45 Summary of 3-Frequency Propagation Data Rocket 8, Star Fish Event. 204
C.46 Summary of 3-Frequency Propagation Data Rocket 9, Star Fish Event. 205
C.47 Summary of 3-Frequency Propagation Data Rocket 11, Blue Gill Event. 207
C.48 Summary of 3-Frequency Propagation Data Rocket 12, Blue Gill Event. 209
C.49 Summary of 3-Frequency Propagation Data Rocket 14, Blue Gill Event. 211
C.50 Summary of 3-Frequency Propagation Data Rocket 15, Blue Gill Event 213
C.51 Summary of 3-Frequency Propagation Data Rocket 17, Blue Gill Event. 214
C.52 Summary of 3-Frequency Propagation Data, Rocket 18, Blue Gill Event. 216
C.53 Summary of 3-Frequency Propagation Data Rocket 19, King Fish Event. 217
C.54 Summary of 3-Frequency Propagation Data Rocket 22, King Fish Event. 219
C.55 Summary of 3-Frequency Propagation Data Rocket 25, King Fish Event. 221
C.56 Summary of 3-Frequency Propagation Data Rocket 27, King Fish Event. 223
C.57 Summary of 3-Frequency Propagation Data Rocket 28, King Fish Event. 225
C.58 Summary of 3-Frequency Propagation Data Rocket 29, King Fish Event 226
C.59 3-Frequency, VHF TM and GMD System Parameters for Star Fish Event. 228

FIGURES

B.1 Trajectory for Rocket 1, Star Fish 49

B.2 Trajectory for Rocket 2, Star Fish 50

B.3 Trajectory for Rocket 4, Star Fish 51

B.4 Trajectory for Rocket 5, Star Fish 52

B.5 Trajectory for Rocket 6, Star Fish 53

B.6 Trajectory for Rocket 7, Star Fish 54

B.7 Trajectory for Rocket 8, Star Fish 55

B.8 Trajectory for Rocket 9, Star Fish 56

B.9 Trajectory for Rocket 10, Blue Gill 57

B.10 Trajectory for Rocket 11, Blue Gill 58

B.11 Trajectory for Rocket 12, Blue Gill 59

B.12 Trajectory for Rocket 13, Blue Gill 60

B.13 Trajectory for Rocket 14, Blue Gill 61

B.14 Trajectory for Rocket 15, Blue Gill 62

B.15 Trajectory for Rocket 17, Blue Gill 63

B.16 Trajectory for Rocket 18, Blue Gill 64

B.17 Trajectory for Rocket 19, King Fish 65

B.18 Trajectory for Rocket 20, King Fish 66

B.19 Trajectory for Rocket 21, King Fish 67

B.20 Trajectory for Rocket 22, King Fish 68

B.21 Trajectory for Rocket 23, King Fish 69

B.22 Trajectory for Rocket 24, King Fish 70

B.23 Trajectory for Rocket 25, King Fish 71

B.24 Trajectory for Rocket 26, King Fish 72

B.25 Trajectory for Rocket 27, King Fish 73

B.26 Trajectory for Rocket 28, King Fish 74

B.27 Trajectory for Rocket 29, King Fish 75

B.28 Slant range versus time for Rocket 1, Star Fish 76

B.29 Slant range versus time for Rocket 2, Star Fish 77

B.30 Slant range versus time for Rocket 4, Star Fish 78

B.31 Slant range versus time for Rocket 5, Star Fish 79

B.32 Slant range versus time for Rocket 6, Star Fish 80

B.33 Slant range versus time for Rocket 7, Star Fish 81

B.34 Slant range versus time for Rocket 8, Star Fish 82

B.35 Slant range versus time for Rocket 9, Star Fish 83

B.36 Slant range versus time for Rocket 10, Blue Gill 84

B.37 Slant range versus time for Rocket 11, Blue Gill 85

B.38 Slant range versus time for Rocket 12, Blue Gill 86

B. 39	Slant range versus time for Rocket 13, Blue Gill	87
B.40	Slant range versus time for Rocket 14, Blue Gill	88
B.41	Slant range versus time for Rocket 15, Blue Gill	89
B.42	Slant range versus time for Rocket 17, Blue Gill	90
B.43	Slant range versus time for Rocket 18, Blue Gill	91
B.44	Slant range versus time for Rocket 19, King Fish	92
B.45	Slant range versus time for Rocket 20, King Fish	93
B.46	Slant range versus time for Rocket 21, King Fish	94
B.47	Slant range versus time for Rocket 22, King Fish	95
B.48	Slant range versus time for Rocket 23, King Fish	96
B.49	Slant range versus time for Rocket 24, King Fish	97
B.50	Slant range versus time for Rocket 25, King Fish	98
B.51	Slant range versus time for Rocket 26, King Fish	99
B.52	Slant range versus time for Rocket 27, King Fish	100
B.53	Slant range versus time for Rocket 28, King Fish	101
B.54	Slant range versus time for Rocket 29, King Fish	102
C.1	Photograph of 37-Mc crossed dipole antenna.	229
C.2	Photograph of 148-Mc helix antennas. .	230
C.3	Photograph of 888-Mc helix antennas. .	231
C.4	Photograph of 54-Mc rotating dipole antenna.	232

C.5 Photograph of 324-Mc helix antenna. . 233

C.6 Photograph of GMD system functional diagram. 234

C.7 Block diagram of GMD system. 235

C.8 Field layout of GMD trackers. 236

C.9 Photograph of GMD recording van interior. 237

C.10 GMD azimuth and elevation versus time for Rocket 1, Star Fish 238

C.11 GMD azimuth and elevation versus time for Rocket 2, Star Fish 239

C.12 GMD azimuth and elevation versus time for Rocket 3, Star Fish 240

C.13 GMD azimuth and elevation versus time for Rocket 4, Star Fish 241

C.14 GMD azimuth and elevation versus time for Rocket 5, Star Fish 242

C.15 GMD azimuth and elevation versus time for Rocket 6, Star Fish 243

C.16 GMD azimuth and elevation versus time for Rocket 7, Star Fish 244

C.17 GMD azimuth and elevation versus time for Rocket 8, Star Fish 245

C.18 GMD azimuth and elevation versus time for Rocket 9, Star Fish 246

C.19 GMD azimuth and elevation versus time for Rocket 10, Blue Gill 247

C.20 GMD azimuth and elevation versus time for Rocket 11, Blue Gill 248

C.21 GMD azimuth and elevation versus time for Rocket 12, Blue Gill 249

C.22 GMD azimuth and elevation versus time for Rocket 13, Blue Gill 250

C.23 GMD azimuth and elevation versus time for Rocket 14, Blue Gill 251

C.24 GMD azimuth and elevation versus time for Rocket 15, Blue Gill 252

C.25 GMD azimuth and elevation versus time for Rocket 17, Blue Gill 253

C.26 GMD azimuth and elevation versus time for Rocket 18, Blue Gill 254

C.27 GMD azimuth and elevation versus time for Rocket 20, King Fish 255

C.28 GMD azimuth and elevation versus time for Rocket 21, King Fish 256

C.29 GMD azimuth and elevation versus time for Rocket 23, King Fish 257

C.30 GMD azimuth and elevation versus time for Rocket 24, King Fish 258

C.31 GMD azimuth and elevation versus time for Rocket 26, King Fish 259

C.32 GMD azimuth and elevation versus time for Rocket 27, King Fish 260

C.33 GMD azimuth and elevation versus time for Rocket 28, King Fish 261

C.34 GMD azimuth and elevation versus time for Rocket 29, King Fish 262

C.35 Block diagram of 3-frequency beacon control in blockhouse. 263

C.36 Photograph of 3-frequency beacon antennas on Honest John-Nike rockets, Project 6.3 264

C.37 Radiation pattern for 37-Mc loop antenna on Honest John-Nike rockets, Project 6.3 265

C.38 Radiation pattern for 148-Mc loop antenna on Honest John-Nike rockets, Project 6.3 266

C.39 Radiation pattern for 888-Mc antenna on Honest John-Nike rockets, Project 6.3. 267

C.40 Photograph of 3-frequency beacon antennas on Javelin and Honest John-Nike-Nike rockets, Project 6.2. 268

C.41 Radiation pattern for 148-Mc shroud antenna on Javelin and Honest John-Nike Nike rockets, Project 6.2. 269

C.42 Radiation pattern for 37-Mc single shroud antenna on Javelin and Honest John-Nike-Nike rockets, Project 6.2. .. 270

C.43 Radiation pattern for 888-Mc stub antennas on Javelin and Honest John-Nike-Nike rockets, Project 6.2. 271

C.44 Three-frequency beacon antennas on Javelin rockets, Project 6.4 272

C.45 Photograph of 3-frequency beacon antennas on Javelin rockets, Project 6.4. 273

C.46 BRL-designed 888-Mc stub antenna. . .. 274

C.47 Circuit diagram of GMD beacon 275

C.48 Photograph of 1680-Mc slot antennas on Nike-Cajun rockets, Project 6.3 276

C.49 Radiation pattern for 1680-Mc slot antennas in plane of longitudinal axis of rocket. 277

C.50 Radiation pattern for 1680-Mc slot antennas off side of rocket. 278

C.51 Dispersive doppler versus time derived from the 37- and 148-Mc doppler Rocket 1, Star Fish 279

C.52 Dispersive doppler versus time derived from the 37- and 148-Mc doppler, Rocket 4, Star Fish 280

C.53 Dispersive doppler versus time derived from the 37- and 148-Mc doppler Rocket 5, Star Fish 281

C.54 Dispersive doppler versus time derived from the 37- and 148-Mc doppler, Rocket 7, Star Fish 282

C.55 Dispersive doppler versus time derived from the 37- and 148-Mc doppler Rocket 8, Star Fish 283

C.56 Dispersive doppler versus time derived from the 37- and 148-Mc doppler, Rocket 9, Star Fish 284

C.57 Dispersive doppler versus time derived from the 37- and 148-Mc doppler Rocket 12, Blue Gill 285

C.58 Dispersive doppler versus time derived from the 37- and 148-Mc doppler, Rocket 14, Blue Gill 286

C.59 Dispersive doppler versus time derived from the 37- and 148-Mc doppler, Rocket 15, Blue Gill 287

C.60 Dispersive doppler versus time derived from the 37- and 148-Mc doppler, Rocket 17, Blue Gill 288

C.61 Dispersive doppler versus time derived from the 37- and 148-Mc doppler, Rocket 19, King Fish 289

C.62 Dispersive doppler versus time derived from the 148- and 888-Mc doppler, Rocket 19, King Fish . . . 290

C.63 Dispersive doppler versus time derived from the 37- and 148-Mc doppler, Rocket 22, King Fish 291

C.64 Dispersive doppler versus time derived from the 37- and 148-Mc doppler, Rocket 25, King Fish 292

C.65 Dispersive doppler versus time derived from the 148- and 888-Mc doppler, Rocket 25, King Fish 293

C.66 Dispersive doppler versus time derived from the 37- and 148-Mc doppler, Rocket 27, King Fish 294

C.67 Dispersive doppler versus time derived from the 37- and 148-Mc doppler, Rocket 28, King Fish 295

C.68 Duration of useful received signal for experiments carried on Rocket 1, Star Fish 296

C.69 Duration of useful received signal for experiments carried on Rocket 2, Star Fish 297

C.70 Duration of useful received signal for experiments carried on Rocket 3, Star Fish 298

C.71 Duration of useful received signal for experiments carried on Rocket 4, Star Fish 299

C.72 Duration of useful received signal for experiments carried on Rocket 5, Star Fish 300

C.73 Duration of useful received signal for experiments carried on Rocket 6, Star Fish 301

C.74 Duration of useful received signal for experiments carried on Rocket 7, Star Fish 302

C.75 Duration of useful received signal for experiments carried on Rocket 8, Star Fish 303

C.76 Duration of useful received signal for experiments carried on Rocket 9, Star Fish 304

C.77 Duration of useful received signal for experiments carried on Rocket 10, Blue Gill 305

C.78 Duration of useful received signal for experiments carried on Rocket 11, Blue Gill 306

C.79 Duration of useful received signal for experiments carried on Rocket 12, Blue Gill 307

C.80 Duration of useful received signal for experiments carried on Rocket 13, Blue Gill 308

C.81 Duration of useful received signal for experiments carried on Rocket 14, Blue Gill 309

C.82 Duration of useful received signal for experiments carried on Rocket 15, Blue Gill 310

C.83 Duration of useful received signal for experiments carried on Rocket 17, Blue Gill 311

C.84 Duration of useful received signal for experiments carried on Rocket 18, Blue Gill 312

C.85 Duration of useful received signal for experiments carried on Rocket 19, King Fish 313

C.86 Duration of useful received signal for experiments carried on Rocket 20, King Fish 314

C.87 Duration of useful received signal for experiments carried on Rocket 21, King Fish 315

C.88 Duration of useful received signal for experiments carried on Rocket 22, King Fish 316

C.89 Duration of useful received signal for experiments carried on Rocket 23, King Fish 317

C.90 Duration of useful received signal for experiments carried on Rocket 24, King Fish 318

C.91 Duration of useful received signal for experiments carried on Rocket 25, King Fish 319

C.92 Duration of useful received signal for experiments carried on Rocket 26, King Fish 320

C.93 Duration of useful received signal for experiments carried on Rocket 27, King Fish 321

C.94 Duration of useful received signal for experiments carried on Rocket 28, King Fish 322

C.95 Duration of useful received signal for experiments carried on Rocket 29, King Fish 323

C.96 Received signal strength versus slant range for 3-frequency beacon, 37 Mc left, Rocket 1, Star Fish 324

C.97 Received signal strength versus slant range for 3-frequency beacon, 37 Mc right, Rocket 1, Star Fish 325

C.98 Received signal strength versus slant range for 3-frequency beacon, 148 Mc left, Rocket 1, Star Fish 326

C.99 Received signal strength versus slant range for 3-frequency beacon, 148 Mc right, Rocket 1, Star Fish 327

C.100 Received signal strength versus slant range for 3-frequency beacon, 888 Mc left, Rocket 1, Star Fish 328

C.101 Received signal strength versus slant range for 3-frequency beacon, 888 Mc right, Rocket 1, Star Fish 329

C.102 Received signal strength versus slant range for 3-frequency beacon, 37 Mc left, Rocket 4, Star Fish 330

C.103 Received signal strength versus slant range for 3-frequency beacon, 37 Mc right, Rocket 4, Star Fish 331

C.104 Received signal strength versus slant range for 3-frequency beacon, 148 Mc left, Rocket 4, Star Fish 332

C.105 Received signal strength versus slant range for 3-frequency beacon, 148 Mc right, Rocket 4, Star Fish 333

C.106 Received signal strength versus slant range for 3-frequency beacon, 888 Mc left, Rocket 4, Star Fish 334

C.107 Received signal strength versus slant range for 3-frequency beacon, 888 Mc right, Rocket 4, Star Fish 335

C.108 Received signal strength versus slant range for 3-frequency beacon, 37 Mc left, Rocket 5, Star Fish 336

C.109 Received signal strength versus slant range for 3-frequency beacon, 37 Mc right, Rocket 5, Star Fish 337

C.110 Received signal strength versus slant range for 3-frequency beacon, 148 Mc left, Rocket 5, Star Fish 338

C.111 Received signal strength versus slant range for 3-frequency beacon, 148 Mc right, Rocket 5, Star Fish 339

C.112 Received signal strength versus slant range for 3-frequency beacon, 888 Mc left, Rocket 5, Star Fish 340

C.113 Received signal strength versus slant range for 3-frequency beacon, 888 Mc right, Rocket 5, Star Fish 341

C.114 Received signal strength versus slant range for 3-frequency beacon, 37 Mc left, Rocket 7, Star Fish 342

C.115 Received signal strength versus slant range for 3-frequency beacon, 37 Mc right, Rocket 7, Star Fish 343

C.116 Received signal strength versus slant range for 3-frequency beacon, 148 Mc left, Rocket 7, Star Fish 344

C.117 Received signal strength versus slant range for 3-frequency beacon, 148 Mc right, Rocket 7, Star Fish 345

C.118 Received signal strength versus slant range for 3-frequency beacon, 888 Mc left, Rocket 7, Star Fish 346

C.119 Received signal strength versus slant range for 3-frequency beacon, 888 Mc right, Rocket 7, Star Fish 347

C.120 Received signal strength versus slant range for 3-frequency beacon, 37 Mc left, Rocket 8, Star Fish 348

C.121 Received signal strength versus slant range for 3-frequency beacon, 37 Mc right, Rocket 8, Star Fish 349

C.122 Received signal strength versus slant range for 3-frequency beacon, 148 Mc left, Rocket 8, Star Fish 350

C.123 Received signal strength versus slant range for 3-frequency beacon, 148 Mc right, Rocket 8, Star Fish 351

C.124 Received signal strength versus slant range for 3-frequency beacon, 888 Mc left, Rocket 8, Star Fish 352

C.125 Received signal strength versus slant range for 3-frequency beacon, 888 Mc right, Rocket 8, Star Fish 353

C.126 Received signal strength versus slant range for 3-frequency beacon, 37 Mc left, Rocket 9, Star Fish 354

C.127 Received signal strength versus slant range for 3-frequency beacon, 37 Mc right, Rocket 9, Star Fish 355

C.128 Received signal strength versus slant range for 3-frequency beacon, 148 Mc left, Rocket 9, Star Fish 356

C.129 Received signal strength versus slant range for 3-frequency beacon, 148 Mc right, Rocket 9, Star Fish 357

C.130 Received signal strength versus slant range for 3-frequency beacon, 888 Mc left, Rocket 9, Star Fish 358

C.131 Received signal strength versus slant range for 3-frequency beacon, 888 Mc right, Rocket 9, Star Fish 359

C.132 Received signal strength versus slant range for 3-frequency beacon, 37 Mc left, Rocket 11, Blue Gill 360

C.133 Received signal strength versus slant range for 3-frequency beacon, 37 Mc right, Rocket 11, Blue Gill 361

C.134 Received signal strength versus slant range for 3-frequency beacon, 148 Mc left, Rocket 11, Blue Gill 362

C.135 Received signal strength versus slant range for 3-frequency beacon, 148 Mc right, Rocket 11, Blue Gill 363

C.136 Received signal strength versus slant range for 3-frequency beacon, 888 Mc left, Rocket 11, Blue Gill . . . 364

C.137 Received signal strength versus slant range for 3-frequency beacon, 888 Mc right, Rocket 11, Blue Gill . .. 365

C.138 Received signal strength versus slant range for 3-frequency beacon, 37 Mc left, Rocket 12, Blue Gill . . . 366

C.139 Received signal strength versus slant range for 3-frequency beacon, 37 Mc right, Rocket 12, Blue Gill . .. 367

C.140 Received signal strength versus slant range for 3-frequency beacon, 148 Mc left, Rocket 12, Blue Gill . . . 368

C.141 Received signal strength versus slant range for 3-frequency beacon, 148 Mc right, Rocket 12, Blue Gill . .. 369

C.142 Received signal strength versus slant range for 3-frequency beacon, 888 Mc left, Rocket 12, Blue Gill . . . 370

C.143 Received signal strength versus slant range for 3-frequency beacon, 888 Mc right, Rocket 12, Blue Gill . .. 371

C.144 Received signal strength versus slant range for 3-frequency beacon, 37 Mc left, Rocket 14, Blue Gill . . . 372

C.145 Received signal strength versus slant range for 3-frequency beacon, 37 Mc right, Rocket 14, Blue Gill . . . 373

C.146 Received signal strength versus slant range for 3-frequency beacon, 148 Mc left, Rocket 14, Blue Gill 374

C.147 Received signal strength versus slant range for 3-frequency beacon,148 Mc right, Rocket 14, Blue Gill . . . 375

C.148 Received signal strength versus slant range for 3-frequency beacon, 888 Mc left, Rocket 14, Blue Gill . . . 376

C.149 Received signal strength versus slant range for 3-frequency beacon, 888 Mc right,Rocket 14, Blue Gill . . . 377

C.150 Received signal strength versus slant range for 3-frequency beacon, 37 Mc left, Rocket 15, Blue Gill . . . 378

C.151 Received signal strength versus slant range for 3-frequency beacon, 37 Mc right, Rocket 15, Blue Gill . .. 379

C.152 Received signal strength versus slant range for 3-frequency beacon, 148 Mc left, Rocket 15, Blue Gill . . . 380

C.153 Received signal strength versus slant range for 3-frequency beacon, 148 Mc right, Rocket 15, Blue Gill . .. 381

C.154 Received signal strength versus slant range for 3-frequency beacon, 888 Mc left, Rocket 15, Blue Gill . . . 382

C.155 Received signal strength versus slant range for 3-frequency beacon, 888 Mc right, Rocket 15, Blue Gill . .. 383

C.156 Received signal strength versus slant range for 3-frequency beacon, 37 Mc left, Rocket 17, Blue Gill . . . 384

C.157 Received signal strength versus slant range for 3-frequency beacon, 37 Mc right, Rocket 17, Blue Gill . .. 385

C.158 Received signal strength versus slant range for 3-frequency beacon, 148 Mc left, Rocket 17, Blue Gill . . . 386

C.159 Received signal strength versus slant range for 3-frequency beacon, 148 Mc right, Rocket 17, Blue Gill . .. 387

C.160 Received signal strength versus slant range for 3-frequency beacon, 888 Mc left, Rocket 17, Blue Gill . . . 388

C.161 Received signal strength versus slant range for 3-frequency beacon, 888 Mc right, Rocket 17, Blue Gill . .. 389

C.162 Received signal strength versus slant range for 3-frequency beacon, 37 Mc left, Rocket 18, Blue Gill . . . 390

C.163 Received signal strength versus slant range for 3-frequency beacon, 37 Mc right, Rocket 18, Blue Gill . .. 391

C.164 Received signal strength versus slant range for 3-frequency beacon, 148 Mc left, Rocket 18, Blue Gill . . . 392

C.165 Received signal strength versus slant range for 3-frequency beacon, 148 Mc right, Rocket 18, Blue Gill . .. 393

C.166 Received signal strength versus slant range for 3-frequency beacon, 888 Mc left, Rocket 18, Blue Gill . . . 394

C.167 Received signal strength versus slant range for 3-frequency beacon, 888 Mc right, Rocket 18, Blue Gill . .. 395

C.168 Received signal strength versus slant range for 3-frequency beacon, 37 Mc left, Rocket 19, King Fish . . . 396

C.169 Received signal strength versus slant range for 3-frequency beacon, 37 Mc right, Rocket 19, King Fish . .. 397

C.170 Received signal strength versus slant range for 3-frequency beacon, 148 Mc left, Rocket 19, King Fish . . . 398

C.171 Received signal strength versus slant range for 3-frequency beacon, 148 Mc right, Rocket 19, King Fish . .. 399

C.172 Received signal strength versus slant range for 3-frequency beacon, 888 Mc left, Rocket 19, King Fish . . . 400

C.173 Received signal strength versus slant range for 3-frequency beacon, 888 Mc right, Rocket 19, King Fish . .. 401

C.174 Received signal strength versus slant range for 3-frequency beacon, 37 Mc left, Rocket 22, King Fish . . . 402

C.175 Received signal strength versus slant range for 3-frequency beacon, 37 Mc right, Rocket 22, King Fish . .. 403

C.176 Received signal strength versus slant range for 3-frequency beacon, 148 Mc left, Rocket 22, King Fish . . . 404

C.177 Received signal strength versus slant range for 3-frequency beacon, 148 Mc right, Rocket 22, King Fish . .. 405

C.178 Received signal strength versus slant range for 3-frequency beacon, 888 Mc left, Rocket 22, King Fish . . . 406

C.179 Received signal strength versus slant range for 3-frequency beacon, 888 Mc right, Rocket 22, King Fish . .. 407

C.180 Received signal strength versus slant range for 3-frequency beacon, 37 Mc left, Rocket 25, King Fish . . . 408

C.181 Received signal strength versus slant range for 3-frequency beacon, 37 Mc right, Rocket 25, King Fish . .. 409

C.182 Received signal strength versus slant range for 3-frequency beacon, 148 Mc left, Rocket 25, King Fish . . . 410

C.183 Received signal strength versus slant range for 3-frequency beacon, 148 Mc right, Rocket 25, King Fish . . . 411

C.184 Received signal strength versus slant range for 3-frequency beacon, 888 Mc left, Rocket 25, King Fish 412

C.185 Received signal strength versus slant range for 3-frequency beacon, 888 Mc right, Rocket 25, King Fish . . . 413

C.186 Received signal strength versus slant range for 3-frequency beacon, 37 Mc left, Rocket 27, King Fish 414

C.187 Received signal strength versus slant range for 3-frequency beacon, 37 Mc right, Rocket 27, King Fish . . . 415

C.188 Received signal strength versus slant range for 3-frequency beacon, 148 Mc left, Rocket 27, King Fish 416

C.189 Received signal strength versus slant range for 3-frequency beacon, 148 Mc right, Rocket 27, King Fish . . . 417

C.190 Received signal strength versus slant range for 3-frequency beacon, 888 Mc left, Rocket 27, King Fish 418

C.191 Received signal strength versus slant range for 3-frequency beacon, 888 Mc right, Rocket 27, King Fish . . . 419

C.192 Received signal strength versus slant range for 3-frequency beacon, 37 Mc left, Rocket 28, King Fish 420

C.193 Received signal strength versus slant range for 3-frequency beacon, 37 Mc right, Rocket 28, King Fish . . . 421

C.194 Received signal strength versus slant range for 3-frequency beacon, 148 Mc left, Rocket 28, King Fish . . . 422

C.195 Received signal strength versus slant range for 3-frequency beacon, 148 Mc right, Rocket 28, King Fish . . . 423

C.196 Received signal strength versus slant range for 3-frequency beacon, 888 Mc left, Rocket 28, King Fish . . . 424

C.197 Received signal strength versus slant range for 3-frequency beacon, 888 Mc right, Rocket 28, King Fish . . . 425

C.198 Received signal strength versus slant range for 3-frequency beacon, 37 Mc left, Rocket 29, King Fish . . . 426

C.199 Received signal strength versus slant range for 3-frequency beacon, 37 Mc right, Rocket 29, King Fish . . . 427

C.200 Received signal strength versus slant range for 3-frequency beacon, 148 Mc left, Rocket 29, King Fish . . . 428

C.201 Received signal strength versus slant range for 3-frequency beacon, 148 Mc right, Rocket 29, King Fish . . . 429

C.202 Received signal strength versus slant range for 3-frequency beacon, 888 Mc left, Rocket 29, King Fish . . . 430

C.203 Received signal strength versus slant range for 3-frequency beacon, 888 Mc right, Rocket 29, King Fish . . . 431

C.204 Received signal strength versus slant range for VHF telemetry, Rocket 1, Star Fish 432

C.205 Received signal strength versus slant range for VHF telemetry, Rocket 2, Star Fish 433

C.206 Received signal strength versus slant range for VHF telemetry, Rocket 4, Star Fish 434

C.207 Received signal strength versus slant range for VHF telemetry, Rocket 5, Star Fish 435

C.208 Received signal strength versus slant range for VHF telemetry, Rocket 6, Star Fish 436

C.209 Received signal strength versus slant range for VHF telemetry, Rocket 7, Star Fish 437

C.210 Received signal strength versus slant range for VHF telemetry, Rocket 8, Star Fish 438

C.211 Received signal strength versus slant range for VHF telemetry, Rocket 9, Star Fish 439

C.212 Received signal strength versus slant range for VHF telemetry, Rocket 10, Blue Gill 440

C.213 Received signal strength versus slant range for VHF telemetry, Rocket 11, Blue Gill 441

C.214 Received signal strength versus slant range for VHF telemetry, Rocket 12, Blue Gill 442

C.215 Received signal strength versus slant range for VHF telemetry, Rocket 13, Blue Gill 443

C.216 Received signal strength versus slant range for VHF telemetry, Rocket 14, Blue Gill 444

C.217 Received signal strength versus slant range for VHF telemetry, Rocket 15, Blue Gill 445

C.218 Received signal strength versus slant range for VHF telemetry, Rocket 17, Blue Gill 446

C.219 Received signal strength versus slant range for VHF telemetry, Rocket 18, Blue Gill 447

C.220 Received signal strength versus slant range for VHF telemetry, Rocket 19, King Fish 448

C.221 Received signal strength versus slant range for VHF telemetry, Rocket 20, King Fish 449

C.222 Received signal strength versus slant range for VHF telemetry, Rocket 22, King Fish 450

C.223 Received signal strength versus slant range for VHF telemetry, Rocket 24, King Fish 451

C.224 Received signal strength versus slant range for VHF telemetry, Rocket 25, King Fish 452

C.225 Received signal strength versus slant range for VHF telemetry, Rocket 26, King Fish 453

C.226 Received signal strength versus slant range for VHF telemetry, Rocket 27, King Fish 454

C.227 Received signal strength versus slant range for VHF telemetry, Rocket 28, King Fish 455

C.228 Received signal strength versus slant range for VHF telemetry, Rocket 29, King Fish 456

C.229 Received signal strength versus slant range for GMD telemetry, Rocket 1, Star Fish 457

C.230 Received signal strength versus slant range for GMD telemetry, Rocket 2, Star Fish 458

C.231 Received signal strength versus slant range for GMD telemetry, Rocket 4, Star Fish 459

C.232 Received signal strength versus slant range for GMD telemetry, Rocket 5, Star Fish 460

C.233 Received signal strength versus slant range for GMD telemetry, Rocket 6, Star Fish 461

C.234 Received signal strength versus slant range for GMD telemetry, Rocket 7, Star Fish 462

C.235 Received signal strength versus slant range for GMD telemetry, Rocket 8, Star Fish 463

C.236 Received signal strength versus slant range for GMD telemetry, Rocket 9, Star Fish 464

C.237 Received signal strength versus slant range for GMD telemetry, Rocket 10, Blue Gill 465

C.238 Received signal strength versus slant range for GMD telemetry, Rocket 11, Blue Gill 466

C.239 Received signal strength versus slant range for GMD telemetry, Rocket 12, Blue Gill 467

C.240 Received signal strength versus slant range for GMD telemetry, Rocket 13, Blue Gill 468

C.241 Received signal strength versus slant range for GMD telemetry, Rocket 14, Blue Gill 469

C.242 Received signal strength versus slant range for GMD telemetry, Rocket 15, Blue Gill 470

C.243 Received signal strength versus slant range for GMD telemetry, Rocket 17, Blue Gill 471

C.244 Received signal strength versus slant range for GMD telemetry, Rocket 18, Blue Gill 472

C.245 Received signal strength versus slant range for GMD telemetry, Rocket 19, King Fish 473

C.246 Received signal strength versus slant range for GMD telemetry, Rocket 20, King Fish 474

C.247 Received signal strength versus slant range for GMD telemetry, Rocket 21, King Fish 475

C.248 Received signal strength versus slant range for GMD telemetry, Rocket 23, King Fish 476

C.249 Received signal strength versus slant range for GMD telemetry, Rocket 24, King Fish 477

C.250 Received signal strength versus slant range for GMD telemetry, Rocket 25, King Fish 478

C.251 Received signal strength versus slant range for GMD telemetry, Rocket 26, King Fish 479

C.252 Received signal strength versus slant range for GMD telemetry, Rocket 27, King Fish 480

C.253 Received signal strength versus slant range for GMD telemetry, Rocket 28, King Fish 481

C.254 Received signal strength versus slant range for GMD telemetry, Rocket 29, King Fish 482

C.255 Calculated received signal strength versus slant range for the 3-frequency beacon, VHF telemetry and GMD, Star Fish 483

C.256 Calculated received signal strength versus slant range for the 3-frequency beacon, VHF telemetry and GMD, Blue Gill and King Fish 484

APPENDIX B

ROCKET VEHICLE PERFORMANCE

B.1 INTRODUCTION

In the determination of a missile's flight path, ground-based instrumentation dispersed over several sites generally allows more flexibility and greater accuracy in data reduction than measuring systems concentrated at a single location. In addition to providing less accuracy, single-site systems frequently fail to yield sufficient data for position determination without the introduction of constraints such as parabolic or elliptical motion. To arrive at a trajectory under single-site conditions, it becomes necessary to assume that the motion of the missile may be characterized by a set of parameters which are functionally related to the measured quantities. A solution is possible if there are at least as many observations as parameters, and if the resulting system of condition equations is sufficiently independent.

The reduction and analysis of a large portion of the observed rocket trajectory data for Projects 6.2, 6.3, and 6.4, was based upon the flight paths

GROUP 1
Excluded from automatic downgrading and declassification

of the missiles as a function of time. For many rockets, the various missile tracking systems operating at or near Johnston Island failed to provide adequate coverage to meet all trajectory requirements. Therefore, it became necessary to develop methods of position determination from a combination of various measurements or observations. Frequently, these observations were neither of sufficient quantity nor quality to permit a high order of accuracy. Fortunately, most of the rocket measurements of atmospheric and event parameters could tolerate moderate errors in position determination, provided that the differential in position varied smoothly. In view of the relatively lax requirements for accuracy and the limited precision of the observations, it was considered reasonable to characterize the drag-free portion of the trajectory by simple parabolic motion.

B.2 TRAJECTORY PARAMETERS

With the assumption of parabolic motion within a plane, the reduction problem became two-

dimensional. If ρ is defined as the horizontal coordinate and y as the vertical, the equations of motion are,

$$\rho = \rho_o + \dot{\rho}_o(t-t_o) \tag{B.1}$$

$$y = y_o+\dot{y}_o(t-t_o)-1/2\ g\ (t-t_o)^2 \tag{B.2}$$

where ρ_o and y_o are the position coordinates, and $\dot{\rho}_o$ and $\dot{y}_o$ are the velocity components for the initial time t_o. The time variable is t, and -g is the vertical component of acceleration resulting from the force of gravity which is assumed constant for each trajectory determination, but variable from rocket to rocket. For convenience, let $T \equiv (t-t_o)$ so that the above equations become

$$\rho = \rho_o+\dot{\rho}_o\ T \tag{B.3}$$

$$y = y_o+\dot{y}_o\ T - 1/2\ g\ T^2 \tag{B.4}$$

The velocity components are obtained by differentiating the last two equations.

$$\dot{\rho} = \dot{\rho}_o \tag{B.5}$$

$$\dot{y} = \dot{y}_o - g\ T \tag{B.6}$$

Hence, if the parameters ρ_o, y_o, $\dot{\rho}_o$, and $\dot{y}_o$ can be evaluated from the observed data, position and velocity are determined as a function of time by the last four equations.

B.3 TRAJECTORY SOLUTIONS

A complete solution, for the problem as formulated, consisted of using the measured data to evaluate ρ_o, y_o, $\dot{\rho}_o$, and $\dot{y}_o$, the trajectory parameters. This required the derivation of a system of equations of condition which related the trajectory parameters to the observed data. Since Equations B.3 through B.6 relate the position and velocity components of the missile to the trajectory parameters and time, it is necessary to initially establish a functional relationship between the measured quantitites and the missile's position and velocity. It was sufficient for the rocket flights here discussed to express the slant range r, and the elevation angle ε, in terms of the position coordinates, while developing $\dot{r}$ in terms of both the position coordinates and the velocity components.

The equations follow:

$$r = \sqrt{\rho^2 + y^2} \tag{B.7}$$

$$\varepsilon = \tan^{-1}(y/\rho) \tag{B.8}$$

$$\dot{r} = (\rho\dot{\rho}+y\dot{y})/r \tag{B.9}$$

Combining the above equations with Equations B.3 through B.6, there result:

$$r = \sqrt{(\rho_o+\dot{\rho}_o T)^2+(y_o+\dot{y}_o T-1/2gT^2)^2} \tag{B.10}$$

$$\varepsilon = \tan^{-1}[(y_o+\dot{y}_o T-1/2gT^2)/(\rho_o+\dot{\rho}_o T)] \tag{B.11}$$

$$\dot{r} = [(\rho_o+\dot{\rho}_o T)(\dot{\rho}_o)+(y_o+\dot{y}_o T-1/2gT^2)(\dot{y}_o-gT)] \times \left[\sqrt{(\rho_o+\dot{\rho}_o T)^2+(y_o+\dot{y}_o T-1/2\ gT^2)^2}\right]^{-1} \tag{B.12}$$

In particular, when $t = t_o$ so that $T = 0$, Equations B.10, B.11, and B.12 reduce to:

$$r_o = \sqrt{\rho_o^2+y_o^2} \tag{B.13}$$

$$\varepsilon_o = \tan^{-1}(y_o/\rho_o) \tag{B.14}$$

$$\dot{r}_o = (\rho_o\dot{\rho}_o+y_o\dot{y}_o)/r_o \tag{B.15}$$

where r_o, ε_o, and $\dot{r}_o$ are, respectively, the slant range, the elevation angle, and the component of velocity in the direction of the radius vector at time $t = t_o$. The equations of condition were obtained by substituting measured data in one or more of Equations B.10 through B.15 or in equations derived from various combinations of these. If more than four observations were available, the system would be over-determined, and in general, would require rather extensive computation. In selecting a set of equations of condition, caution was required to avoid a system in which the equations were so nearly dependent that they failed to yield a reliable solution. For example, observations of slant range for four times at the same site generally provided a very weak solution. Likewise, poor results were experienced from a set of observations consisting of elevation angle measurements for four times at a single location. However, several combinations of single-site observations provided useful results. Computational methods for three of these will be considered in detail below.

If measurements of either slant range or its first time derivative are available for the major

portion of a missile's trajectory, together with the elevation angle for at least the initial portion of the flight above the effective atmosphere, its trajectory may be determined from measurements of r_o, $\dot{r}_o$, and ϵ_o for time t_o and a slant range, r, for any time, t, other than t_o. If only the slant range is measured, $\dot{r}$ may be obtained by either numerical or graphical differentiation. On the other hand, if $\dot{r}$ is the measured quantity, integration may be used to derive the necessary values for r. The latter process requires a continuous record of $\dot{r}$ from launch. Preferably, t_o should occur on the upward leg of the trajectory and t on the downward leg. Both times are, of course, restricted to that portion of the trajectory where the missile is in free flight and above the effective atmosphere.

With ϵ_o and r_o as input, initial position for time t_o may be readily obtained from the equations,

$$\rho_o = r_o \cos \epsilon_o \qquad \text{(B.16)}$$

$$y_o = r_o \sin \epsilon_o \qquad \text{(B.17)}$$

Solutions for the remaining trajectory parameters require Equation B.15 which may be written in the form,

$$\dot{\rho}_o = (r_o\dot{r}_o - y_o\dot{y}_o)/\rho_o \qquad \text{(B.18)}$$

Substituting for $\dot{\rho}_o$ in Equation B.10, yields,

$$r = \sqrt{[\rho_o + \{(r_o\dot{r}_o - y_o\dot{y}_o)/\rho_o\}T]^2 + [y_o + \dot{y}_o T - (1/2)gT^2]^2} \qquad \text{(B.19)}$$

After squaring and simplifying, this reduces to

$$A\dot{y}_o^2 + B\dot{y}_o + C = 0 \qquad \text{(B.20)}$$

Where,

$$A = 1 + (y_o/\rho_o)^2$$

$$B = -[(gT + (2r_o\dot{r}_o y_o)/\rho_o^2]$$

$$C = \{[r_o\dot{r}_o/\rho_o]^2 + [(r_o^2 - r^2)/T^2] + [2r_o\dot{r}_o/T] - g[y_o - (gT^2)/4]\}$$

One of the solutions for Equation B.20 yields a false result and may be neglected. The valid solution for $\dot{y}_o$ is obtained from:

$$\dot{y}_o = [-B - \sqrt{B^2 - 4AC}\ ]/2A \qquad \text{(B.21)}$$

$\dot{\rho}_o$ may now be evaluated with Equation B.18 to complete the solution.

If a reliable estimate of $\dot{r}_o$ is available, the method can be altered slightly to accept as input ε_o, r_o, and measurements of slant range, r_1 and r_2, for two times, t_1 and t_2, such that $t_o < t_1 < t_2$. If $T_1 \equiv (t_1-t_o)$ and $T_2 \equiv (t_2-t_o)$, the equations of condition may be written as

$$[\rho_o+\dot{\rho}_o T_1]^2+[y_o+\dot{y}_o T_1-(1/2)gT_1^2]^2 = r_1^2 \qquad (B.22)$$

$$[\rho_o+\dot{\rho}_o T_2]^2+[y_o+\dot{y}_o T_2-(1/2)gT_2^2]^2 = r_2^2 \qquad (B.23)$$

Since ρ_o and y_o may be determined by Equations B.16 and B.17, the above system contains the unknowns $\dot{\rho}_o$ and $\dot{y}_o$. The solution of Equations B.22 and B.23 may be obtained rather quickly by employing an iterative type of computation in which an initial approximation to the result is improved by a series of corrections until the desired number of significant figures is obtained.

A reduction problem, which occurred frequently in the trajectory determinations here discussed, required a trajectory determination from a series of elevation angle measurements recorded as a function of time. However, a system of equations derived

from observations of elevation angle alone is weak and the results unreliable. Fortunately, these reductions were required for rockets that were highly consistent in performance throughout the powered portion of flight. Hence, slant range could be rather accurately related to flight time near burnout. When such an estimate of slant range was combined with three observations of elevation angle, the resulting set of equations provided relatively reliable results.

When elevation angles alone were available, the input for the computation consisted of r_o, the slant range for time t_o, and three elevation angles, ε_o, ε_1, and ε_2, corresponding to times t_o, t_1, and t_2. The times were related so that $t_o < t_1 < t_2$ with t_o occurring on the upward leg of the trajectory and t_2 on the downward leg if possible. All three times were, of course, selected for a drag-free portion of the trajectory.

Proceeding with the derivations, the assumed value for r_o and the observed ε_o may be substituted directly into Equations B.16 and B.17 to determine

the position of the rocket at the initial time, t_o. With ρ_o and y_o known, Equations B.22 and B.23 may be solved for the unknowns, $\dot{\rho}_o$ and y_o. The resulting solution consists of

$$\dot{\rho}_o = [D(y_o + 1/2\ gT_1T_2)+E\rho_o]/F \qquad (B.24)$$

$$\dot{y}_o = [(\tan \varepsilon_2(\rho_o+\dot{\rho}_oT_2)-y_o)/T_2]+gT_2/2 \qquad (B.25)$$

where,

$$D = (T_2-T_1)$$

$$E = (T_1 \tan \varepsilon_2-T_2 \tan \varepsilon_1)$$

$$F = T_1T_2(\tan \varepsilon_1-\tan \varepsilon_2)$$

B.4 RESULTS

The trajectories, which are presented in graphical form in Figures B.1 through B.54, were determined from the best observations available for the particular rocket. Where possible, the computed trajectories were derived from flight paths obtained by missile tracking systems such as radar or the Cubic system. For these flight paths, parabolic trajectories were fitted to the tracking results. In

the absence of data from radar or the Cubic system, flight paths were computed by one of the methods previously described. In general, elevation angle measurements were preferred to observations of slant range for input data; the latter, in turn, were given preference over rate of change in slant range. This order of priority was dictated by the methods of measurement which resulted in better accuracy in the angle measurements than in the observations of slant range. In Figures C.10 through C.34 are plotted the azimuth-elevation data derived from the GMD tracking system and used as the principal source of angle measurements for the trajectory determinations.

The parameters which characterized the motion of each rocket are presented in Table B.1. In addition, the source of the input data for the trajectory determination of each rocket is indicated. Elevation angle input is represented by ε and slant range by r. The value for g is an average value based on the apogee of the flight

path. In practice, initial estimates were adjusted by an iterative procedure until the values for g were consistent with the computed trajectory. It should be observed that trajectories for Rockets 8 and 9 were well determined by radar. These trajectories were of sufficient duration that, to obtain a better fit to the observations, ρ was redefined by the equation:

$$\rho = \rho_o + \dot{\rho}_o T + (1/2)\ddot{\rho}_o T^2 \qquad \text{(B.26)}$$

For Rocket 8, $\ddot{\rho}_o = -0.000546$ km/sec^2, and for Rocket 9, $\ddot{\rho}_o = -0.000478$ km/sec^2.

A three-dimensional trajectory may be obtained from the parameters of Table B.1 by adding the following equations to the previous development:

$$x = \rho \cos \alpha \qquad \text{(B.27)}$$

$$z = \rho \sin \alpha \qquad \text{(B.28)}$$

where α is the azimuth angle measured clockwise from north. A right-hand coordinate system is formed by x, y, and z, in which y is the vertical, x is positive north, and z is positive to the east.

The origin of the system is located at Point John. The unit of length in the table is the kilometer, and the unit of time is the second. t_o is the time after launch.

B.5 DISCUSSION

The accuracy of the computed trajectories is primarily a function of the type of input data used to determine the trajectory parameters. The most accurate reductions consist of the results derived from radar and Cubic tracking measurement. Of moderate accuracy are those based on elevation angle measurements. Finally, the reductions of uncertain quality are those derived soley from measurements of slant range.

The predominant error, in the parabolic flight paths fitted to the reductions of radar and Cubic tracking data, entered as a result of assuming parabolic motion. The tracking error of either system is negligible in comparison to the error introduced by the curve-fitting procedure. Hence, the error in the computed trajectory is essentially equivalent to the error in fitting.

Generally, the uncertainty in position for such trajectories varies from 0.5 km on the upward leg of the trajectory to 1.5 km on the downward leg.

In considering the quality of the trajectory determination for other types of input data, direct evaluation of the errors is impossible, since there exists no well-defined trajectory for comparison. However, Table B.2 offers a method for indirectly evaluating the accuracy of those trajectories which were derived from measurements of elevation angles. Presented in Table B.2 are estimates of altitudes at which the rockets began to nose-over upon reentry into the effective atmosphere on the downward leg of the trajectory. This reentry phase is primarily a function of the aerodynamic characteristics of the rocket. The entries in Table B.2 were obtained by estimating nose-over times from the occurrence of discontinuities in magnetometer records and also in GMD and AGC field strength measurements. For many rockets, these times could be determined from all three sources with an accuracy of from 1 to 5 seconds. Missile altitudes corresponding to

nose-over times were extracted from the computed trajectories for entry in Table B.2. When more than one measurement of nose-over time was available for a rocket, an average value was used. It is observed that the values are quite well clustered for each rocket type. Since for every rocket, the reentering vehicle consists of the payload and last stage, it is reasonable to include the Honest John-Nike and Honest John-Nike-Nike missiles together for comparison. Excellent agreement in nose-over altitude is apparent for both types of rockets regardless of the source of the reduction data. This strongly suggests that the accuracy of the trajectories based solely on elevation angle data is equivalent to that of trajectories derived from radar or Cubic tracking data. However, other error evaluations indicate that the latter may be slightly more accurate. Hence, reasonable estimates of positional error for trajectories determined from observations of elevation angles would vary from 1 to 2 km over the initial portion of the trajectory, to 2 to 3 km near reentry.

Only two nose-over altitudes were available for rockets of the D-4 type. These altitudes were 84.7 km for Rocket 22, and 59.7 km for Rocket 25. These values are not necessarily in poor agreement if it is considered that Rocket 25 was well behaved, whereas the poor performance of Rocket 22 resulted in such erratic motion that the missile very probably did not reenter tail first. The low nose-over altitude for Rocket 25 is quite reasonable, since the reentry vehicle for this rocket had no tail fins.

It is difficult to estimate errors for reductions derived from range-only measurements. Huge errors could result from a shift in the frequency of the transmitter. If such a shift were abrupt, it could be observed and corrected. However, no satisfactory method was available for the detection of gradual shifts in the transmitter frequency. A reasonable estimate of positional error in such reductions would be 1 to 5 km on the upward leg of the trajectory growing to 5 to 15 km near reentry.

Rocket 19 required special attention. The only observation available consisted of a recording of doppler frequency as a function of time. This record was known to be of poor quality as a result of frequency drift. In measuring nose-over altitudes, it was observed that Rocket 19 turned over at 345 seconds after launch, whereas Rocket 26 nosed over at 346 seconds. These rockets were identical and were programmed to fly identical trajectories. The flight path for Rocket 26 was well determined by radar tracking. Therefore, it was concluded that the best estimate for the trajectory of Rocket 19 could be obtained by using the results for Rocket 26, shifted to the appropriate azimuth for Rocket 19.

In conclusion, positional errors probably vary from 0.5 to 1.5 km for Rockets 8, 9, 11, 15, 17, 19, 20, 24, 26, 27, 28, and 29; from 1 to 3 km for Rockets 2, 4, 6, 7, 10, 12, 13, 14, 18, 21, 23, and 25; and from 1 to 15 km for Rockets 1, 5, and 22.

TABLE B.1 SOURCE OF INPUT DATA FOR DETERMINING ROCKET TRAJECTORIES, PROJECTS 6.2, 6.3, 6.4

Rocket Number	t_o	ρ_o	y_o	$\dot{\rho}_o$	$\dot{y}_o$	g	α	Input Data
1	110	29.00	84.30	0.7990	2.6544	0.00867	130.0	r
2	30	4.64	30.44	0.1964	1.1540	0.00953	114.0	ϵ
4	40	5.35	33.78	0.1811	0.9910	0.00958	111.5	ϵ and r
5	110	43.20	98.00	1.3156	2.7125	0.00860	148.0	r
6	30	2.55	30.70	0.1750	1.1582	0.00953	103.0	ϵ
7	110	30.18	82.34	1.4491	2.6854	0.00868	120.0	ϵ
8	110	58.31	137.74	1.6350	2.7767	0.008213	26.2	Radar
9	110	40.71	140.62	1.1686	2.9372	0.008113	23.5	Radar
10	40	9.10	39.72	0.3000	1.0523	0.00962	101.8	ϵ
11	40	8.68	32.52	0.2993	0.9450	0.00949	86.5	Cubic
12	35	7.20	27.10	0.3053	1.0187	0.00954	19.7	ϵ
13	35	6.52	33.93	0.2370	1.0986	0.00957	87.5	ϵ
14	40	4.70	34.10	0.1715	1.0710	0.00960	100.8	ϵ
15	40	9.03	30.52	0.4964	1.4186	0.00945	21.0	Radar
17	35	7.39	23.15	0.3457	1.0576	0.00951	116.0	Radar
18	40	6.80	29.30	0.1594	0.6402	0.00966	35.6	ϵ
19	35	5.73	29.83	0.2937	1.5786	0.00940	135.0	a
20	35	3.80	28.03	0.2347	1.5936	0.00950	109.2	Cubic
21	30	3.09	28.93	0.1480	1.2081	0.00953	79.0	ϵ
22	110	35.66	49.00	0.9771	1.3201	0.00945	100.0	r
23	30	6.22	28.77	0.3210	1.2687	0.00949	100.5	ϵ
24	35	7.69	27.38	0.4602	1.5483	0.00951	19.4	Cubic
25	110	31.19	107.56	0.7931	2.7864	0.00855	163.0	ϵ
26	35	5.73	29.83	0.2937	1.5786	0.00940	113.5	Radar
27	35	6.54	27.93	0.2528	1.5715	0.00951	109.7	Cubic
28	40	9.51	33.06	0.4599	1.4914	0.00939	17.5	Radar
29	50	5.90	30.55	0.1695	0.8434	0.00960	91.0	Radar

[a]Based on results for Rocket 26

SECRET

TABLE B.2 ESTIMATED NOSE-OVER ALTITUDES FOR SELECTED ROCKETS OF PROJECTS 6.2, 6.3, AND 6.4

Rocket Number	Input Data	Rocket Type	Nose-over Altitude	Apogee
2	ϵ	NC[a]	83.6 km	100.3 km
6	ϵ	NC	79.9	101.1
10	ϵ	NC	84.0	97.4
13	ϵ	NC	78.8	97.1
21	ϵ	NC	80.0	105.5
			average 81.3	
4	ϵ and r	HJN[b]	63.5	85.0
11	Cubic	HJN	66.2	79.7
12	ϵ	HJN	67.4	81.6
14	ϵ	HJN	68.1	93.9
17	Radar	HJN	65.2	82.1
			average 66.1	
19	d	HJN_2[c]	66.9	162.6
20	Cubic	HJN_2	64.9	161.8
24	Cubic	HJN_2	63.4	154.0
26	Radar	HJN_2	66.9	162.6
27	Cubic	HJN_2	63.7	158.0
28	Radar	HJN_2	69.2	152.0
			average 65.8	

[a] Nike-Cajun

[b] Honest John-Nike

[c] Honest John-Nike-Nike

[d] Based on results of Rocket 26

SECRET

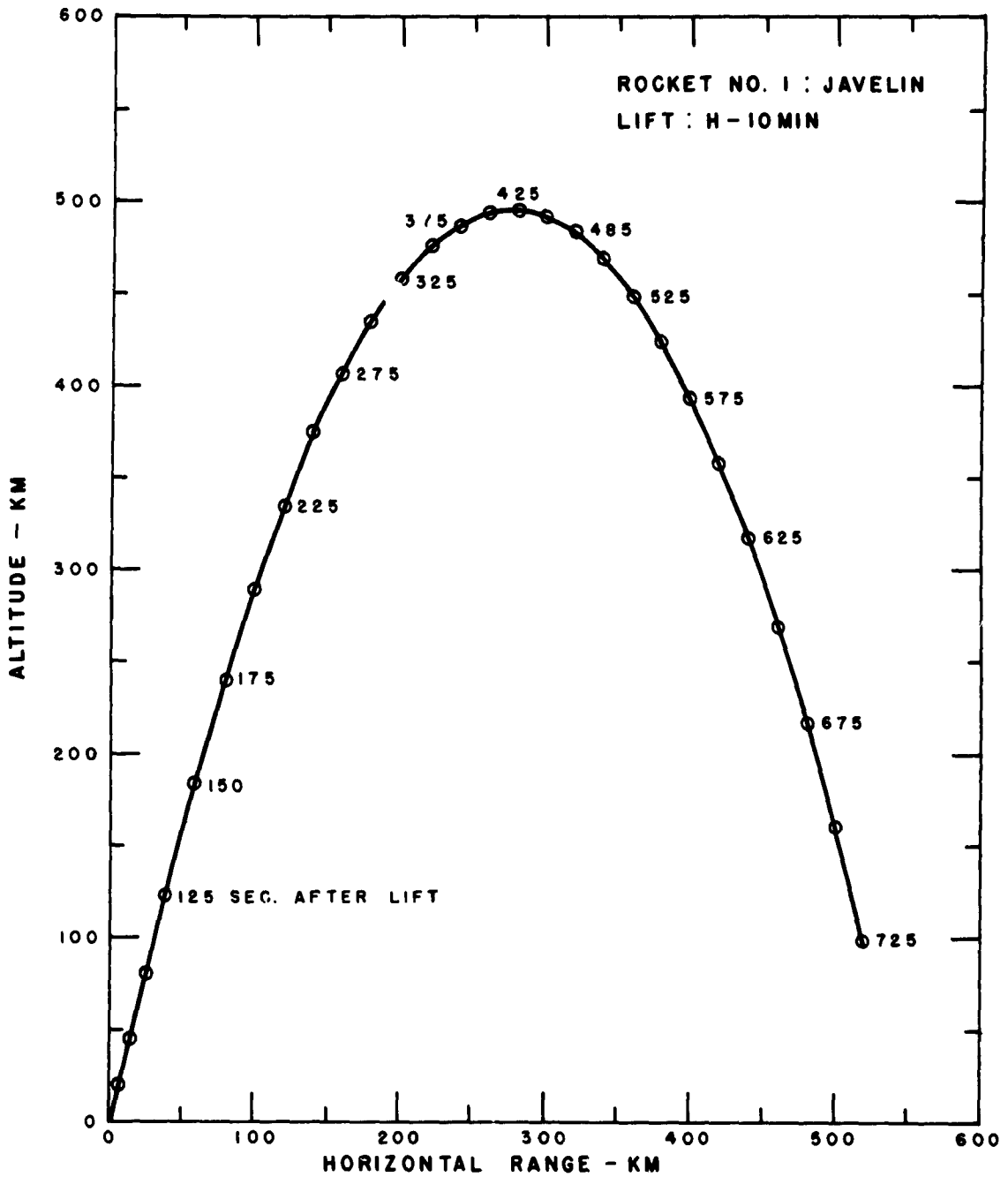

Figure B.1 Trajectory for Rocket 1, Star Fish..

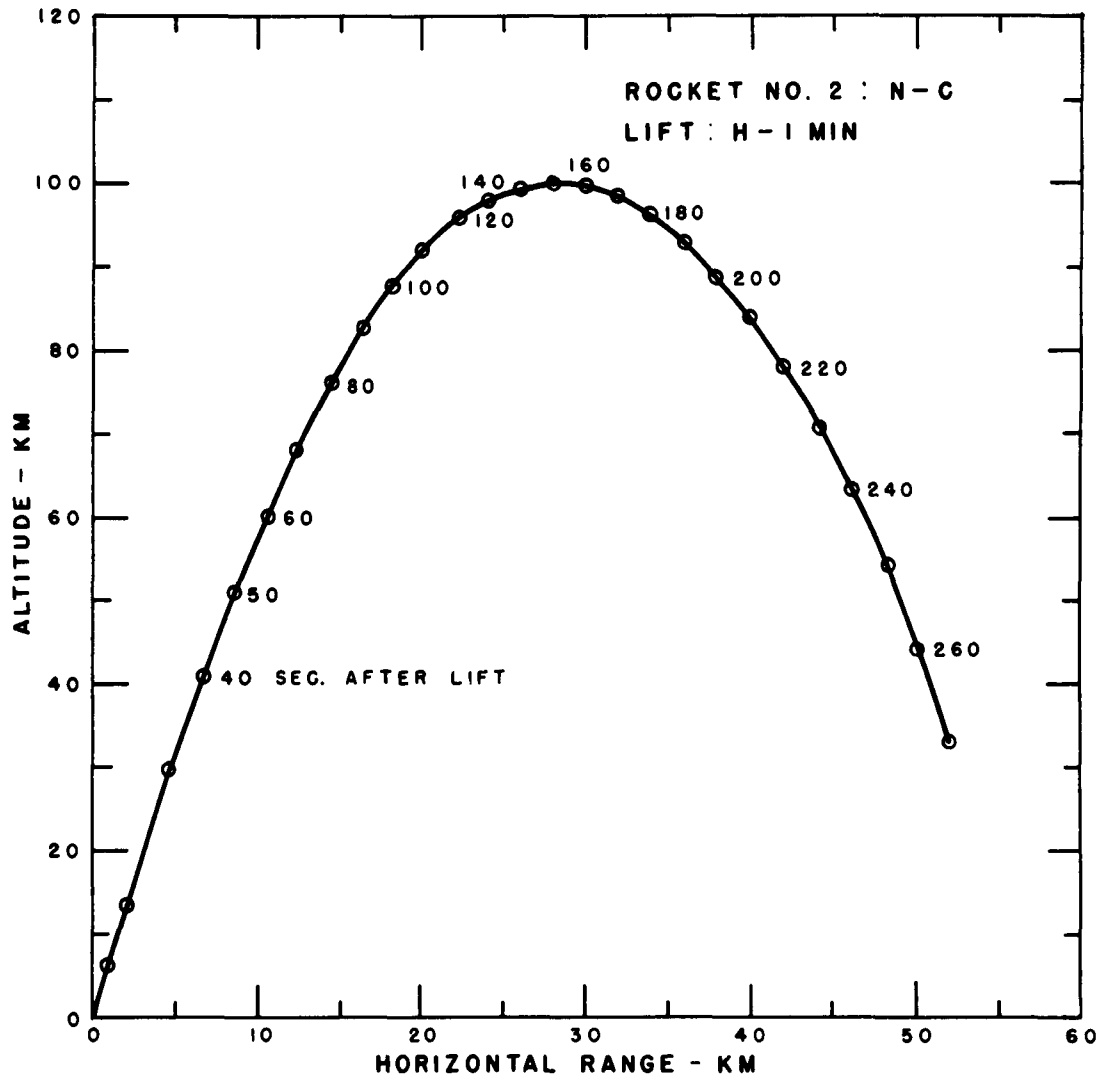

Figure B.2 Trajectory for Rocket 2, Star Fish.

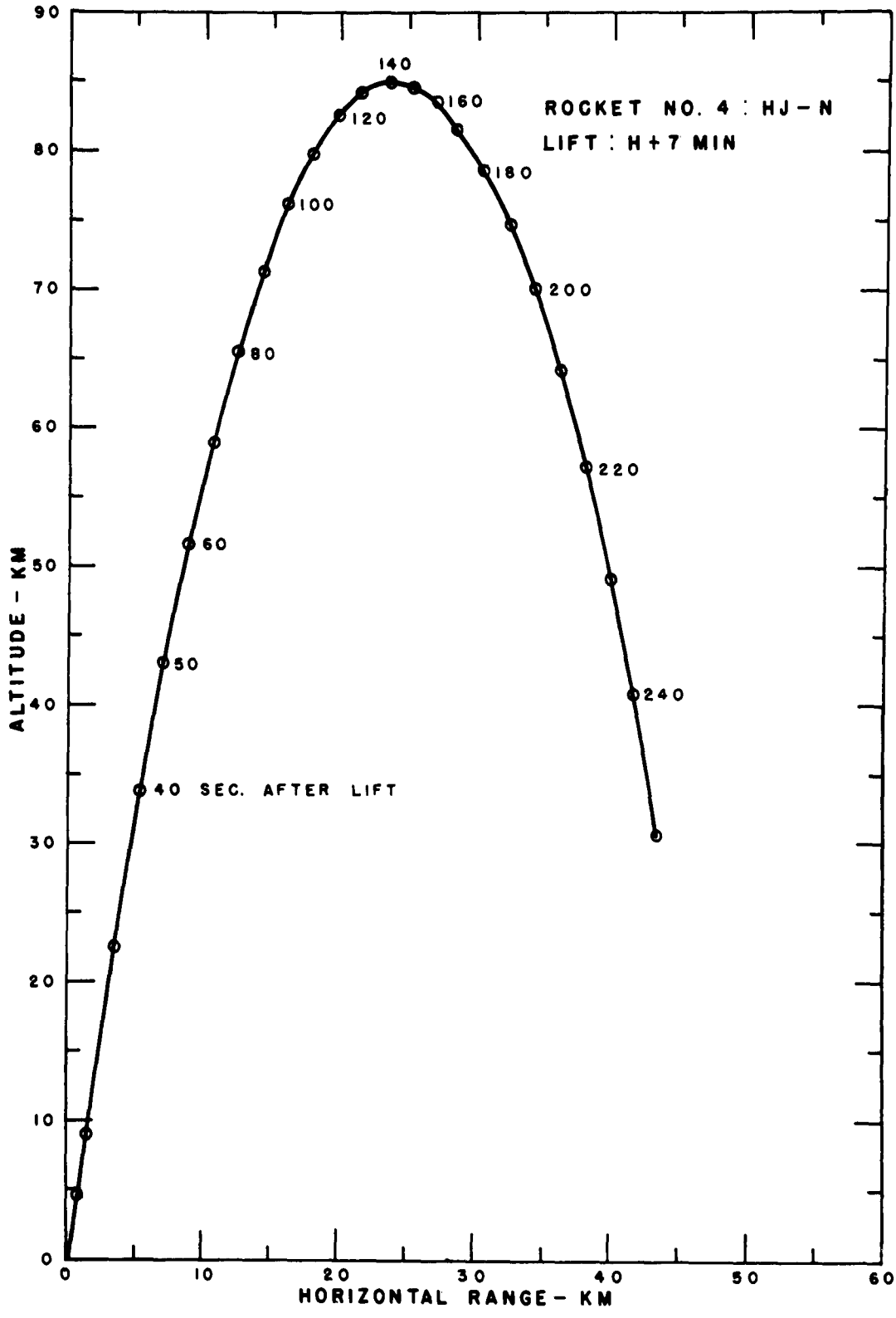

Figure B.3 Trajectory for Rocket 4, Star Fish.

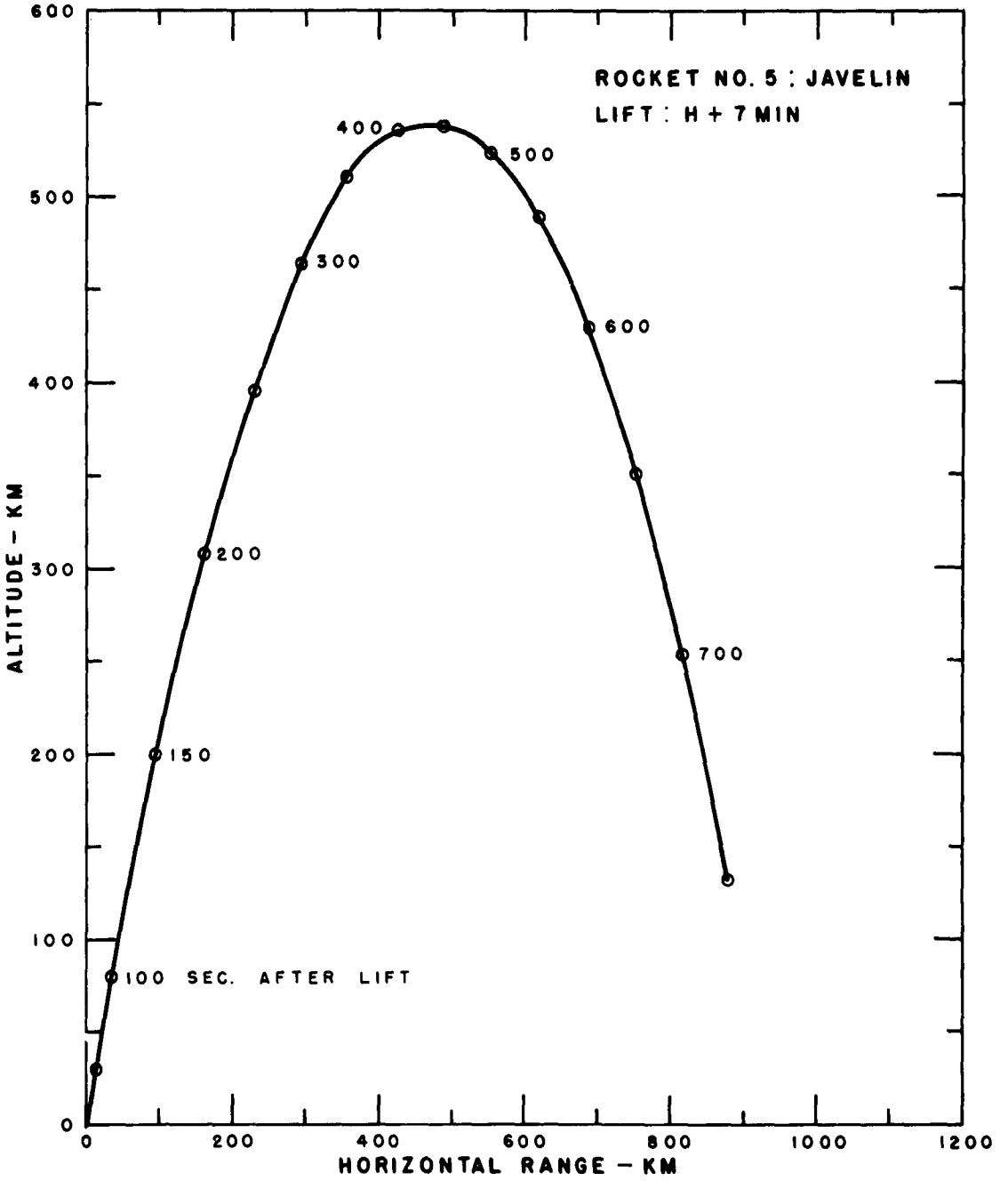

Figure B.4 Trajectory for Rocket 5, Star Fish.

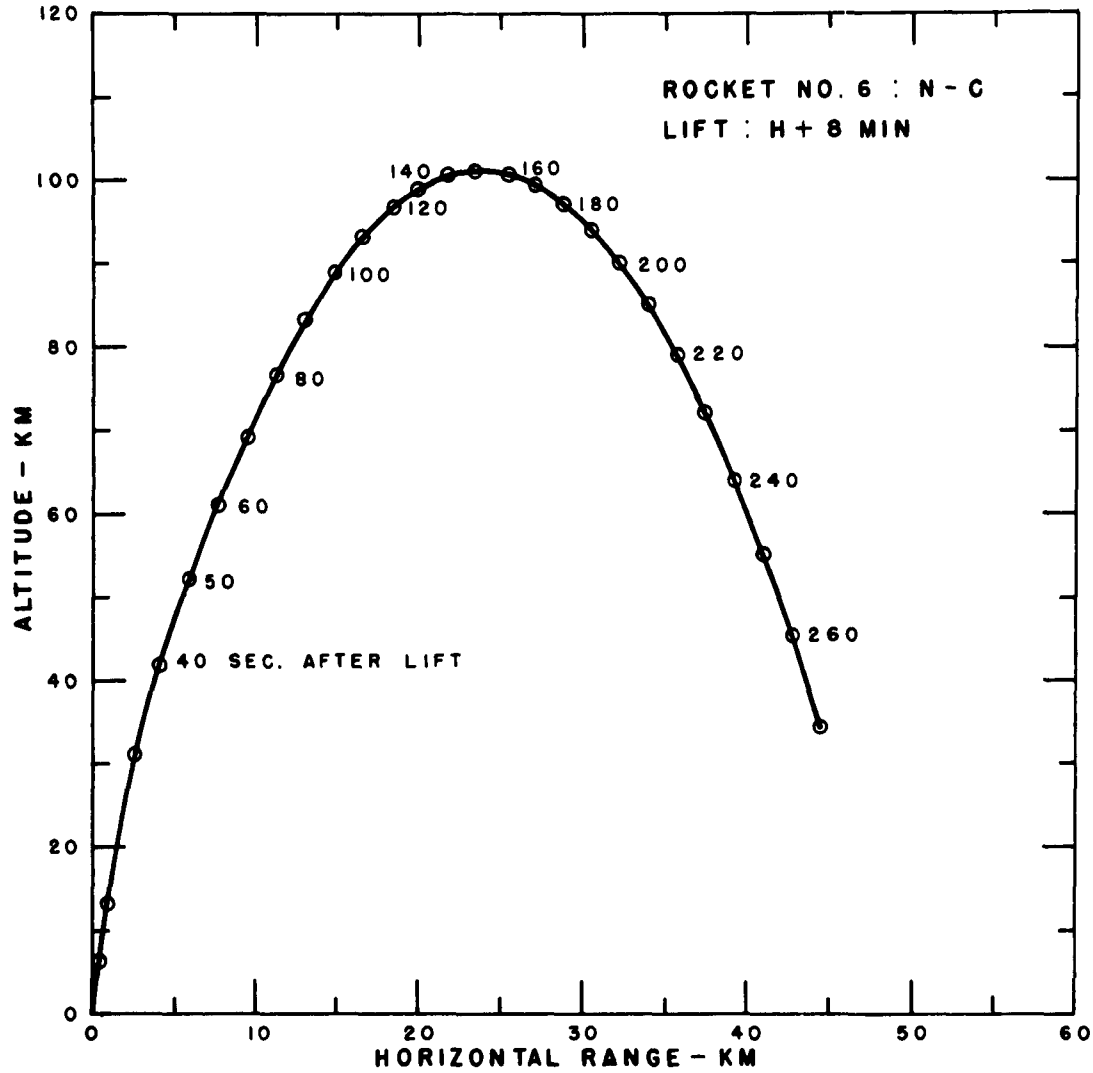

Figure B.5 Trajectory for Rocket 6, Star Fish.

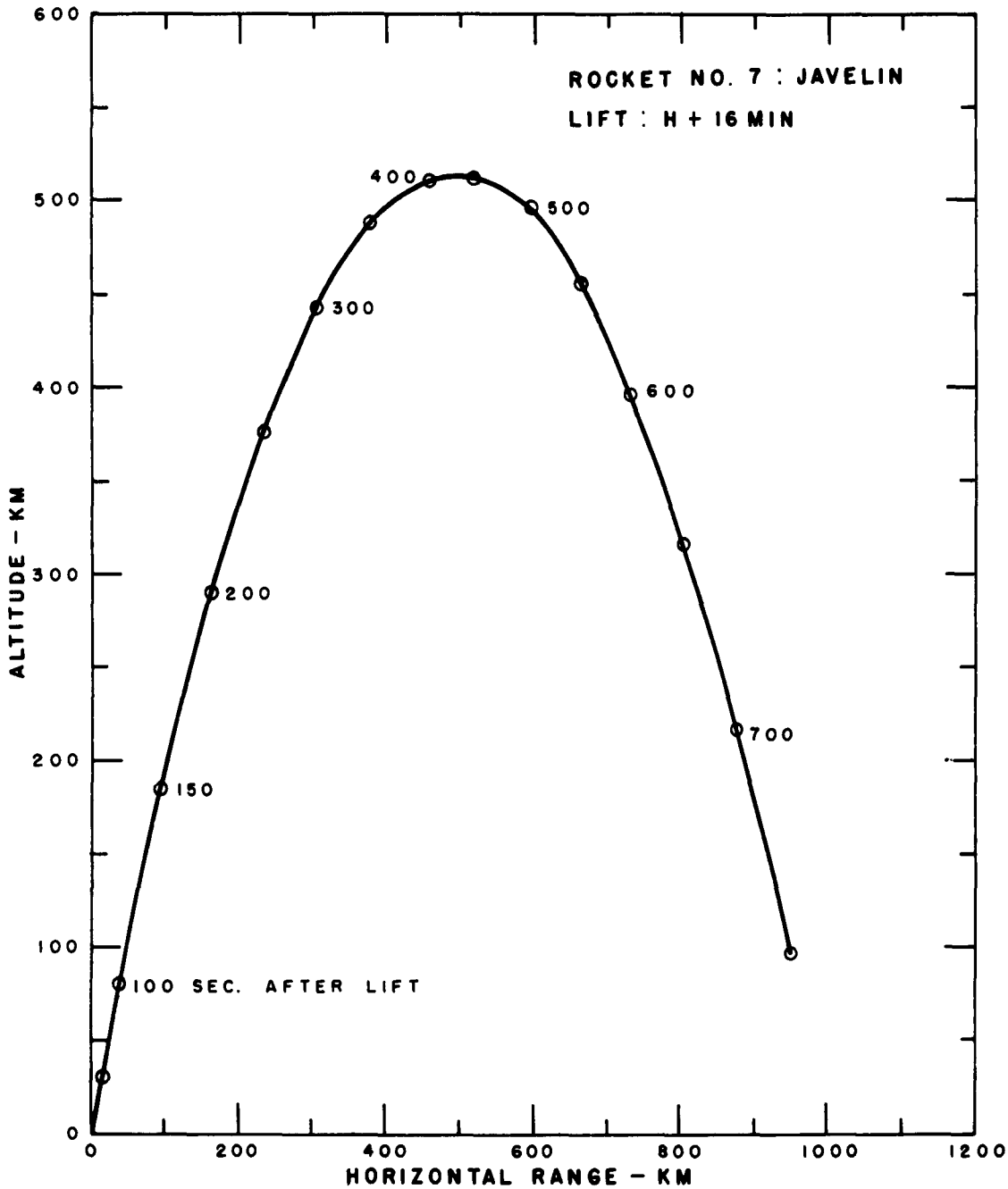

Figure B.6 Trajectory for Rocket 7, Star Fish.

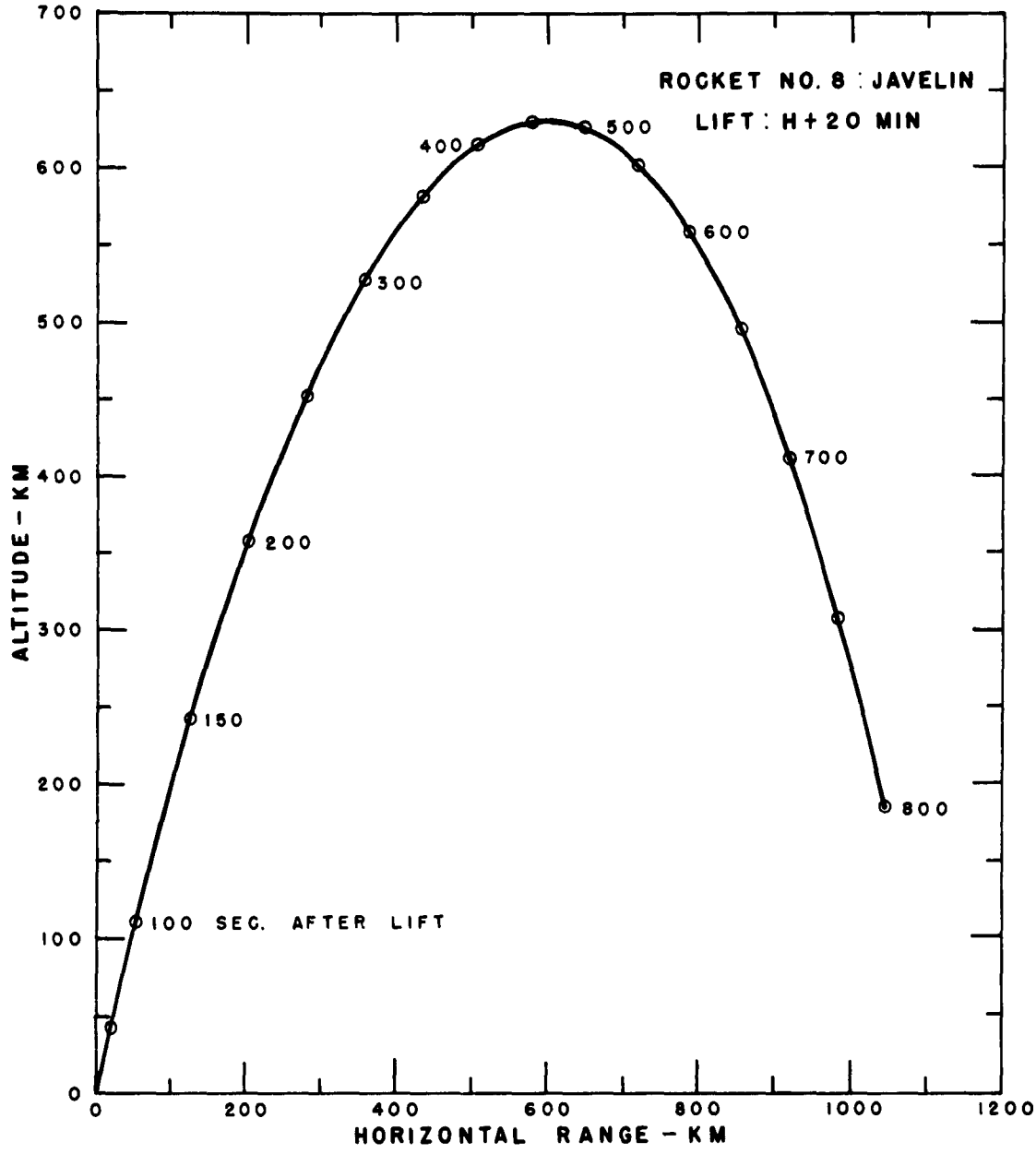

Figure B.7 Trajectory for Rocket 8, Star Fish.

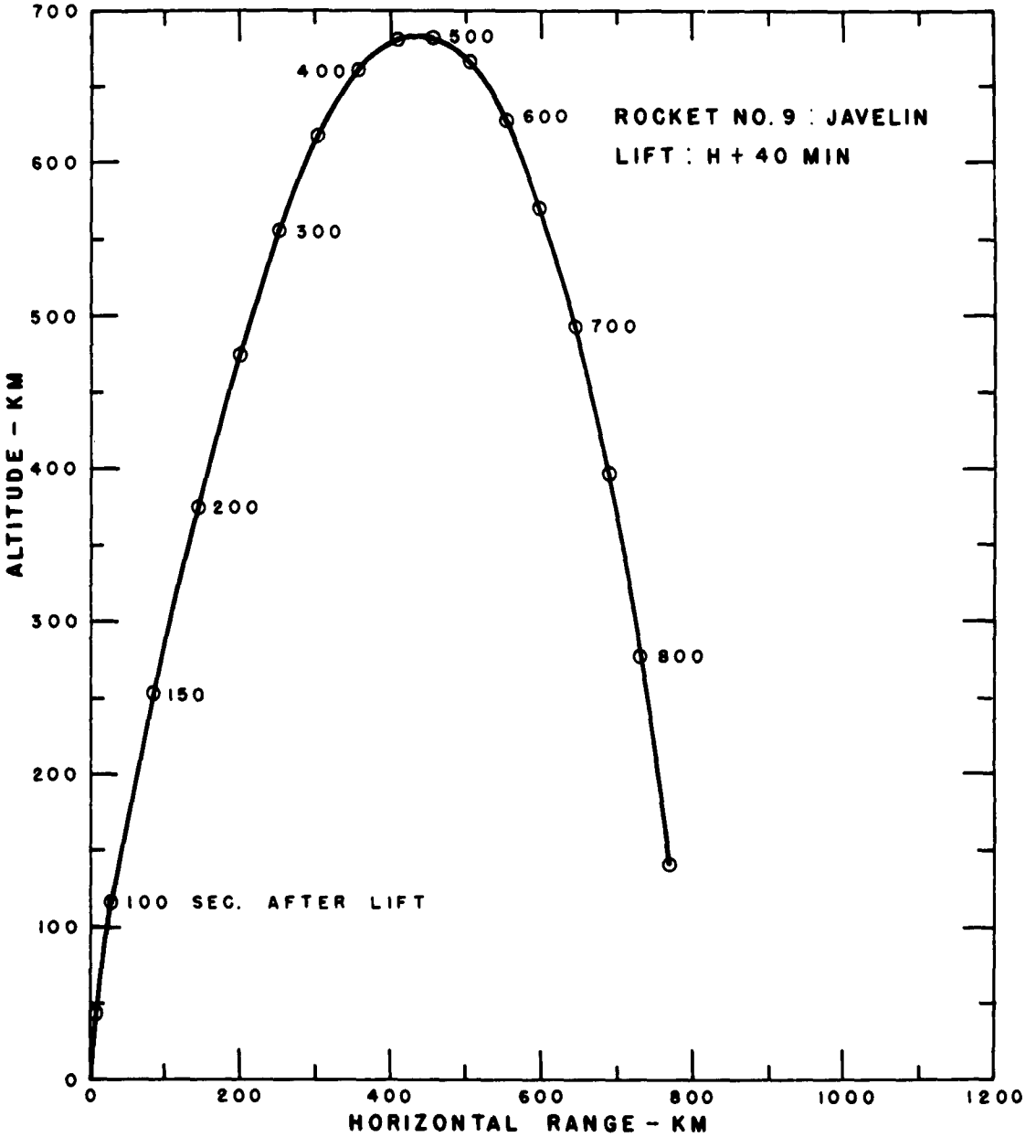

Figure B.8 Trajectory for Rocket 9, Star Fish.

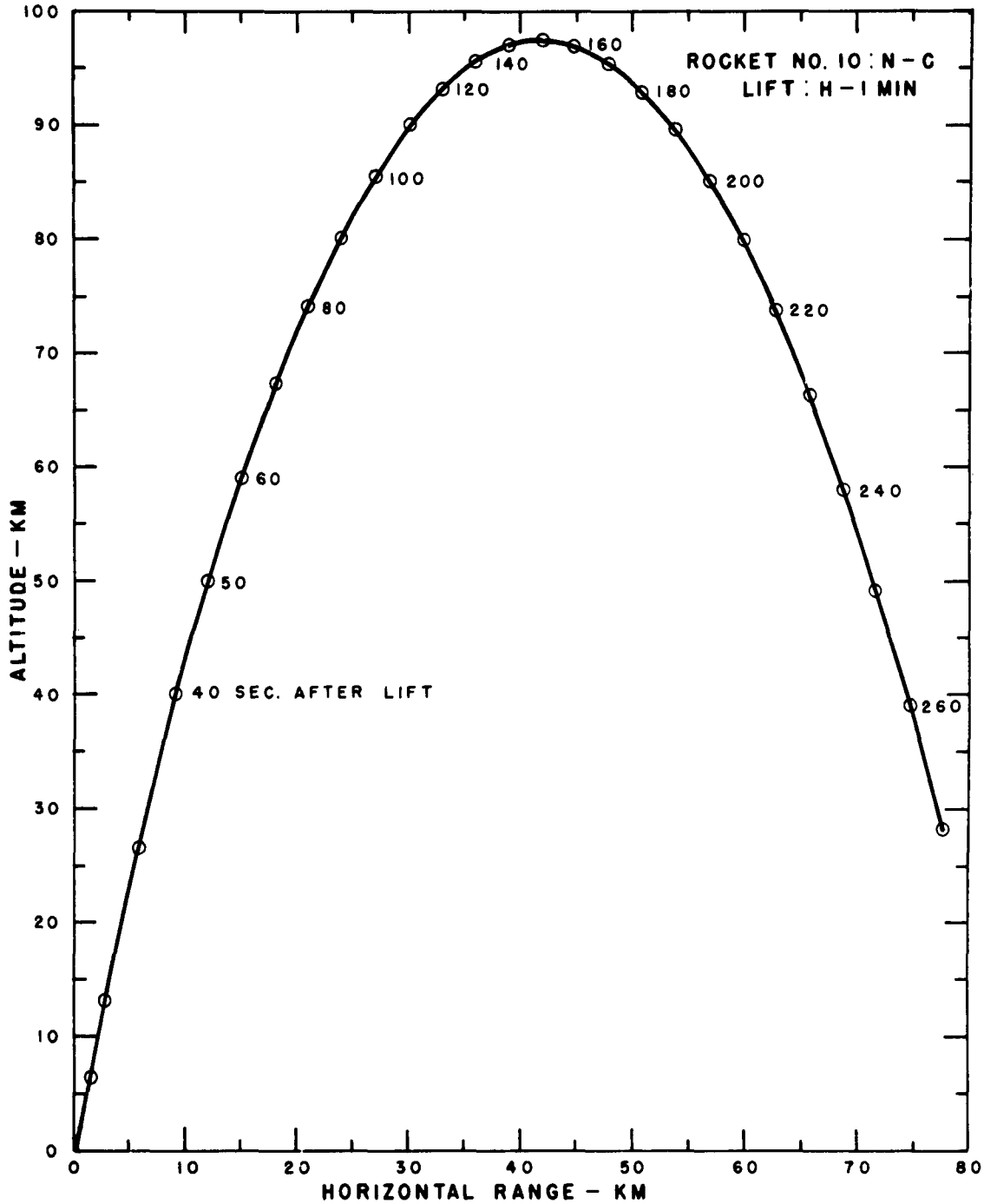

Figure B.9 Trajectory for Rocket 10, Blue Gill.

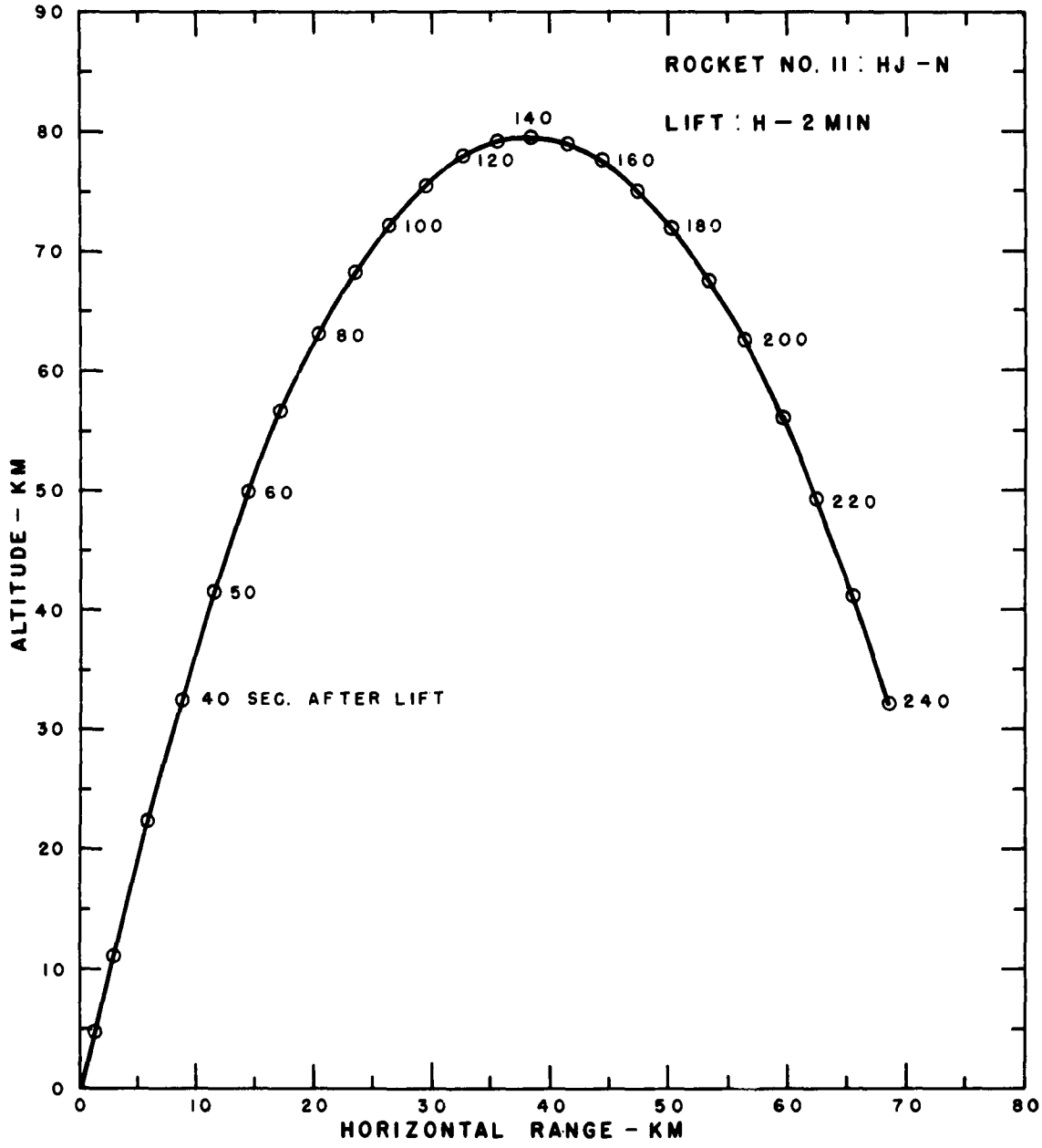

Figure B.10 Trajectory for Rocket 11, Blue Gill.

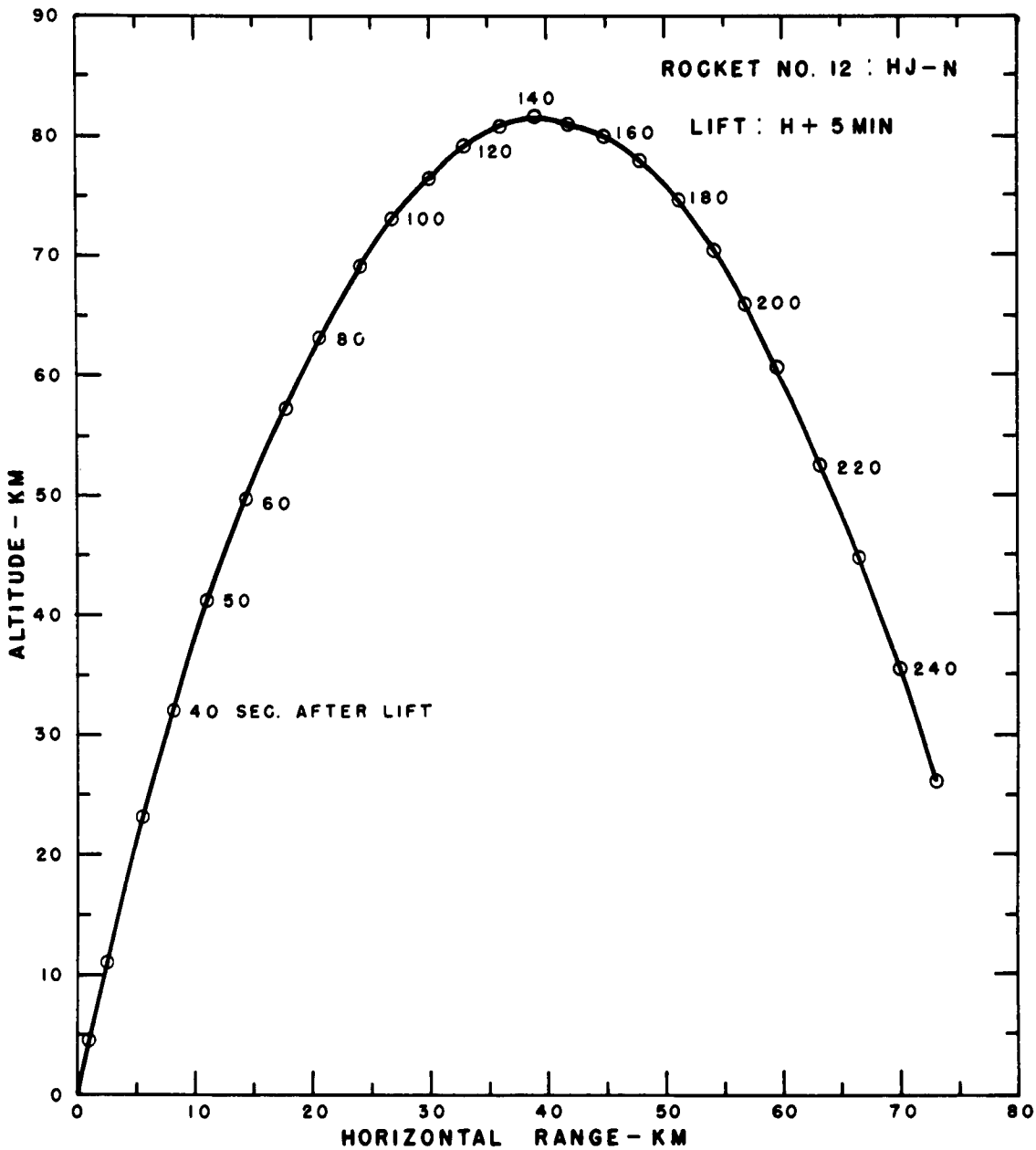

Figure B.11 Trajectory for Rocket 12, Blue Gill.

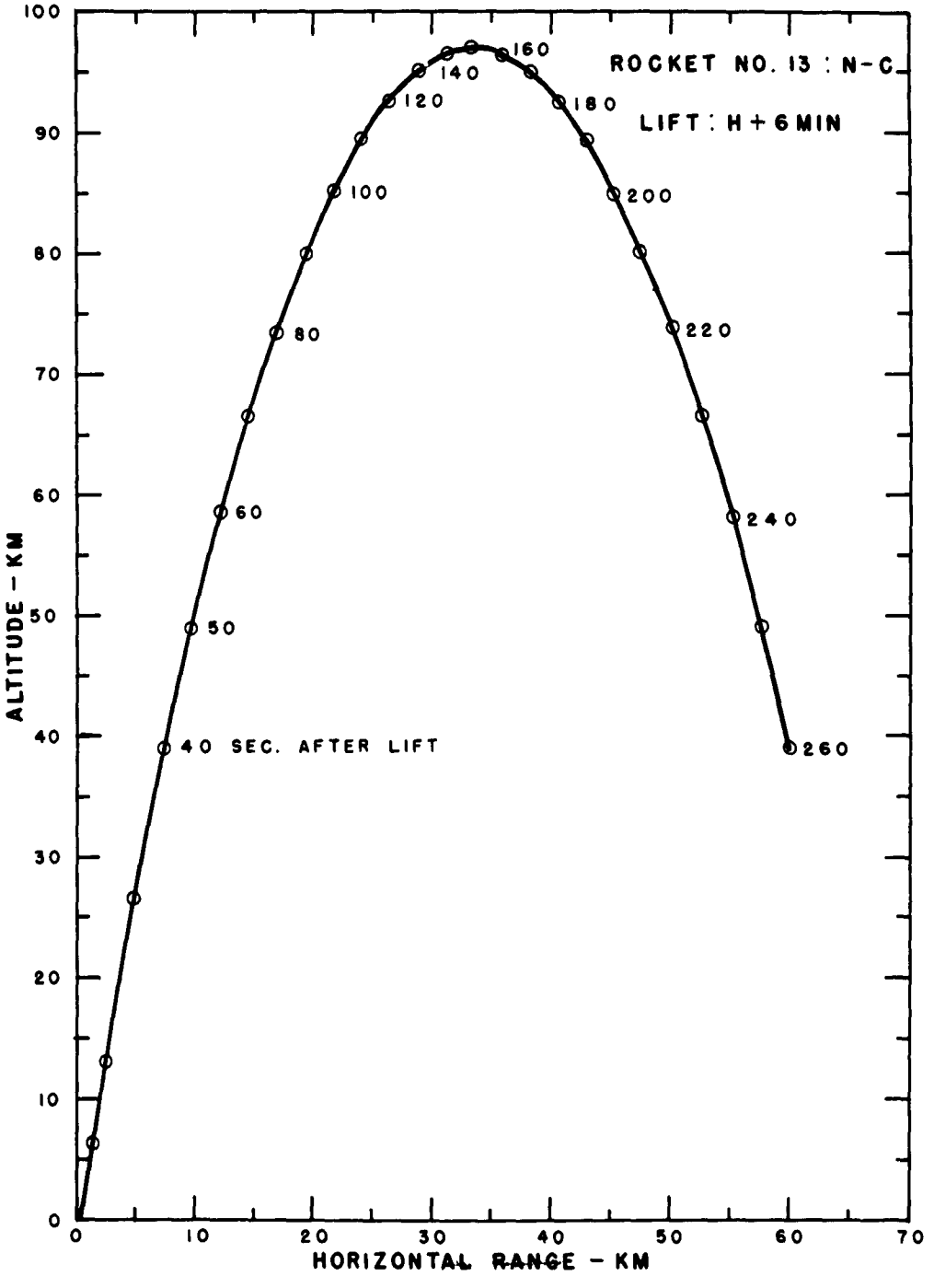

Figure B.12 Trajectory for Rocket 13, Blue Gill.

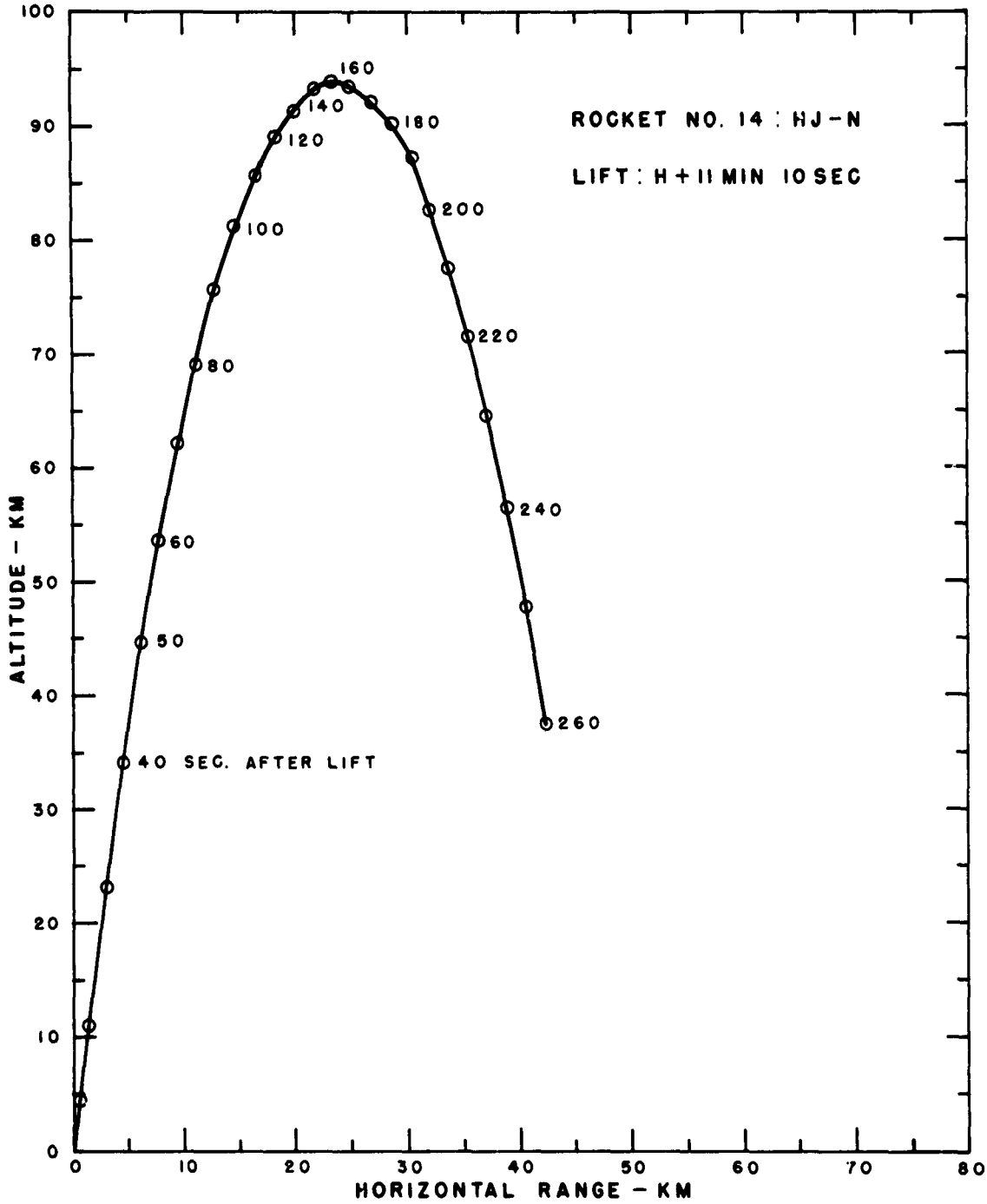

Figure B.13 Trajectory for Rocket 14, Blue Gill.

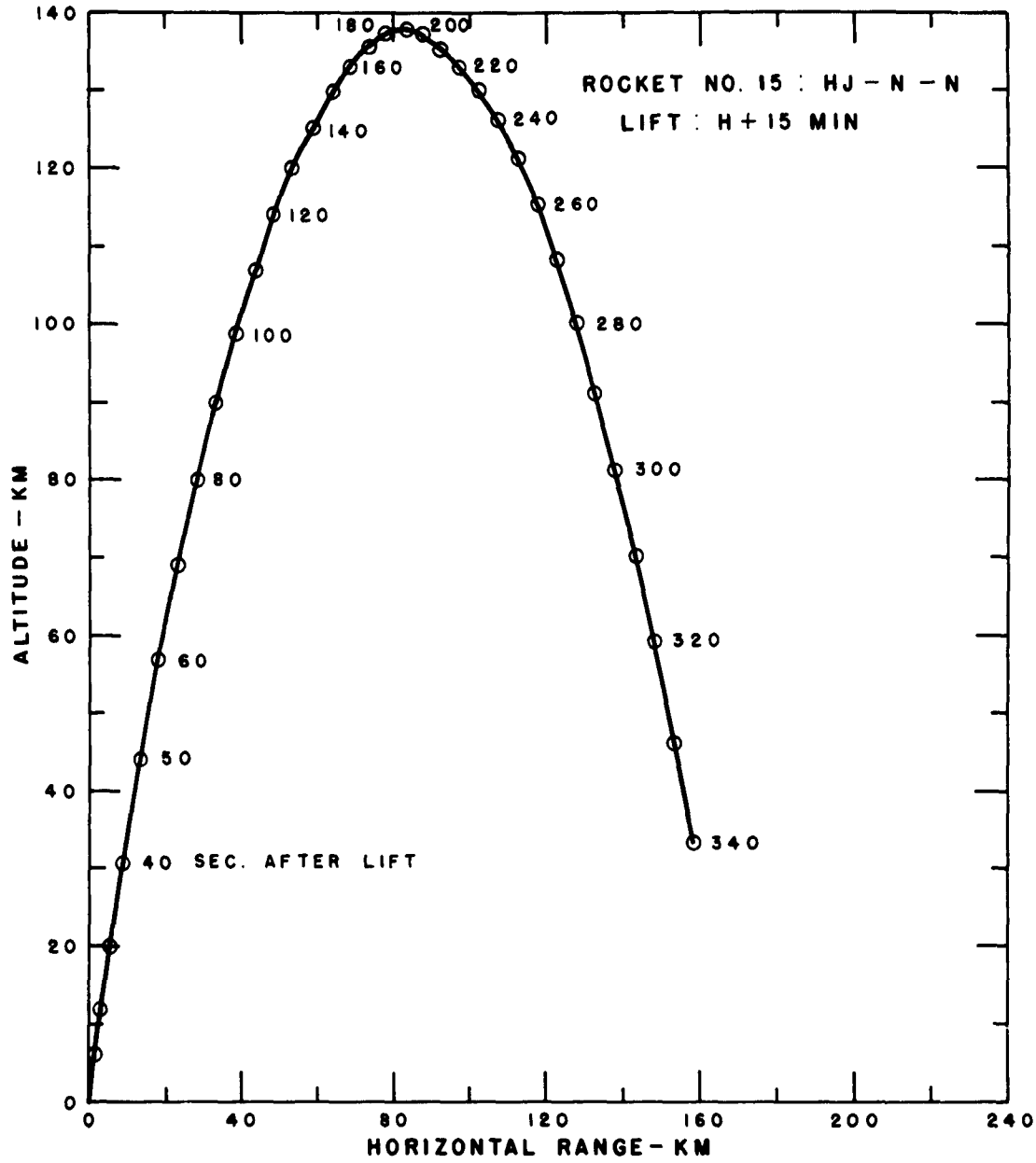

Figure B.14 Trajectory for Rocket 15, Blue Gill.

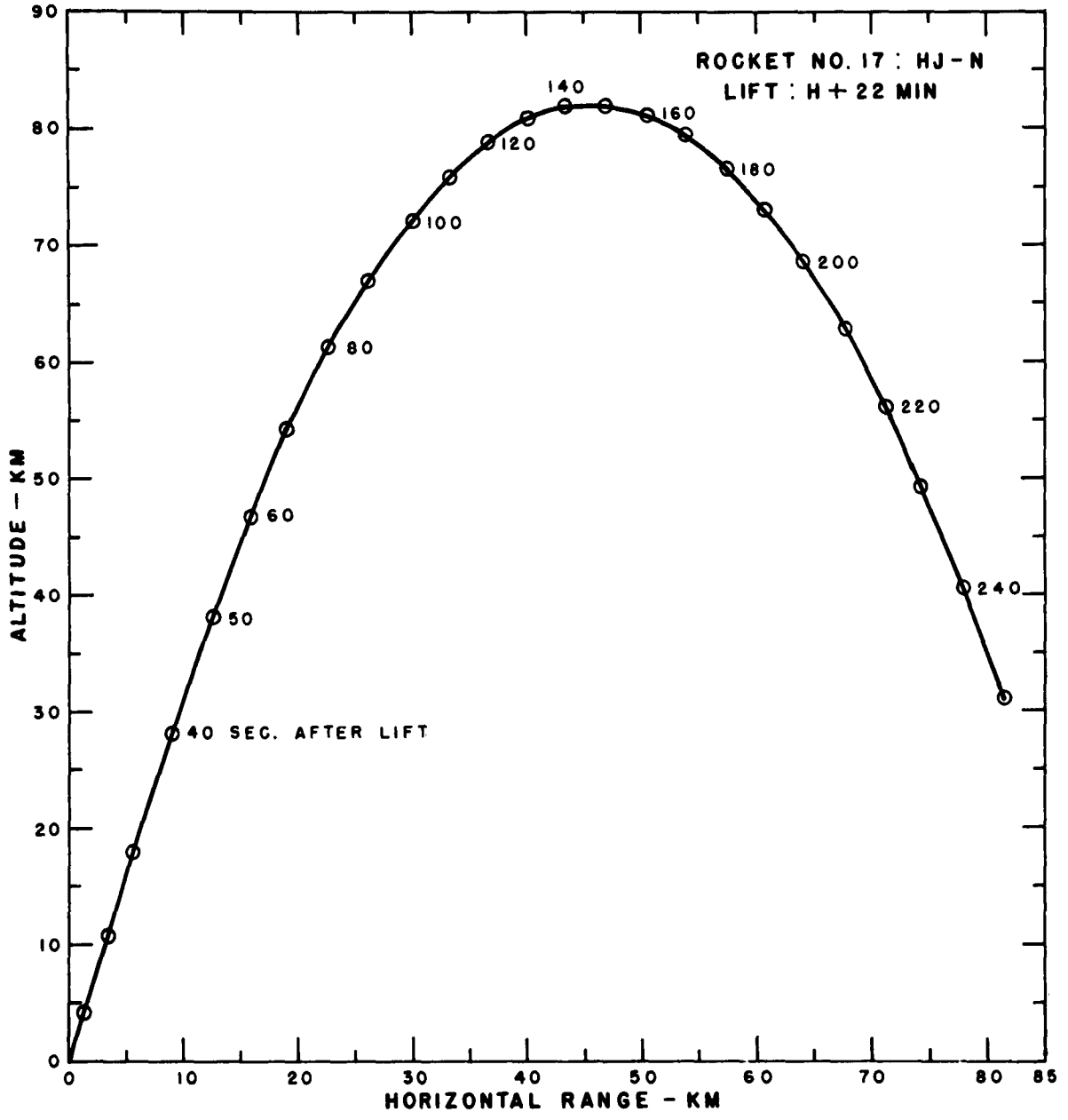

Figure B.15 Trajectory for Rocket 17. Blue Gill.

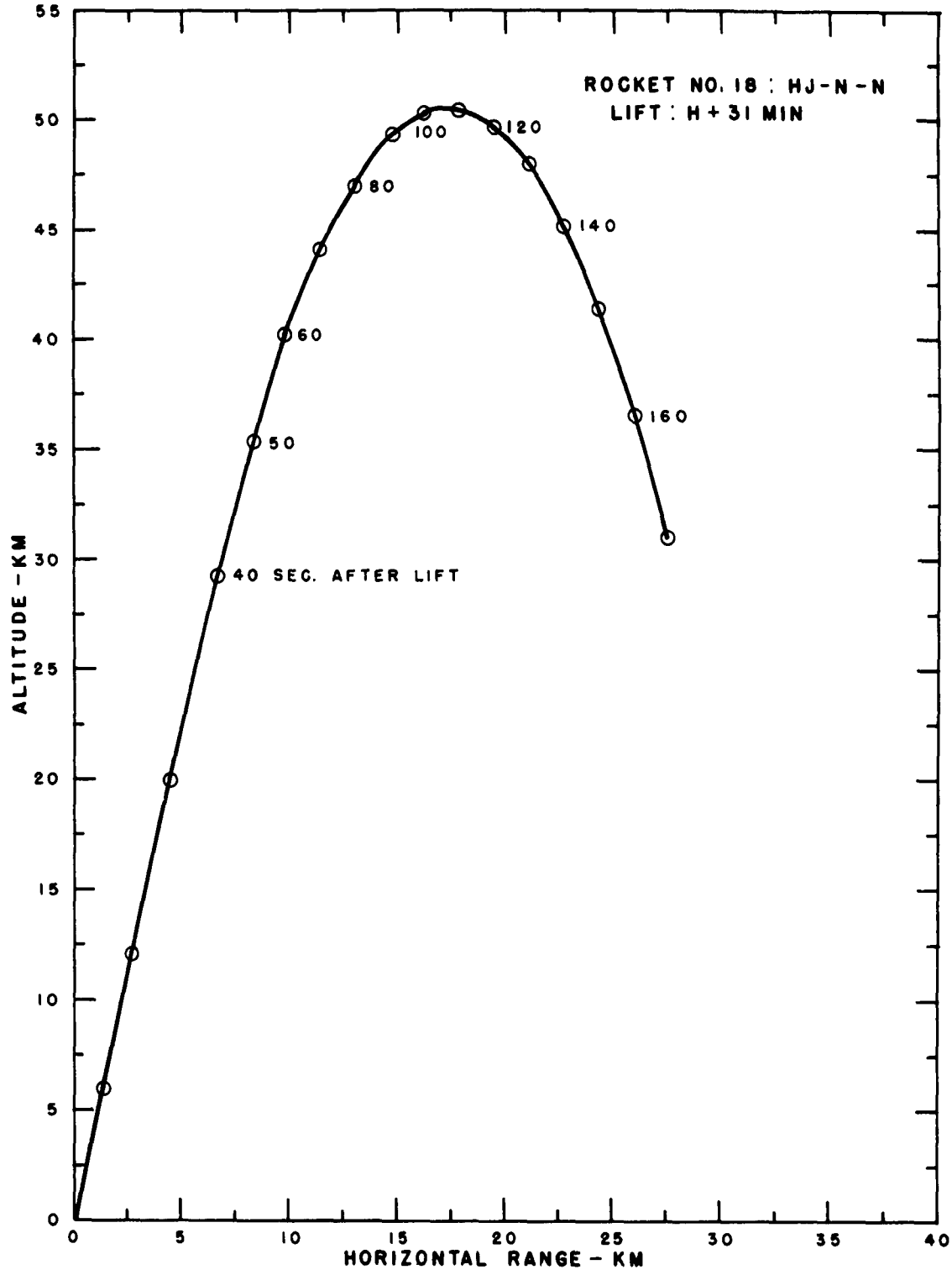

Figure B.16 Trajectory for Rocket 18, Blue Gill.

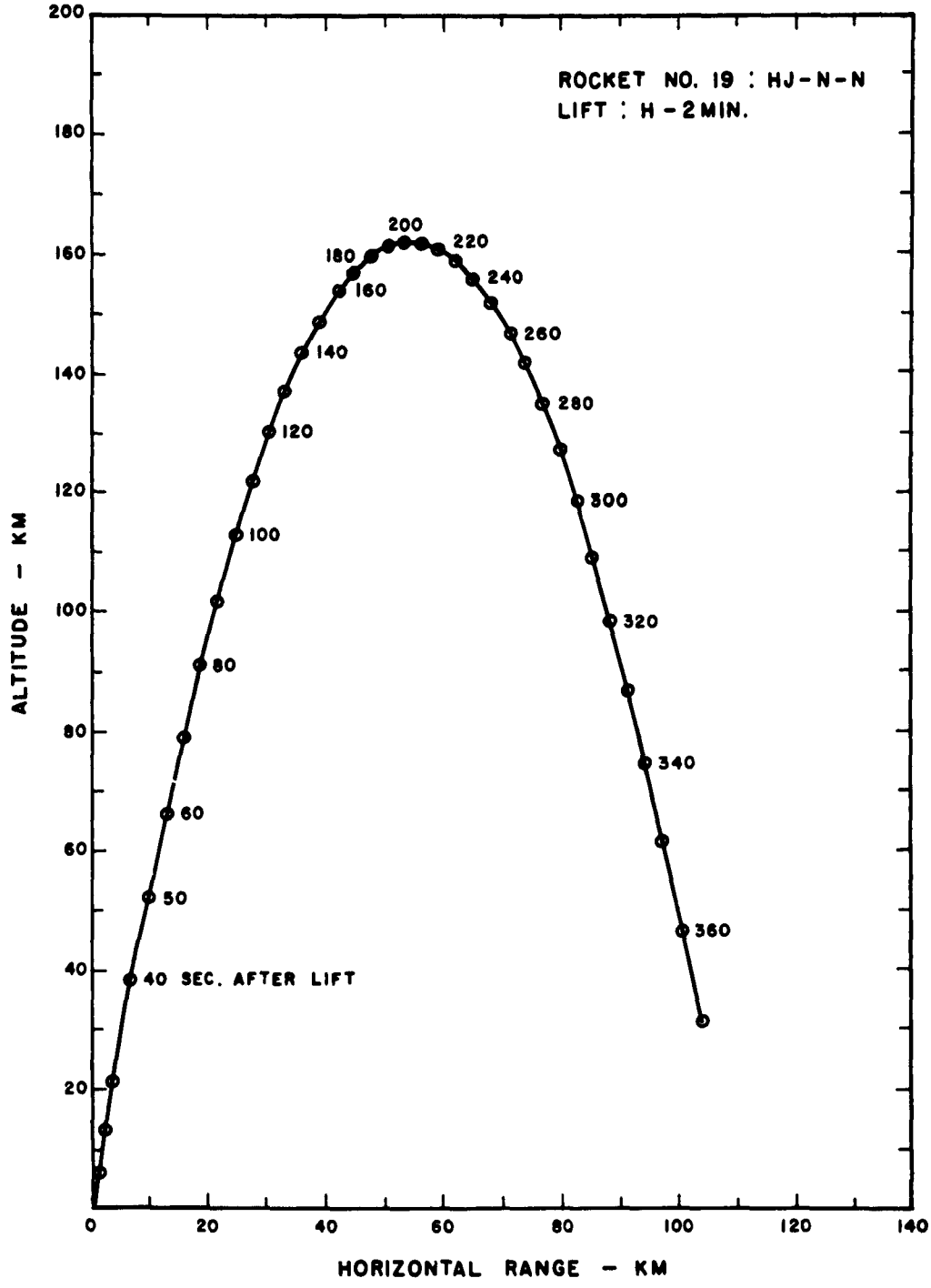

Figure B.17 Trajectory for Rocket 19, King Fish.

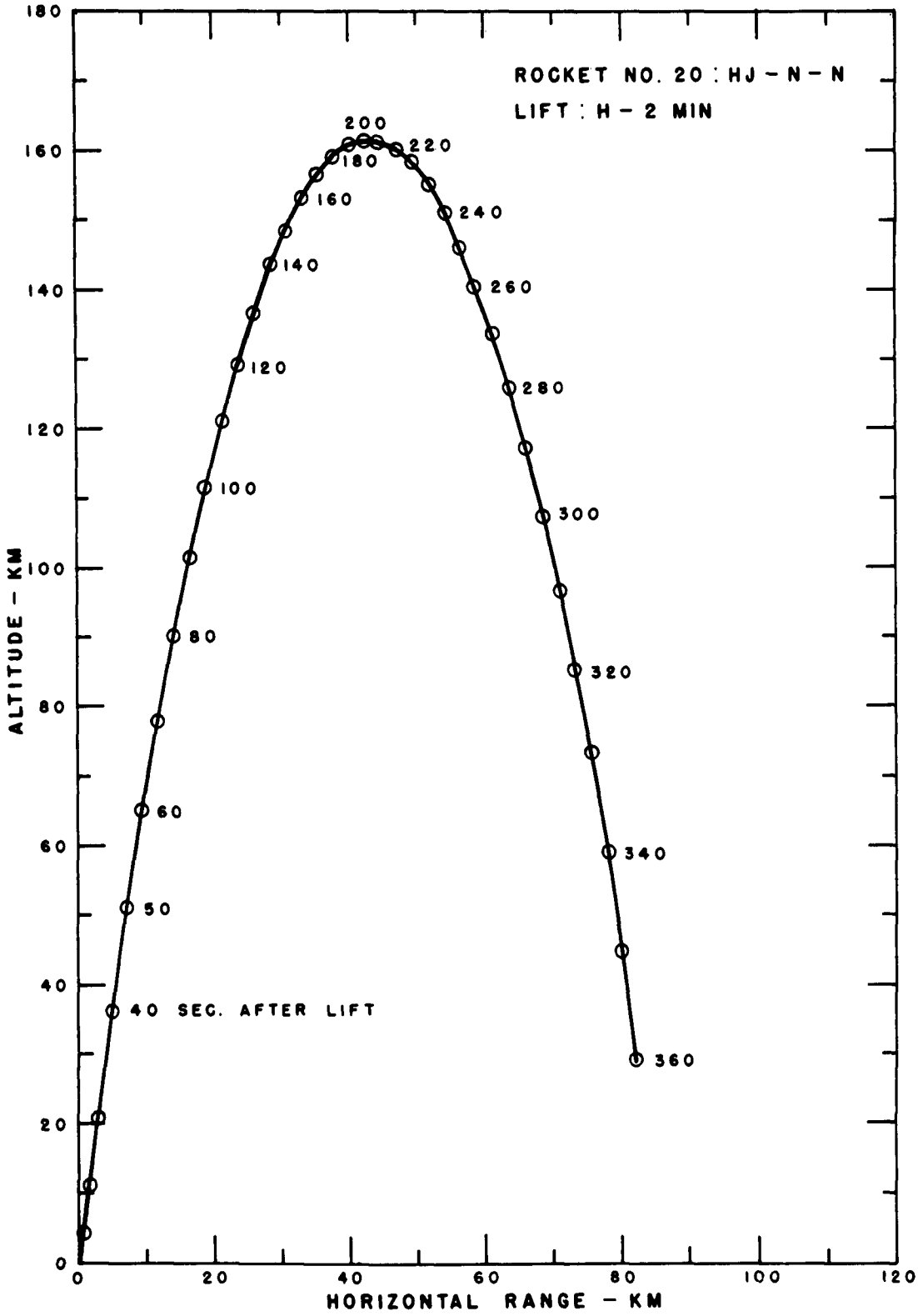

Figure B.18 Trajectory for Rocket 20, King Fish.

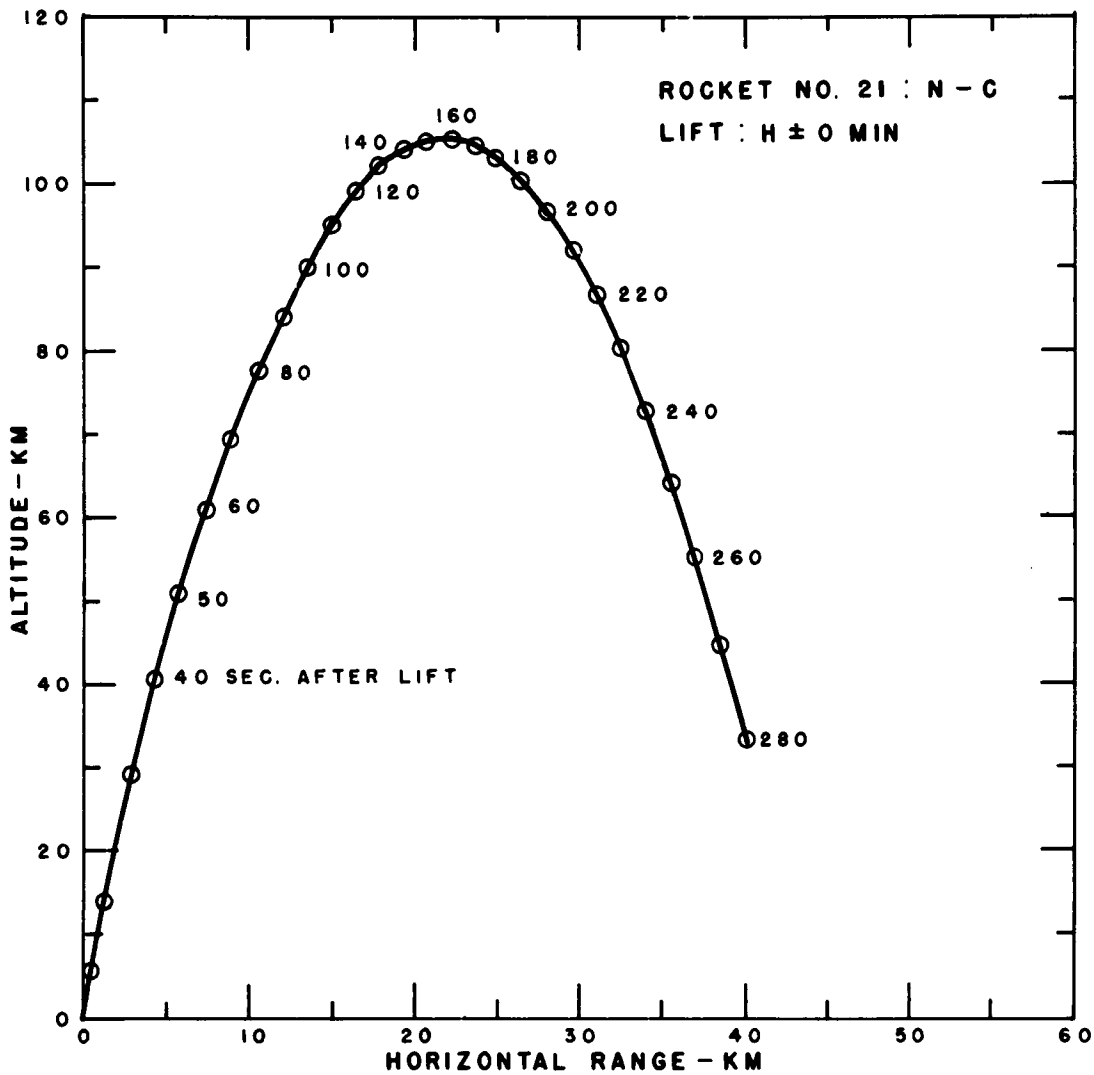

Figure B.19 Trajectory for Rocket 21, King Fish.

SECRET

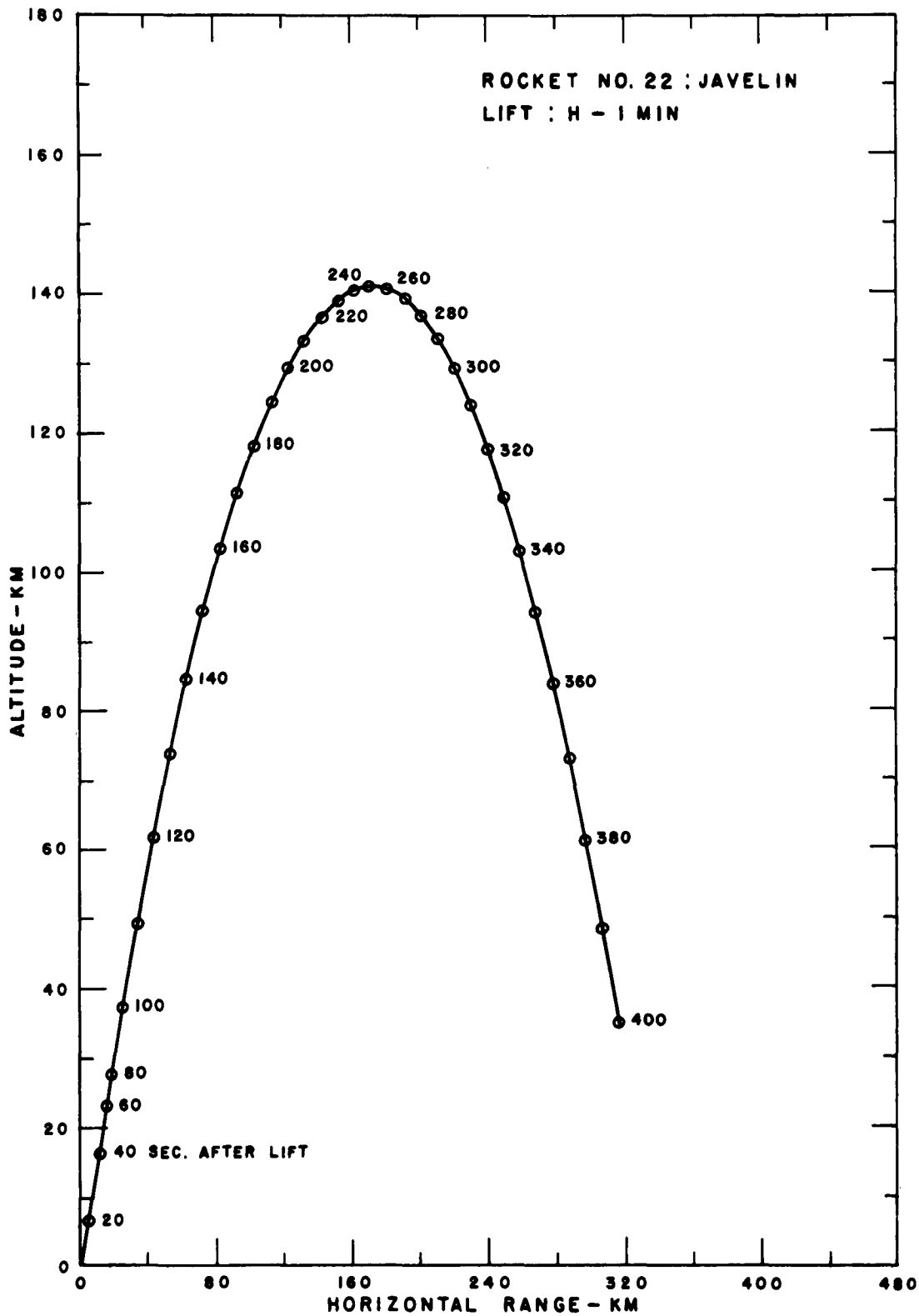

Figure B.20 Trajectory for Rocket 22, King Fish.

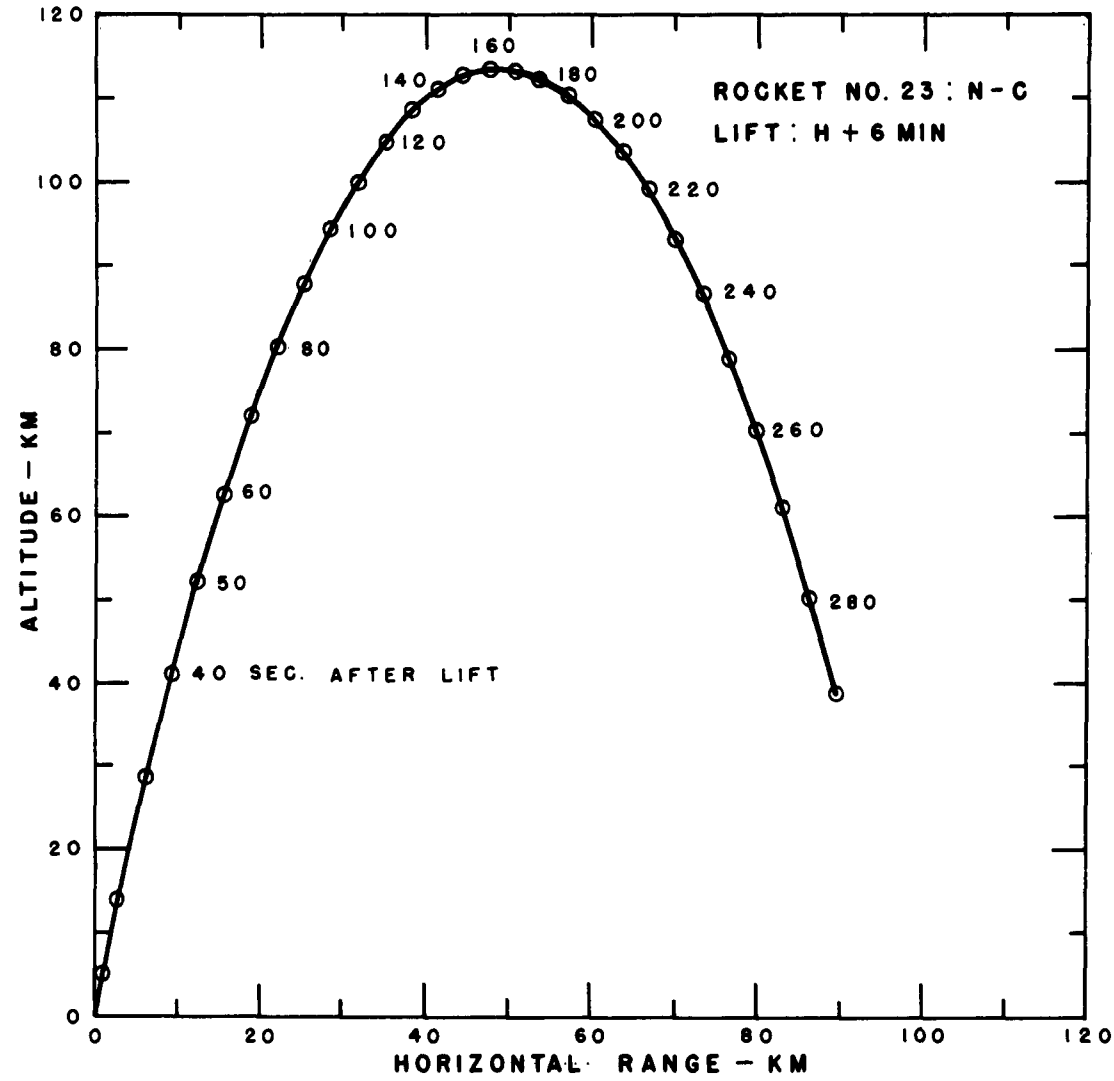

Figure B.21 Trajectory for Rocket 23, King Fish.

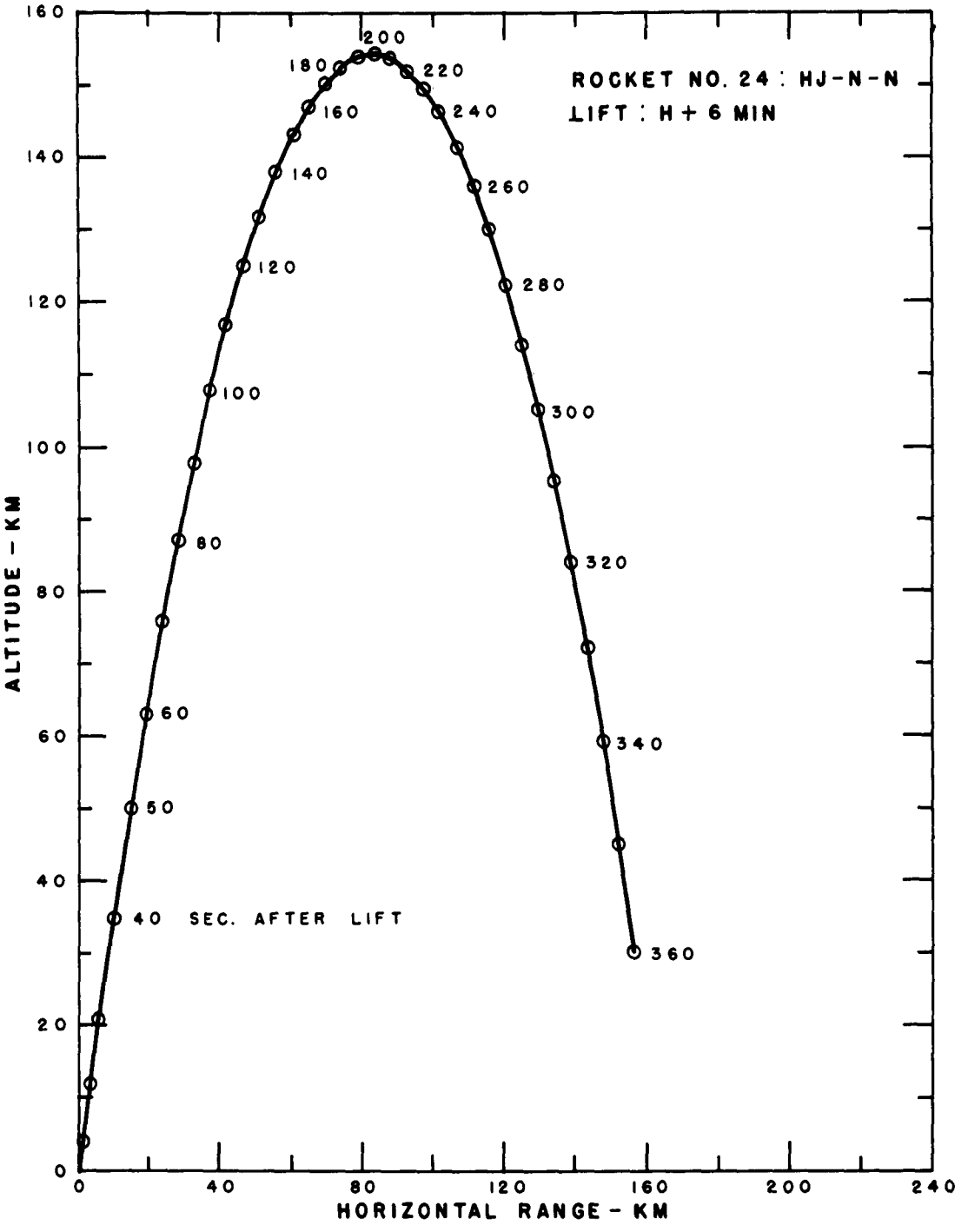

Figure B.22 Trajectory for Rocket 24, King Fish.

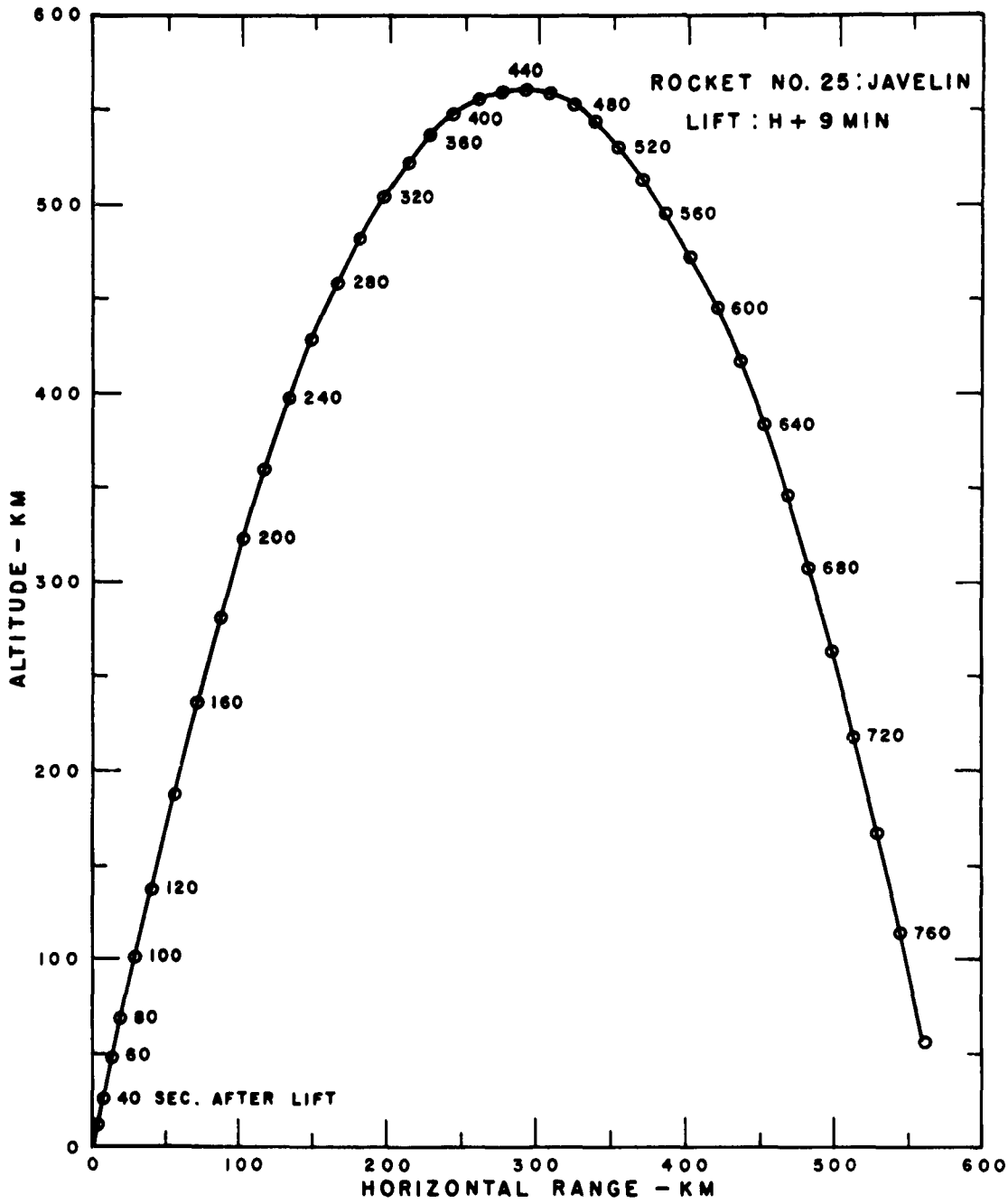

Figure B.23 Trajectory for Rocket 25, King Fish.

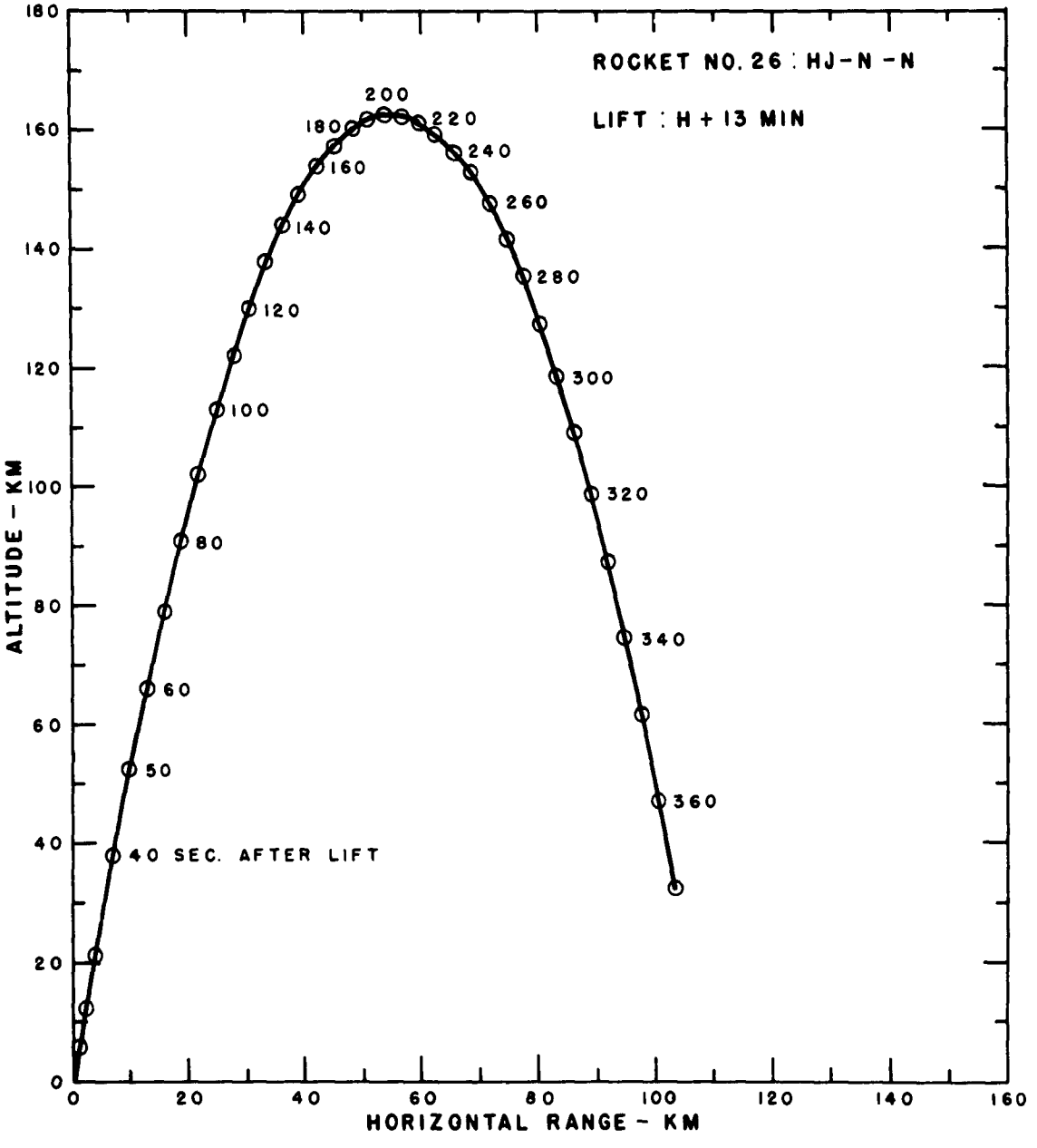

Figure B.24 Trajectory for Rocket 26, King Fish.

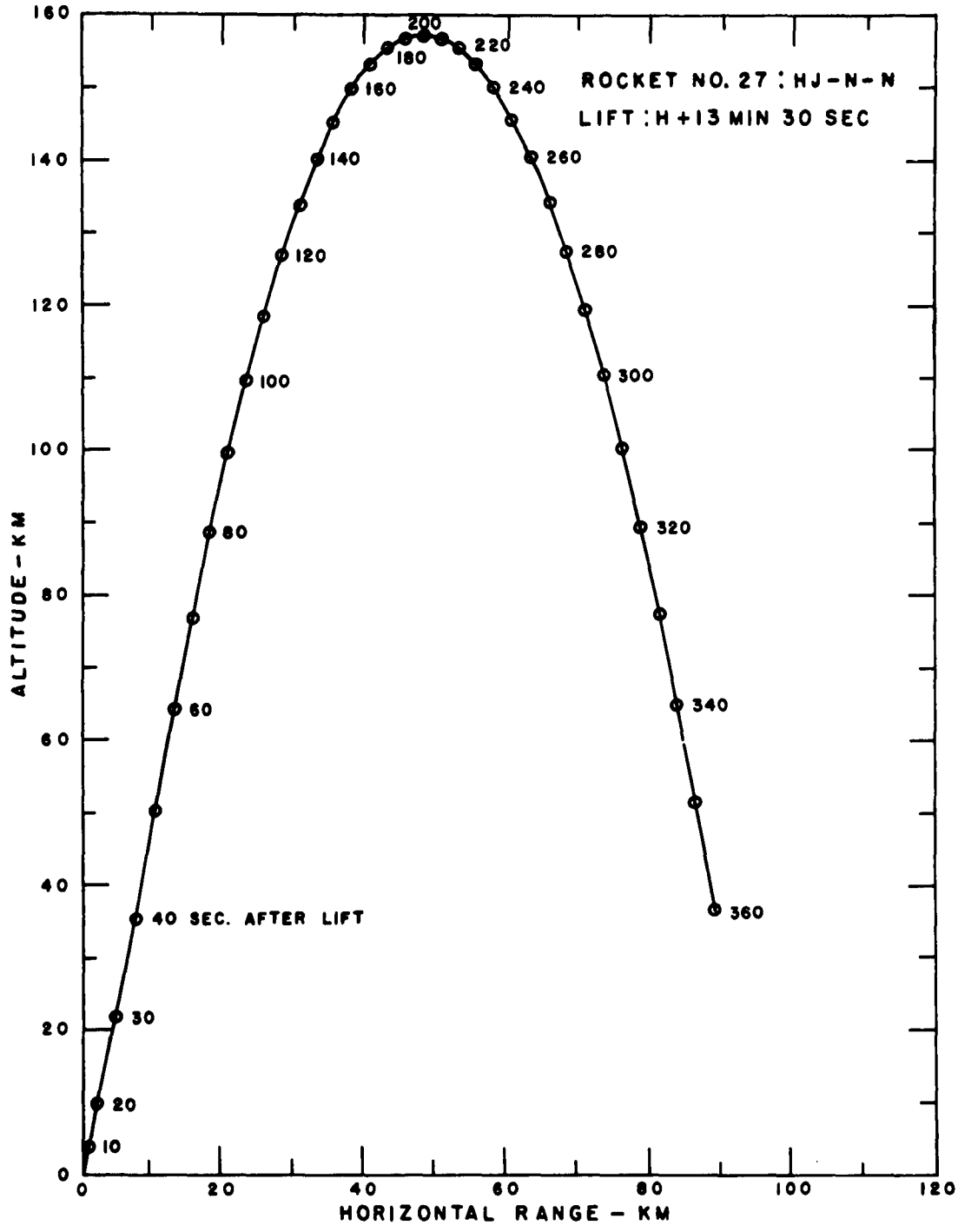

Figure B.25 Trajectory for Rocket 27, King Fish.

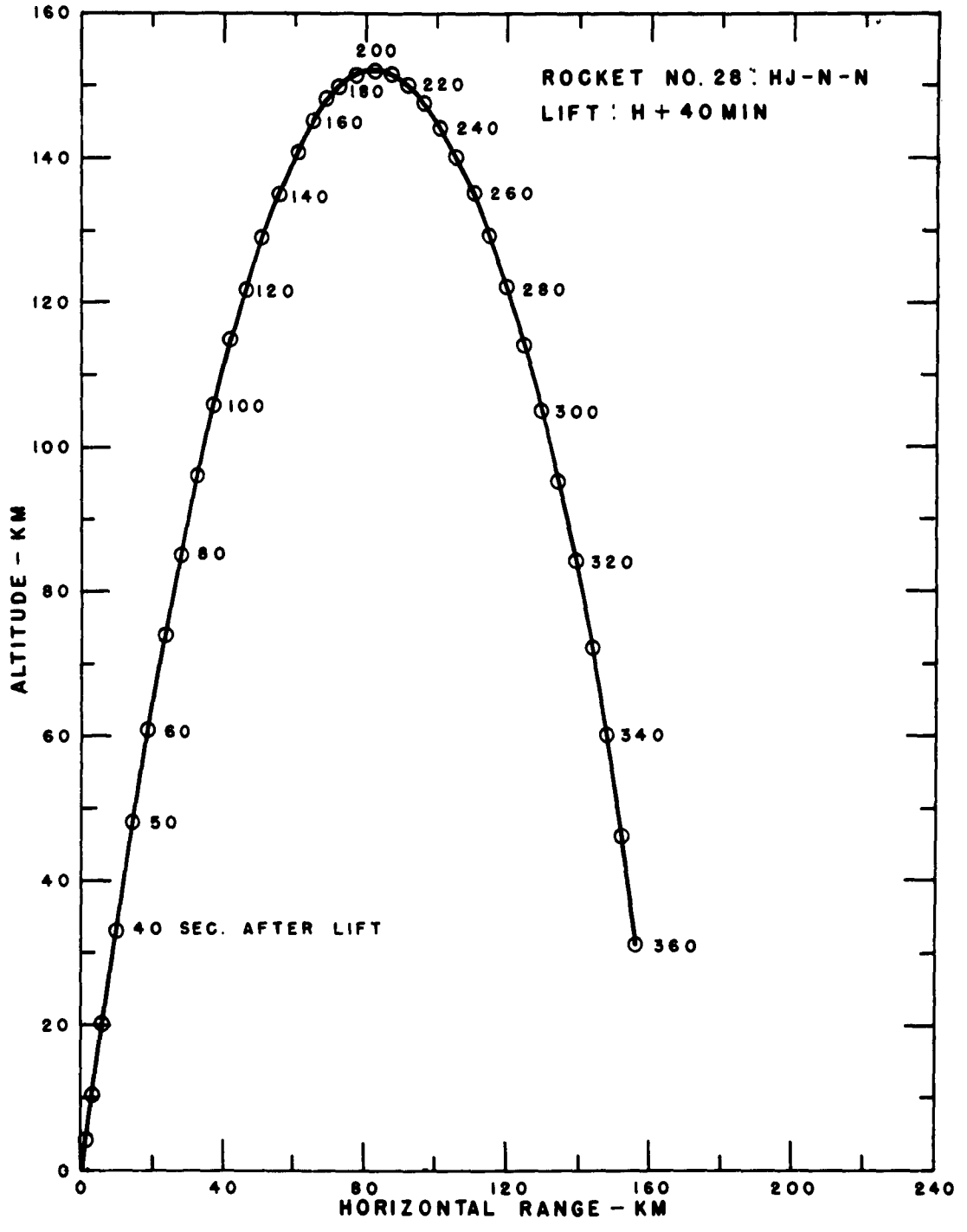

Figure B.26 Trajectory for Rocket 28, King Fish.

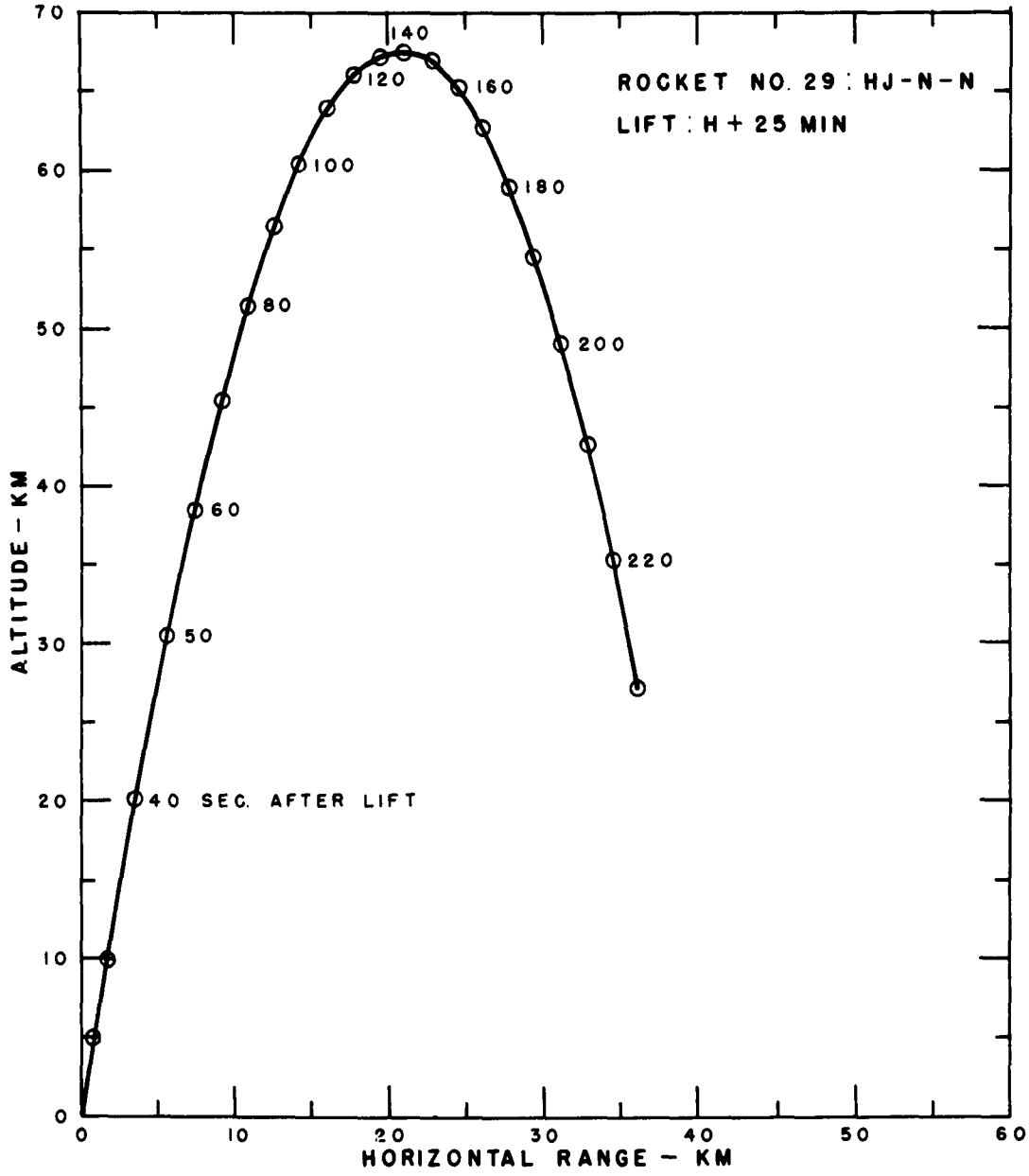

Figure B.27 Trajectory for Rocket 29, King Fish.

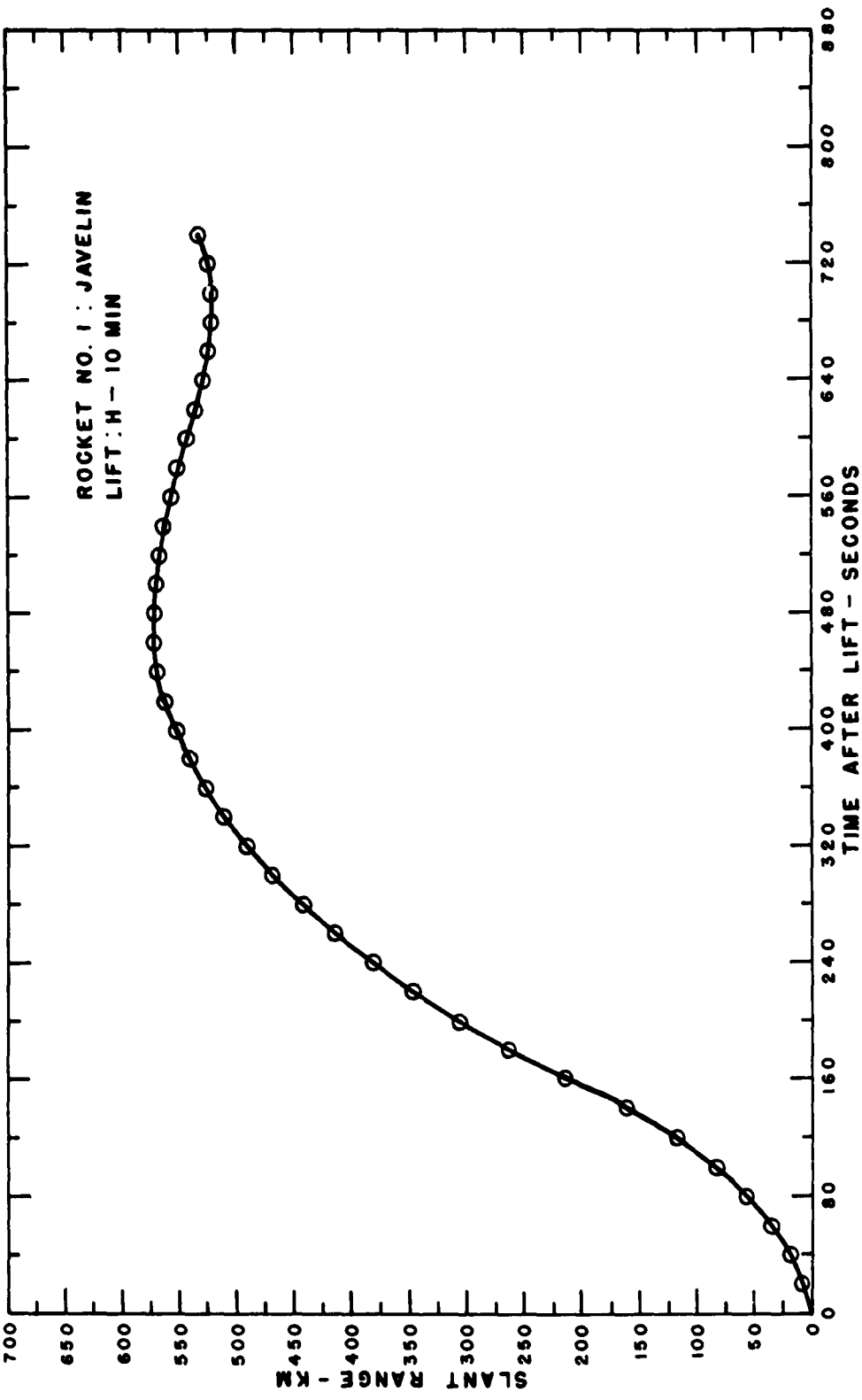

Figure B.28 Slant range versus time for Rocket 1, Star Fish.

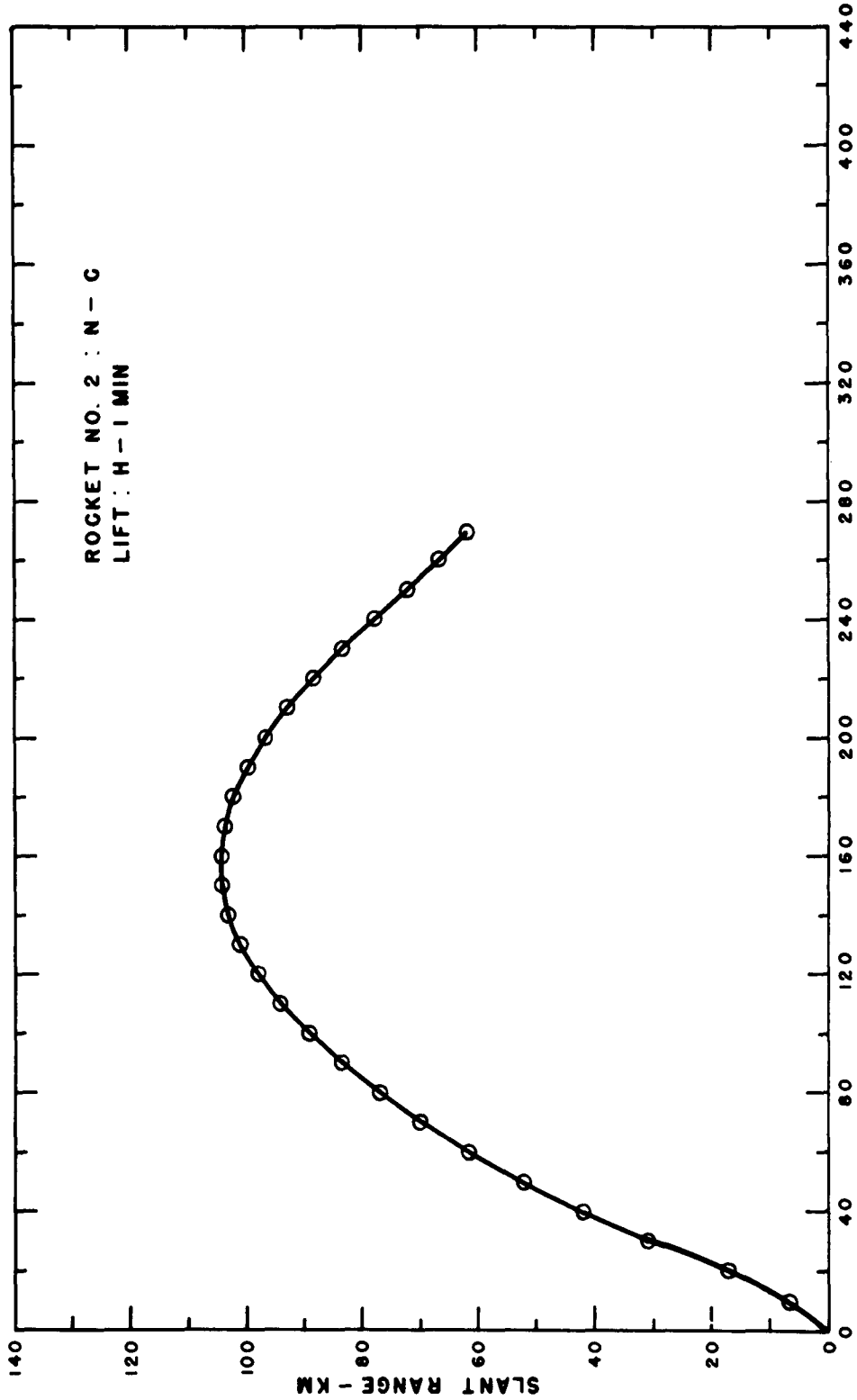

Figure B.29 Slant range versus time for Rocket 2, Star Fish.

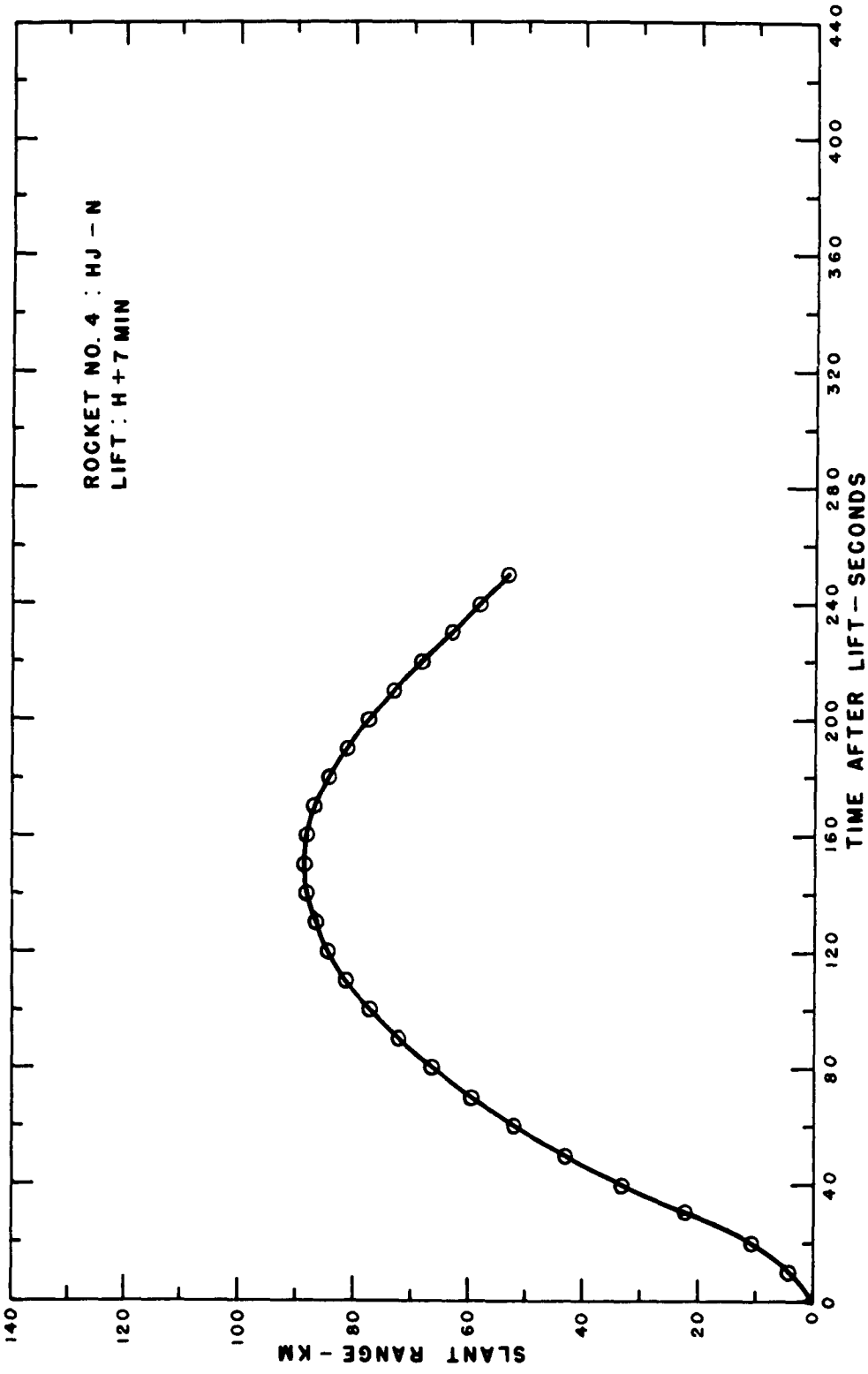

Figure B.30 Slant range versus time for Rocket 4, Star Fish.

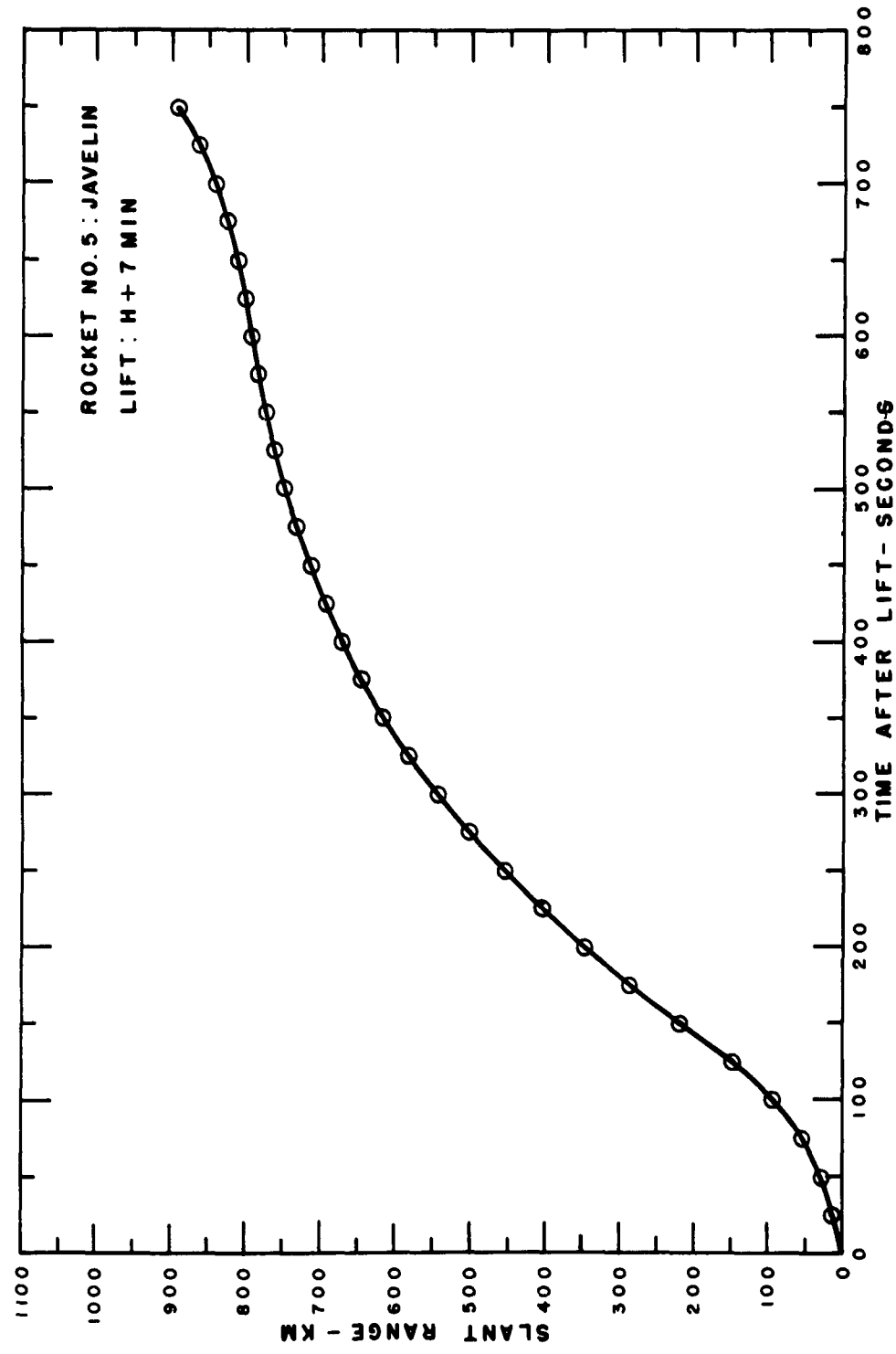

Figure B.31 Slant range versus time for Rocket 5, Star Fish.

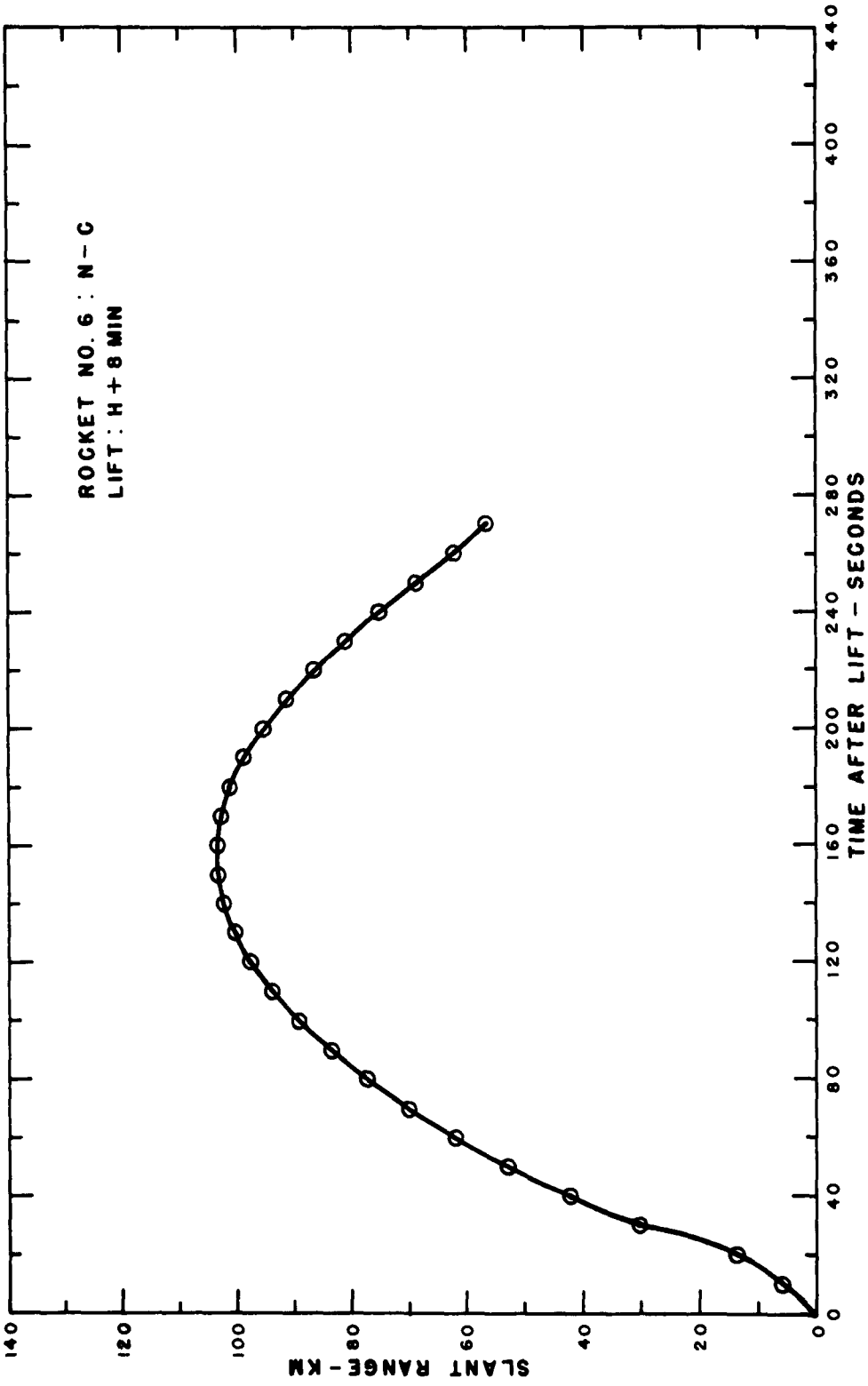

Figure B.32 Slant range versus time for Rocket 6, Star Fish.

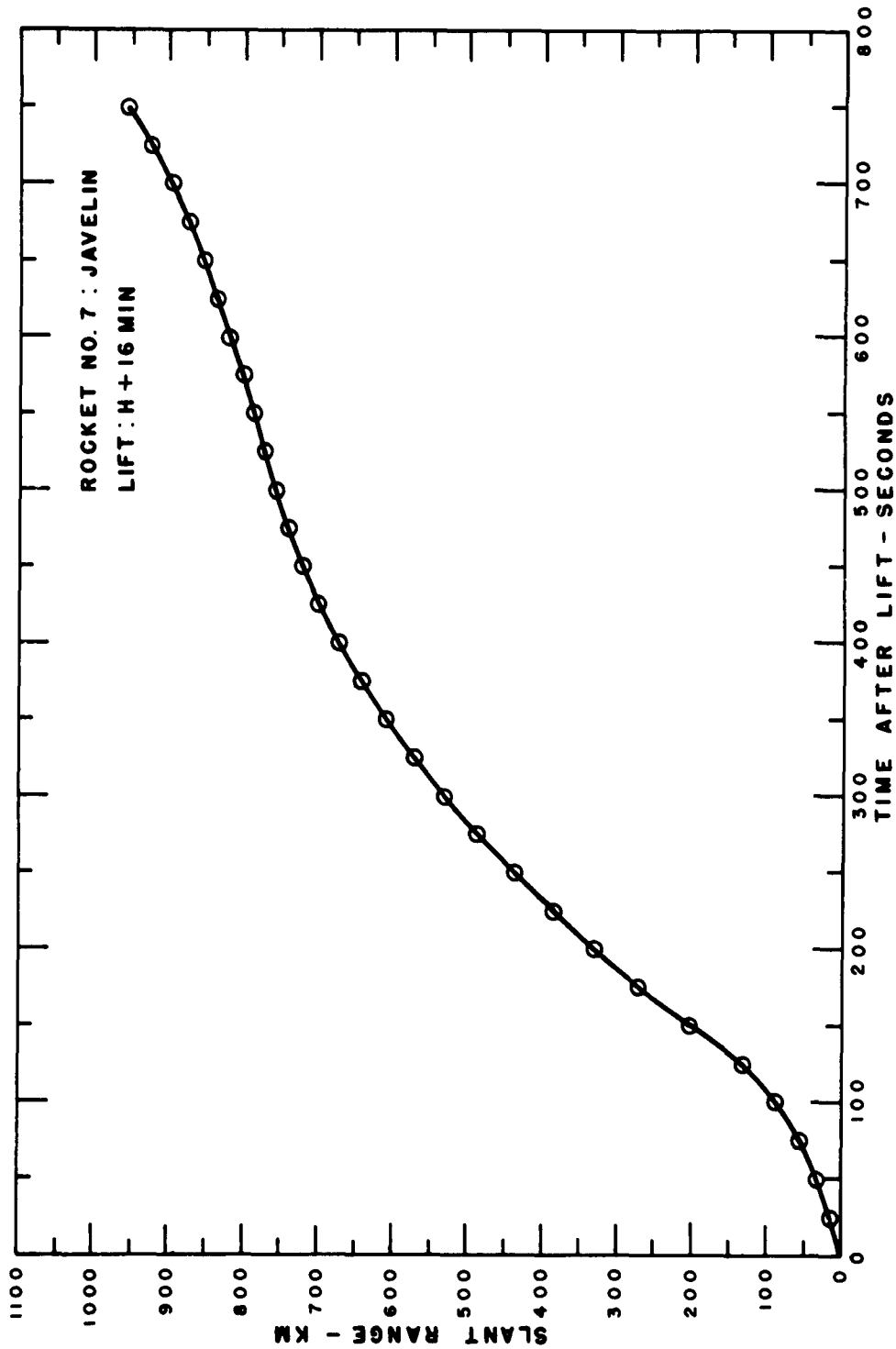

Figure B.33 Slant range versus time for Rocket 7, Star Fish.

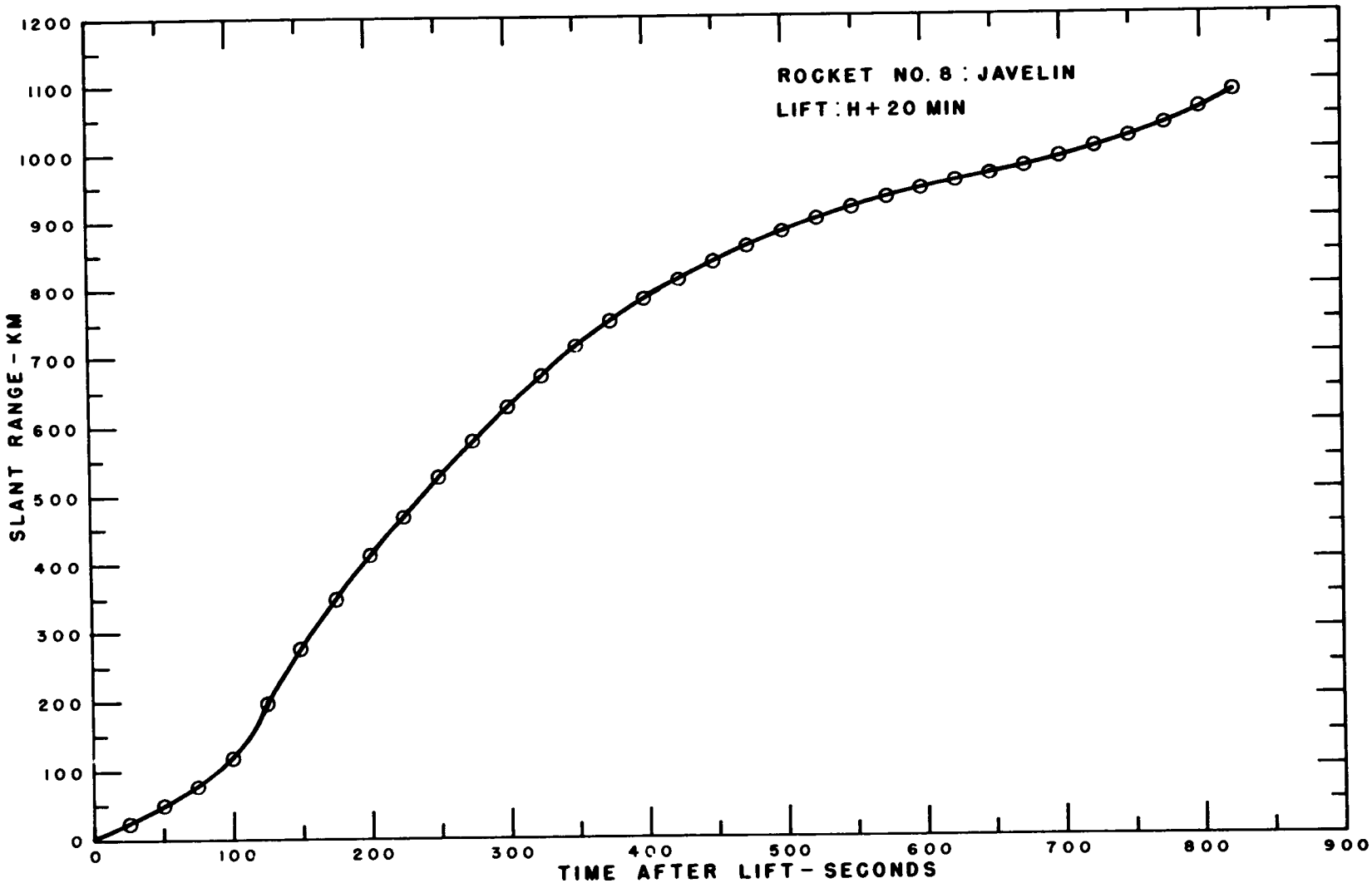

Figure B.34 Slant range versus time for Rocket 8, Star Fish.

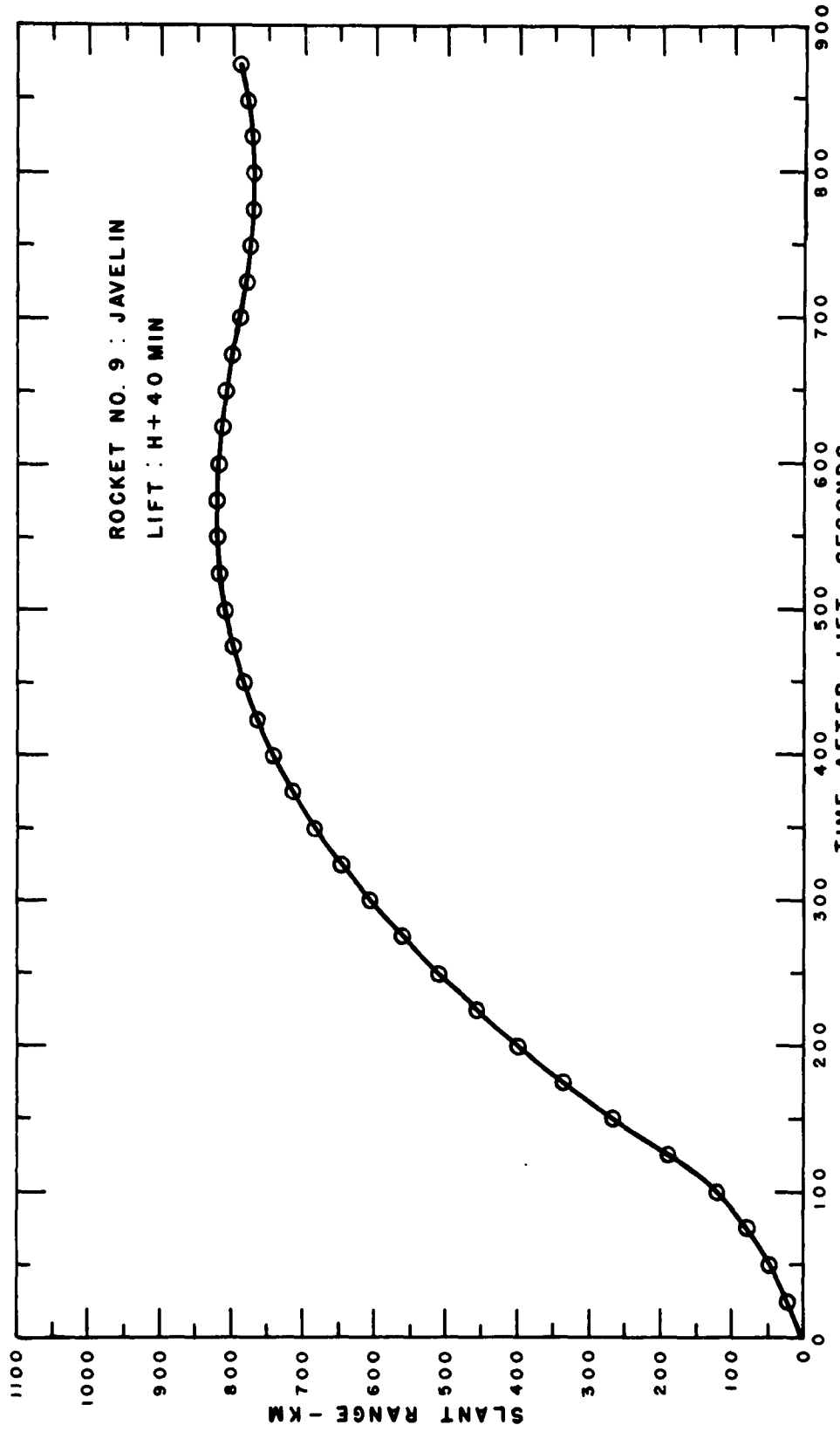

Figure B.35 Slant range versus time for Rocket 9, Star Fish.

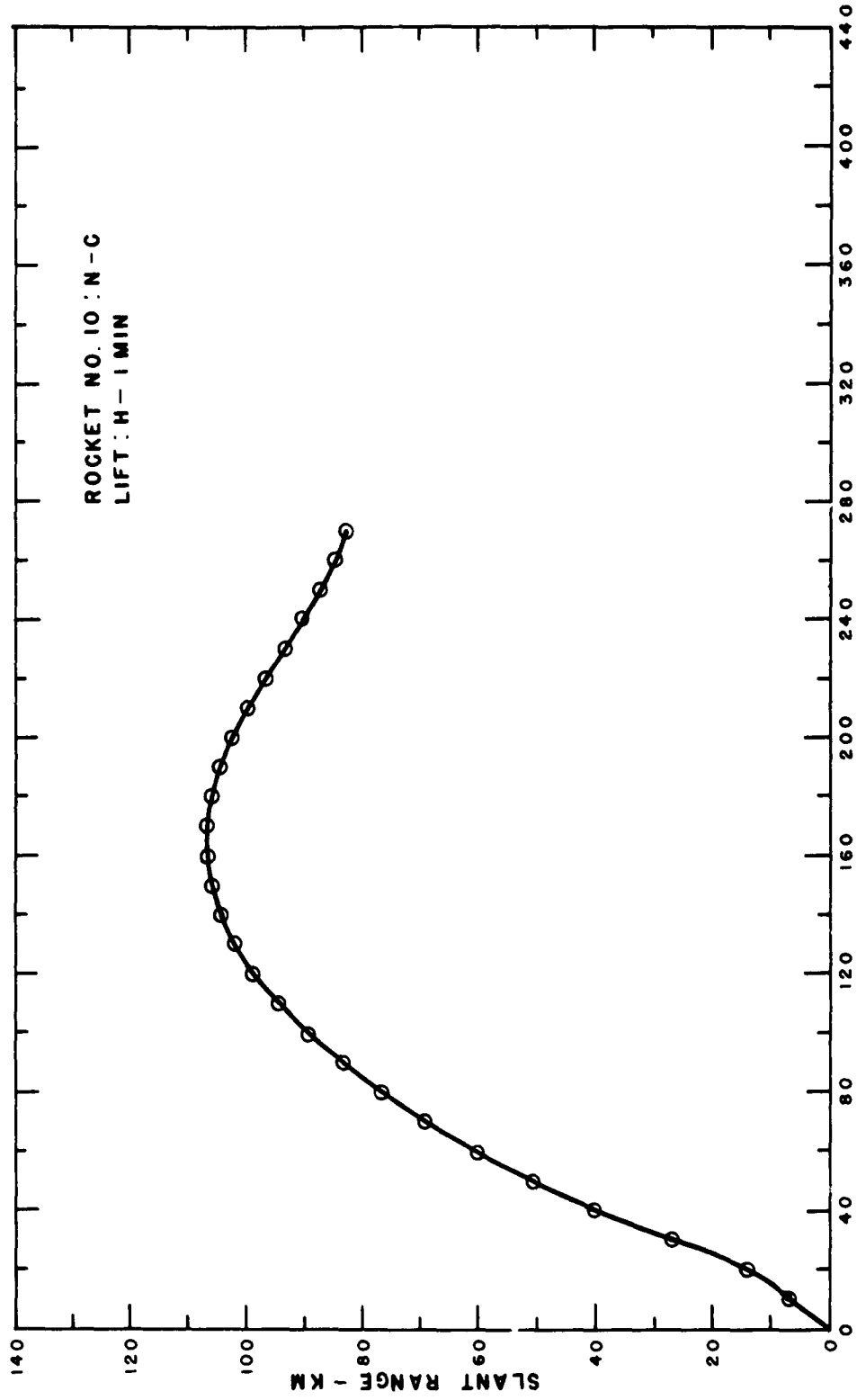

Figure B.36 Slant range versus time for Rocket 10, Blue Gill.

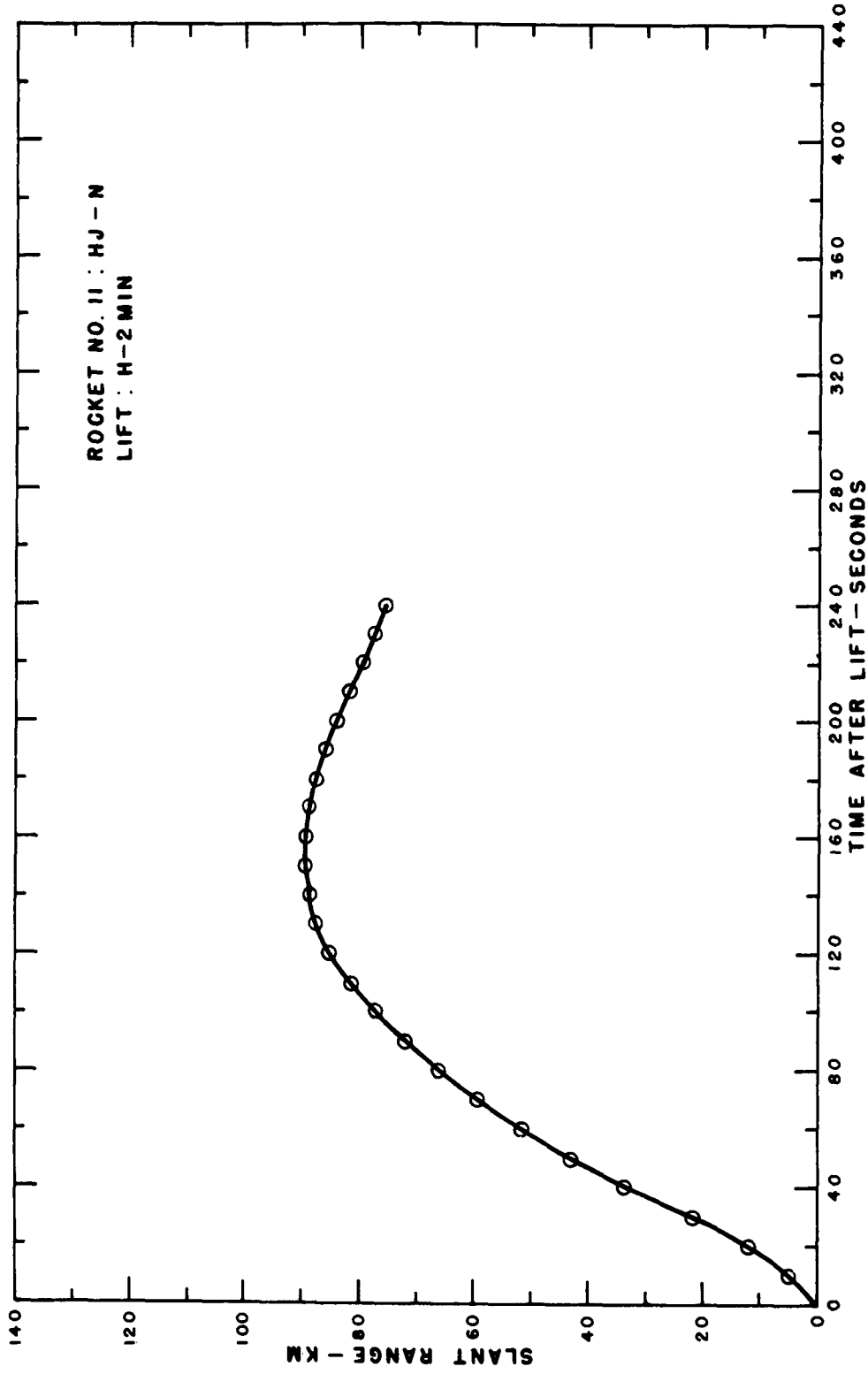

Figure B.37 Slant range versus time for Rocket 11, Blue Gill.

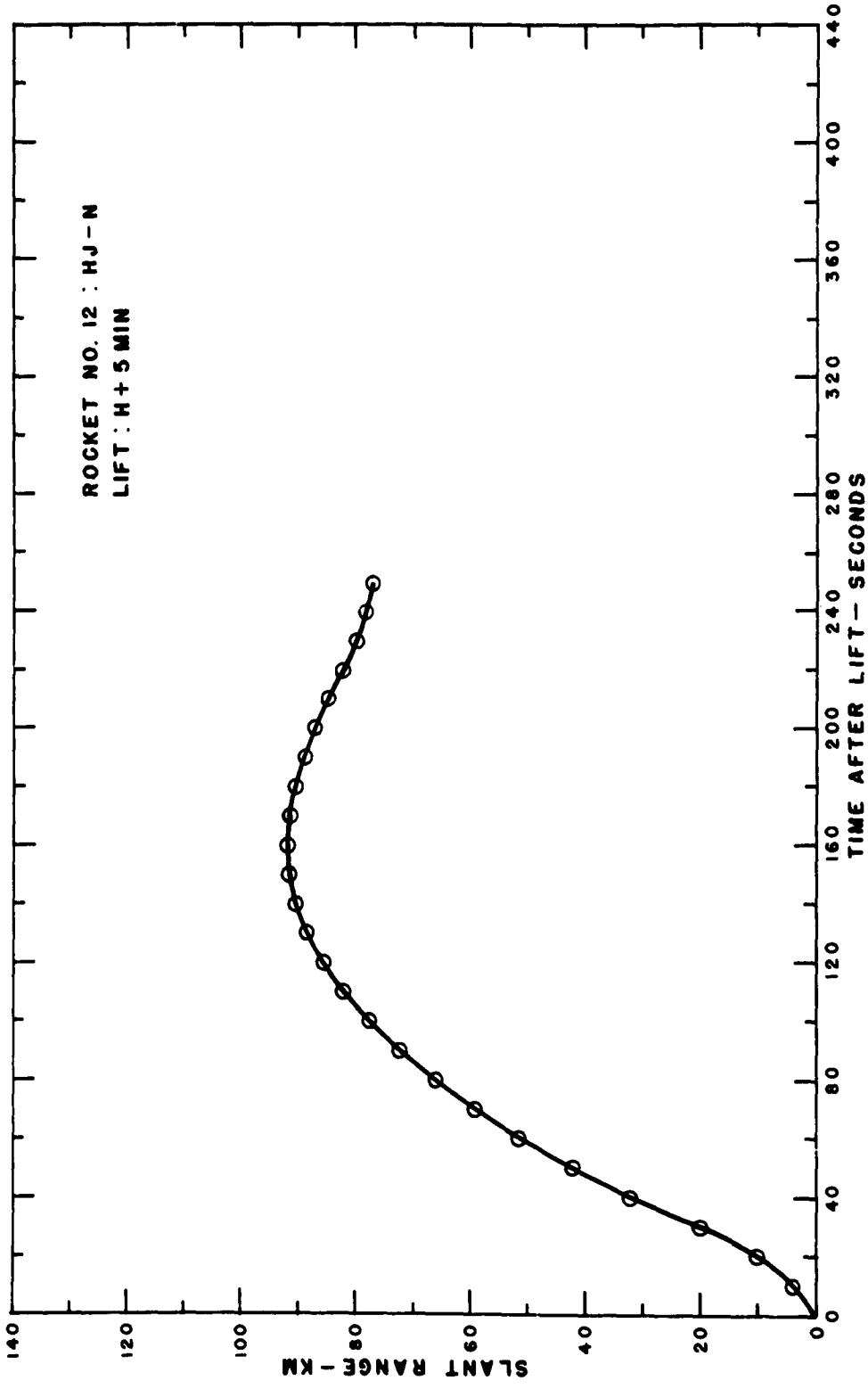

Figure B.38 Slant range versus time for Rocket 12, Glue Gill.

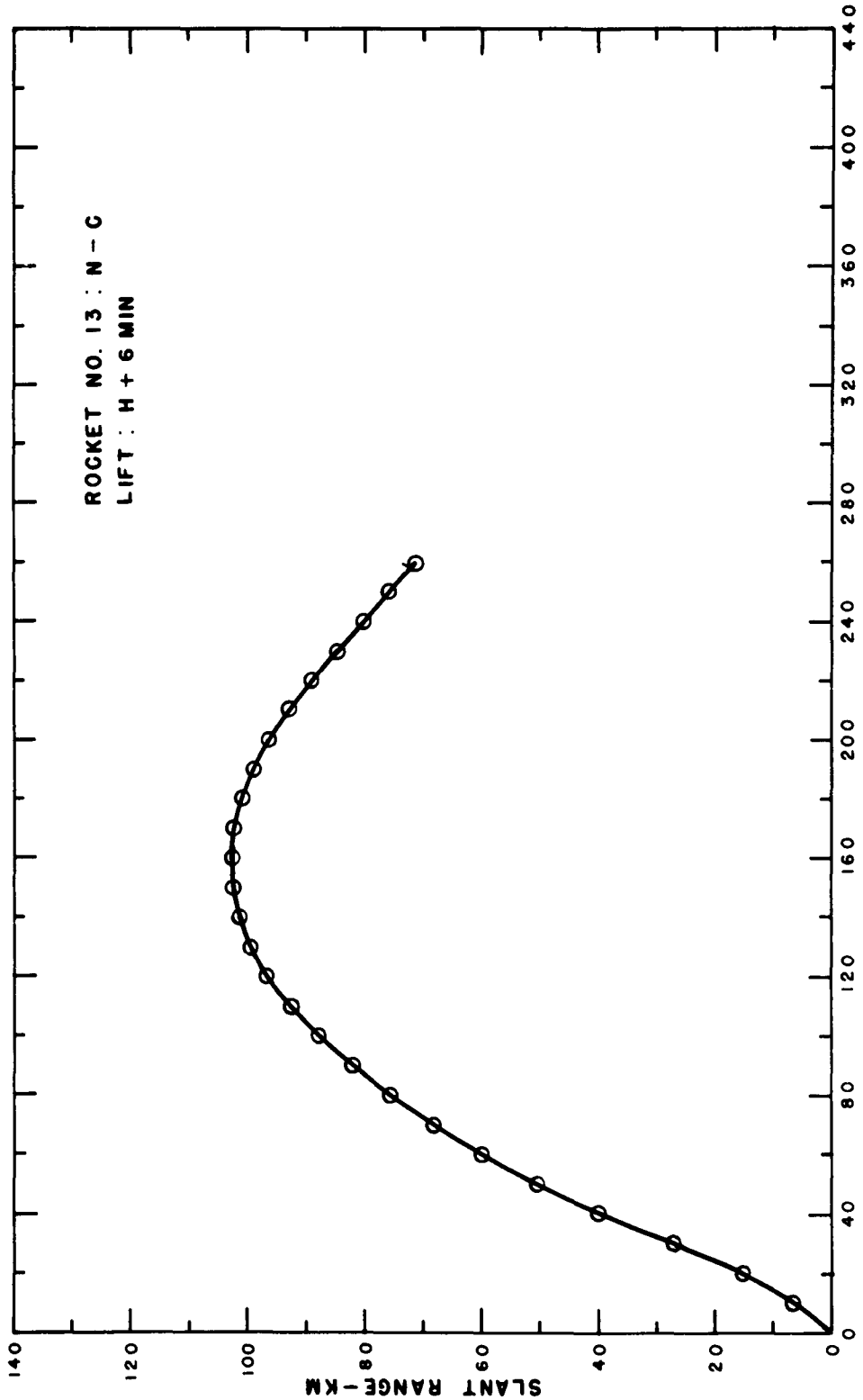

Figure B.39 Slant range versus time for Rocket 13, Blue Gill.

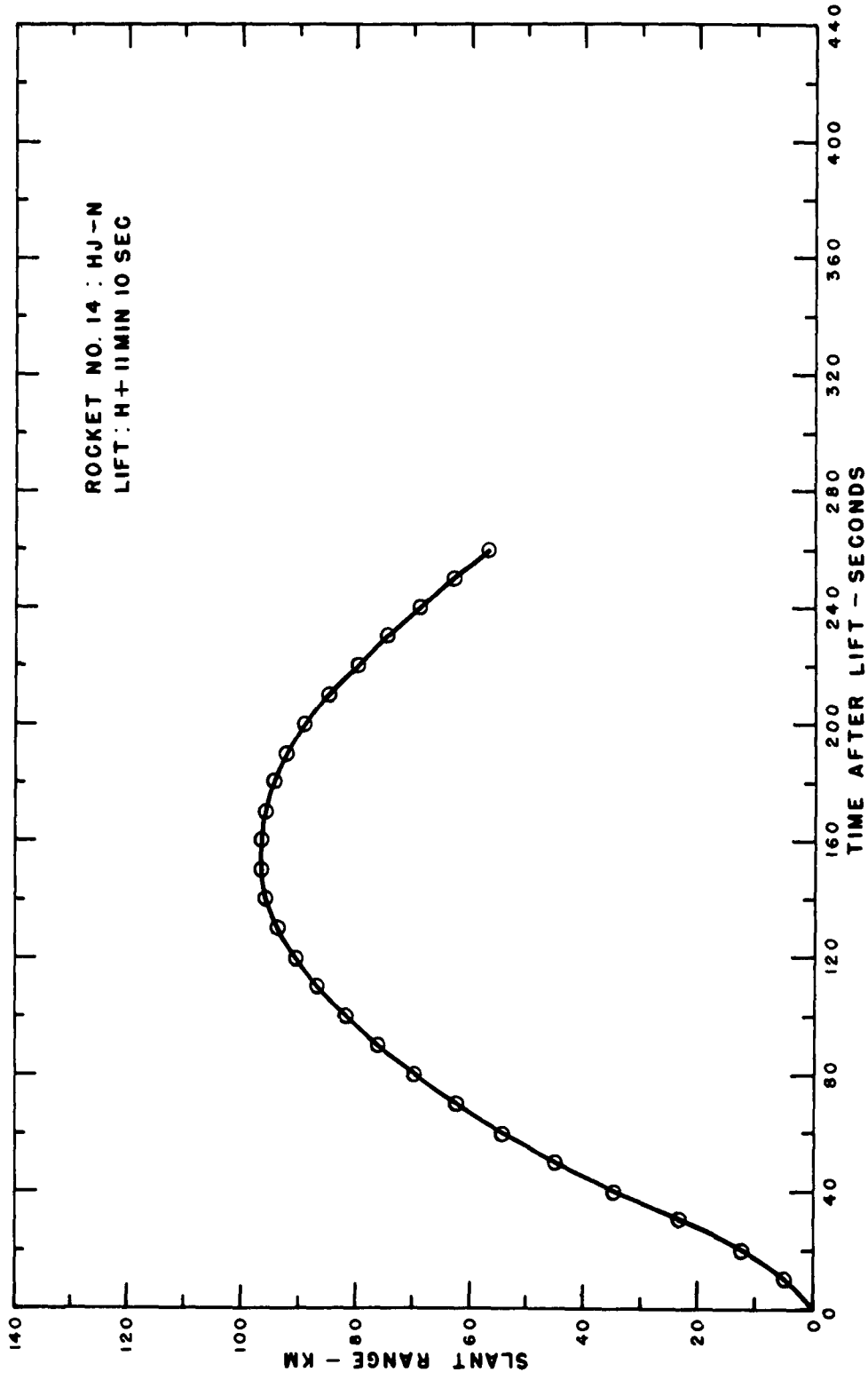

Figure B.40 Slant range versus time for Rocket 14, Blue Gill.

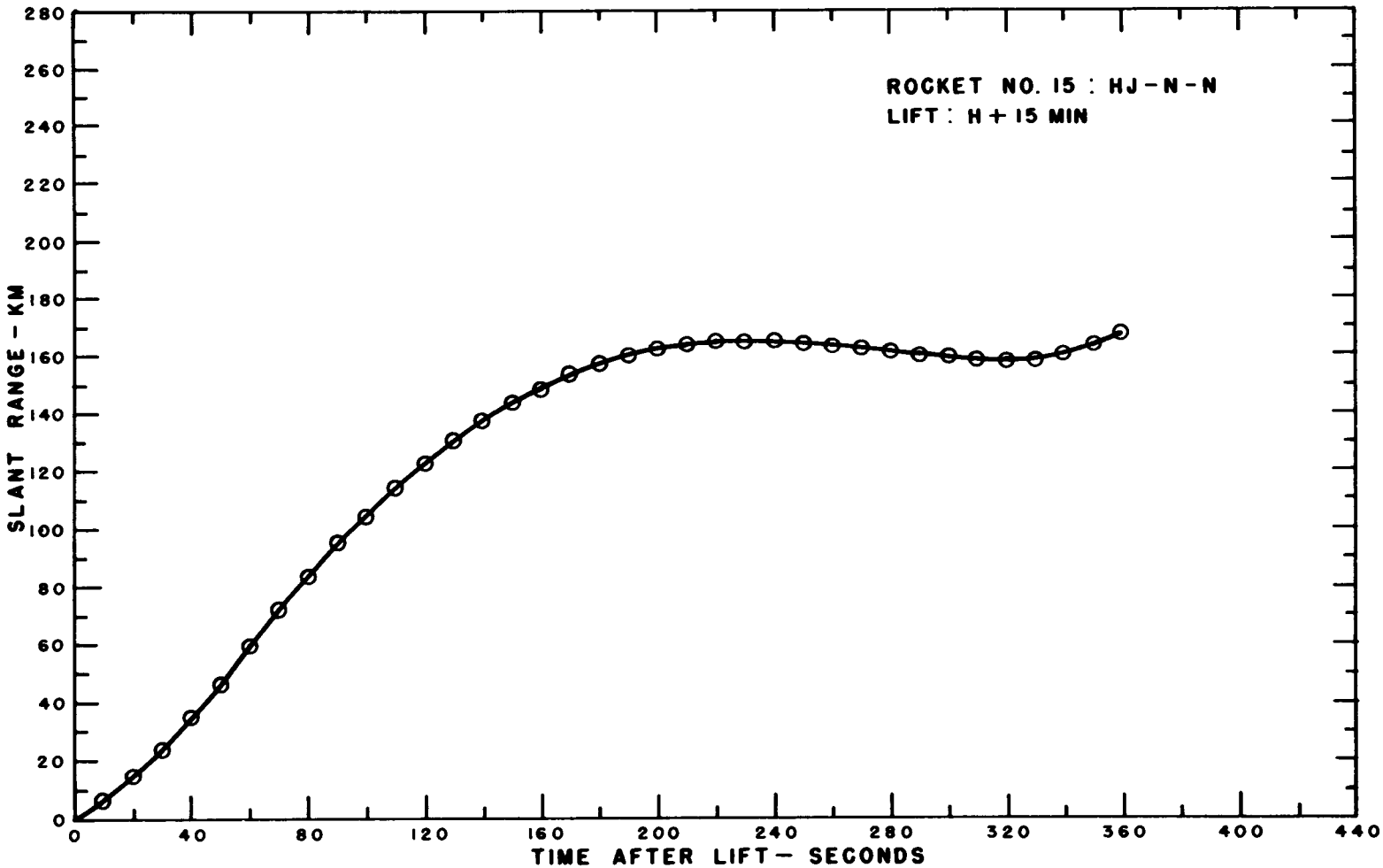

Figure B.41 Slant range versus time for Rocket 15, Blue Gill.

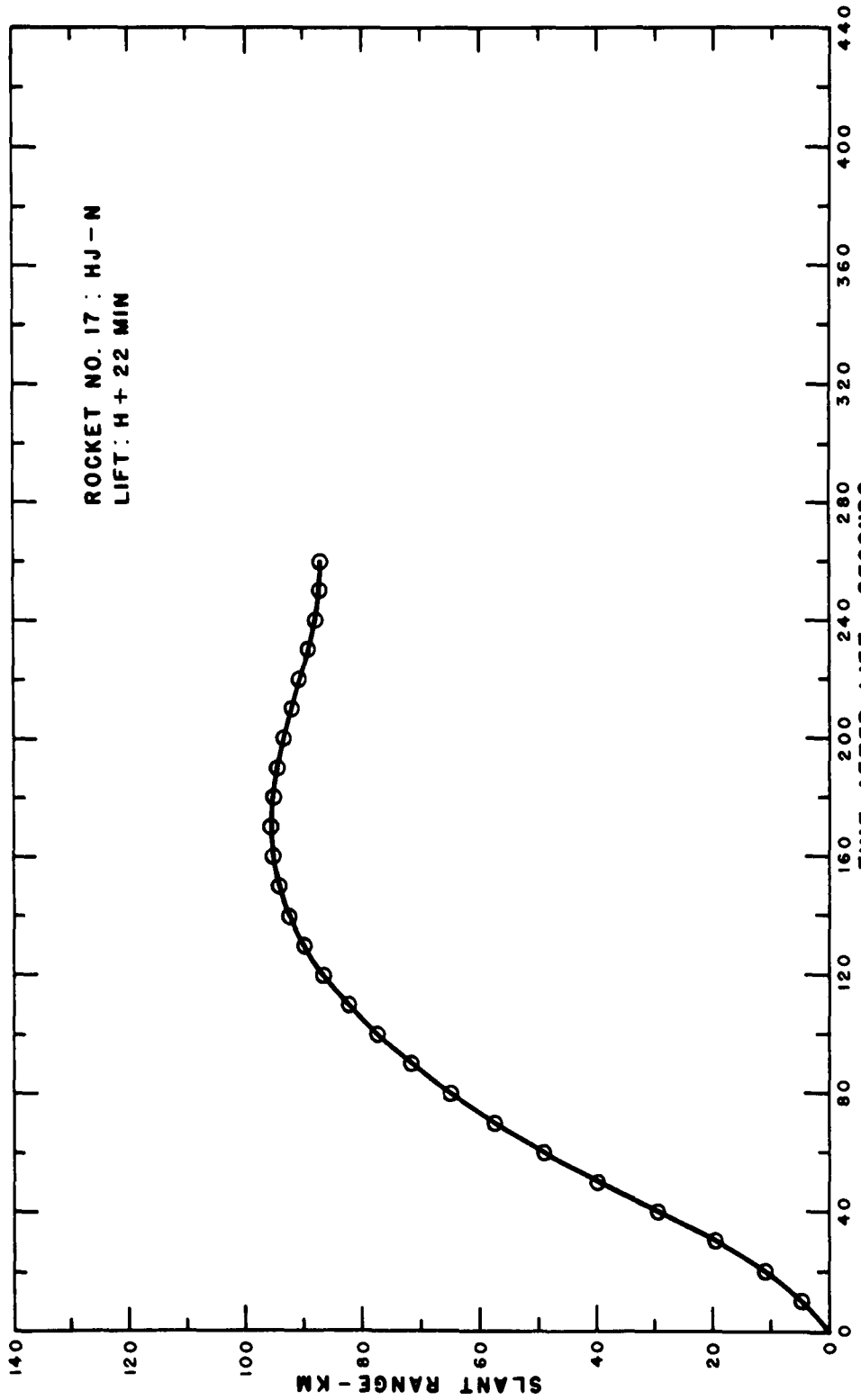

Figure B.42 Slant range versus time for Rocket 17, Blue Gill.

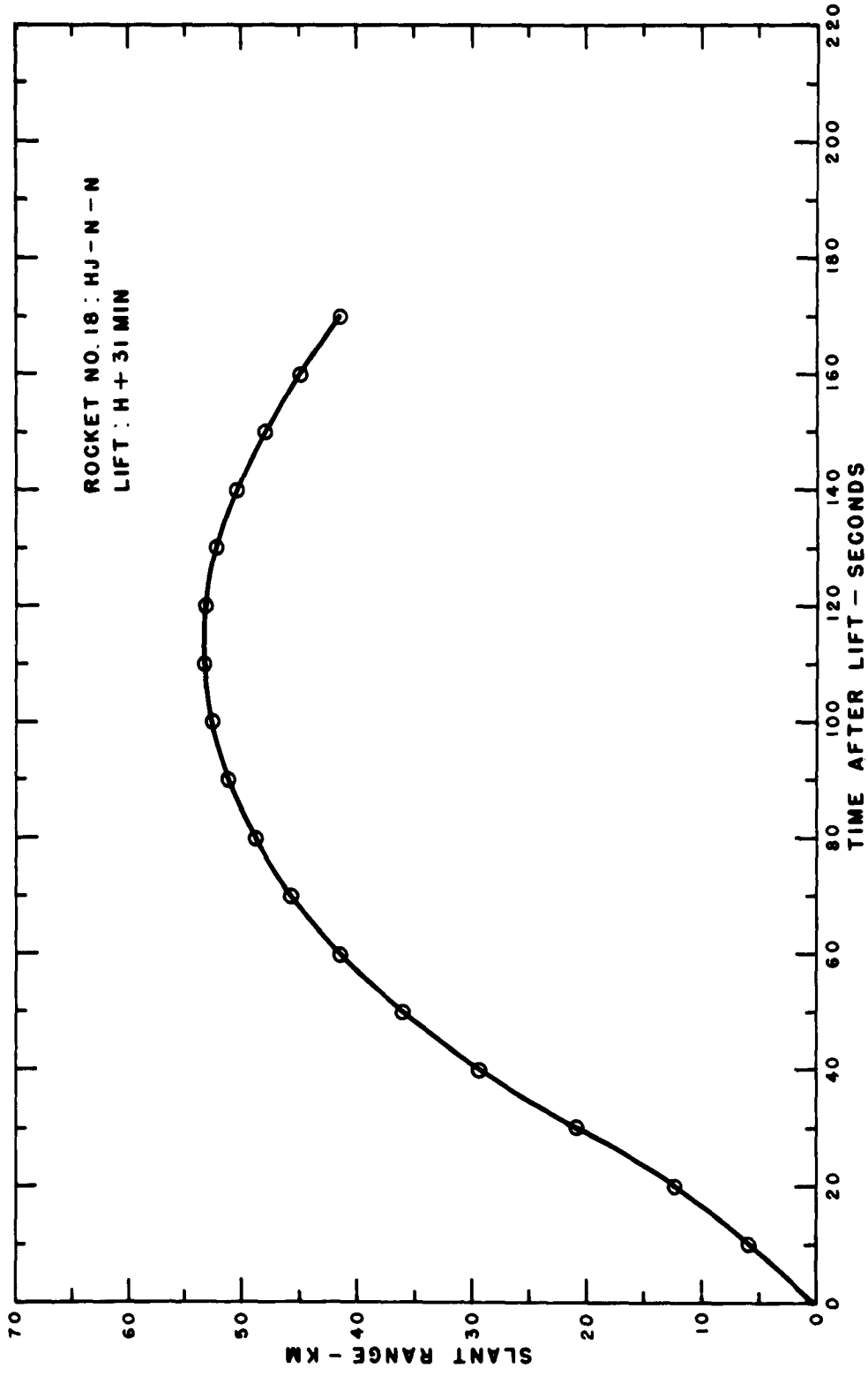

Figure B.43 Slant range versus time for Rocket 18, Blue Gill.

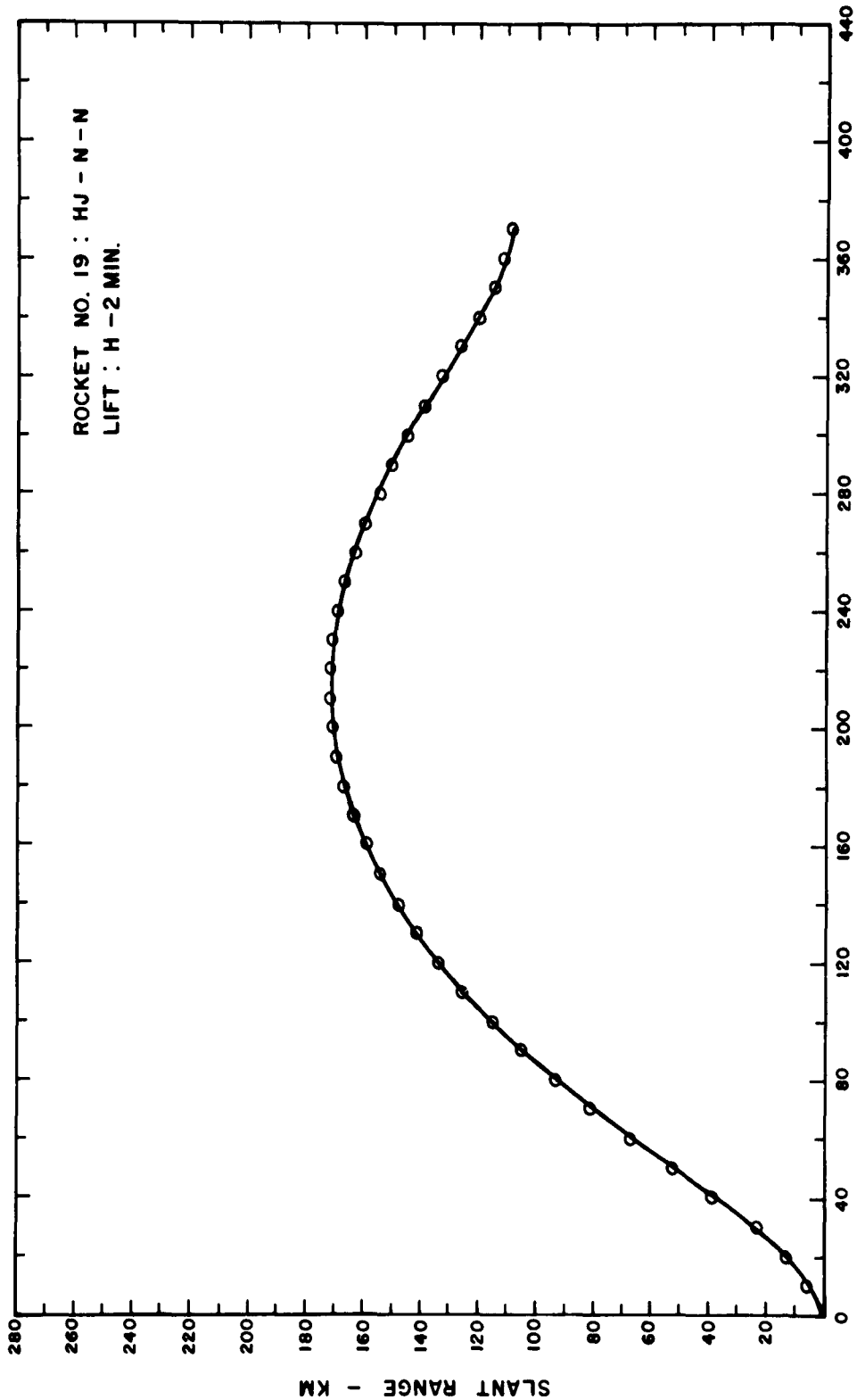

Figure B.44 Slant range versus time for Rocket 19, King Fish.

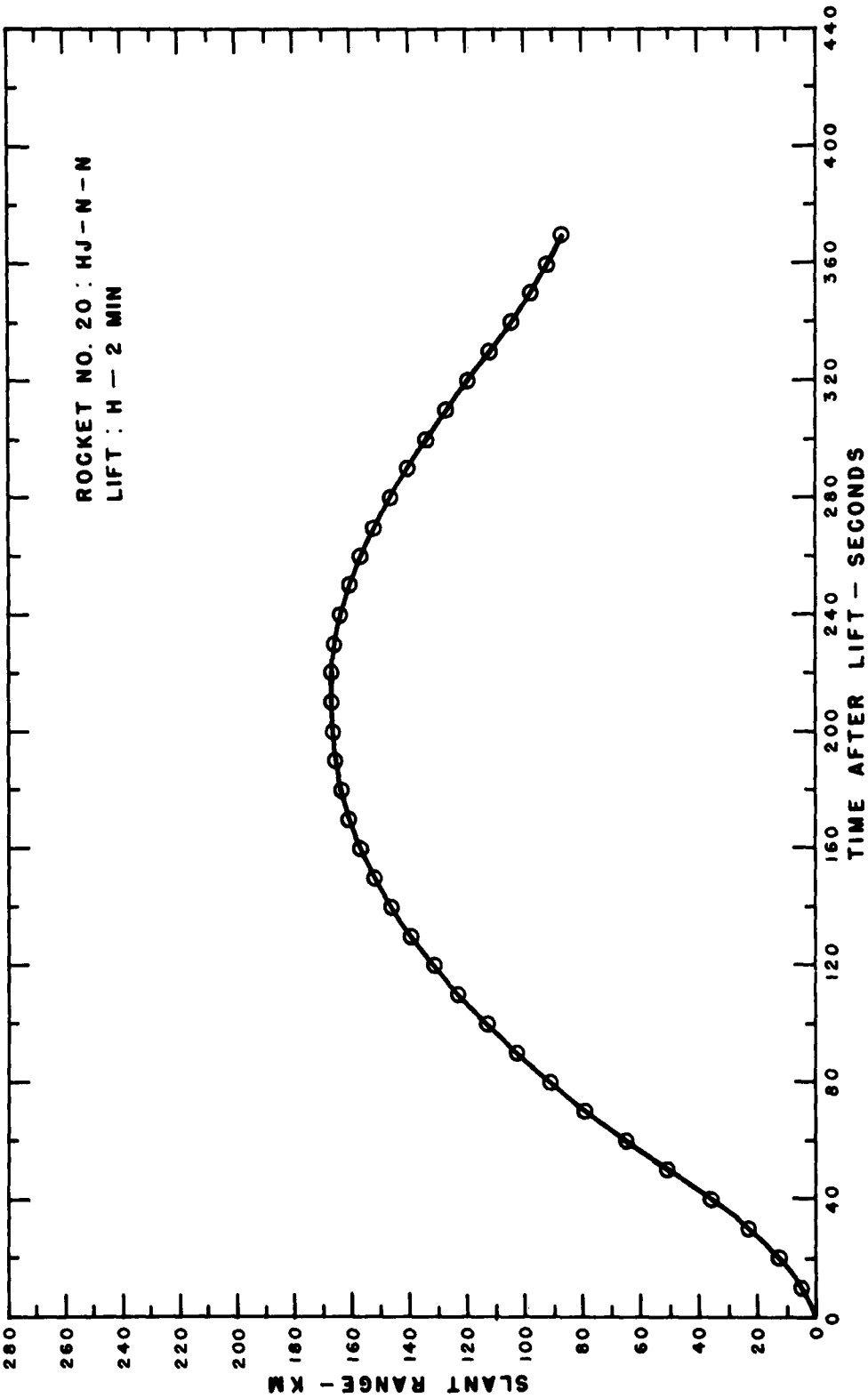

Figure B.45 Slant range versus time for Rocket 20, King Fish.

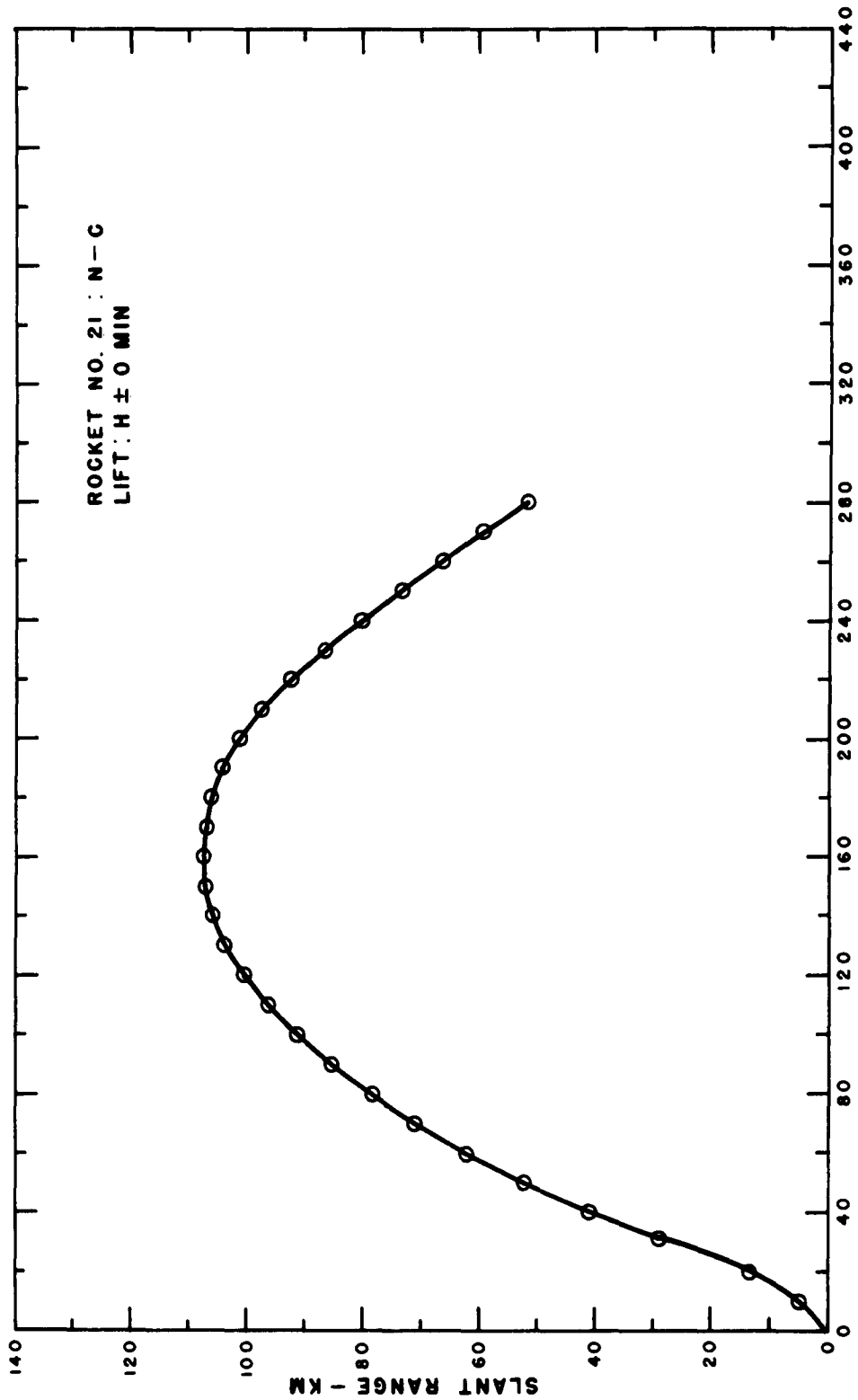

Figure B.46 Slant range versus time for Rocket 21, King Fish.

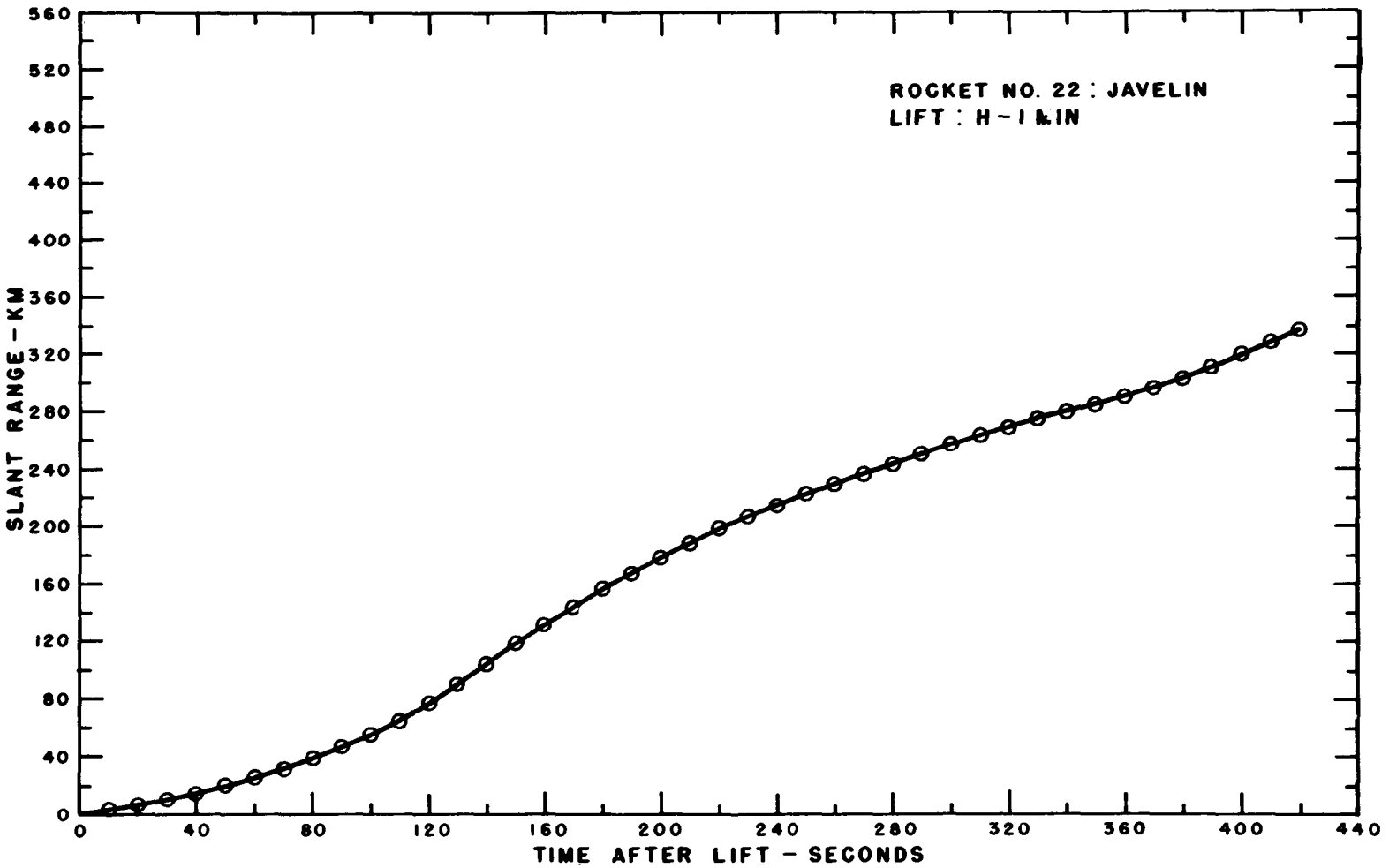

Figure B.47 Slant range versus time for Rocket 22, King Fish.

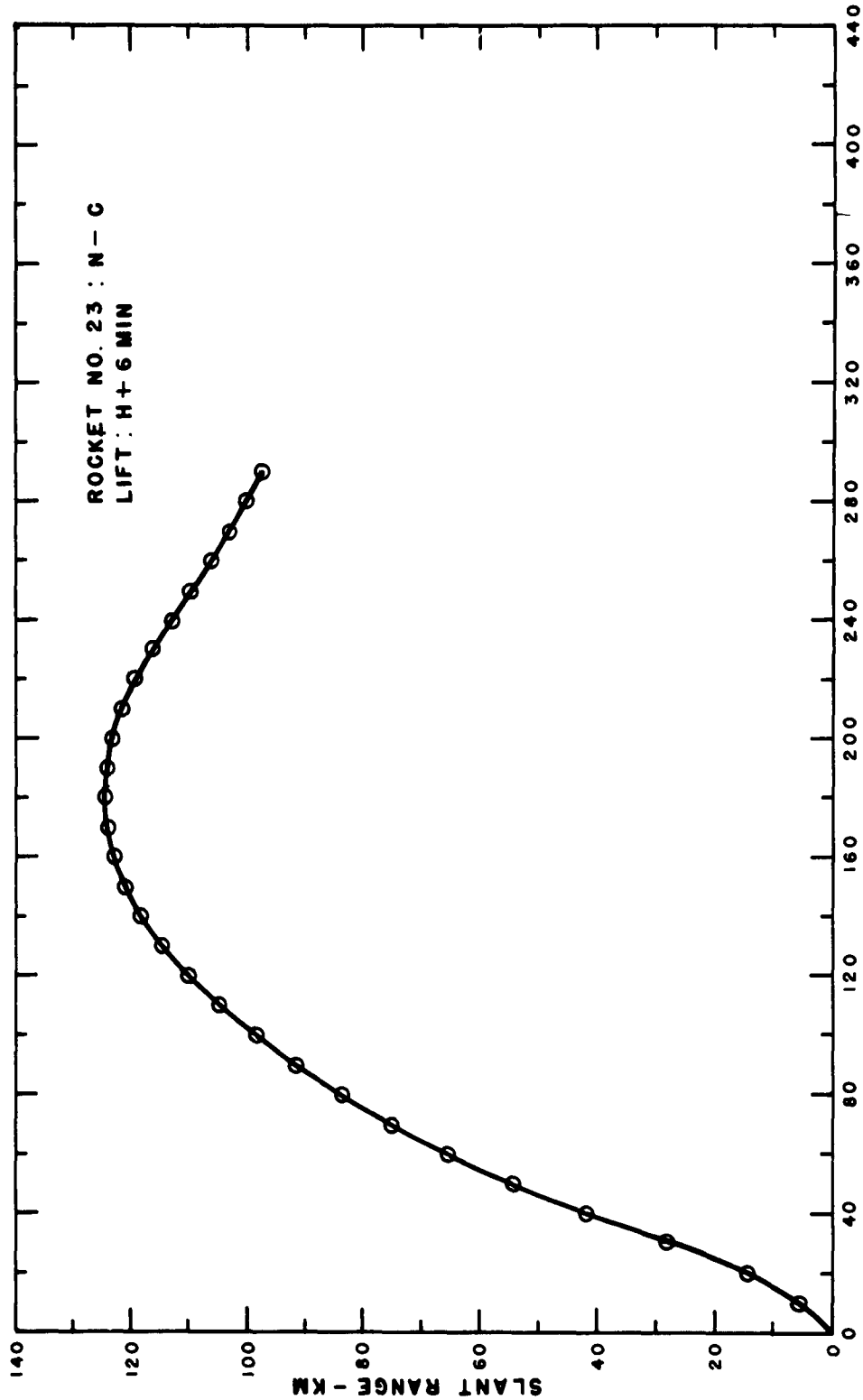

Figure B.48 Slant range versus time for Rocket 23, King Fish.

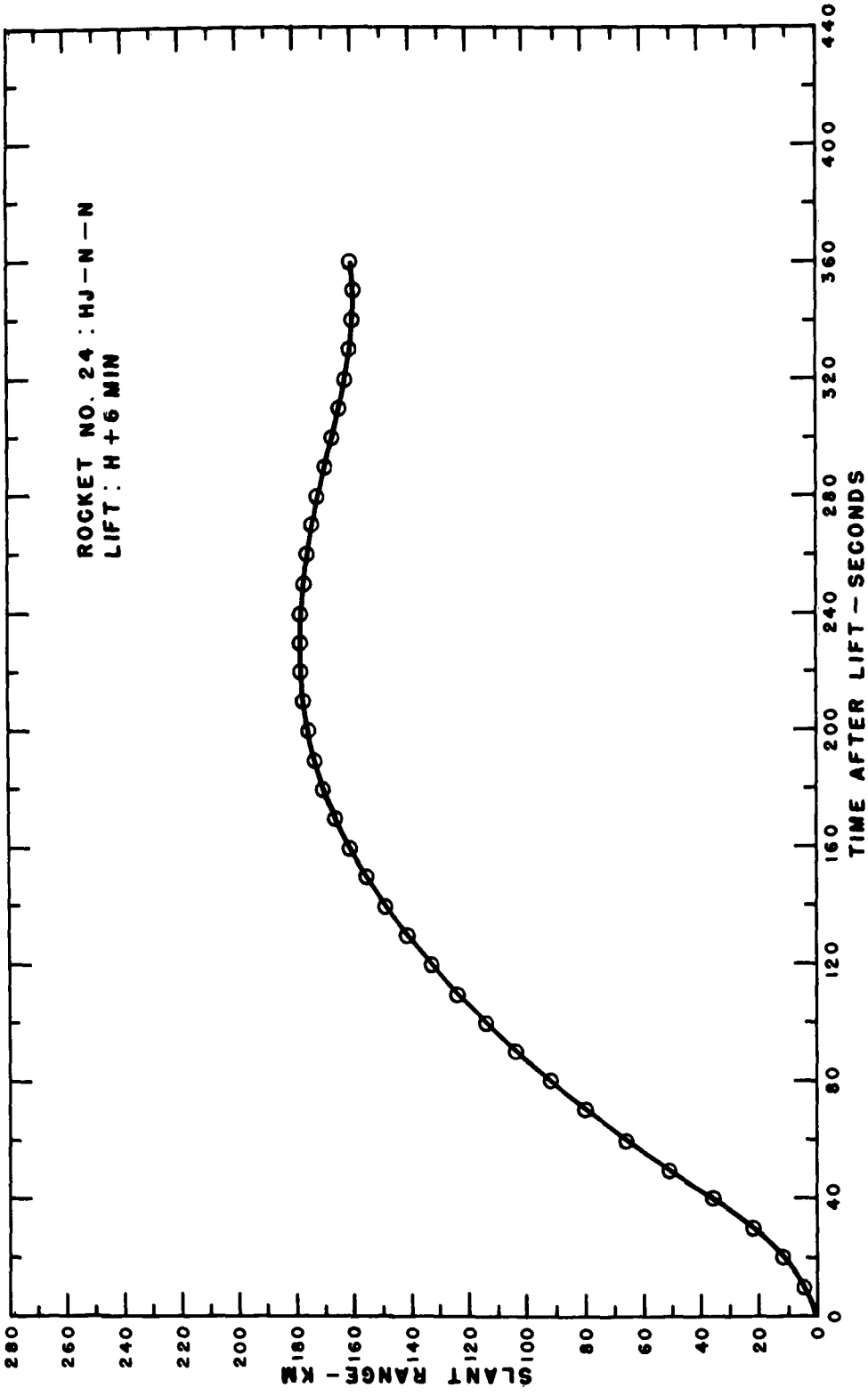

Figure B.49 Slant range versus time for Rocket 24, King Fish.

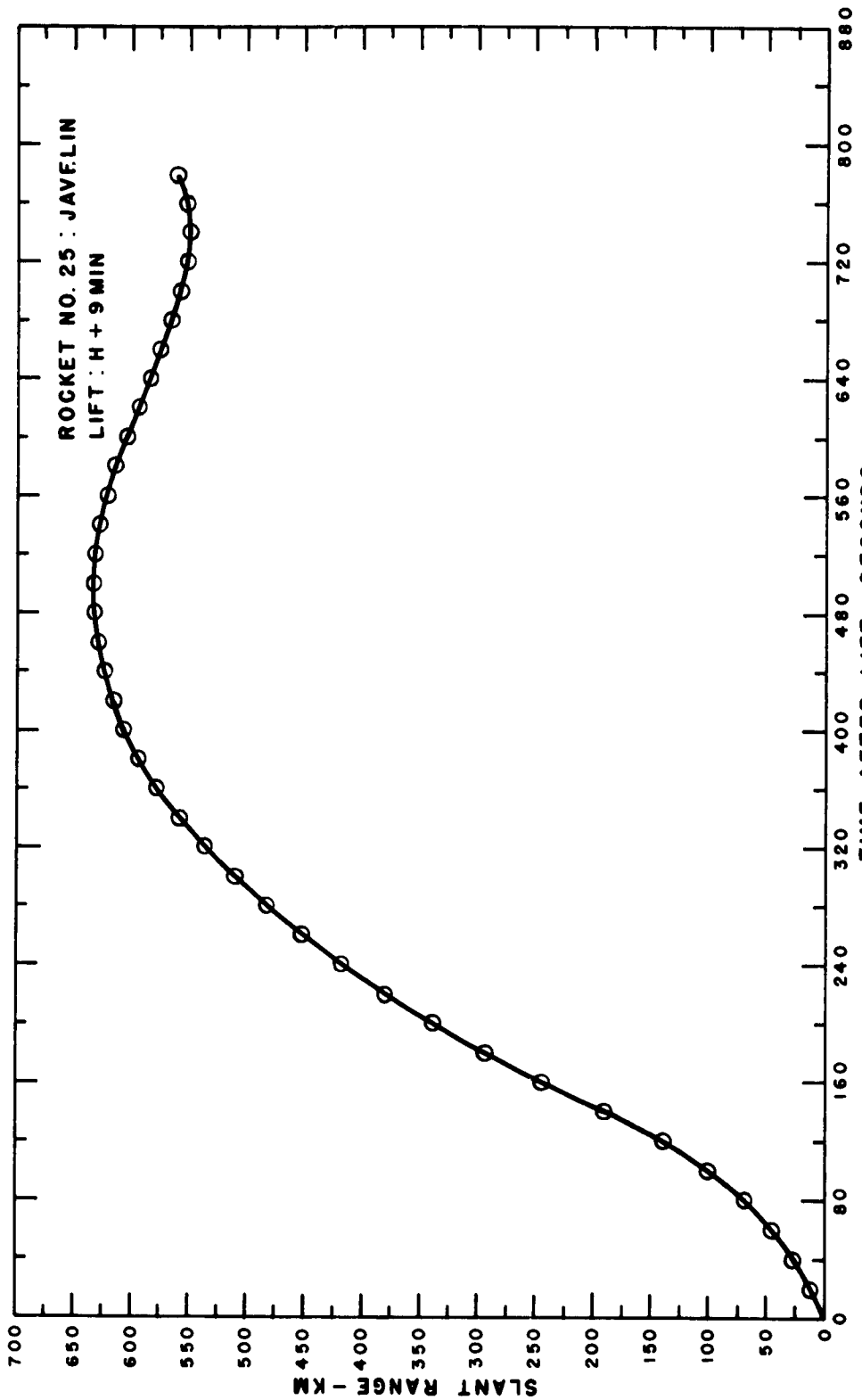

Figure B.50 Slant range versus time for Rocket 25, King Fish.

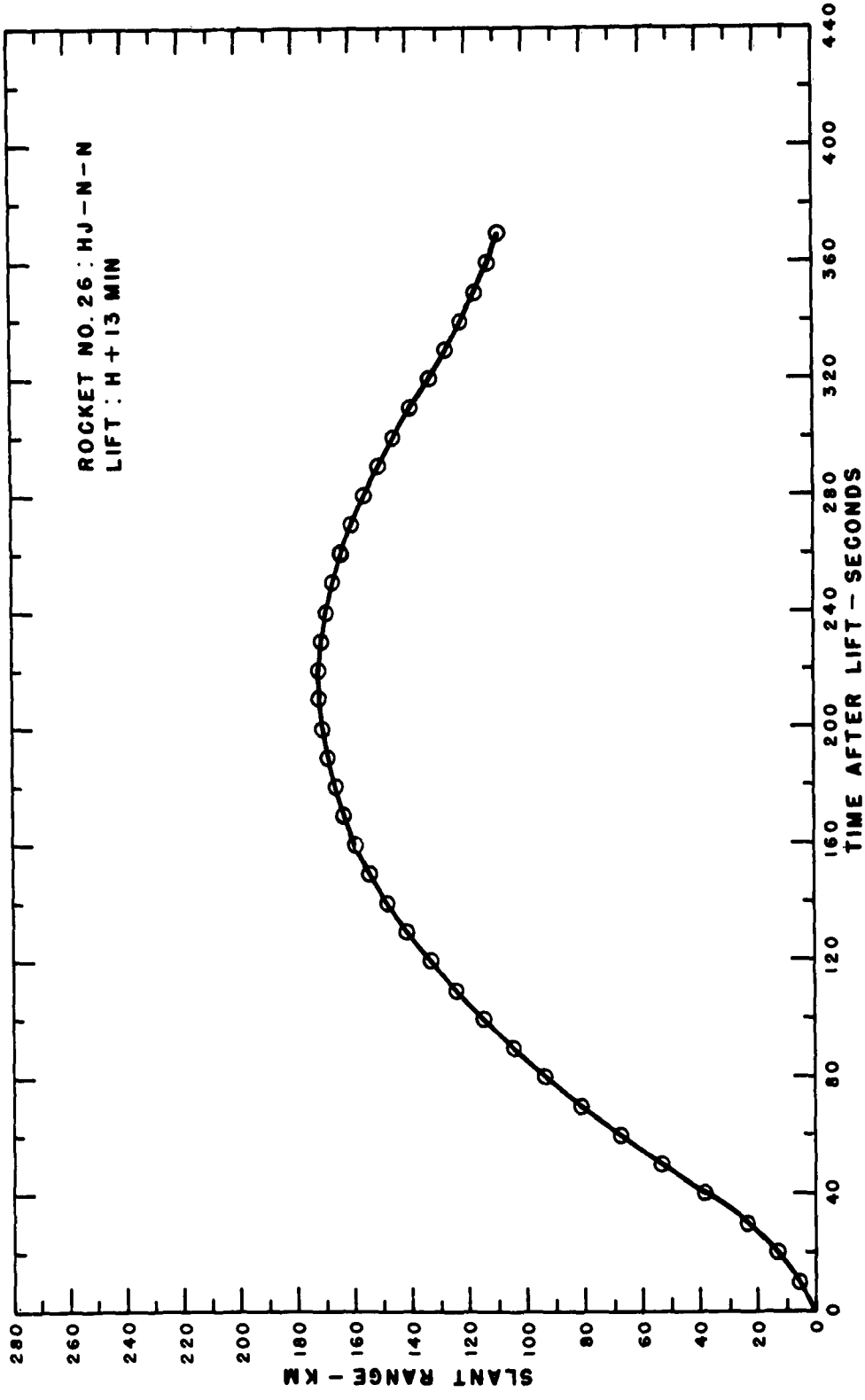

Figure B.51 Slant range versus time for Rocket 26, King Fish.

SECRET

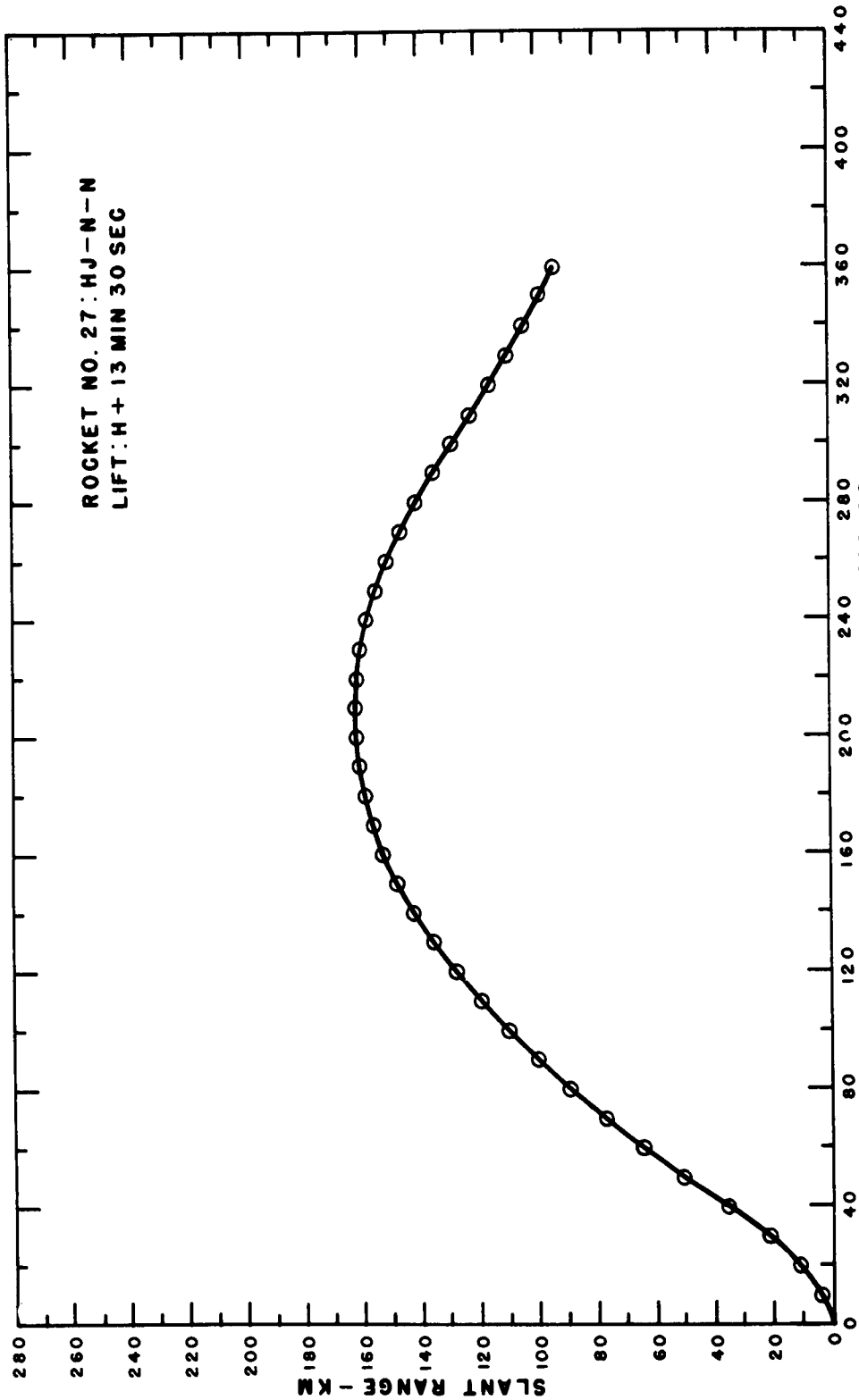

Figure B.52 Slant range versus time for Rocket 27, King Fish.

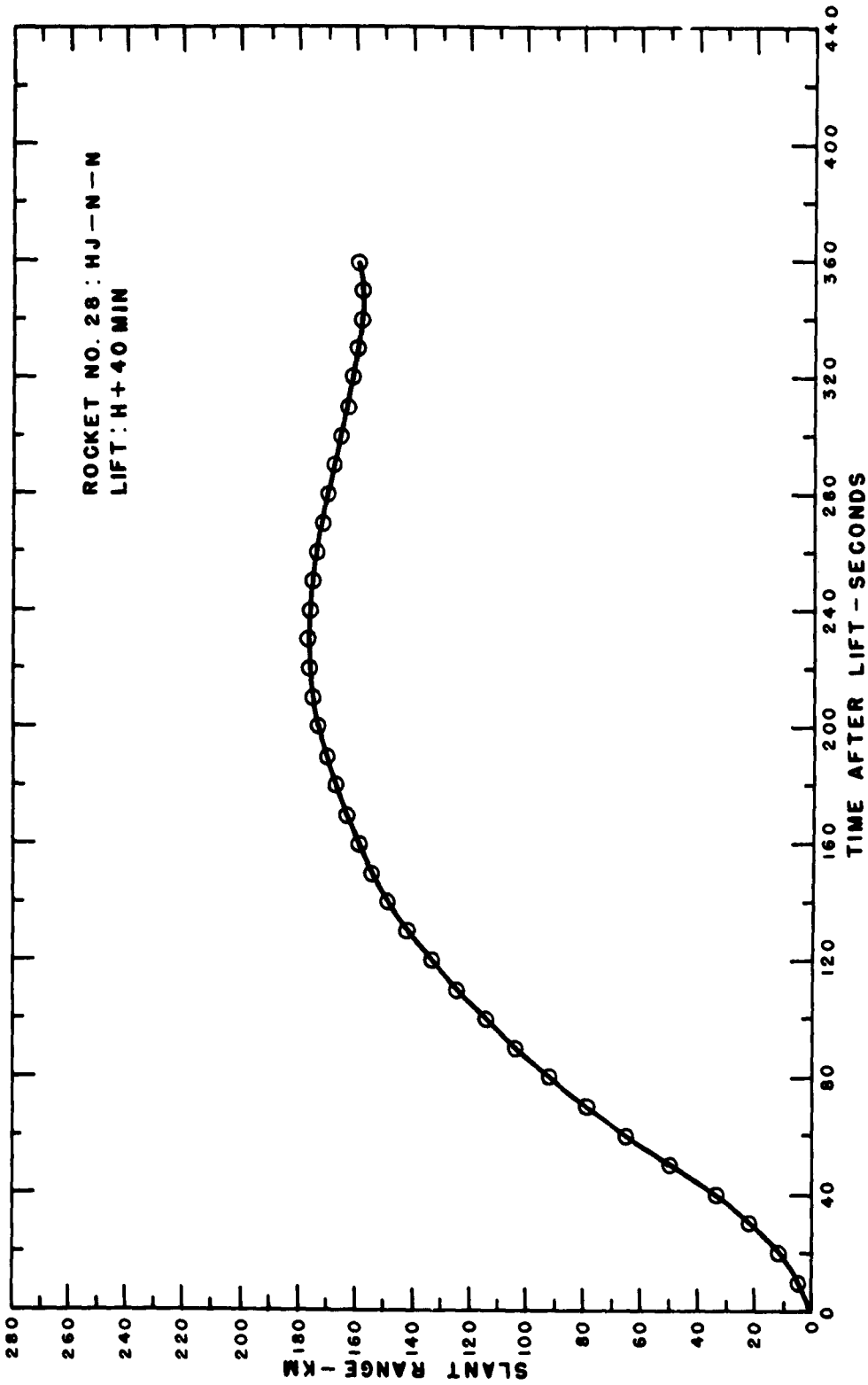

Figure B.53 Slant range versus time for Rocket 28, King Fish.

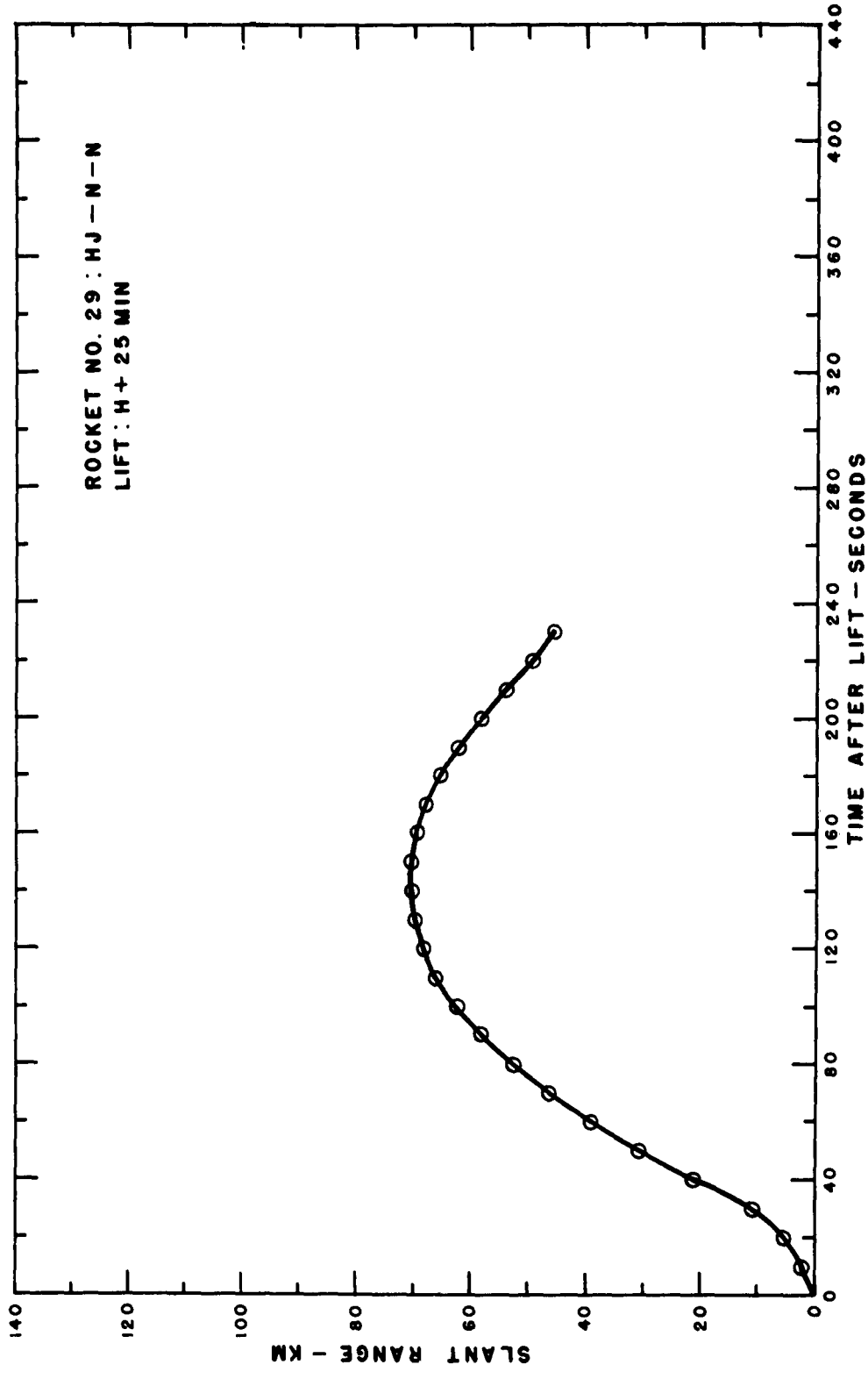

Figure B.54 Slant range versus time for Rocket 29, King Fish.

APPENDIX C

PROPAGATION EXPERIMENT: INSTRUMENTATION AND PERFORMANCE

C.1 GROUND INSTRUMENTATION AND PERFORMANCE

C.1.1 Three-Frequency Experiment Ground Instrumentation.

The ground receiving antennas for reception of signals at 37, 148, and 888 Mc are shown in Figures C.1, C.2, and C.3, respectively. The performance of these antennas was satisfactory regarding their basic physical and electrical properties; however, because of their fixed beam orientation, they were often receiving signals considerably off from their main lobe axis, with attendant reduction in gain and highly elliptical polarization. There is also a possibility that their beam patterns were significantly distorted because of their close proximity to each other and to adjacent reflecting objects such as metal masts, trailers, and overhead power lines and transformers. Since the three-frequency experiment is basically a differential measurement of the carrier frequency signal phase, any differential distortion of the radiation phase patterns of the ground antennas as a function of angle to reception can introduce errors. The characteristics of

the ground antennas are summarized in Table C.1

The helix lengths were shortened for Blue Gill and King Fish events. This was done to broaden the antenna pattern for improved reception off axis of the helix in the event that the rocket flight direction differed appreciably from predicted, as was the case for Star Fish. An additional set of 148-Mc helixes was installed for Blue Gill and King Fish to cover the large differences in launch angles of the rockets carrying the three-frequency experiment. The proper antennas were connected to the receivers by means of remotely controlled coaxial relays. The 888-Mc antennas were put on mounts remotely controlled in azimuth and elevation for proper orientation to cover the different rocket flight directions.

The ground antennas were designed and tested by BRL and built by the General Development Corporation, Elkton, Maryland.

Preamplifiers were placed at each antenna to provide sufficient gain to overcome the loss in the long feed cables to the receivers and give maximum

signal-to-noise performance. The 37- and 148-Mc preamplifiers, designed and built at BRL (Reference 69), had 40-db gain and a 3 to 4 noise figure. The 888-Mc preamplifiers, supplied by the Applied Research Corporation, had 30-db gain and a 7- to 8-db noise figure.

The receivers were of the triple conversion superheterodyne type with the original design providing for all of the local oscillator signals to be derived from one frequency standard, to provide phase-coherent doppler data at the three frequencies. However, the synthesizer which provided the nine harmonically related frequencies was found to have excessive phase jitter on the highest local oscillator frequency for the 148- and 888-Mc receivers. A last-minute change in the design was made at Johnston Island using separate local oscillator frequency sources which cured the phase jitter problem but left the 37- and 148-Mc doppler outputs noncoherent, i.e., the dispersive doppler data had to be corrected for local oscillator frequency drift. The receivers were used in this manner for Star Fish—for later events additional

design changes were made which cured the phase jitter problem and restored the phase-coherent doppler outputs. Considerable difficulty was experienced with birdies (spurious signals) in the 888-Mc receiver output, which was serious because of the possibility of locking the tracking filter on to a false signal. The trouble was minimized by separation of common power supplies from local oscillator signal sources. The commercial 888-Mc receivers were very unstable, requiring frequent adjustment of the input RF stages and the automatic gain control (AGC) dc amplifier stages.

Electronic, phase-locked tracking filters (Reference 30) were used at the last intermediate frequency (IF) output of each receiver channel. These frequencies were 4, 16, and 96 kc at 37, 148, and 888 Mc, respectively. These were very narrow bandpass filters whose center frequency tracked the input frequency. This was accomplished automatically by the use of a phase-locked, servo-controlled circuit. A large signal-to-noise improvement in the output as compared to the input was obtained. Bandwidths of 25, 50, and 100 cps

were used at 37, 148, and 888 Mc, respectively, during the burning phases of the rockets. Reduced bandwidths were used thereafter for maximum signal-to-noise improvement. Another feature of the tracking filters was their constant-amplitude output which was necessary for the doppler adding and differential mixing circuits. The filter enabled tracking of signals which were less than the noise at the receiver output. The tracking filters were models IV and VIII, Interstate Engineering Corporation, Anahiem, California, and Model 207, Electrac Corporation, Anahiem, California.

The outputs of the tracking filters on the 37-, 148-, and 888-Mc channels were the respective biased doppler frequencies. In order to remove rocket spin and faraday effects, the biased doppler from 37-Mc right- and left-hand circularly polarized channels were added and doubled, giving 8 kc plus twice the 37-Mc doppler frequency. Similarly, the biased doppler from the 148-Mc oppositely polarized channels was divided by four, added, then divided by two, giving 8 kc plus one-half the 148-Mc doppler frequency. The 37- and 148-Mc added outputs

were combined in a differential mixer giving the desired dispersive doppler data, i.e., one-half the doppler at 148 Mc minus 2 times the doppler at 37 Mc.

A similar mixing process was used between the 148- and 888-Mc received signals giving the desired dispersive doppler data.

Faraday rotation data was obtained by the procedure outlined below.

If the right hand (RH) and left hand (LH) 37-Mc tracking filter outputs are differenced, the resulting electrical signal contains information given by the expression;

$$(f_f+f_d+f_s) - (f_d- f_f- f_s) = 2(f_f+ f_s)_{37} \qquad (C.1)$$

where, f_f is the faraday rotation frequency, f_d is true doppler frequency, and f_s is the rocket spin frequency. In a similar fashion, differencing RH and LH 148-Mc tracking filter outputs gives

$$2(f_f+f_s)_{148} \qquad (C.2)$$

Differencing Equations C.1 and C.2 gives,

$$2(f_f+f_s)_{148} - 2(f_f+f_s)_{37} \qquad (C.3)$$

However, $(f_s)_{148} = (f_s)_{37}$ (spin effect is independent of frequency), so that the expression may be rewritten,

$$(f_f)_{148} - (f_f)_{37}$$

It follows then, the differencing operation represented by the expression C.3 furnishes the difference in faraday rotation rates at 148 and 37 Mc. A similar mixing process was used to obtain the difference in faraday rotation between 888 and 148 Mc. A block diagram of the complete mixing system is shown in Figure 5.7.

The complete data-handling system was conceived, designed, and built at BRL.

A combination of paper chart and magnetic tape recorders was used for data recording. Receiver AGC, spin, faraday, and dispersive doppler data were recorded on two 8-channel Brush recorders, one in each receiver trailer. Four

Ampex FR 114 tape recorders were used, employing 2000-foot reels of tape run at 60 inches per second to record the biased dippler frequencies which were as high as 110 kc on the 888-Mc channel.

The received signal strengths were recorded for the following frequencies: 36.44, 36.94, 145.76, 147.76, 874.56, and 886.56 Mc. Paper chart recorders were used to record the AGC voltages from the receivers and tracking filters. Chart deflection was calibrated against input signal to the receiver preamplifier in decibels below 1 milliwatt (dbm). The calibration signal was fed out to the preamplifier in the antenna field through a coaxial cable whose attenuation was measured and accounted for in calibrating the chart recorder. A remotely controlled coaxial relay was used to disconnect the antenna and connect the calibrate cable to the preamplifier input. The remotely controlled relay permitted quick checks of the calibration just prior to and following the rocket flights, to minimize errors due to

receiver drift. Calibration signals were obtained from an HP 608D signal generator for the 37- and 147-Mc signals, and from a special crystal-controlled generator for 888 Mc.

The basic source of standard frequencies was a radio-frequency oscillator, Borg Corporation Type 0-471 (XN-1)/U, which produced frequencies of 100 kc, 1 Mc, and 5 Mc with an accuracy of 2 parts in 10^8. Since frequencies other than the basic 100 kc from the Borg standard were required in various parts of the instrumentation system, both divider and multiplier circuits were used to cover the necessary range.

The Electronic Engineering Company's time code generator, Model ZA-1935, produced outputs of 10 kc and 1 cps CW or pulsed, as well as 1 pulse/minute and 1 pulse/10 minutes, all derived from the 100 kc of the Borg standard. In addition, the unit generated a time code suitable for recording on magnetic tape and displayed this time code on decimal indicators of hours, minutes, and seconds. These were set to correspond with

Universal Time received from WWVH.

There are two major functions performed by the station timing system: (1) synchronized control of data recording equipment, and (2) indication of time on the recorded outputs. Pulse shapers and inverters produced the desired polarity, duration, and amplitude of signals for the timing applications.

An analysis of the 888-Mc channel performance disclosed several factors that caused the noisy signals and short records. The 888-Mc channel was originally designed for a 500-mw transmitter, but the contractor could not meet the 500-mw output specification in the time allotted, and instead delivered transmitters which gave between 80- and 150-mw output, thereby introducing a 7-db reduction in the system margin. The wide divergence of rocket flight trajectories from those predicted caused off-beam reception in

the 888-Mc ground helixes which introduced another 3- to 6-db reduction in signal. The local oscillator injection signal for the 888-Mc receiver had phase jitter that caused a 4- to 6-db reduction in receiver sensitivity. The 888-Mc rocket antennas had radiation patterns which were quite deeply lobed because of the large dimensions of the rocket compared with the transmitted wavelength and the interfering effects of the many other protruding antennas nearby. The total effect of all of these factors added up to between 20 and 30 db of additional loss when they occurred simultaneously, which would account for the noisy signals and short records observed in many instances.

C.1.2 Satellite Experiment Ground Instrumentation. The transmissions received on the ground were the 54- and 324-Mc harmonically related CW signals from

the Transit 4A and 4B satellites. Three independent tracking channels were used, two on 54 Mc and one on 324 Mc (Figure 5.8).

On both 54-Mc receiving channels, the antennas used were standard dipoles with half-wavelength elements placed horizontally, one-half wavelength above the ground plane. One of the dipoles was stationary throughout a satellite pass. The second dipole was mounted on a pedestal which was motor driven to rotate in azimuth at about 30 rpm during the pass, this rate being large compared to the predicted magnitude of the faraday rotation rate (Figure C.4). The tracking channel associated with the 54-Mc rotating dipole was used primarily to obtain faraday rotation data. The antenna rotation allowed determination of the direction of faraday rotation and enabled more faraday phase and rate fixes than were obtainable with a non-rotating dipole.

Each time the direction of the incoming linearly polarized signal (or major axis of an elliptically polarized signal) became perpendicular to the length of the dipole, there was a minimum in signal strength concurrent with a sudden 180° phase shift.

The antenna pedestal was equipped with a rotary joint to feed the RF signal from the antenna to the preamplifier. In addition, a contact switch on the pedestal closed a few milliseconds for each revolution of the antenna and provided a marker pulse for determination of the antenna orientation and rotation rate.

It had been anticipated that the rotating joint feeding the signal from the rotating dipole to the base might introduce an intolerable amount of noise into the signal. However, it was found that noise introduced had a negligible effect on the remainder of the system. In many cases, the rotating dipole data channel was able to track the satellite over longer periods of time than the fixed dipole channel.

The antenna used for receiving the 324-Mc signal was a right-hand, 8-turn helix (Figure C.5). The first antennas tried were 324-Mc dipoles, but these were unsatisfactory because the satellite

radiated such a small amount of power at this frequency that an antenna with some gain was required. Because of the rotation direction of the component of circular polarization of the radiated signal at the satellite, a right-hand-polarized antenna was needed.

Each antenna fed a preamplifier unit situated at the antenna location. These preamplifiers were designed and built at BRL. They had an overall gain of 40 db, a noise figure of 4 db, and a passband of 2 Mc. They exhibited excellent stability and reliability under field conditions over long periods of operation.

The output of the preamplifiers was fed through long coaxial cables into the tracking station where it served as the input to the receivers. In the 54-Mc channels, the Nems-Clarke Model 2501 special-purpose receivers were used directly. These were designed for the reception of AM and CW signals, tunable over a range of 55 to 260 Mc, and had a noise figure of 6 db maximum at antenna input. They were provided with a 50-ohm antenna input and an additional 50-ohm input to the second RF amplifier, to allow for the injection of a known reference signal for comparison with the received signal.

In the 324-Mc channel, it was necessary to extend the operating range of the Model 2501 receiver. This was accomplished by the addition of a range extender unit, Nems-Clarke Model REU-300B. This unit was designed to operate in a 50-ohm system, had a noise figure of 14 db, and was tunable from 250 to 900 Mc.

A frequency synthesizer manufactured by Rodhe and Schwarz provided the required RF injection frequency into the receiver for the reception of doppler information. The unit produced a continually adjustable frequency over the range of 30 cps to 30 Mc from an internal or external 100-kc source. Besides the adjustable frequency, other outputs provided were 10-kc and 1-kc CW, and 10-kc and 1-kc pulses. During tracking operations, the output frequency remained constant to within $\pm$ 1 cps over a 20-minute period of time.

A frequency multiplier was used in conjunction with the synthesizer for frequencies above 30 Mc. In the case of the 54- and 324-Mc Transit frequencies, the frequency multiplier used the 27-Mc

output of the synthesizer as input to two channels. The first channel simply doubled the frequency to 54 Mc, while the second channel doubled, then tripled, and again doubled the frequency to produce 324 Mc.

The basic function of the tracking filter used (Reference 70) was to provide the detection of doppler signals much weaker than the noise at the output of the receiver. A signal-to-noise improvement between 20 and 30 db was obtained by use of an extremely narrow filter bandwidth relative to the input signal bandwidth.

The outputs of the tracking filters on the 54-Mc and 324-Mc channels were audio-frequencies, and corresponded to the biased doppler frequencies. The 54-Mc doppler was multiplied by six and subtracted from the 324-Mc doppler to obtain the dispersive doppler. The equipment for doing this was the multiplier-mixer unit (References 13 and 14) designed and constructed at the BRL.

The total doppler change during a pass of the Transit satellite was about 2 kc on the 54-Mc carrier and 12 kc on 324-Mc carrier. To accommodate

the same type of tracking filter in each channel, the frequency of the local oscillator was set to provide an output frequency bias on the 54-Mc channel of 2.5 kc at the time when the true doppler frequency was zero. The bias frequency on the 324-Mc channel was then 15 kc. Therefore, during the actual tracking operation, the doppler effect caused the output frequency to vary between 1.5 kc and 3.5 kc on the 54-Mc channel and between 9 kc and 21 kc on the 324-Mc channel. Consequently, the two biased doppler frequencies varied by amounts exceeding one octave, so that conventional frequency multipliers could be used in this application.

The cross polarization nulls due to faraday rotation of the 54-Mc signal received by the rotating dipole antenna were superimposed on the cross polarization nulls due to the antenna rotation. The faraday fading frequency varied from a maximum of about 0.3 cps when the satellite was south of Johnston Island to zero when the satellite was north of the Island. The antenna rotation frequency was about 0.5 cps, giving an antenna fading

rate of 1 cps. Hence, the faraday frequency acted as a small frequency modulation on the antenna rotation carrier. Therefore, the frequency of the resultant signal, as it appeared at the correlation output of the tracking filter, varied between the limits of 0.7 cps to 1.3 cps. During periods of very low signal level, there was also present at the correlation output varying amourts of noise due to phase jitter which was not related to faraday rotation. Since this noise was usually of a frequency high compared with 1 cps, a very low pass filter of 2-cps cutoff was introduced to eliminate it. Using conventional construction, this filter would have been too large to be practical. Therefore, a filter was designed to employ electronic multiplication of reactances, resulting in very satisfactory elimination of the noise. The resultant signal, as it was used with automatic digitization equipment, introduced considerably fewer spurious pulses than did a nonfiltered signal

The information recorded may be summarized as follows: (1) doppler frequency on three data channels, (2) AGC voltage on three data channels,

(3) dispersive doppler, (4) one-pulse-per-second timing, (5) WWVH time, (6) local oscillator frequency, and (7) low pass filtered correlation.

The biased doppler frequency on one 54-Mc data channel and the 324-Mc data channels was also recorded on analog charts of frequency versus time. To accomplish this, the output of the tracking filter was put into a frequency integrator. The dc output of the integrator, being proportional to the input frequency, was recorded on a Varian Associates paper strip chart recorder to give the desired data.

The dispersive doppler frequency was recorded on a paper strip chart recorder along with the timing pulses, the AGC voltages, low pass filtered correlation, and timing pulses. A Brush Instruments Company 8-channel strip chart recorder was used.

It was important to have available on magnetic tape the signals obtained by each receiving channel during the satellite passes. This record served as a backup in case of equipment failure in the system and could be used to recover the original data at a later time. Also, the data on the magnetic tape was later used as input to automatic digitizing

equipment in order to obtain the dispersive doppler and faraday rotation throughout the pass. A magnetic tape recorder, Ampex Model FR-114, was used at the receiving station and at the data-handling station to record and play back the received signals.

After a few satellite passes had been made, it became evident that good signals could be obtained on the large majority of passes which were within ± 600 miles of the Johnston Island site. Because part of the tracking equipment was also used for another experiment, it was decided to confine the satellite tracking operations to only those passes that were within the above range. Improved signal on the 324-Mc channel could have been obtained when the satellite was close to the horizon if the antenna could have been operated in a tracking mode. This was confirmed by using an existing high-gain tracking antenna of the Cubic Corporation facility on some selected passes.

The stability of the internal oscillator in the circuit for extending the frequency range of the commercial receiver used at 324 Mc was not

completely satisfactory. A long warm-up time was necessary to insure adequate signal reception. Installation of a crystal-controlled local oscillator would eliminate this difficulty on any future operations.

In Tables C.2 through C.13 are summarized the kinds of recordings made in the BRL trailers for both the rocket and satellite propagation experiments.

C.1.3 GMD Telemetry and Tracking Ground Instrumentation. The purpose of using the GMD radiosonde ground set was twofold: (1) the GMD served as a backup telemetry system, (2) the GMD served as a backup angular tracking system. In the nose cones employed on Nike-Cajun rockets, there was insufficient space for the Cubic Corporation (AME/DME) tracking beacon, and the GMD beacon furnished the only source of tracking information for these vehicles.

The GMD set, originally designed to track a balloon-borne radiosonde transmitter in the 1660- to 1700-Mc frequency range, was modified for rocket tracking. A pictorial view of the tracker is shown in Figure C.6. Figure C.7 shows

the components of the GMD tracking and telemetry system. Three GMD sets were used, identified as sets A, B, and C. The physical location of the three GMD antennas relative to the control blockhouse (Building 200) and the telemetry vans is shown in Figure C.8. The control and recording instruments inside of the GMD van are shown in Figure C.9. Firing of the rockets automatically initiated a one-second-interval recording of azimuth and elevation data.

Modifications made to the GMD system were: (1) a series resistor and output shunt capacitor were attached to the receiver AGC in order to record received signal strength, (2) the control recorders were modified to accept a 1/sec printing rate, (3) an automatic start relay system was built into each recorder in order that the printer would start as each rocket lifted, (4) tunnel diode RF preamplifiers were used on Rockets 11 through 29, inclusive, with the exception of Rockets 13 and 17. The preamplifiers increased the signal-to-noise ratio of the GMD recievers by a factor of 10 db.

Signal strength recordings were made on Brush type Mark II records. Each receiver AGC was calibrated from -20 to -110 dbm in 2-db steps. Response time tests of the receiver-recorder combination were also made. A signal decrease of 100 db deflected the recorder pen from full scale to zero in 90 msec; an increase of 100 db deflected the pen from zero to full scale in 10 msec.

In order to calibrate the tracking mode of the system, a position and angle survey was made for each GMD set. The position of each set was surveyed with respect to the Johnston Island grid system. The reference used for angle measures was the line from Point Joe to Point John which had a true bearing of 65 degrees, 13 minutes, 19 seconds. In the Johnston Island grid system, the position of each set was as follows: (1) A set, North (N) 199, 670, East (2) 199, 705; (2) B set, N 199, 714, E 199,682; (3) C set, N 199, 660, E 199, 516. The accuracy of the survey was $\pm$1.0 foot.

Azimuth angles of each set were referenced to true north; in order to determine these angles accurately, a reference 1670-Mc beacon was placed

on the northeast corner of the balcony on the airport control tower. The true azimuth angles for each tracker were measured by placing a transit over the reference beacon and measuring the angle between the star Polaris and each GMD set. These measured angles were corrected for a bearing of true north. The elevation angle between the tracker and the reference beacon was also measured with a transit. The accuracy of the measurements was ± one minute of arc. Prior to each series of rocket flights, the sets were locked on the reference beacon signal, and the measured angles were set on the dials of the tracker and control recorder.

In Tables C.14 through C.40 are summarized the GMD telemeter-tracking operations for each rocket of Projects 6.2, 6.3, and 6.4 carrying the GMD beacon. Figures C.10 through C.34 present the GMD azimuth and elevation tracking data.

C.2 ROCKET INSTRUMENTATION AND PERFORMANCE

C.2.1 Three-Frequency Experiment Rocket Instrumentation.

The rocket-borne instrumentation for the three-frequency experiment consisted of a transmitting

beacon and associated antennas. A block diagram of the beacon is shown in Figure 5.1, and a photograph in Figure 5.2. The beacon was 5.5 inches in diameter by 5 inches long and weighed 7.7 pounds. The fundamental frequency of 37 Mc was generated by a transistorized, crystal-controlled oscillator. The output of the crystal oscillator was amplified by a transistor amplifier to provide two outputs at 37 Mc. One output was connected to the antenna and provided a signal power of 150 mw. The other output signal was fed to a 4-times frequency multiplier consisting of two cascaded transistor doublers. The 148-Mc output from the multiplier was amplified by a transistor amplifier to a power level of two watts. One hundred fifty mw of this power was diverted to the antenna, and the remainder was fed to a 6-times frequency multiplier. The multiplier consisted of a cascaded varactor doubler and tripler giving an output at 888 Mc of 150 mw.

The closely controlled temperature for the crystal oscillator was obtained by using the heat-

of-fusion principle (Reference 70). The crystal was submerged in eutectic alloy, Cerrolow 117, which was partially melted prior to rocket lift-off. The alloy had a melting point of 47°C, which, by the heat-of-fusion principle, provided a constant temperature until all of the alloy was melted. A carefully predetermined amount of alloy was melted prior to launch by an externally controlled heating element to bring the mixture up to a constant temperature and to take care of any heat loss in the early part of the flight. During the preflight thermal preparation, a careful balance was maintained between the amount of solid and melted alloy to insure that at take-off sufficient alloy was melted to furnish heat lost during the first minute of flight, while leaving sufficient reserve of solid material for absorbing heat in the remainder of the flight.

The three-frequency beacon was powered by mercury batteries with voltages of 4, 16, and 60 volts. The 4-volt battery powered the oscillator and had sufficient capacity to operate

it for 500 hours. The oscillator was turned on well in advance of firing to insure stable operation. The 16- and 60-volt batteries could power the beacon for 1 hour.

A Ledex stepping relay was used for turning the beacon on and off remotely. Monitor detectors were used on the 37- and 888-Mc outputs, giving 4 volts at normal output. The dc voltage from these detectors was telemetered via the payload telemetering system. The inside temperature of the beacon can was also telemetered. Only Rockets 11, 12, 14, 17, and 22 showed appreciable changes in any of the telemetered monitors; comments on these changes are given in Tables C.41 through C.58.

Remote indicators in the blockhouse were available for monitoring beacon temperature, oscillator temperature, Ledex relay position, oscillator heater voltage, and battery voltages. A diagram of the beacon control system located at the blockhouse is shown in Figure C.35.

The 37- and 148-Mc portion of the beacon was originally designed at the University of Michigan

under a previous contract with the BRL. Modifications, improvements, fabrication, and testing of the beacons were done by the BRL. The 888-Mc portion of the beacon was designed and built by the Applied Research Corporation, Port Washington, New York, under contract with the BRL.

Preflight tests of the beacons indicated two problem areas: (1) low output power or complete malfunctioning of the 6-times frequency multiplier unit, and (2) malfunctioning of 37-Mc transmitting transistor. The short time available for design and production of the frequency multiplier units forced the selection of a type of circuitry easily produced in quantity; however, the units had poor operating efficiency, low output power, and critical tuning adjustments. These difficulties were somewhat alleviated for the Blue Gill and King Fish firings for which additional frequency multipliers were made, utilizing an improved type of circuitry having a higher output power.

Frequency drifts of 10 to 20 cps during flight were observed in some beacon oscillators,

because crystals were not available with turning points (df/dt = 0) at the melting point of the alloy (47°C). Most of the crystals had turning points between 50° and 60°C. Operation at 47°C in these cases placed the operating point on the steep negative slope of the crystal frequency versus temperature coefficient (10 cps per degree centigrade). The alloy method was very simple and reliable, but securing large quantities of crystals with turning points coincident with the alloy melting point was very expensive.

Sudden, permanent shifts of beacon crystal frequency of 20 to 30 cps were caused by acceleration during rocket burning and after burnout. Most of the frequency shifts occurred at burnout of the second Nike booster (approximately 60 g). The frequency variations, however, did not interfere with the primary purpose of the three-frequency beacon (i.e., electron density measurements) but did interfere with its secondary function of doppler ranging.

Tables C.41 through C.58 present comments on the 37-, 148-, and 888-Mc doppler and signal AGC,

and on the high and low-frequency dispersive doppler. Also given is the quality of the beacon performance, which was monitored in the beacon and telemetered on Channel 12 of the telemeter system (10.5 kc). These telemetered data were: (1) the RF voltage at the 37-Mc output stage, (2) 888-Mc RF voltage at the output of the 6-times frequency multiplier, and (3) temperature of the beacon package. In five rockets where the 37-Mc output power was initially low, the output power at 888 Mc was normal. This was possible because the input signal to the frequency multiplier was taken off ahead of the 37-Mc output stage.

Rocket antenna systems were designed to fit the 9-inch-base-diameter Honest John-Nike payload housing and the 18-inch-base-diameter Javelin (more properly, Argo D-4) and Honest John-Nike-Nike payload housings. One system used loop antennas at 37 and 148 Mc and swept-back stub antennas at 888 Mc. The other system used shroud antennas (Reference 71) at 37 and 148 Mc and stub antennas at 888 Mc. A fiberglas nose cone was

used over the antennas with each system. The location and types of all rocket antennas used on Projects 6.2, 6.3, and 6.4 are shown in Figures 5.3 and 5.4. These figures show the location of the three-frequency experiment antennas relative to the other antennas on the rockets.

The Honest John-Nike antenna system for Project 6.3, is shown in the photograph, Figure C.36. Trapezoidal-shaped loops formed of 1-inch-wide copper strip were used at 37 and 148 Mc. They were mounted mutually perpendicular, to minimize mutual coupling and radiation pattern interference. Basically, the trapezoidal loops were balanced loop antennas resonated with a capacitor at the gap and matched to 50 ohms. The 37-Mc loop was tap fed near the base at the 50-ohm point. The design of these loops was based on the theory that a single-turn balanced loop with a circumference of 0.3 wavelength or less has a radiation pattern that is omni-directional in the plane of the loop; also, its pattern is independent of the physical shape of

the loop. The pattern is negligibly affected by the presence of a large, long rocket body if the diameter of the rocket is less than one-half wavelength. Radiation patterns of the 37-Mc loop on the Honest John-Nike rocket on Project 6.3 are shown in Figure C.37. The effect on the pattern of the metal rods used with the AFCRL ion trap and impedance probe experiments is also shown in Figure C.37.

The loop used at 148 Mc was fed at the gap through a two-capacitor matching circuit; radiation patterns for the Project 6.3 Honest John-Nike rockets are shown in Figure C.38. The 37-inch metal rods below the 148-Mc loop caused difficulty in obtaining a good radiation pattern off the rocket tail. The rods reflected the signal nose-ward. An acceptable radiation pattern was obtained by aligning the 148-Mc loop parallel to the 10-foot rods and insulating the rods from the rocket body. The 10-foot rods were effectively insulated from each other and the rocket body at 148 Mc by the inductor connected in series with them for matching to the 3- to 12-Mc region for the RF impedance probe experiment.

Two stub antennas, phased 180 degrees, were used at 888 Mc on the Project 6.3 Honest John-Nike rockets. The stubs were mounted diametrically opposite on the metal cylinder housing the three-frequency beacon, and were swept back at an angle of 45 degrees with respect to the missile axis. Figure C.39 shows the radiation pattern of this stub antenna system.

The Javelin and Honest John-Nike-Nike (Project 6.2) antenna system consisted of shroud antennas at 37 and 148 Mc, and stub antennas at 888 Mc (Figure C.40). A metal nose cone was used inside the fiberglas nose cone to serve as a ground plane for the shroud antennas. The 148-Mc antenna system consisted of two shrouds mounted diametrically opposite on the metal nose cone. The shrouds were electrically phased 180 degrees with respect to each other; the radiation pattern is shown in Figure C.41. For the 37-Mc antenna, a single shroud was used, providing a nearly omnidirectional pattern in the plane of the shroud (Figure C.42). Stub antennas were used at 888 Mc, mounted diametrically opposite on the lower portion of the

metal cone (Figure C.40). These stubs were electrically phased 180 degrees with respect to each other; radiation patterns are shown in Figure C.43.

The rockets for Javelin Project 6.4 used the same antennas as described above except that the antennas were mounted at different places on the rocket. Figures C.44 and C.45 show the locations of these antennas. The radiation patterns of the shroud antennas at the new locations remained approximately the same as before. The stub antennas were moved to the upper portion of the metal nose cone, but patterns are not available for this location. The 888-Mc stub antennas were redesigned for the King Fish event to improve the mechanical mounting. The redesigned stub is shown in Figure C.46.

The 37- and 148-Mc loop antennas were designed and built by the BRL. The 37- and 148-Mc shroud antennas were designed at the BRL and built by the General Development Corporation, Elkton, Maryland. The 888-Mc antennas used on the Star Fish and Blue Gill events were designed and built by the Marquardt Corporation, Pomona, California;

those used on King Fish were designed and built by the BRL. All antennas were tested and installed by the BRL.

C.2.2 GMD Rocket Instrumentation. The GMD beacon consisted of a cylindrical container 4 inches long by 4 inches in diameter, with an approximate weight of four pounds. The beacon was packaged in a design compatible with the three vehicle configurations discussed in Section C.2.1. The unit consisted of a modulator amplifier, a transmitter using a 7533 cavity oscillator tube, a silver-zinc 6-volt battery, a power change-over Ledex switch, and a dc-to-dc converter with Zener-regulated voltage output. A circuit diagram of the beacon is shown in Figure C.47. The CW transmitter was capable of being frequency modulated by a composite signal in the standard IRIG subcarrier band. The composite of eight FM modulated data signals was used to FM modulate the transmitter. The RF power output was 1 watt. Three frequencies, 1660, 1670, and 1680 Mc, were used to avoid interference when three rockets were in flight simultaneously.

The beacon unit was capable of power change-over from external to internal source by means of a 28-volt pulse to a control circuit. Provision was made for battery checking and for charging through the external connector. The beacons were designed and built by the Marquardt Corporation, Pomona, California.

The GMD beacon antenna system consisted of three or four slot antennas and a matching and phasing network. Three slots were used on the 6- and 9-inch-diameter nose cones, and four slots were used on the 18-inch-diameter nose cones. The antenna assembly was matched to the transmitter with a VSWR of 1 to 1.5 or better. The antennas were designed and built by the Marquardt Corporation, Pomona, California. A typical slot antenna is shown in Figure C.48, and antenna locations for the different rocket nose cones used in Projects 6.2, 6.3, and 6.4 are shown in Figures 5.3 and 5.4. Antenna radiation patterns are shown in Figures C.49 and C.50.

C.3 ROCKET DISPERSIVE DOPPLER

C.3.1 Star Fish Event. For the rockets launched in the Star Fish event, lack of coherency in the ground-generated receiver injection frequencies produced an unknown bias frequency on the 37- and 148-Mc dispersive doppler data. The expressions "37- and 148-Mc dispersive doppler" and "148- and 888-Mc dispersive doppler" designate the dispersive doppler obtained by combining the frequencies indicated. Unfortunately, the bias frequency was not only unknown but changed as a result of slight drifts in the ground-based local oscillator during the course of a rocket flight. The bias frequency was present on the paper analog chart recordings of dispersive doppler from the time the rocket beacons were turned on (usually one minute before rocket lift) until signal was no longer being received. Since the rockets did not enter regions of ionization for 1 to 2 minutes after rocket lift, 2 to 3 minutes of bias were available for study and analysis of frequency and frequency drift. In an attempt to

define and eliminate the bias, a least squares approximation (usually a straight line) of the bias frequencies was made with the constraint that the integral under the least squares curve was equal to the numerically integrated bias frequencies measured. The least squares curve was then extrapolated for the remainder of the rocket flight. Deviations from the extrapolated curve were then taken as true dispersive doppler data. Consequently, no great degree of accuracy can be claimed for the dispersive doppler data thus obtained, but later comparisons with data from other sources indicated strongly that the dispersive doppler results can be accepted with a fair level of confidence.

Plots of the integrated dispersive doppler and dispersive doppler frequencies for the Star Fish event are shown in Figures C.51 through C.56. Comments on the data for the individual rockets are in the following paragraphs.

The 37- and 148-Mc dispersive doppler data for Rocket 1 (Figure C.51) was obtained from magnetic tape recordings of the doppler signals by appropriately multiplying and differencing digitally the

data in a computer. The rocket entered regions of ionization at 163 seconds after rocket lift, and continuous dispersive doppler data was obtained until 600 seconds after rocket lift, at which time the 37-Mc signal was lost and not recovered for the remainder of the flight. The absolute accuracy of the integrated dispersive doppler may be subject to question because of the long time interval over which the extrapolated least squares bias curve was employed, but it is felt that accuracy within ± 15 percent is maintained at least up through rocket apogee. Because of the poor quality of the 888-Mc doppler, no usable 148- and 888-Mc dispersive doppler was obtained for this rocket.

The 37- and 148-Mc dispersive doppler data for Rocket 4 (Figure C.52) was measured exclusively from the paper analog chart recordings. The rocket entered regions of ionization at 65 seconds after rocket lift, and continuous dispersive doppler data was available until the rocket left the regions of ionization at 222 seconds after rocket lift. Since the dispersive doppler data was complete, the additional constraint that the integrated dispersive

doppler must be zero before the rocket enters and after it leaves ionized regions could be used to define and eliminate the bias. As a result, a reasonably high level of confidence may be placed in the dispersive doppler data. There was no usable 148- and 888-Mc dispersive doppler for this rocket.

The 37- and 148-Mc dispersive doppler measurements for Rocket 5 (Figure C.53) were obtained exclusively from the paper analog chart recordings. The rocket entered regions of ionization at 85 seconds after rocket lift, and dispersive doppler data was available until 230 seconds after rocket lift, at which time the 37-Mc signal became so distorted in phase that measurements were no longer possible. There was no usable 148-Mc and 888-Mc dispersive doppler for this rocket.

The 37- and 148-Mc dispersive doppler measurements for Rocket 7 (Figure C.54) were obtained from the paper analog chart recordings. The rocket entered ionization at 105 seconds after rocket lift, and dispersive doppler data was available until 205 seconds after rocket lift, at which time loss of the 148-Mc signal caused loss of dispersive doppler.

Attempts to recover the 148-Mc doppler from magnetic tape recordings were unsuccessful. Since the least squares bias curve required extrapolation for only 100 seconds, the dispersive doppler data should be reasonably accurate. There was no usable 148- and 888-Mc dispersive doppler for this rocket.

The 37- and 148-Mc dispersive doppler data for Rocket 8 (Figure C.55) was derived from magnetic tape recordings of the doppler signals by appropriately multiplying and differencing digitally the recorded signals in a computer. The rocket entered regions of ionization at 151 seconds after rocket lift, and data was continuous until 245 seconds after rocket lift, at which time the 37-Mc signal became so distorted in phase that further recovery of data was impossible. The dispersive doppler was also measured from the paper analog chart recordings and was in excellent agreement with that from magnetic tape recordings of doppler signals but was of somewhat shorter duration. Measurements of the 148- and 888-Mc dispersive doppler were made, but the data appeared to contain a rocket-spin-induced error which could not be successfully isolated.

The 37- and 148-Mc dispersive doppler for Rocket 9 (Figure C.56) was measured from a combination of paper analog chart recordings and magnetic tape records of the doppler signals. The rocket entered regions of ionization at 121 seconds after rocket lift, and data was continuous until 740 seconds after rocket lift, at which time the 37-Mc signal was lost. The accuracy of the data is subject to question because of the long extrapolation time for the least squares bias curve. Excellent 148- and 888-Mc dispersive doppler was available for this rocket from 121 seconds to 240 seconds after rocket lift. The agreement between the 37- and 148-Mc and the 148- and 888-Mc dispersive doppler was extremely good over this time period, which lends confidence to the bias correction used for the 37- and 148-Mc dispersive doppler.

C.3.2 Blue Gill Event. For the Blue Gill series of rockets, the lack of coherency in the ground-generated receiver injection frequencies was eliminated, so that the problem of a bias on the 37- and 148-Mc dispersive doppler no longer existed. For all except one of the rockets for

this series, the 37-Mc signal was blacked out or heavily attenuated for extended time periods. This was expected, and it was hoped to fill in these periods with 148- and 888-Mc dispersive doppler. However, a combination of spin-induced errors and low 888-Mc signal levels defeated, for all practical purposes, any usage of the 148- and 888-Mc dispersive doppler. Plots of the integrated dispersive doppler and dispersive doppler frequencies for the Blue Gill event are shown in Figures C.57 through C.60. Comments on the data for the individual rockets are in the following paragraphs.

For Rocket 11, the 37-Mc signal blacked out at H-zero which occurred 120 seconds after rocket lift and was not reacquired until 220 seconds after rocket lift. The rocket had encountered no ionization before blackout occurred, and the quality of the doppler data was so poor after reacquisition of the 37-Mc signal that no 37- and 148-Mc dispersive doppler was obtained. The 888-Mc signal suffered so much distortion in phase that the 148- and 888-Mc dispersive doppler could not be measured.

For Rocket 12 (Figure C.57), the 37-Mc signal fell below receiver threshold 81 seconds after rocket lift and was reacquired 163 seconds after rocket lift. The rocket entered regions of ionization 60 seconds after rocket lift and left ionization 196 seconds after rocket lift. Excellent 37- and 148-Mc dispersive doppler was obtained from 60 to 81 seconds and from 163 to 196 seconds. The 148- and 888-Mc dispersive doppler data was good and in excellent agreement with the 37- and 148-Mc data from 60 to 81 seconds, at which time the 148-Mc signal became phase distorted to the extent that measurement of dispersive doppler was impossible.

For Rocket 14 (Figure C.58), the 37-Mc signal fell below receiver threshold 79 seconds after rocket lift and was reacquired 230 seconds after rocket lift. The rocket entered regions of ionization 60 seconds after rocket lift and left ionization at 244 seconds. Excellent 37- and 148-Mc dispersive doppler data was obtained from the paper analog chart recording from 60 to 79 seconds and from 230 to 244 seconds. The paper analog chart recording was not made during rocket flight, and the 888-Mc doppler could not be recovered from magnetic tape,

so there was no 148- and 888-Mc dispersive doppler available for this rocket.

For Rocket 15 (Figure C.59), 37- and 148-Mc dispersive doppler data was measured from the paper analog chart recordings. The rocket entered regions of ionization 54 seconds after rocket lift and left ionization at 312 seconds. The dispersive doppler data was continuous over this entire interval and was of excellent quality except for a 10-second period between 85 and 95 seconds. Since the dispersive doppler frequency was very low during this period, it is felt very little error was made in measurement, and the results should carry a high level of confidence. Because of very distorted data, there was no 148- and 888-Mc dispersive doppler for this rocket.

For Rocket 17 (Figure C.60), the 37- and 148-Mc dispersive doppler was measured from the paper analog chart recordings. The rocket entered regions of ionization 67 seconds after rocket lift, and dispersive doppler data was available until 110 seconds, at which time the 37-Mc signal fell below receiver threshold. The 37-Mc signal was reacquired 200

seconds after rocket lift, but at this time the 148-Mc was so badly distorted that no further dispersive doppler was obtained. Phase distortions on the 888-Mc signal prevented the acquisition of any usable 148- and 888-Mc dispersive doppler.

For Rocket 18, indications are that the level of ionization in the regions traversed by this rocket were so low that no measurable dispersive doppler was produced.

C.3.3 King Fish Event. For the King Fish series of rockets, considerably more complete, reliable data was obtained than for the two events discussed earlier. For Rockets 19 and 25, extensive usable 148- and 888-Mc dispersive doppler was measured after some corrections were made for a rocket-spin function error which appeared on the dispersive doppler channel. Plots of the integrated dispersive doppler and dispersive doppler frequencies for the King Fish event are shown in Figures C.61 through C.67. Comments on the data for individual rockets are in the following paragraphs.

Rocket 19 (Figures C.61 and C.62) was in the air at time of burst, and all three frequencies blacked out at burst time. The 37-Mc signal was out

for about 41 seconds, the 148-Mc signal was out for about 22.5 seconds, and the 888-Mc signal was out for about 2 seconds. The rocket was not in a region of ionization prior to burst time. The 37- and 148-Mc dispersive doppler was excellent in quality after reacquisition of the 37-Mc signal at 161 seconds after rocket lift until the rocket left ionization at 340 seconds. The 148- and 888-Mc dispersive doppler channel for Rocket 19 showed data even prior to the time the rocket entered regions of ionization. After some study, it was discovered that this apparent dispersive doppler frequency was a direct function of the rocket spin rate. Realistic data was obtained from the time the 148-Mc signal recovered at 142.5 seconds after rocket lift until 330 seconds after rocket lift, and a correction was then made to the data based on the rocket spin rate function determined from pre-burst observations. The resulting 148- and 888-Mc dispersive doppler showed excellent agreement with the 37- and 148-Mc dispersive doppler.

For Rocket 22 (Figure C.63), the 37- and 148-Mc dispersive doppler data was measured from the paper analog chart recording. The rocket entered regions

of ionization at 110 seconds after rocket lift, and excellent continuous dispersive doppler data was obtained from that time to 350 seconds after rocket lift. There was no usable 148- and 888-Mc dispersive doppler for this rocket.

Rocket 25 (Figures C.64 and C.65) entered regions of ionization 82 seconds after rocket lift. The 37- and 148-Mc dispersive doppler data was obtained from doppler data digitized from magnetic tape recordings from 82 seconds to 255 seconds after rocket lift, after which time accurate recovery of 37-Mc doppler from magnetic tape was not possible. Even prior to 255 seconds, the 37-Mc doppler was considerably distorted in phase, which could easily result in some errors in the derived dispersive doppler. The confidence level placed on the 37- and 148-Mc dispersive doppler must necessarily be degraded because of the poor quality of the 37-Mc signal. The paper analog chart recording for Rocket 25 yielded 148- and 888-Mc dispersive doppler. As with Rocket 19, the data was biased by a frequency which was a function of the rocket spin rate. The data was corrected for this bias,

and dispersive doppler was thus obtained from 82 seconds after rocket lift to 290 seconds after rocket lift. There is reasonably good agreement between the 37- and 148-Mc and 148- and 888-Mc dispersive doppler, but considerably more confidence should be placed in the 148- and 888-Mc data.

Rocket 27 (Figure C.66) entered regions of ionization at 56 seconds after rocket lift and left ionization at 339 seconds. Good continuous 37- and 148-Mc dispersive doppler data was obtained over this entire interval. The quality of the 148- and 888-Mc dispersive doppler data was questionable, and, in view of complete coverage by 37- and 148-Mc data, no attempts at measuring 148- and 888-Mc dispersive doppler were made.

Rocket 28 (Figure C.67) entered regions of ionization 63 seconds after rocket lift and left ionization approximately 330 seconds after rocket lift. Excellent 37- and 148-Mc dispersive doppler was obtained from 63 to 162 seconds and 295 to 330 seconds except that an uncertainty of one cycle in the integrated dispersive doppler exists over the latter interval. A combination of spin modulation

on the dispersive doppler with intermittent loss of the 148-Mc signal to below-receiver threshold made it impossible to retrieve dispersive doppler data between 162 and 295 seconds. There was no usable 148- and 888-Mc dispersive doppler data for this rocket.

The ionization level in the regions traversed by Rocket 29 was apparently too low to produce any dispersive doppler.

C.4 SIGNAL DURATION AND STRENGTH

C.4.1 Signal Duration Graphs. The duration of received signals from all rocket-borne transmitters used in Projects 6.2, 6.3, and 6.4 are shown in Figures C.68 through C.95. The minimum useful signal level was taken as that level for each system which would provide readable output data.

C.4.2 Signal Strength Graphs. Received signal strength recordings versus time were made of all of the three-frequency beacon experiment signals, the VHF telemetry, and the GMD signals. These analog signal strength recordings were read and the data replotted as a function of slant range between the rocket and the launch site. The signal strength measurements are shown in Figures C.96 through C.254. A predicted value of

signal strength versus slant range has been included to permit interpretation of signal changes from causes other than increasing slant range. The system parameters used to prepare the predicted signal strength versus slant range curve for the Star Fish event are given in Table C.59.

The propagation attenuation at 1 km (item 6, Table C.59) was calculated using the equation;

$$A = 37.8 + 20 \log F + 20 \log D, \qquad (C.4)$$

where, A is the free-space attenuation in db assuming isotropic antennas, F is the frequency in Mc, and D is the distance from transmitter to receiver in miles. The received signal strength in dbm (item 7, Table C.59) was the algebraic sum of items 3, 4, 5 and 6 in Table C.59. To construct the predicted signal strength versus slant range curve, use was made of the relation between attenuation and distance given in Equation C.4 which states that the attenuation increases 20 db for each decade increase in distance. Certain of the telemetry transmitters had 10-watt output; instead of the 2-watt level assumed in Table C.59, which increased the predicted signal levels by 7 db. Also, certain of the rockets used linearly polarized telemetry antennas instead of the circular polarized antennas assumed in Table C.59, which decreased the predicted signal values by 3 db. The

predicted 148- and 888-Mc signal levels for the Blue Gill and King Fish events were reduced 5 db because of the shortened helix antenna length used. Figure C.255 shows the predicted signal levels versus slant range for the three-frequency, VHF TM, and GMD systems used on the Star Fish event. Figure C.256 shows similar information for the Blue Gill and King Fish events.

TABLE C.1 CHARACTERISTICS OF THREE-FREQUENCY GROUND ANTENNAS

Event	Frequency	Antenna	Length	Turns	Beamwidth	Gain Over Linear Isotropic
All	37	Crossed Dipole	Half wave $\lambda/4$ above ground	--	70°	1
Star Fish	148	Helix	11'	8	30°	7
Blue Gill King Fish	148	Helix	7'6"	5.5	45°	4
Star Fish	888	Helix	2'8"	8	30°	7
Blue Gill King Fish	888	Helix	1'4"	4	45°	4

SECRET

TABLE C.2 DESCRIPTION OF MAGNETIC TAPE DATA RECORDED IN BRL VAN 2, STAR FISH EVENT

Tape Unit 1 (Ampex FR 114)				Tape Unit 2 (Ampex FR 114)			
Channel	Data (Beacon)		Recorder Amplifier	Channel	Data (Beacon)		Recorder Amplifier
1	Receiver Out	36.94 L[a]	DC	1	Track. Filter Out	36.94 L	DC
2	Receiver Out	36.94 R[a]	DC	2	Track. Filter Out	36.94 R	DC
3	Receiver Out	147.76 L	DC	3	Track. Filter Out	147.76 L	DC
4	Receiver Out	147.76 R	DC	4	Track. Filter Out	147.76 R	DC
5	Receiver Out	886.56 L	DC	5	Track. Filter Out	886.56 L	DC
6	Receiver Out	886.56 R	DC	6	Track. Filter Out	886.56 R	DC
7	ΔFaraday 36.94 and	147.76[b]	FM	7	ΔDoppler 36.94 and	147.76[c]	FM
8	ΔFaraday 147.76 and	886.56	FM	8	ΔDoppler 147.76 and	886.56	FM
9	Doppler	36.94	DC	9	Spin and Faraday	36.94	FM
10	Doppler	147.76	DC	10	Spin and Faraday	147.76	FM
11	Doppler	886.56	DC	11	Spin and Faraday	886.56	FM
12	10 KC		DC	12	10 KC		
13	1 pps/voice		DC	13	1 pps/voice		
14	WWVH		DC	14	WWVH		

[a] L denotes left-hand polarization; R denotes right-hand.

[b] ΔFaraday denotes difference in faraday rotation between indicated frequencies.

[c] ΔDoppler denotes dispersive doppler for the indicated frequencies.

TABLE C.2 CONTINUED

Tape Unit 1 (Ampex FR 114)

Channel	Date (Satellite)	Recorder Amplifier
1	Receiver Out, 54 Mc (rotating)	DC
2	Receiver Out, 54 Mc (fixed)	DC
3	Receiver Out, 324 Mc	DC
4	Track. Filter Out, 54 Mc (rotating)	DC
5	Track. Filter Out, 54 Mc (fixed)	DC
6	Track. Filter Out, 324 Mc	DC
7	Filtered correlation out, 54 Mc (rotating)	FM
8	ΔDoppler, 54 and 324 Mc	FM
9	Antenna marker out, 54 Mc (rotating)	DC
10	--	--
11	--	--
12	10 KC	DC
13	1 pps/voice	DC
14	WWVH	DC

SECRET

TABLE C.3 DESCRIPTION OF MAGNETIC TAPE DATA RECORDED IN BRL VAN 3, STAR FISH EVENT

Tape Unit 1 (Ampex FR 114)				Tape Unit 2 (Ampex FR 114)			
Channel	Data (Beacon)		Recorder Amplifier	Channel	Data (Beacon)		Recorder Amplifier
1	Receiver Out	36.44 L[a]	DC	1	Receiver AGC	36.44 L	FM
2	Receiver Out	36.44 R[a]	DC	2	Receiver AGC	36.44 R	FM
3	Receiver Out	145.76 L	DC	3	Receiver AGC	145.76 L	FM
4	Receiver Out	145.76 R	DC	4	Receiver AGC	145.76 R	FM
5	Receiver Out	874.56 L	DC	5	Receiver AGC	874.56 L	FM
6	Receiver Out	874.56 R	DC	6	Receiver AGC	874.56 R	FM
7	Track. Filter Out	36.44	DC	7	--		--
8	Track. Filter Out	145.76	DC	8	--		--
9	Track. Filter Out	874.56	DC	9	--		--
10	--		--	10	GMD Telemeter A[b]		FM
11	--		--	11	GMD Telemeter B		FM
12	10 KC		DC	12	GMD Telemeter C		FM
13	1 pps/voice		DC	13	1 pps/voice		DC
14	WWVH		DC	14	WWVH		DC

[a] L denotes left-hand polarization; R denotes right-hand.

[b] Letters A, B, and C denotes the telemeter video signals from GMD sets A, B, and C.

SECRET

TABLE C.4 DESCRIPTION OF CHART DATA RECORDED IN BRL VAN 2, STAR FISH EVENT

Chart Recorder 1 (Brush)			Chart Recorder 2 (Brush)		
Channel	Date (Beacon)		Channel	Data (Beacon)	
1	Receiver AGC	36.94 L[a]	1	Spin and faraday	36.94
2	Receiver AGC	36.94 R[a]	2	Spin and faraday	147.76
3	Receiver AGC	147.76 L	3	Spin and faraday	886.56
4	Receiver AGC	147.76 R	4	ΔDoppler	36.94 and 147.76[c]
5	Receiver AGC	886.56 L	5	ΔDoppler	147.76 and 886.56
6	Receiver AGC	886.56 R	6	ΔFaraday	36.94 and 147.76[b]
7	--		7	ΔFaraday	147.76 and 886.56
8	--		8	--	
EM	Timing		EM	Timing	
EM	Timing		EM	Timing	
Chart Recorder 1 (Varian)					
1	Doppler frequency vs Time	36.94			
2	Doppler frequency vs Time	147.76			
EM	Timing				

[a] L denotes left-hand polarization; R denotes right-hand.

[b] ΔFaraday denotes difference in faraday rotation between indicated frequencies.

[c] ΔDoppler denotes dispersive doppler for the indicated frequencies.

SECRET

TABLE C.4 CONTINUED

Chart Recorder 1 (Brush)		Chart Recorder 1 (Varian)	
Channel	Date (Satellite)	Channel	Date (Satellite)
1	Track. filter AGC, 54 Mc (rotating)	1	54 Mc
2	Track. filter correlation, 54 Mc (rotating)	2	324 Mc
3	Filtered correlation, 54 Mc (rotating)	EM	Timing
4	Timing		
5	Track. filter AGC, 54 Mc (fixed)		
6	Track. filter correlation, 54 Mc (fixed)		
7	Track. filter AGC, 324 Mc		
8	--		
EM	Antenna marker, 54 Mc (rotating)		
EM	Timing		
Chart Recorder 1 (Brush Mark II)			
1	Mixer Output, 54 and 324 Mc		
2	--		
EM	Timing		

SECRET

TABLE C.5 DESCRIPTION OF CHART DATA RECORDED IN BRL VAN 3, STAR FISH EVENT

Chart Recorder 1 (Varian)		Chart Recorder 1 (Brush Mark II)	
Channel	Data (Beacon)	Channel	Data (Beacon)
1	Doppler frequency vs Time 36.44	1	EG and G relays and rocket lift pulses
2	Doppler frequency vs Time 145.76	2	EG and G relays and rocket lift pulses
EM	Timing	EM	Timing

TABLE C.6 DESCRIPTION OF MAGNETIC TAPE DATA RECORDED IN BRL VAN 2, BLUE GILL EVENT

Recording of satellite data was the same as for the Star Fish event.

Tape Unit 1 (Ampex FR 114)				Tape Unit 2 (Ampex FR 114)			
Channel	Data (Beacon)		Recorder Amplifier	Channel	Data (Beacon)		Recorder Amplifier
1	Receiver Out	36.94 L[a]	DC	1	Track. filter out	36.94 L	DC
2	Receiver Out	36.94 R	DC	2	Track. filter out	36.94 R	DC
3	Receiver Out	147.76 L	DC	3	Track. filter out	147.76 L	DC
4	Receiver Out	147.76 R	DC	4	Track. filter out	147.76 R	DC
5	Receiver Out	886.56 L	DC	5	Track. filter out	886.56 L	DC
6	Receiver Out	886.56 R	DC	6	Track. filter out	886.56 R	DC
7	ΔFaraday 36.94 and 147.76[b]		FM	7	ΔDoppler 36.94 and 147.76[c]		FM
8	ΔFaraday 147.76 and 886.56		FM	8	ΔDoppler 147.76 and 886.56		FM
9	Doppler	36.94	DC	9	Spin and faraday	36.94	FM
10	Doppler	147.76	DC	10	Spin and faraday	147.76	FM
11	Doppler	886.56	DC	11	Spin and faraday	886.56	FM
12	10KC		DC	12	10KC		DC
13	1 pps/voice		DC	13	1 pps/voice		DC
14	1 per minute tone		DC	14	1 per minute tone		DC

[a] L denotes left-hand polarization; R denotes right-hand.

[b] ΔFaraday denotes difference in faraday rotation between indicated frequencies.

[c] ΔDoppler denotes dispersive doppler for the indicated frequencies.

SECRET

TABLE C.7 DESCRIPTION OF MAGNETIC TAPE DATA RECORDED IN BRL VAN 3, BLUE GILL EVENT

Tape Unit 1 (Ampex FR 114)				Tape Unit 2 (Ampex FR 114)			
Channel	Data (Beacon)		Recorder Amplifier	Channel	Date (Beacon)		Recorder Amplifier
1	Receiver Out	36.44 L[a]	DC	1	Receiver Out	36.44 L[a]	DC
2	Receiver Out	36.44 R	DC	2	Receiver Out	36.44 R	DC
3	Receiver Out	145.76 L	DC	3	Receiver Out	145.76 L	DC
4	Receiver Out	145.76 R	DC	4	Receiver Out	145.76 R	DC
5	Receiver Out	874.56 L	DC	5	GMD Telemeter A[b]		FM
6	Receiver Out	874.56 R	DC	6	GMD Telemeter B		FM
7	Track. filter out	36.44 R	DC	7	Track. filter out	36.44 R	DC
8	Track. filter out	145.76 R	DC	8	Track. filter out	145.76 R	DC
9	Track. filter out	874.56 R	DC	9	Track. filter out	874.56 R	DC
10	Track. filter out	874.56 L	DC	10	Track. filter out	874.56 L	DC
11	--		--	11	GMD Telemeter C		FM
12	10KC		DC	12	10KC		DC
13	1 pps/voice		DC	13	1 pps/voice		DC
14	1 per minute tone		DC	14	1 per minute tone		DC

[a] L denotes left-hand polarization; R denotes right-hand.

[b] Letters A, B, and C denotes the telemeter video signals from GMD sets A, B and C.

TABLE C.8 DESCRIPTION OF CHART DATA RECORDED IN BRL VAN 2, BLUE GILL EVENT

Recording of satellite data was the same as for Star Fish event.

Chart Recorder 1 (Brush)

Channel	Data (Beacon)	
1	Receiver AGC	36.94 L[a]
2	Receiver AGC	36.94 R
3	Receiver AGC	147.76 L
4	Receiver AGC	147.76 R
5	Receiver AGC	886.56 L
6	Receiver AGC	886.56 R
7	Track. filter AGC	36.94 R
8	Track. filter AGC	886.56 L
EM	Timing	
EM	Timing	

Chart Recorder 2 (Brush)

Channel	Data (Beacon)	
1	Spin and faraday	36.94
2	Spin and faraday	147.76
3	Spin and faraday	886.56
4	ΔDoppler	36.94 and 147.76[c]
5	ΔDoppler	147.76 and 886.56
6	ΔFaraday	36.94 and 147.76[b]
7	ΔFaraday	147.76 and 886.56
8	Track. filter AGC	147.76 R
EM	Timing	
EM	Timing	

Chart Recorder 1 (Varian)

1	Doppler frequency vs Time	36.94
2	Doppler frequency vs Time	147.76
EM	Timing	

[a] L denotes left-hand polarization; R denotes right-hand.

[b] ΔFaraday denotes difference in faraday rotation between indicated frequencies.

[c] ΔDoppler denotes dispersive doppler for the indicated frequencies.

SECRET

TABLE C.9 DESCRIPTION OF CHART DATA RECORDED IN BRL VAN 3, BLUE GILL EVENT

Chart Recorder 1 (Brush)			Chart Recorder 1 (Brush Mark II)	
Channel	Data (Beacon)		Channel	Data (Beacon)
1	Receiver AGC	36.44 L[a]	1	Track. filter AGC 874.56 L
2	Receiver AGC	36.44 R	2	Track. filter AGC 874.56 R
3	Receiver AGC	145.76 L	EM	Timing
4	Receiver AGC	145.76 R		
5	Receiver AGC	874.56 L	Chart Recorder 2 (Brush Mark II)	
6	Receiver AGC	874.56 R	1	EG and G relays and rocket lift pulses
7	Track. filter AGC	36.44 R	2	EG and G relays and rocket lift pulses
8	Track. filter AGC	145.76 R	EM	Timing
EM	Timing			
EM	Timing		Chart Recorder 1 (Varian)	
			1	Doppler frequency vs Time 36.44
			2	Doppler frequency vs Time 145.76
			EM	Timing

[a] L denotes left-hand polarization; R denotes right-hand.

SECRET

TABLE C10 DESCRIPTION OF MAGNETIC TAPE DATA RECORDED IN BRL VAN 2, KING FISH EVENT

Recording of satellite data was the same as for Star Fish event.

Tape Unit 1 (Ampex FR 114)				Tape Unit 2 (Ampex FR 114)			
Channel	Data (Beacon)		Recorder Amplifier	Channel	Data (Beacon)		Recorder Amplifier
1	Receiver out	36.94 L[a]	DC	1	Track. filter out	36.94 L	DC
2	Receiver out	36.94 R	DC	2	Track. filter out	36.94 R	DC
3	Receiver out	147.76 L	DC	3	Track. filter out	147.76 L	DC
4	Receiver out	147.76 R	DC	4	Track. filter out	147.76 R	DC
5	Receiver out	886.56 L	DC	5	Track. filter out	886.56 L	DC
6	Receiver out	886.56 R	DC	6	Track. filter out	886.56 R	DC
7	Track. filter out	886.56 L	DC	7	ΔDoppler 36.94 and 147.76[b]		FM
8	Track. filter out	886.56 R	DC	8	ΔDoppler 147.76 and 886.56		FM
9	Doppler	36.94	DC	9	Spin and faraday	36.94	FM
10	Doppler	147.76	DC	10	Spin and faraday	147.76	FM
11	Doppler	886.56	DC	11	Spin and faraday	886.56	FM
12	10KC		DC	12	10KC		DC
13	1 pps/voice		DC	13	1 pps/voice		DC
14	1 per minute tone		DC	14	1 per minute tone		DC

[a] L denotes left-hand polarization; R denotes right-hand.

[b] ΔDoppler denotes dispersive doppler for the indicated frequencies.

SECRET

TABLE C.11 DESCRIPTION OF MAGNETIC TAPE DATA RECORDED IN BRL VAN 3, KING FISH EVENT

Tape Unit 1 (Ampex FR 114)				Tape Unit 2 (Ampex FR 114)			
Channel	Data (Beacon)		Recorder Amplifier	Channel	Data (Beacon)		Recorder Amplifier
1	Receiver out	36.44 L[a]	DC	1	Receiver out	36.44 L	DC
2	Receiver out	36.44 R	DC	2	Receiver out	36.44 R	DC
3	Receiver out	145.76 L	DC	3	Receiver out	145.76 L	DC
4	Receiver out	145.76 R	DC	4	Receiver out	145.76 R	DC
5	Receiver out	874.56 L	DC	5	GMD Telemeter A[b]		FM
6	Receiver out	874.56 R	DC	6	GMD Telemeter B		FM
7	Track. filter out	36.44 R	DC	7	Track. filter out	36.44 R	DC
8	Track. filter out	145.76 R	DC	8	Track. filter out	145.76 R	DC
9	Track. filter out	874.56 R	DC	9	Track. filter out	874.56 R	DC
10	Track. filter out	874.56 L	DC	10	Track. filter out	874.56 L	DC
11	--		--	11	GMD Telemeter C		FM
12	10KC		DC	12	10KC		DC
13	1 pps/voice		DC	13	1 pps/voice		DC
14	1 per minute tone		DC	14	1 per minute tone		DC

[a] L denotes left-hand polarization; R denotes right-hand.

[b] Letters A, B, and C denotes the telemeter video signals from GMD sets A, B, and C.

SECRET

TABLE C.12 DESCRIPTION OF CHART DATA RECORDED IN BRL VAN 2, KING FISH EVENT

Recording of satellite data was the same as for Star Fish event.

Chart Recorder 1 (Brush)		Chart Recorder 2 (Brush)	
Channel	Data (Beacon)	Channel	Data (Beacon)
1	Receiver AGC 36.94 L[a]	1	Spin and faraday 36.94
2	Receiver AGC 36.94 R	2	Spin and faraday 147.76
3	Receiver AGC 147.76 L	3	Spin and faraday 886.56
4	Receiver AGC 147.76 R	4	ΔDoppler[b] 36.94 and 147.76
5	Receiver AGC 886.56 L	5	ΔDoppler 147.76 and 886.56
6	Receiver AGC 886.56 R	6	Track. filter AGC 886.56 L
7	Track. filter AGC 36.94 L	7	Track. filter AGC 886.56 R
8	Track. filter AGC 36.94 R	8	Track. filter AGC 147.76 R
EM	Timing	EM	Timing
EM	Timing	EM	Timing
Chart Recorder 1 (Brush Mark II)		Chart Recorder 1 (Varian)	
1	Track. filter AGC 147.76 L	1	Doppler frequency vs Time 36.94
2	Track. filter AGC 147.76 R	2	Doppler frequency vs Time 147.76
EM	Timing	EM	Timing

[a] L denotes left-hand polarization; R denotes right-hand.

[b] ΔDoppler denotes dispersive doppler for the indicated frequencies.

SECRET

TABLE C.13 DESCRIPTION OF CHART DATA RECORDED IN BRL VAN 3, KING FISH EVENT

Chart Recorder 1 (Brush)			Chart Recorder 1 (Brush Mark II)	
Channel	Data (Beacon)		Channel	Data (Beacon)
1	Receiver AGC	36.44 L[a]	1	Track. filter AGC 874.56 L
2	Receiver AGC	36.44 R	2	Track. filter AGC 874.56 R
3	Receiver AGC	145.76 L	EM	Timing
4	Receiver AGC	145.76 R		
5	Receiver AGC	874.56 L	Chart Recorder 2 (Brush Mark II)	
6	Receiver AGC	874.56 R	1	EG and G relays and rocket lift pulses
7	Track. filter AGC	36.44 R	2	EG and G relays and rocket lift pulses
8	Track. filter AGC	145.76 R	EM	Timing
EM	Timing		Chart Recorder 1 (Varian)	
EM	Timing		1	Doppler frequency vs Time 36.44
			2	Doppler frequency vs Time 145.76
			EM	Timing

[a] L denotes left-hand polarization; R denotes right-hand.

SECRET

TABLE C.14 SUMMARY OF GMD TELEMETRY AND TRACKING DATA, ROCKET 1, STAR FISH EVENT

Low-noise preamplifier not used.

Angular tracking accuracy: ± 0.20 degree.

Project: 6.4
Rocket No: 1
GMD frequency: 1670 Mc

Data	Type of recording	Van	Recorder	Channel	Reel
Telemetry[a]	Magnetic tape	EOS	2	9	35
Telemetry	(not recorded)	--	--	--	--
Elevation angle[b]	Paper tape	4	B	Left	NA
Azimuth angle[b]	Paper tape	4	B	Right	NA
AGC[c]	Paper chart	4	1	2	NA
AGC[c]	Paper chart	4	2	1	NA

[a] Data to 121 seconds. Data very noisy and unreadable except for period from 37 to 68 seconds.

[b] Tracking poor. Good sections from 40 to 80 seconds and 100 to 130 seconds.

[c] Signal very weak. Strength varied from -90 dbm to infinity.

SECRET

TABLE C.15 SUMMARY OF GMD TELEMETRY AND TRACKING DATA, ROCKET 2, STAR FISH EVENT

Low-noise preamplifier not used.

Angular tracking accuracy: ± 0.20 degree.

Project: 6.3
Rocket No: 2
GMD frequency: 1660 Mc

Data	Type of recording	Van	Recorder	Channel	Reel
Telemetry[a]	Magnetic tape	EOS	2	8	33
Telemetry	(not recorded)	--	--	--	--
Elevation angle[b]	Paper tape	4	A	Left	NA
Azimuth angle[b]	Paper tape	4	A	Right	NA
AGC[c]	Paper chart	4	1	1	NA
AGC	(not recorded)	--	--	--	--

[a] Data to 307 seconds. Data very noisy from 0 to 12, 25 to 80, and 278 to 321 seconds. The 14.5- and 22-kc channels were readable through the first two periods of noise, but the 70-kc channel was not. No channel was readable during the third period of noise.

[b] Tracking excellent from 30 seconds to splash.

[c] Signal good from lift to splash.

SECRET

TABLE C.16 SUMMARY OF GMD TELEMETRY AND TRACKING DATA, ROCKET 3, STAR FISH EVENT

Low-noise preamplifier not used.

Angular tracking accuracy: ± 0.20 degree.

Project: 6.3
Rocket No: 3
GMD frequency: 1680 Mc

Date	Type of recording	Van	Recorder	Channel	Reel
Telemetry[a]	Magnetic tape	EOS	2	10	33
Telemetry	(not recorded)	--	--	--	--
Elevation angle[b]	Paper tape	4	C	Left	NA
Azimuth angle[b]	Paper tape	4	C	Right	NA
AGC[c]	Paper chart	4	2	2	NA
AGC	(not recorded)	--	--	--	--

[a] Data to 63 seconds. Signal was lost at lift but re-appears strong from 39 to 63 seconds.

[b] Tracking excellent from 30 seconds to splash.

[c] Signal very good from lift to splash (108 seconds). Signal: -75 dbm.

SECRET

TABLE C.17 SUMMARY OF GMD TELEMETRY AND TRACKING DATA, ROCKET 4, STAR FISH EVENT

Low-noise preamplifier not used.

Angular tracking accuracy: ± 0.20 degree.

Project: 6.3
Rocket No: 4
GMD frequency: 1660 Mc

Date	Type of recording	Van	Recorder	Channel	Reel
Telemetry[a]	Magnetic tape	EOS	2	8	33
Telemetry[a]	Magnetic tape	3	2	10	1
Elevation angle[b]	Paper tape	4	A	Left	NA
Azimuth angle[b]	Paper tape	4	A	Right	NA
AGC[c]	Paper chart	4	1	1	NA
AGC	(Not recorded)	--	--	--	--

[a] Data to 251 seconds. The data continuous, but the recorder was shut off. Data was noisy from 0 to 28 and from 211 to 241 seconds. The low-frequency channels have noise spikes throughout, but the data is readable.

[b] Tracking excellent from 15 seconds to 277 seconds. Would have tracked to splash but GMD in Rocket No. 7 turned on at that time.

[c] Signal good from lift to 277 seconds.

SECRET

TABLE C.18 SUMMARY OF GMD TELEMETRY AND TRACKING DATA, ROCKET 5, STAR FISH EVENT

Low-noise preamplifier not used.

Angular tracking accuracy: $\pm$ 0.20 degree.

Project: 6.4
Rocket No: 5
GMD frequency: 1670 Mc

Data	Type of recording	Van	Recorder	Channel	Reel
Telemetry[a]	Magnetic tape	EOS	1	9	31
Telemetry[a]	Magnetic tape	3	2	11	1
Elevation angle[b]	Paper tape	4	B	Left	NA
Azimuth angle[b]	Paper tape	4	B	Right	NA
AGC[c]	Paper chart	4	1	2	NA
AGC[c]	Paper chart	4	2	1	NA

[a] Data to 126 seconds. Data was noisy from 0 to 20 and 74 to 92 seconds. Data is unreadable from 0 to 20 seconds and partly readable from 74 to 92 seconds. The data beyond 92 seconds gradually fades into noise.

[b] Tracking good from 25 to 134 seconds.

[c] Signal fair to good from lift to 134 seconds.

TABLE C.19 SUMMARY OF GMD TELEMETRY AND TRACKING DATA, ROCKET 6, STAR FISH EVENT

Low-noise preamplifier not used.

Angular tracking accuracy: ± 0.20 degree.

Project: 6.3
Rocket No: 6
GMD frequency: 1680 Mc

Data	Type of recording	Van	Recorder	Channel	Reel
Telemetry[a]	Magnetic tape	EOS	1	10	31
Telemetry[a]	Magnetic tape	3	2	12	1
Elevation angle[b]	Paper tape	4	C	Left	NA
Azimuth angle[b]	Paper tape	4	C	Right	NA
AGC[c]	Paper chart	4	2	2	NA
AGC	(not recorded)	--	--	--	--

[a] Data to 331 seconds. The data continues, but the recorder was shut off. Intense noise was present from 0 to 14, 21 to 33, and 274 to 331 seconds, and data was not readable during these periods.

[b] Tracking excellent from 50 seconds to splash.

[c] Signal very good from lift to splash (329 seconds).

TABLE C.20 SUMMARY OF GMD TELEMETRY AND TRACKING DATA, ROCKET 7, STAR FISH EVENT

Low-noise preamplifier not used.

Angular tracking accuracy: ± 0.20 degree.

Project: 6.4
Rocket No: 7
GMD frequency: 1660 Mc

Data	Type of recording	Van	Recorder	Channel	Reel
Telemetry[a]	Magnetic tape	EOS	2	8	34
Telemetry[a]	Magnetic tape	3	2	10	1
Elevation angle[b]	Paper tape	4	A	Left	NA
Azimuth angle[b]	Paper tape	4	A	Right	NA
AGC[c]	Paper chart	4	1	1	NA
AGC	(not recorded)	--	--	--	--

[a] No usable data. The signal goes into noise at lift and does not re-appear.

[b] Tracking fair from 60 to 150 seconds.

[c] Signal fair to poor from lift to 190 seconds.

SECRET

TABLE C.21 SUMMARY OF GMD TELEMETRY AND TRACKING DATA, ROCKET 8, STAR FISH EVENT

Low-noise preamplifier not used.

Angular tracking accuracy: ± 0.20 degree.

Project: 6.2
Rocket No: 8
GMD frequency: 1670

Data	Type of recording	Van	Recorder	Channel	Reel
Telemetry[a]	Magnetic tape	EOS	2	9	34
Telemetry[a]	Magnetic tape	3	2	11	1
Elevation angle[b]	Paper tape	4	B	Left	NA
Azimuth angle[b]	Paper tape	4	B	Right	NA
AGC[c]	Paper chart	4	1	2	NA
AGC[c]	Paper chart	4	2	1	NA

[a] Data to 128 seconds. The data was noisy from 68 to 72 and 80 to 86 seconds and was not readable during these periods. Some noise appeared early on the low-frequency channels, but the data was readable.

[b] Tracking good from 20 to 140 seconds.

[c] Signal fair to good from lift to 134 seconds.

TABLE C.22 SUMMARY OF GMD TELEMETRY AND TRACKING DATA, ROCKET 9, STAR FISH EVENT

Low-noise preamplifier not used.

Angular tracking accuracy: ± 0.20 degree.

Project: 6.2
Rocket No: 9
GMD frequency: 1680 Mc

Data	Type of recording	Van	Recorder	Channel	Reel
Telemetry[a]	Magnetic tape	EOS	1	8,9,10	32
Telemetry[a]	Magnetic tape	3	2	10,11,12	1
Elevation angle[b]	Paper tape	4	A,B,C	Left	NA
Azimuth angle[b]	Paper tape	4	A,B,C	Right	NA
AGC[c]	Paper chart	4	1	1,2	NA
AGC[c]	Paper chart	4	2	1,2	NA

[a] Data to 111 seconds. All channels were noisy throughout, but some periods provided usable data.

[b] Tracking poor from 20 to 131 seconds.

[c] Signal fair to good from lift to 131 seconds.

SECRET

TABLE C.23 SUMMARY OF GMD TELEMETRY AND TRACKING DATA, **ROCKET 10, BLUE GILL EVENT**

Low-noise preamplifier used on Rockets 11, 12, 14, 15, and 18.

Angular tracking accuracy: $\pm$ 0.20 degree.

Project: 6.3
Rocket No: 10
GMD frequency: 1660 Mc

Data	Type of recording	Van	Recorder	Channel	Reel
Telemetry[a]	Magnetic tape	EOS	1	8	74
Telemetry	(not recorded)	--	--	--	--
Elevation angle[b]	Paper tape	4	A	Left	NA
Azimuth angle[b]	Paper tape	4	A	Right	NA
AGC[c]	Paper chart	4	1	1	NA
AGC	(not recorded)	--	--	--	--
AGC (High speed)[c]	Paper chart	4	3	A	NA

[a] Data to 324 seconds. The signal was lost from 5 to 18 and 24 to 88 seconds because of a double shift in the airborne transmitter frequency. The tape recorder stopped from 60 to 156 seconds, so this data was lost. The remaining data was excellent except for some noise on the low-frequency channels.

[b] Angle track was excellent.

[c] Signal good from lift to splash (323 seconds) except for RF drop out from 4 to 17 seconds and 23 to 38 seconds.

SECRET

TABLE C.24 SUMMARY OF GMD TELEMETRY AND TRACKING DATA, **ROCKET 11, BLUE GILL EVENT**

Low-noise preamplifier used on Rockets 11, 12, 14, 15, and 18.

Angular tracking accuracy: ± 0.20 degree.

Project: 6.3
Rocket No: 11
GMD frequency: 1670 Mc

Data	Type of recording	Van	Recorder	Channel	Reel
Telemetry[a]	Magnetic tape	EOS	1	9	74
Telemetry	(not recorded)	--	--	--	--
Elevation angle[b]	Paper tape	4	B	Left	NA
Azimuth angle[b]	Paper tape	4	B	Right	NA
AGC[c]	Paper chart	4	1	2	NA
AGC[c]	Paper chart	4	2	1	NA
AGC[c] (High speed)	Paper chart	4	3	B	NA

[a] Data to 281 seconds. The data was noisy from 0 to 29 seconds and from 68 to 70 seconds. The tape recorder stopped from 120 to 216 seconds, so this data was lost. The data was good up to the recorder cut off at 120 seconds and was very noisy and unreadable from 216 seconds to the end.

[b] Angle track was excellent.

[c] Signal good from lift to splash at 292 seconds.

TABLE C.25 SUMMARY OF GMD TELEMETRY AND TRACKING DATA, ROCKET 12, BLUE GILL EVENT

Low-noise preamplifier used on Rockets 11, 12, 14, 15, and 18.

Angular tracking accuracy: ± 0.20 degree.

Project: 6.3
Rocket No: 12
GMD frequency: 1680 Mc

Data	Type of recording	Van	Recorder	Channel	Reel
Telemetry[a]	Magnetic tape	EOS	1	10	74
Telemetry	(not recorded)	--	--	--	--
Elevation angle[b]	Paper tape	4	C	Left	NA
Azimuth angle[b]	Paper tape	4	C	Right	NA
AGC[c]	Paper chart	4	2	2	NA
AGC	(not recorded)	--	--	--	--
AGC (High speed)[c]	Paper chart	4	3	C	NA

[a] Data to 270 seconds. Excellent record. There were several noise bursts at the beginning of the record. Constant noise started to appear at 190 seconds and increased to the end.

[b] Angle track was excellent.

[c] Signal good from lift to splash (277 seconds).

TABLE C.26 SUMMARY OF GMD TELEMETRY AND TRACKING DATA, ROCKET 13, BLUE GILL EVENT

Low-noise preamplifier used on Rockets 11, 12, 14, 15, and 18.

Angular tracking accuracy: ± 0.20 degree.

Project: 6.3
Rocket No: 13
GMD frequency: 1660 Mc

Data	Type of recording	Van	Recorder	Channel	Reel
Telemetry[a]	Magnetic tape	EOS	1	8	74
Telemetry	(not recorded)	--	--	--	--
Elevation angle[b]	Paper tape	4	A	Left	NA
Azimuth angle[b]	Paper tape	4	A	Right	NA
AGC[c]	Paper chart	4	1	1	NA
AGC	(not recorded)	--	--	--	--

[a] Data to 306 seconds. Some noise appears at lift on the lowest frequency channel and continues until 85 seconds where loss of signal occurs. At 109 seconds, the signal reappears, but the signal-to-noise ratio is very low, and the data is unreadable.

[b] Angle track was good.

[c] Signal good from lift to splash (328 seconds) except for RF drop-out from 85 to 109 seconds. When signal was recovered at 109 seconds, the frequency was 8 Mc below the nominal 1660 Mc. The frequency remained at 1652 Mc until splash.

SECRET

TABLE C.27 SUMMARY OF GMD TELEMETRY AND TRACKING DATA, ROCKET 14, BLUE GILL EVENT

Low-noise preamplifier used on Rockets 11, 12, 14, 15, and 18.

Angular tracking accuracy: ± 0.20 degree.

Project: 6.3
Rocket No: 14
GMD frequency: 1670 Mc

Data	Type of recording	Van	Recorder	Channel	Reel
Telemetry[a]	Magnetic tape	EOS	1	9	74
Telemetry	(not recorded)	--	--	--	--
Elevation angle[b]	Paper tape	4	B	Left	NA
Azimuth angle[b]	Paper tape	4	B	Right	NA
AGC[c]	Paper chart	4	1	2	NA
AGC[c]	Paper chart	4	2	1	NA

[a] Data to 301 seconds. Excellent record. The data continues beyond 301 seconds, but the recorder was shut off at this point. Noise appears on the low-frequency channels from 0 to 30 and 201 to 301 seconds, but the data is readable.

[b] Angle track was excellent.

[c] Signal good from lift to splash (302 seconds).

TABLE C.28 SUMMARY OF GMD TELEMETRY AND TRACKING DATA, **ROCKET 15, BLUE GILL EVENT**

Low-noise preamplifier used on Rockets 11, 12, 14. 15, and 18.

Angular tracking accuracy: $\pm$ 0.20 degree.

Project: 6.2
Rocket No: 15
GMD frequency: 1680 Mc

Data	Type of recording	Van	Recorder	Channel	Reel
Telemetry[a]	Tape	EOS	2	10	77
Telemetry	(not recorded)	--	--	--	--
Elevation angle[b]	Paper tape	4	C	Left	NA
Azimuth angle[b]	Paper tape	4	C	Right	NA
AGC[c]	Paper chart	4	2	2	NA
AGC	(not recorded)	--	--	--	--

[a] Data to 306 seconds. There are many periods of noise through the record. The analog data is readable during these periods, but the commutated data is not.

[b] Angle track was excellent after acquisition at 55 seconds.

[c] Signal fair from lift to splash (350 seconds).

SECRET

TABLE C.29 SUMMARY OF GMD TELEMETRY AND TRACKING DATA, **ROCKET 17, BLUE GILL EVENT**

Low-noise preamplifier used on Rockets 11, 12, 14, 15, and 18.

Angular tracking accuracy: $\pm$ 0.20 degree.

Project: 6.3
Rocket No: 17
GMD frequency: 1660 Mc

Data	Type of recording	Van	Recorder	Channel	Reel
Telemetry[a]	Magnetic tape	EOS	1	8	75
Telemetry	(not recorded)	--	--	--	--
Elevation angle[b]	Paper tape	4	A	Left	NA
Azimuth angle[b]	Paper tape	4	A	Right	NA
AGC[c]	Paper chart	4	1	1	NA
AGC	(not recorded)	--	--	--	--

[a] Data to 289 seconds. Noise appears at 117 seconds on the low-frequency channels and increases until the end of the record. All data is readable to 245 seconds.

[b] Angle track was excellent.

[c] Signal good from lift to splash (288 seconds).

SECRET

TABLE C.30 SUMMARY OF GMD TELEMETRY AND TRACKING DATA, ROCKET 18, BLUE GILL EVENT

Low-noise preamplifier used on Rockets 11, 12, 14, 15, and 18.

Angular tracking accuracy: ± 0.20 degree.

Project: 6.2
Rocket No: 18
GMD frequency: 1680 Mc

Data	Type of recording	Van	Recorder	Channel	Reel
Telemetry[a]	Magnetic tape	EOS	1	8,9,10	75
Telemetry	(not recorded)	--	--	--	--
Elevation angle[b]	Paper tape	4	A,B,C	Left	NA
Azimuth angle[b]	Paper tape	4	A,B,C	Right	NA
AGC[c]	Paper chart	4	1	1,2	NA
AGC[c]	Paper chart	4	2	1,2	NA

[a] Data to 241 seconds. The data is noisy but readable. The period from 8 to 50 seconds has the highest signal-to-noise ratio.

[b] Angle track was excellent.

[c] Signal fair from lift to splash (249 seconds).

SECRET

TABLE C.31 SUMMARY OF GMD TELEMETRY AND TRACKING DATA, ROCKET 19, KING FISH EVENT

Low-noise preamplifier used on all rockets.

Angular tracking accuracy: ± 0.20 degree.

Project: 6.2
Rocket No: 19
GMD frequency: 1660 Mc

Data	Type of recording	Van	Recorder	Channel	Reel
Telemetry[a]	Magnetic tape	EOS	1	8	98
Telemetry[a]	Magnetic tape	3	2	5	81
Elevation angle[b]	Paper tape	4	A	Left	NA
Azimuth angle[b]	Paper tape	4	A	Right	NA
AGC[c]	Paper chart	4	1	1	NA
AGC	(not recorded)	--	--	--	--

[a]Data to 34 seconds. No useful data after the first 16 seconds. At 16 seconds the signal-to-noise ratio is very low, and the data becomes unreadable.

[b]No tracking was accomplished.

[c]Signal very poor out to 70 seconds.

TABLE C.32 SUMMARY OF GMD TELEMETRY AND TRACKING DATA, ROCKET 20, KING FISH EVENT

Low-noise preamplifier used on all rockets.

Angular tracking accuracy: ± 0.20 degree.

Project: 6.3
Rocket No: 20
GMD frequency: 1670 Mc

Data	Type of recording	Van	Recorder	Channel	Reel
Telemetry[a]	Magnetic tape	EOS	1	10	98
Telemetry[a]	Magnetic tape	3	2	11	81
Elevation angle[b]	Paper tape	4	C	Left	NA
Azimuth angle[b]	Paper tape	4	C	Right	NA
AGC[c]	Paper chart	4	2	2	NA
AGC	(not recorded)	--	--	--	--

[a]Data to 396 seconds. Noise appears at 64 seconds on the lower frequency channels, and the signal-to-noise ratio decreases through the record.

[b]Tracking was excellent from 20 seconds to splash.

[c]Signal good from lift to splash (397 seconds).

SECRET

TABLE C.33 SUMMARY OF GMD TELEMETRY AND TRACKING DATA, ROCKET 21, KING FISH EVENT

Low-noise preamplifier used on all rockets.

Angular tracking accuracy: ± 0.20 degree.

Project: 6.3
Rocket No: 21
GMD frequency: 1680 Mc

Data	Type of recording	Van	Recorder	Channel	Reel
Telemetry[a]	Magnetic tape	EOS	1	9	98
Telemetry[a]	Magnetic tape	3	2	6	81
Elevation angle[b]	Paper tape	4	B	Left	NA
Azimuth angle[b]	Paper tape	4	B	Right	NA
AGC[c]	Paper chart	4	1	2	NA
AGC[c]	Paper chart	4	2	1	NA

[a]Data to 317 seconds. Excellent record. All data is readable with only occasional noise spikes.

[b]Tracking was excellent from 10 seconds to cut-off.

[c]Signal excellent from lift to cut-off (317 seconds).

TABLE C.34 SUMMARY OF GMD TELEMETRY AND TRACKING DATA, ROCKET 23, KING FISH EVENT

Low-noise preamplifier used on all rockets.

Angular tracking accuracy: ± 0.20 degree.

Project: 6.3
Rocket No: 23
GMD frequency: 1680 Mc

Data	Type of recording	Van	Recorder	Channel	Reel
Telemetry[a]	Magnetic tape	EOS	1	9	98
Telemetry[a]	Magnetic tape	3	2	6	81
Elevation angle[b]	Paper tape	4	B	Left	NA
Azimuth angle[b]	Paper tape	4	B	Right	NA
AGC[c]	Paper chart	4	1	2	NA
AGC[c]	Paper chart	4	2	1	NA

[a] Data to 339 seconds. Excellent record. All data is readable with only occasional noise spikes.

[b] Tracking was excellent from 10 seconds to splash.

[c] Signal excellent from lift to splash (345 seconds).

SECRET

TABLE C.35 SUMMARY OF GMD TELEMETRY AND TRACKING DATA, ROCKET 24, KING FISH EVENT

Low-noise preamplifier used on all rockets.

Angular tracking accuracy: ± 0.20 degree.

Project: 6.3
Rocket No : 24
GMD frequency: 1670 Mc

Data	Type of recording	Van	Recorder	Channel	Reel
Telemetry[a]	Magnetic tape	EOS	1	10	98
Telemetry[a]	Magnetic tape	3	2	11	81
Elevation angle[b]	Paper tape	4	C	Left	NA
Azimuth angle[b]	Paper tape	4	C	Right	NA
AGC[c]	Paper chart	4	2	2	NA
AGC	(not recorded)	--	--	--	--

[a]Data to 338 seconds. The signal-to-noise ratio is low, 0 to 36 seconds. All of the lower frequency channels are noisy throughout, and the signal-to-noise ratio on the 10.5- and 14.5-Mc channels is low.

[b]Tracking was excellent from 20 seconds to splash.

[c]Signal good from lift to splash (369 seconds).

SECRET

TABLE C.36 SUMMARY OF GMD TELEMETRY AND TRACKING DATA, ROCKET 25, KING FISH EVENT

Low noise preamplifier used on all rockets.

Angular tracking accuracy: ± 0.20 degree.

Project: 6.4
Rocket No : 25
GMD frequency: 1660 Mc

Data	Type of recording	Van	Recorder	Channel	Reel
Telemetry[a]	Magnetic tape	EOS	1	8	98
Telemetry[a]	Magnetic tape	3	2	5	81
Elevation angle[b]	Paper tape	4	A	Left	NA
Azimuth angle[b]	Paper tape	4	A	Right	NA
AGC[c]	Paper chart	4	1	1	NA
AGC	(not recorded)	--	--	--	--

[a]Data to 78 seconds. The data is noisy with only a few readable periods.

[b]No tracking was accomplished.

[c]Signal fair from lift to 187 seconds.

TABLE C.37 SUMMARY OF GMD TELEMETRY AND TRACKING DATA, ROCKET 26, KING FISH EVENT

Low-noise preamplifier used on all rockets.

Angular tracking accuracy: ± 0.20 degree.

Project: 6.2
Rocket No: 26
GMD frequency: 1680 Mc

Data	Type of recording	Van	Recorder	Channel	Reel
Telemetry[a]	Magnetic tape	EOS	1	9	98
Telemetry[a]	Magnetic tape	3	2	6	81
Elevation angle[b]	Paper tape	4	B	Left	NA
Azimuth angle[b]	Paper tape	4	B	Left	NA
AGC[c]	Paper chart	4	1	2	NA
AGC[c]	Paper chart	4	2	1	NA

[a] Data to 412 seconds. The data is noisy but readable up to 180 seconds where the signal-to-noise becomes too low to obtain any useful data.

[b] Tracking was excellent from 25 seconds to splash.

[c] Signal good from lift to splash (412 seconds).

TABLE C.38 SUMMARY OF GMD TELEMETRY AND TRACKING DATA, ROCKET 27, KING FISH EVENT

Low-noise preamplifier used on all rockets.

Angular tracking accuracy: ±0.20 degree.

Project: 6.3
Rocket No: 27
GMD frequency: 1670 Mc

Data	Type of recording	Van	Recorder	Channel	Reel
Telemetry[a]	Magnetic tape	EOS	1	10	98
Telemetry[a]	Magentic tape	3	2	11	81
Elevation angle[b]	Paper tape	4	C	Left	NA
Azimuth angle[b]	Paper tape	4	C	Right	NA
AGC[c]	Paper chart	4	2	2	NA
AGC	(not recorded)	--	--	--	--

[a] Data to 391 seconds. The data is very noisy and unreadable from 0 to 33 seconds. All channels except the 70-kc channel are noisy throughout.

[b] Tracking was excellent from 20 seconds to splash.

[c] Signal was good from lift to splash (392 seconds).

SECRET

TABLE C.39 SUMMARY OF GMD TELEMETRY AND TRACKING DATA, ROCKET 28, KING FISH EVENT

Low-noise preamplifier used on all rockets.

Angular tracking accuracy: ± 0.20 degree.

Project: 6.3
Rocket No: 28
GMD frequency: 1680 Mc

Data	Type of recording	Van	Recorder	Channel	Reel
Telemetry[a]	Magnetic tape	EOS	1	8,9,10	99
Telemetry[a]	Magnetic tape	3	2	5,6,11	81
Elevation angle[b]	Paper tape	4	A,B,C	Left	NA
Azimuth angle[b]	Paper tape	4	A,B,C	Right	NA
AGC[c]	Paper chart	4	1	1,2	NA
AGC[c]	Paper chart	4	2	1,2	NA

[a] Data to 346 seconds. Noise appears early on the low-frequency channels, and the signal-to-noise ratio decreases until the end of the record. The signal-to-noise ratio on the 70-kc channel is high throughout.

[b] Tracking was good from 20 seconds to splash on GMD-A and GMD-C. GMD-B had some tracking oscillations up to 250 seconds but was good thereafter.

[c] Signal was good from lift to splash (370 seconds).

SECRET

TABLE C.40 SUMMARY OF GMD TELEMETRY AND TRACKING DATA, ROCKET 29, KING FISH EVENT

Low-noise preamplifier used on all rockets.

Angular tracking accuracy: ± 0.20 degree.

Project: 6.2
Rocket No: 29
GMD frequency: 1660 Mc

Data	Type of recording	Van	Recorder	Channel	Reel
Telemetry[a]	Magnetic tape	EOS	1	8,9,10	99
Telemetry[a]	Magnetic tape	3	2	5,6,11	81
Elevation angle[b]	Paper tape	4	A,B,C	Left	NA
Azimuth angle[b]	Paper tape	4	A,B,C	Right	NA
AGC[c]	Paper chart	4	1	1,2	NA
AGC[c]	Paper chart	4	2	1,2	NA

[a] Data to 275 seconds. The signal-to-noise on all channels is low throughout, but the analog data is readable through this noise. The 70-kc commutated channel is not readable during the noisy periods.

[b] Tracking was excellent from 30 seconds to splash on GMD-A and GMD-B. GMD-C had an overload relay go out at 65 seconds, but tracking was resumed at 205 seconds.

[c] Signal was good from lift to splash (270 seconds).

SECRET

TABLE C.41 SUMMARY OF 3-FREQUENCY PROPAGATION DATA, ROCKET 1, **STAR FISH**

PROJECT: 6.4
EVENT: Star Fish
ROCKET NO: 1
LAUNCH TIME & DATE: 0850:09 GMT 9 Jul 62

Data Recorded	Type of Recording	Van Number	Recorder Number	Channel Number	Reel Number	Remarks
Low-Frequency Dispersive Doppler $\left[2(37\ \text{Mc}) - \frac{148\ \text{Mc}}{2}\right]$	Magnetic tape	2	2	7	4	Bias frequency existed on dispersive doppler.
	Brush chart	2	2	4	-	Bias eliminated with reasonable confidence, and dispersive doppler acquired 168 to 600 seconds.
High-Frequency Dispersive Doppler $\left[\frac{148\ \text{Mc}}{2} - \frac{888\ \text{Mc}}{12}\right]$	Magnetic tape	2	2	8	4	No usable data because of poor quality of 888-Mc signal.
	Brush chart	2	2	5	-	
Doppler Frequency (37 Mc)	Magnetic tape	2	1	9	1	Duration was from rocket lift to 600 seconds.
	Varian chart	2	1	1	-	Data was of good quality and was used for derivation of dispersive doppler.
Doppler Frequency (148 Mc)	Magnetic tape	2	1	10	1	Duration was from rocket lift to 770 seconds.
	Varian chart	2	1	2	-	Data was of good quality and was used for trajectory determination and derivation of dispersive doppler.
Doppler Frequency (888 Mc)	Magnetic tape	2	1	11	1	Not used. Quality not evaluated. Duration was from rocket lift to 140 seconds.

SECRET

TABLE C.41 CONTINUED

PROJECT: 6.4
EVENT: Star Fish
ROCKET NO: 1
LAUNCH TIME & DATE: 0850:09 GMT 9 Jul 62

Data Recorded	Type of Recording	Van Number	Recorder Number	Channel Number	Reel Number	Remarks
Signal Level (AGC) (37 Mc)	Brush chart	2	1	1, 2	-	Smooth signal decay to burst. Signal drops below receiver AGC threshold at burst (600 seconds). Only weak, intermittent signal following burst. Spin modulation 2- to 4-db left-hand (LH) and right-hand (RH) polarization.
Signal Level (AGC) (148 Mc)	Brush chart	2	1	3, 4	-	Smooth signal decay to burst. Signal drops below receiver AGC threshold 600 to 617 seconds LH, 600 to 609 seconds RH. Recovers almost to pre-burst level. Spin modulation 2 to 15 db LH, 2 to 6 db RH. Signal ends 764 seconds LH, 768 seconds RH.
Signal Level (AGC) (888 Mc)	Brush chart	2	1	5, 6	-	Sharp signal decay 10 to 15 seconds LH, minimum signal below receiver AGC threshold after 20 seconds. Signal ends 24 seconds LH. Minimum signal below threshold after 15 seconds RH, ends 28 seconds RH.
					NOTE:	Actual frequencies employed were 36.94 Mc, 147.76 Mc, and 886.56 Mc.

TABLE C.4c SUMMARY OF 3-FREQUENCY PROPAGATION DATA, ROCKET 4, STAR FISH

PROJECT: 6.3
EVENT: Star Fish
ROCKET NO: 4
LAUNCH TIME & DATE: 0907:09 GMT 9 Jul 62

Data Recorded	Type of Recording	Van Number	Recorder Number	Channel Number	Reel Number	Remarks
Low-Frequency Dispersive Doppler	Magnetic tape Brush chart	2 2	2 2	7 4	4 -	Bias frequency existed on dispersive doppler. Bias eliminated with reasonable confidence, and dispersive doppler acquired during entire period of ionization from 65 to 222 seconds.
High-Frequency Dispersive Doppler	Magnetic tape Brush chart	2 2	2 2	8 5	4 -	No usable data. Based on low-frequency dispersive doppler; only about one-third of a cycle of high-frequency dispersive doppler could be expected.
Doppler Frequency (37 Mc)	Magnetic tape Varian chart	2 2	1 1	9 1	1 -	Duration was from rocket lift to 290 seconds. Much frequency drift especially during rocket staging.
Doppler Frequency (148 Mc)	Magnetic tape Varian chart	2 2	1 1	10 2	1 -	Duration was from rocket lift to 290 seconds. Much frequency drift especially during rocket staging.
Doppler Frequency (888 Mc)	Magnetic tape	2	1	11	1	Not used. Quality not evaluated. Duration from rocket lift to 290 seconds.

SECRET

TABLE C.42 CONTINUED

PROJECT: 6.3
EVENT: Star Fish
ROCKET NO: 4
LAUNCH TIME & DATE: 0907:09 GMT 9 Jul 62

Data Recorded	Type of Recording	Van Number	Recorder Number	Channel Number	Reel Number	Remarks
Signal Level (37 Mc)	Brush chart	2	1	1, 2	-	Smooth signal decay to peak altitude 145 seconds LH and RH. Spin modulation 1 to 2 db LH, 3 to 5 db RH. Signal ends 286 seconds LH, 289 seconds RH.
Signal Level (148 Mc)	Brush chart	2	1	3, 4	-	Smooth signal decay to 145 seconds LH. Sharp drop at 65 seconds RH when ion trap and RF probe deployed. Spin modulation 3 to 6 db LH, 1 to 2 db RH. Signal ends 289 seconds LH and RH.
Signal Level (888 Mc)	Brush chart	2	1	5, 6	-	Smooth signal decay to 67 seconds (ion trap, RF probe deployment). Signal abruptly drops below receiver AGC theshold 67 to 84 seconds LH and RH. Abruptly recovers to normal at 84 seconds. Spin modulation 3 to 22 db LH, 8 to 15 db RH. Signal ends 200 seconds LH, 235 seconds RH.
					NOTE:	Actual frequencies employed were 36.94 Mc, 147.76 Mc, and 886.56 Mc. RH and LH denote right- and left-hand polarization.

SECRET

TABLE C.43 SUMMARY OF 3-FREQUENCY PROPAGATION DATA, ROCKET 5, **STAR FISH**

PROJECT: 6.4
EVENT: Star Fish
ROCKET NO: 5
LAUNCH TIME & DATE: 0907:09 GMT 9 Jul 62

Data Recorded	Type of Recording	Van Number	Recorder Number	Channel Number	Reel Number	Remarks
Low-Frequency Dispersive Doppler	Not recorded directly; derived from other taped data	3	1	1 to 6	7	Bias existed on dispersive doppler. Bias was eliminated with reasonable confidence, and dispersive doppler acquired from 85 to 230 seconds at which time 37-Mc signal became too noisy.
High-Frequency Dispersive Doppler	Not recorded directly; derived from other taped data	3	1	1 60 6	7	No usable data.
Doppler Frequency (37 Mc)	Magnetic tape	3	1	1, 2	7	Duration was from rocket lift to 687 seconds.
	Varian chart	3	1	1	-	Some frequency drift, no discontinuities.
Doppler Frequency (148 Mc)	Magnetic tape	3	1	3, 4	7	Duration was from rocket lift to 687 seconds.
	Varian chart	3	1	2	-	Some frequency drift, no discontinuities. Data was used for trajectory determination.
Doppler Frequency (888 Mc)	Magnetic tape	3	1	5, 6	7	Not used. Quality not evaluated. Duration from rocket lift to 200 seconds.

SECRET

TABLE C.43 CONTINUED

PROJECT: 6.4
EVENT: Star Fish
ROCKET NO: 5
LAUNCH TIME & DATE: 0907:09 GMT 9 Jul 62

Data Recorded	Type of Recording	Van Number	Recorder Number	Channel Number	Reel Number	Remarks
Signal Level (37 Mc)	Magnetic tape	3	2	1, 2	8	Only maximum signal plotted because of questionable calibration at minimum signal level. Smooth decay, 2-db drop at 4th-stage ignition 70 seconds RH. Signal ends 685 seconds LH, 580 seconds RH.
Signal Level (148 Mc)	Magnetic tape	3	2	3, 4	8	Only maximum signal plotted (see 37-Mc AGC above). Sharp drop and recovery at 4th-stage ignition, both LH and RH. Signal ends 665 seconds LH, 685 seconds RH.
Signal Level (888 Mc)	Magnetic tape	3	2	5, 6	8	Smooth decay, sharp drop at 4th-stage ignition, both LH and RH. Spin modulation 4 to 20 db LH, 1 to 2 db RH. Signal ends 145 seconds LH, 105 seconds RH (abruptly).
					NOTE:	Actual frequencies employed were 36.44 Mc, 145.76 Mc, and 874.56 Mc. RH and LH denote right- and left-hand polarization.

SECRET

TABLE C.44 SUMMARY OF 3-FREQUENCY PROPAGATION DATA, ROCKET 7, STAR FISH

PROJECT: 6.4
EVENT: Star Fish
ROCKET NO: 7
LAUNCH TIME & DATE: 0916:09 GMT 9 Jul 62

Data Recorded	Type of Recording	Van Number	Recorder Number	Channel Number	Reel Number	Remarks
Low-Frequency Dispersive Doppler	Magnetic tape Brush chart	2 2	2 2	7 4	5 -	Bias existed on dispersive doppler. Bias was eliminated with reasonable confidence. Dispersive doppler data 105 to 205 seconds. Lost 148-Mc signal at 205 seconds.
High-Frequency Dispersive Doppler	Magnetic tape Brush chart	2 2	2 2	8 5	5 -	No usable data.
Doppler Frequency (37 Mc)	Magnetic tape Varian chart	2 2	1 1	9 1	2 -	Duration was from rocket lift to 695 seconds. Much frequency drift especially during rocket staging.
Doppler Frequency (148 Mc)	Magnetic tape Varian chart	2 2	1 1	10 2	2 -	Duration was from rocket lift to 205 seconds. Much frequency drift especially during rocket staging.
Doppler Frequency (888 Mc)	Magnetic tape	2	1	11	2	Not used. Quality not evaluated. Duration from rocket lift to 70 seconds.

TABLE C.44 CONTINUED

PROJECT: 6.4
EVENT: Star Fish
ROCKET NO: 7
LAUNCH DATE & TIME: 0916:09 GMT 9 Jul 62

Data Recorded	Type of Recording	Van Number	Recorder Number	Channel Number	Reel Number	Remarks
Signal Level (37 Mc)	Brush chart	2	1	1, 2	-	Smooth signal decay entire flight. Spin modulation 2 to 4 db LH and RH. Signal ends 687 seconds LH, 692 seconds RH.
Signal Level (148 Mc)	Brush chart	2	1	3, 4	-	Smooth signal decay to 4th-stage ignition 70 seconds. Sharp drop LH and to receiver AGC threshold RH. Signal lost 70 to 74 seconds, 94 to 103 seconds RH. Intermittent recovery 74 to 94 seconds RH. Spin modulation 2 to 4 db LH and RH. Signal ends 110 seconds (4th-stage burnout) LH, 501 seconds RH.
Signal Level (888 Mc)	Brush chart	2	1	5, 6	-	Sharp signal decay to 4th-stage ignition 70 seconds LH, smooth decay to 70 seconds RH. Spin modulation 1 to 2 db LH, 2 to 6 db RH. No signal after 71 seconds LH and RH.

NOTE: Actual frequencies employed were 36.94 Mc, 147.76 Mc, and 886.56 Mc. RH and LH denote right- and left-hand polarization.

SECRET

TABLE C.45 SUMMARY OF 3-FREQUENCY PROPAGATION DATA, ROCKET 8, **STAR FISH**

PROJECT: 6.2
EVENT: Star Fish
ROCKET NO: 8
LAUNCH TIME & DATE: 0920:12 GMT 9 Jul 62

Data Recorded	Type of Recording	Van Number	Recorder Number	Channel Number	Reel Number	Remarks
Low-Frequency Dispersive Doppler	Not recorded directly; derived from other taped data.	3	1	1 to 6	7	Bias existed on dispersive doppler. Bias was eliminated with reasonable confidence. Dispersive doppler data 151 to 245 seconds. 37 Mc too noisy after 245 seconds.
High-Frequency Dispersive Doppler	Not recorded directly; derived from other taped data.	3	1	1 to 6	7	High-frequency dispersive doppler contained a rocket-spin-induced error which could not be successfully eliminated.
Doppler Frequency (37 Mc)	Magnetic tape	3	1	1, 2	7	Duration was from rocket lift to 510 seconds. The data was of good quality for 245 seconds and was used for derivation of dispersive doppler.
	Varian chart	3	1	1	-	
Doppler Frequency (148 Mc)	Magnetic tape	3	1	3, 4	7	Duration was from rocket lift to 830 seconds. The data was of good quality and was used for derivation of dispersive doppler.
	Varian chart	3	1	2	-	
Doppler Frequency (888 Mc)	Magnetic tape	3	1	5, 6	7	Not used. Quality not evaluated. Duration from rocket lift to 208 seconds.
Signal Level (37 Mc)	Magnetic tape	3	2	1, 2	8	Smooth signal decay entire flight. Spin modulation 2 to 8 db LH, 2 to 5 db RH. Signal ends 475 seconds LH, 250 seconds RH.
Signal Level (148 Mc)	Magnetic tape	3	2	3, 4	8	Smooth signal decay entire flight. Spin modulation 1 to 2 db LH, 1 to 4 db RH. Signal ends 650 seconds LH, 653 seconds RH.
Signal Level (888 Mc)	Magnetic tape	3	2	5, 6	8	Smooth signal decay entire flight. Spin modulation 2 to 6 db LH, 1 to 4 db RH. Signal ends 110 seconds (4th-stage burnout) LH, 265 seconds RH.

NOTE: Actual frequencies employed were 36.44 Mc, 145.76 Mc, and 874.56 Mc. RH and LH denote right- and left-hand polarization.

TABLE C.46 SUMMARY OF 3-FREQUENCY PROPAGATION DATA, ROCKET 9, **STAR FISH**

PROJECT: 6.2
EVENT: Star Fish
ROCKET NO: 9
LAUNCH TIME & DATE: 0940:09 GMT 9 Jul 62

Data Recorded	Type of Recording	Van Number	Recorder Number	Channel Number	Reel Number	Remarks
Low-Frequency Dispersive Doppler	Magnetic tape Brush chart	2 2	2 2	7 4	6 -	Bias existed on dispersive doppler. Bias eliminated with reasonable confidence. Dispersive doppler data 121 to 740 seconds. 37-Mc signal lost at 740 seconds.
High-Frequency Dispersive Doppler	Magnetic tape Brush chart	2 2	2 2	8 5	6 -	Good dispersive doppler data acquired from 121 to 240 seconds. Quality of data too poor to be usable after 240 seconds.
Doppler Frequency (37 Mc)	Magnetic tape Varian chart	2 2	1 1	9 1	3 -	Duration was from rocket lift to 810 seconds. Data was of fair quality and was partially used in derivation of dispersive doppler.
Doppler Frequency (148 Mc)	Magnetic tape Varian chart	2 2	1 1	10 2	3 -	Duration was from rocket lift to 860 seconds. Data was of good quality and was partially used in derivation of dispersive doppler.
Doppler Frequency (888 Mc)	Magnetic tape	2	1	11	3	Not used. Quality not evaluated. Duration from rocket lift to 420 seconds.

SECRET

TABLE C.46 CONTINUED

PROJECT: 6.2
EVENT: Star Fish
ROCKET NO: 9
LAUNCH TIME & DATE: 0940:09 GMT 9 Jul 62

Data Recorded	Type of Recording	Van Number	Recorder Number	Channel Number	Reel Number	Remarks
Signal Level (37 Mc)	Brush chart	2	1	1, 2	-	Only maximum signal plotted because of questionable calibration at minimum signal level. Smooth decay entire flight. Signal ends 800 seconds LH and RH.
Signal Level (148 Mc)	Brush chart	2	1	3, 4	-	Only maximum signal plotted (see 37-Mc AGC above). Smooth decay to 226 seconds. Lost signal 226 to 348 seconds LH. Signal ends 800 seconds LH and RH.
Signal Level (888 Mc)	Brush chart	2	1	5, 6	-	Sharp decay of maximum signal 10 to 30 seconds LH. Minimum signal below tracking filter AGC threshold 70 to 150 seconds LH. Spin modulation 2 to 10 db LH, 2 to 5 db RH. Signal ends 150 seconds LH, 350 seconds RH.
					NOTE:	Actual frequencies employed were 36.94 Mc, 147.76 Mc, and 886.56 Mc. RH and LH denote right- and left-hand polarization.

SECRET

TABLE C.47 SUMMARY OF 3-FREQUENCY PROPAGATION DATA, ROCKET 11, BLUE GILL

PROJECT: 6.3
EVENT: Blue Gill
ROCKET NO: 11
LAUNCH TIME & DATE: 0957:49 GMT 26 Oct 62

Data Recorded	Type of Recording	Van Number	Recorder Number	Channel Number	Reel Number	Remarks
Low-Frequency Dispersive Doppler	Magnetic tape	2	2	7	2	No ionization before 37-Mc blackout at 120 seconds. Signal too noisy to yield usable dispersive doppler after 37-Mc recovery.
	Brush chart	2	2	4	-	
High-Frequency Dispersive Doppler	Magnetic tape	2	2	8	2	No usable data.
	Brush chart	2	2	5	-	
Doppler Frequency (37 Mc)	Magnetic tape	2	1	9	1	Not used. Quality not evaluated. Duration from rocket lift to 120 seconds and from 210 to 282 seconds.
	Varian chart	2	1	1	-	
Doppler Frequency (148 Mc)	Magnetic tape	2	1	10	1	Not used. Quality not evaluated. Duration from rocket lift to 282 seconds.
	Varian chart	2	1	2	-	
Doppler Frequency (888 Mc)	Magnetic tape	2	1	11	1	Not used. Quality not evaluated. Duration from rocket lift to 248 seconds.

SECRET

TABLE C.47 CONTINUED

PROJECT: 6.3
EVENT: Blue Gill
ROCKET NO: 11
LAUNCH TIME & DATE: 0957:49 GMT 26 Oct 62

Data Recorded	Type of Recording	Van Number	Recorder Number	Channel Number	Reel Number	Remarks
Signal Level (37 Mc)	Brush chart	2	1	1, 2	-	Signal lost at burst 120 to 191 seconds LH, 120 to 186 seconds RH. Spin modulation 2 to 3 db both channels. Signal ends 272 seconds LH, 274 seconds RH.
Signal Level (148 Mc)	Brush chart	2	1	3, 4	-	Signal lost at burst 120 to 132 seconds LH, 120 to 129 seconds RH. Spin modulation 1 to 2 db LH, 2 to 4 db RH. Signal ends 302 seconds LH, 306 seconds RH.
Signal Level (888 Mc)	Brush chart	2	1	5, 6	-	Signal attenuation at burst 20 to 22 db LH, 8 to 10 db RH. Recovery 3 to 4 seconds. Spin modulation 2 to 10 db LH. Minimum signal below receiver AGC threshold after 20 seconds RH. Signal ends 257 seconds LH, 255 seconds RH.
						Telemetered Performance of 3-Frequency Beacon: Output power of 37-Mc stage was low, but 888-Mc output was normal. Slight package heating occurred on re-entry.
					NOTE:	Actual frequencies employed were 36.94 Mc, 147.76 Mc, and 886.56 Mc. RH and LH denote right- and left-hand polarization.

SECRET

TABLE C.48 SUMMARY OF 3-FREQUENCY PROPAGATION DATA, ROCKET 12, BLUE GILL

PROJECT: 6.3
EVENT: Blue Gill
ROCKET NO: 12
LAUNCH TIME & DATE: 1004:49 GMT 26 Oct 62

Data Recorded	Type of Recording	Van Number	Recorder Number	Channel Number	Reel Number	Remarks
Low-Frequency Dispersive Doppler	Magnetic tape Brush chart	3 2	1, 2 2	1 to 4 4	4 -	Good dispersive doppler data from 60 to 81 seconds and from 163 to 196 seconds.
High-Frequency Dispersive Doppler	Magnetic tape Brush chart	3 2	1, 2 2	3 to 6 5	4 -	No usable data.
Doppler Frequency (37 Mc)	Magnetic tape Varian chart	3 3	1, 2 1	1, 2 1	4 -	Not used. Quality not evaluated. Duration from rocket lift to 81 seconds and from 163 to 286 seconds.
Doppler Frequency (148 Mc)	Magnetic tape Varian chart	3 3	1, 2 1	3, 4 2	4 -	Not used. Quality not evaluated. Duration from rocket lift to 286 seconds.
Doppler Frequency (888 Mc)	Magnetic tape	3	1, 2	5, 6	4	Not used. Quality not evaluated. Duration from rocket lift to 270 seconds.
Signal Level (37 Mc)	Brush chart	3	1	1, 2	-	Signal attenuation due to absorption 60 to 80 seconds LH and RH. Signal below receiver AGC threshold 80 to 154 seconds LH, 80 to 155 seconds RH. Spin modulation 1 to 2 db. Signal ends 280 seconds LH and RH.

SECRET

TABLE C.48 CONTINUED

PROJECT: 6.3
EVENT: Blue Gill
ROCKET NO: 12
LAUNCH TIME & DATE: 1004:49 GMT 26 Oct 62

Data Recorded	Type of Recording	Van Number	Recorder Number	Channel Number	Reel Number	Remarks
Signal Level (148 Mc)	Brush chart	3	1	3, 4	-	Signal attenuation due to absorption 60 to 80 seconds LH, 60 to 90 seconds RH. Never reaches receiver AGC threshold. Spin modulation 1 to 2 db LH, 2 to 4 db RH. Signal ends 280 seconds LH and RH.
Signal Level (888 Mc)	Brush chart	3	1	5, 6	-	Smooth signal decay, no absorption effect visible. Spin modulation 2 to 6 db LH, 8 to 15 db RH. Signal ends 278 seconds LH, 270 seconds RH.
						Telemetered Performance of 3-Frequency Beacon: 37-Mc power dropped to zero 24 seconds after launch, but 888-Mc power remained normal. All telemetry signals were obscured by noise between 3 and 4 minutes after launch but recovered 266 seconds after launch (re-entry). Possible commutator failures.
						NOTE: Actual frequencies employed were 36.44 Mc, 145.76 Mc, and 874.56 Mc. RH and LH denote right and left-hand polarization.

SECRET

TABLE C.49 SUMMARY OF 3-FREQUENCY PROPAGATION DATA, ROCKET 14, BLUE GILL

PROJECT: 6.3
EVENT: Blue Gill
ROCKET NO: 14
LAUNCH TIME & DATE: 1010:59 GMT 26 Oct 62

Data Recorded	Type of Recording	Van Number	Recorder Number	Channel Number	Reel Number	Remarks
Low-Frequency Dispersive Doppler	Magnetic tape Brush chart	3 2	1, 2 2	1 to 4 4	4 -	Good dispersive doppler data except during 37-Mc blackout. Dispersive doppler data from 60 to 79 seconds and 230 to 244 seconds.
High-Frequency Dispersive Doppler	Magnetic tape Brush chart	3 2	1, 2 2	3 to 6 5	4 -	No usable data.
Doppler Frequency (37 Mc)	Magnetic tape Varian chart	3 3	1, 2 1	1, 2 1	4 -	Not used. Quality not evaluated. Duration from rocket lift to 79 seconds and from 230 to 302 seconds.
Doppler Frequency (148 Mc)	Magnetic tape Varian chart	3 3	1, 2 1	3, 4 2	4 -	Not used. Quality not evaluated. Duration from rocket lift to 302 seconds.
Doppler Frequency (888 Mc)	Magnetic tape	3	1, 2	5, 6	4	Not used. Quality not evaluated. Duration from rocket lift to 50 seconds.

SECRET

TABLE C.49 CONTINUED

PROJECT: 6.3
EVENT: Blue Gill
ROCKET NO: 14
LAUNCH TIME & DATE: 1010:59 GMT 26 Oct 62

Data Recorded	Type of Recording	Van Number	Recorder Number	Channel Number	Reel Number	Remarks
Signal Level (37 Mc)	Brush chart	3	1	1, 2	-	Signal attenuation due to absorption 60 to 80 seconds LH and RH. Signal below receiver AGC threshold 80 to 226 seconds LH, 80 to 220 seconds RH. Spin modulation 1 to 2 db. Signal ends 300 seconds LH, 302 seconds RH.
Signal Level (148 Mc)	Brush chart	3	1	3, 4	-	Signal attenuation due to absorption 60 to 100 seconds LH and RH. Never reaches receiver AGC threshold. Spin modulation 1 to 2 db. Signal ends 302 seconds LH, 301 seconds RH.
Signal Level (888 Mc)	Brush chart	3	1	5, 6	-	Signal less than -110 dbm on launcher. Spin modulation 4 to 8 db LH, 4 to 6 db RH. Signal ends 51 seconds LH (abruptly), 29 seconds RH.
						Telemetered Performance of 3-Frequency Beacon: Output power at 37 and 888 Mc were low before launch. All telemetry signals became unreadable 7 to 10 seconds after launch. Possible malfunction of monitor channel.
					NOTE:	Actual frequencies employed were 36.44 Mc, 145.76 Mc, and 874.56 Mc. RH and LH denote right- and left-hand polarization.

TABLE C.50 SUMMARY OF 3-FREQUENCY PROPAGATION DATA, ROCKET 15, **BLUE GILL**

PROJECT: 6.2
EVENT: Blue Gill
ROCKET NO: 15
LAUNCH TIME & DATE: 1014:49 GMT 26 Oct 62

Data Recorded	Type of Recording	Van Number	Recorder Number	Channel Number	Reel Number	Remarks
Low-Frequency Dispersive Doppler	Magnetic tape Brush chart	2 2	2 2	7 4	2 -	Good dispersive doppler for entire period rocket was in regions of ionization (54 to 312 seconds).
High-Frequency Dispersive Doppler	Magnetic tape Brush chart	2 2	2 2	8 5	2 -	No usable data.
Doppler Frequency (37 Mc)	Magnetic tape Varian chart	2 2	1 1	9 1	1 -	Not used. Quality not evaluated. Duration from rocket lift to 368 seconds.
Doppler Frequency (148 Mc)	Magnetic tape Varian chart	2 2	1 1	10 2	1 -	Not used. Quality not evaluated. Duration from rocket lift to 360 seconds.
Doppler Frequency (888 Mc)	Magnetic tape	2	1	11	1	Not used. Quality not evaluated. Duration from rocket lift to 96 seconds.
Signal Level (37 Mc)	Brush chart	2	1	1, 2	-	Sharp signal attenuation at third-stage burnout, 30 to 40 seconds followed by normal decay 40 to 60 seconds, LH and RH. Attenuation due to absorption 60 to 79 seconds LH, 60 to 85 seconds RH. Intermittent signal 79 to 125 seconds LH, 85 to 101 seconds RH. Signal ends 370 seconds LH and RH.
Signal Level (148 Mc)	Brush chart	2	1	3, 4	-	Sharp signal attenuation at third-stage burnout, 30 to 40 seconds followed by normal decay LH and RH. Spin modulation 1 to 4 db LH and RH. Signal ends 105 seconds LH, 330 seconds RH.
Signal Level (888 Mc)	Brush chart	2	1	5, 6	-	Sharp signal attenuation at third-stage burnout, 30 to 40 seconds LH and RH, followed by normal decay to 93 seconds and abrupt loss at 96 seconds LH. Signal ends 40 seconds RH. Spin modulation 2 to 8 db LH, 10 to 18 db RH.

NOTE: Actual frequencies employed were 36.94 Mc, 147.76 Mc, and 886.56 Mc. RH and LH denote right- and left-hand polarization.

SECRET

TABLE C.51 SUMMARY OF 3-FREQUENCY PROPAGATION DATA, ROCKET 17, BLUE GILL

PROJECT: 6.3
EVENT: Blue Gill
ROCKET NO: 17
LAUNCH TIME & DATE: 1021:49 GMT 26 Oct 62

Data Recorded	Type of Recording	Van Number	Recorder Number	Channel Number	Reel Number	Remarks
Low-Frequency Dispersive Doppler	Magnetic tape	3	1, 2	1 to 4	4	Good dispersive doppler from 67 to 110 seconds, at which time 37-Mc signal blacked out. No data retrieved after 37-Mc recovery.
	Brush chart	2	2	4	-	
High-Frequency Dispersive Doppler	Magnetic tape	3	1, 2	3 to 6	4	No usable data.
	Brush chart	2	2	5	-	
Doppler Frequency (37 Mc)	Magnetic tape	3	1, 2	1, 2	4	Not used. Quality not evaluated.
	Varian chart	3	1	1	-	
Doppler Frequency (148 Mc)	Magnetic tape	3	1, 2	3, 4	4	Not used. Quality not evaluated.
	Varian chart	3	1	2	-	
Doppler Frequency (888 Mc)	Magnetic tape	3	1, 2	5, 6	4	Not used. Quality not evaluated.
Signal Level (37 Mc)	Brush chart	3	1	1, 2	-	Signal attenuation due to absorption 60 to 100 seconds LH and RH. Signal below receiver threshold 100 to 194 seconds LH, 100 to 197 seconds RH. Spin modulation 1 to 2 db LH and RH. Signal ends 287 seconds LH, 291 seconds RH.

SECRET

TABLE C.51 CONTINUED

PROJECT: 6.3
EVENT: Blue Gill
ROCKET NO: 17
LAUNCH TIME & DATE: 1021:49 GMT 26 Oct 62

Data Recorded	Type of Recording	Van Number	Recorder Number	Channel Number	Reel Number	Remarks
Signal Level (148 Mc)	Brush chart	3	1	3, 4	-	Slight signal attenuation due to absorption 60 to 100 seconds LH only. Never reaches receiver AGC threshold. Spin modulation 1 to 2 db LH, 2 to 8 db RH. Signal ends 284 seconds LH and RH.
Signal Level (888 Mc)	Brush chart	3	1	5, 6	-	Smooth signal decay, no absorption effect visible. Minimum signal below receiver AGC threshold after 25 seconds LH. Spin modulation 15 to 25 db LH, 2 to 10 db RH. Signal ends 265 seconds LH, 255 seconds RH.
						Telemetered Performance of 3-Frequency Beacon: Output at 37 Mc was low for entire flight, but other signals were normal.
					NOTE:	Actual frequencies employed were 36.44 Mc, 145.76 Mc, and 874.56 Mc. RH and LH denote right- and left-hand polarization.

SECRET

TABLE C.52 SUMMARY OF 3-FREQUENCY PROPAGATION DATA, ROCKET 18, BLUE GILL

PROJECT: 6.2
EVENT: Blue Gill
ROCKET NO: 18
LAUNCH TIME & DATE: 1030:49 GMT 26 Oct 62

Data Recorded	Type of Recording	Van Number	Recorder Number	Channel Number	Reel Number	Remarks
Low-Frequency	Magnetic tape	2	2	7	2	Level of ionization too low to produce dispersive doppler.
Dispersive Doppler	Brush chart	2	2	4	-	
High-Frequency	Magnetic tape	2	2	8	2	Level of ionization too low to produce dispersive doppler.
Dispersive Doppler	Brush chart	2	2	5	-	
Doppler Frequency (37 Mc)	Magnetic tape	2	1	9	1	Not used. Quality not evaluated. Duration from rocket lift to 244 seconds.
	Varian chart	2	1	1	-	
Doppler Frequency (148 Mc)	Magnetic tape	2	1	10	1	Not used. Quality not evaluated. Duration from rocket lift to 244 seconds.
	Varian chart	2	1	2	-	
Doppler Frequency (888 Mc)	Magnetic tape	2	1	11	1	Not used. Quality not evaluated. Duration from rocket lift to 246 seconds.
Signal Level (37 Mc)	Brush chart	2	1	1, 2	-	Sharp signal attenuation after third-stage burnout, 28 to 30 seconds LH and RH, followed by normal decay to end. Spin modulation 2 to 8 db LH, 4 to 10 db RH. Signal ends 238 seconds LH, 230 seconds RH.
Signal Level (148 Mc)	Brush chart	2	1	3, 4	-	Slight signal attenuation after third-stage burnout, 28 to 31 seconds LH and RH followed by slow recovery. Spin modulation 1 to 10 db LH and RH. Signal ends 238 seconds LH, 230 seconds RH.
Signal Level (888 Mc)	Brush chart	2	1	5, 6	-	Signal nulls 30 to 40 db during third-stage burning 25 to 30 seconds LH. Signal lost 85 to 147 seconds LH, 100 to 110 seconds RH. Spin modulation 4 to 6 db LH, 20 to 30 db RH. Signal ends 246 seconds LH, 206 seconds RH.

NOTE: Actual frequencies employed were 36.94 Mc, 147.76 Mc, and 886.56 Mc. RH and LH denote right- and left-hand polarization.

TABLE C.53 SUMMARY OF 3-FREQUENCY PROPAGATION DATA, ROCKET 19, KING FISH

PROJECT: 6.2
EVENT: King Fish
ROCKET NO: 19
LAUNCH TIME & DATE: 1208:06 GMT 1 Nov 62

Data Recorded	Type of Recording	Van Number	Recorder Number	Channel Number	Reel Number	Remarks
Low-Frequency Dispersive Doppler	Magnetic tape Brush chart	2 2	2 2	7 4	6 -	No ionization prior to 37-Mc blackout at 120 seconds. Good dispersive doppler after 37-Mc recovery, 161 to 340 seconds.
High-Frequency Dispersive Doppler	Magnetic tape Brush chart	2 2	2 2	8 5	6 -	No ionization prior to 148-Mc blackout at 120 seconds. Good dispersive doppler after 148-Mc recovery, 142 to 330 seconds.
Doppler Frequency (37 Mc)	Magnetic tape Varian chart	2 2	1 1	9 1	5 -	Duration from rocket lift to 405 seconds. Excessive frequency drift—otherwise good. Used to derive dispersive doppler to verify analog dispersive doppler.
Doppler Frequency (148 Mc)	Magnetic tape Varian chart	2 2	1 1	10 2	5 -	Duration from rocket lift to 405 seconds. Excessive frequency drift—otherwise good. Used to derive dispersive doppler to verify analog chart dispersive doppler.
Doppler Frequency (888 Mc)	Magnetic tape	2	1	11	5	Duration from rocket lift to 405 seconds. Excessive frequency drift—otherwise fairly good. Used to derive dispersive doppler to verify analog dispersive doppler.

SECRET

TABLE C.53 CONTINUED

PROJECT: 6.2
EVENT: King Fish
ROCKET NO: 19
LAUNCH TIME & DATE: 1208:06 GMT 1 Nov 62

Data Recorded	Type of Recording	Van Number	Recorder Number	Channel Number	Reel Number	Remarks
Signal Level (37 Mc)	Brush chart	2	1	1, 2	-	Smooth signal decay to burst (120 seconds). Signal drops below receiver AGC threshold 120 to 165 seconds LH, 120 to 164 seconds RH. Both recover to pre-burst level by 190 seconds. Spin modulation 2 to 6 db LH and RH. Signal ends 405 seconds LH, 404 seconds RH.
Signal Level (148 Mc)	Brush chart	2	1	3, 4	-	LH signal unreadable after 65 seconds due to severe interference. Smooth signal decay to burst (120 seconds), drops below receiver AGC threshold 120 to 125 seconds RH. Recovers to pre-burst level by 170 seconds RH. Spin modulation 2 to 4 db LH, 3 to 15 db RH. Signal ends 65 seconds LH, 410 seconds RH.
Signal Level (888 Mc)	Brush chart	2	1	5, 6	-	Both LH and RH drop to tracking filter AGC threshold at burst (120 seconds) but recover to pre-burst level within 1 to 2 seconds. Spin modulation 4 to 6 db LH, 6 to 20 db RH. Signal ends 405 seconds LH, 407 seconds RH.
					NOTE:	Actual frequencies employed were 36.94 Mc and 886.56 Mc. RH and LH denote right-and left-hand polarization.

SECRET

TABLE C.54 SUMMARY OF 3-FREQUENCY PROPAGATION DATA, ROCKET 22, **KING FISH**

PROJECT: 6.4
EVENT: King Fish
ROCKET NO: 22
LAUNCH TIME & DATE: 1209:06 GMT 1 Nov 62

Data Recorded	Type of Recording	Van Number	Recorder Number	Channel Number	Reel Number	Remarks
Low-Frequency Dispersive Doppler	Magnetic tape Brush chart	3 2	1, 2 2	1 to 4 4	7 -	Good dispersive doppler throughout period of ionization from 110 to 350 seconds.
High-Frequency Dispersive Doppler	Magnetic tape Brush chart	3 2	1, 2 2	3 to 6 5	7 -	No usable data.
Doppler Frequency (37 Mc)	Magnetic tape Varian chart	3 3	1, 2 1	1, 2 1	7 -	Duration from rocket lift to 405 seconds. No apparent frequency drift—good quality.
Doppler Frequency (148 Mc)	Magnetic tape Varian chart	3 3	1, 2 1	3, 4 2	7 -	Duration from rocket lift to 410 seconds. No apparent frequency drift—good quality—used for trajectory determination.
Doppler Frequency (888 Mc)	Magnetic tape	3	1	5, 6	7	Not used. Quality not evaluated.
Signal Level (37 Mc)	Brush chart	3	1	1, 2	-	Smooth signal decay to fourth-stage ignition, when LH and RH spin modulation increases from 2 db to 10 to 12 db, 70 to 110 seconds. Spin modulation 1 to 2 db by 140 seconds. Signal ends 406 seconds LH, 405 seconds RH (second stage failed to ignite).
Signal Level (148 Mc)	Brush chart	3	1	3, 4	-	Smooth signal decay to fourth-stage ignition, when minimum signal drops 8 to 10 db by 80 seconds LH and RH. Spin modulation 1 to 2 db by 100 seconds. Signal ends 404 seconds LH and RH (second stage failed to ignite).

TABLE C.54 CONTINUED

PROJECT: 6.4
EVENT: King Fish
ROCKET NO: 22
LAUNCH TIME & DATE: 1209:06 GMT 1 Nov 62

Data Recorded	Type of Recording	Van Number	Recorder Number	Channel Number	Reel Number	Remarks
Signal Level (888 Mc)	Brush chart	3	1	5, 6	-	LH signal smooth to 141 seconds (nose cone ejection) when maximum signal increases 6 db. Minimum signal below receiver AGC threshold after 30 seconds LH. Smooth signal decay to 95 seconds RH. Signal abruptly drops below receiver AGC threshold 95 seconds, abrupt recovery at 145 seconds RH. Signal ends 360 seconds LH, 395 seconds RH (second stage failed to ignite). Telemetered Performance of 3-Frequency Beacon: The 37-Mc output power gradually increased from a low-pre-launch value of 50 mw to 180 mw 94 seconds after launch and again decreased to 80 mw at 6 minutes after launch. The 888-Mc output power remained relatively constant. An unexplained abrupt increase in beacon package temperature occurred at 150 seconds after launch (from 25°C to 60°C). NOTE: Actual frequencies employed were 36.44 Mc, 145.76 Mc, and 874.56 Mc. RH and LH denote right- and left-hand polarization.

SECRET

TABLE C.55 SUMMARY OF 3-FREQUENCY PROPAGATION DATA, ROCKET 25, **KING FISH**

PROJECT: 6.4
EVENT: King Fish
ROCKET NO: 25
LAUNCH TIME & DATE: 1219:08 GMT 1 Nov 62

Data Recorded	Type of Recording	Van Number	Recorder Number	Channel Number	Reel Number	Remarks
Low-Frequency Dispersive Doppler	Magnetic tape	2	2	7	6	Dispersive doppler data available from 82 to 255 seconds. Accuracy of data somewhat questionable because of poor quality of 37-Mc signal.
	Brush chart	2	2	4	-	
High-Frequency Dispersive Doppler	Magnetic tape	2	2	8	6	Good dispersive doppler data from 82 to 290 seconds. No usable data after 290 seconds.
	Brush chart	2	2	5	-	
Doppler Frequency (37 Mc)	Magnetic tape	2	1	9	5	Not used. Quality not evaluated. Duration from rocket lift to 770 seconds.
	Varian chart	2	1	1	-	
Doppler Frequency (148 Mc)	Magnetic tape	2	1	10	5	Not used. Quality not evaluated. Duration from rocket lift to 775 seconds.
	Varian chart	2	1	2	-	
Doppler Frequency (888 Mc)	Magnetic tape	2	1	11	5	Not used. Quality not evaluated. Duration from rocket lift to 785 seconds.
Signal Level (37 Mc)	Brush chart	2	1	1, 2	-	Smooth signal decay to third-stage ignition (25 seconds) when abrupt drop 10 to 12 db lasts until fourth-stage ignition (70 seconds). Sharp recovery at 70 seconds LH and RH. Spin modulation 2 to 20 db LH, 2 to 6 db RH. Signal ends 773 seconds LH, 775 seconds RH.

SECRET

TABLE C.55 CONTINUED

PROJECT: 6.4
EVENT: King Fish
ROCKET NO: 25
LAUNCH TIME & DATE: 1219:08 GMT 1 Nov 62

Data Recorded	Type of Recording	Van Number	Recorder Number	Channel Number	Reel Number	Remarks
Signal Level (148 Mc)	Brush chart	2	1	3, 4	-	Smooth signal decay to third-stage ignition (25 seconds), sharp drop 5 to 6 db, sharp recovery at 70 seconds LH and RH. Spin modulation 2 to 3 db LH, 1 to 2 db RH. Signal ends 770 seconds LH, 773 seconds RH.
Signal Level (888 Mc)	Brush chart	2	1	5, 6	-	Smooth signal decay to third-stage ignition (25 seconds), sharp drop 4 to 6 db, sharp recovery at 70 seconds LH and RH. Minimum signal below receiver AGC threshold after 70 seconds RH. Spin modulation 1 to 2 db LH, 2 to 20 db RH. Signal ends 784 seconds LH, 150 seconds RH.
					NOTE:	Actual frequencies employed were 36.94 Mc, 147.76 Mc, and 886.56 Mc. RH and LH denote right- and left-hand polarization.

TABLE C.56 SUMMARY OF 3-FREQUENCY PROPAGATION DATA, ROCKET 27, KING FISH

PROJECT: 6.3
EVENT: King Fish
ROCKET NO: 27
LAUNCH TIME & DATE: 1223:36 GMT 1 Nov 62

Data Recorded	Type of Recording	Van Number	Recorder Number	Channel Number	Reel Number	Remarks
Low-Frequency Dispersive Doppler	Magnetic tape Brush chart	3 2	1, 2 2	1 to 4 4	7 -	Continuous dispersive doppler data of good quality for entire duration of period of ionization from 56 to 340 seconds.
High-Frequency Dispersive Doppler	Magnetic tape Brush chart	3 2	1, 2 2	3 to 6 5	7 -	Dispersive doppler data was of poor quality. Measurements not made in view of excellent low-frequency dispersive doppler.
Doppler Frequency (37 Mc)	Magnetic tape Varian chart	3 3	1, 2 1	1, 2 1	7 -	Not used. Quality not evaluated. Duration from rocket lift to 390 seconds.
Doppler Frequency (148 Mc)	Magnetic tape Varian chart	3 3	1, 2 1	3, 4 2	7 -	Not used. Quality not evaluated. Duration from rocket lift to 390 seconds.
Doppler Frequency (888 Mc)	Magnetic tape	3	1	5, 6	7	Not used. Quality not evaluated. Duration from rocket lift to 390 seconds.
Signal Level (37 Mc)	Brush chart	3	1	1, 2	-	Smooth decay to 62 seconds (ion trap, RF probe deployment) when 2- to 4-db drop occurs, LH and RH. Slow recovery to 120 seconds. Spin modulation 2 to 6 db LH, 2 to 4 db RH. Signal ends 390 seconds LH and RH.

TABLE C.56 CONTINUED

PROJECT: 6.3
EVENT: King Fish
ROCKET NO: 27
LAUNCH TIME & DATE: 1223:36 GMT 1 Nov 62

Data Recorded	Type of Recording	Van Number	Recorder Number	Channel Number	Reel Number	Remarks
Signal Level (148 Mc)	Brush chart	3	1	3, 4	-	Smooth signal decay to 62 seconds (ion trap, RF probe deployment) when 4-to 6-db drop occurs LH and RH. Slow recovery to 120 seconds. Spin modulation 2 to 3 db LH and RH. Signal ends 390 seconds LH, 391 seconds RH.
Signal Level (888 Mc)	Brush chart	3	1	5, 6	-	Smooth signal decay, no ion trap effect. Minimum signal below receiver AGC threshold after 30 seconds LH. Spin modulation 4 to 20 db LH, 2 to 5 db RH. Signal ends 380 seconds LH, 391 seconds RH.
					NOTE:	Actual frequencies employed were 36.44 Mc, 145.76 Mc, and 874.56 Mc. RH and LH denote right- and left-hand polarization.

SECRET

TABLE C.57 SUMMARY OF 3-FREQUENCY PROPAGATION DATA, ROCKET 28, **KING FISH**

PROJECT: 6.3
EVENT: King Fish
ROCKET NO: 28
LAUNCH TIME & DATE: 1250:06 GMT 1 Nov 62

Data Recorded	Type of Recording	Van Number	Recorder Number	Channel Number	Reel Number	Remarks
Low-Frequency Dispersive Dopper	Magnetic tape Brush chart	3 2	1, 2 2	1 to 4 4	7 -	Good dispersive doppler from 63 to 162 seconds and 295 to 330 seconds. Quality of data made measurement impossible 162 to 295 seconds.
High-Frequency Dispersive Doppler	Magnetic tape Brush chart	3 2	1, 2 2	3 to 6 5	7 -	No usable data.
Doppler Frequency (37 Mc)	Magnetic tape Varian chart	3 3	1, 2 1	1, 2 1	7 -	Not used. Quality not evaluated. Duration from rocket lift to 395 seconds.
Doppler Frequency (148 Mc)	Magnetic tape Varian chart	3 3	1, 2 1	3, 4 2	7 -	Not used. Quality not evaluated. Duration from rocket lift to 390 seconds.
Doppler Frequency (888 Mc)	Magnetic tape	3	1	5, 6	7	Not used. Quality not evaluated. Duration from rocket lift to 385 seconds.
Signal Level (37 Mc)	Brush chart	3	1	1, 2	-	Smooth signal decay, no ion trap effect. Spin modulation 1 to 2 db LH, 1 to 4 db RH. Signal ends 389 seconds LH and RH.
Signal Level (148 Mc)	Brush chart	3	1	3, 4	-	Smooth signal decay to 62 seconds (ion trap, RF probe deployment) when 2- to 3-db drop occurs, LH and RH. Recovery by 200 seconds LH, 80 seconds RH. Spin modulation 2 to 4 db LH, 4 to 16 db RH. Signal ends 385 seconds LH, 384 seconds RH.
Signal Level (888 Mc)	Brush chart	3	1	5, 6	-	Smooth signal decay, no ion trap effect. Minimum signal below receiver AGC threshold 30 to 60 seconds, 300 seconds to end, LH. Spin modulation 6 to 20 db LH, 2 to 5 db RH. Signal ends 370 seconds LH, 363 seconds RH.

NOTE: Actual frequencies employed were 36.44 Mc, 145.76 Mc, and 874.56 Mc. RH and LH denote right- and left-hand polarization.

SECRET

TABLE C.58 SUMMARY OF 3-FREQUENCY PROPAGATION DATA, ROCKET 29, KING FISH

PROJECT: 6.2
EVENT: King Fish
ROCKET NO: 29
LAUNCH TIME & DATE: 1235:06 GMT 1 Nov 62

Data Recorded	Type of Recording	Van Number	Recorder Number	Channel Number	Reel Number	Remarks
Low-Frequency	Magnetic tape	2	2	7	6	Level of ionization too low to produce any
Dispersive Doppler	Brush chart	2	2	4	-	dispersive doppler.
High-Frequency	Magnetic tape	2	2	8	6	Level of ionization too low to produce any
Dispersive Doppler	Brush chart	2	2	5	-	dispersive doppler.
Doppler Frequency (37 Mc)	Magnetic tape	2	1	9	5	Not used. Quality not evaluated. Duration from
	Varian chart	2	1	1	-	rocket lift to 275 seconds.
Doppler Frequency (148 Mc)	Magnetic tape	2	1	10	5	Not used. Quality not evaluated. Duration from
	Varian chart	2	1	2	-	rocket lift to 275 seconds.
Doppler Frequency (888 Mc)	Magnetic tape	2	1	11	5	Not used. Quality not evaluated. Duration from rocket lift to 275 seconds.
Signal Level (37 Mc)	Brush chart	2	1	1, 2	-	Severe signal drop after 30 seconds LH; no signal after 50 seconds LH. Smooth signal decay RH. Spin modulation 1 to 2 db LH, 1 to 5 RH. Signal ends 50 seconds LH, 274 seconds RH (second stage failed to ignite).

TABLE C.58 CONTINUED

PROJECT: 6.2
EVENT: King Fish
ROCKET NO: 29
LAUNCH TIME & DATE: 1235:06 GMT 1 Nov 62

Data Recorded	Type of Recording	Van Number	Recorder Number	Channel Number	Reel Number	Remarks
Signal Level (148 Mc)	Brush chart	2	1	3, 4	-	Smooth signal decay LH and RH. Spin modulation 2 to 5 db LH, 2 to 8 db RH. Signal ends 274 seconds LH, 275 seconds RH (second stage failed to ignite).
Signal Level (888 Mc)	Brush chart	2	1	5, 6	-	Smooth signal decay to 65 seconds. Signal below receiver AGC threshold 65 to 95 seconds LH, 65 to 140 seconds RH. Recovery almost to launch value at 225 seconds LH and RH. Spin modulation 2 to 4 db LH, 2 to 8 db RH. Signal ends 274 seconds LH, 275 seconds RH (second stage failed to ignite).
					NOTE:	Actual frequencies employed were 36.94 Mc, 147.76 Mc, and 886.56 Mc. RH and LH denote right- and left-hand polarization.

SECRET

TABLE C.59 THREE-FREQUENCY, VHF TM AND GMD SYSTEM PARAMETERS FOR STAR FISH

	Three-Frequency Experiment			VHF TM	GMD
Frequency, Mc	37	148	888	240	1680
Rocket Transmitter Power, mw	135	160	130	2000	1000
Rocket Transmitter Power, dbm	21	22	21	33	30
Rocket Transmitter Gain over Isotropic, db	-13	-1	-3	0	-3
Receiver Antenna Gain over Isotropic, db	1	7	7	12	26
Propagation Attenuation at 1 km, db	-65	-77	-93	-81	-98
Received signal at 1 km, dbm	-54	-49	-68	-36	-45

Figure C.1 Photograph of 37-Mc crossed dipole antenna. (BRL photo)

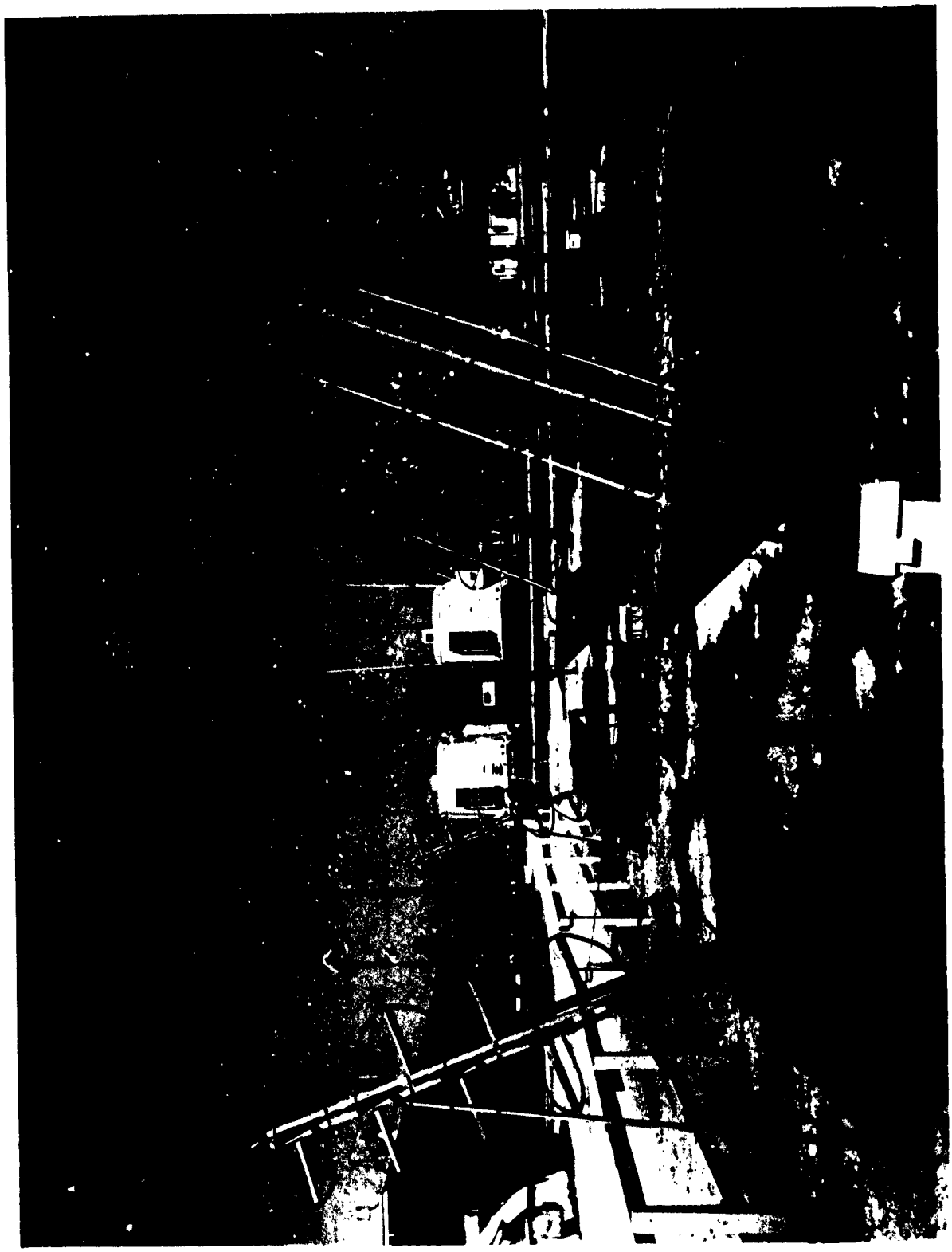

Figure C.2 Photograph of 148-Mc helix antennas. (BRL photo)

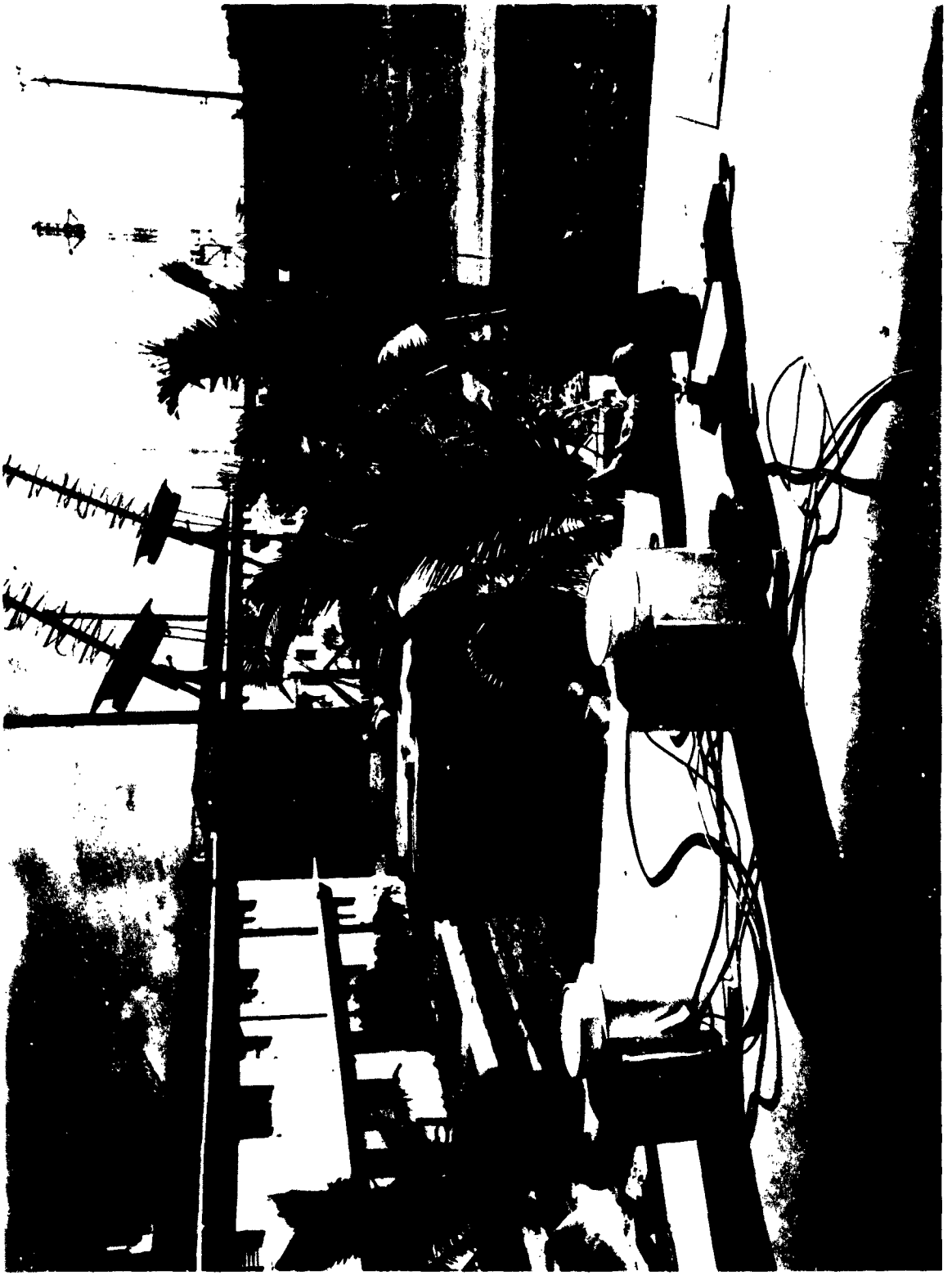

Figure C.3 Photograph of 888-Mc helix antennas. (BRL photo)

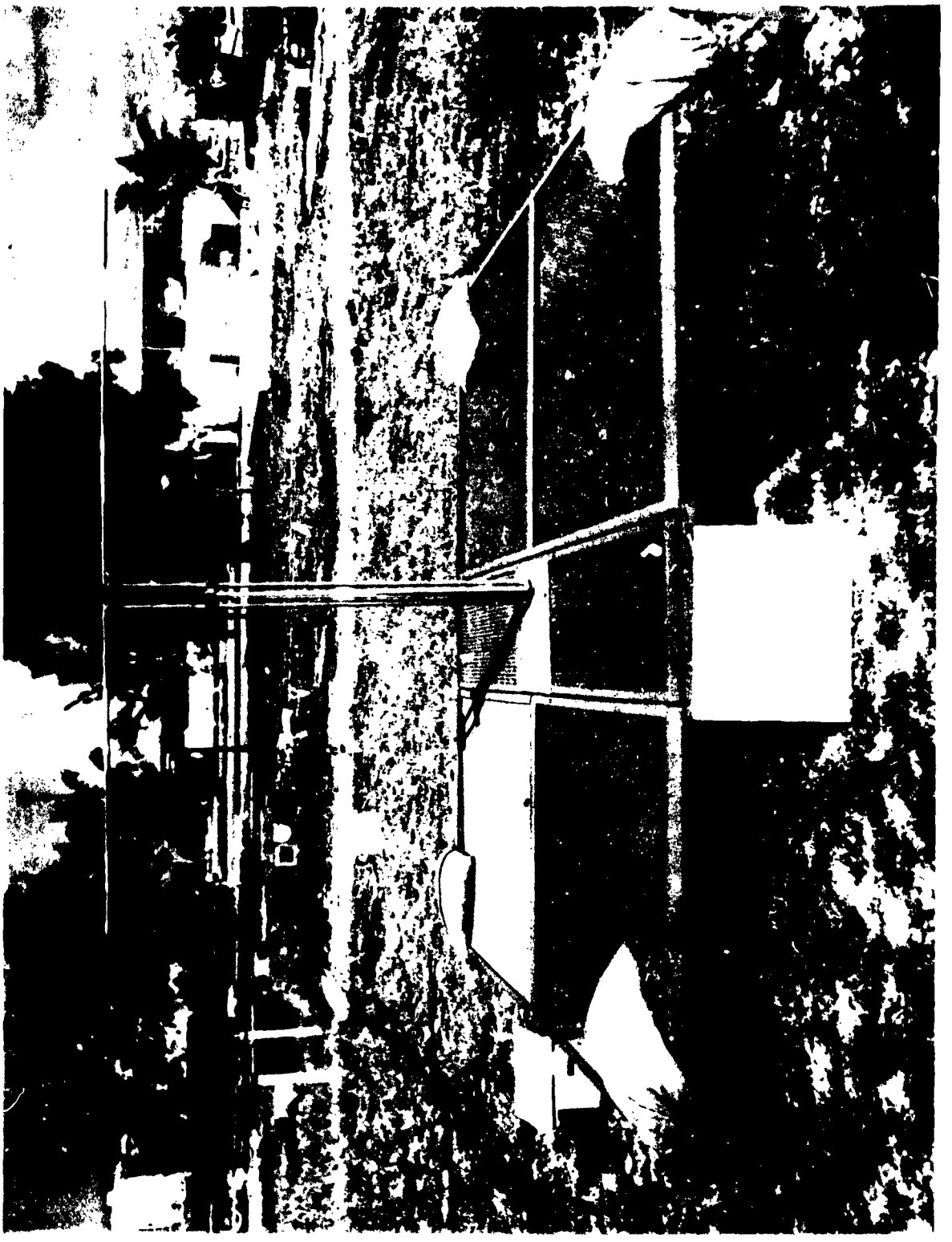

Figure C.4 Photograph of 54-Mc rotating dipole antenna. (BRL photo)

Figure C.5 Photograph of 324-Mc helix antenna. (BRL photo)

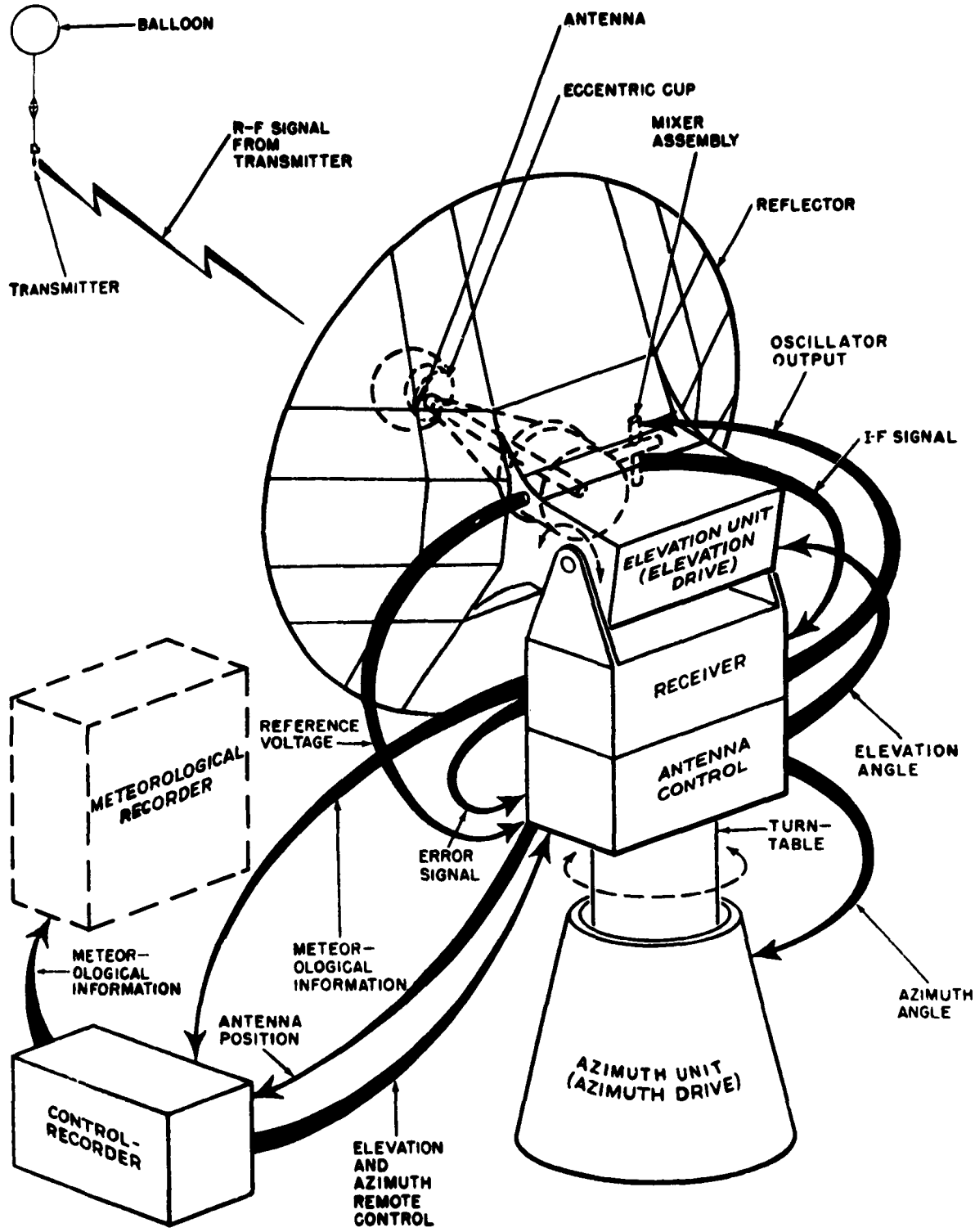

Figure C.6 GMD system functional diagram.

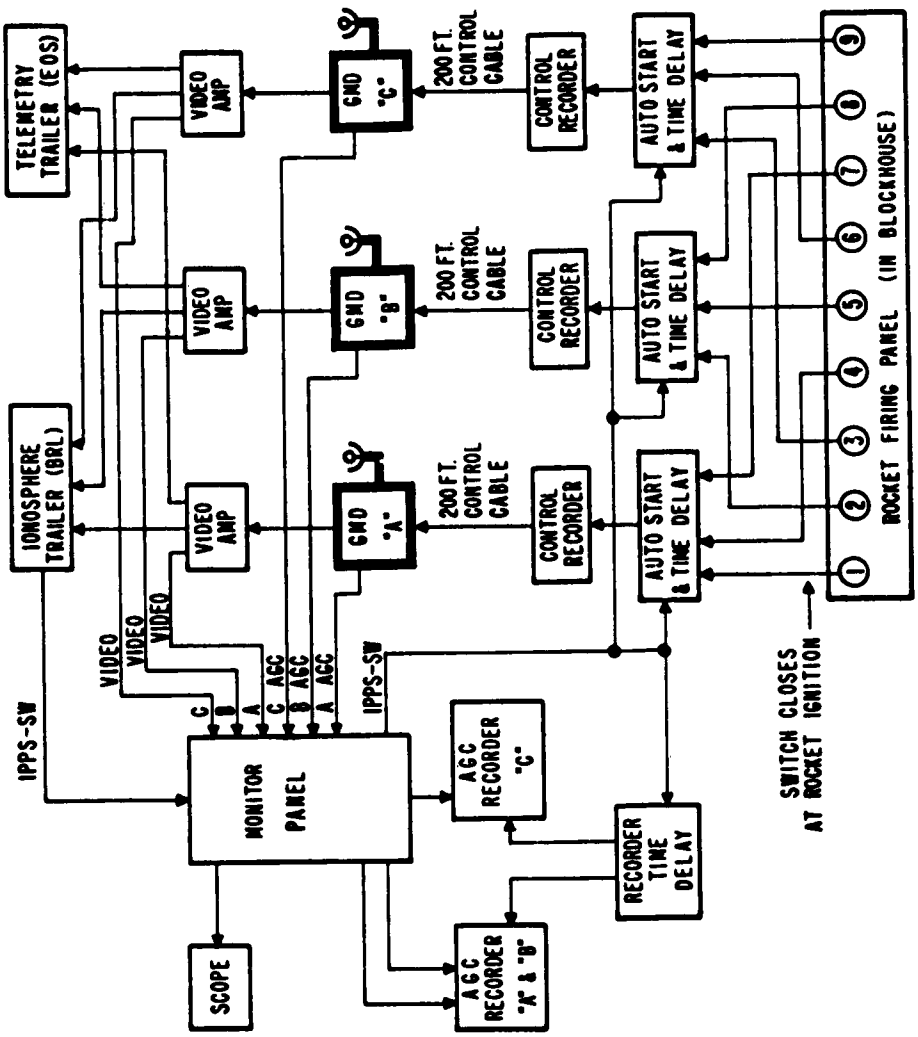

Figure C.7 Block diagram of GMD system.

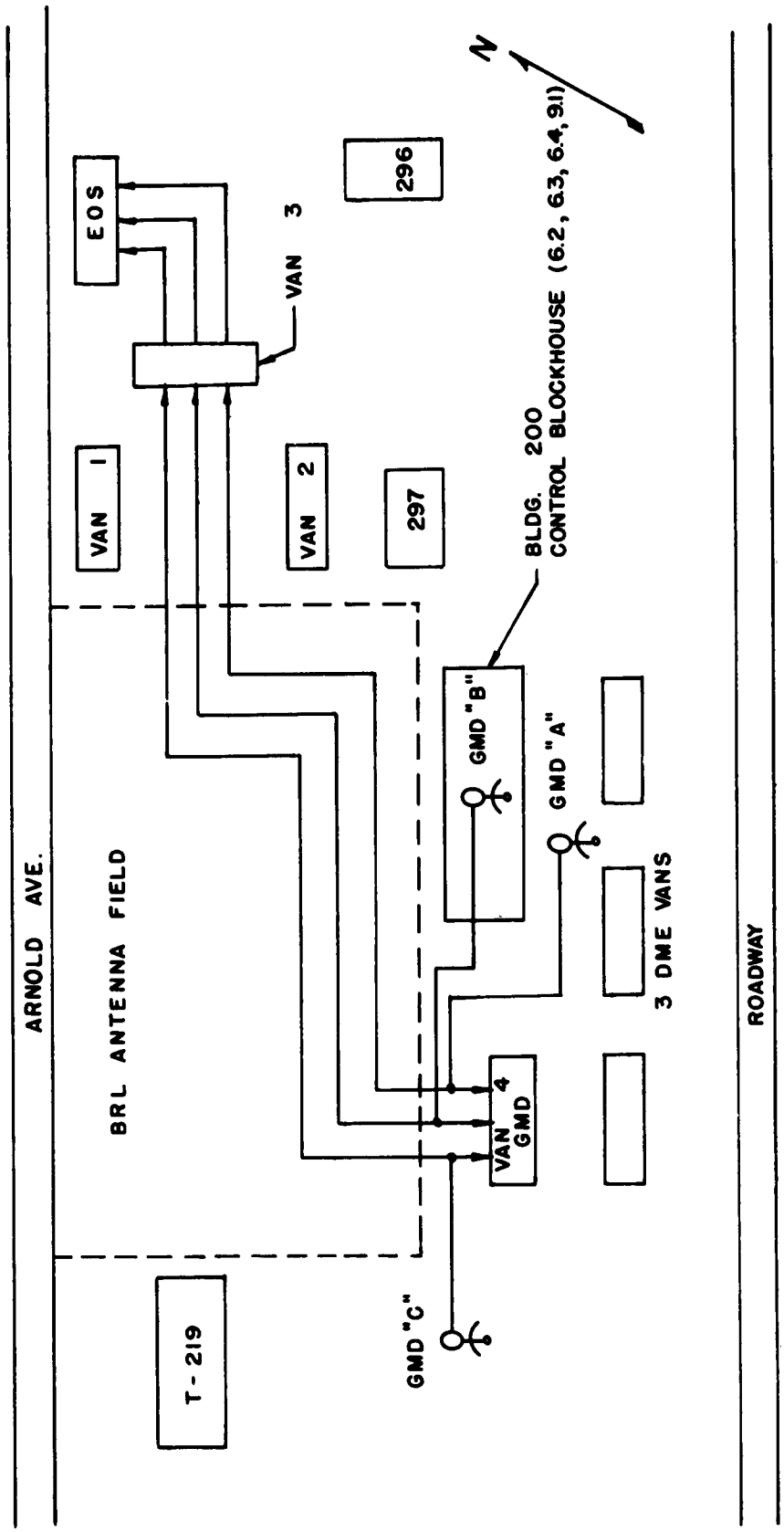

Figure C.8 Field layout of GMD trackers.

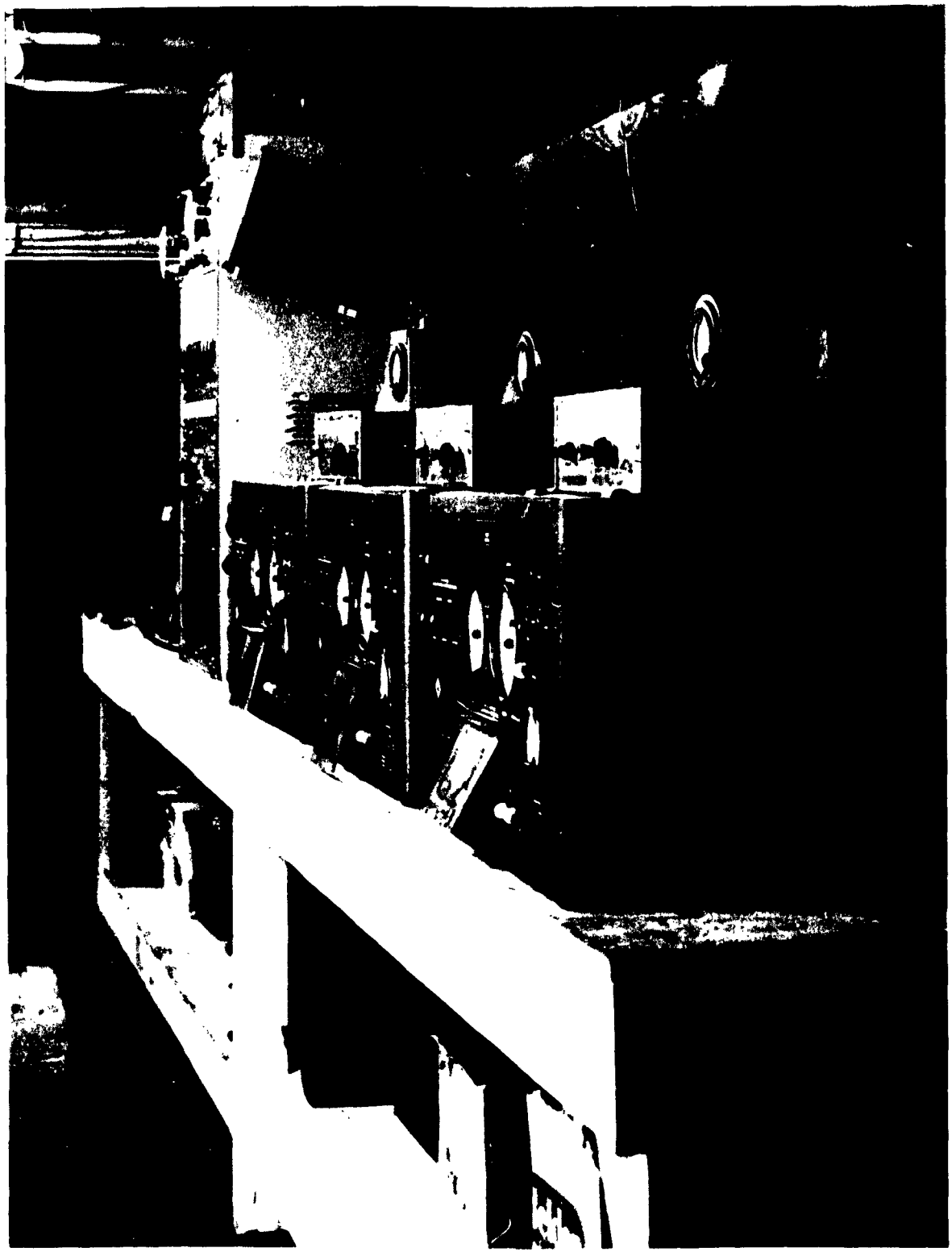

Figure C.9 GMD recording van interior. (BLR photo)

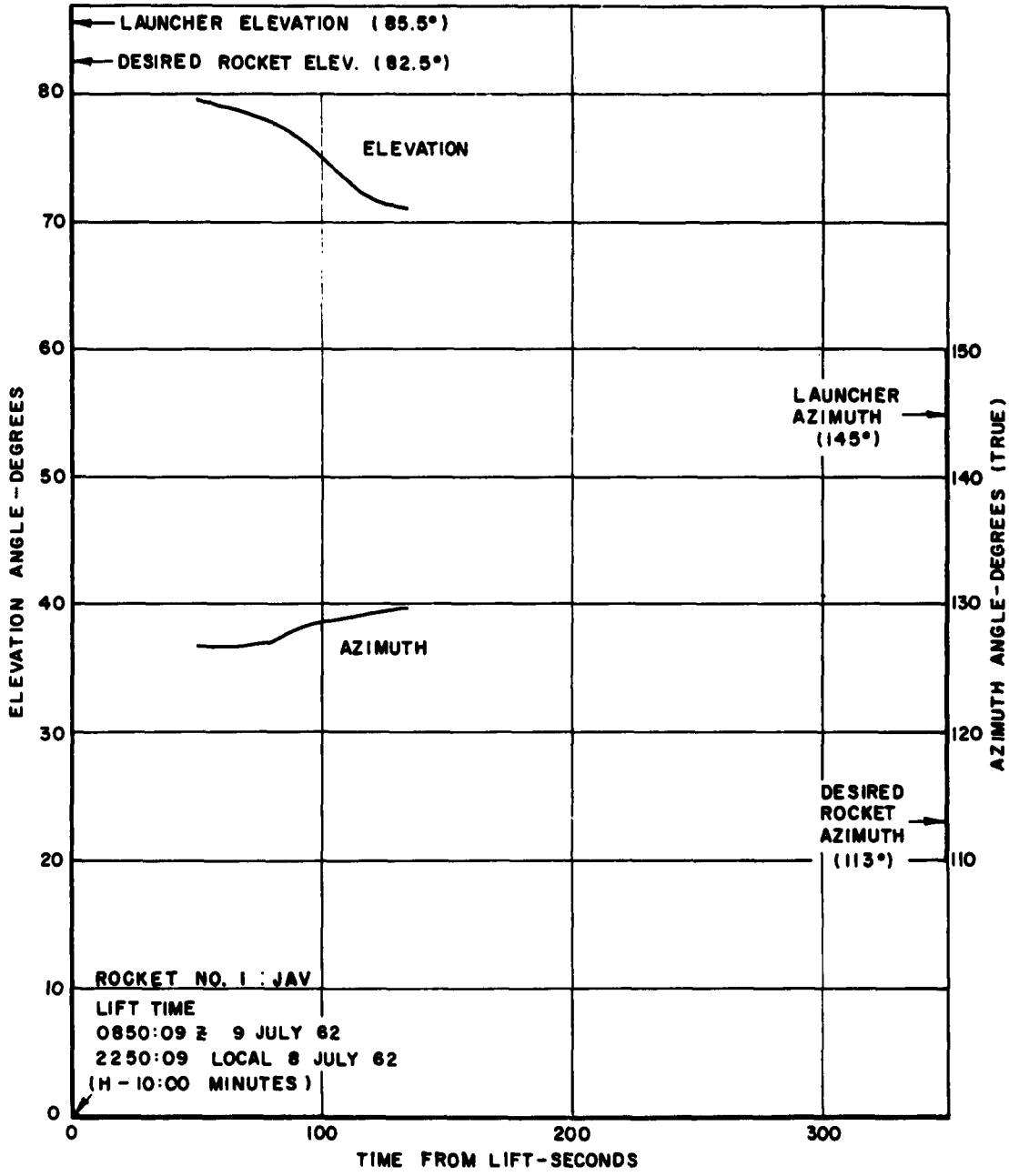

Figure C.10 GMD azimuth and elevation versus time for Rocket 1, Star Fish.

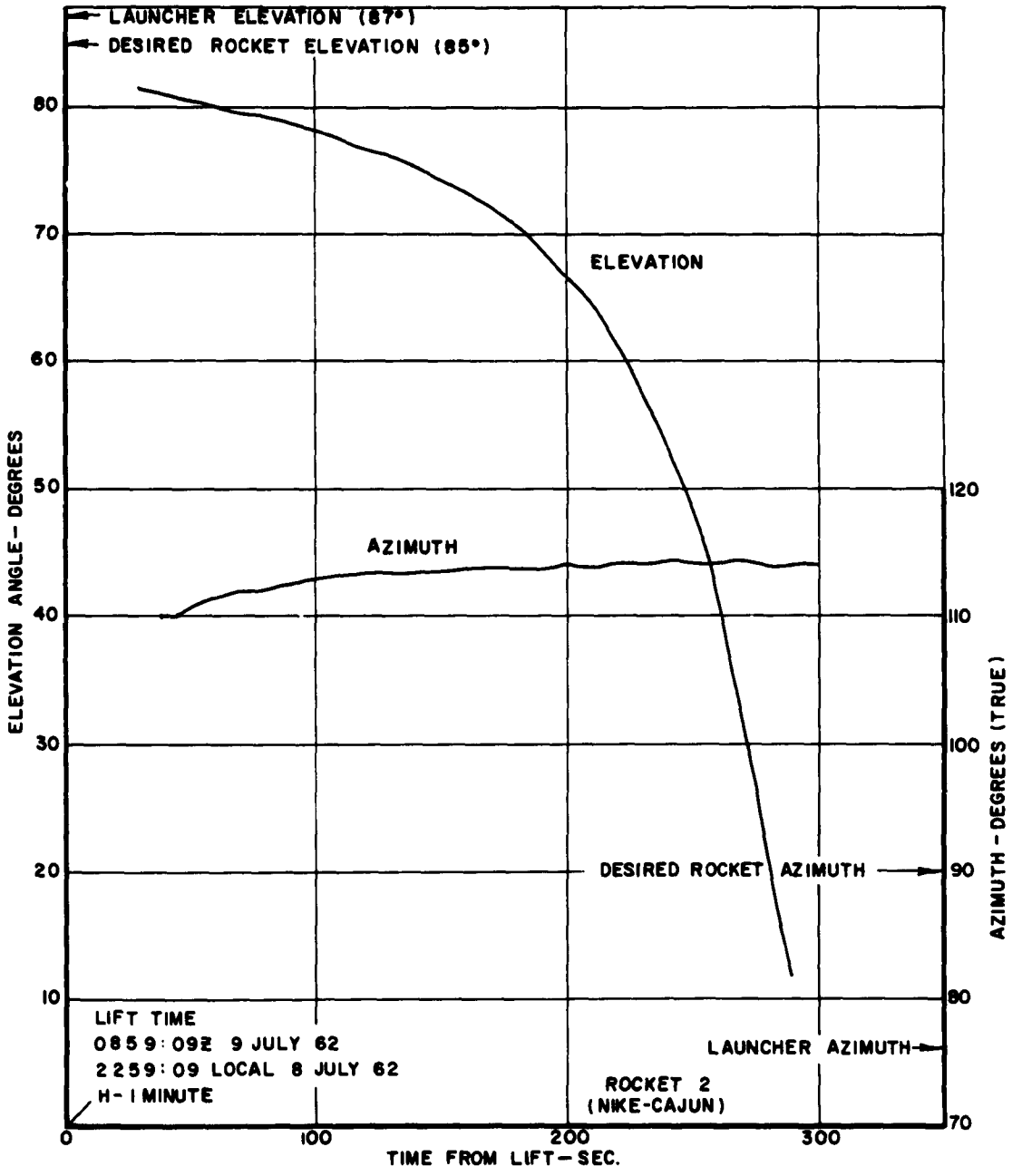

Figure C.11 GMD azimuth and elevation versus time for Rocket 2, Star Fish.

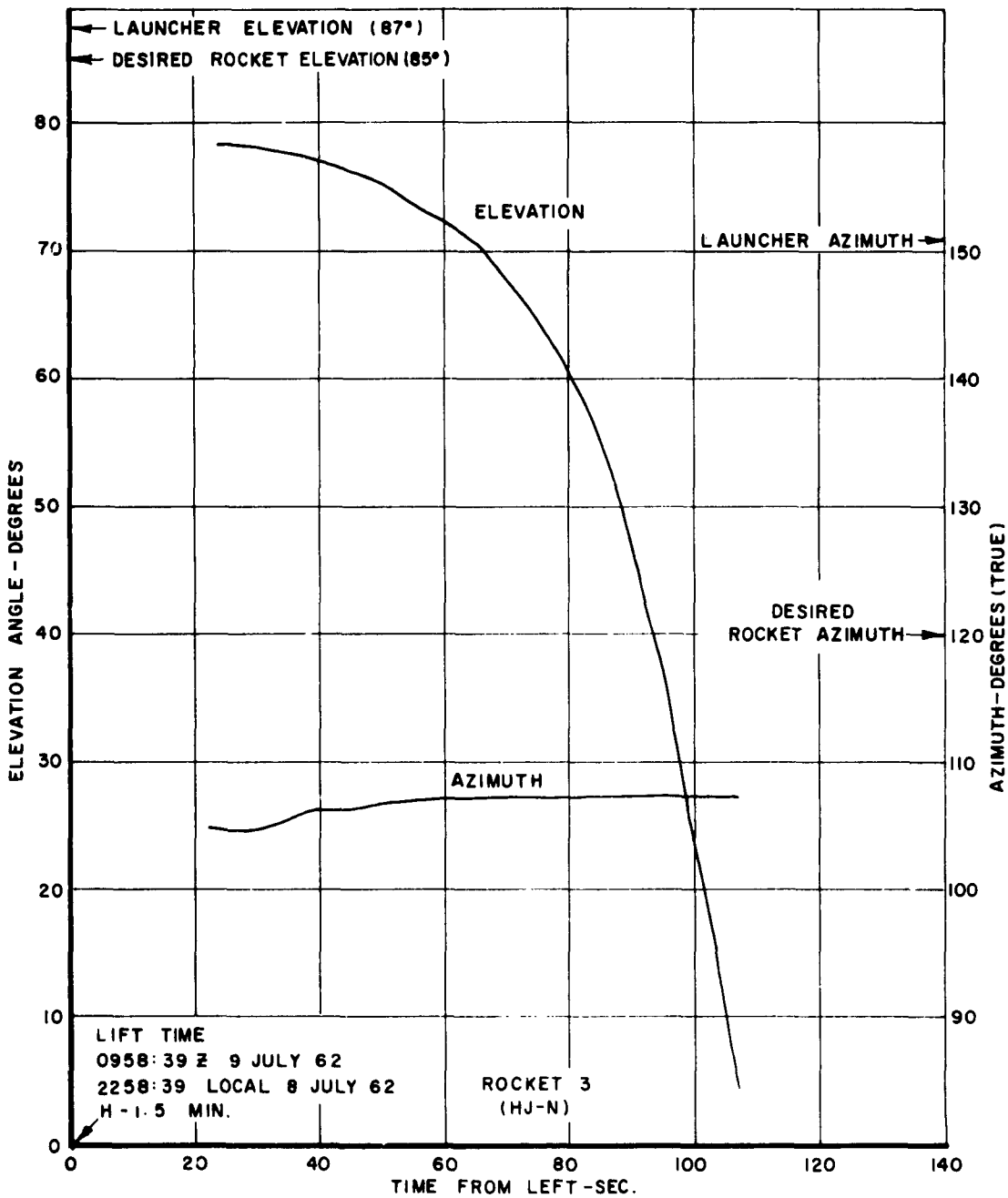

Figure C.12 GMD azimuth and elevation versus time for Rocket 3, Star Fish.

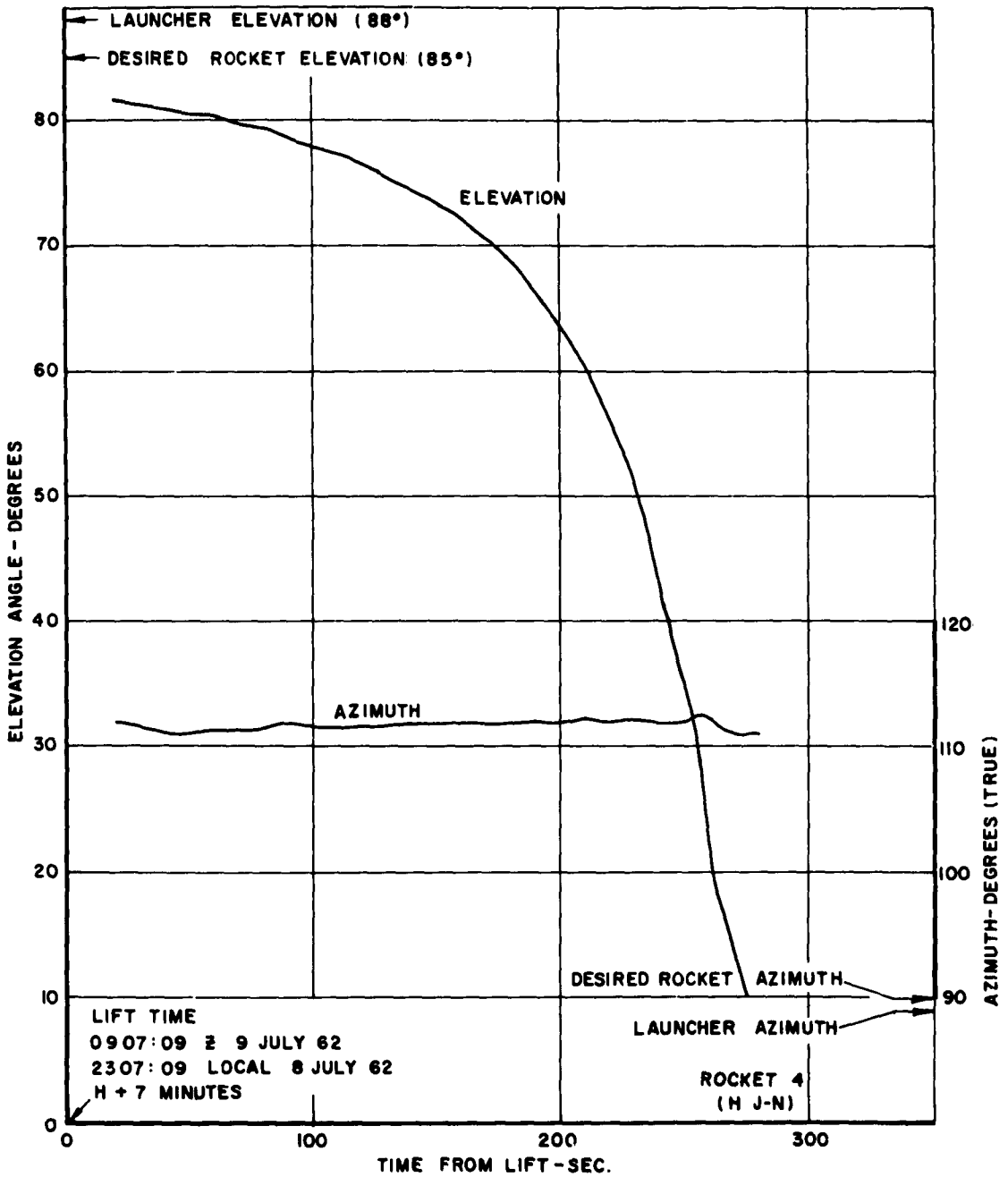

Figure C.13 GMD azimuth and elevation versus time for Rocket 4, Star Fish.

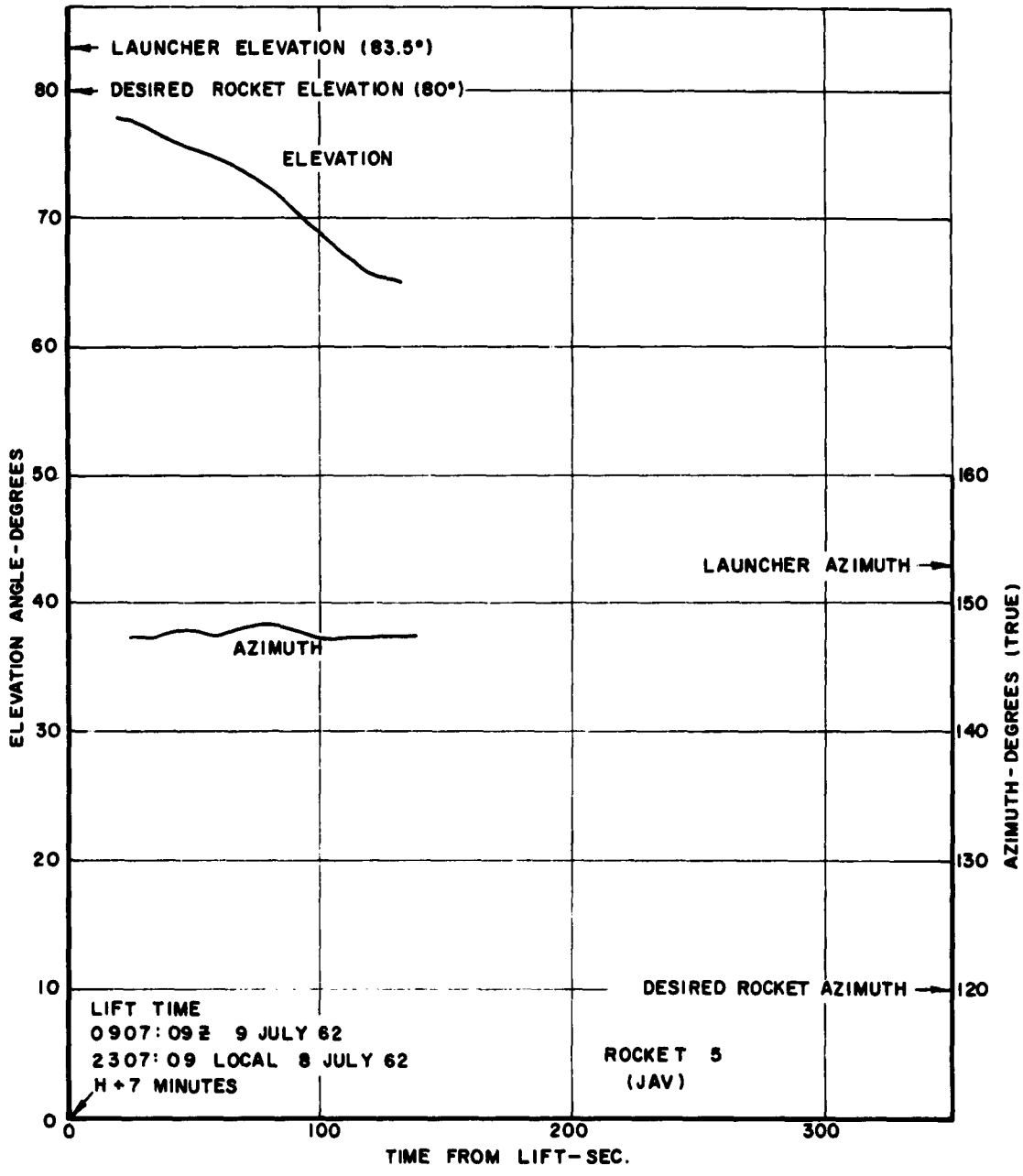

Figure C.14 GMD azimuth and elevation versus time for Rocket 5, Star Fish.

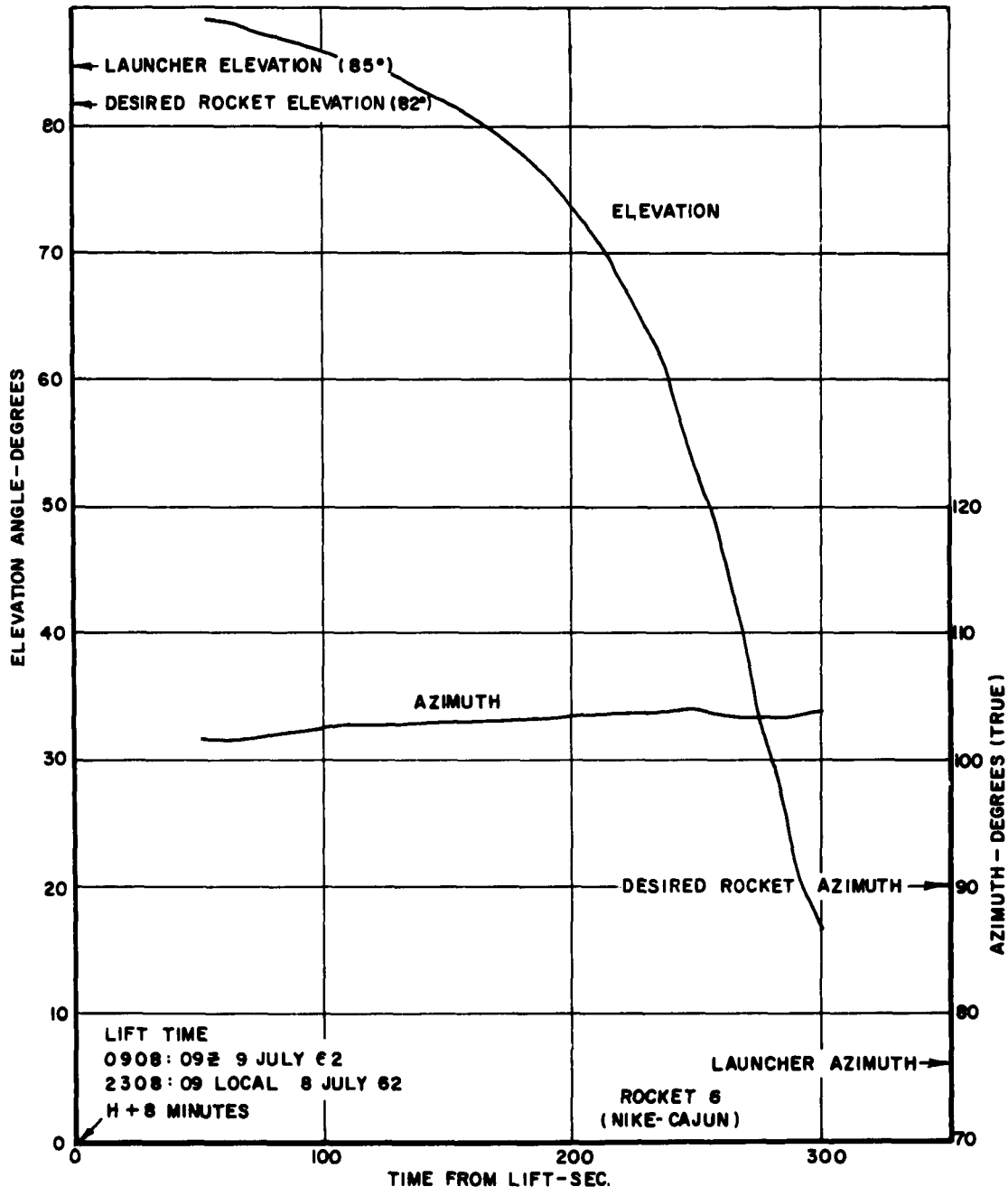

Figure C.15 GMD azimuth and elevation versus time for Rocket 6, Star Fish.

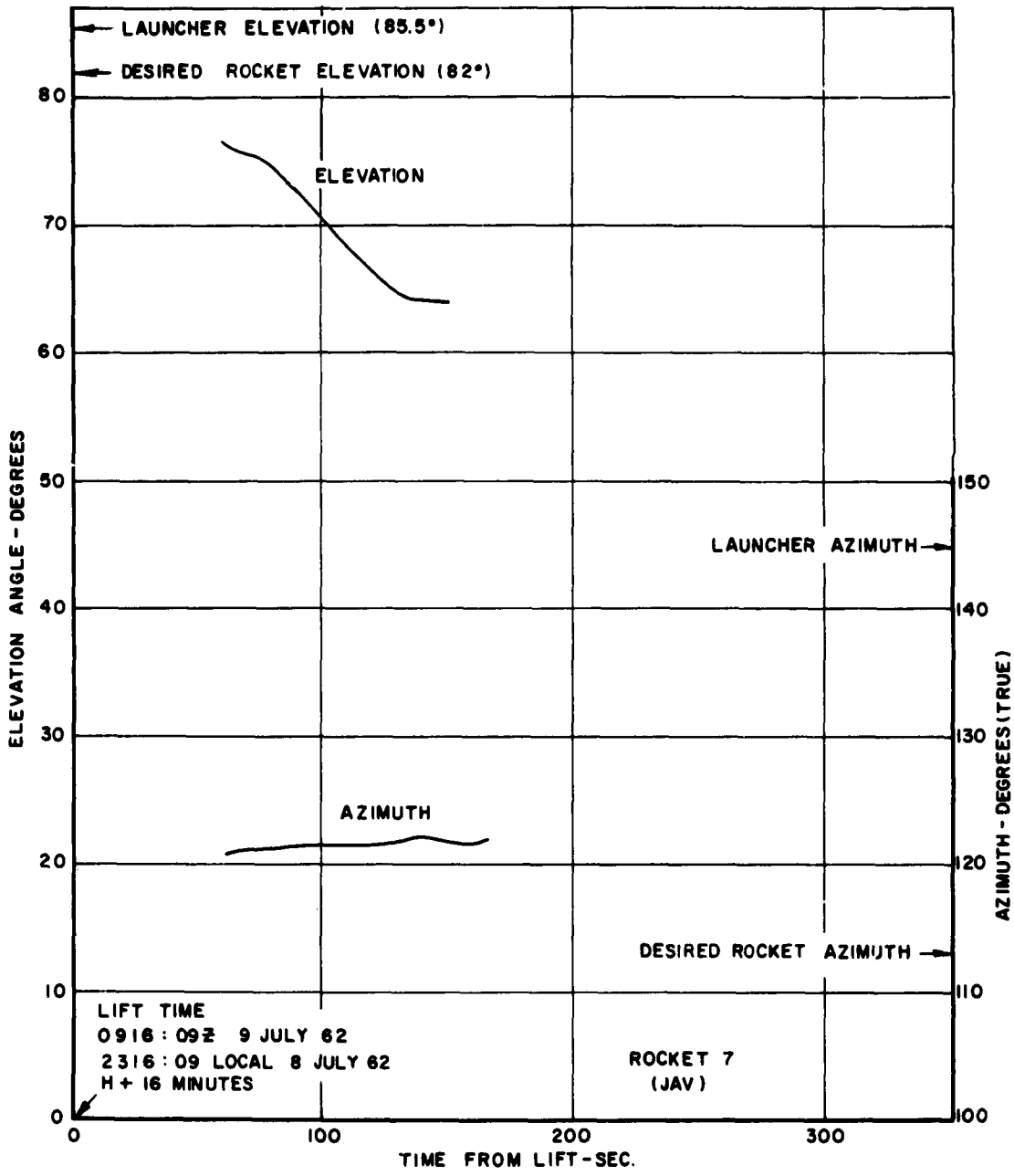

Figure C.16 GMD azimuth and elevation versus time for Rocket 7, Star Fish.

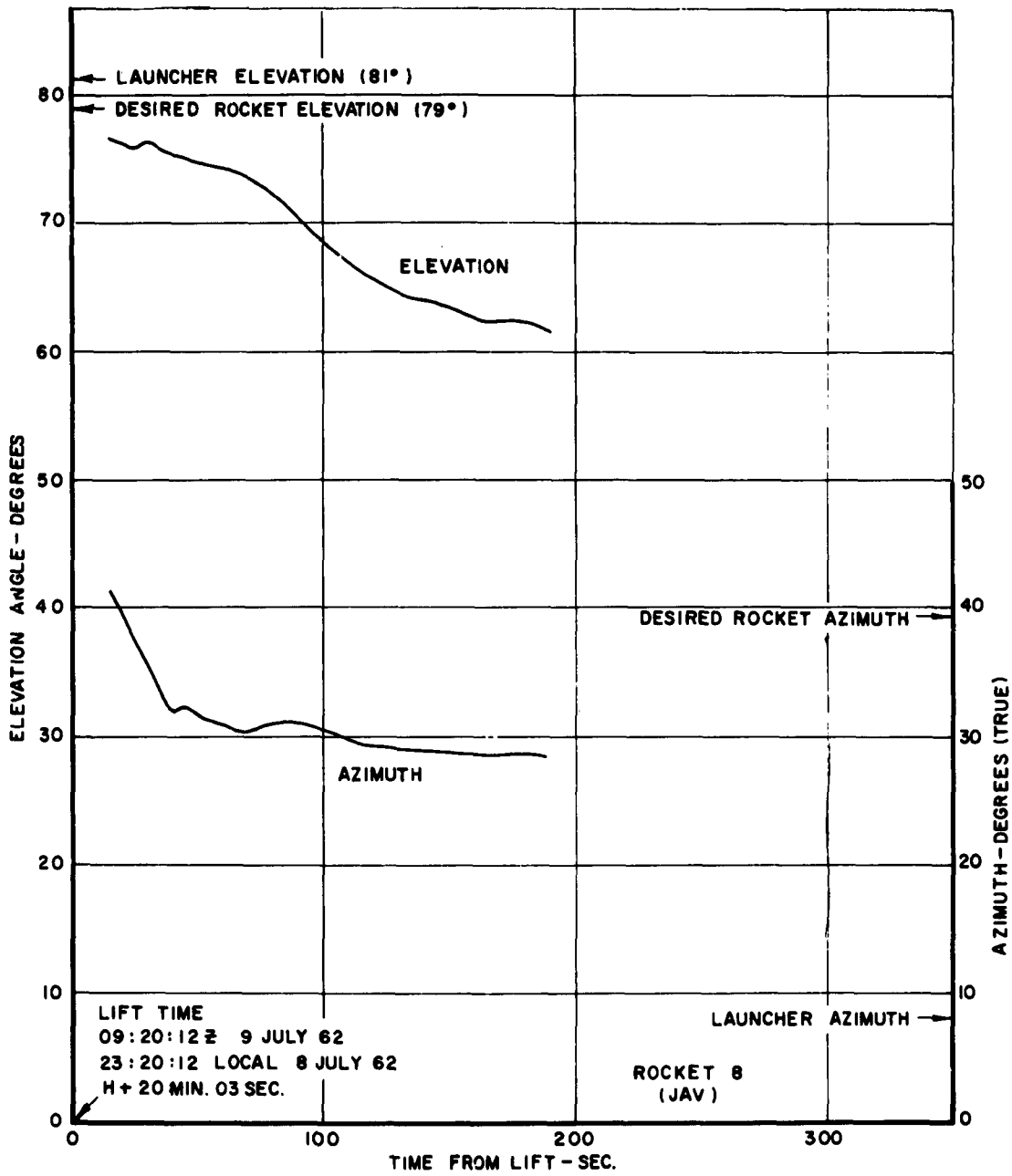

Figure C.17 GMD azimuth and elevation versus time for Rocket 8, Star Fish.

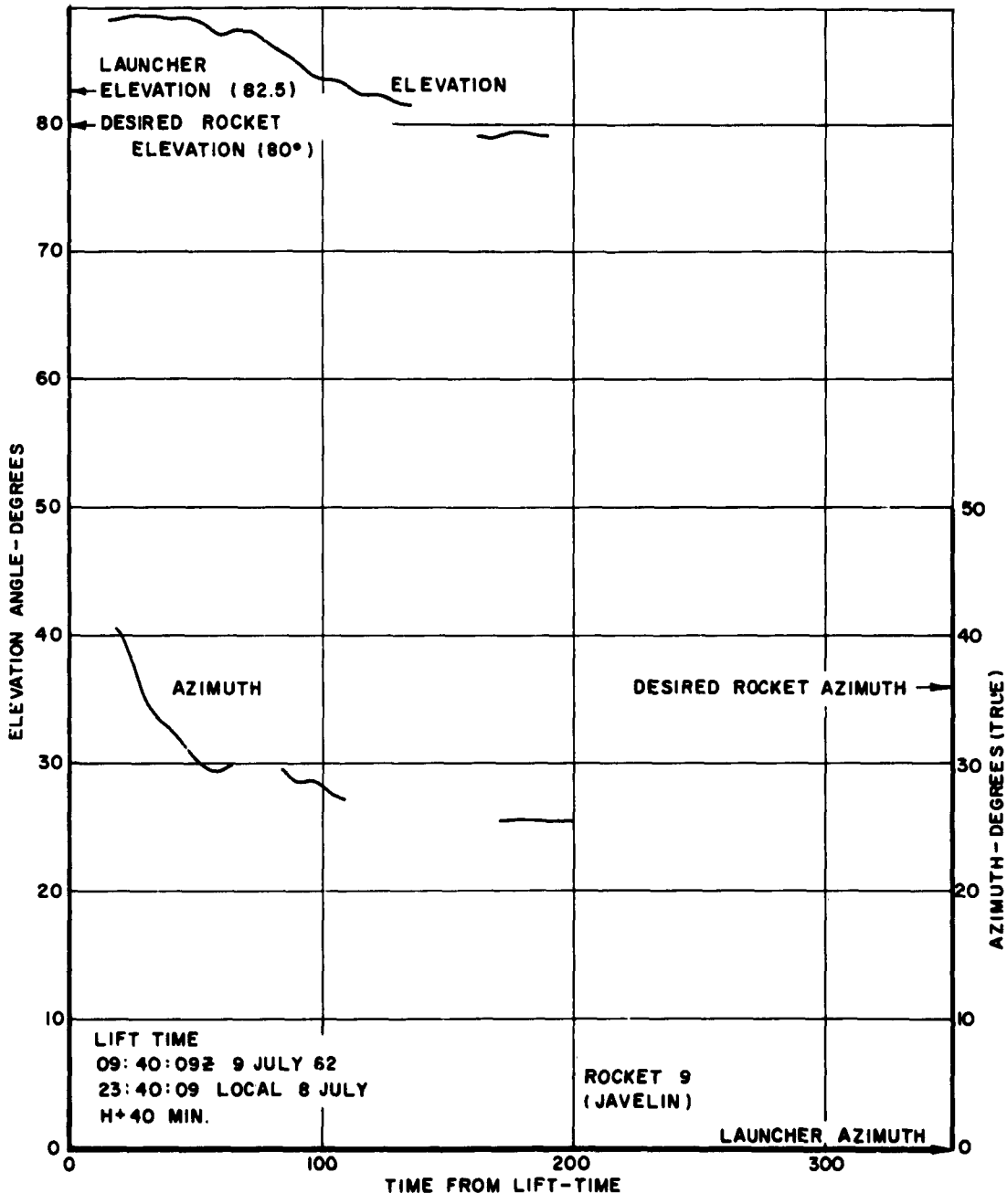

Figure C.18 GMD azimuth and elevation versus time ior Rocket 9, Star Fish.

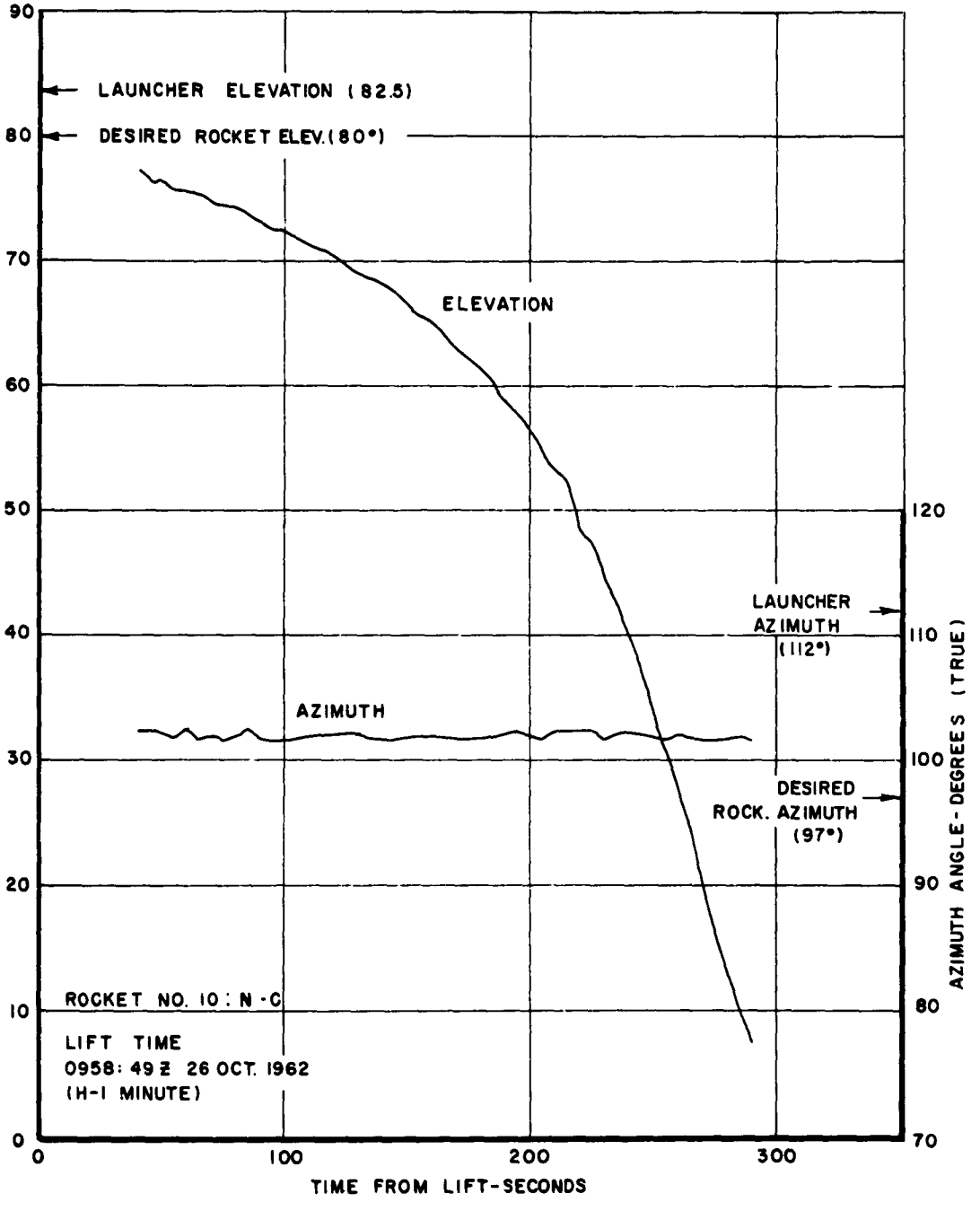

Figure C.19 GMD azimuth and elevation versus time for Rocket 10, Blue Gill.

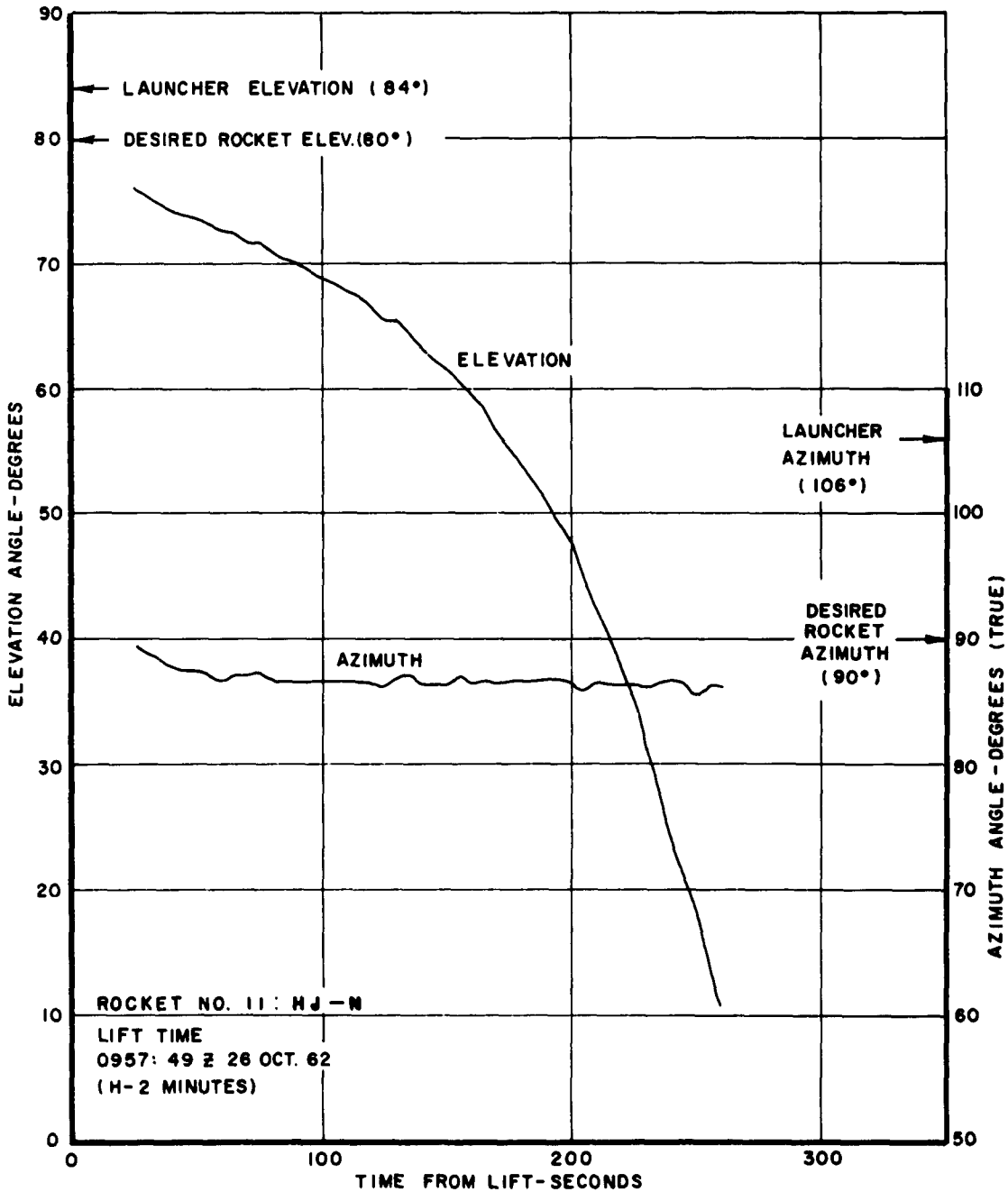

Figure C.20 GMD azimuth and elevation versus time for Rocket 11, Blue Gill.

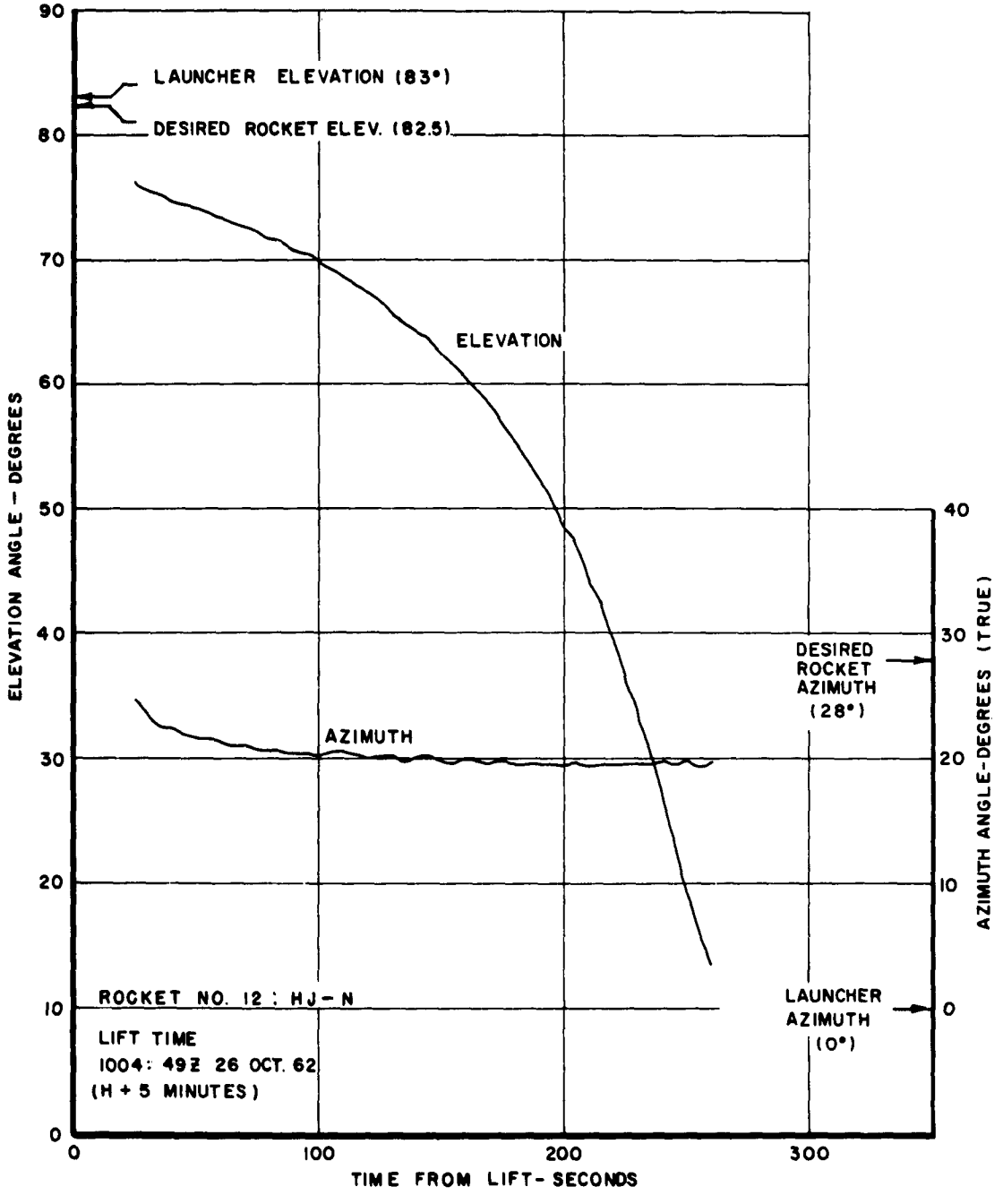

Figure C.21 GMD azimuth and elevation versus time for Rocket 12, Blue Gill.

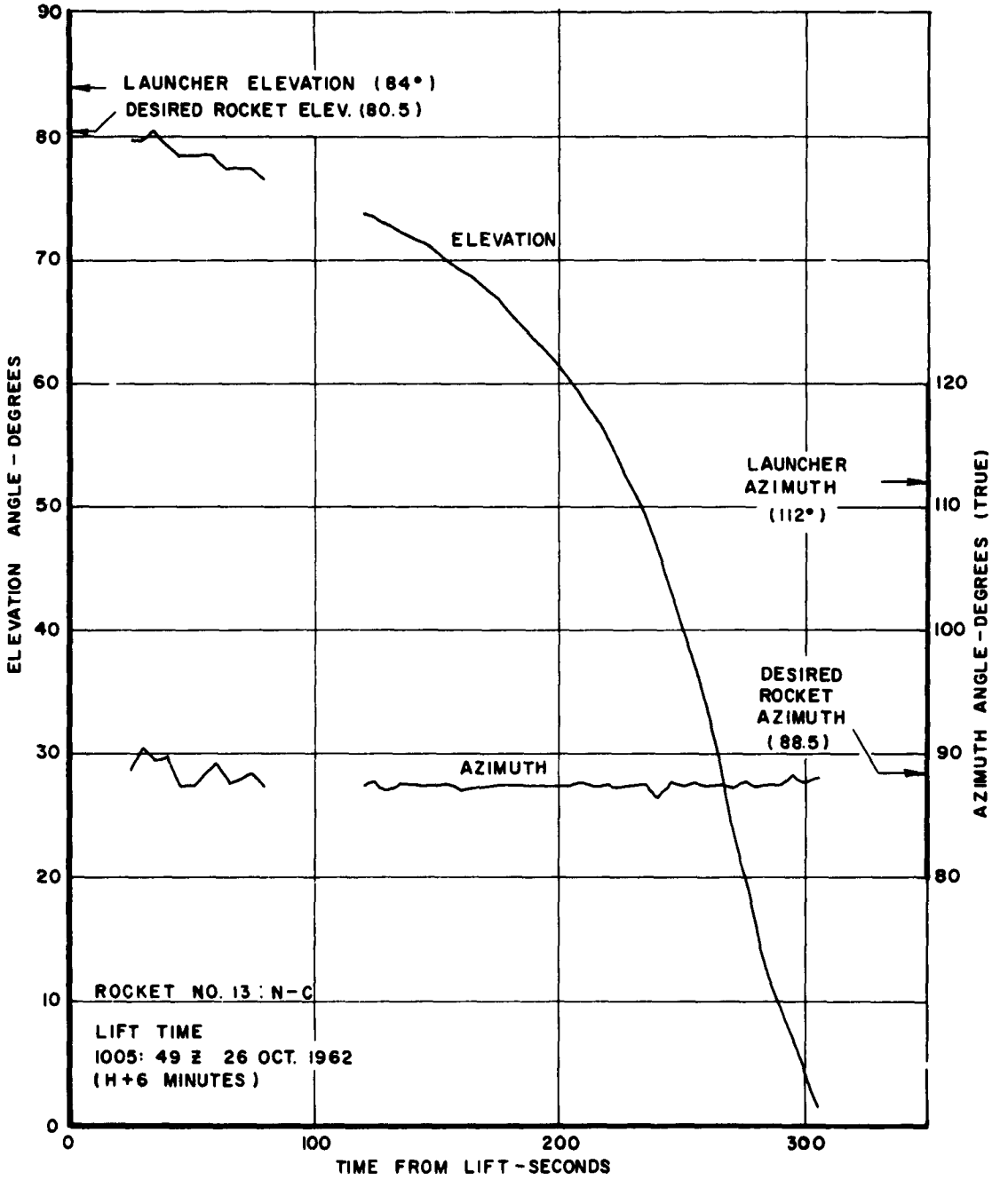

Figure C.22 GMD azimuth and elevation versus time for Rocket 13, Blue Gill.

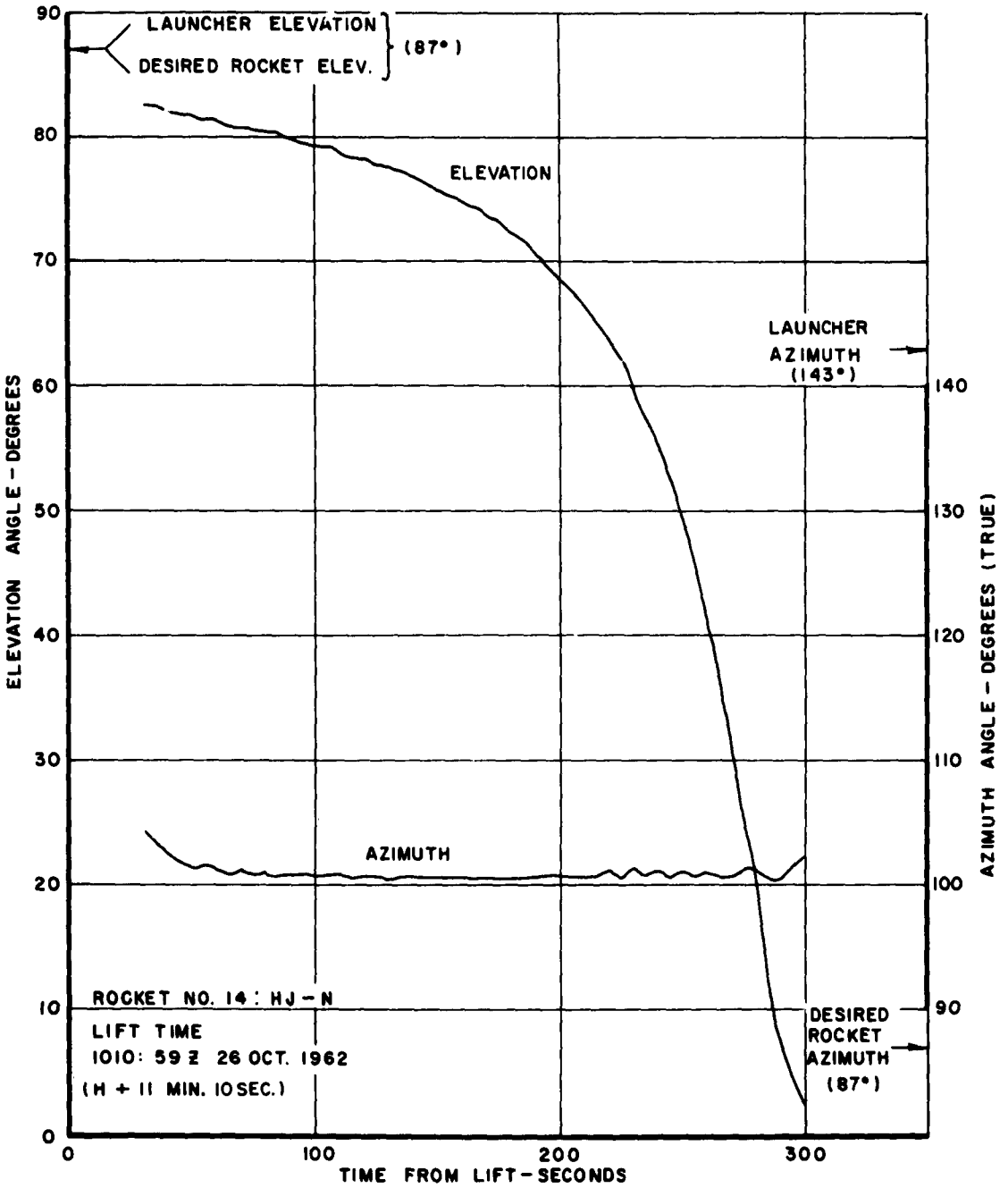

Figure C.23 GMD azimuth and elevation versus time for Rocket 14, Blue Gill.

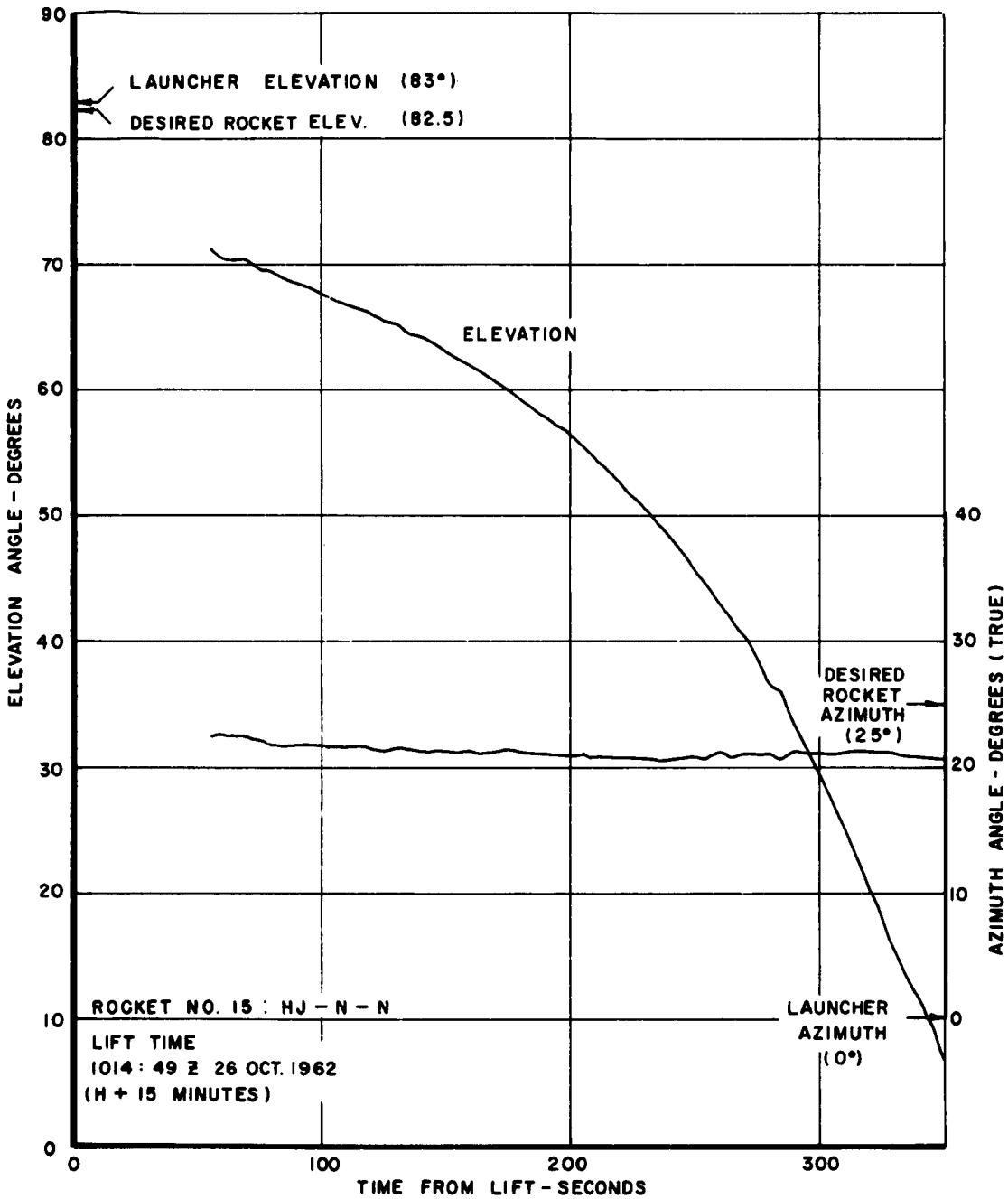

Figure C.24 GMD azimuth and elevation versus time for Rocket 15, Blue Gill.

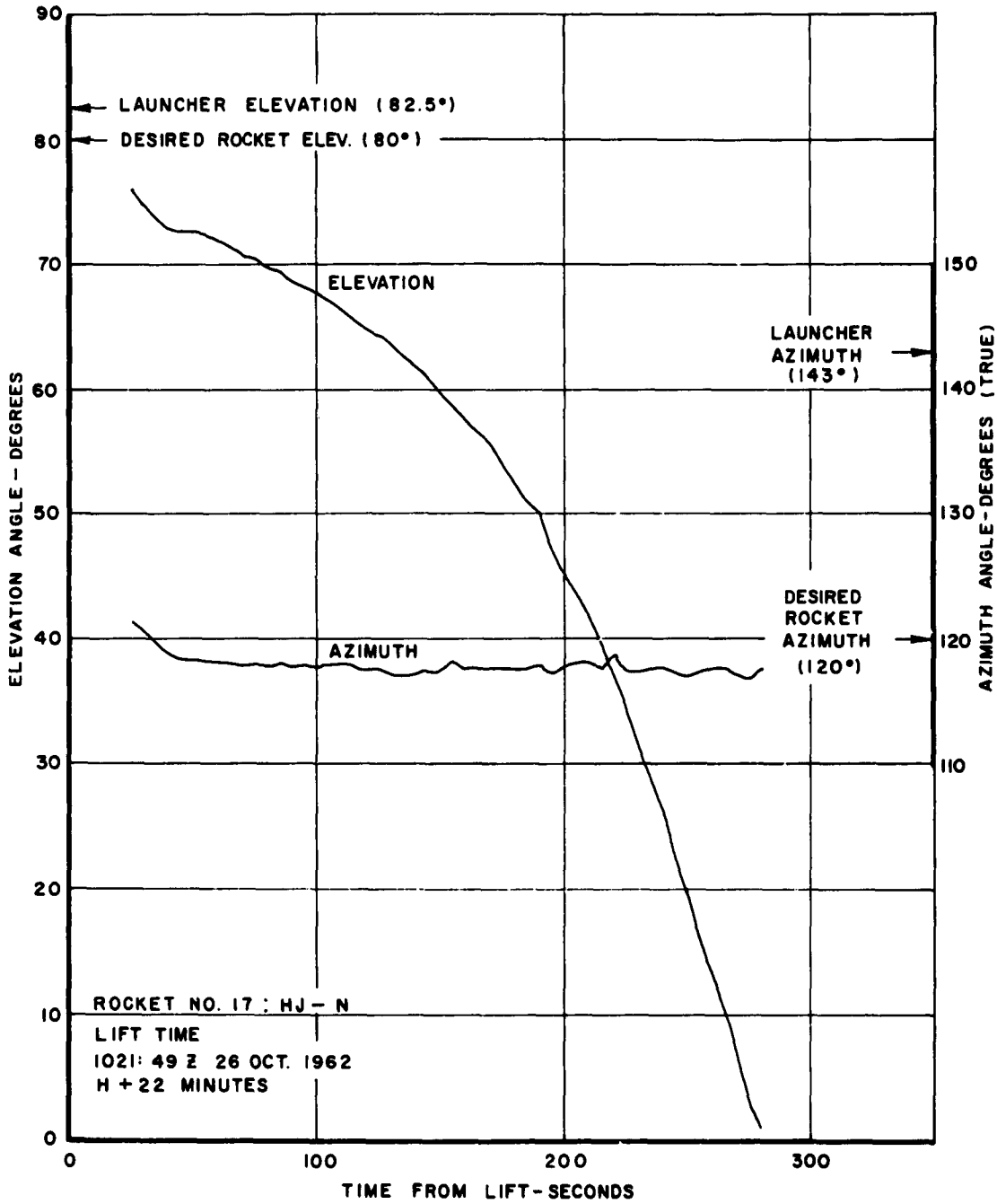

Figure C.25 GMD azimuth and elevation versus time for Rocket 17, Blue Gill.

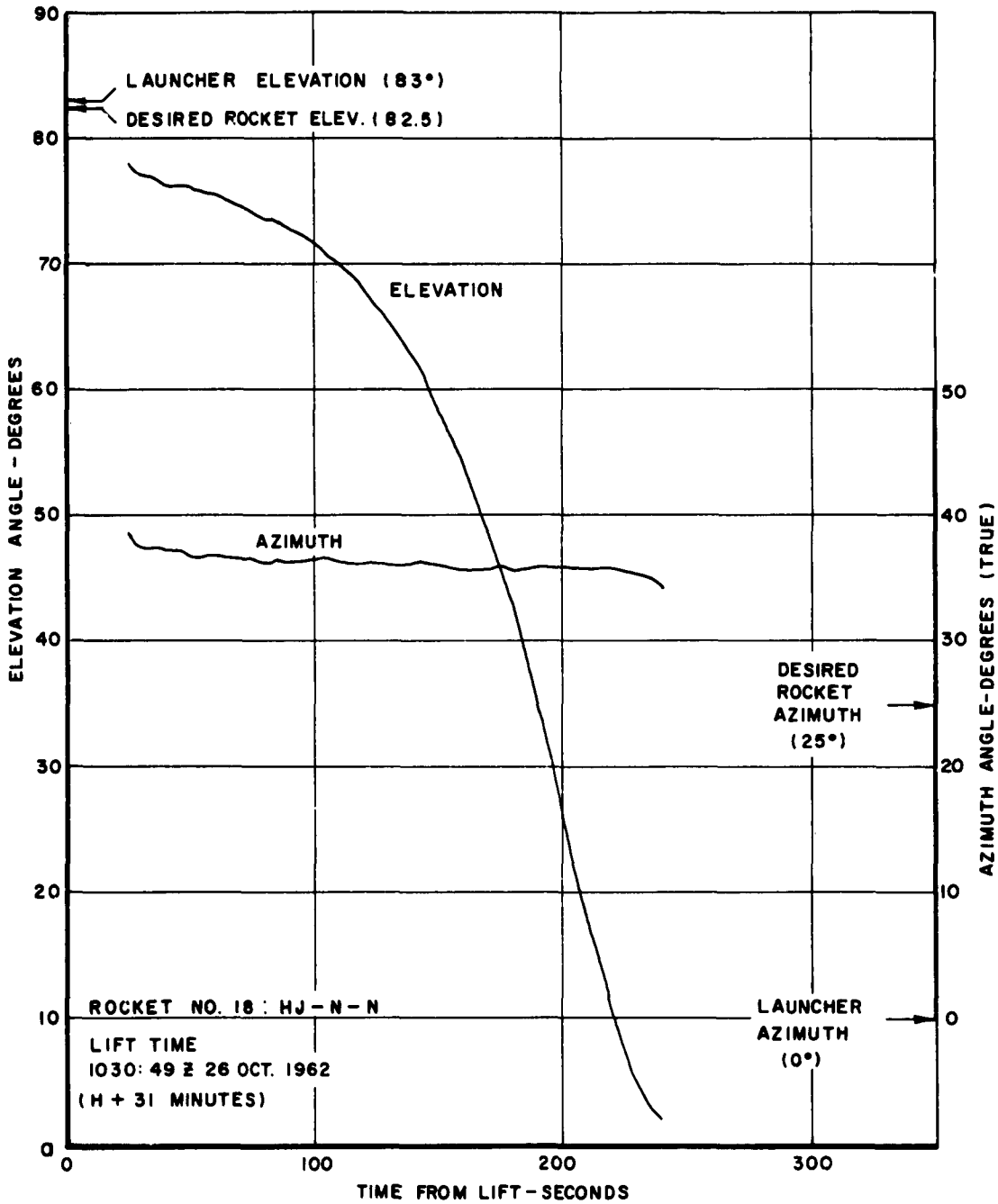

Figure C.26 GMD azimuth and elevation versus time for Rocket 18, Blue Gill.

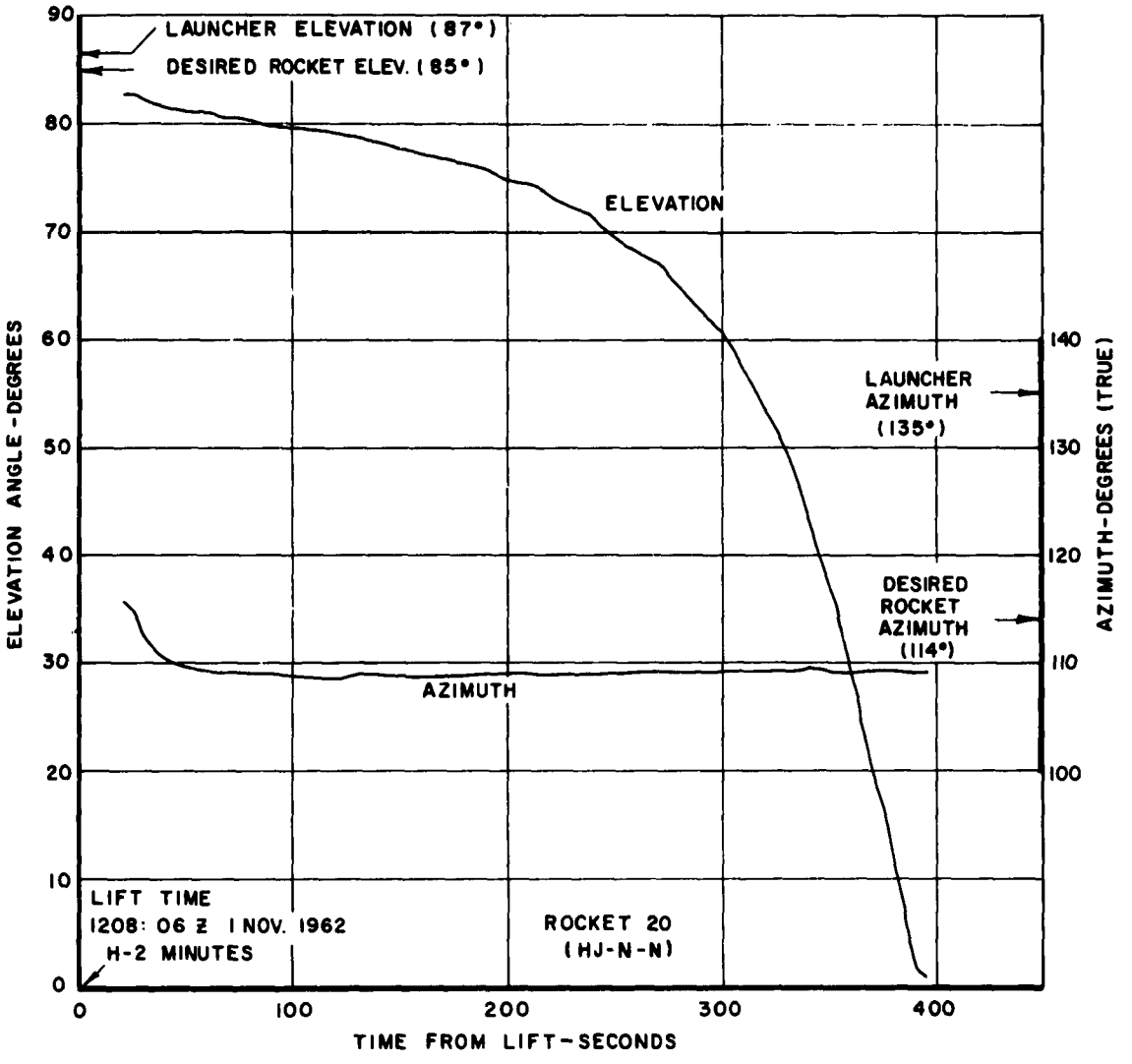

Figure C.27 GMD azimuth and elevation versus time for Rocket 20, King Fish.

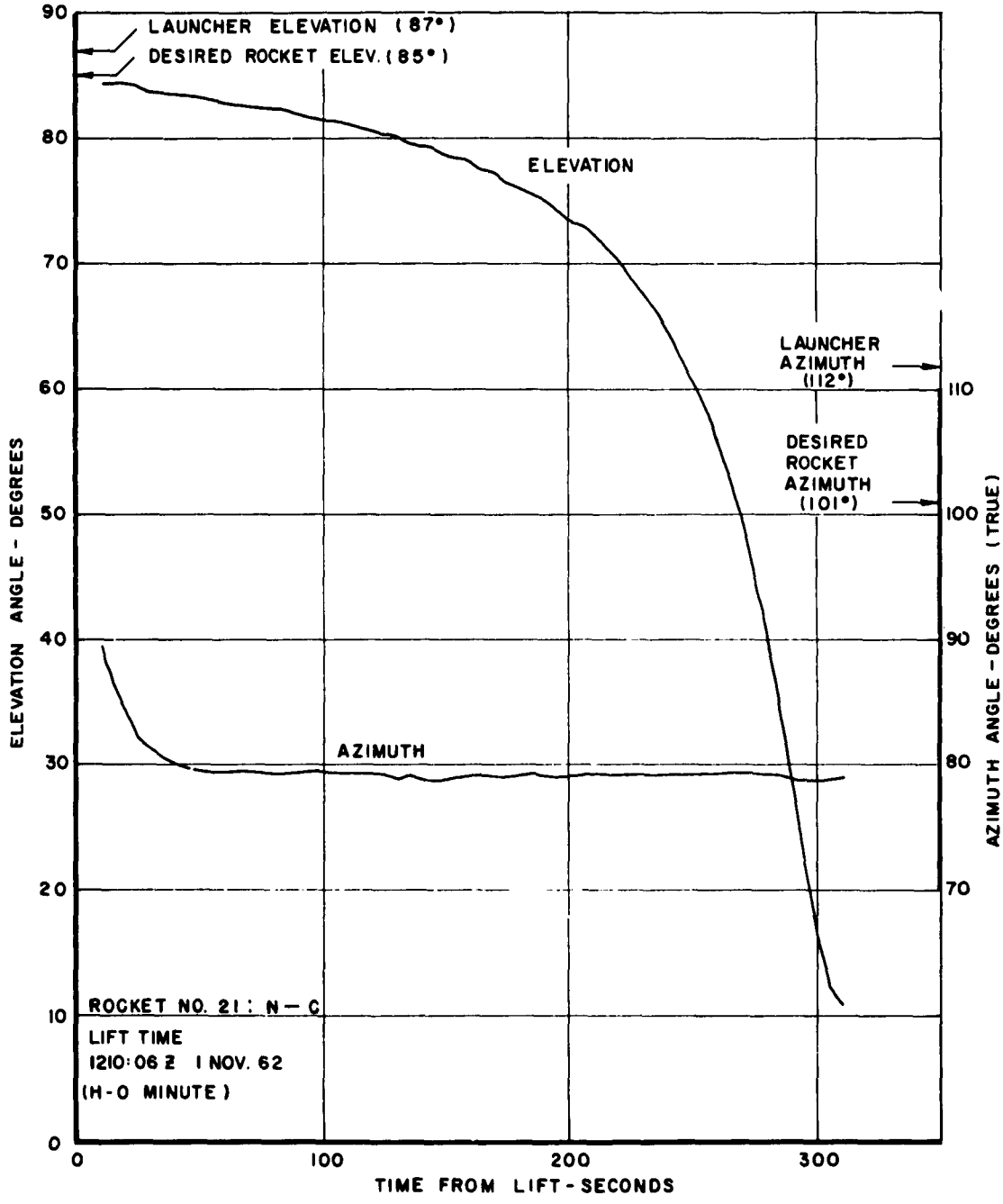

Figure C.28 GMD azimuth and elevation versus time for Rocket 21, King Fish.

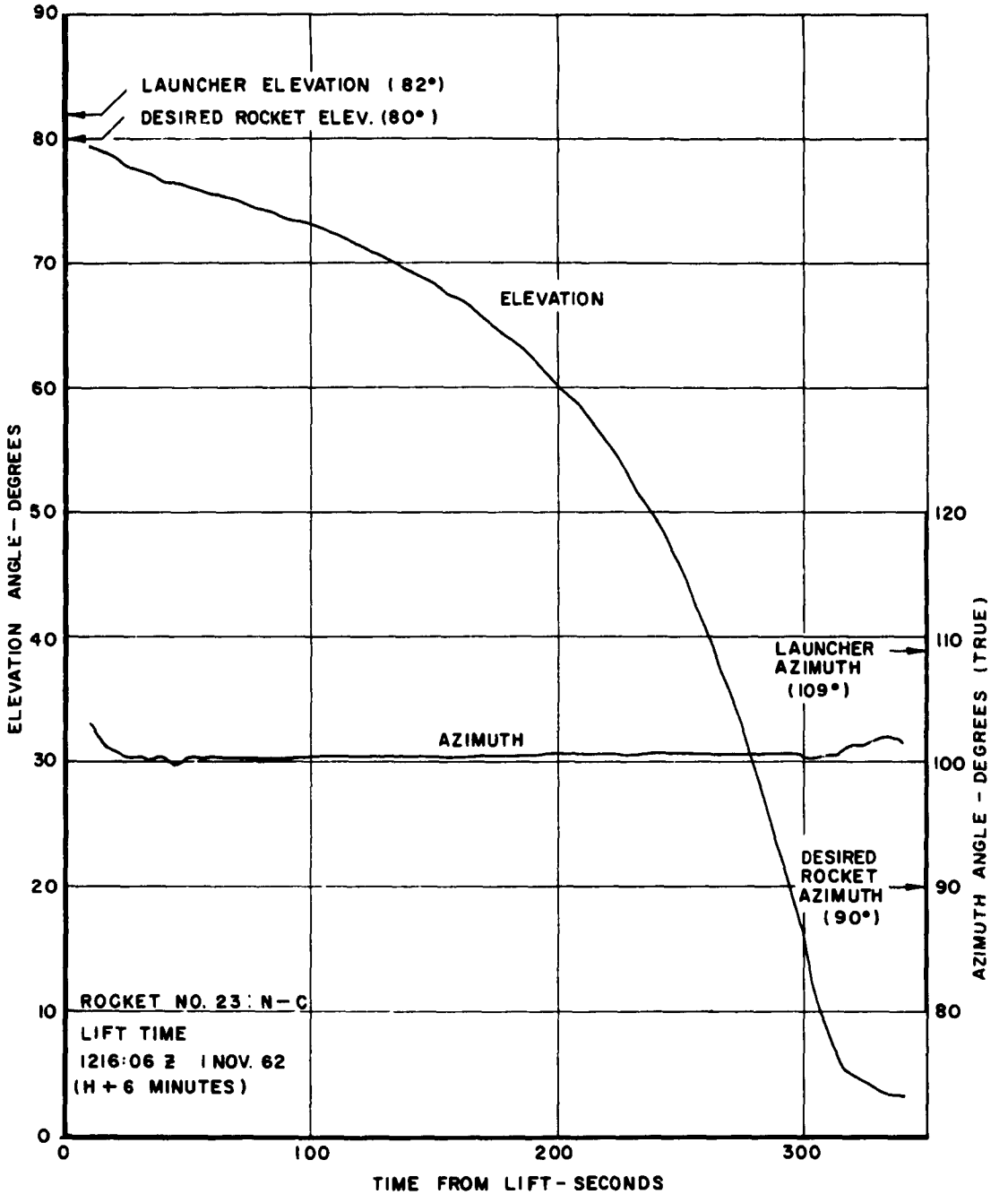

Figure C.29 GMD azimuth and elevation versus time for Rocket 23, King Fish.

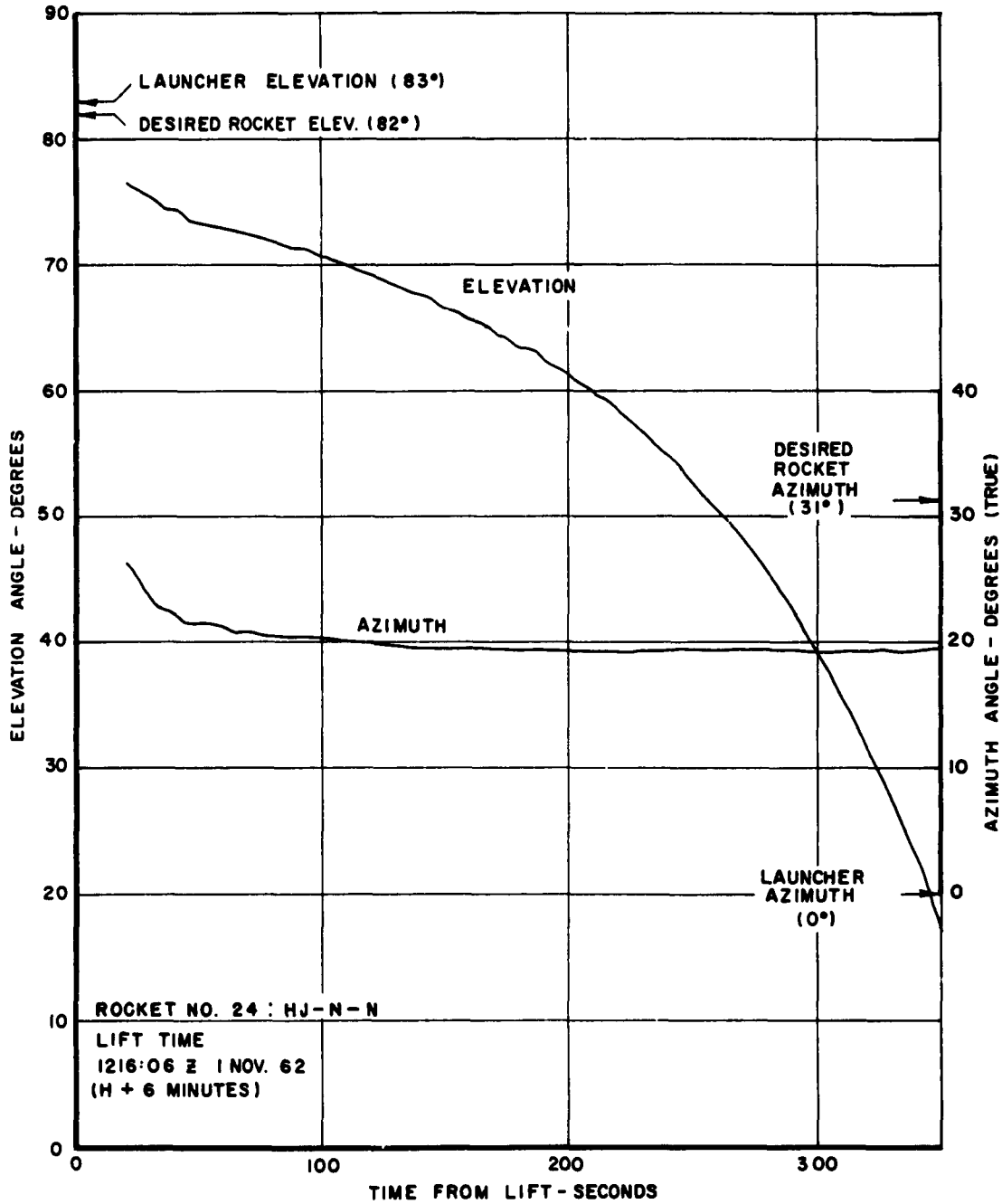

Figure C.30 GMD azimuth and elevation versus time for Rocket 24, King Fish.

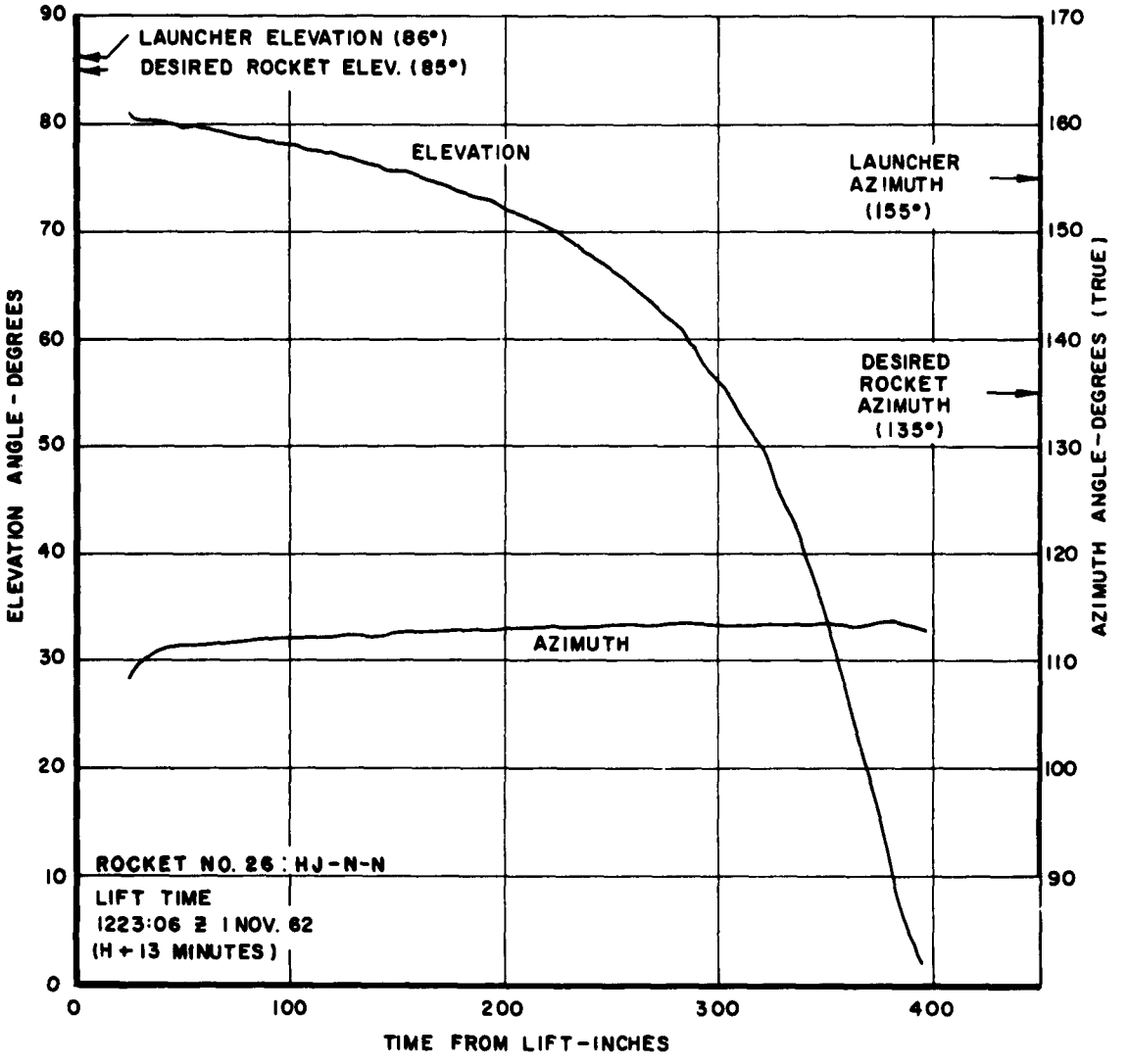

Figure C.31 GMD azimuth and elevation versus time for Rocket 26, King Fish.

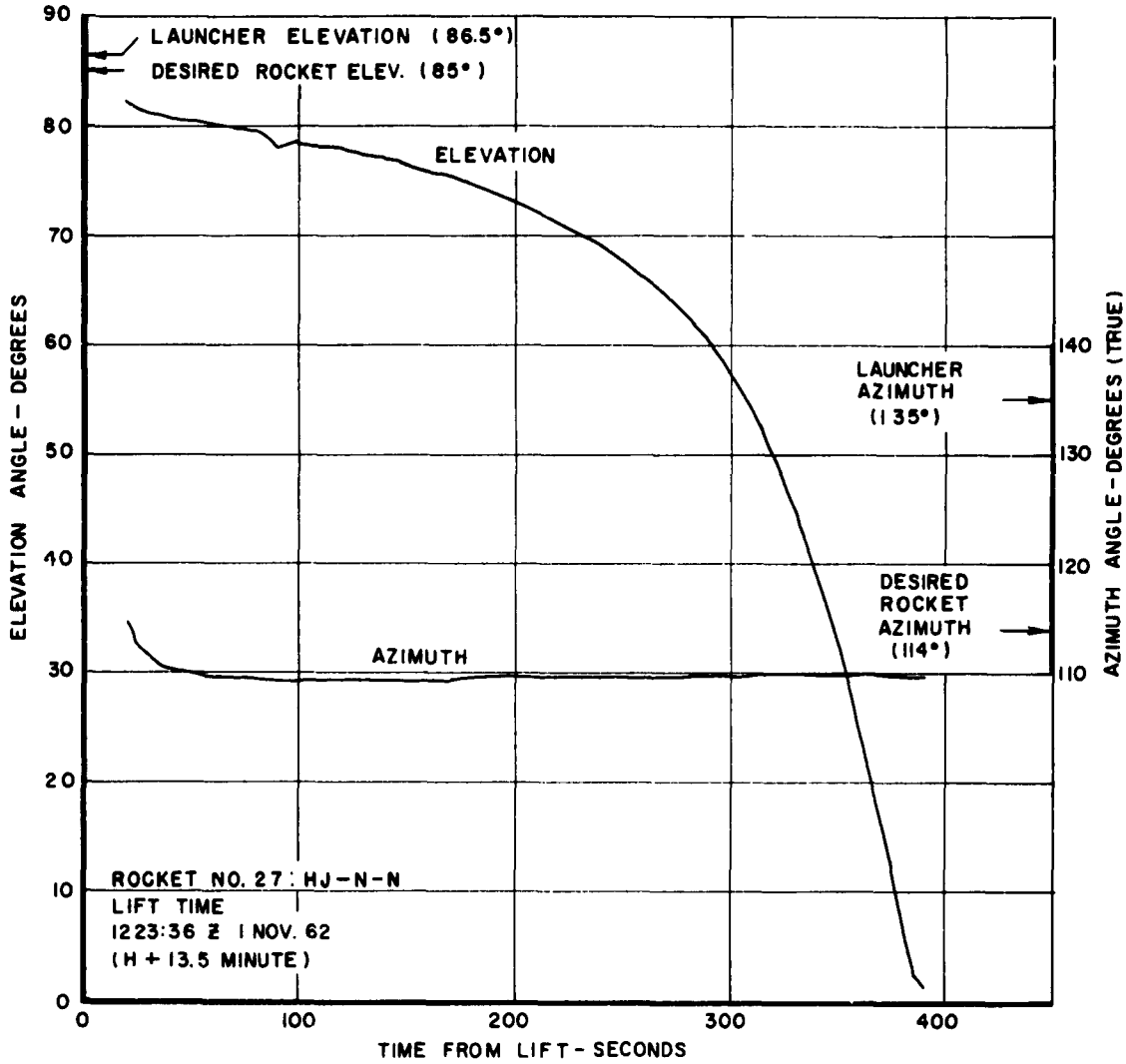

Figure C.32 GMD azimuth and elevation versus time for Rocket 27, King Fish.

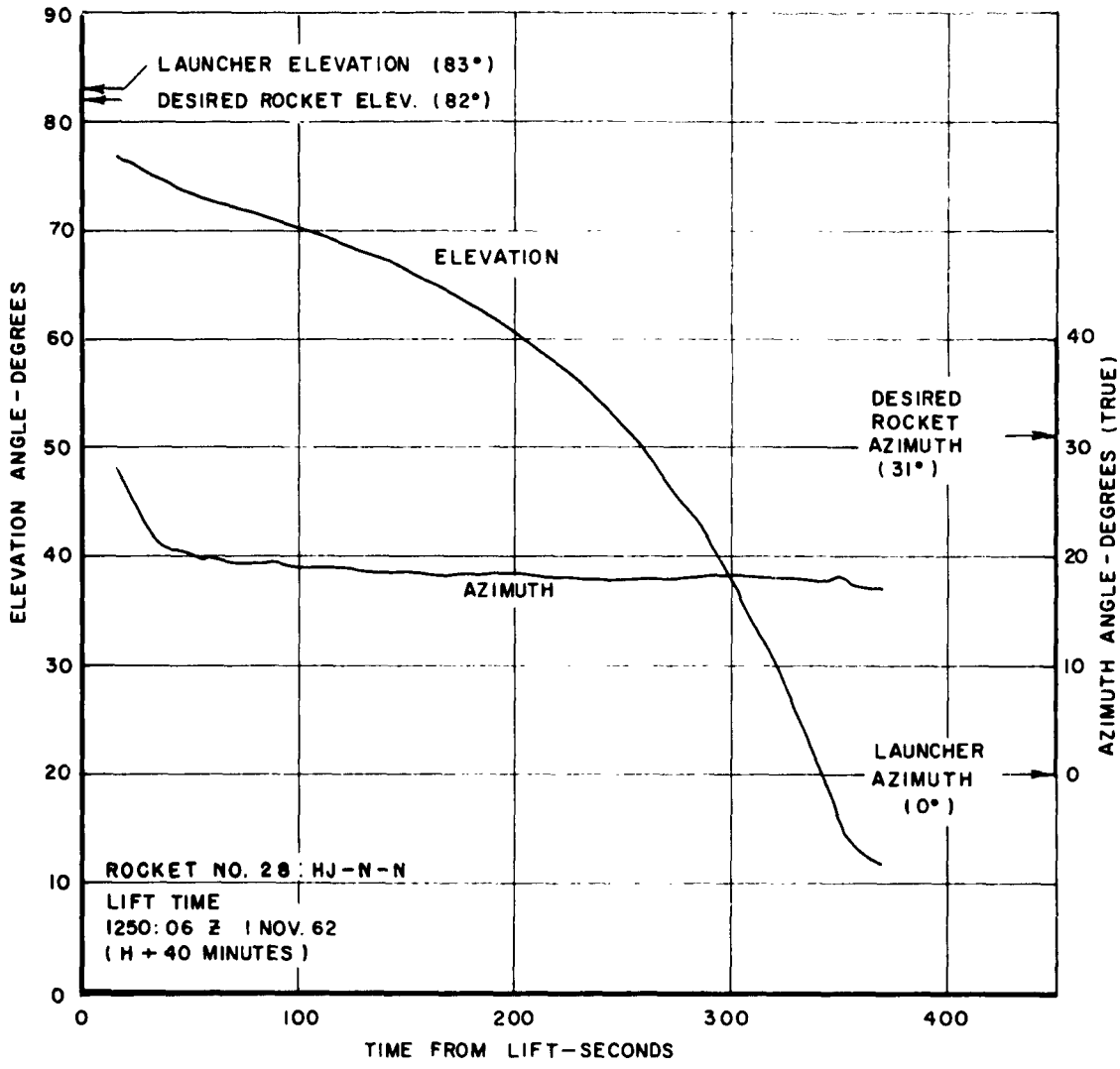

Figure C.33 GMD azimuth and elevation versus time for Rocket 28, King Fish.

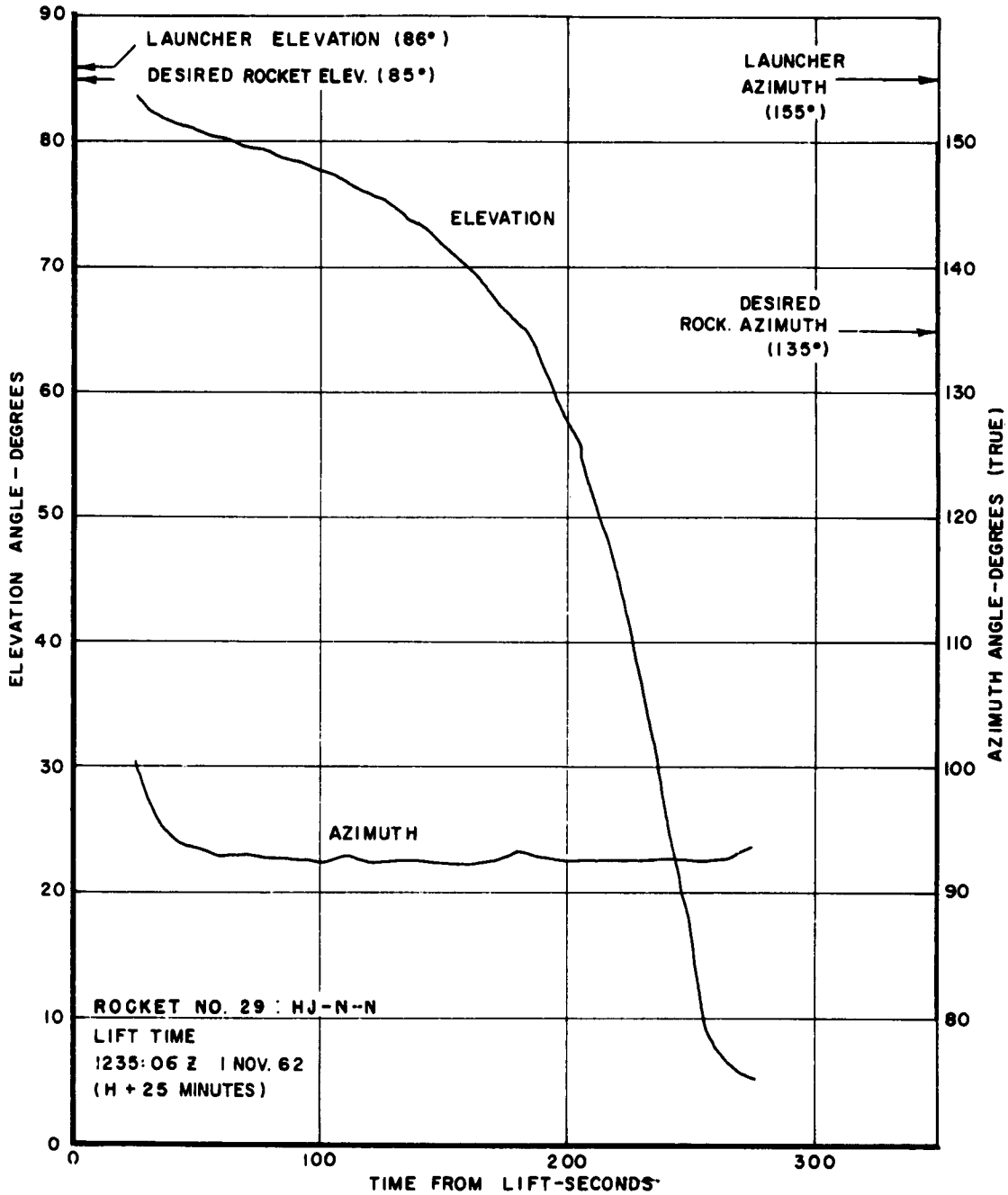

Figure C.34 GMD azimuth and elevation versus time for Rocket 29, King Fish.

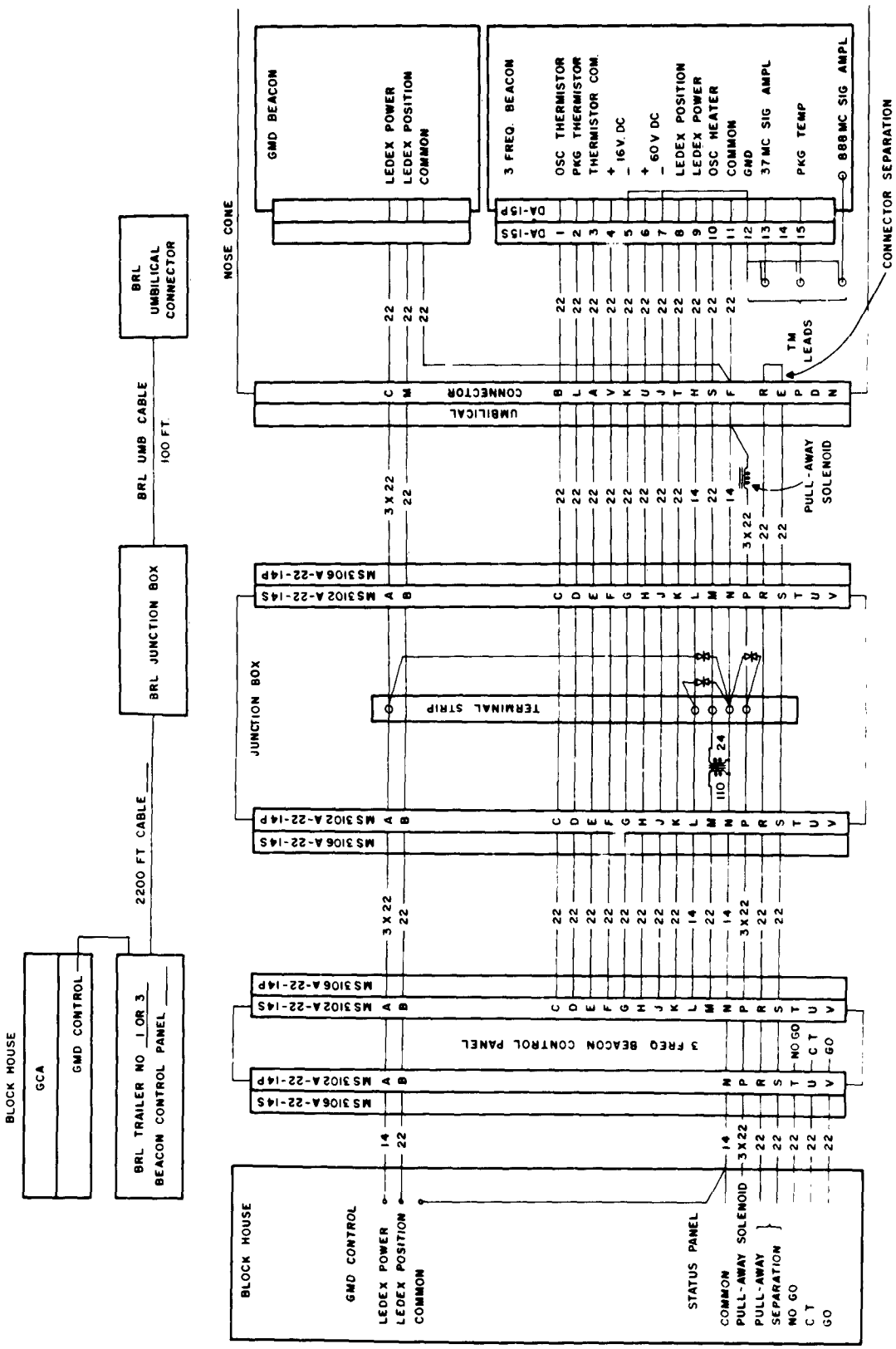

Figure C.35 Block diagram of 3-frequency beacon control in blockhouse.

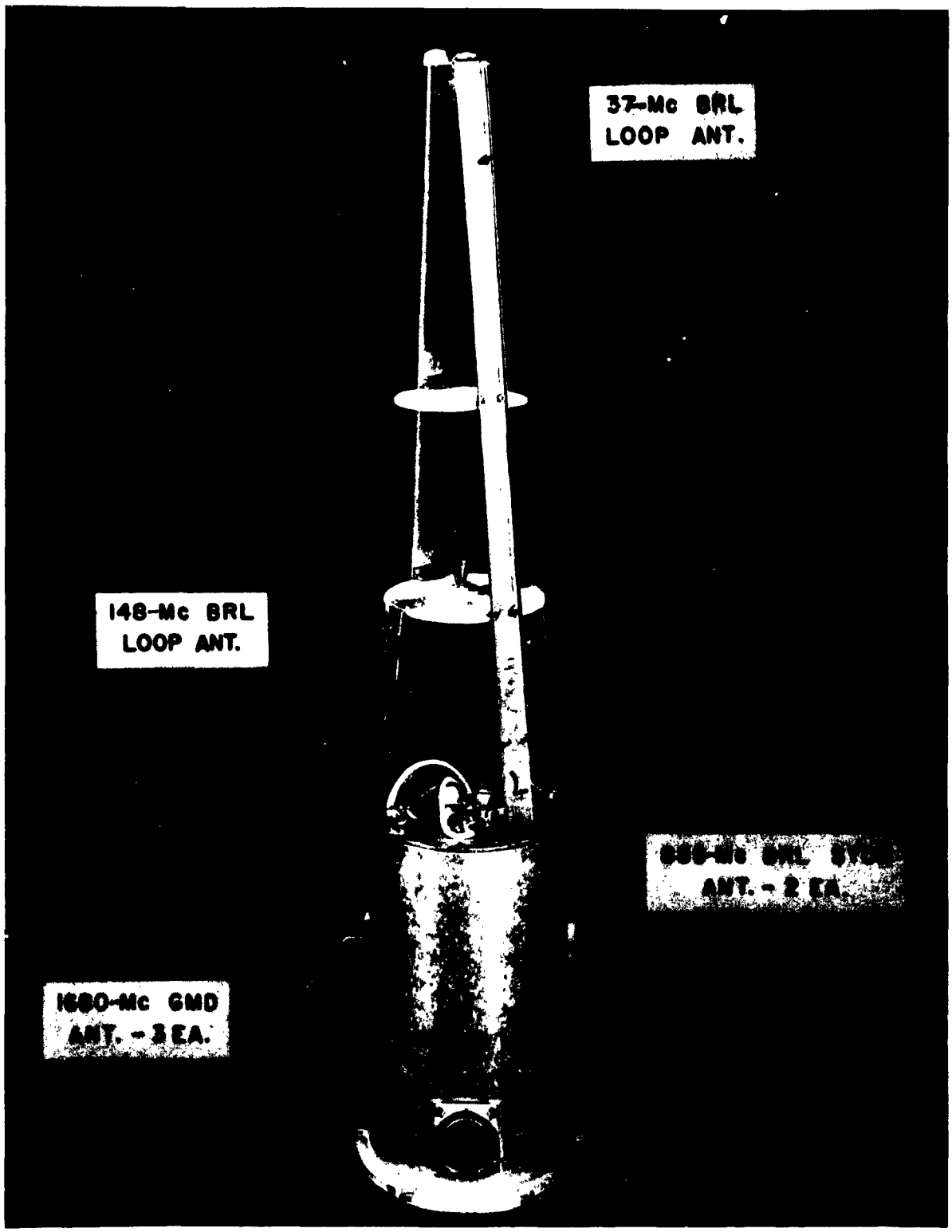

F gure C.36 Photograph of 3-frequency beacon antennas on Honest John-Nike rockets, Project 6.3. (BRL photo)

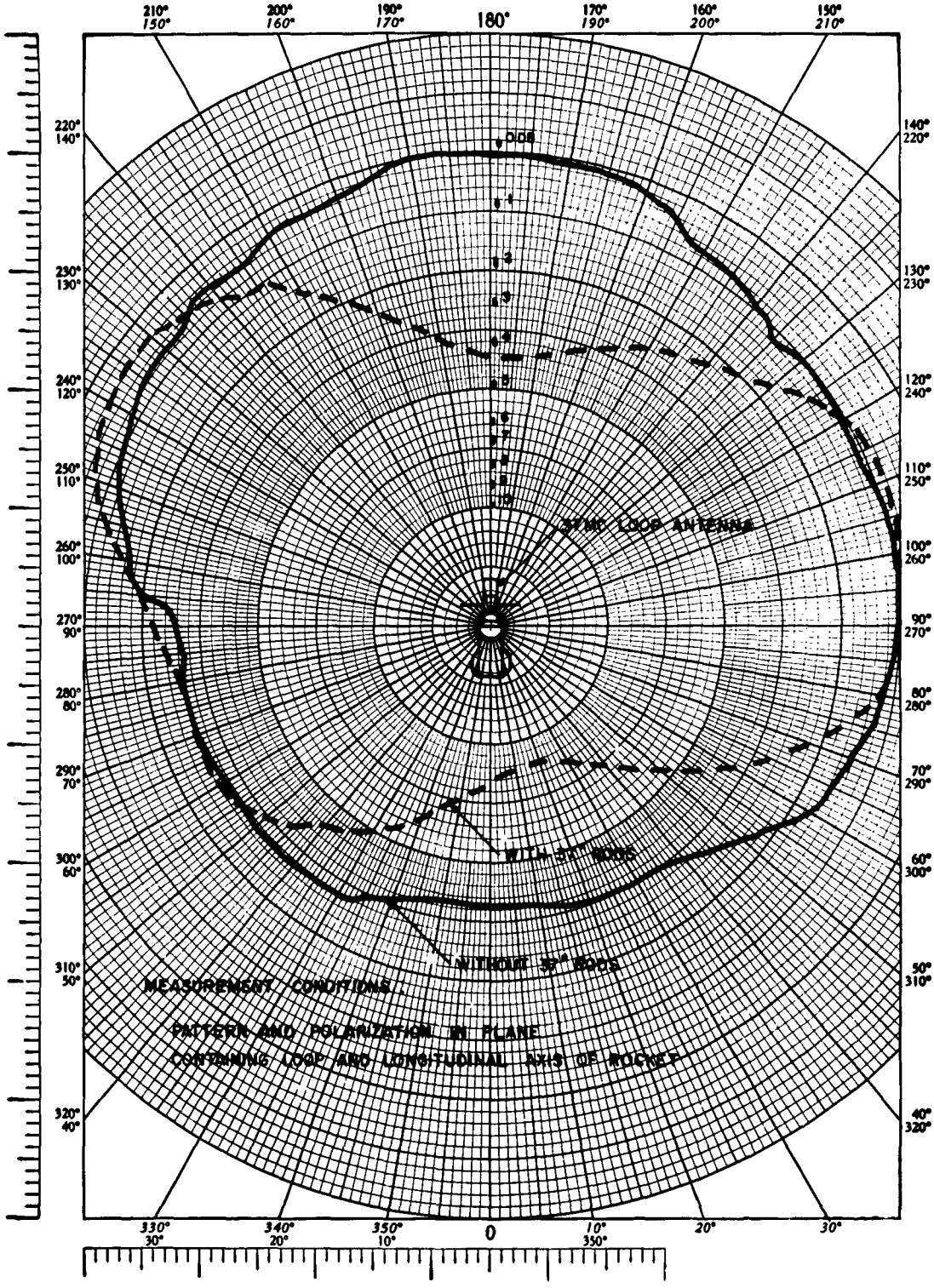

Figure C.37 Radiation pattern for 37-Mc loop antenna on Honest John-Nike rockets, Project 6.3.

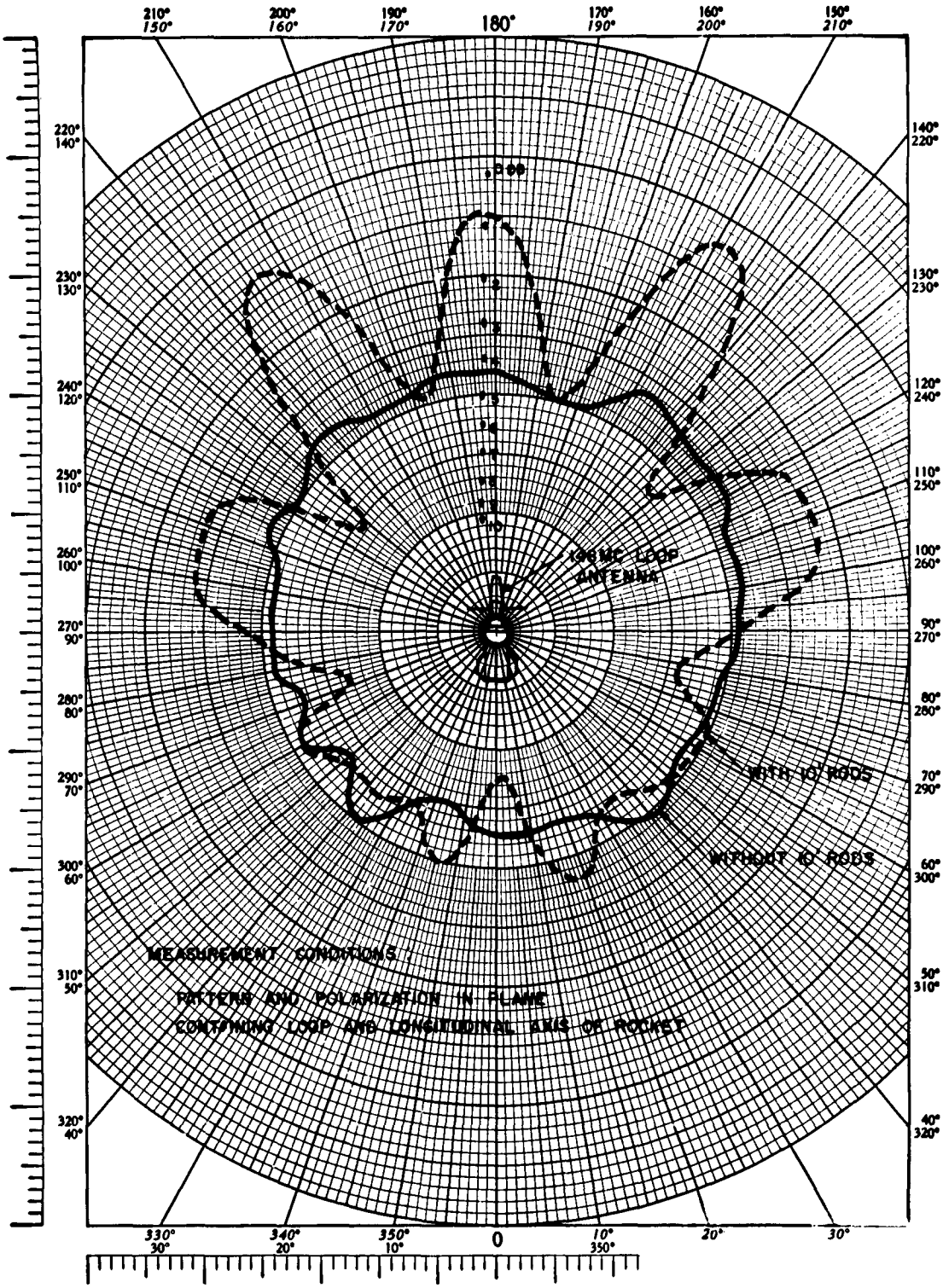

Figure C.38 Radiation pattern for 148-Mc loop antenna on Honest John-Nike rockets, Project 6.3.

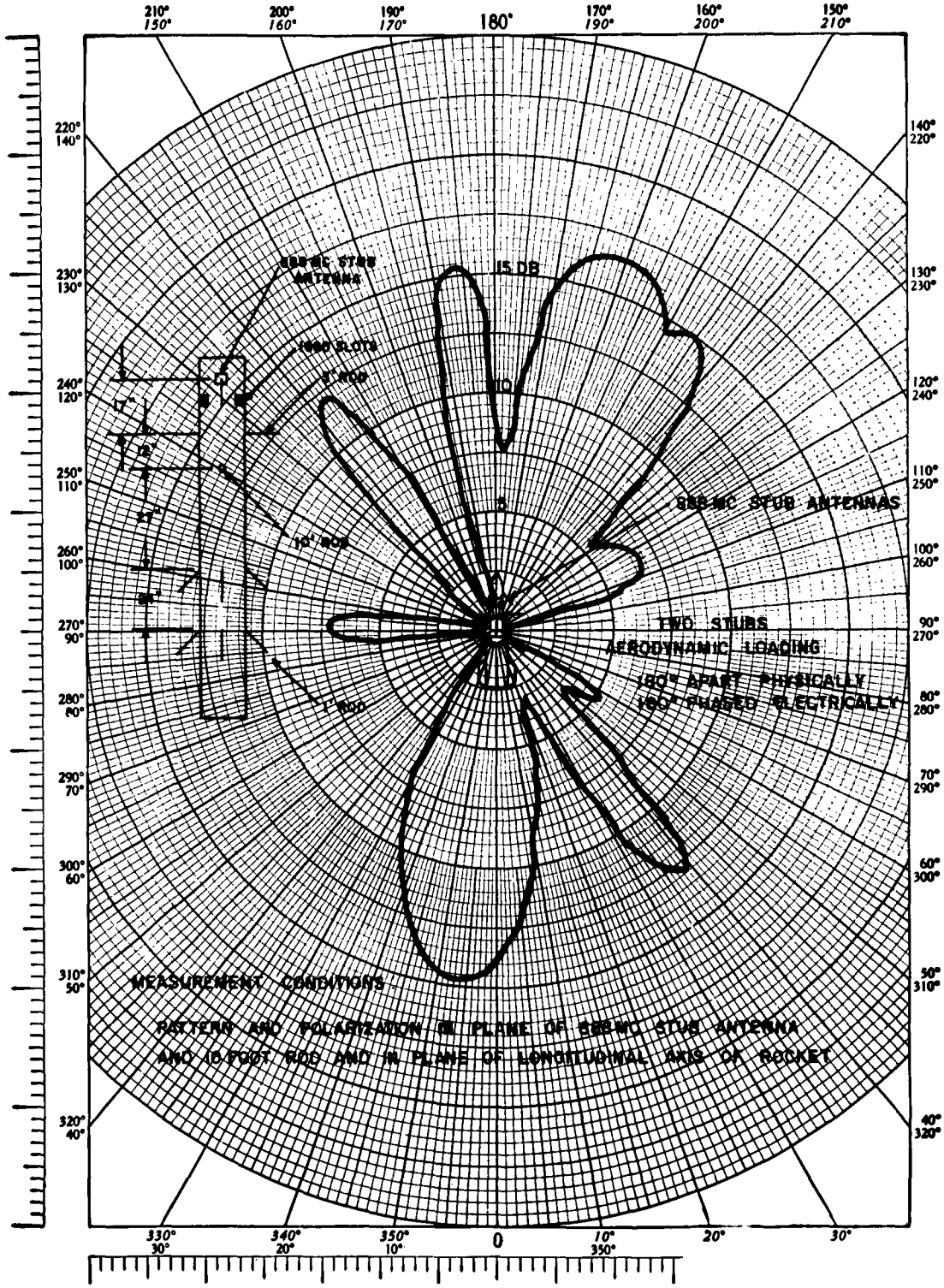

Figure C.39 Radiation pattern for 888-Mc antenna on Honest John-Nike rockets, Project 6.3.

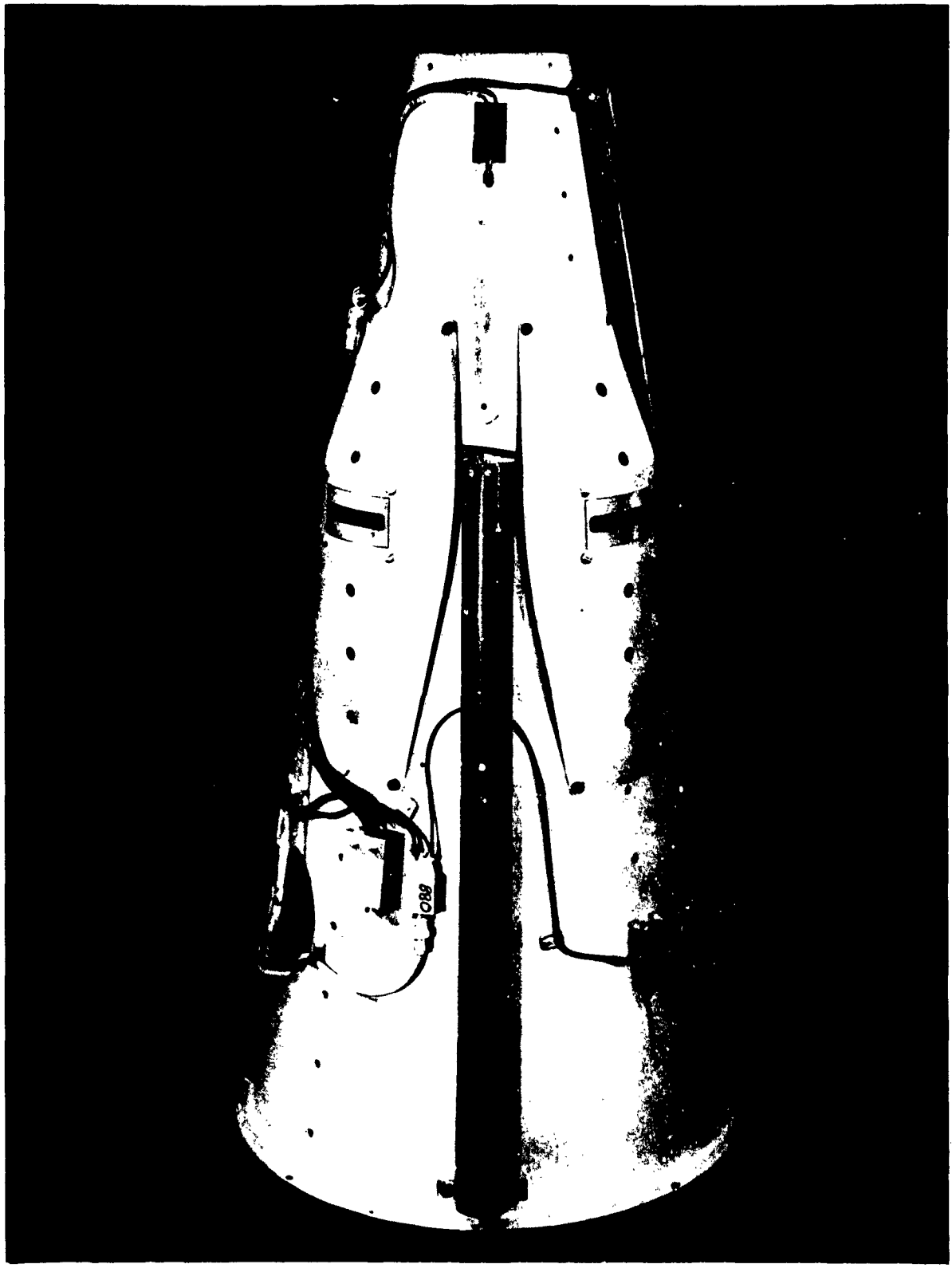

Figure C.40 Photograph of 3-frequency beacon antennas on Javelin and Honest John-Nike-Nike rockets, Project 6.2. (BRL photo)

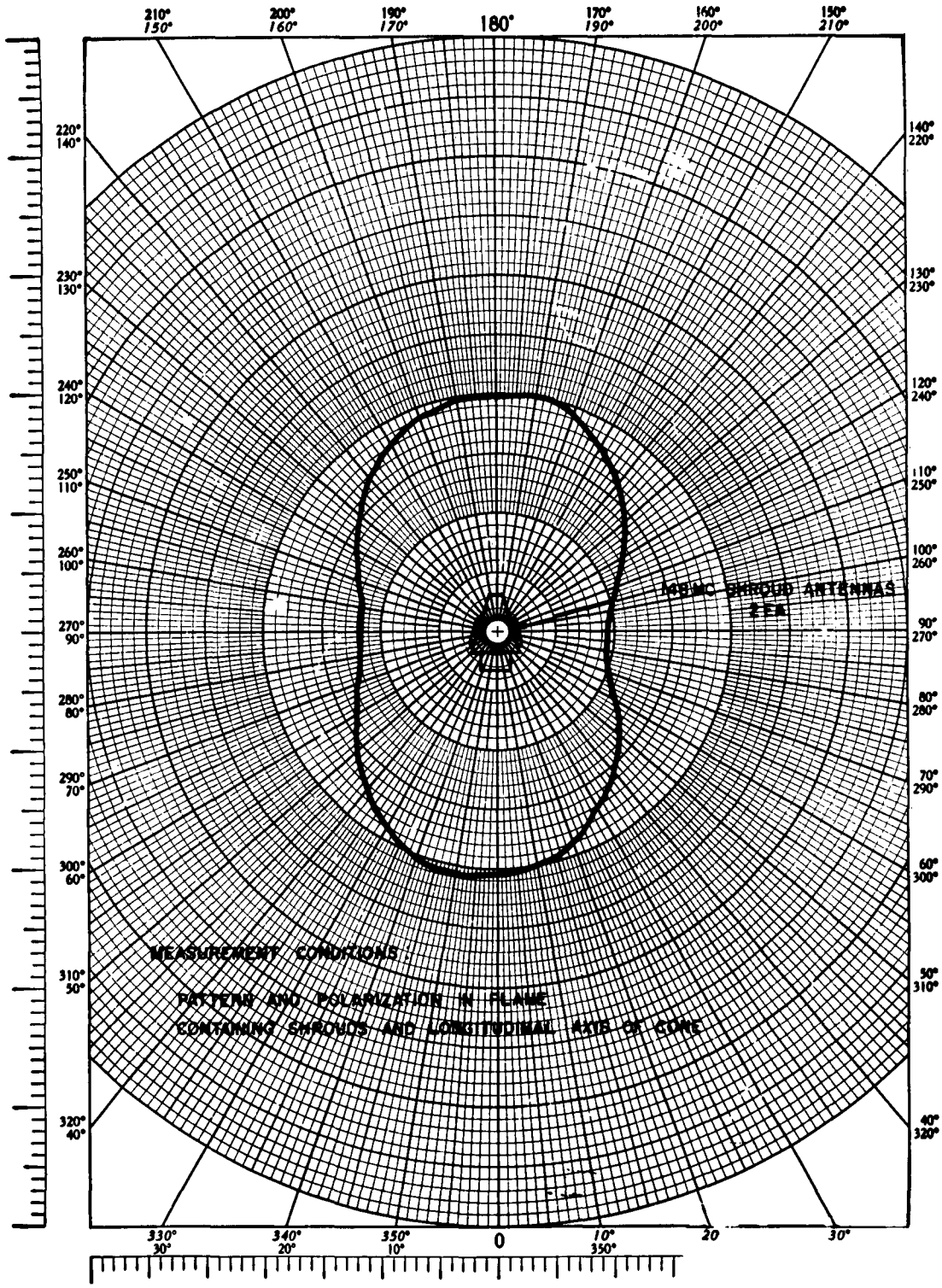

Figure C.41 Radiation pattern for 148-Mc shroud antenna on Javelin and Honest John-Nike-Nike rockets, Project 6.2.

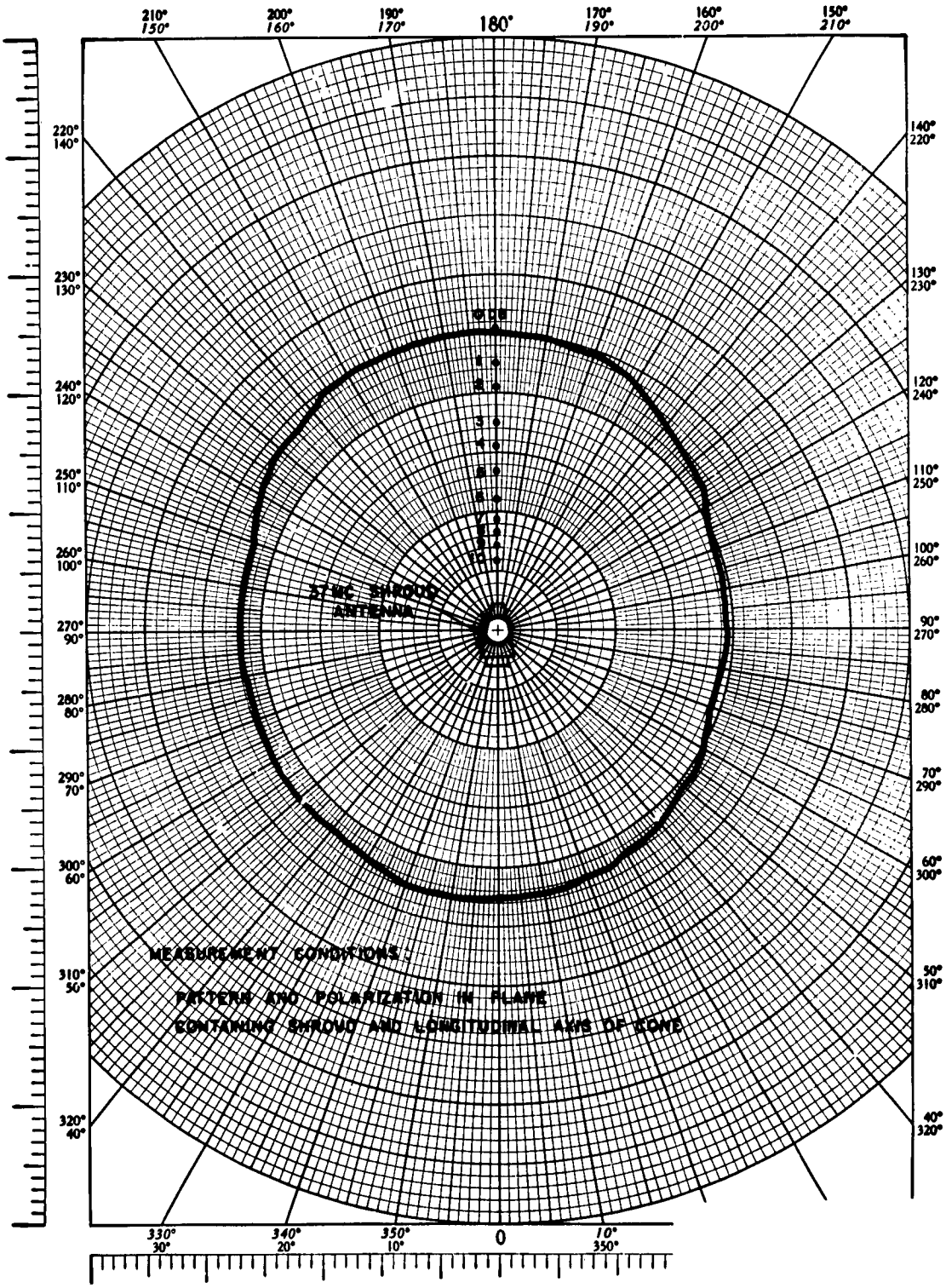

Figure C.42 Radiation pattern for 37-Mc single shroud antenna on Javelin and Honest John-Nike-Nike rockets, Project 6.2.

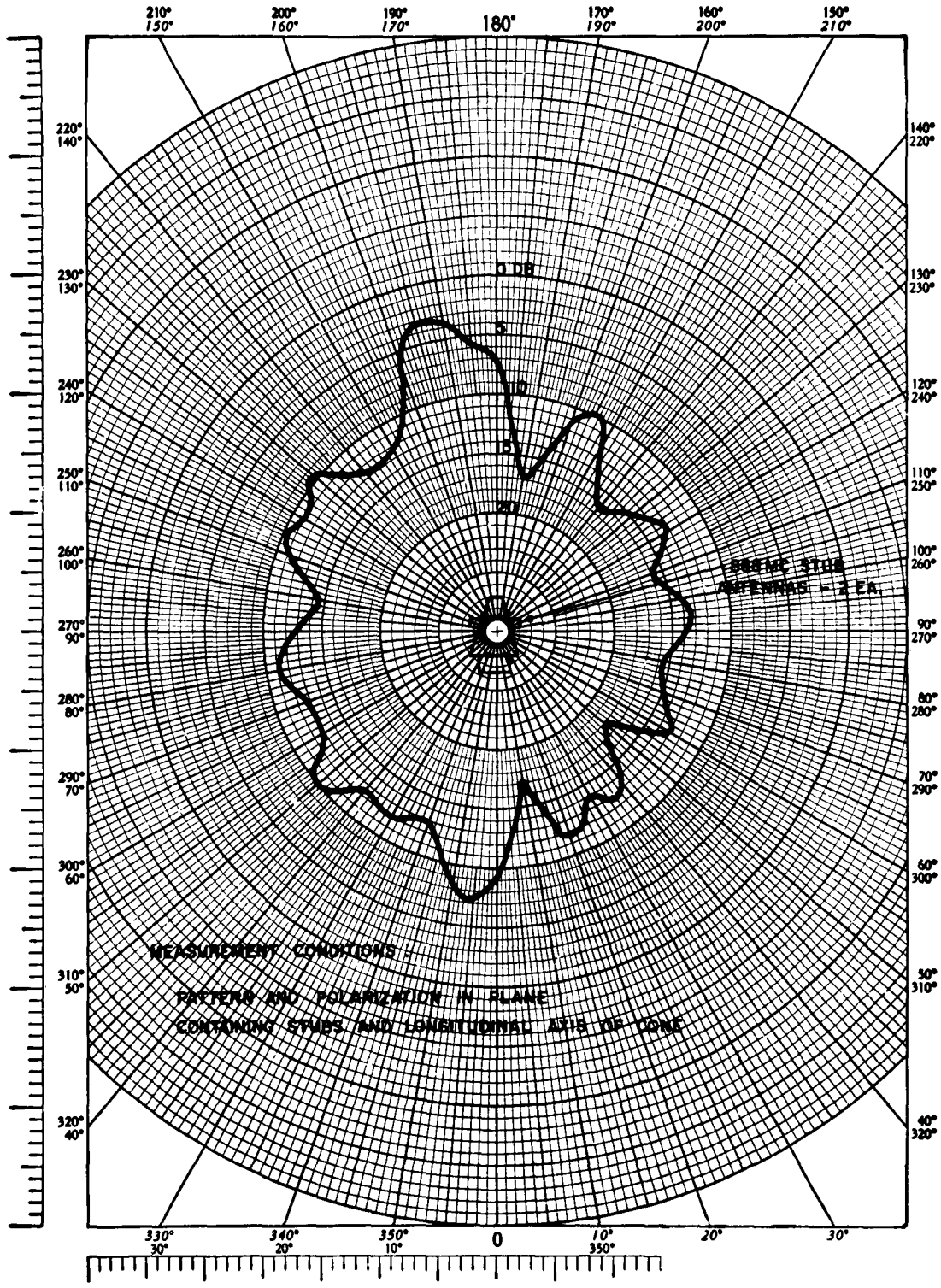

Figure C.43 Radiation pattern for 888-Mc stub antennas on Javelin and Honest John-Nike-Nike rockets, Project 6.2.

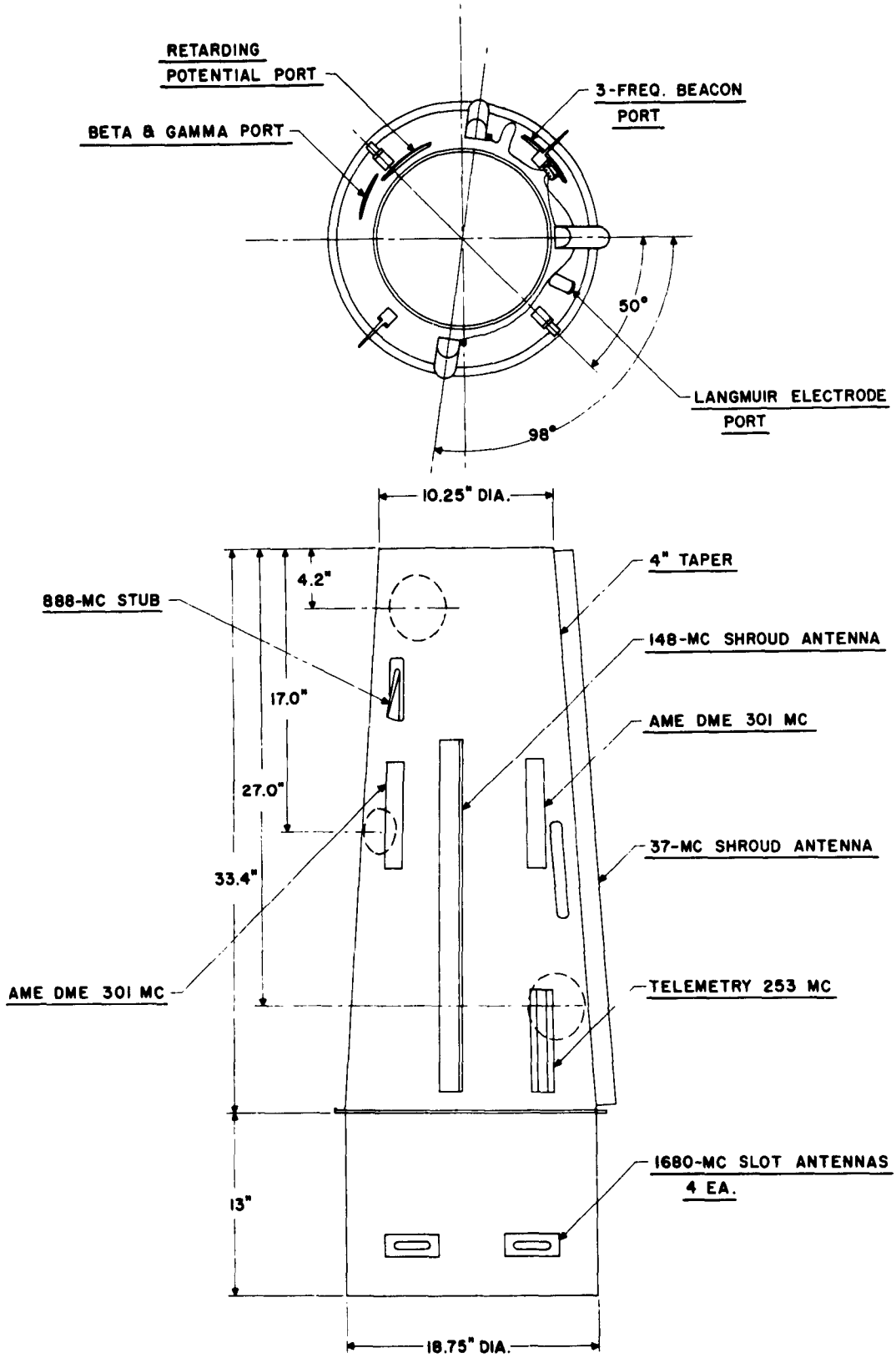

Figure C.44 Three-frequency beacon antennas on Javelin rockets, Project 6.4.

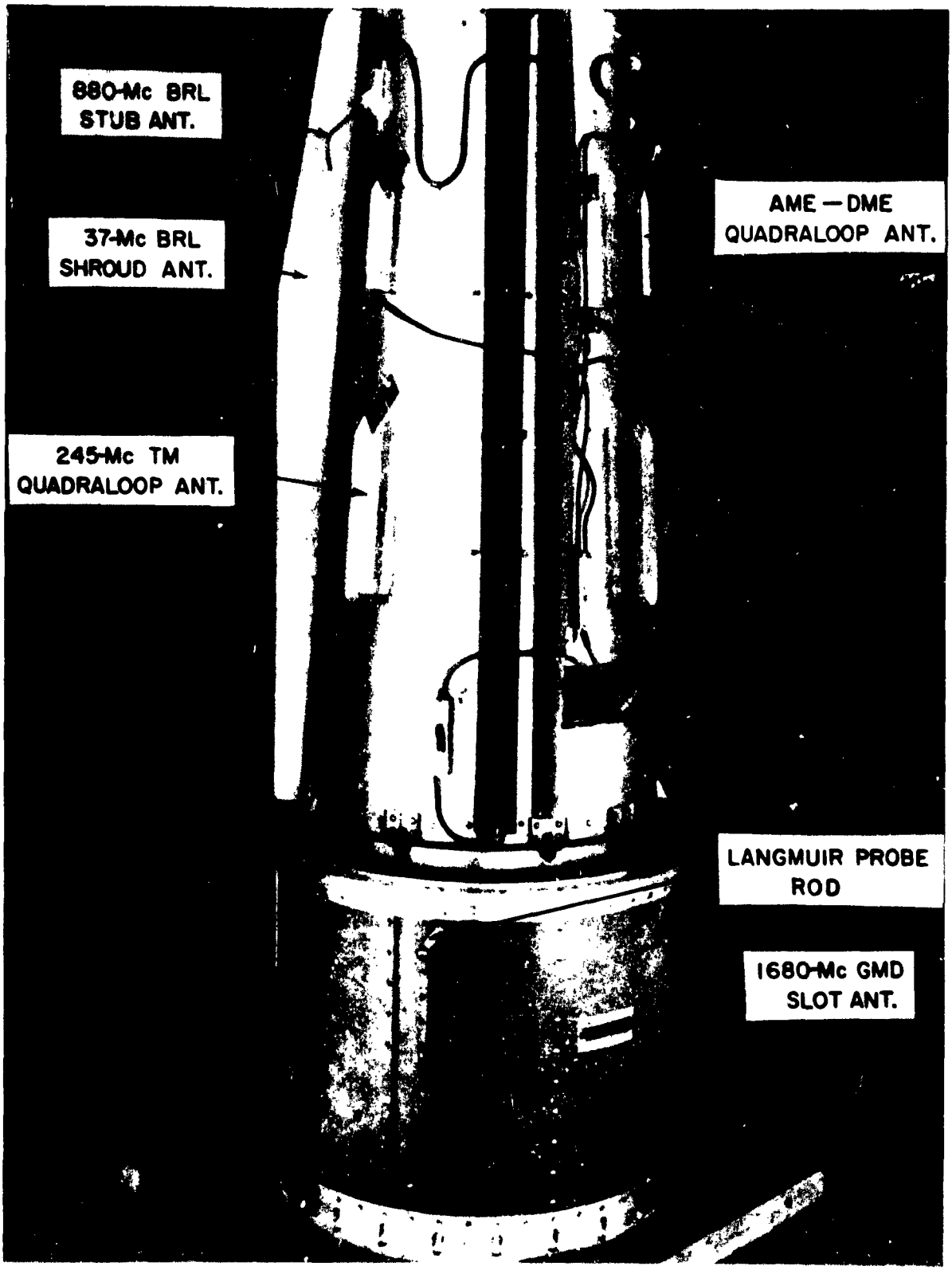

Figure C.45 Photograph of 3-frequency beacon antennas on Javelin rockets, Project 6.4. (BRL photo).

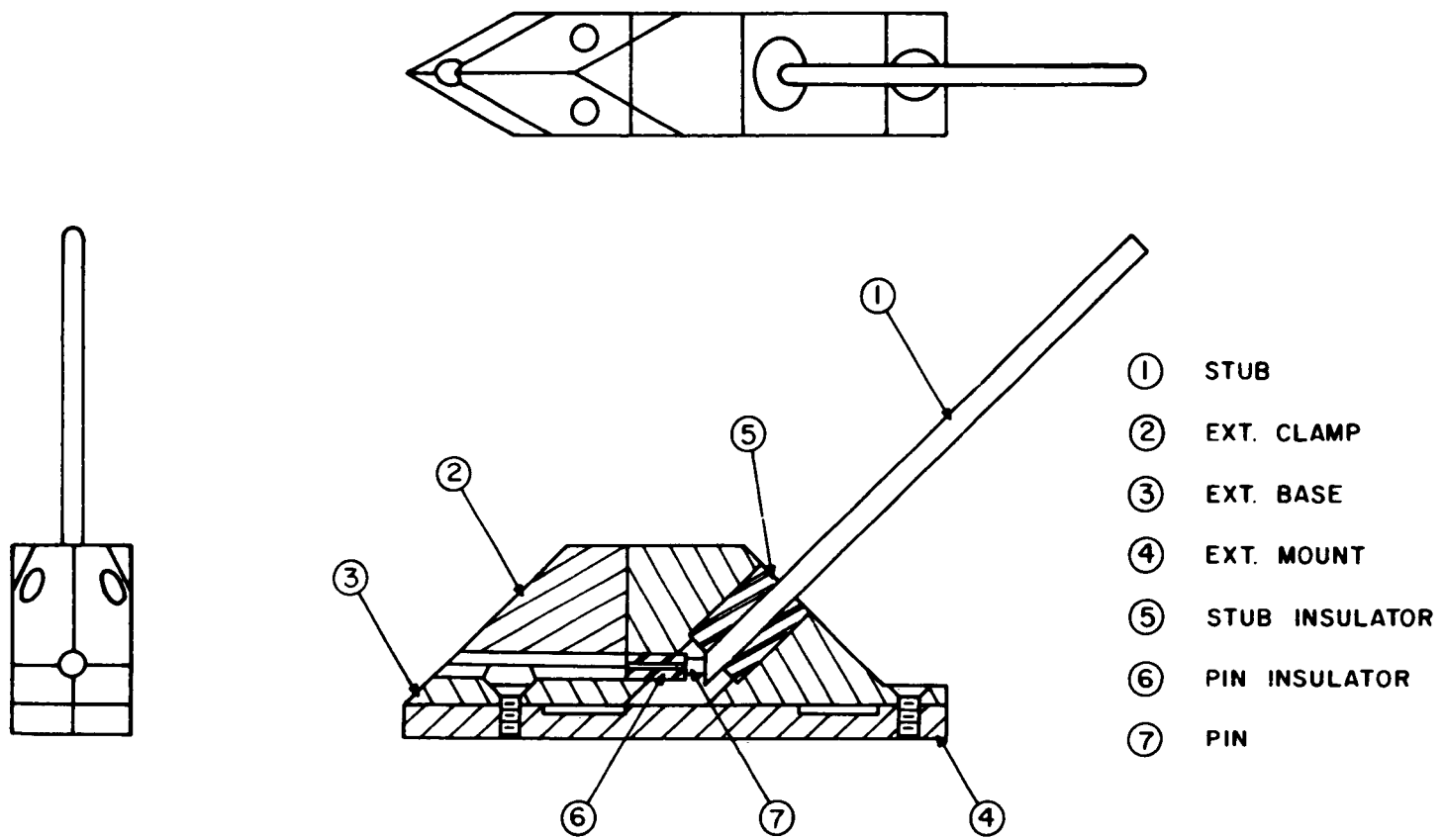

Figure C.46 BRL-designed 888-Mc stub antenna.

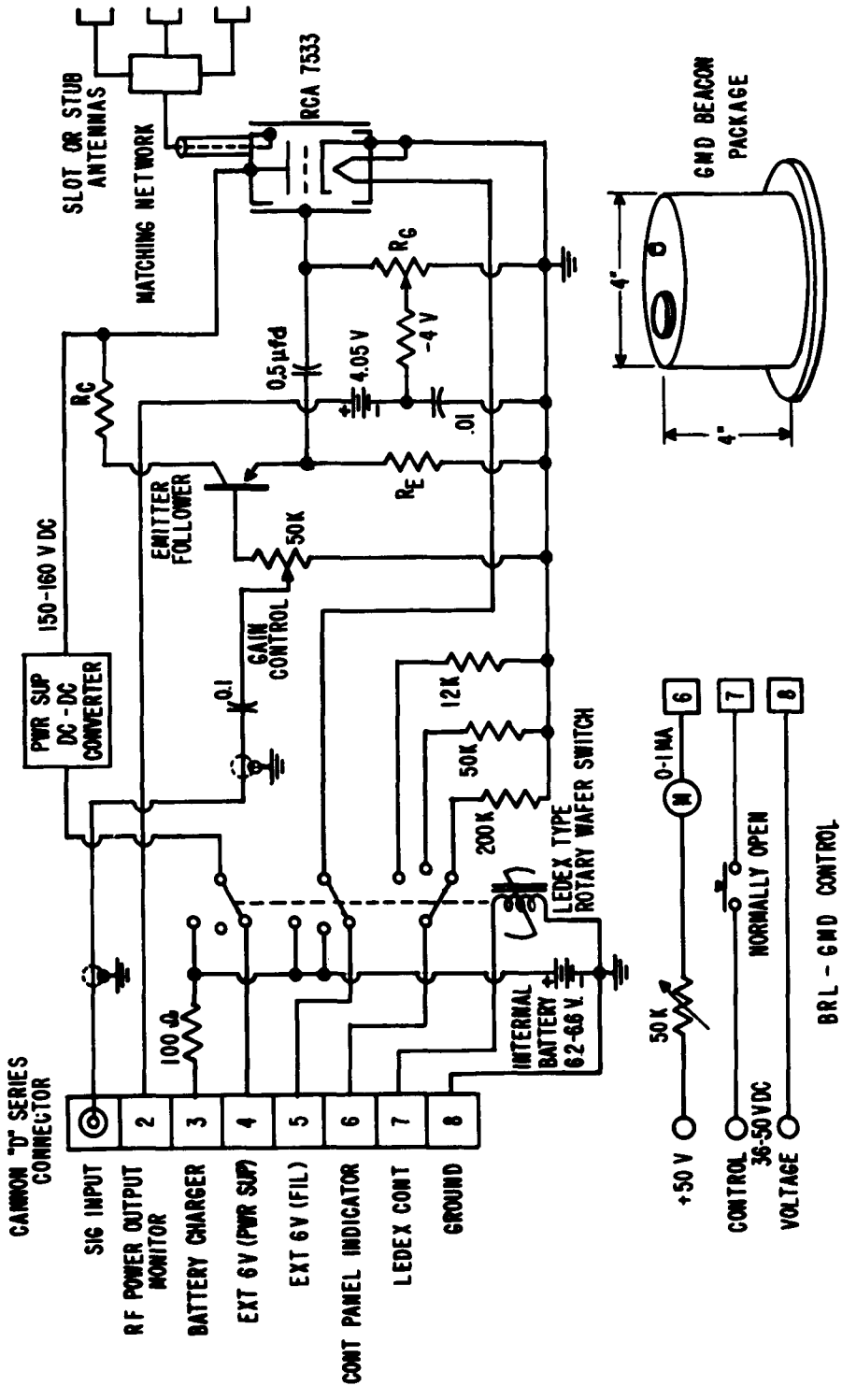

Figure C.47 Circuit diagram of GMD beacon.

Figure C.48 Photograph of 1380-Mc slot antennas on Nike-Cajun rockets. Project 6.3. (BRL photo)

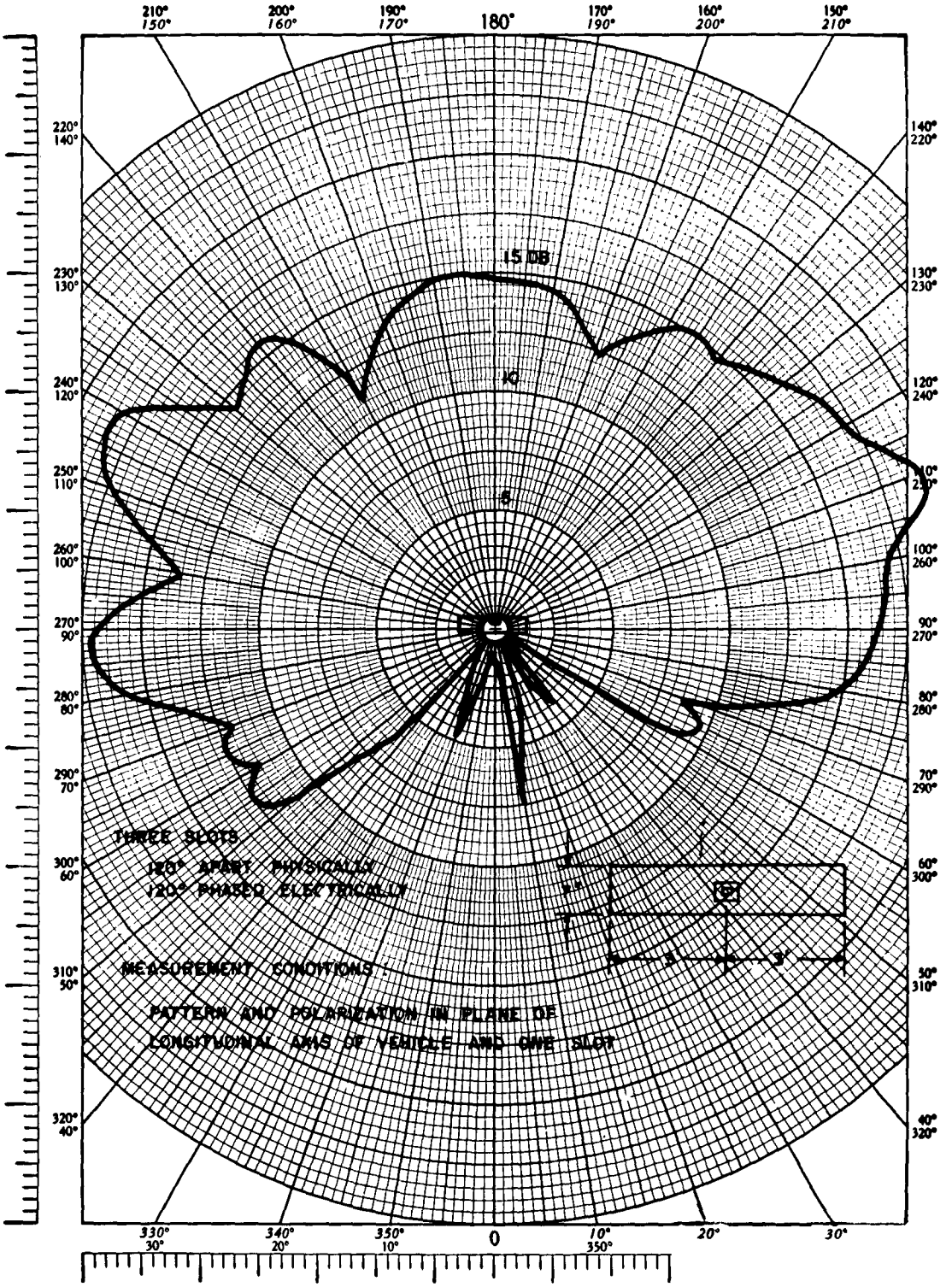

Figure C.49 Radiation pattern for 1680-Mc slot antennas in plane of longitudinal axis of rocket.

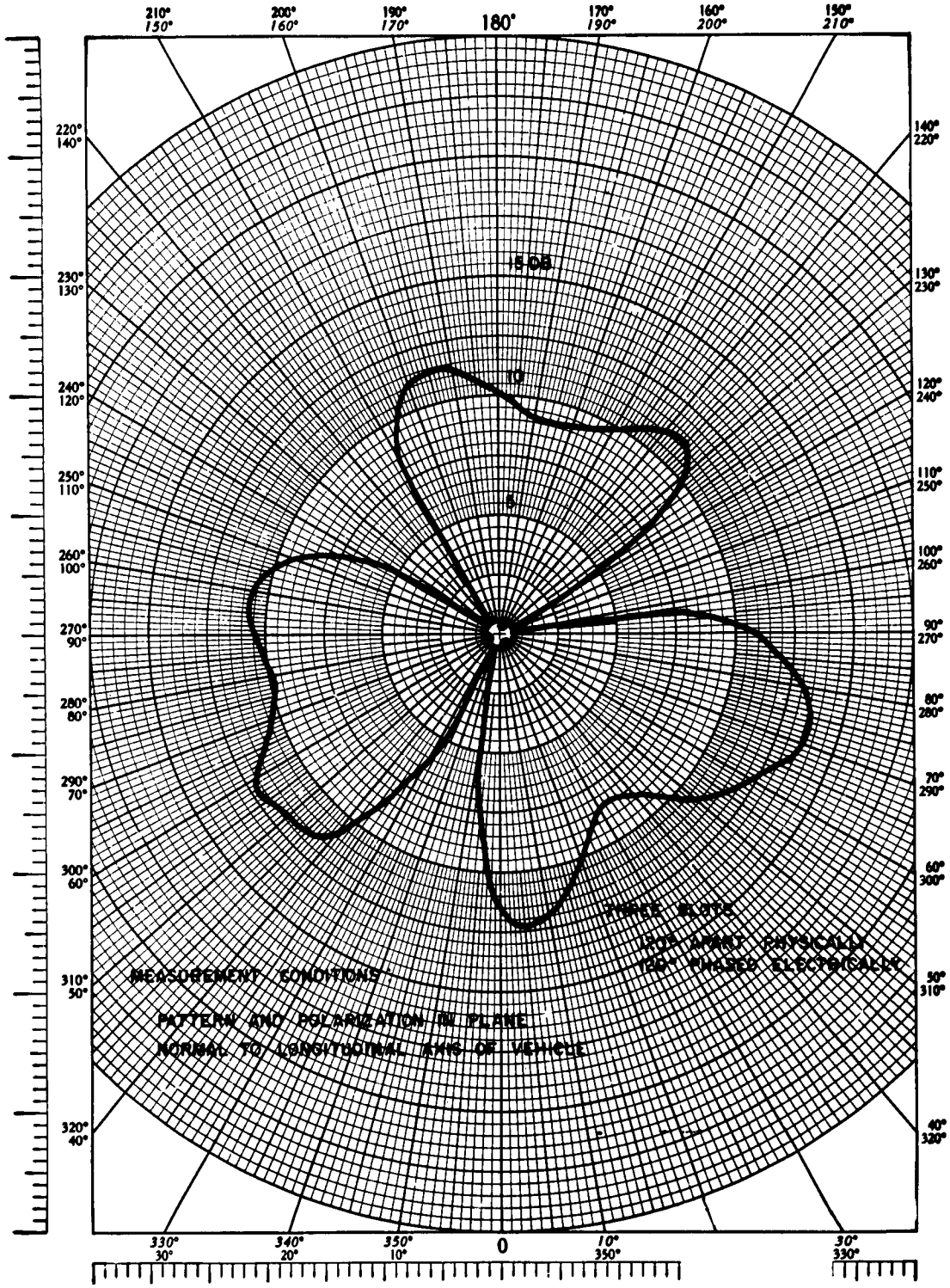

Figure C.50 Radiation pattern for 1680-Mc slot antennas off side of rocket.

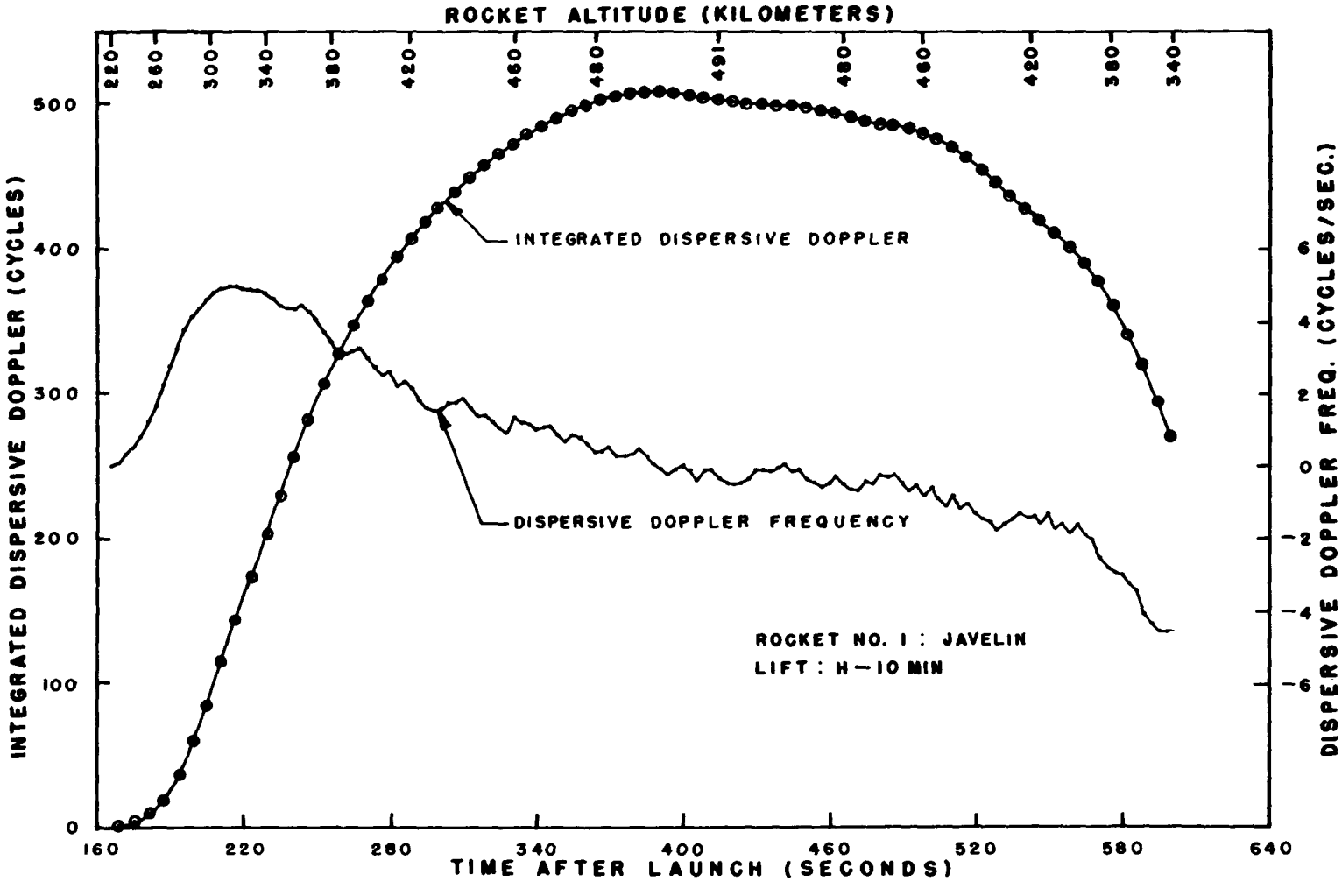

Figure C.51 Dispersive doppler versus time derived from the 37- and 148-Mc doppler Rocket 1, Star Fish.

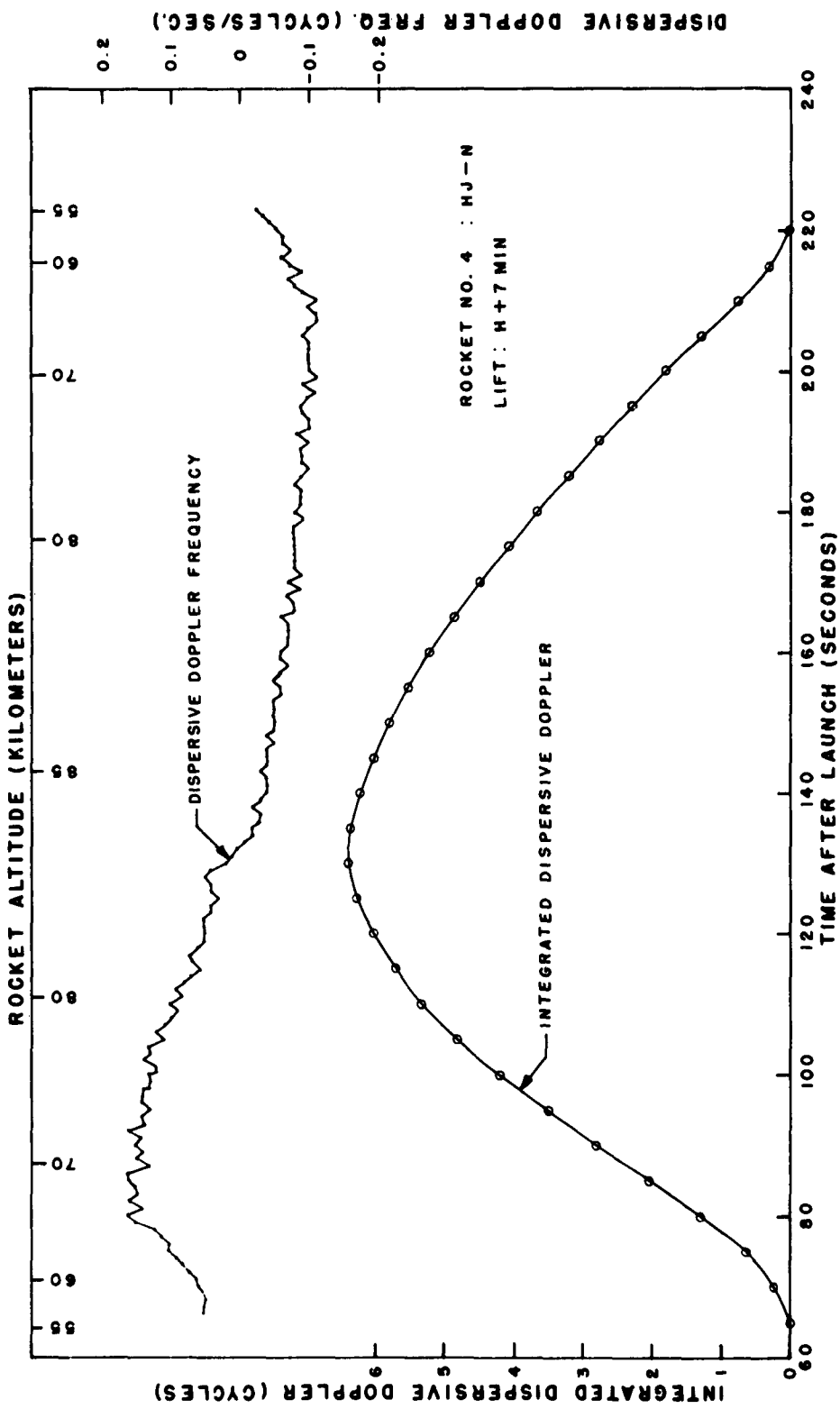

Figure C.52 Dispersive doppler versus time derived from the 37- and 148-Mc doppler, Rocket 4, Star Fish.

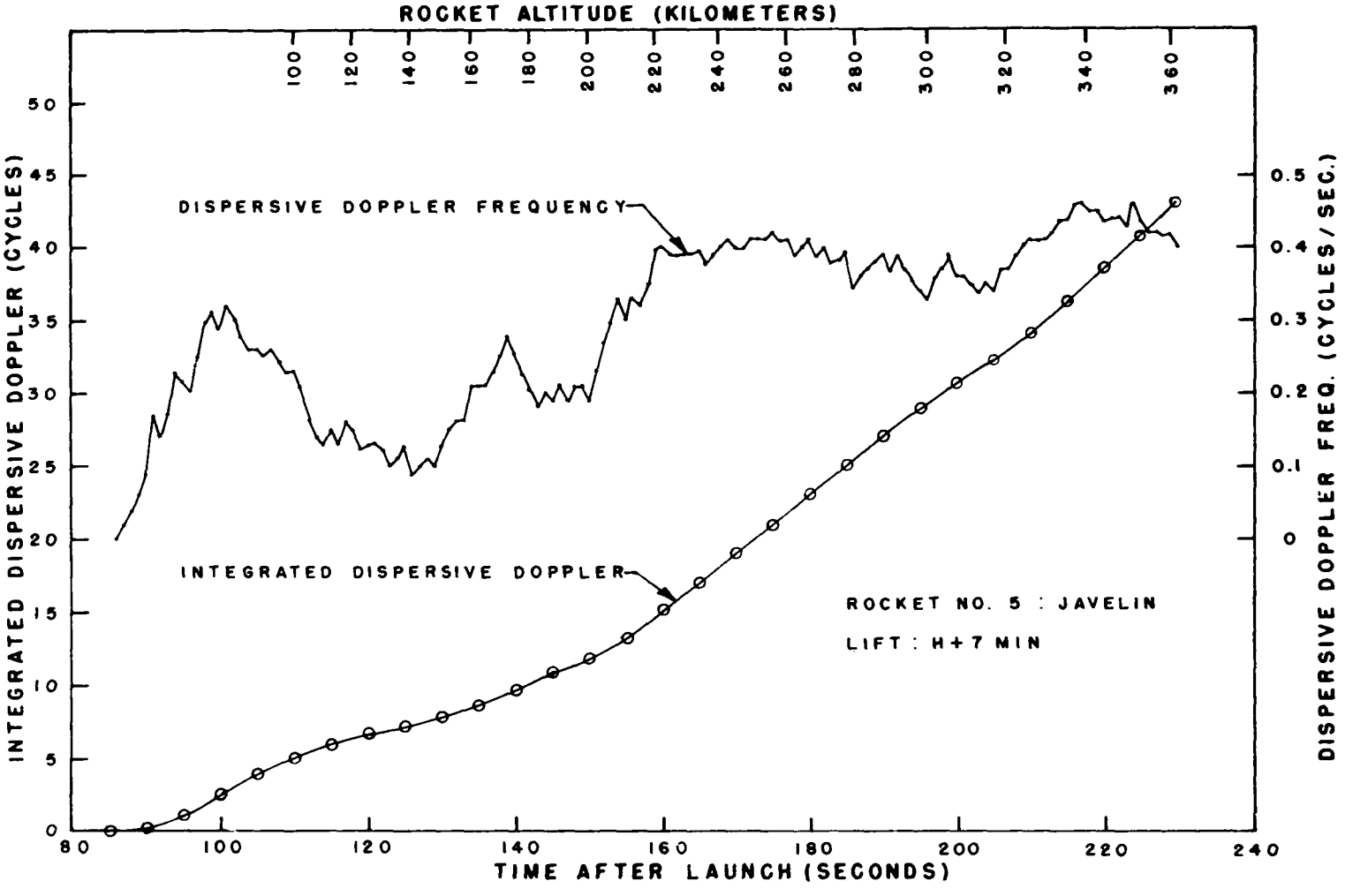

Figure C.53 Dispersive doppler versus time derived from the 37- and 148-Mc doppler, Rocket 5, Star Fish.

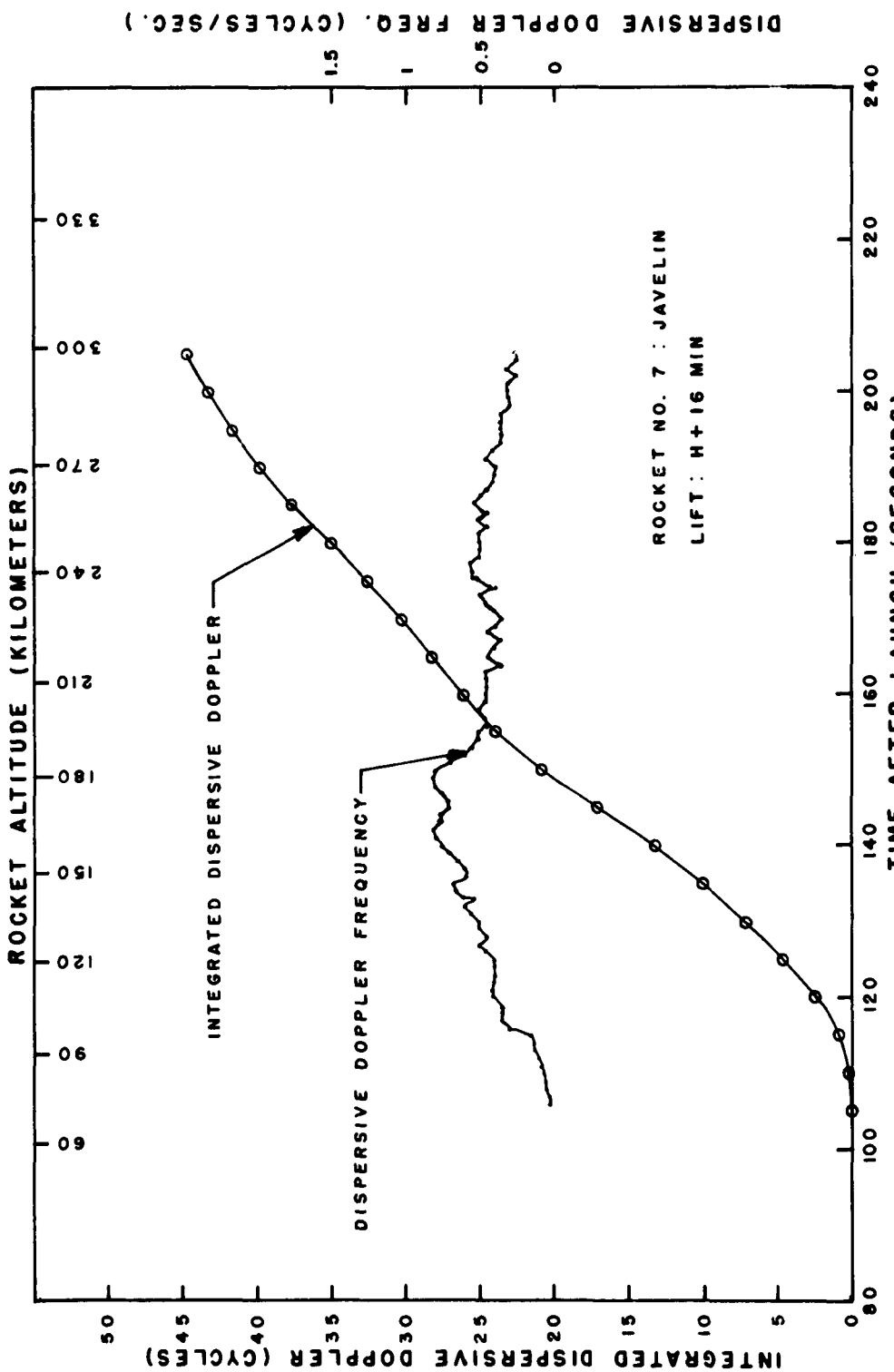

Figure C.54 Dispersive doppler versus time derived from the 37- and 148-Mc doppler, Rocket 7, Star Fish.

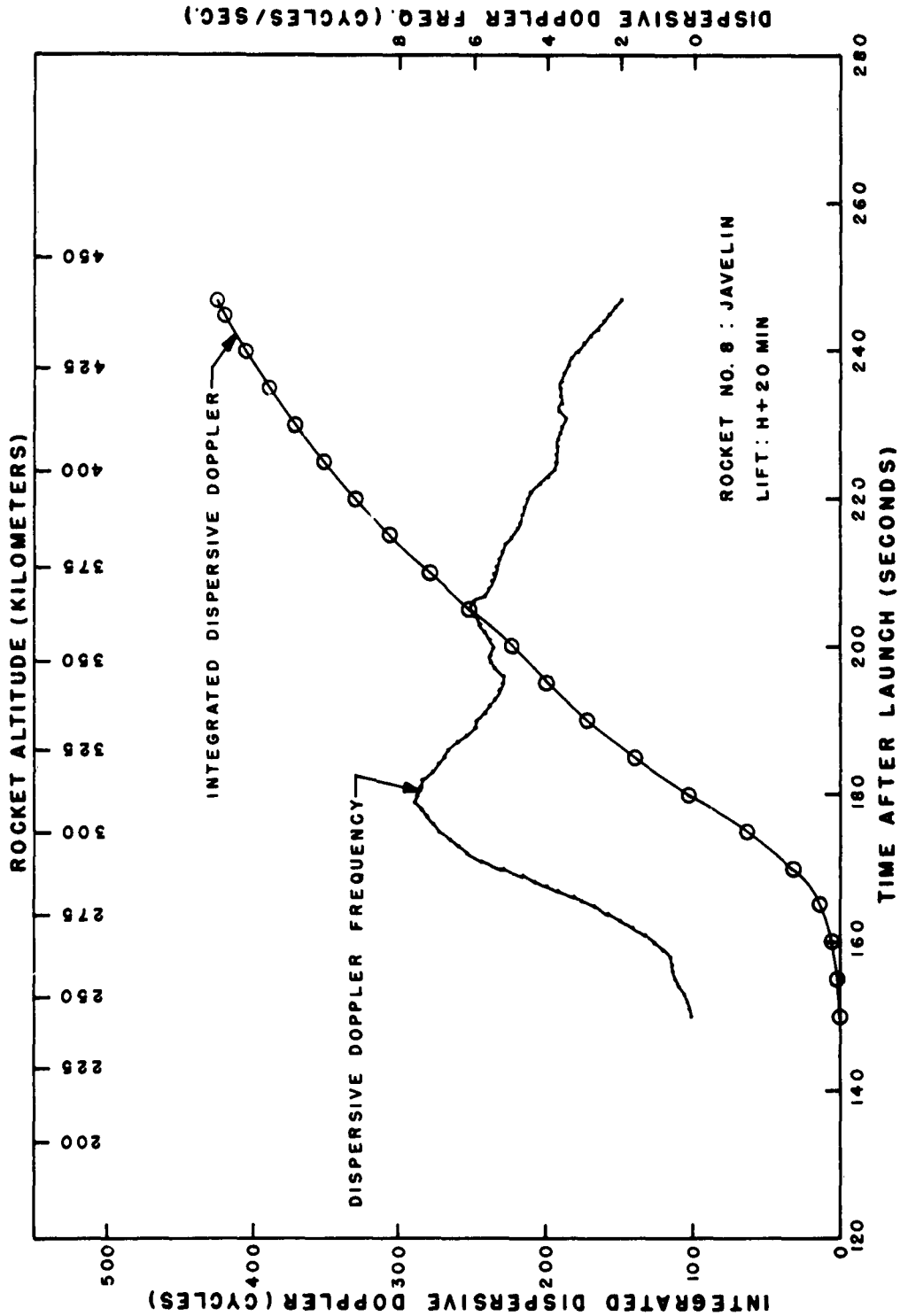

Figure C.55 Dispersive doppler versus time derived from the 37- and 148-Mc doppler, Rocket 8, Star Fish.

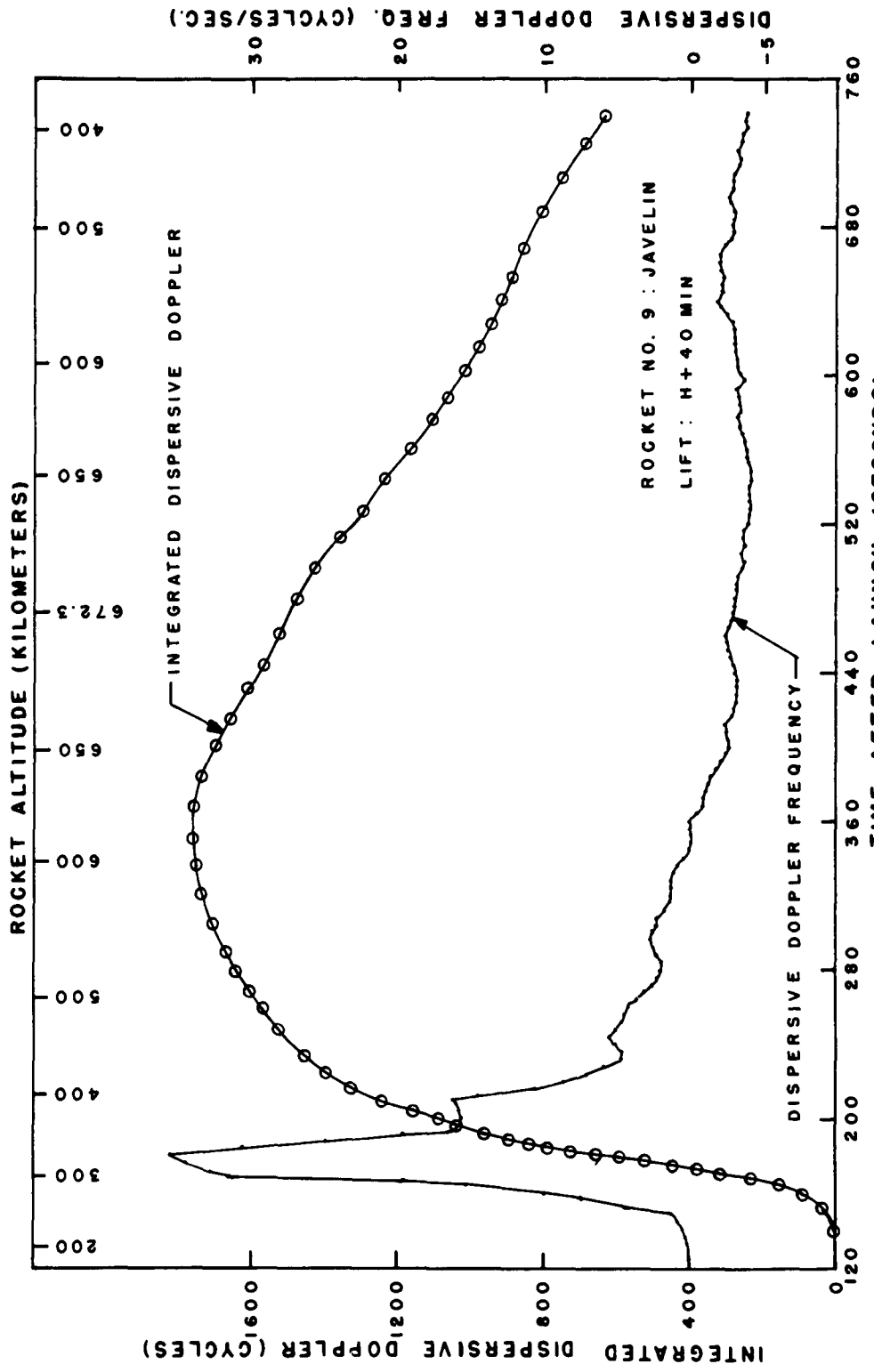

Figure C.56 Dispersive doppler versus time derived from the 37- and 148-Mc doppler, Rocket 9, Star Fish.

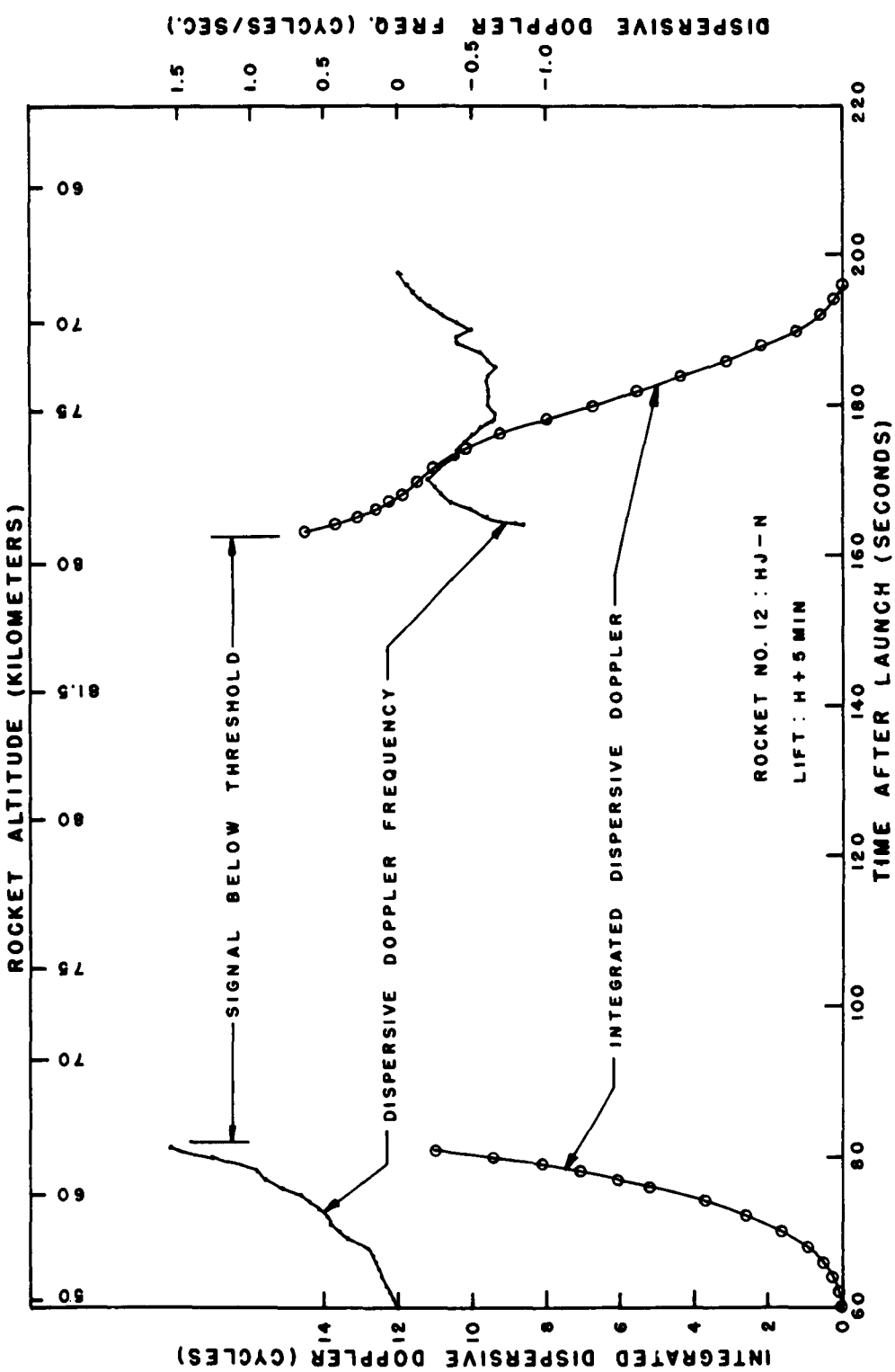

Figure C.57 Dispersive doppler versus time derived from the 37- and 148-Mc doppler, Rocket 12, Blue Gill.

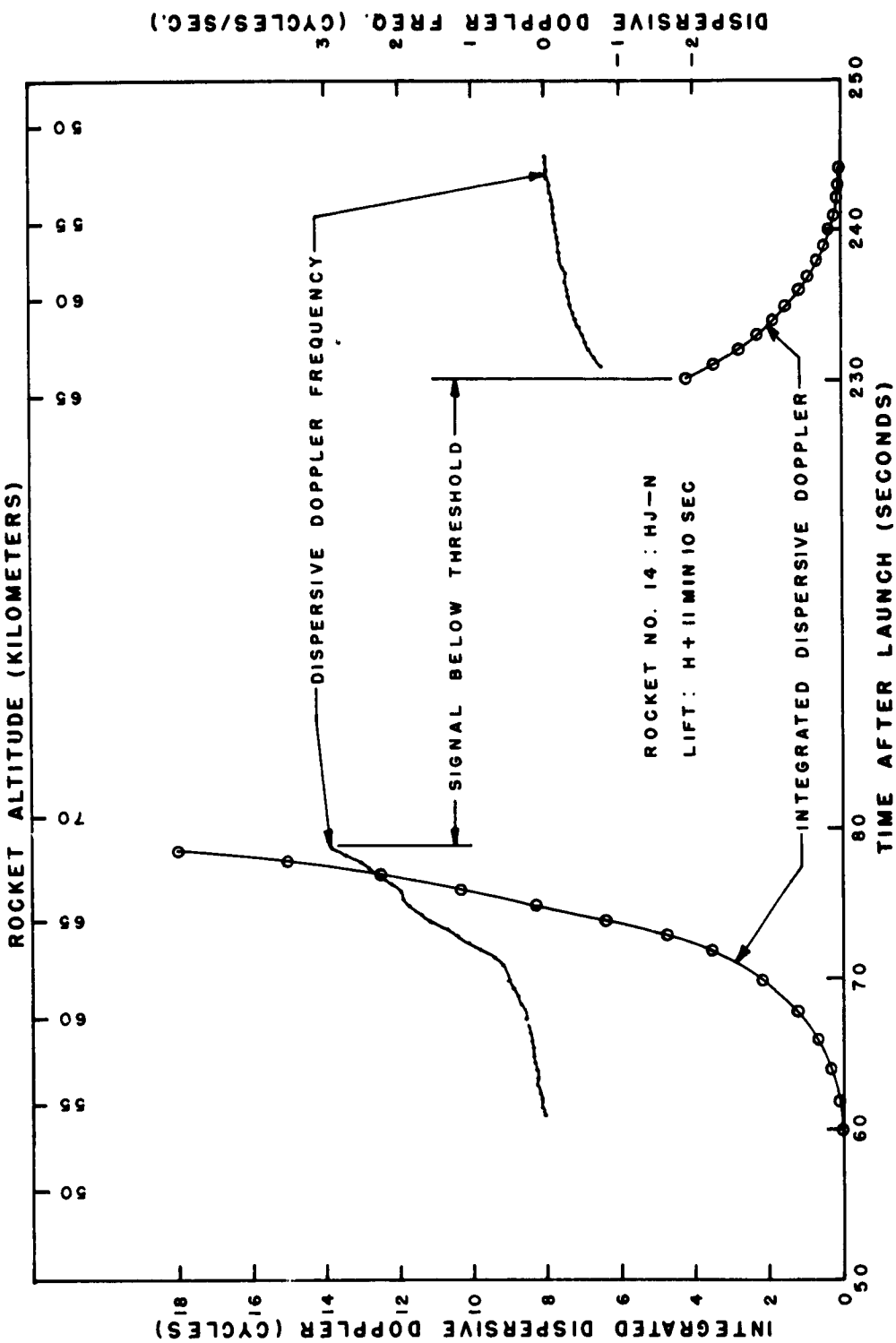

Figure C.58 Dispersive doppler versus time derived from the 37- and 148-Mc doppler, Rocket 14, Blue Gill.

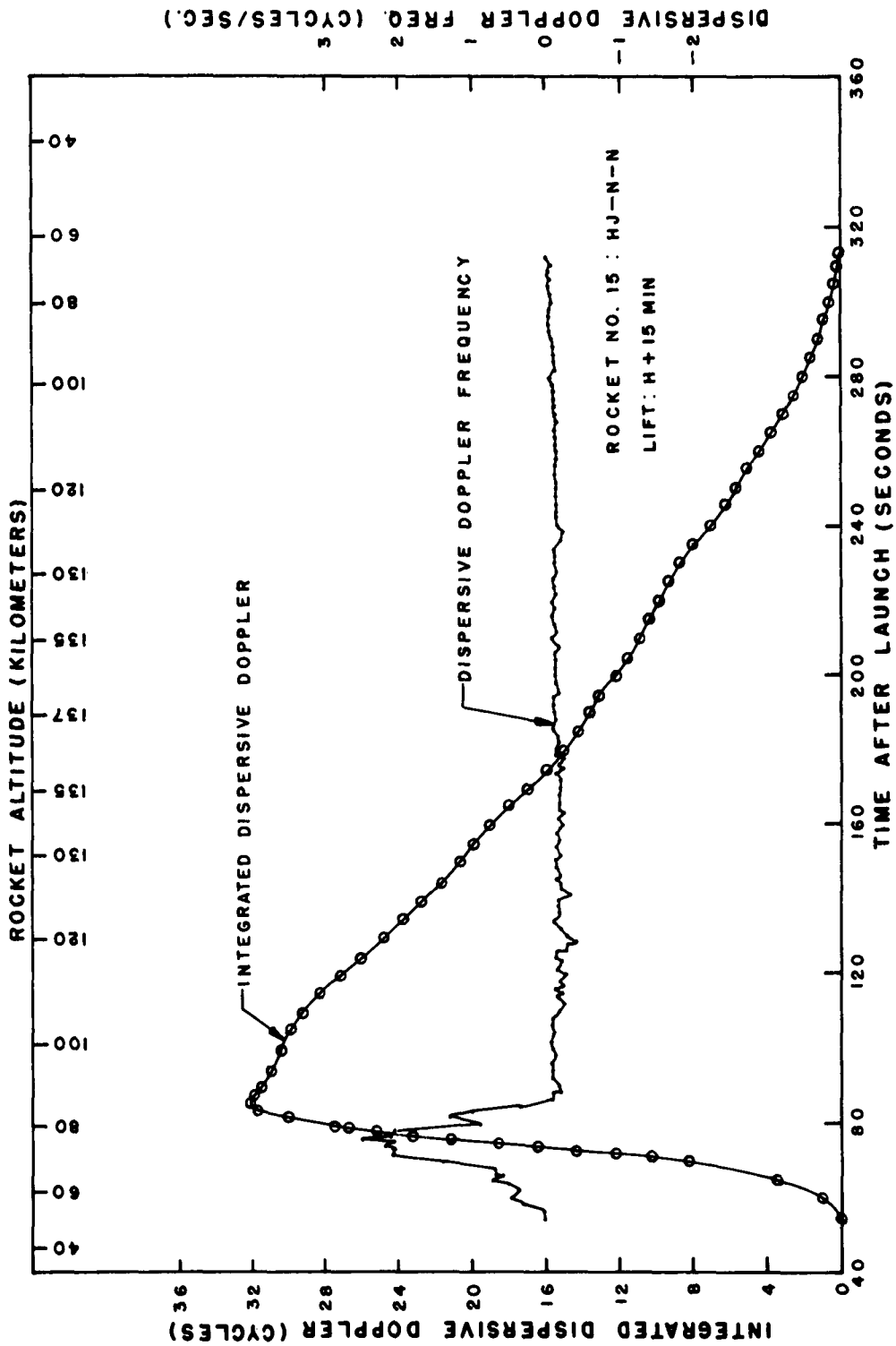

Figure C.59 Dispersive doppler versus time derived from the 37- and 148-Mc doppler, Rocket 15, Blue Gill.

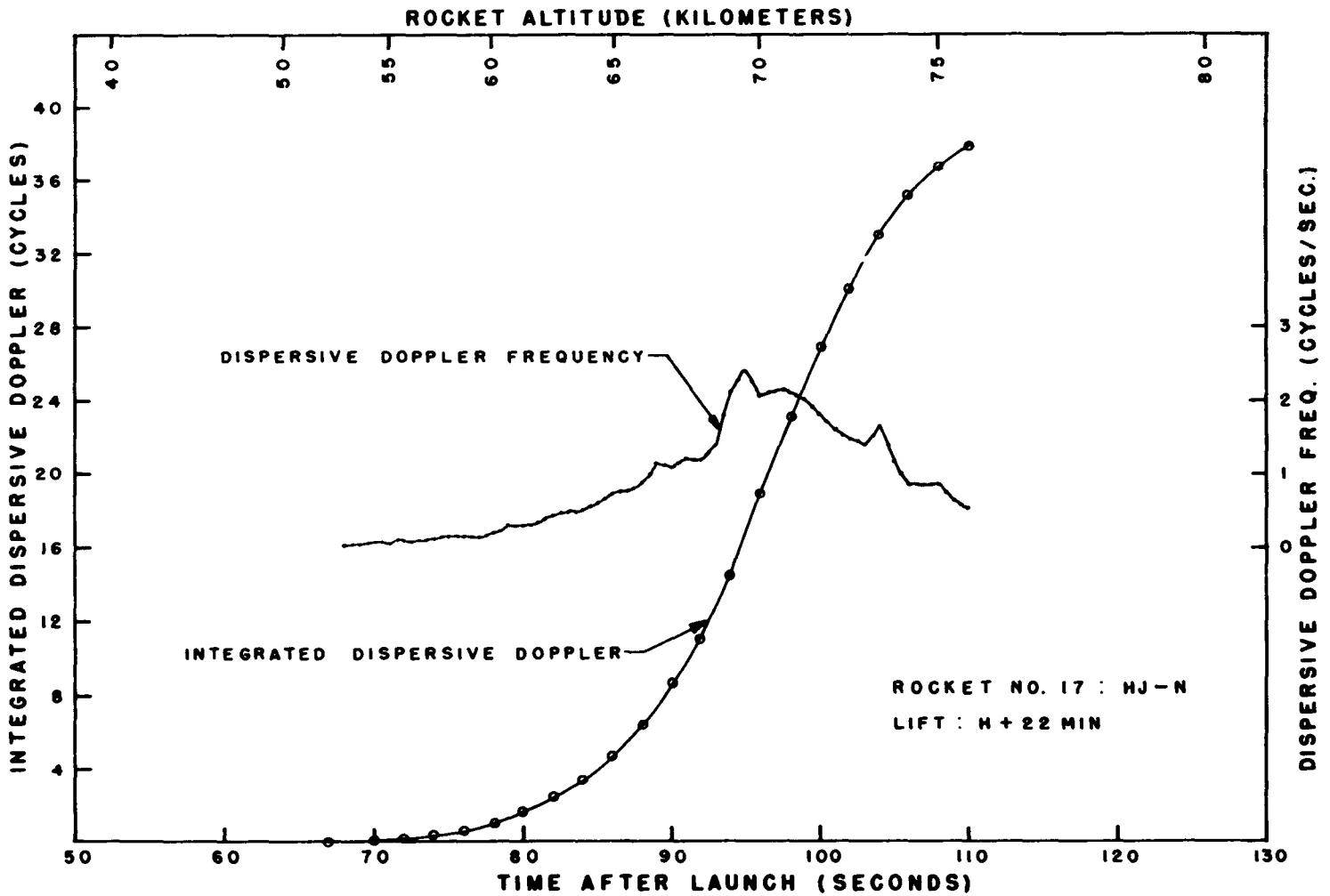

Figure C.60 Dispersive doppler versus time derived from the 37- and 148-Mc doppler, Rocket 17, Blue Gill.

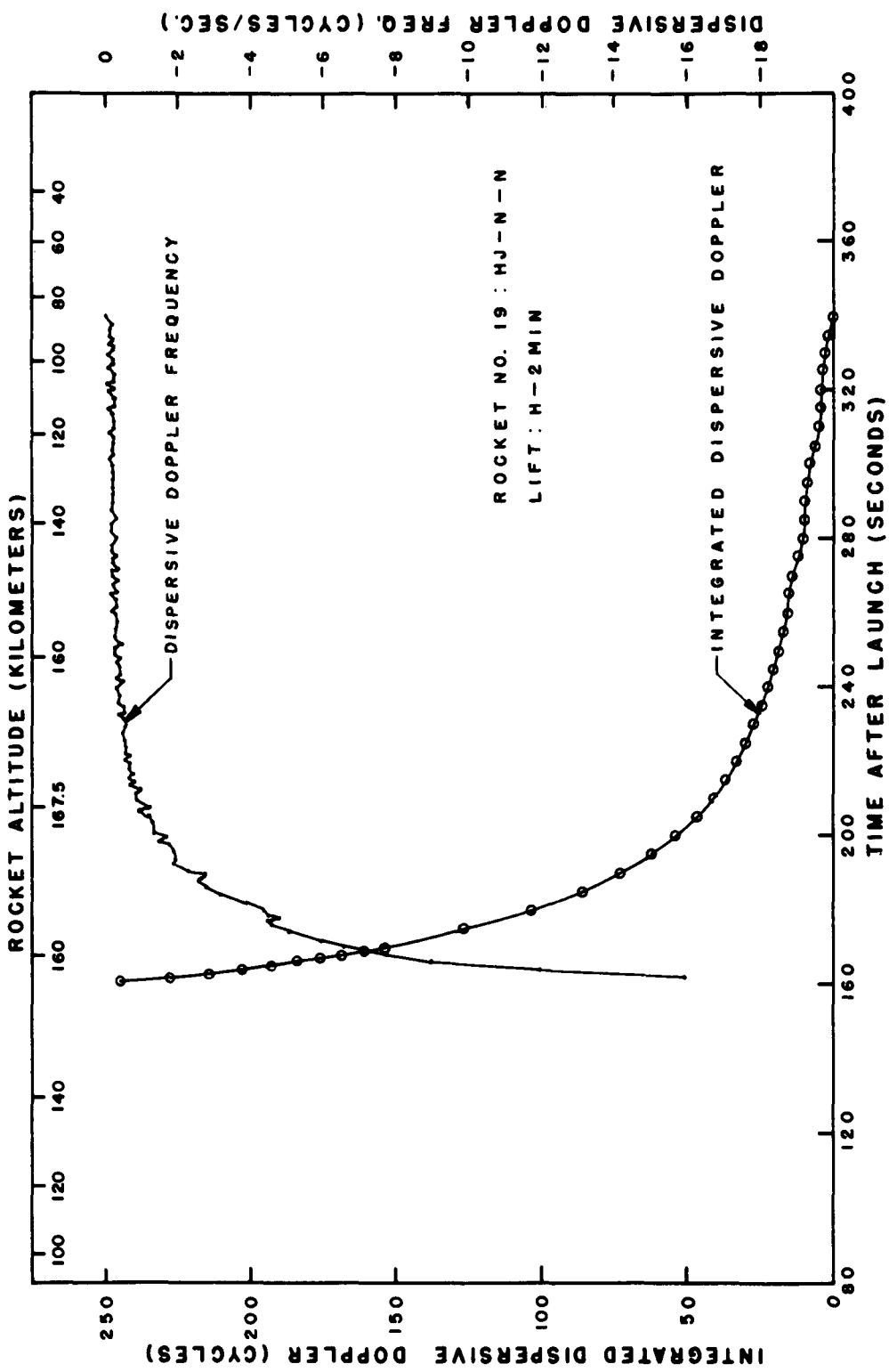

Figure C.61 Dispersive doppler versus time derived from the 37- and 148-Mc doppler, Rocket 19, King Fish.

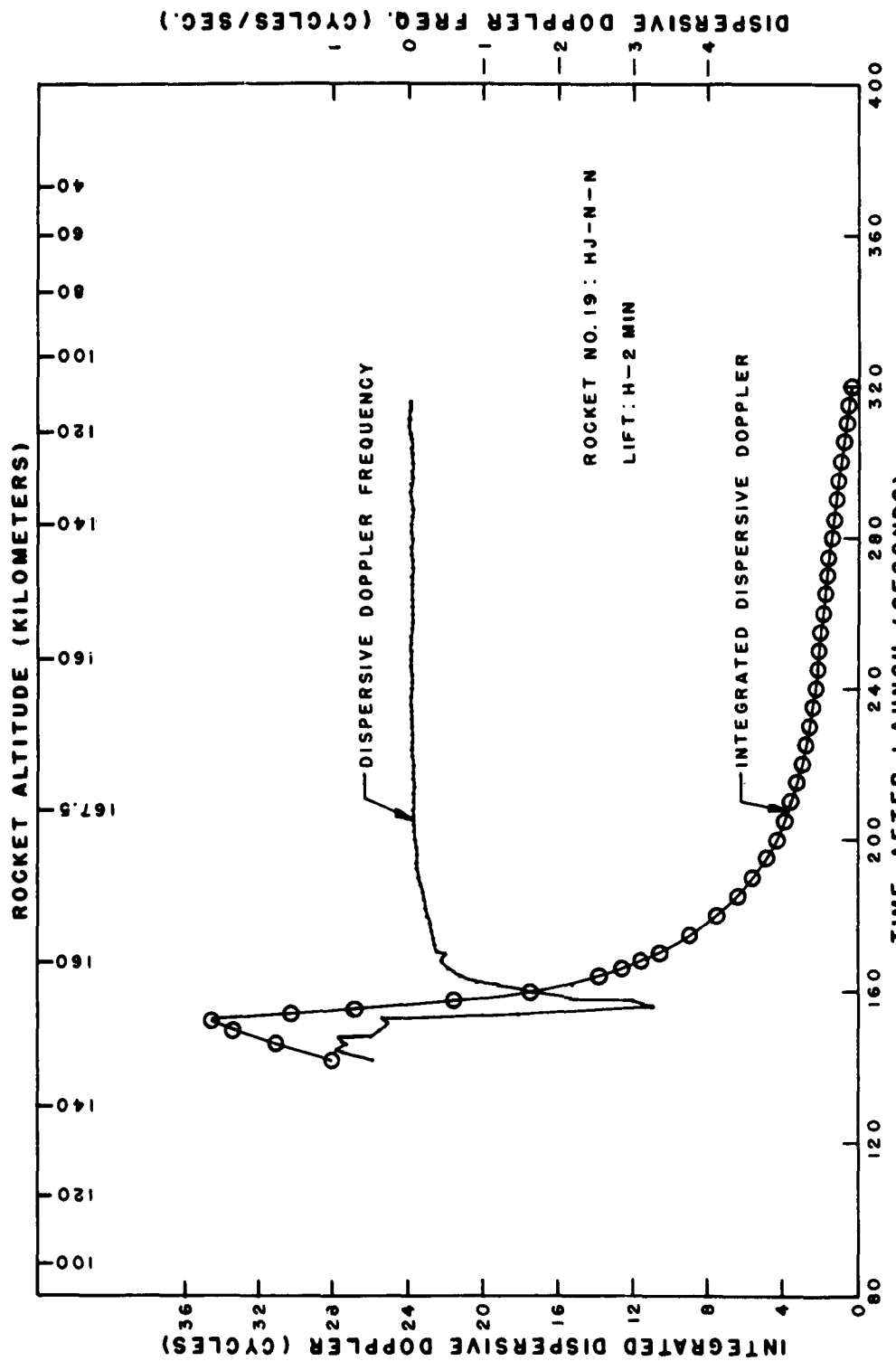

Figure C.62 Dispersive doppler versus time derived from the 148- and 888-Mc doppler, Rocket 19, King Fish.

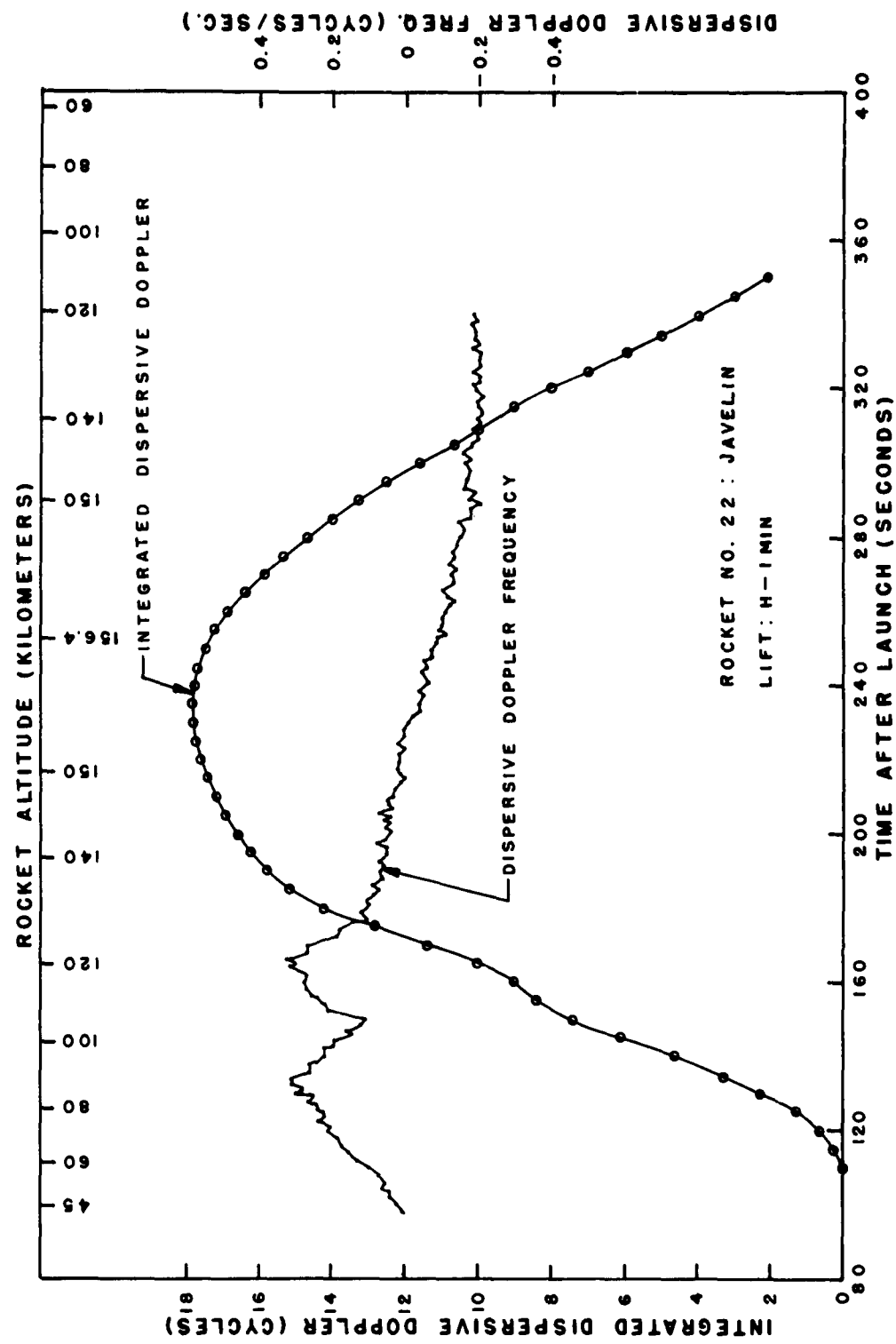

Figure C.63 Dispersive doppler versus time derived from the 37- and 148-Mc doppler, Rocket 22, King Fish.

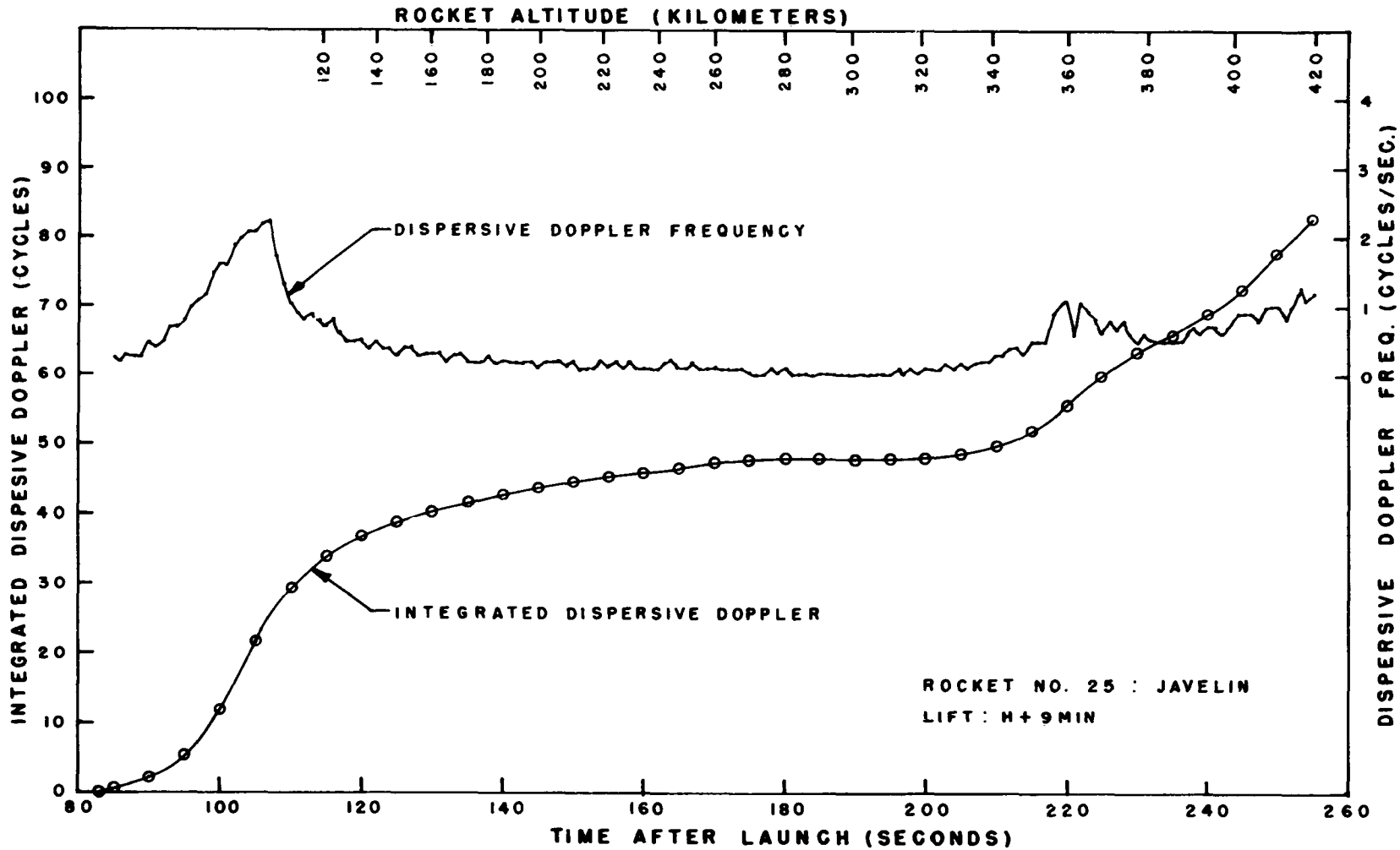

Figure C.64 Dispersive doppler versus time derived from the 37- and 148-Mc doppler, Rocket 25, King Fish.

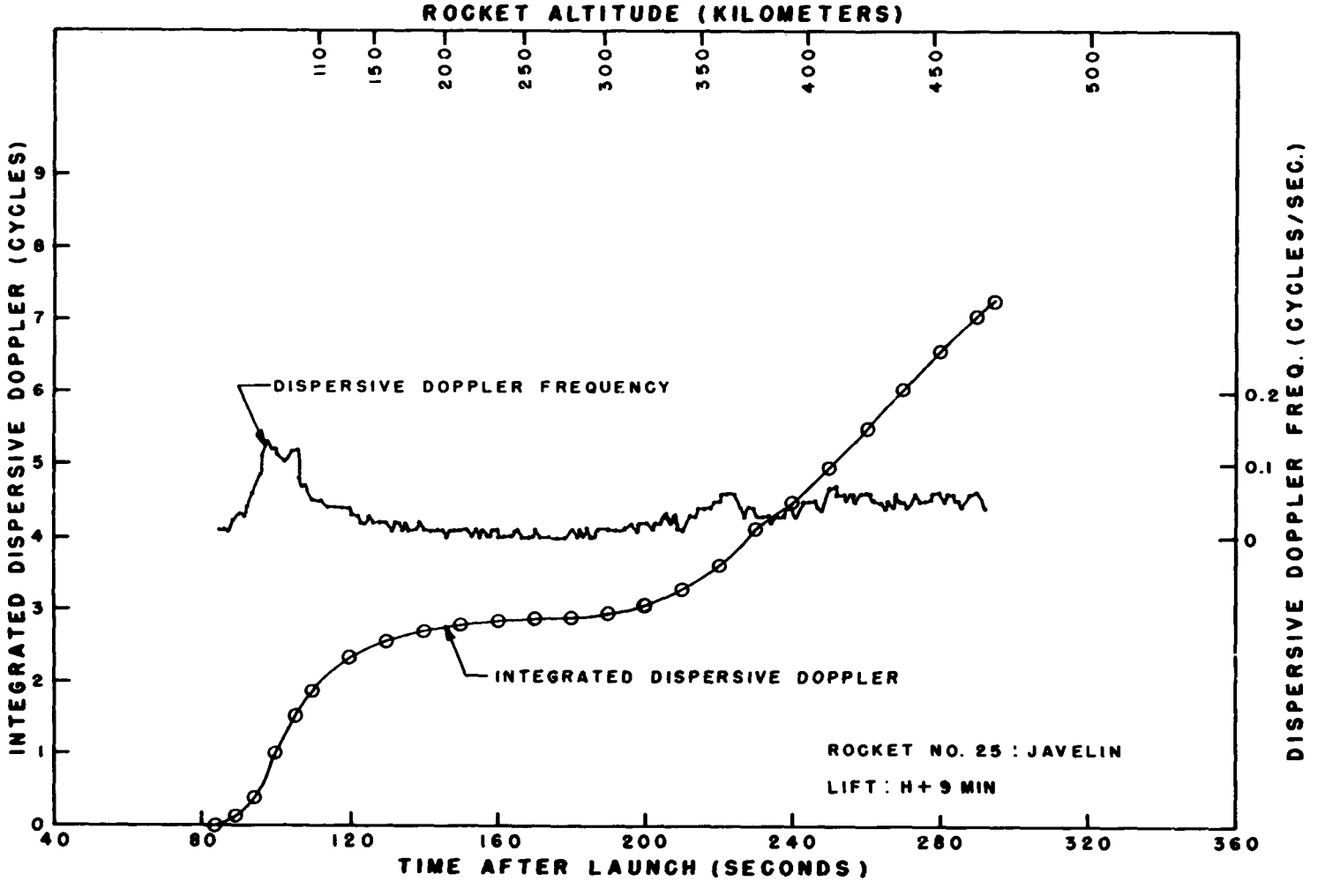

Figure C.65 Dispersive doppler versus time derived from the 148- and 888-Mc doppler, Rocket 25, King Fish.

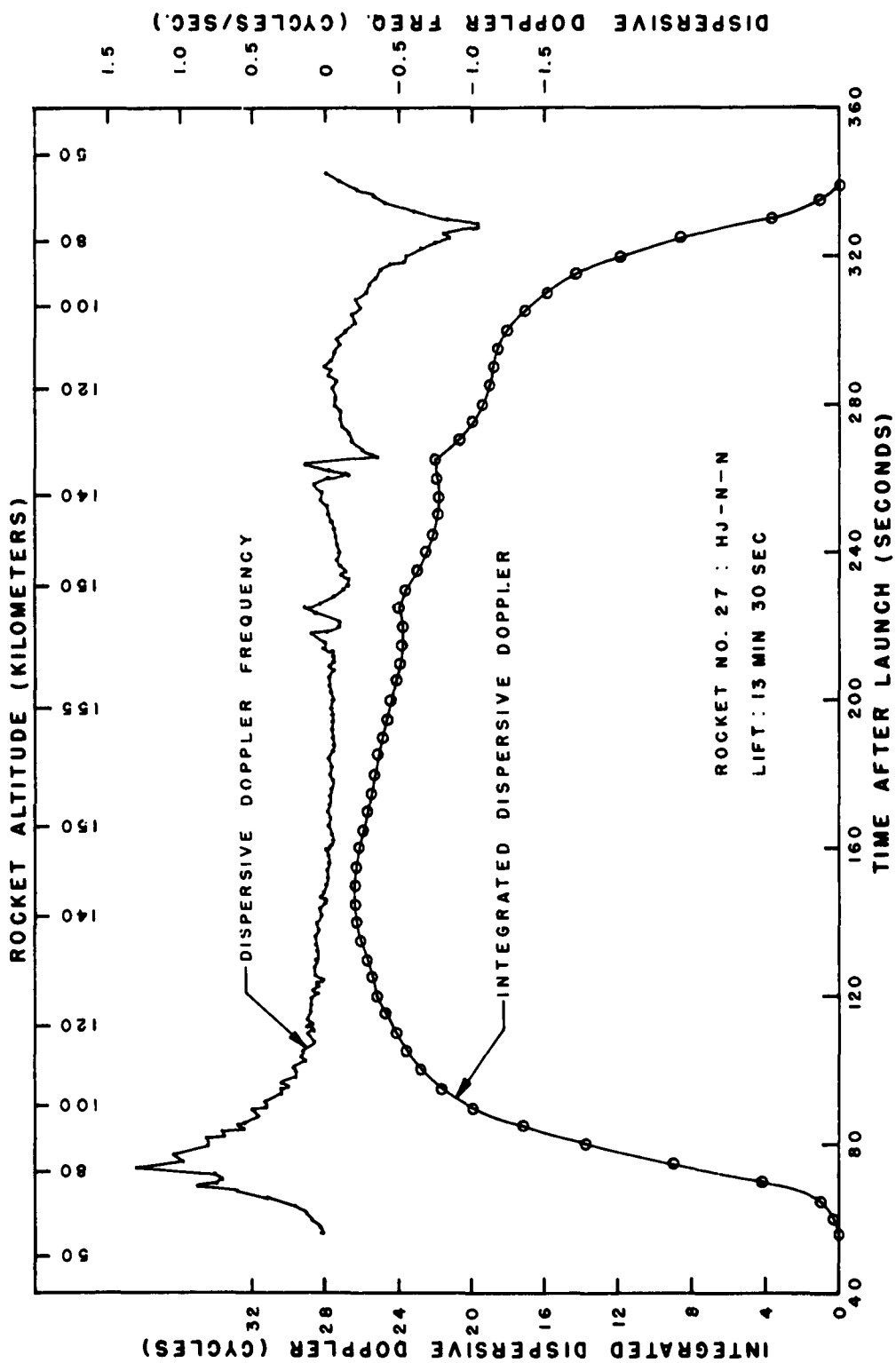

Figure C.66 Dispersive doppler versus time derived from the 37- and 148-Mc doppler, Rocket 27, King Fish.

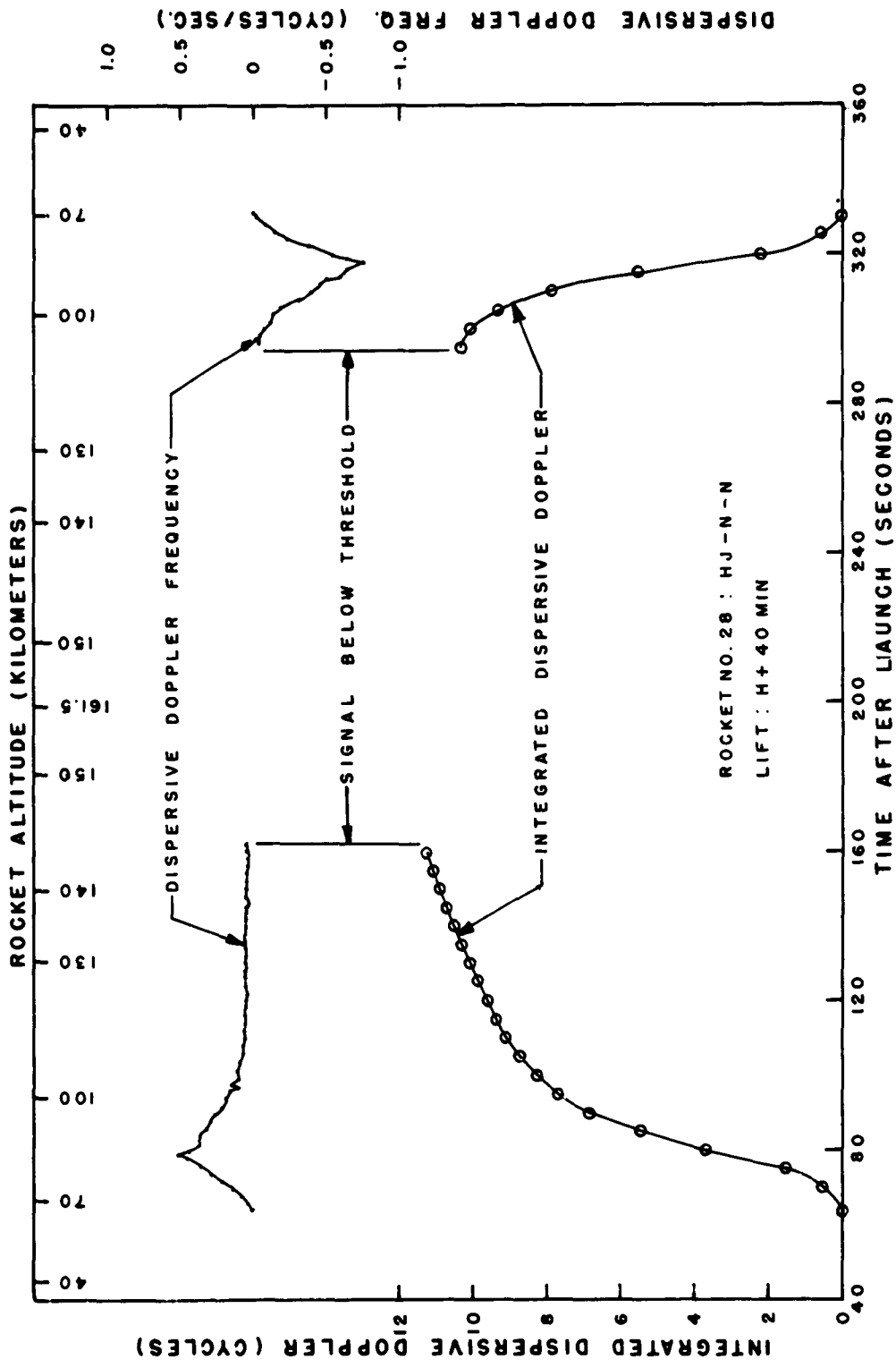

Figure C.67 Dispersive doppler versus time derived from the 37- and 148-Mc doppler, Rocket 28, King Fish.

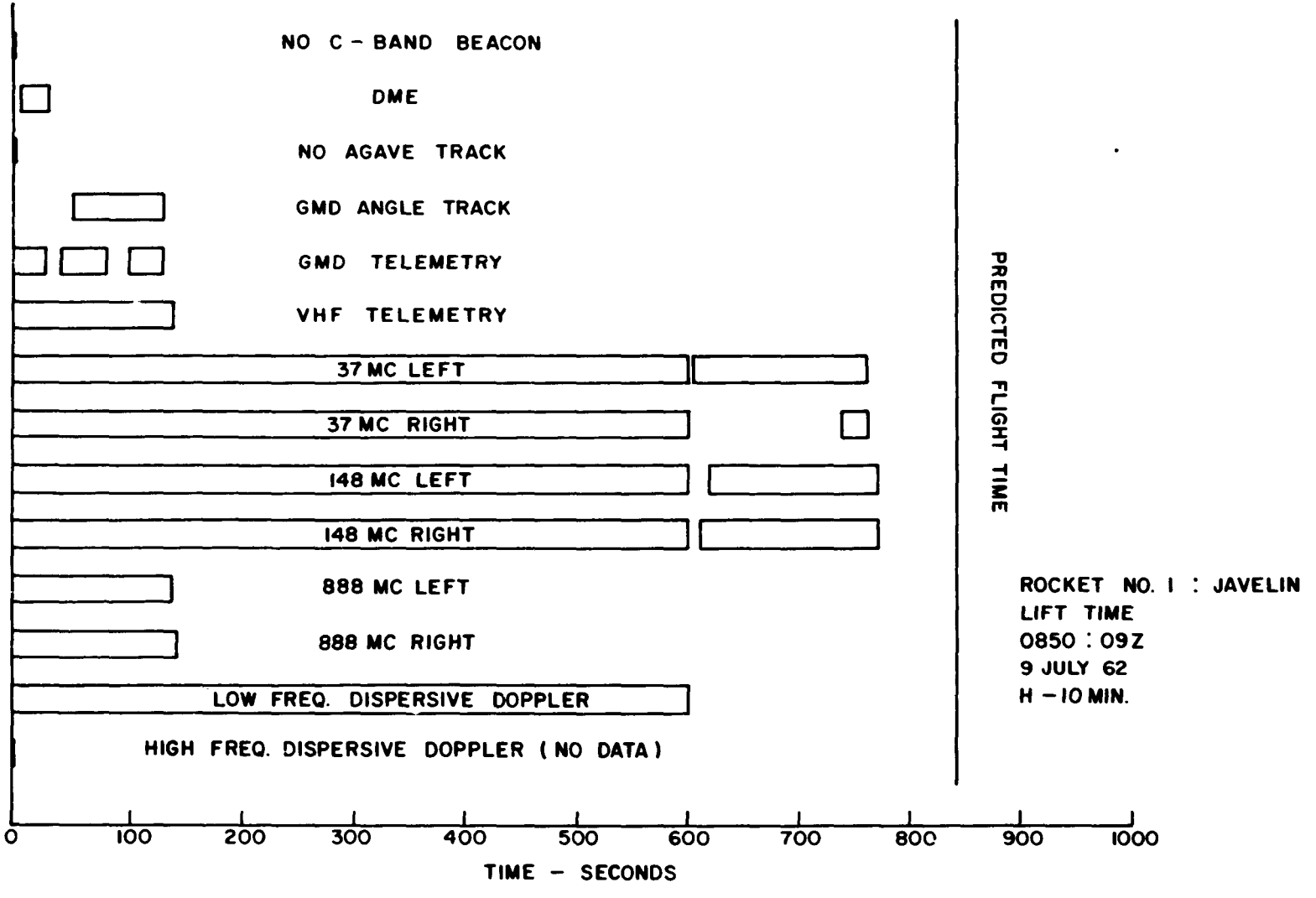

Figure C.68 Duration of useful received signal for experiments carried on Rocket 1, Star Fish.

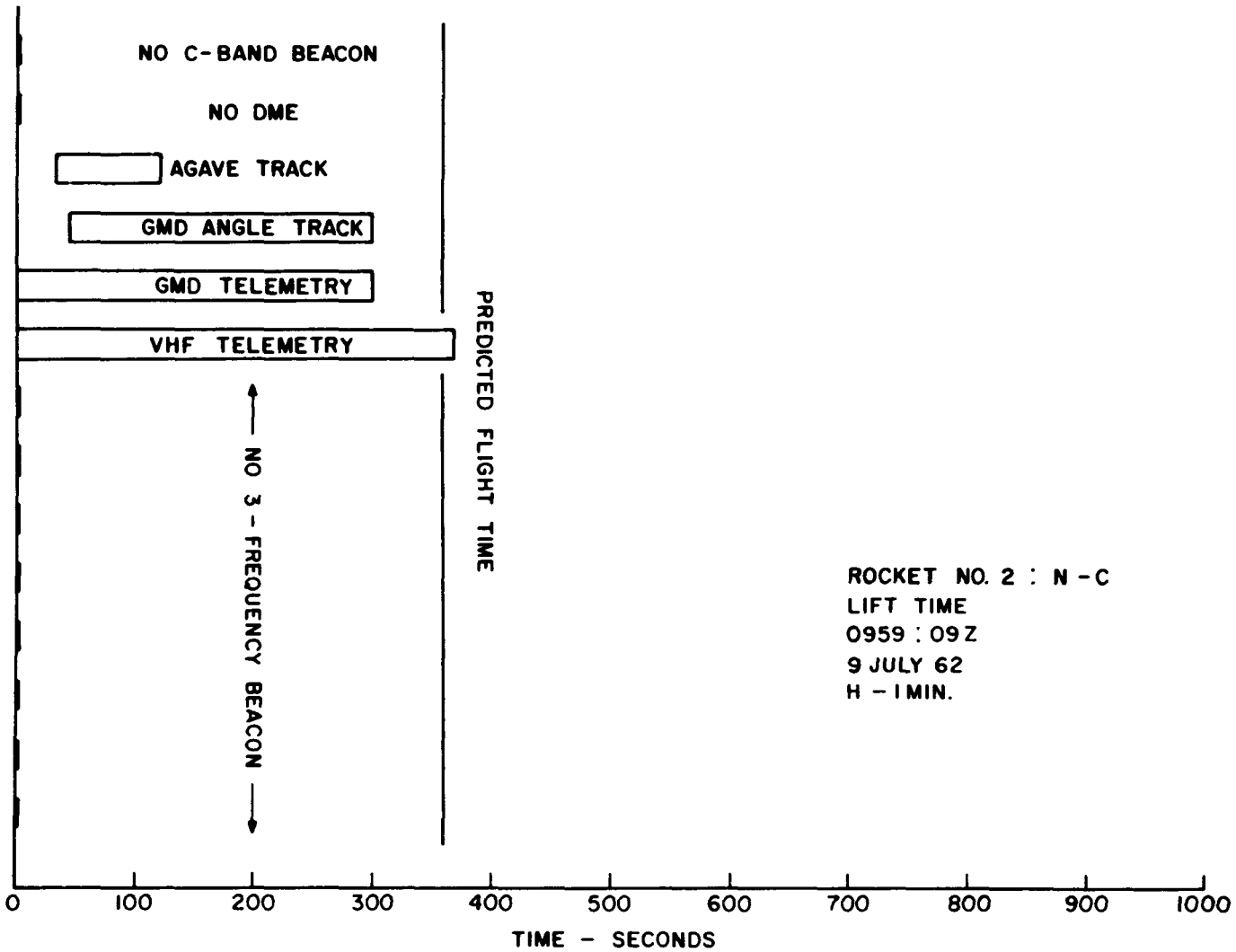

Figure C.69 Duration of useful received signal for experiments carried on Rocket 2, Star Fish.

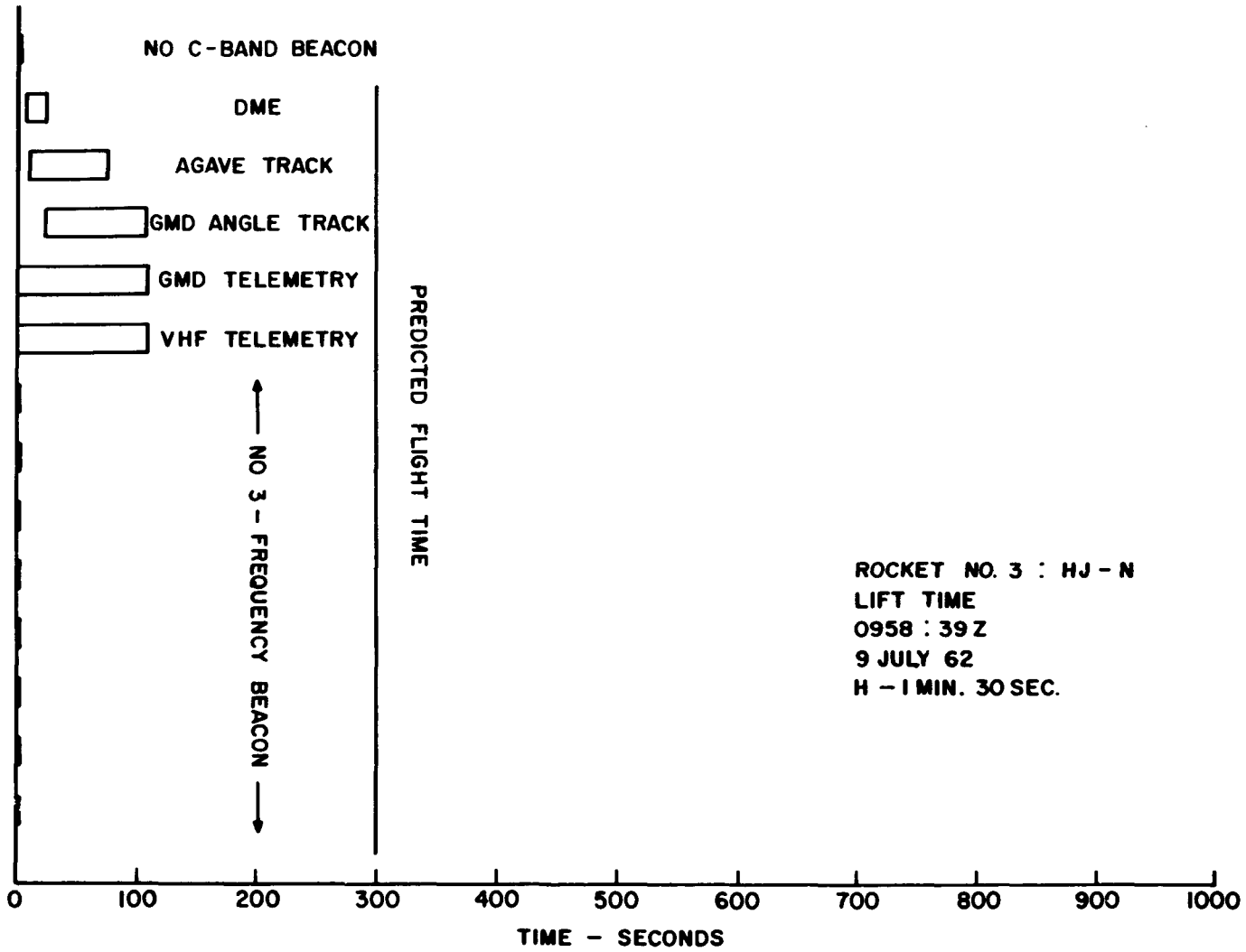

Figure C.70 Duration of useful received signal for experiments carried on Rocket 3, Star Fish.

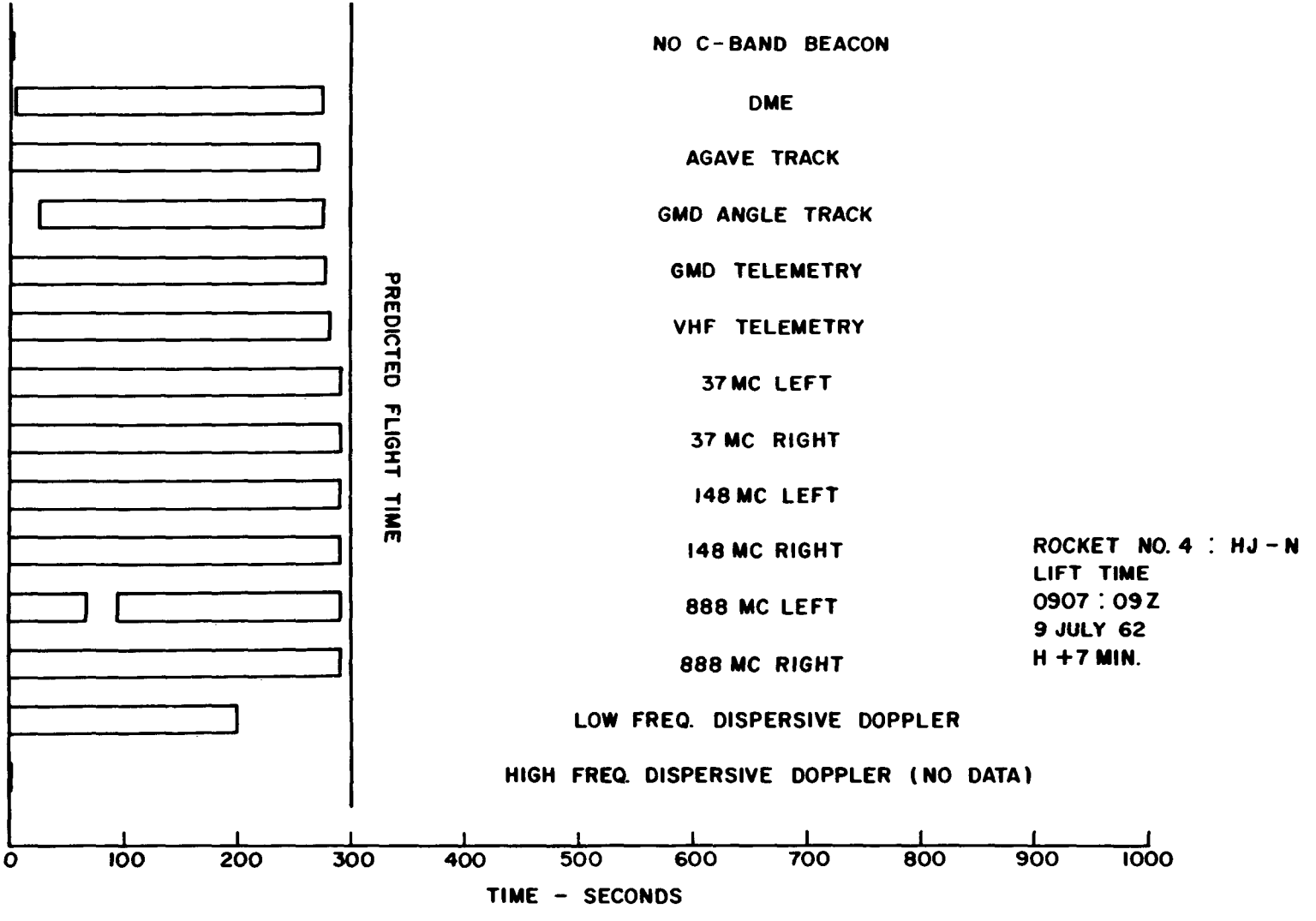

Figure C.71 Duration of useful received signal for experiments carried on Rocket 4, Star Fish.

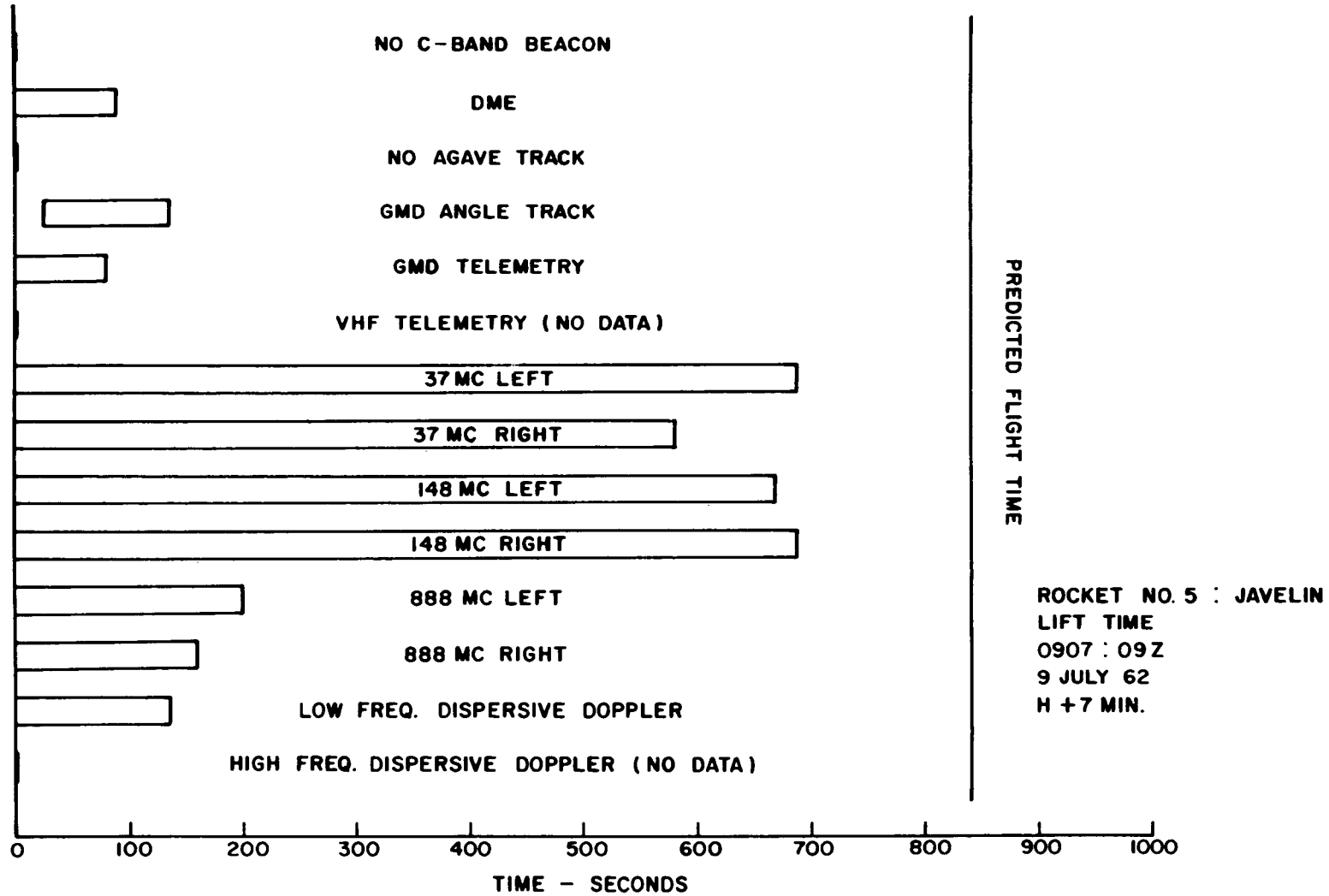

Figure C.72 Duration of useful received signal for experiments carried on Rocket 5, Star Fish.

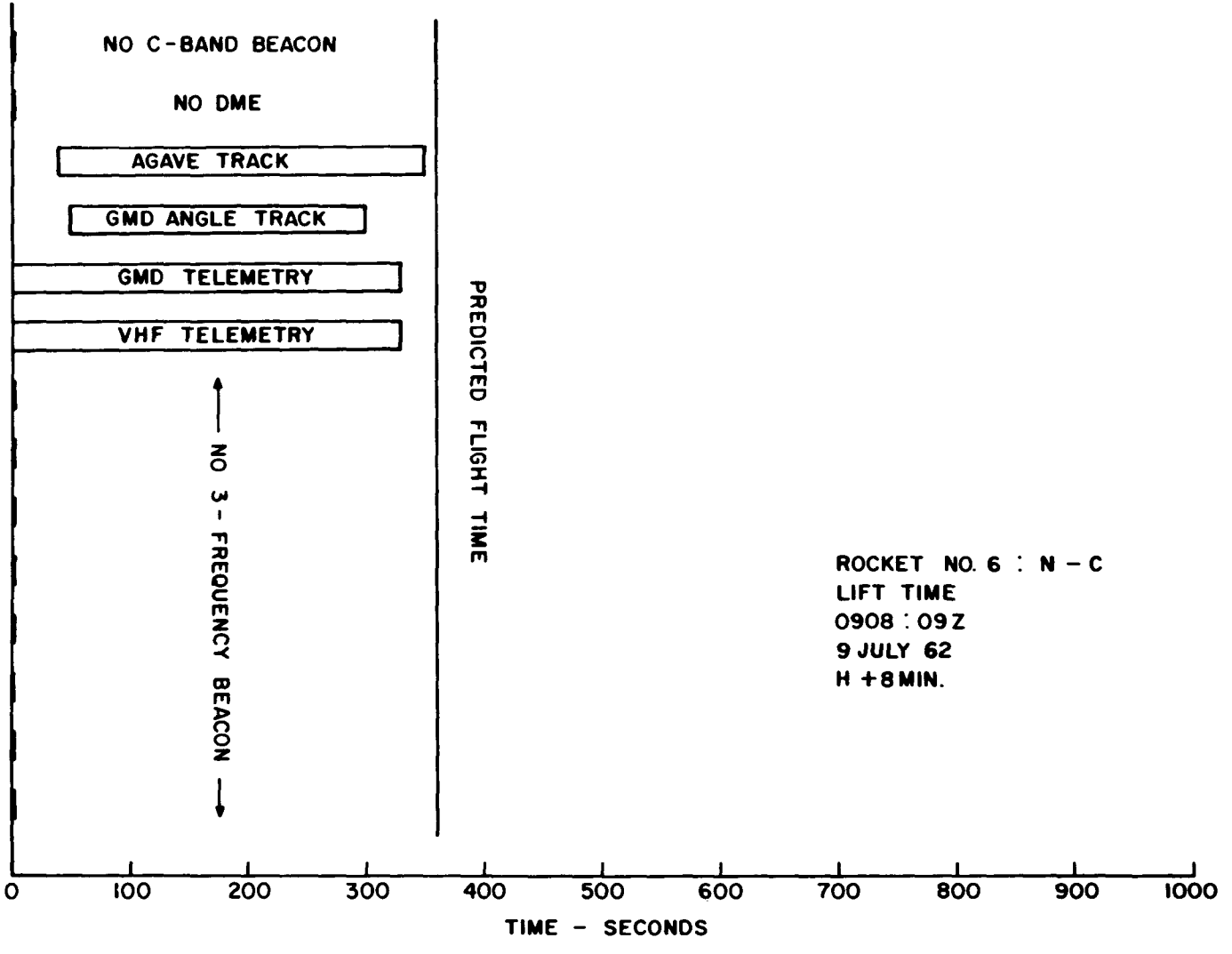

Figure C.73 Duration of useful received signal for experiments carried on Rocket 6, Star Fish.

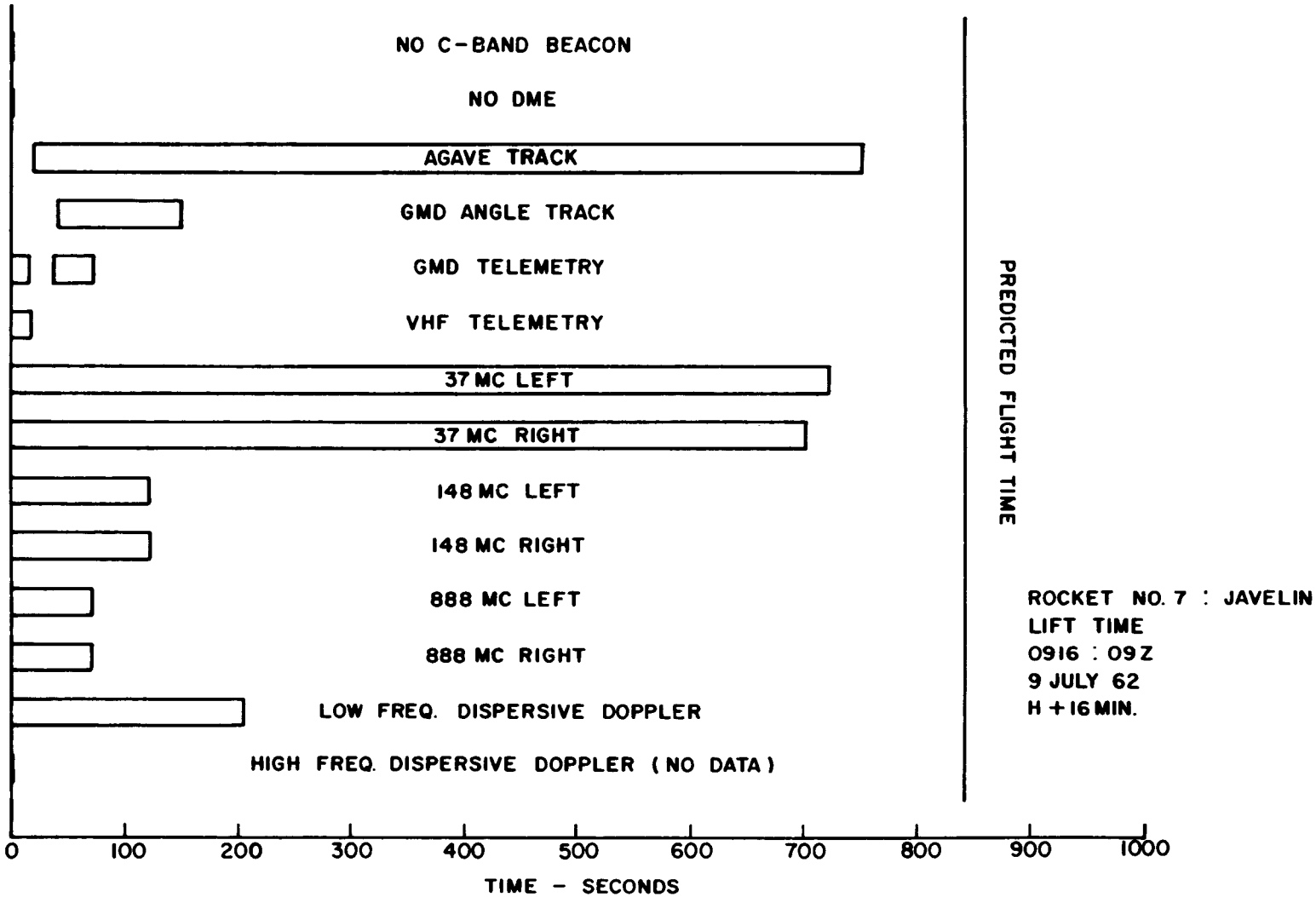

Figure C.74 Duration of useful received signal for experiments carried on Rocket 7, Star Fish.

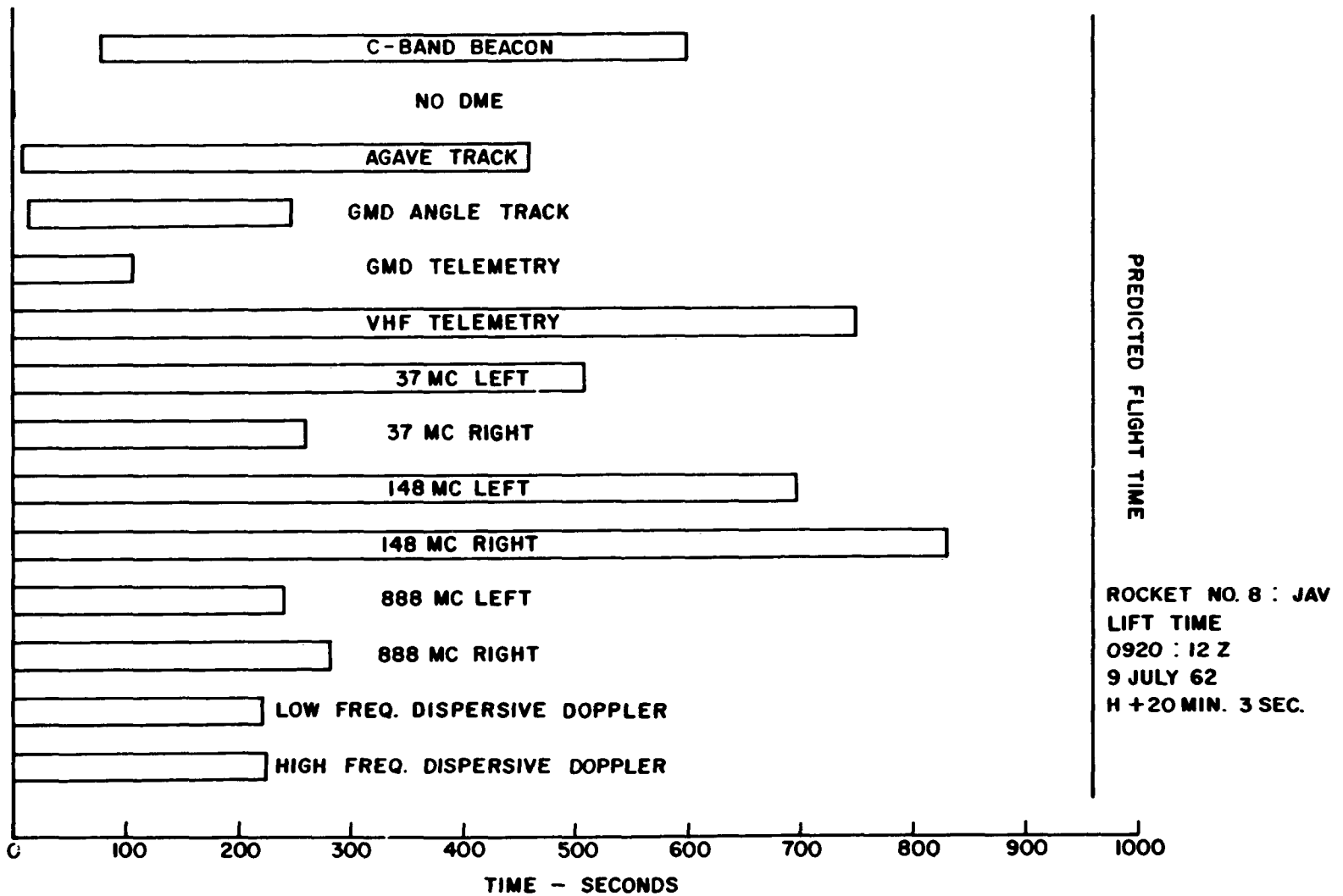

Figure C.75 Duration of useful received signal for experiments carried on Rocket 8, Star Fish.

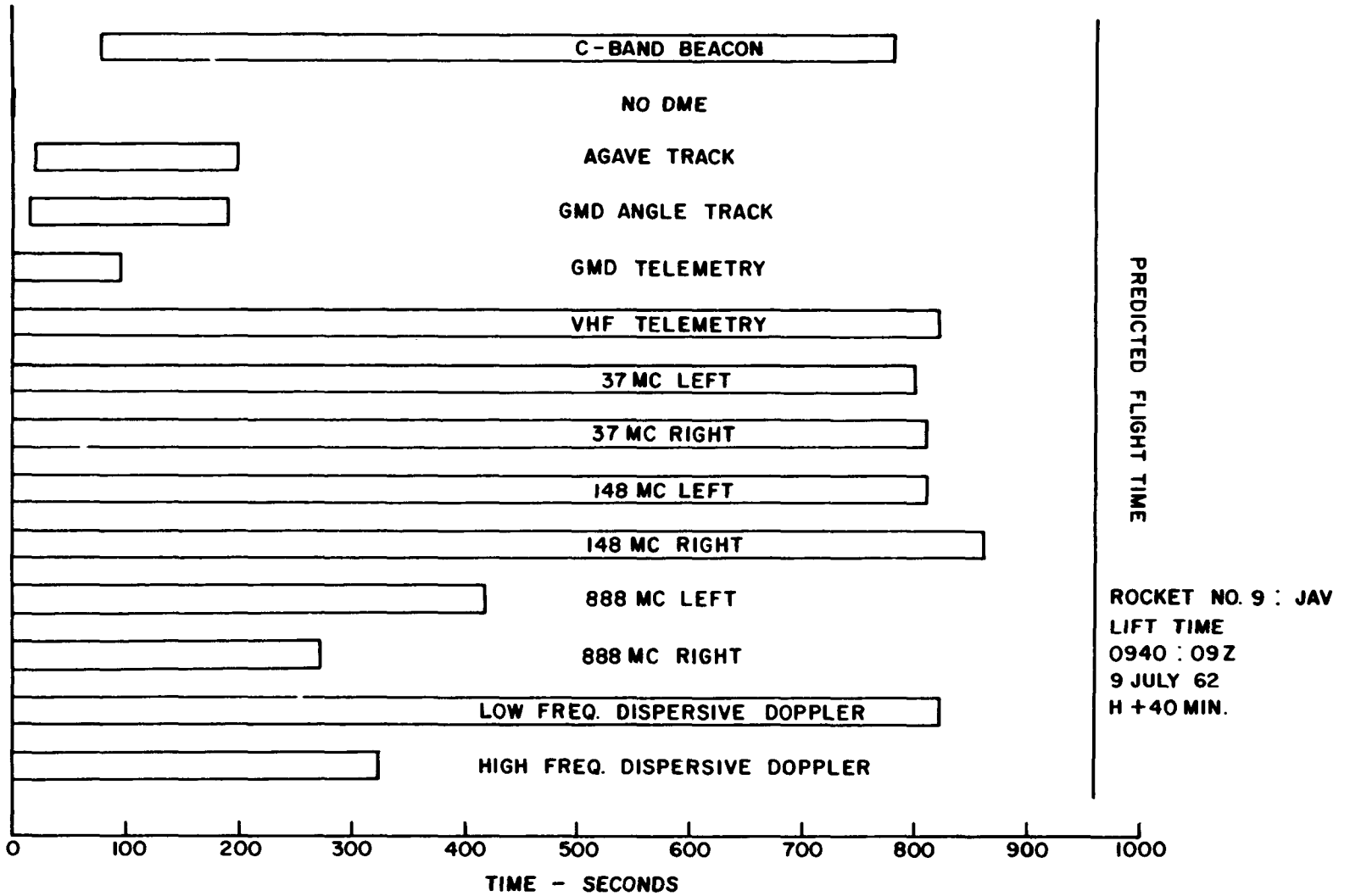

Figure C.76 Duration of useful received signal for experiments carried on Rocket 9, Star Fish.

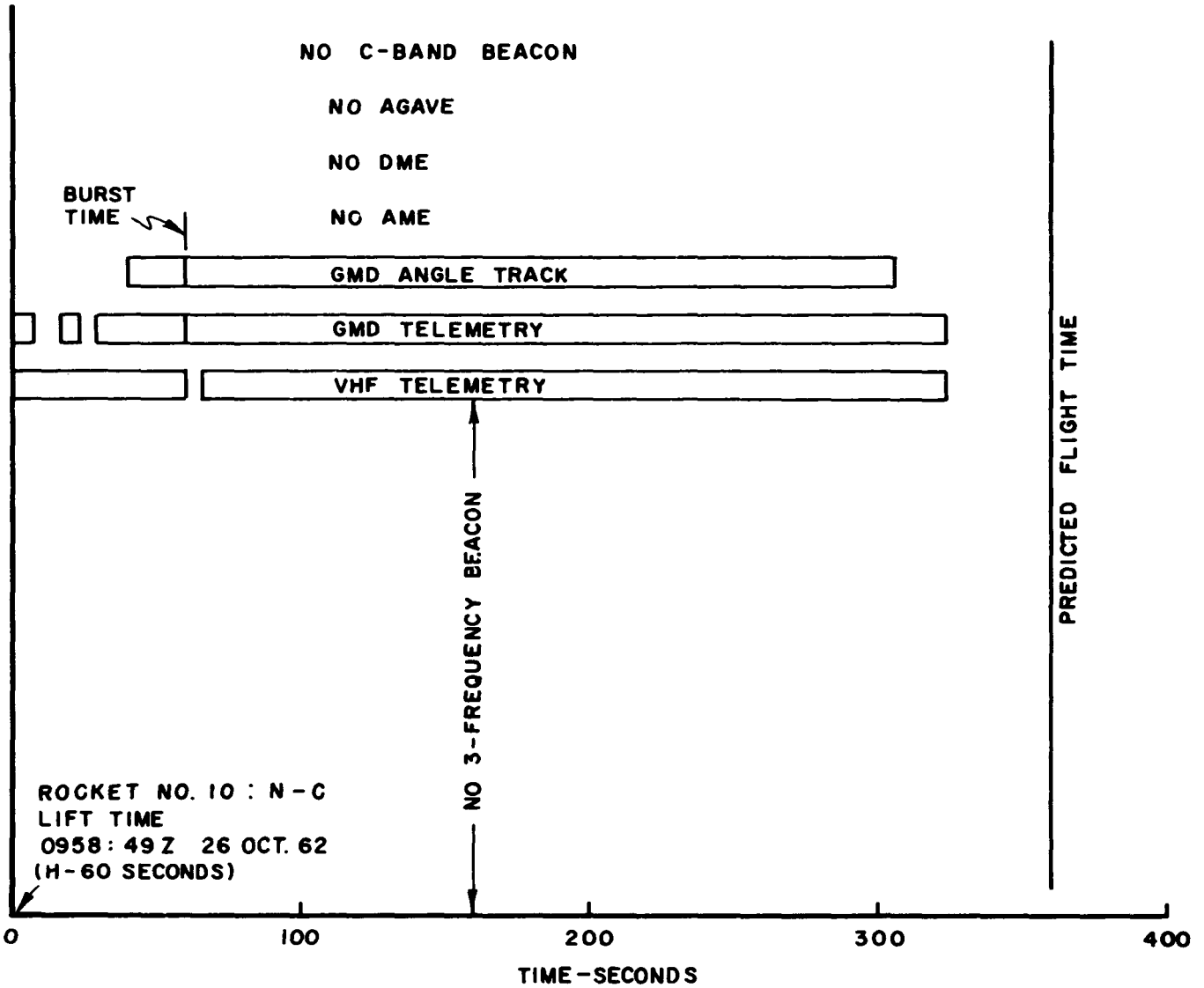

Figure C.77 Duration of useful received signal for experiments carried on Rocket 10, Blue Gill.

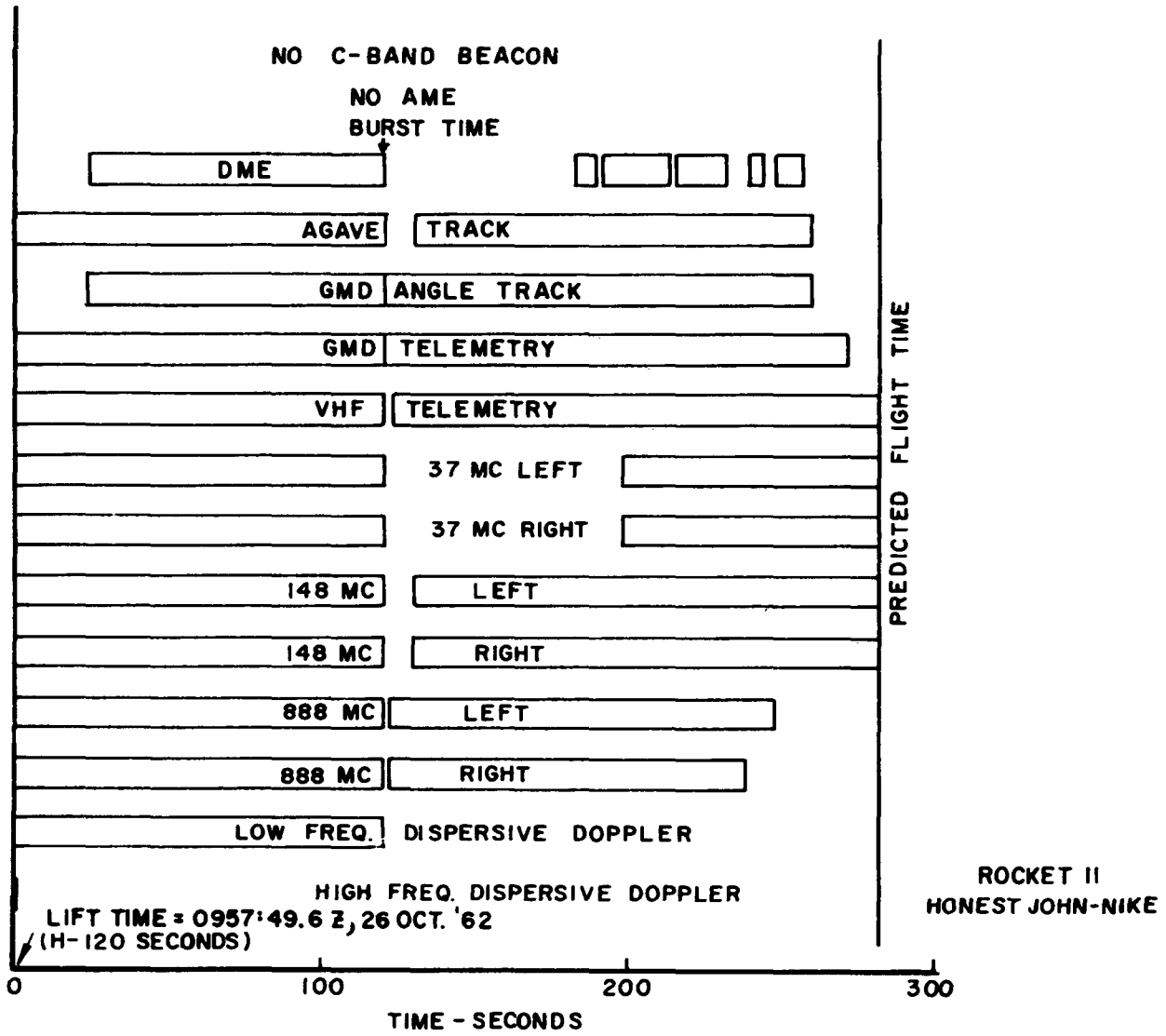

Figure C.78 Duration of useful received signal for experiments carried on Rocket 11, Blue Gill.

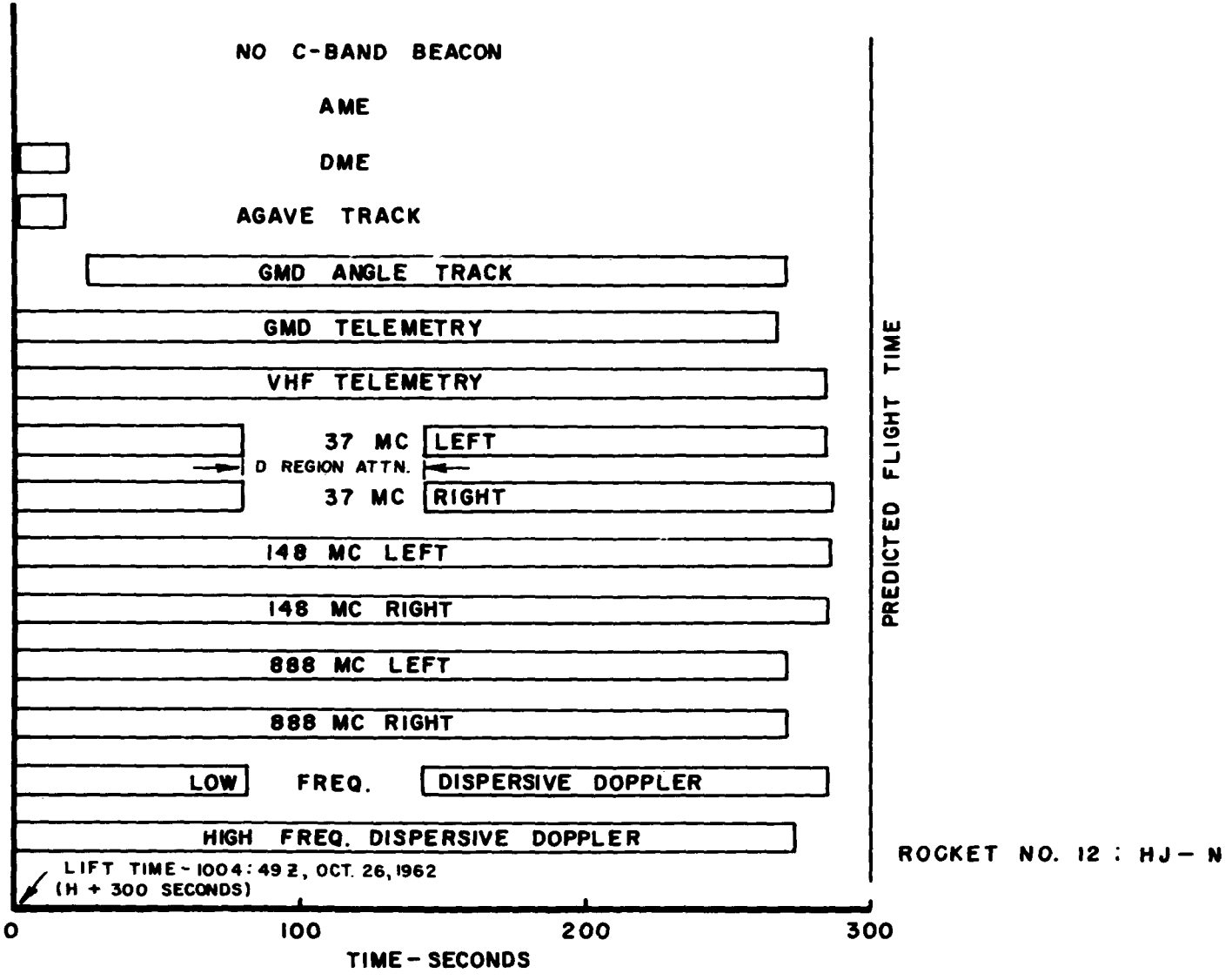

Figure C.79 Duration of useful received signal for experiments carried on Rocket 12, Blue Gill.

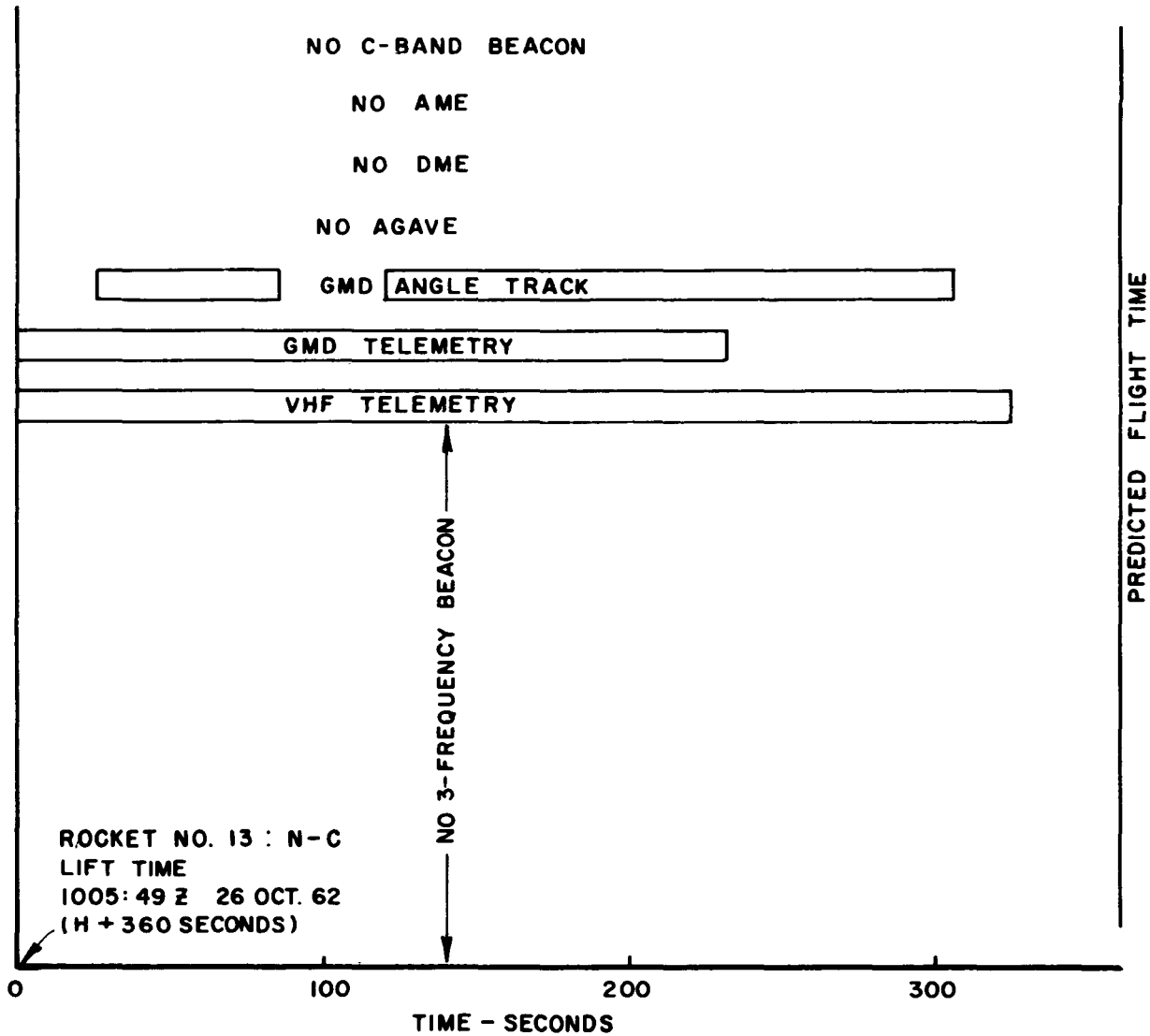

Figure C.80 Duration of useful received signal for experiments carried on Rocket 13, Blue Gill.

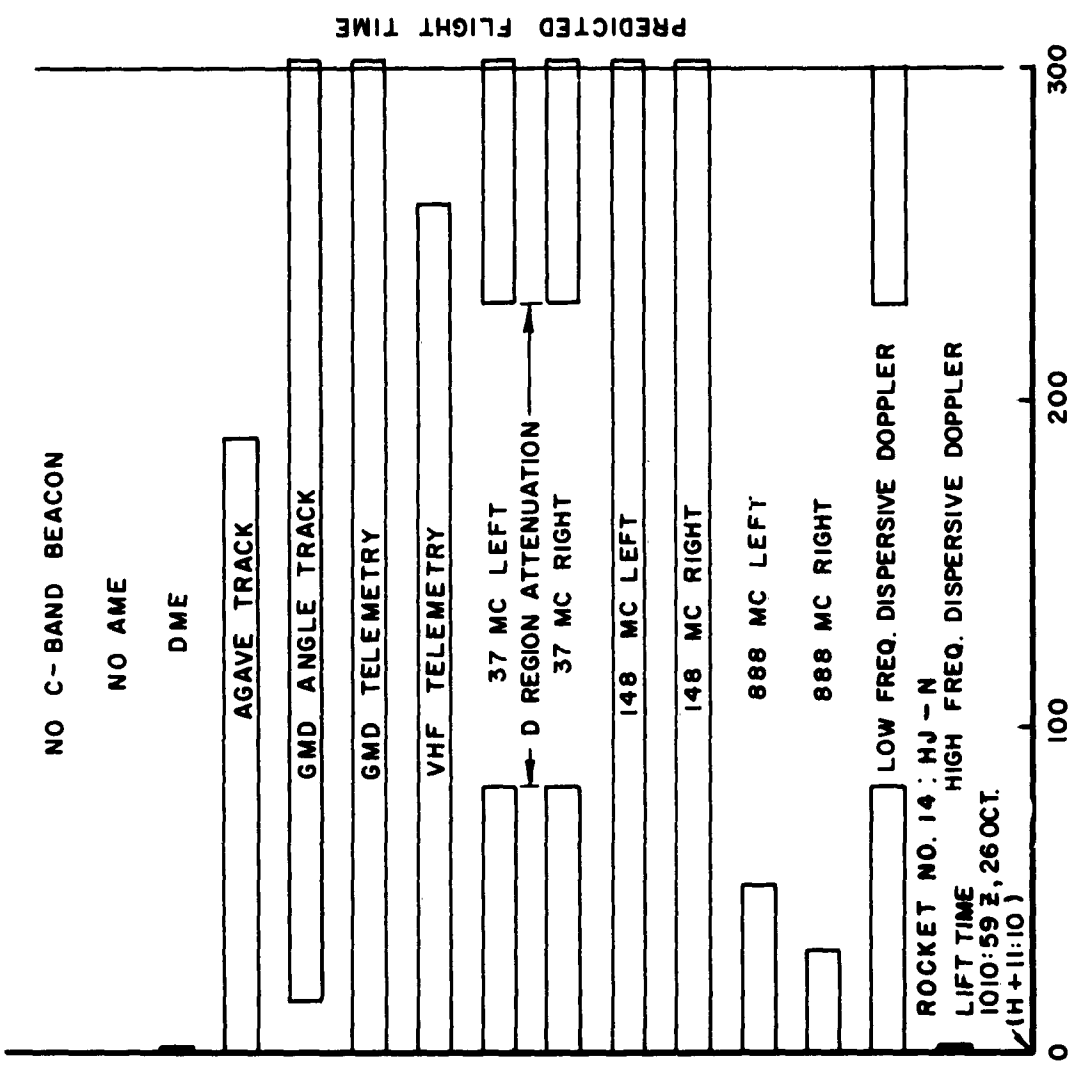

Figure C.81 Duration of useful received signal for experiments carried on Rocket 14, Blue Gill.

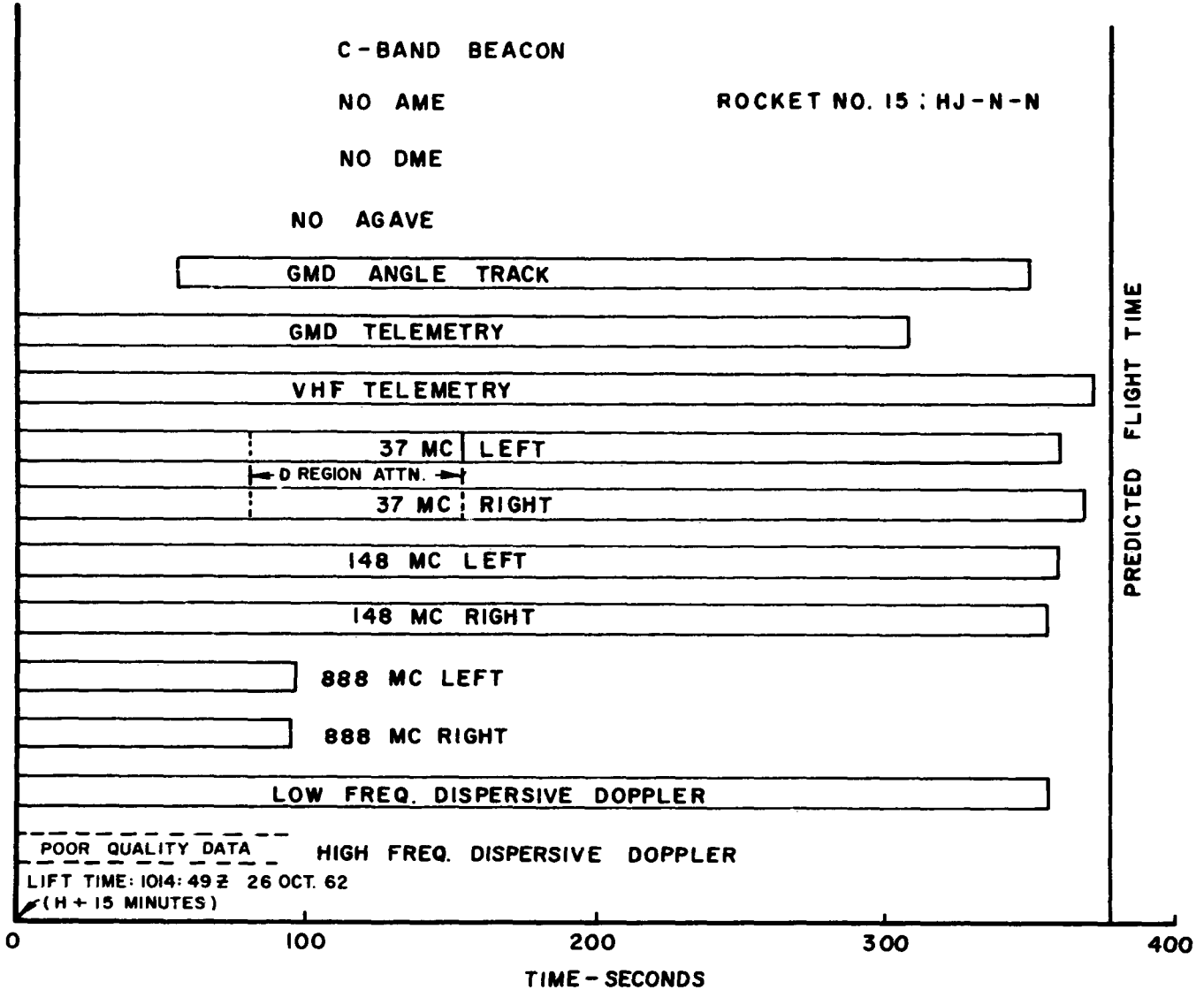

Figure C.82 Duration of useful received signal for experiments carried on Rocket 15, Blue Gill.

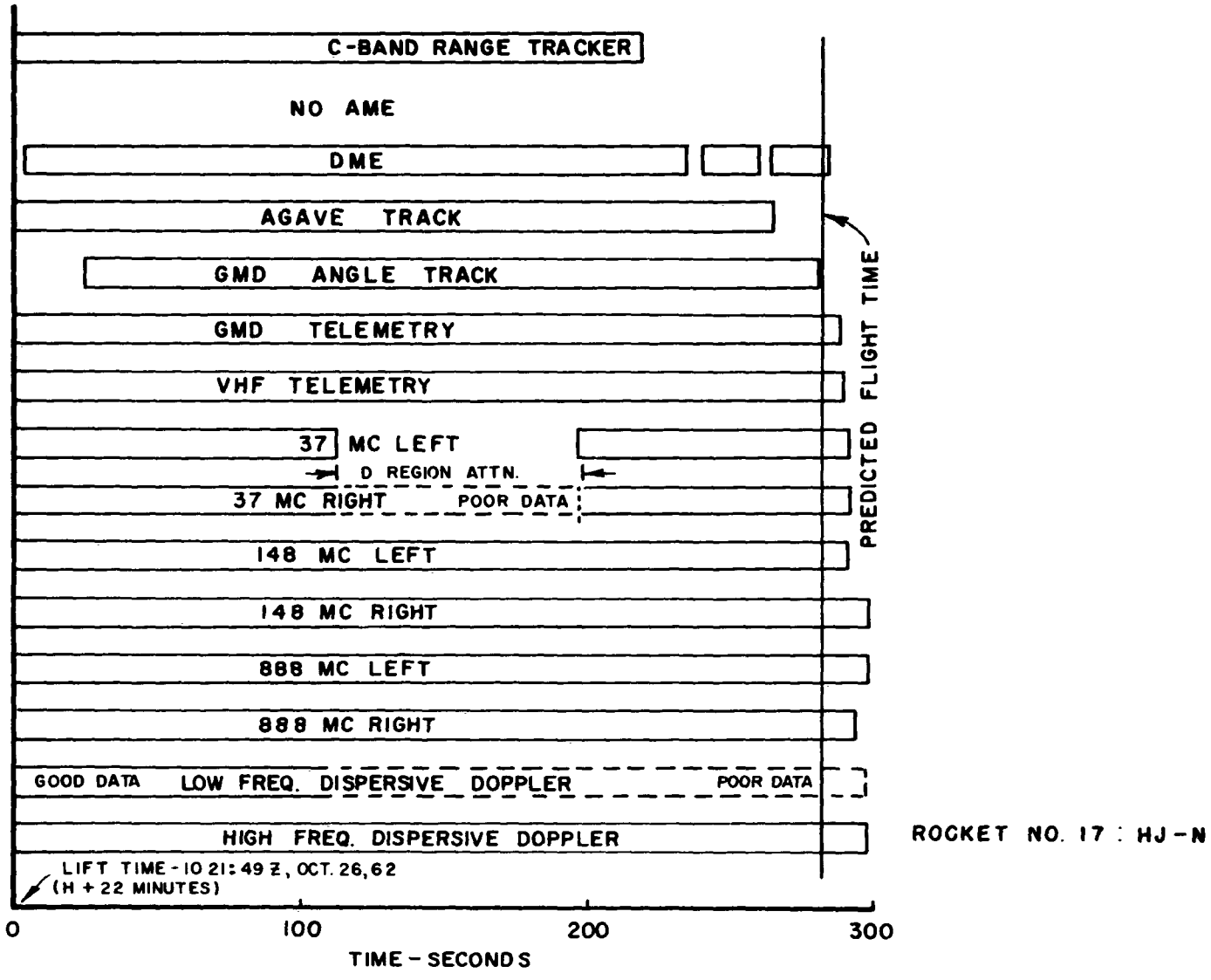

Figure C.83 Duration of useful received signal for experiments carried on Rocket 17, Blue Gill.

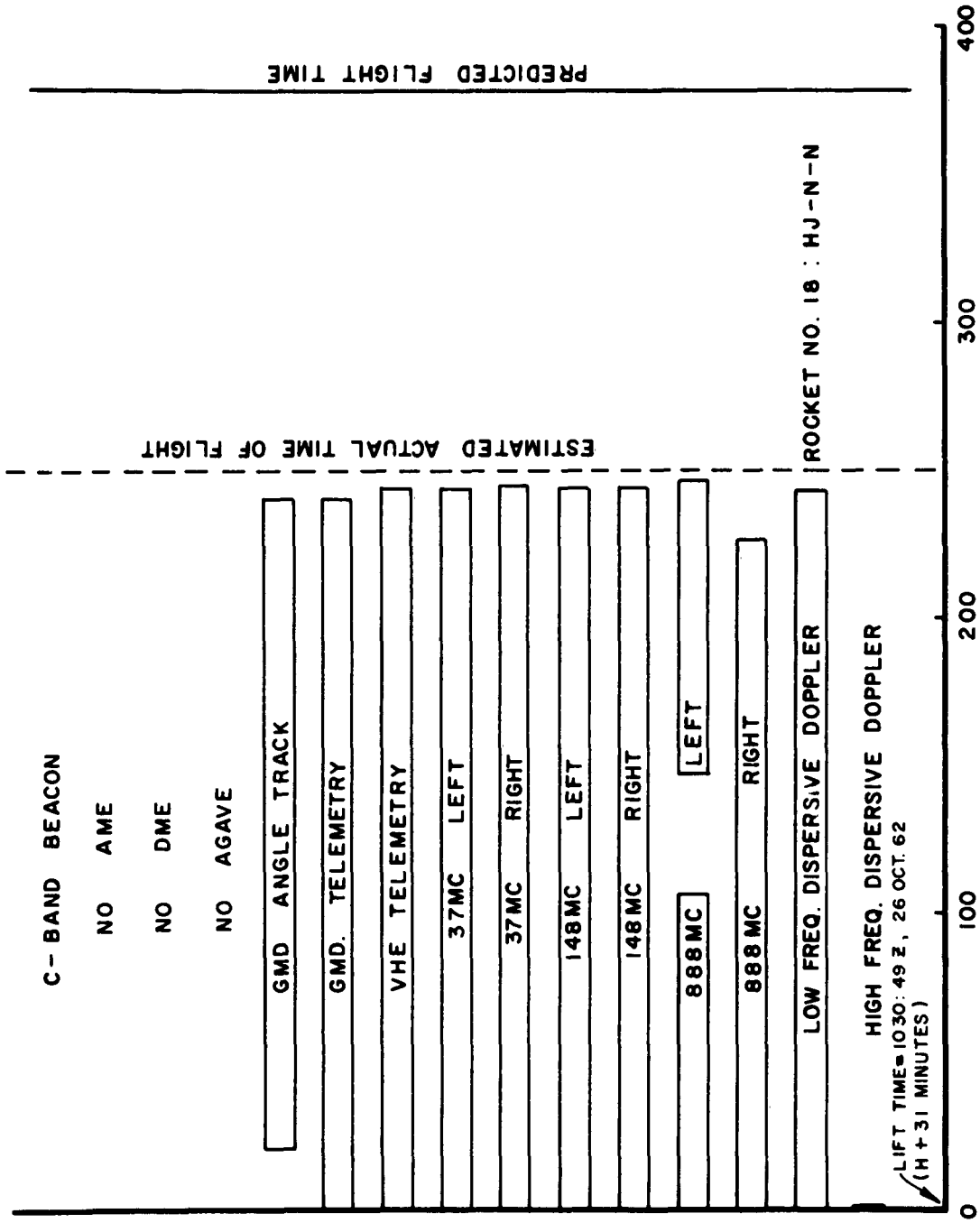

Figure C.84 Duration of useful received signal for experiments carried on Rocket 18, Blue Gill.

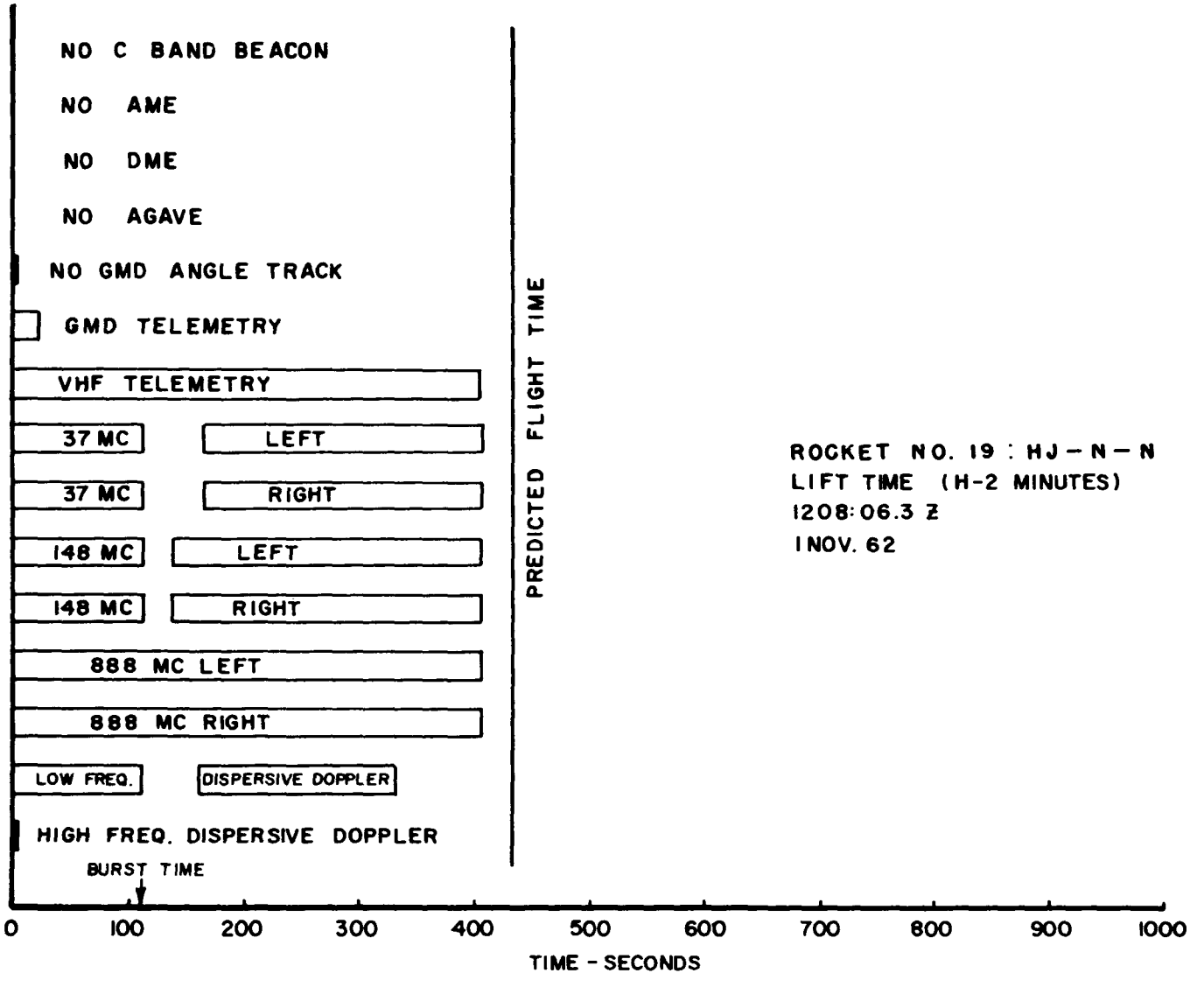

Figure C.85 Duration of useful received signal for experiments carried on Rocket 19, King Fish.

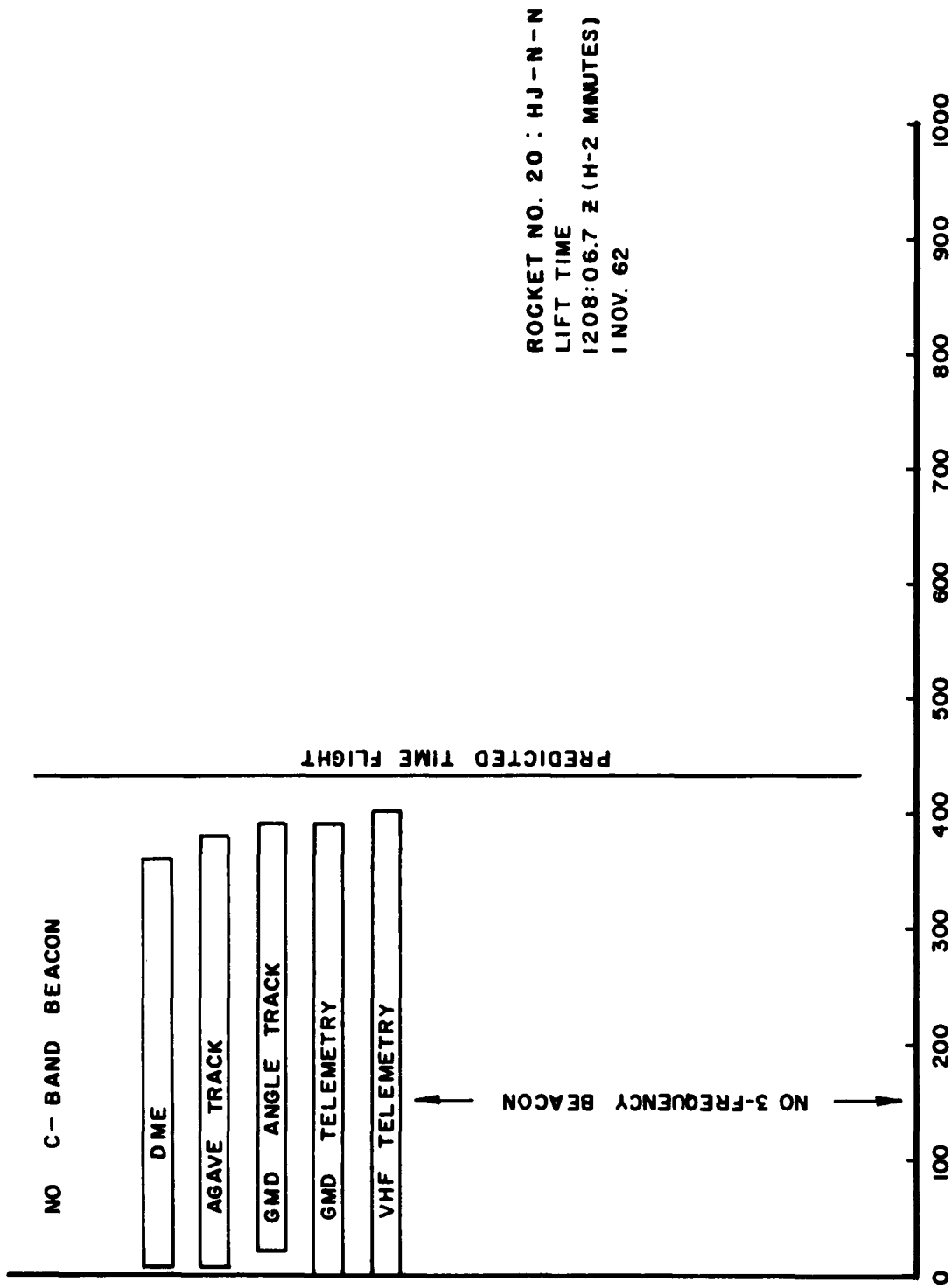

Figure C.86 Duration of useful received signal for experiments carried on Rocket 20, King Fish.

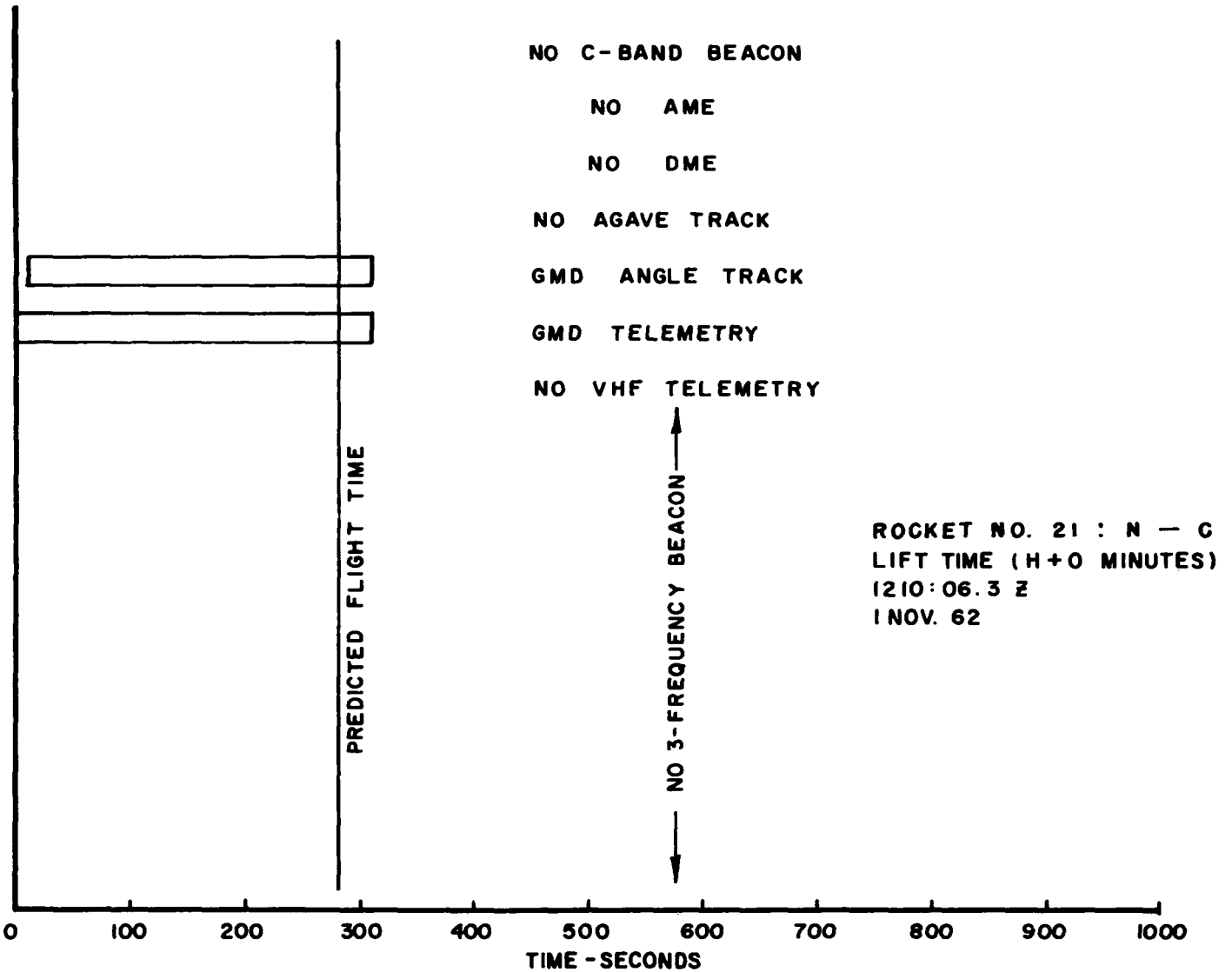

Figure C.87 Duration of useful received signal for experiments carried on Rocket 21, King Fish.

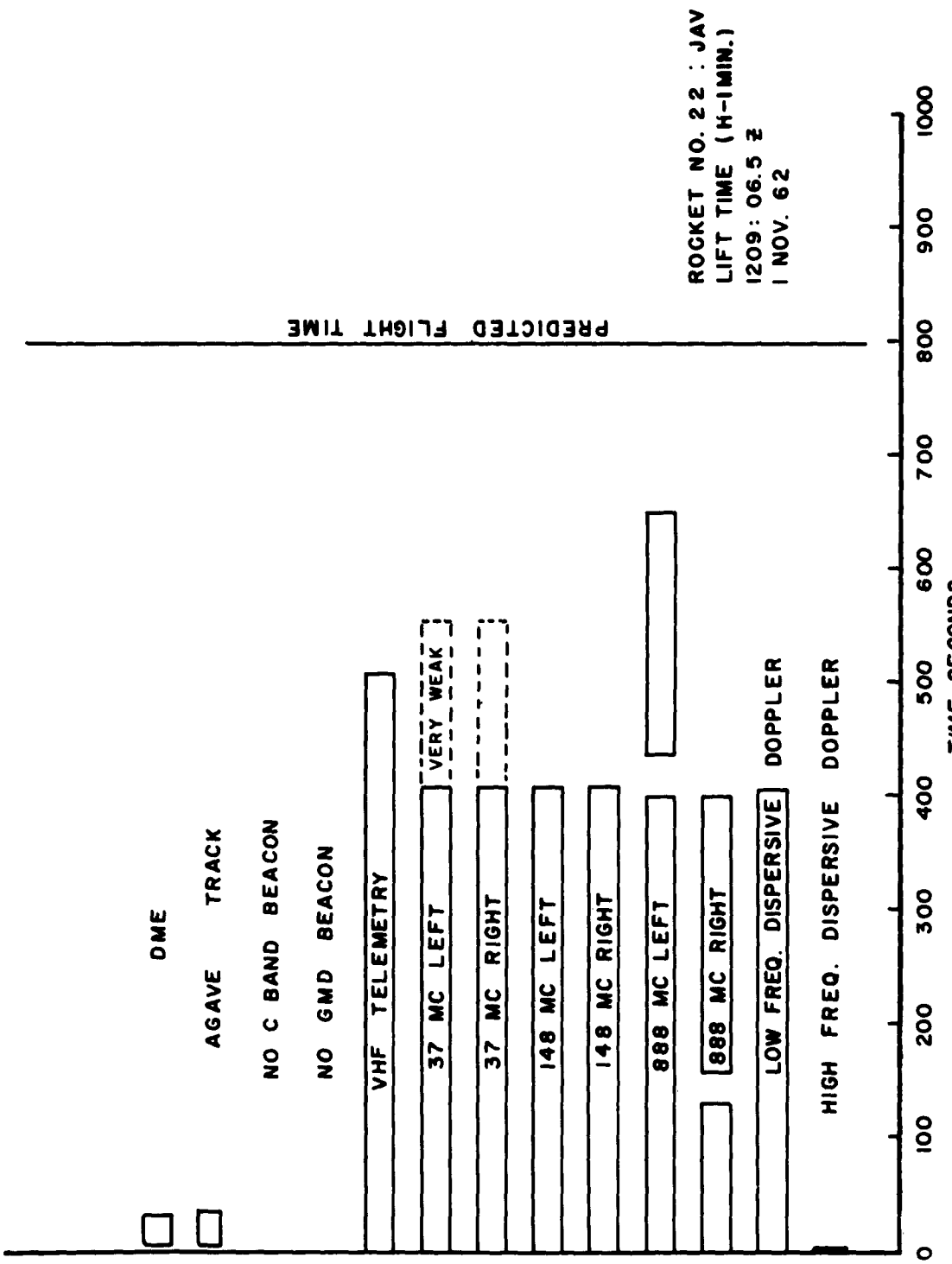

Figure C.88 Duration of useful received signal for experiments carried on Rocket 22, King Fish.

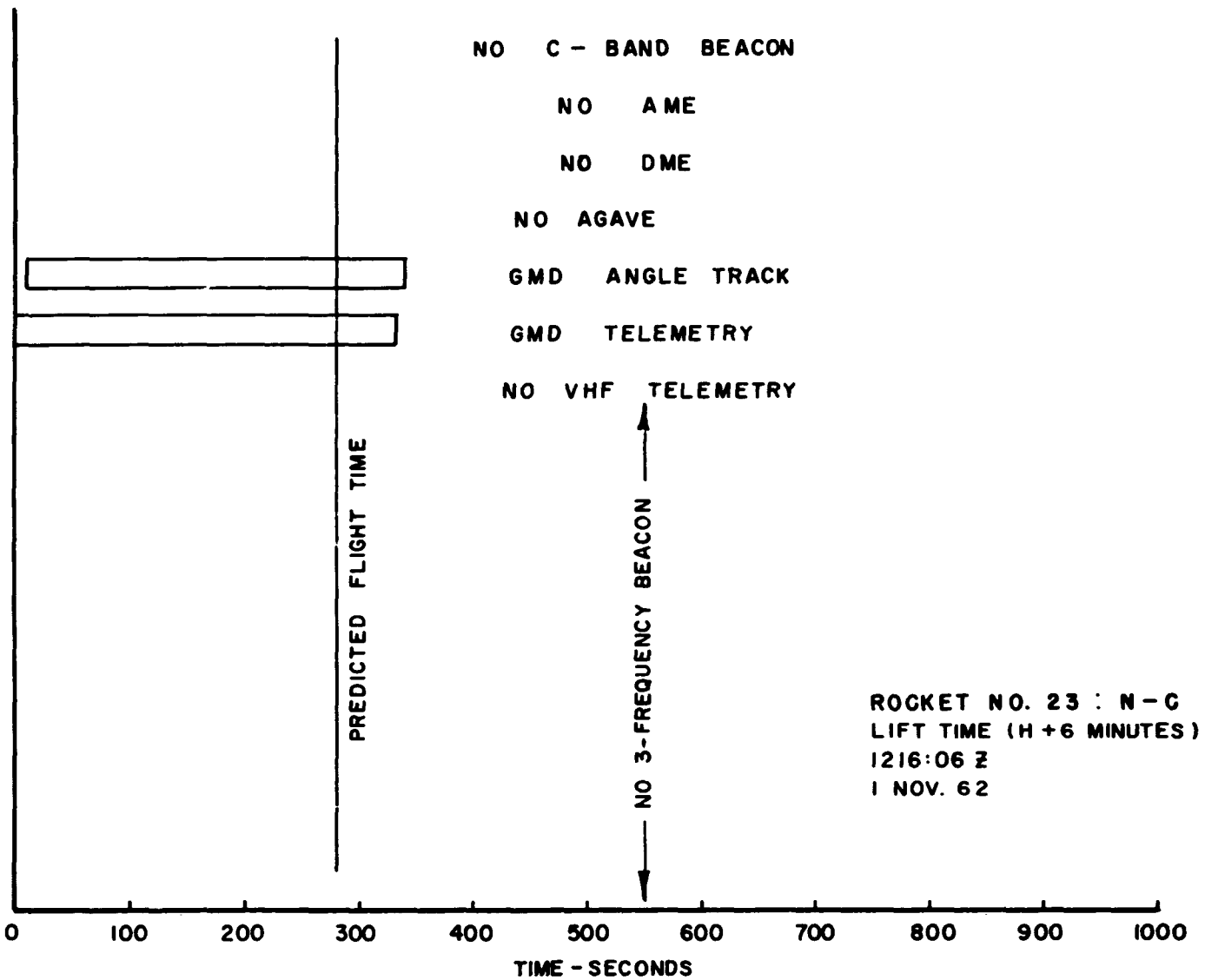

Figure C.89 Duration of useful received signal for experiments carried on Rocket 23, King Fish.

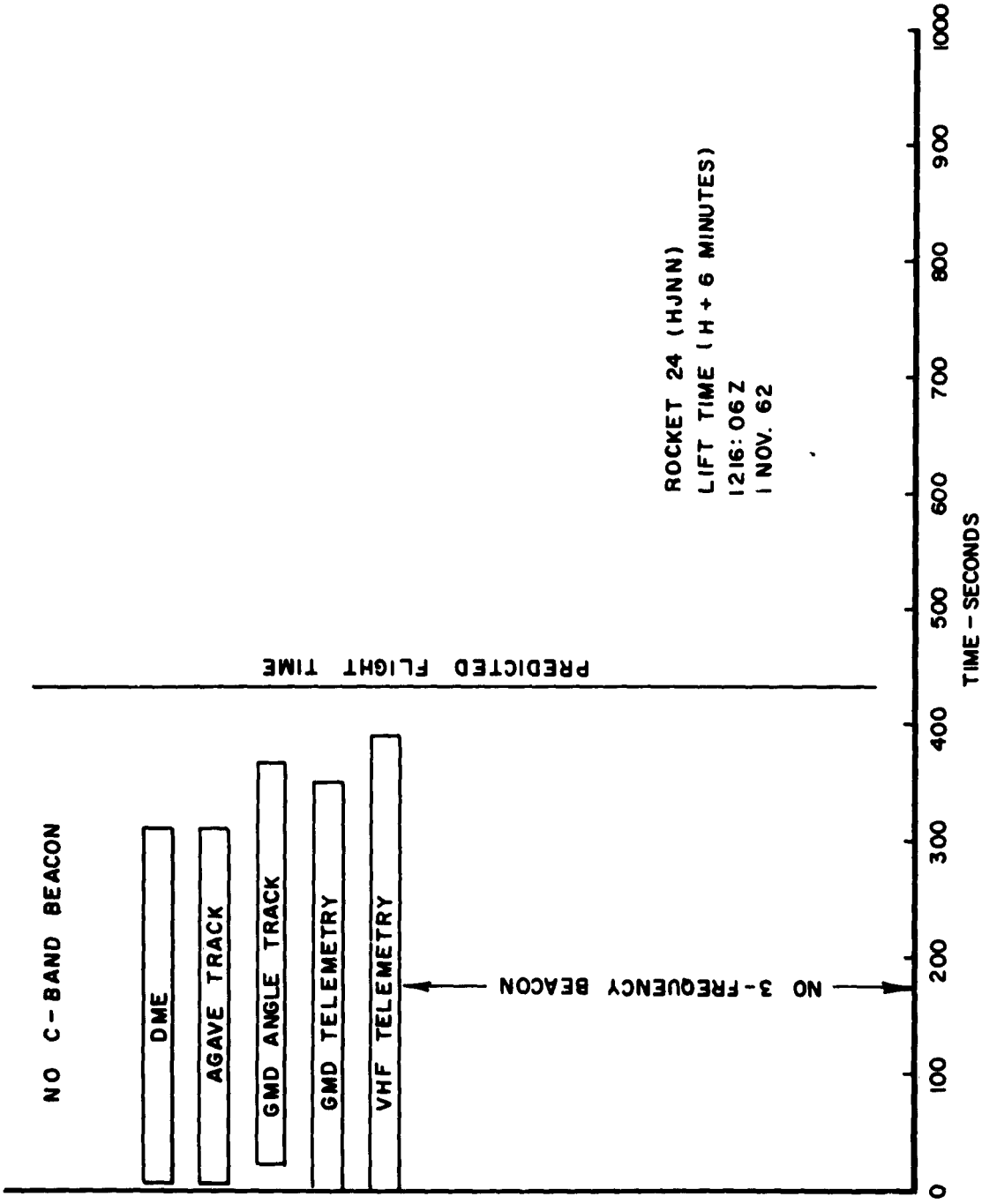

Figure C.90 Duration of useful received signal for experiments carried on Rocket 24, King Fish.

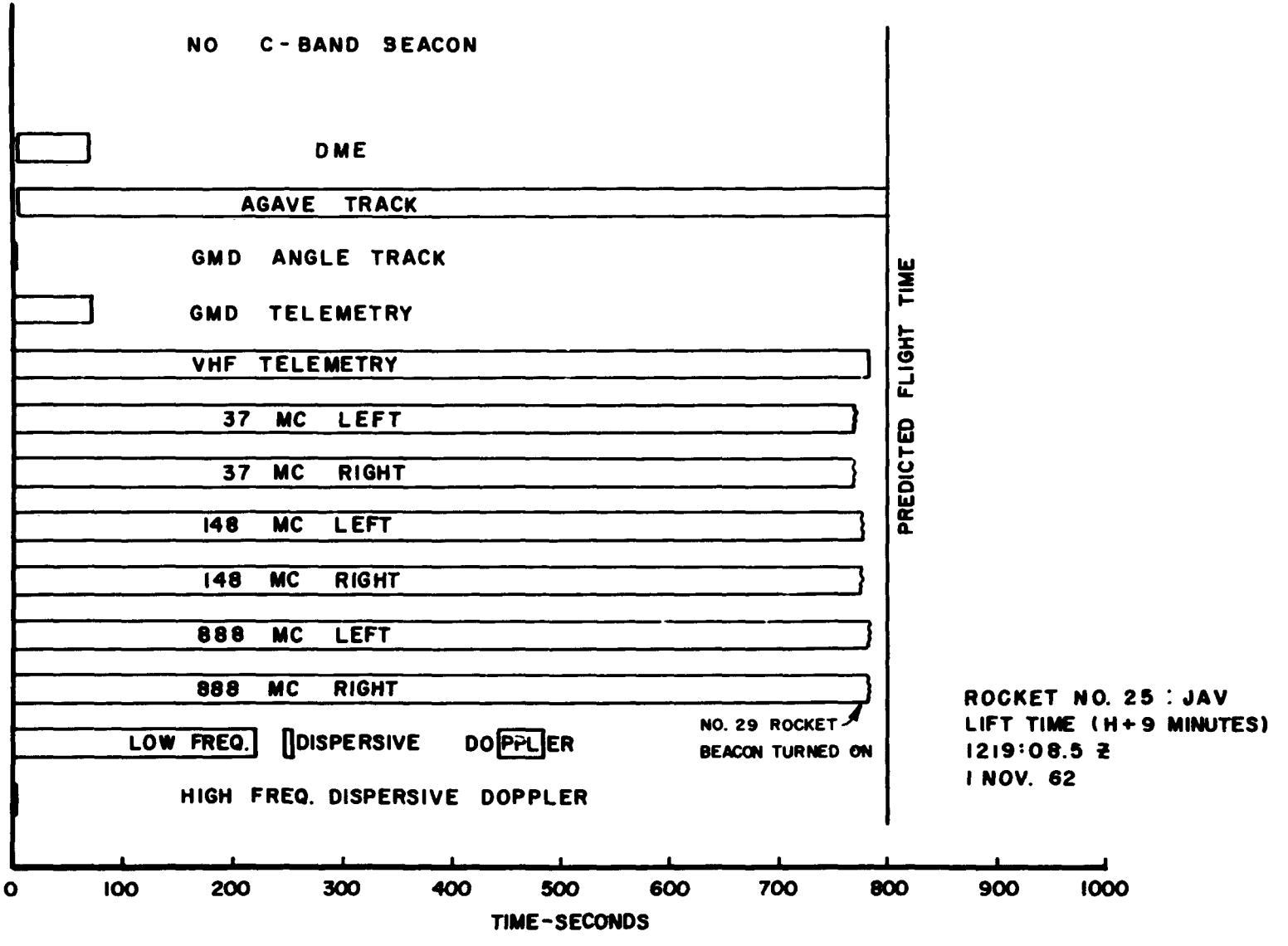

Figure C.91 Duration of useful received signal for experiments carried on Rocket 25, King Fish.

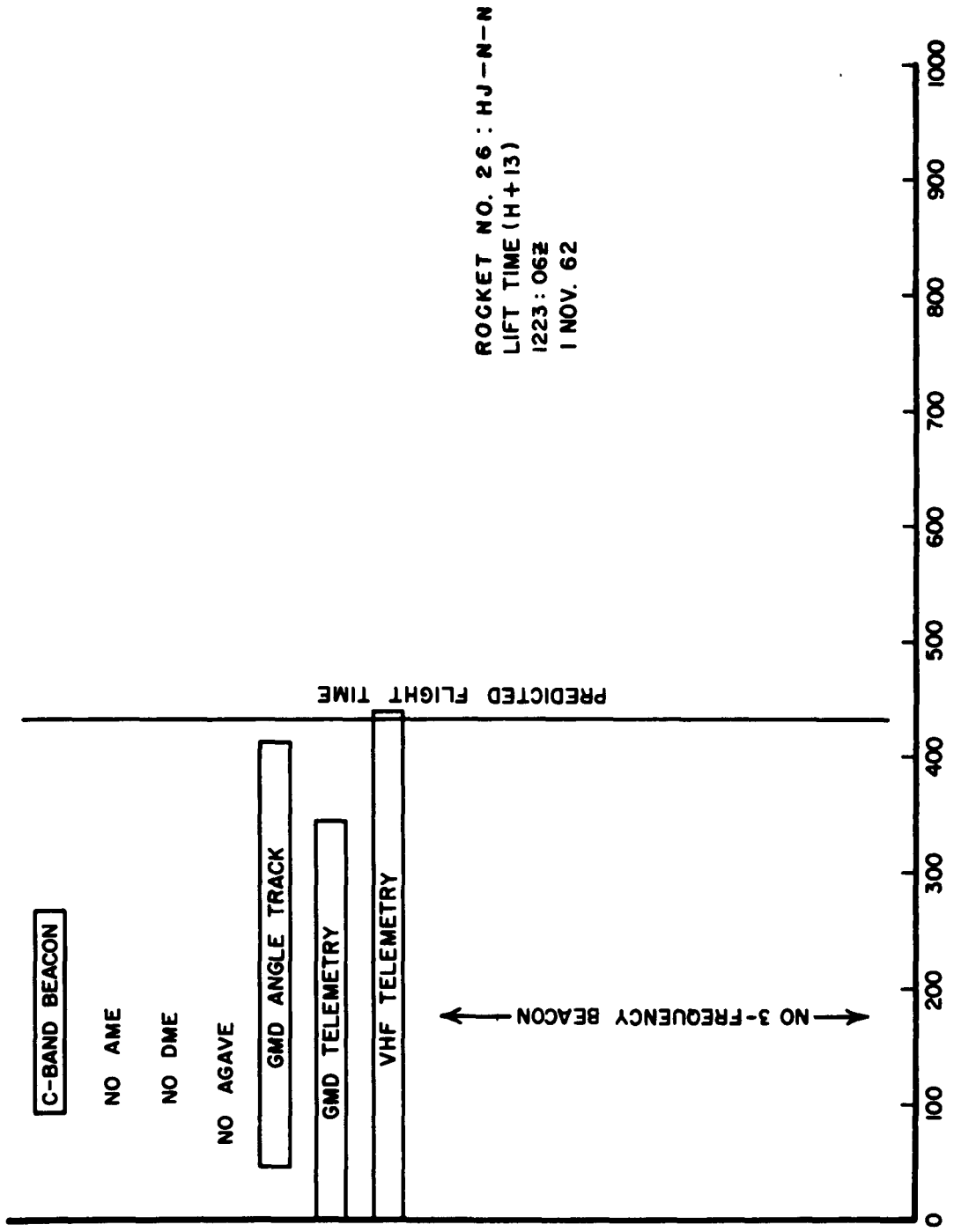

Figure C.92 Duration of useful received signal for experiments carried on Rocket 26, King Fish.

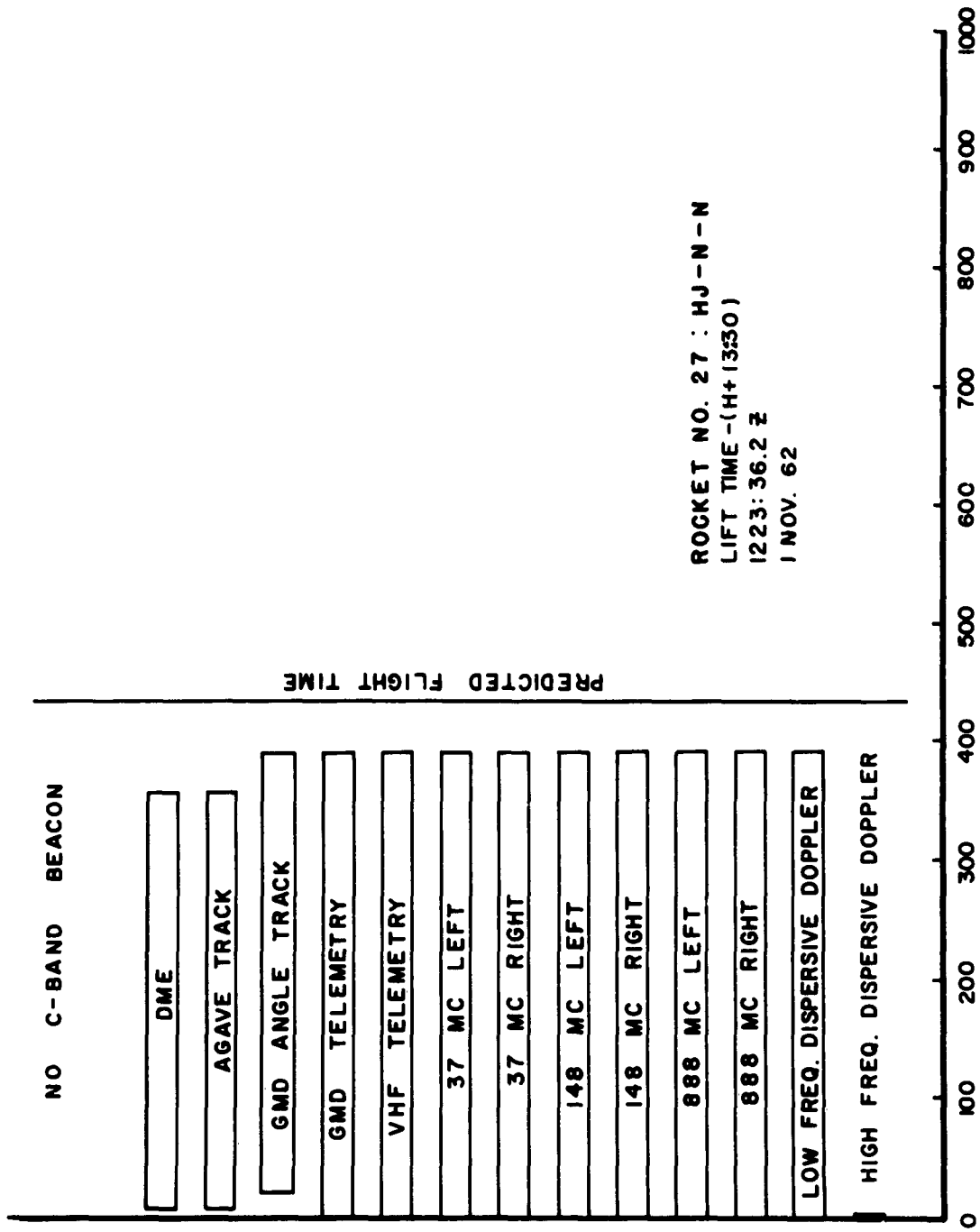

Figure C.93 Duration of useful received signal for experiments carried on Rocket 27, King Fish.

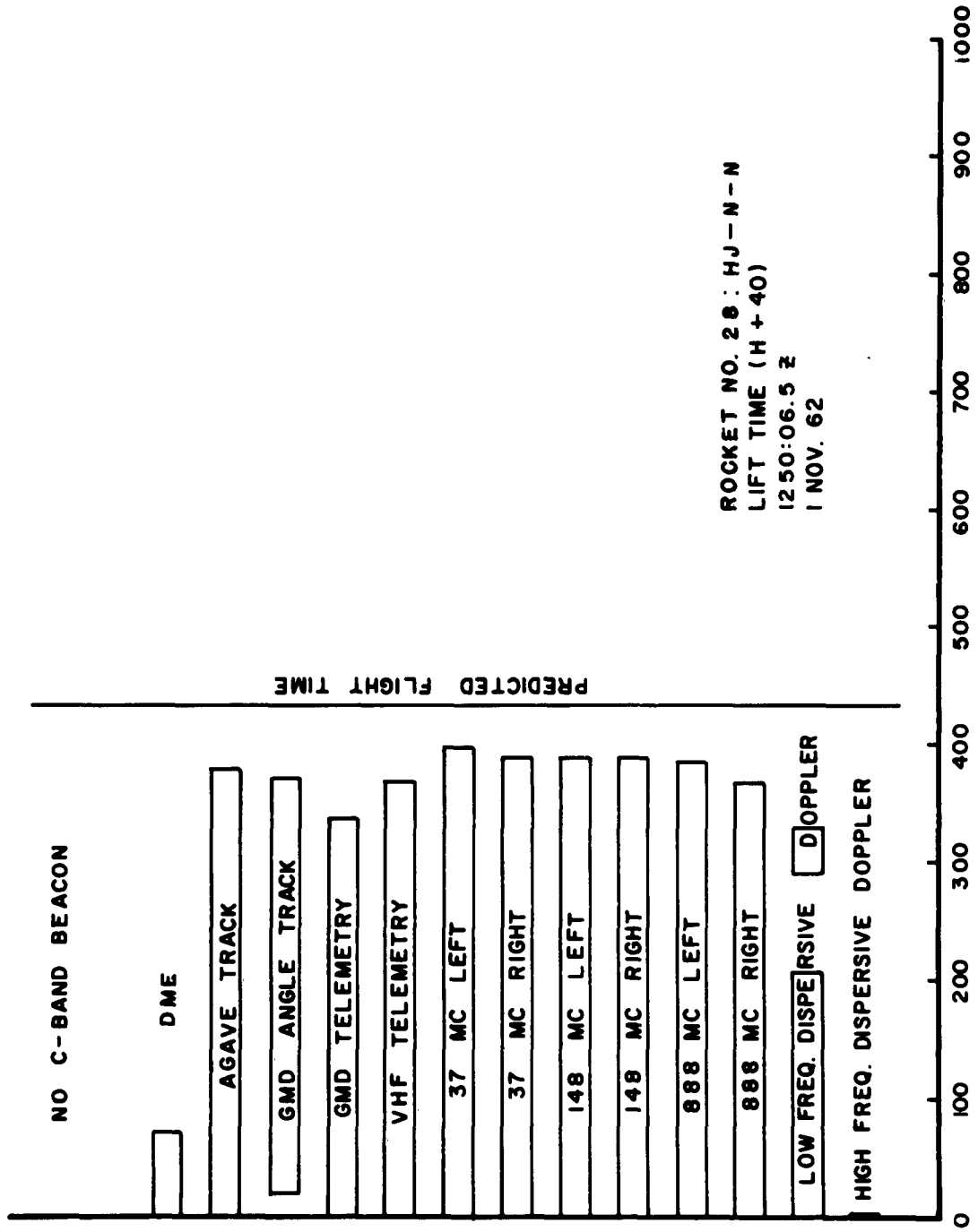

Figure C.94 Duration of useful received signal for experiments carried on Rocket 28, King Fish.

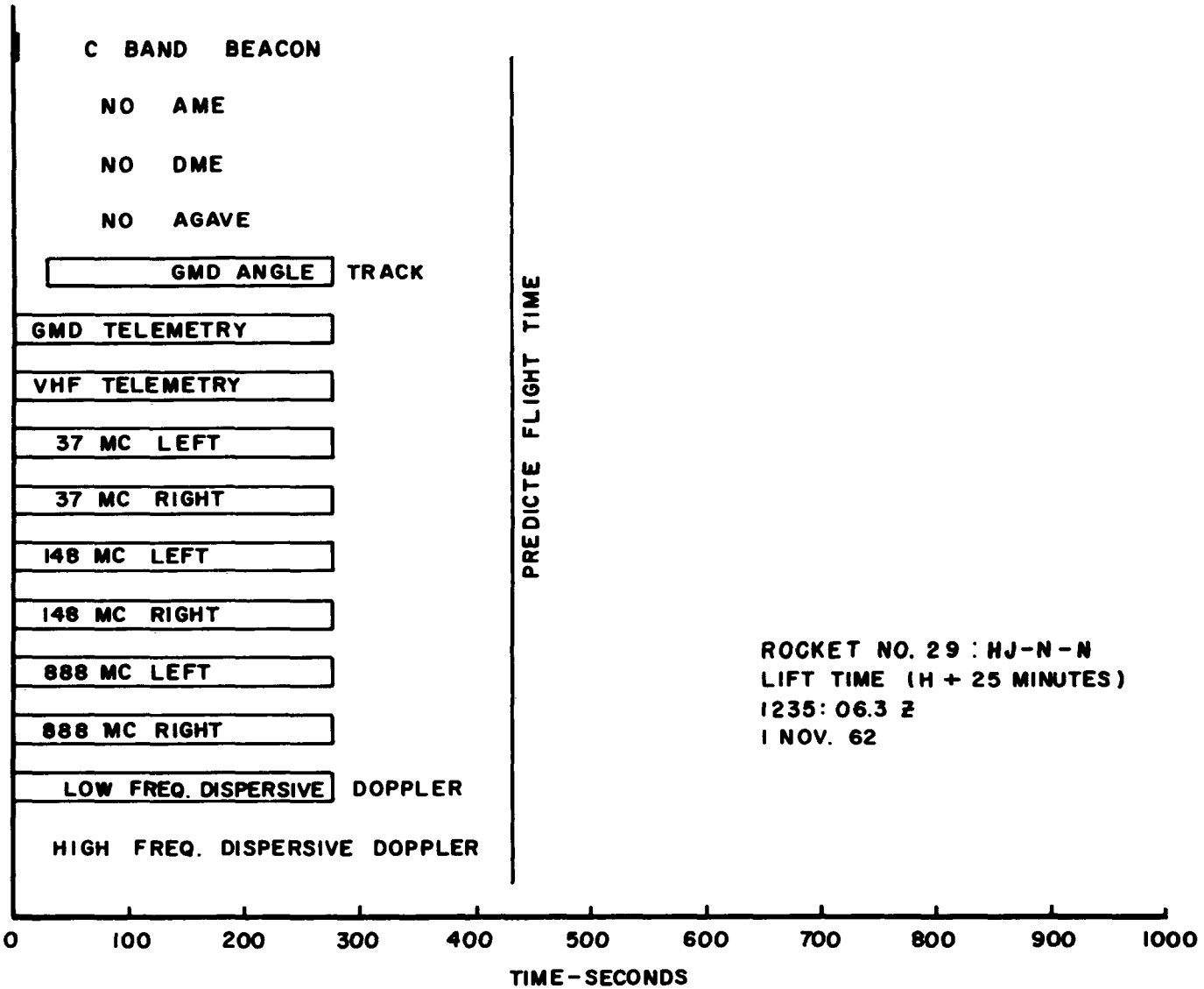

Figure C.95 Duration of useful received signal for experiments carried on Rocket 29, King Fish.

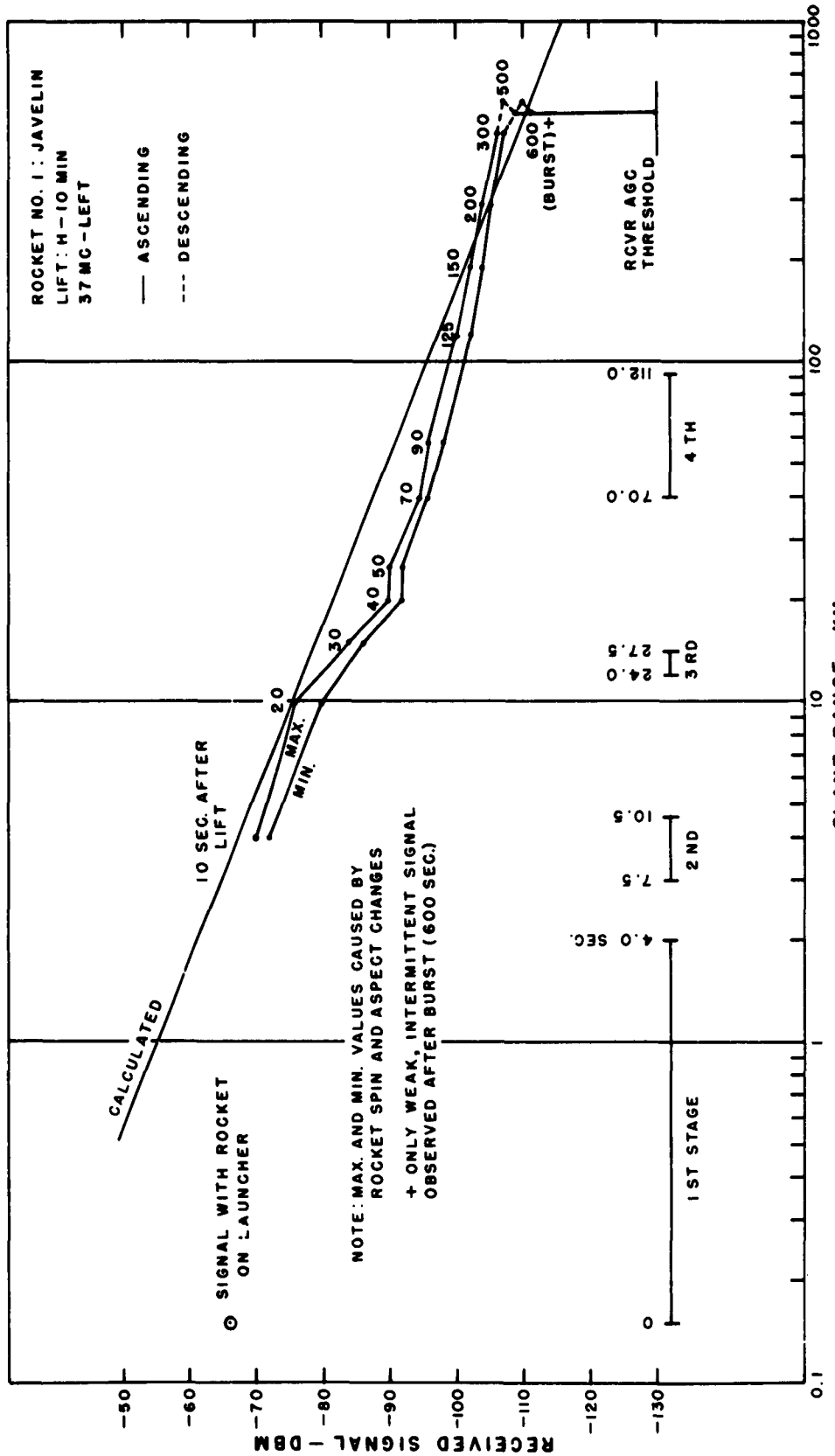

Figure C.96 Received signal strength versus slant range for 3-frequency beacon, 37 Mc left, Rocket 1, Star Fish.

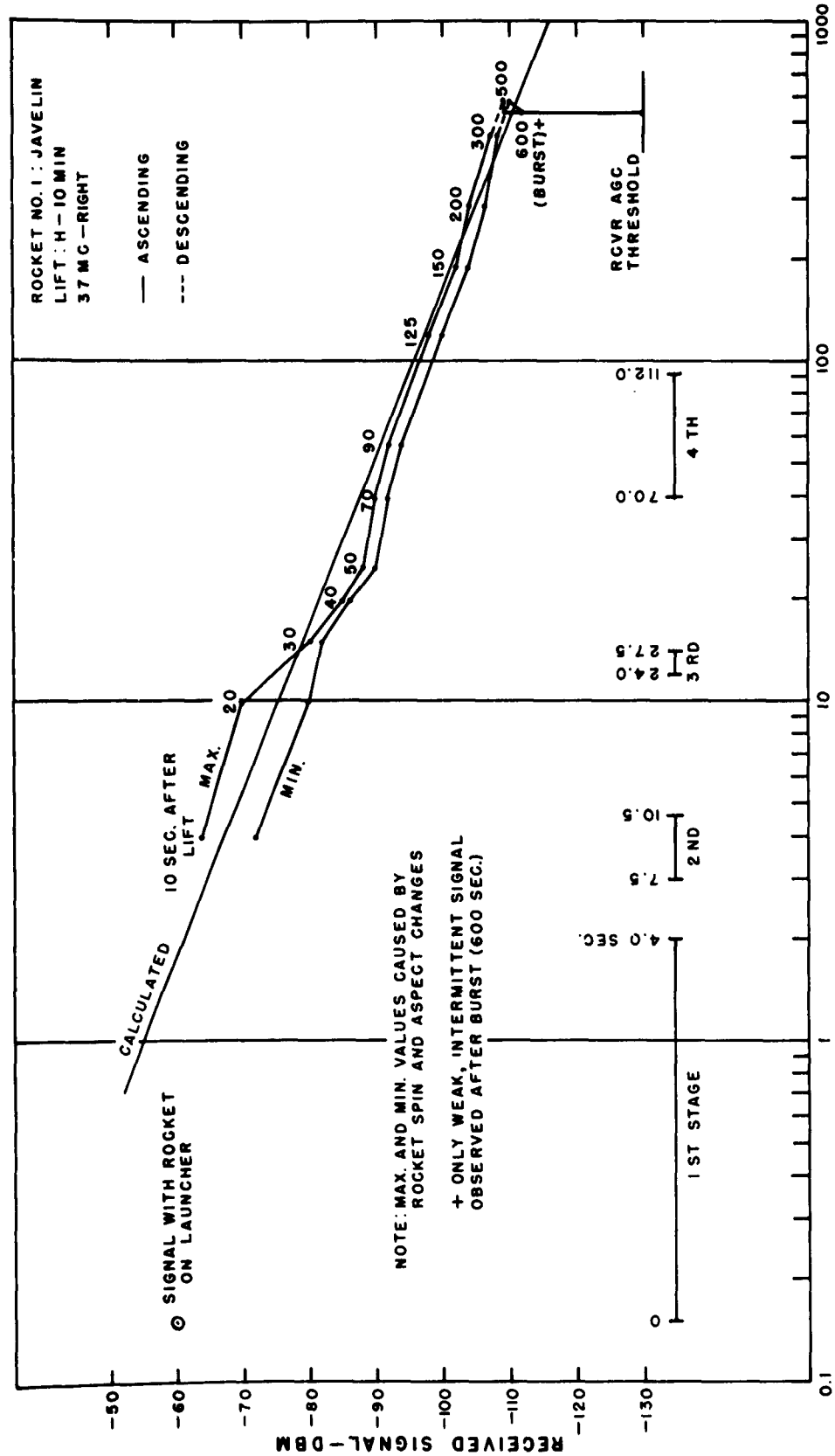

Figure C.97 Received signal strength versus slant range for 3-frequency beacon, 37 Mc right, Rocket 1, Star Fish.

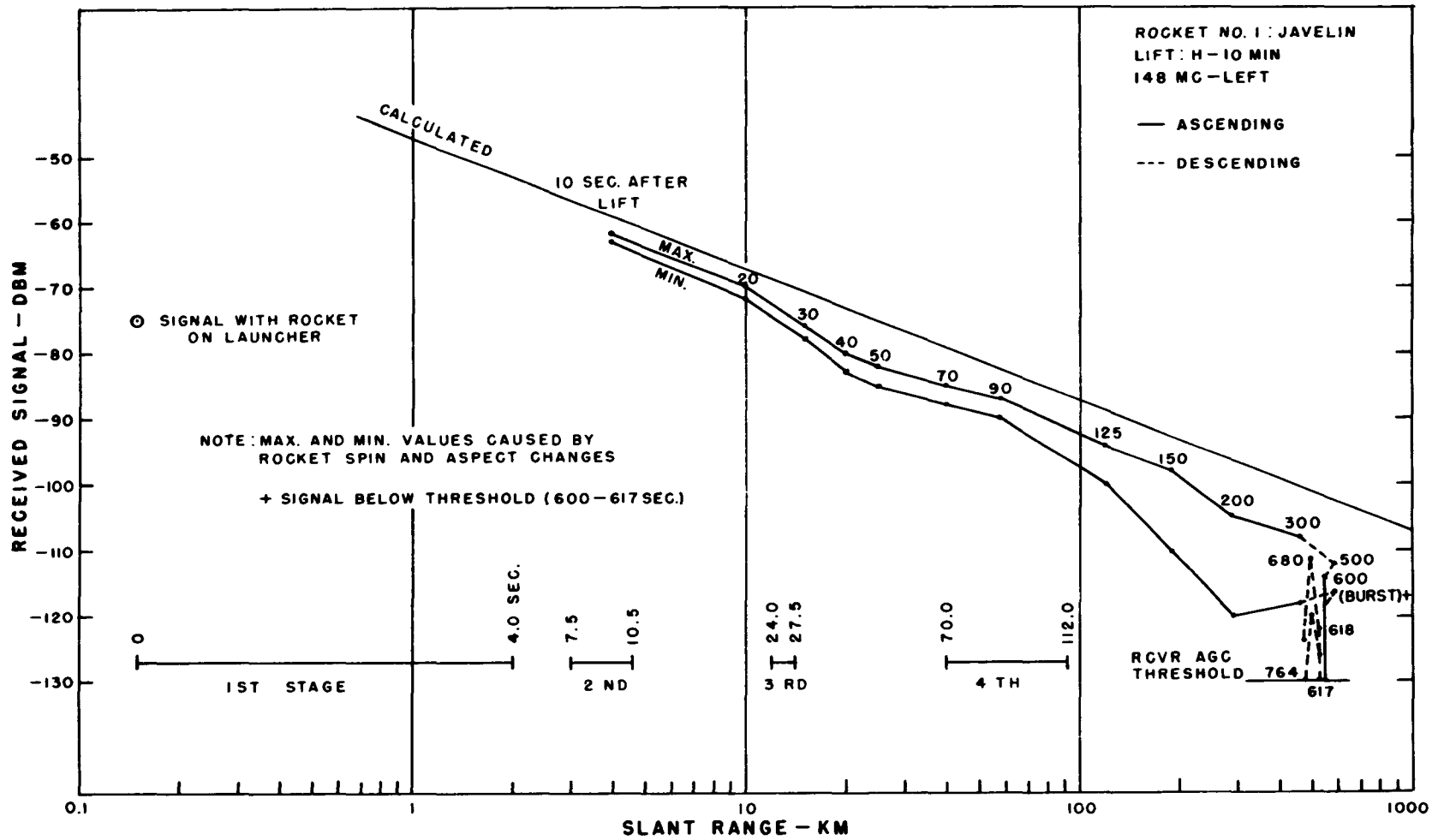

Figure C.98 Received signal strength versus slant range for 3-frequency beacon, 148 Mc left, Rocket 1, Star Fish.

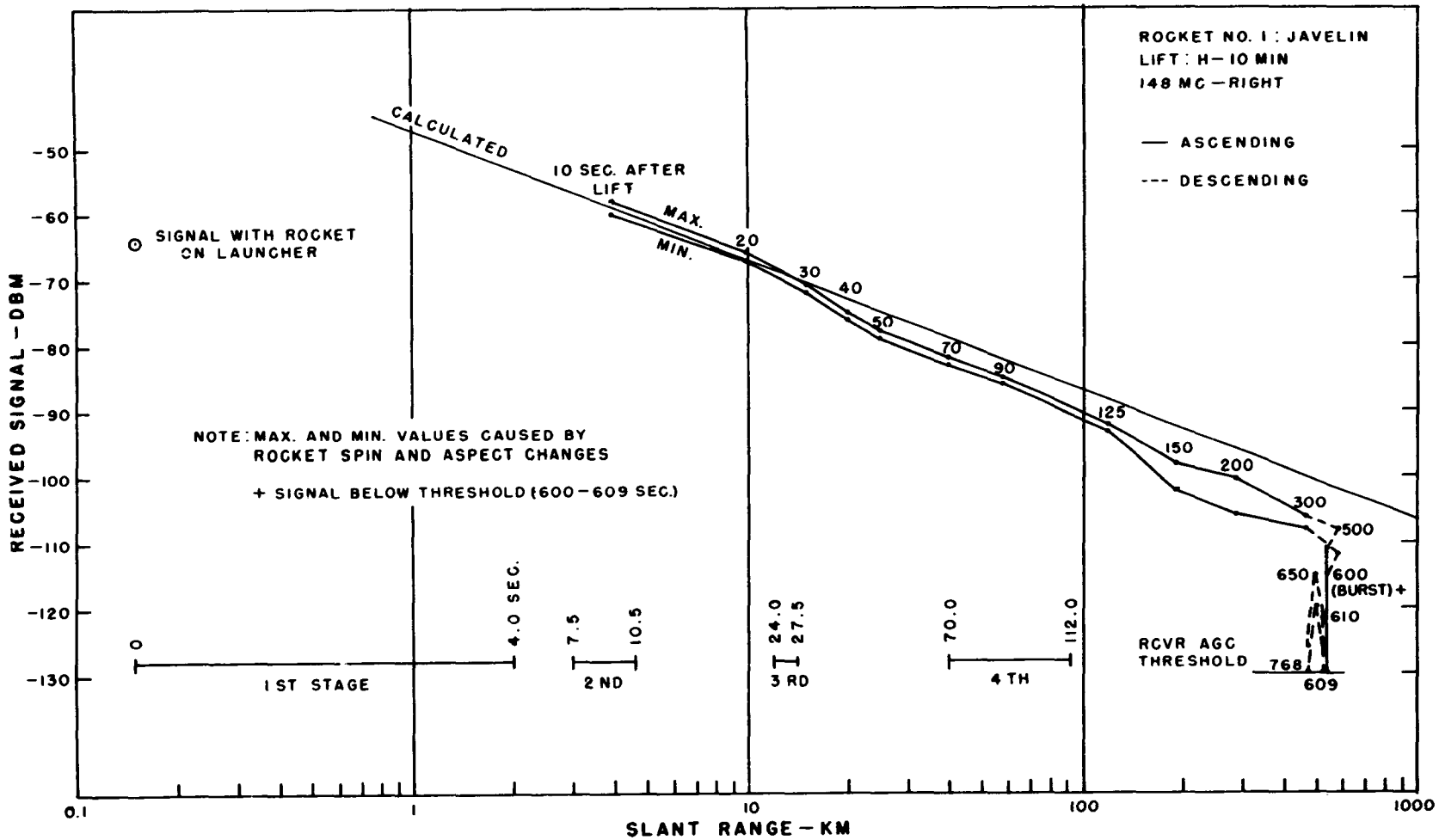

Figure C.99 Received signal strength versus slant range for 3-frequency beacon, 148 Mc right, Rocket 1, Star Fish.

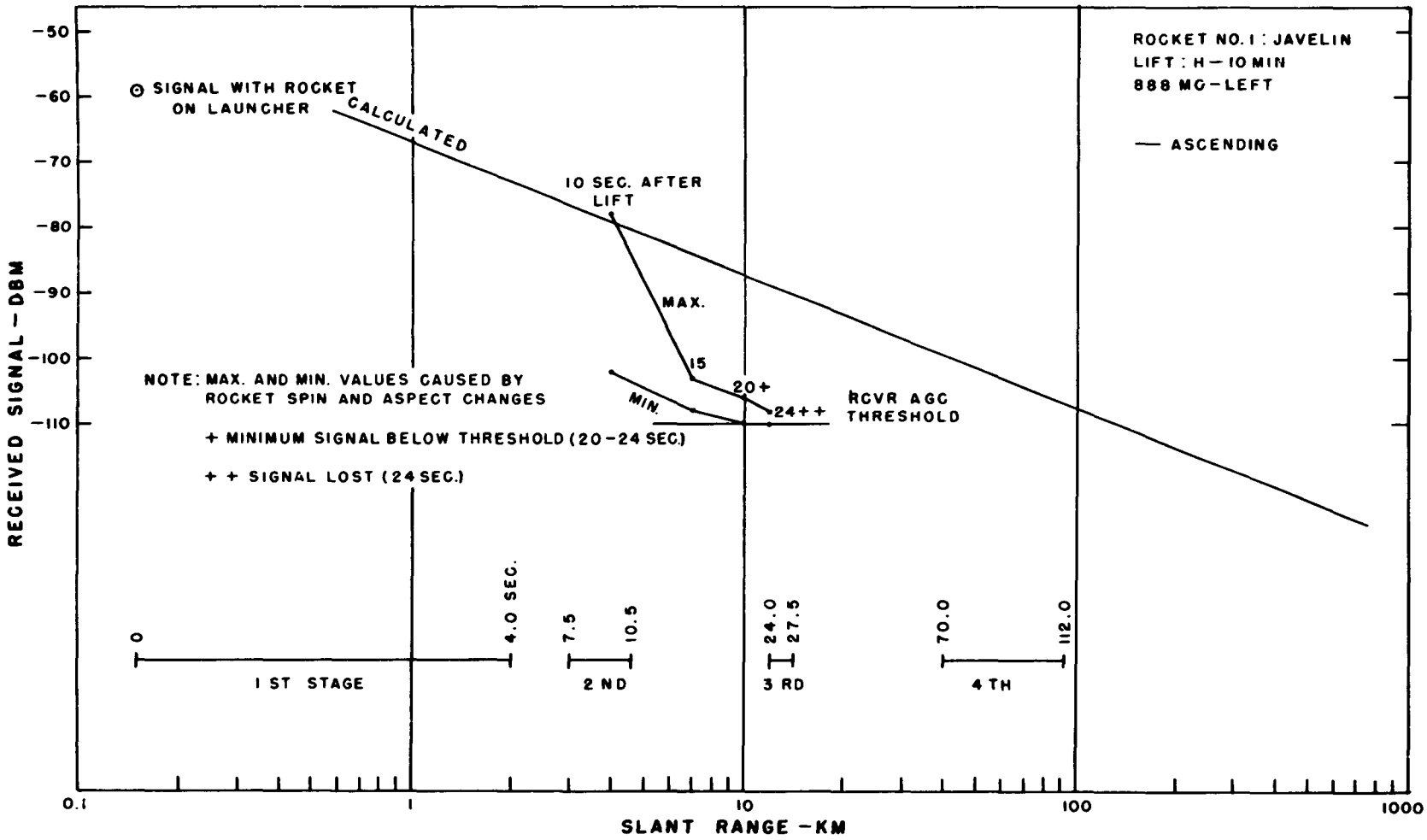

Figure C.100 Received signal strength versus slant range for 3-frequency beacon, 888 Mc left, Rocket 1, Star Fish.

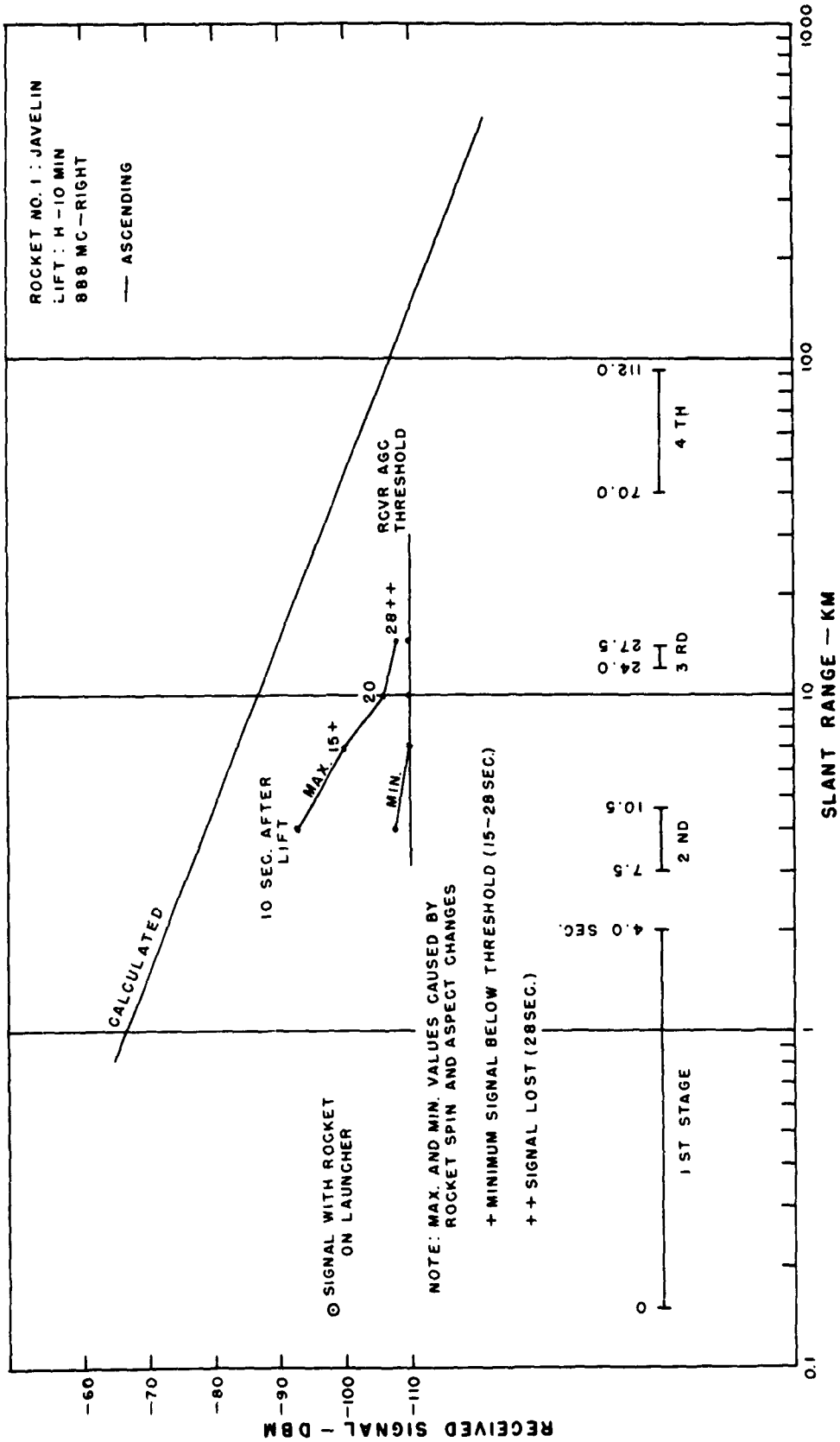

Figure C.101 Received signal strength versus slant range for 3-frequency beacon, 888 Mc right, Rocket 1, Star Fish.

SECRET

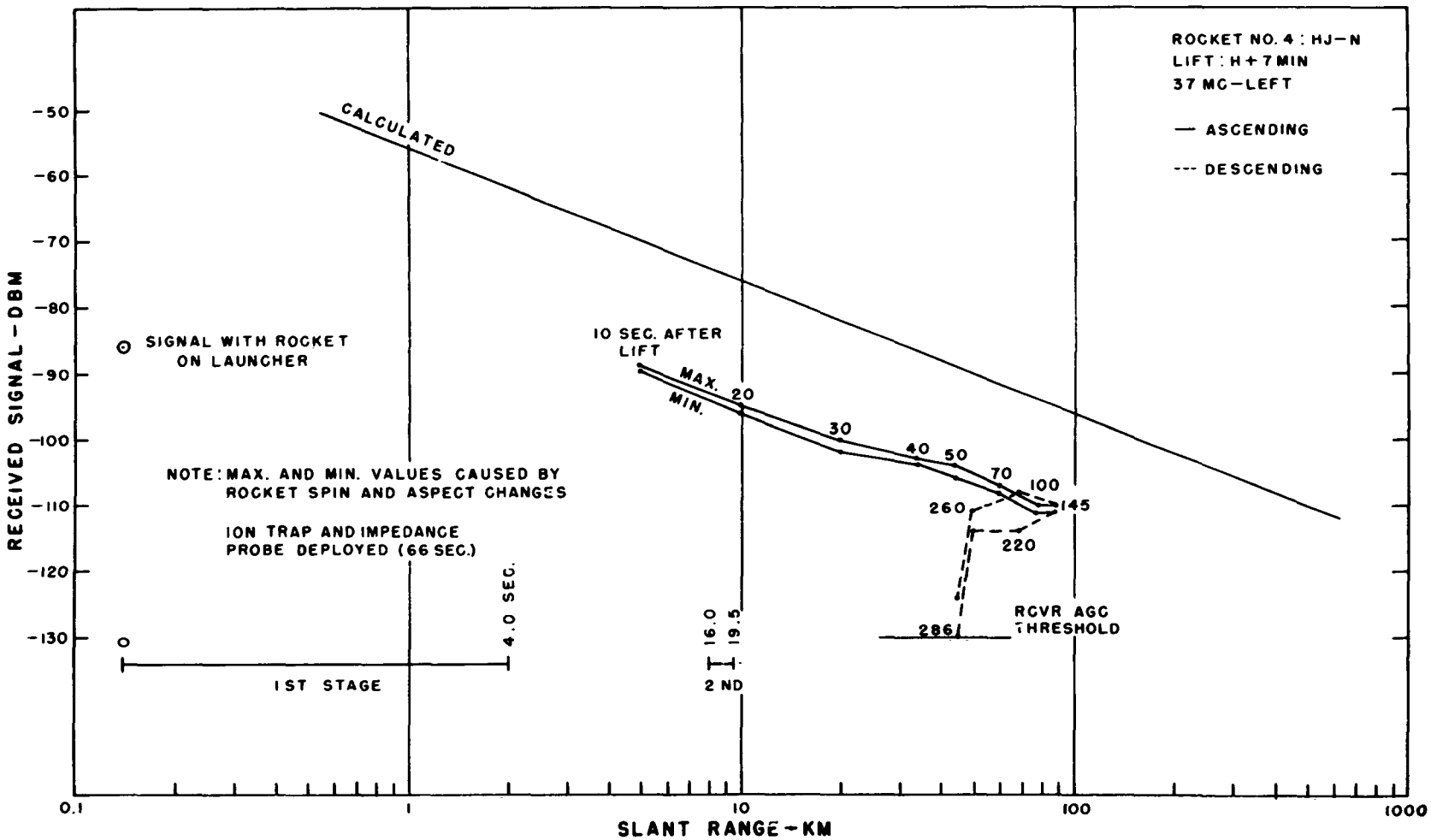

Figure C.102 Received signal strength versus slant range for 3-frequency beacon, 37 Mc left, Rocket 4, Star Fish.

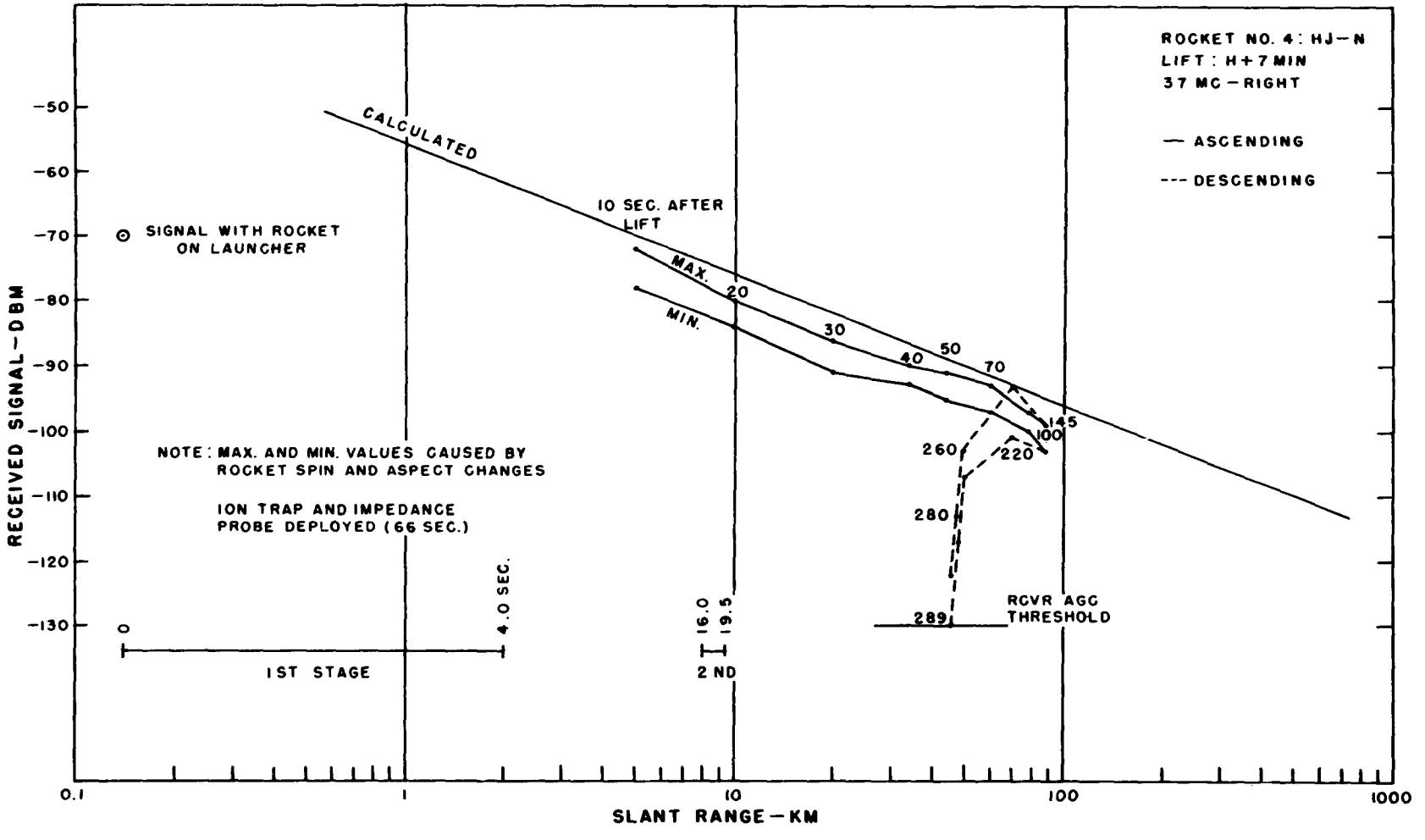

Figure C.103 Received signal strength versus slant range for 3-frequency beacon, 37 Mc right, Rocket 4, Star Fish.

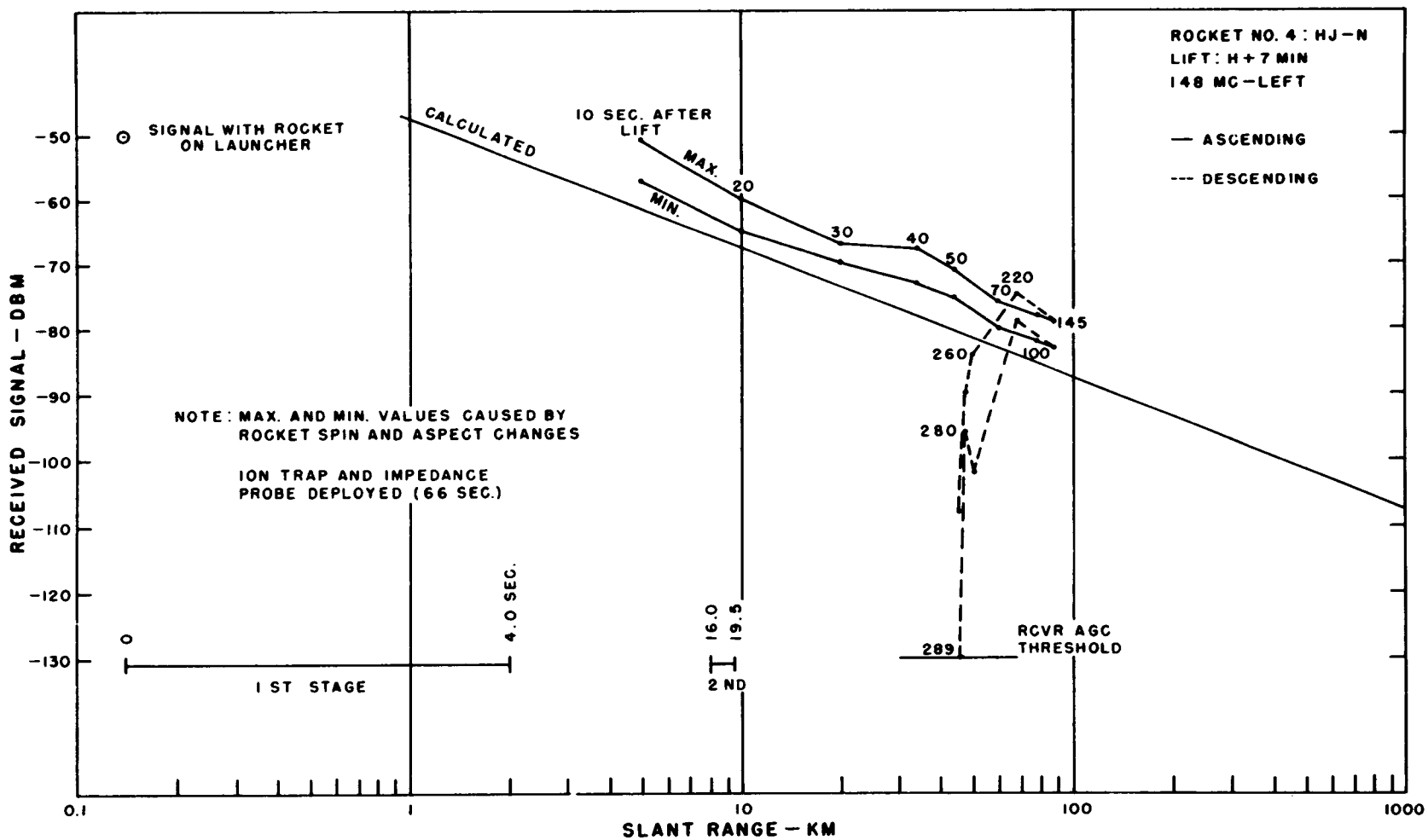

Figure C.104 Received signal strength versus slant range for 3-frequency beacon, 148 Mc left, Rocket 4, Star Fish.

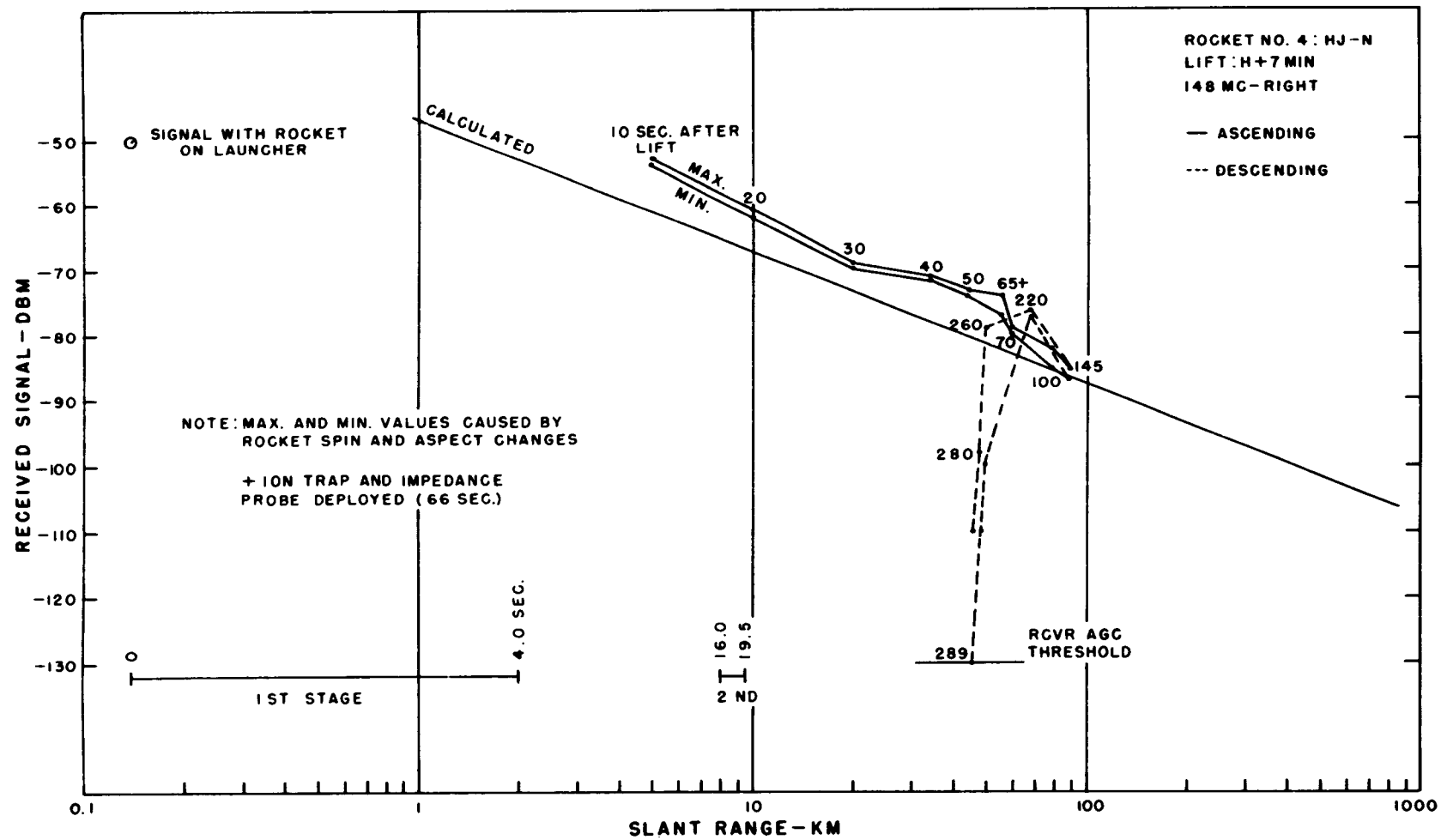

Figure C.105 Received signal strength versus slant range for 3-frequency beacon, 148 Mc right, Rocket 4, Star Fish.

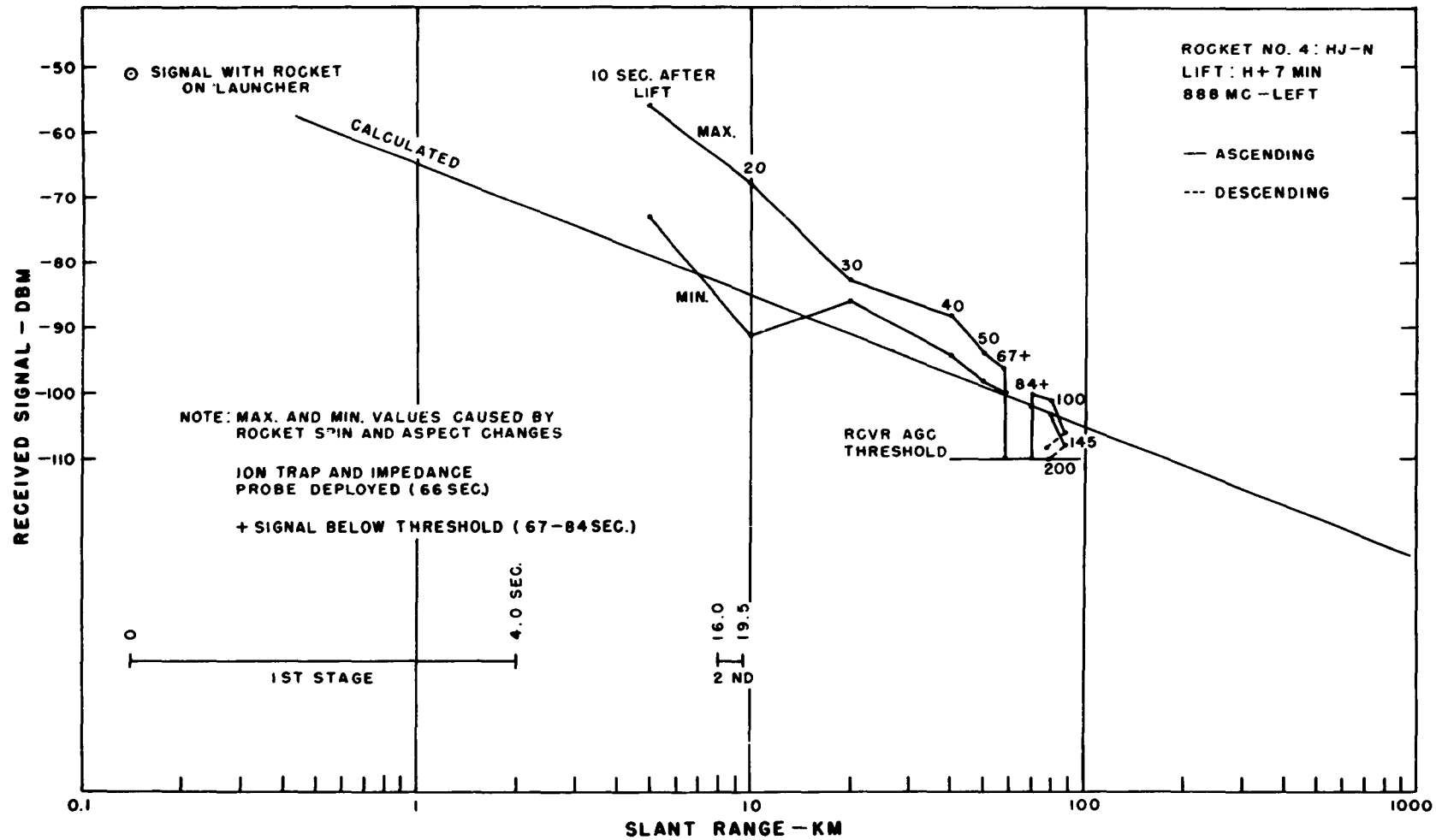

Figure C.106 Received signal strength versus slant range for 3-frequency beacon, 888 Mc left, Rocket 4, Star Fish.

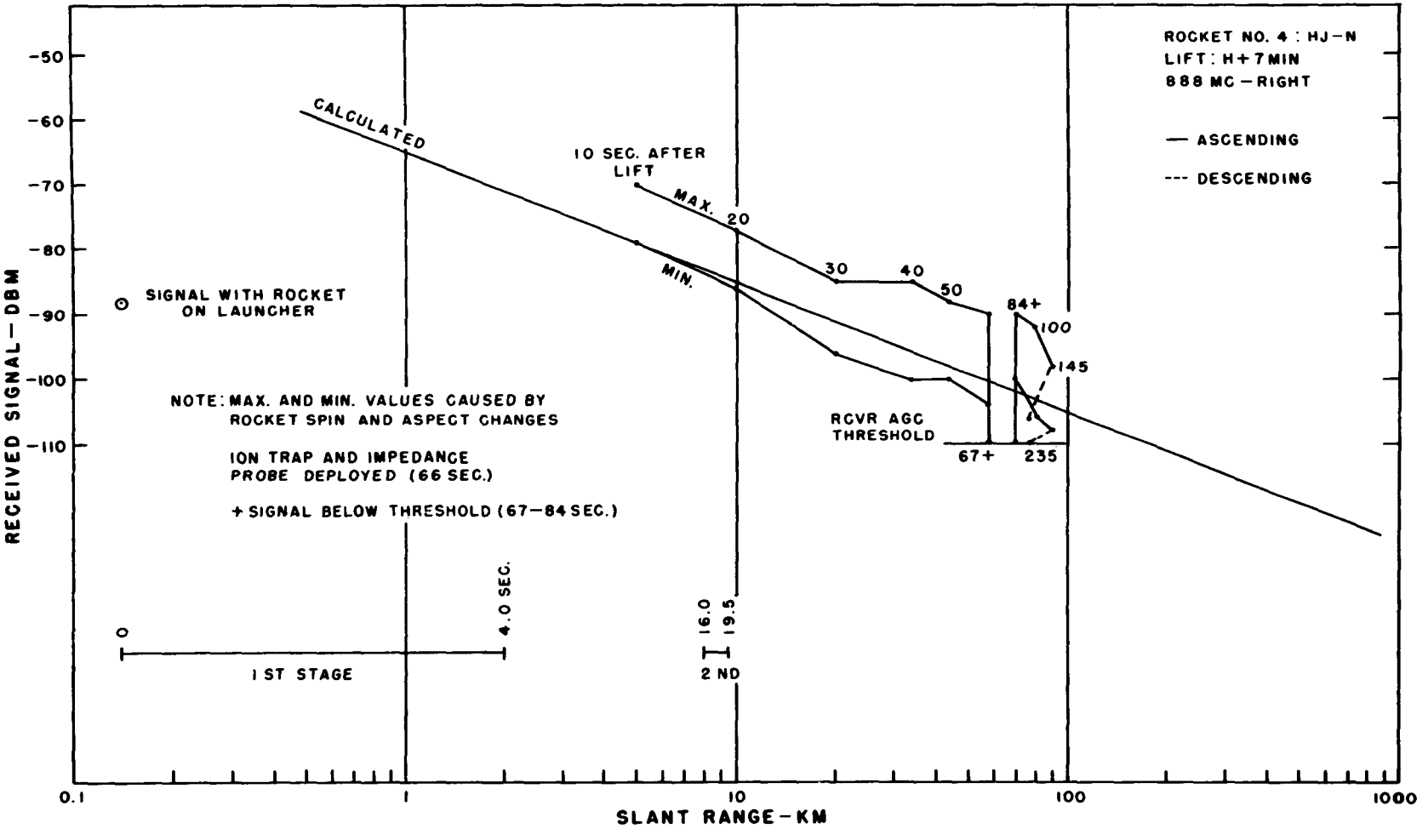

Figure C.107 Received signal strength versus slant range for 3-frequency beacon, 888 Mc right, Rocket 4, Star Fish.

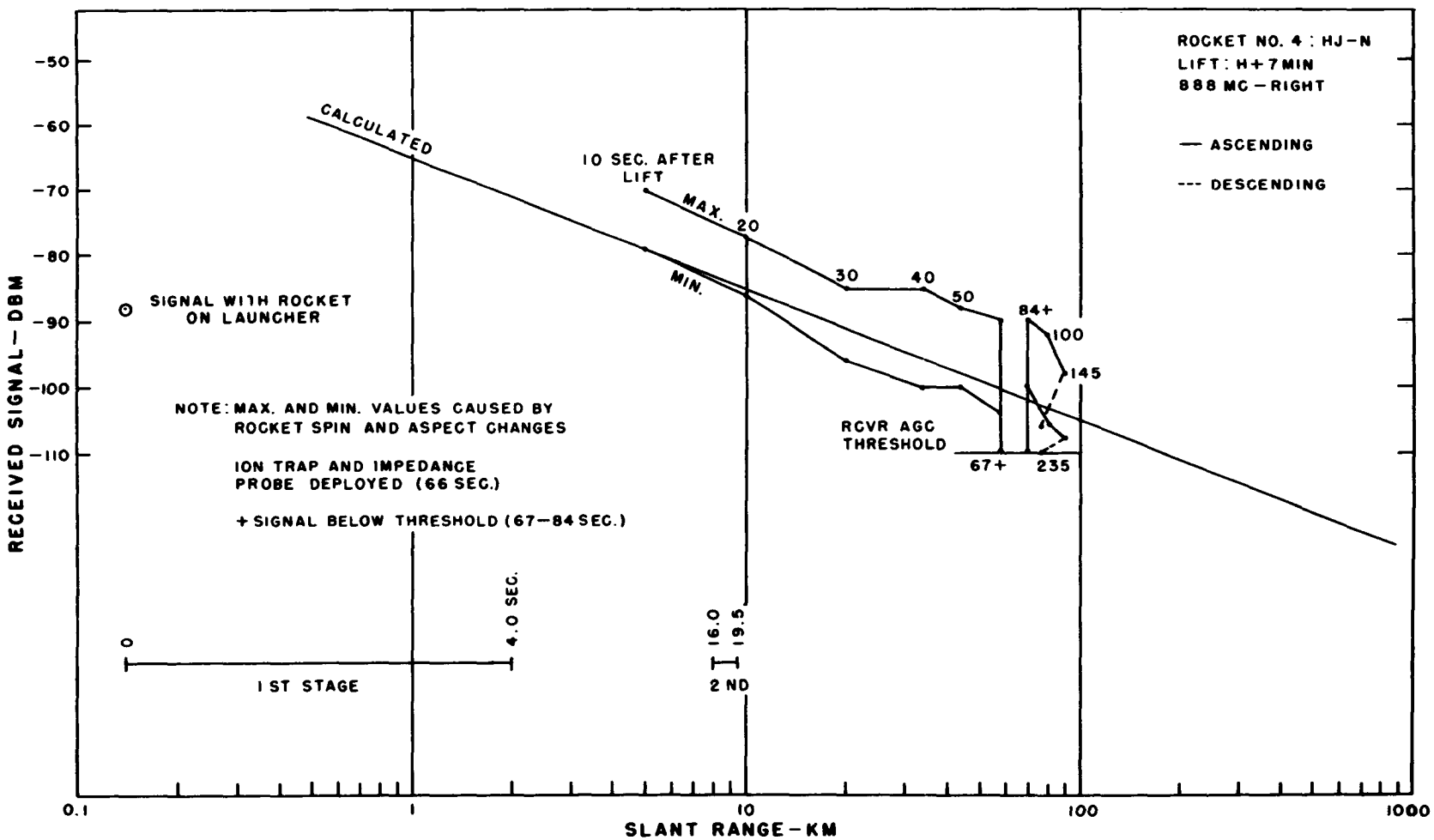

Figure C.107 Received signal strength versus slant range for 3-frequency beacon, 888 Mc right, Rocket 4, Star Fish.

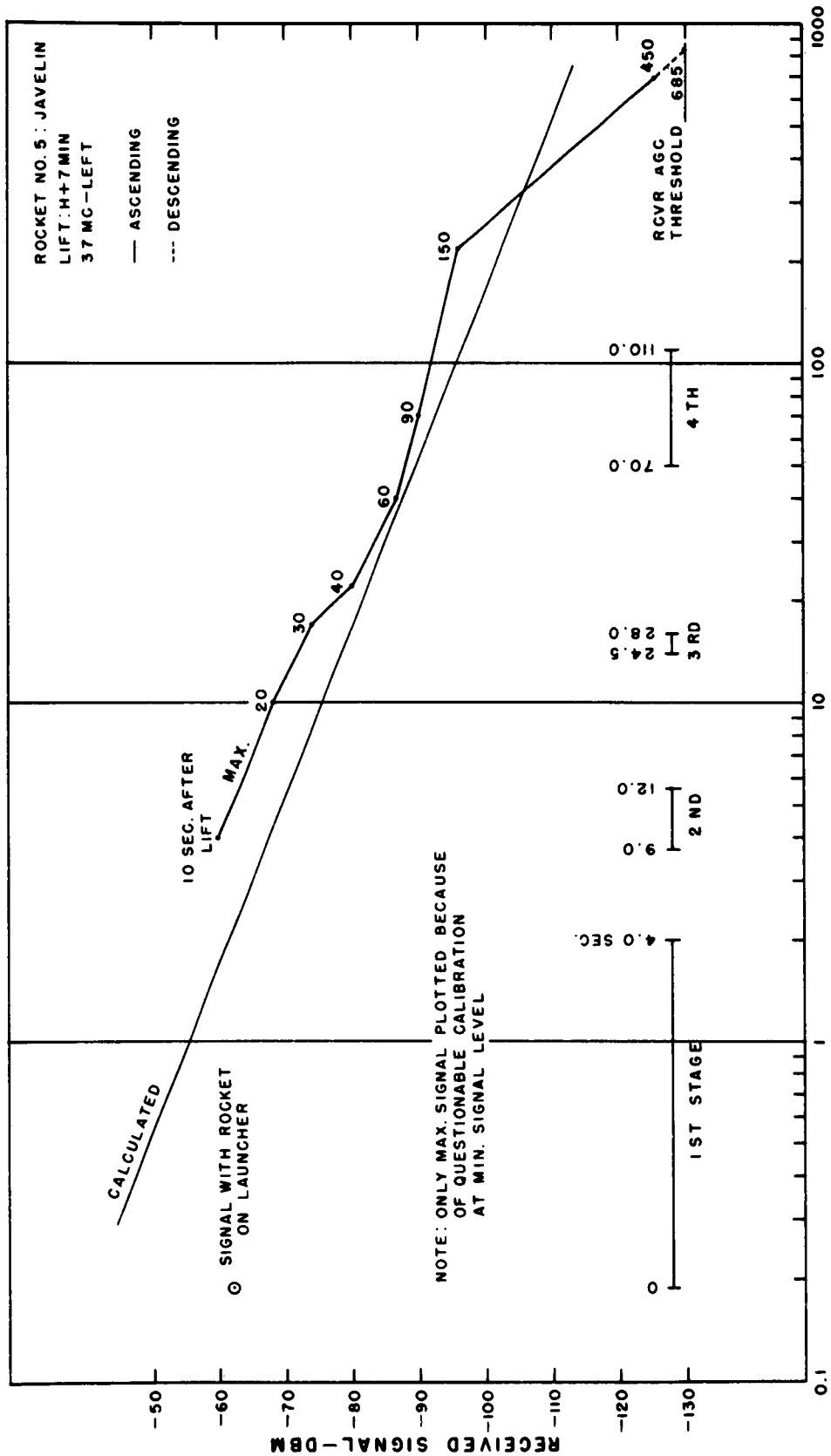

Figure C.108 Received signal strength versus slant range for 3-frequency beacon, 37 Mc left, Rocket 5, Star Fish.

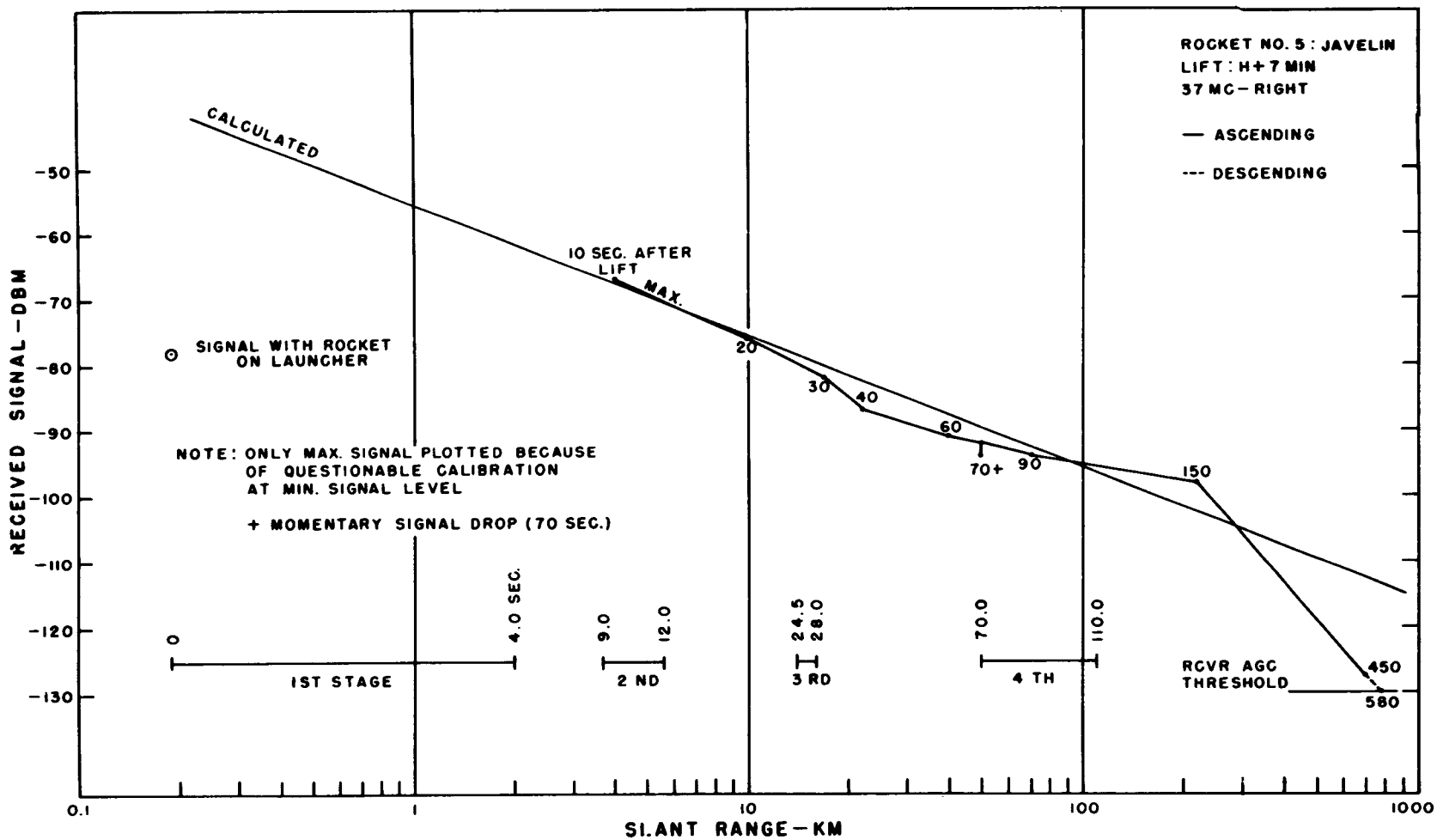

Figure C.109 Received signal strength versus slant range for 3-frequency beacon, 37 Mc right, Rocket 5, Star Fish.

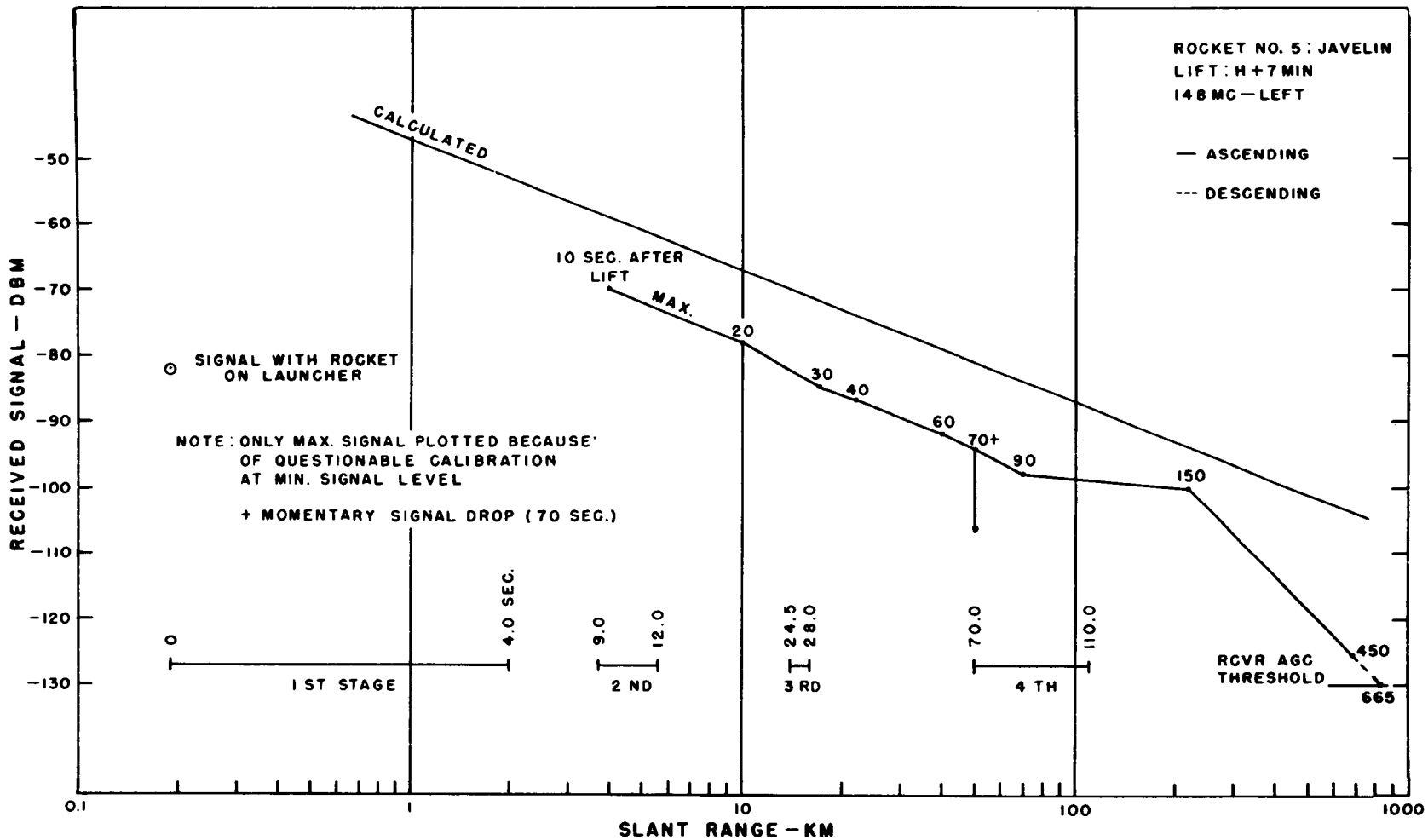

Figure C.110 Received signal strength versus slant range for 3-frequency beacon, 148 Mc left, Rocket 5, Star Fish.

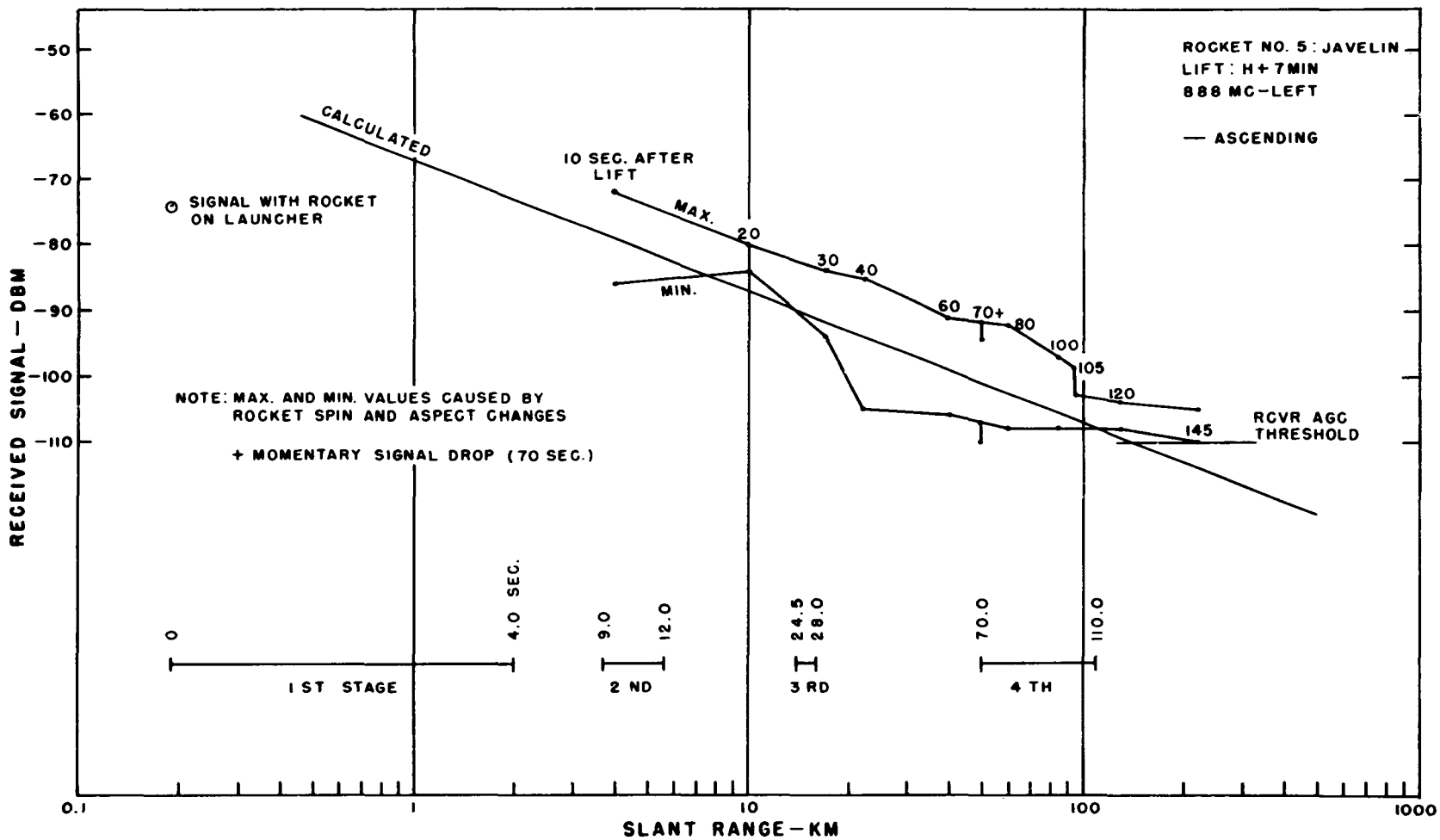

Figure C.111 Received signal strength versus slant range for 3-frequency beacon, 148 Mc right, Rocket 5, Star Fish.

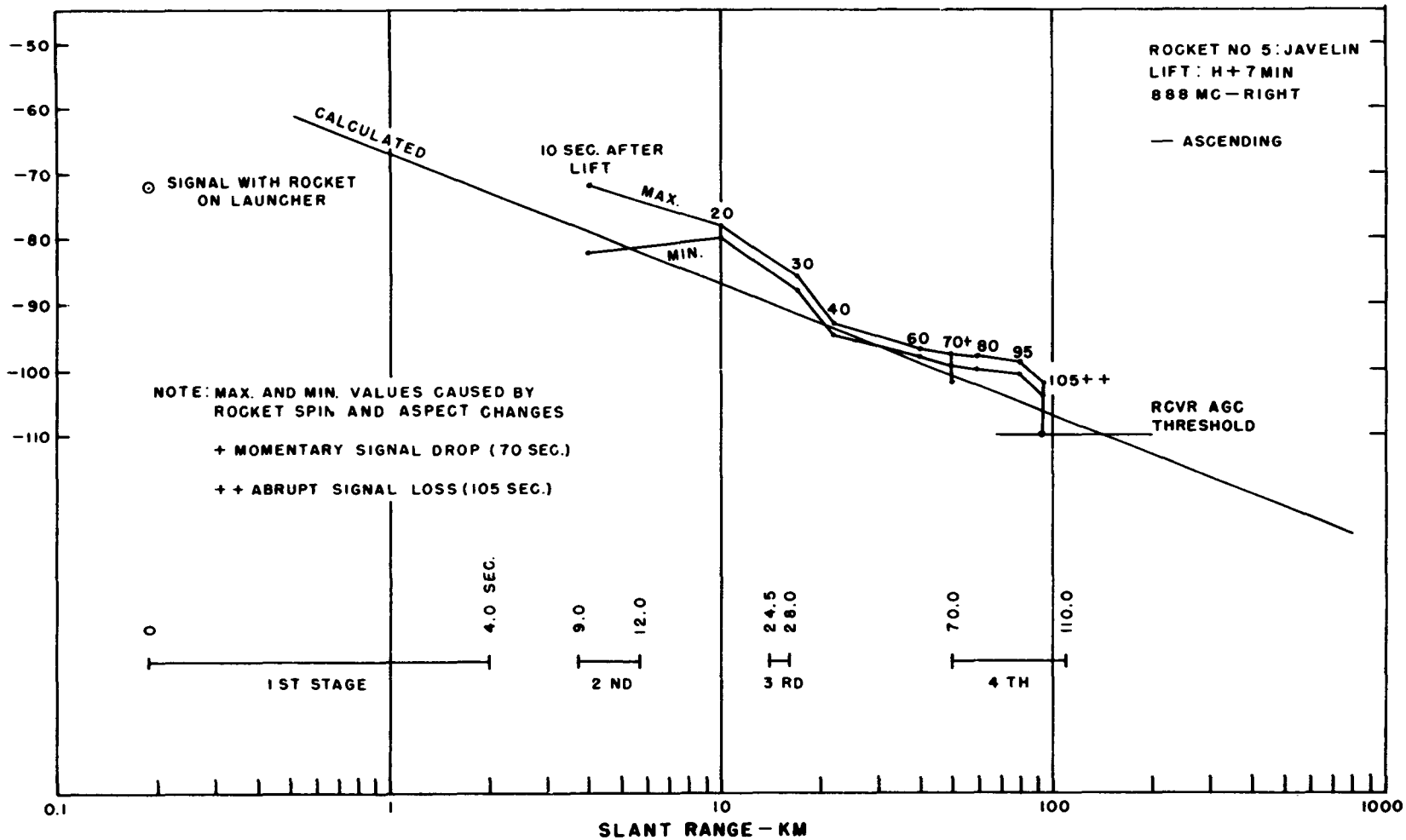

Figure C.112 Received signal strength versus slant range for 3-frequency beacon, 888 Mc left, Rocket 5, Star Fish.

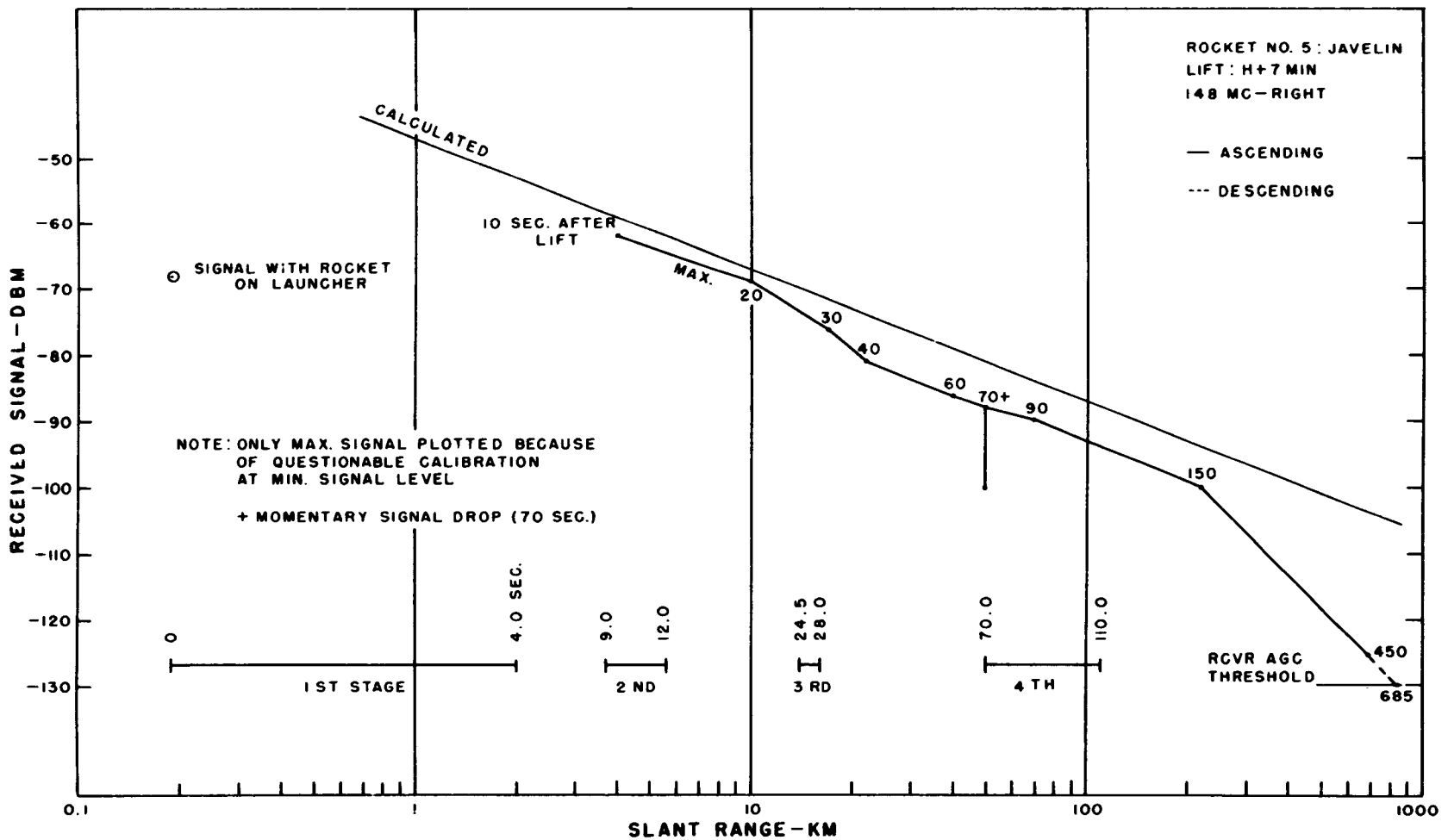

Figure C.113 Received signal strength versus slant range for 3-frequency beacon, 888 Mc right, Rocket 5, Star Fish.

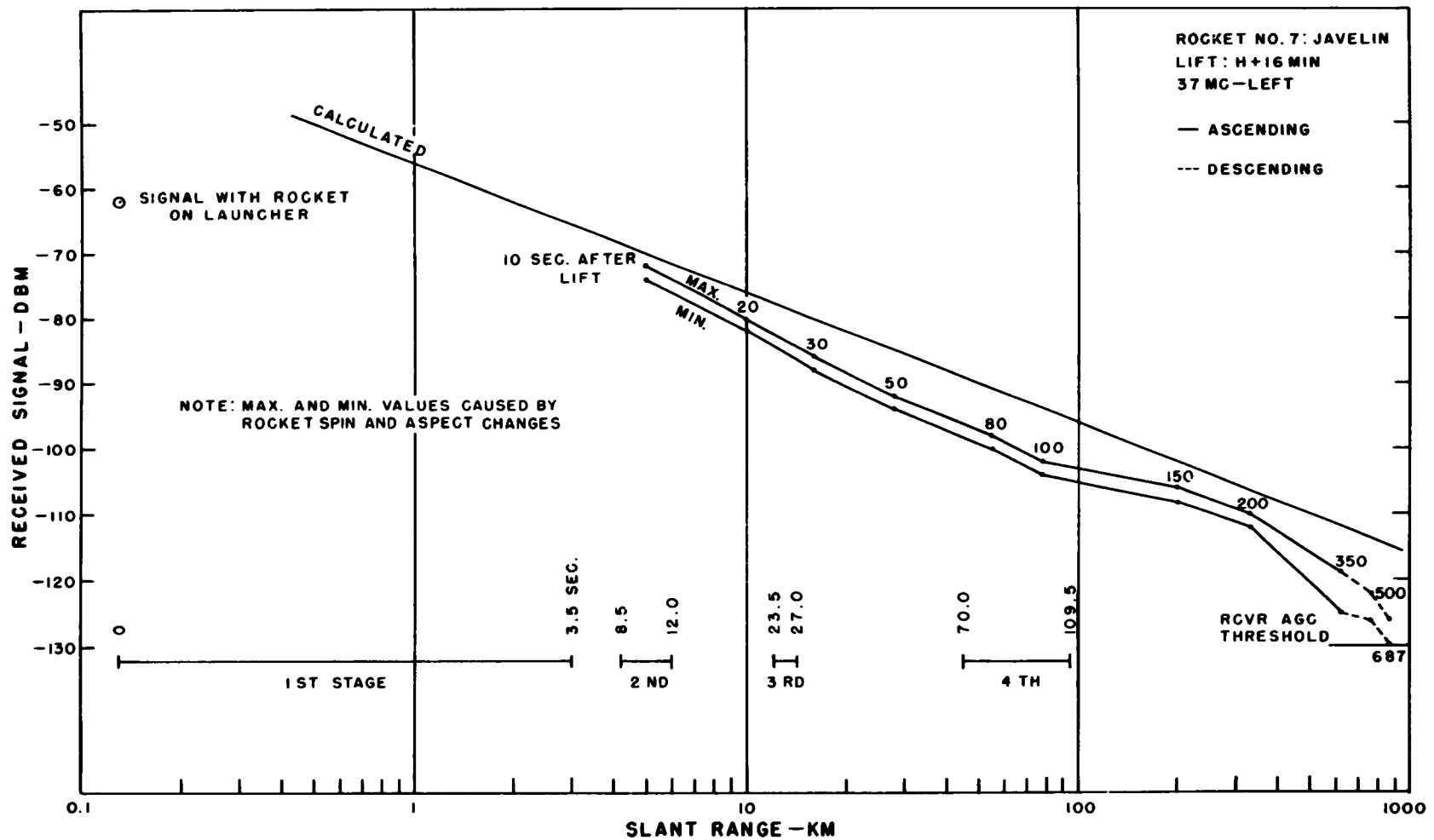

Figure C.114 Received signal strength versus slant range for 3-frequency beacon, 37 Mc left, Rocket 7, Star Fish.

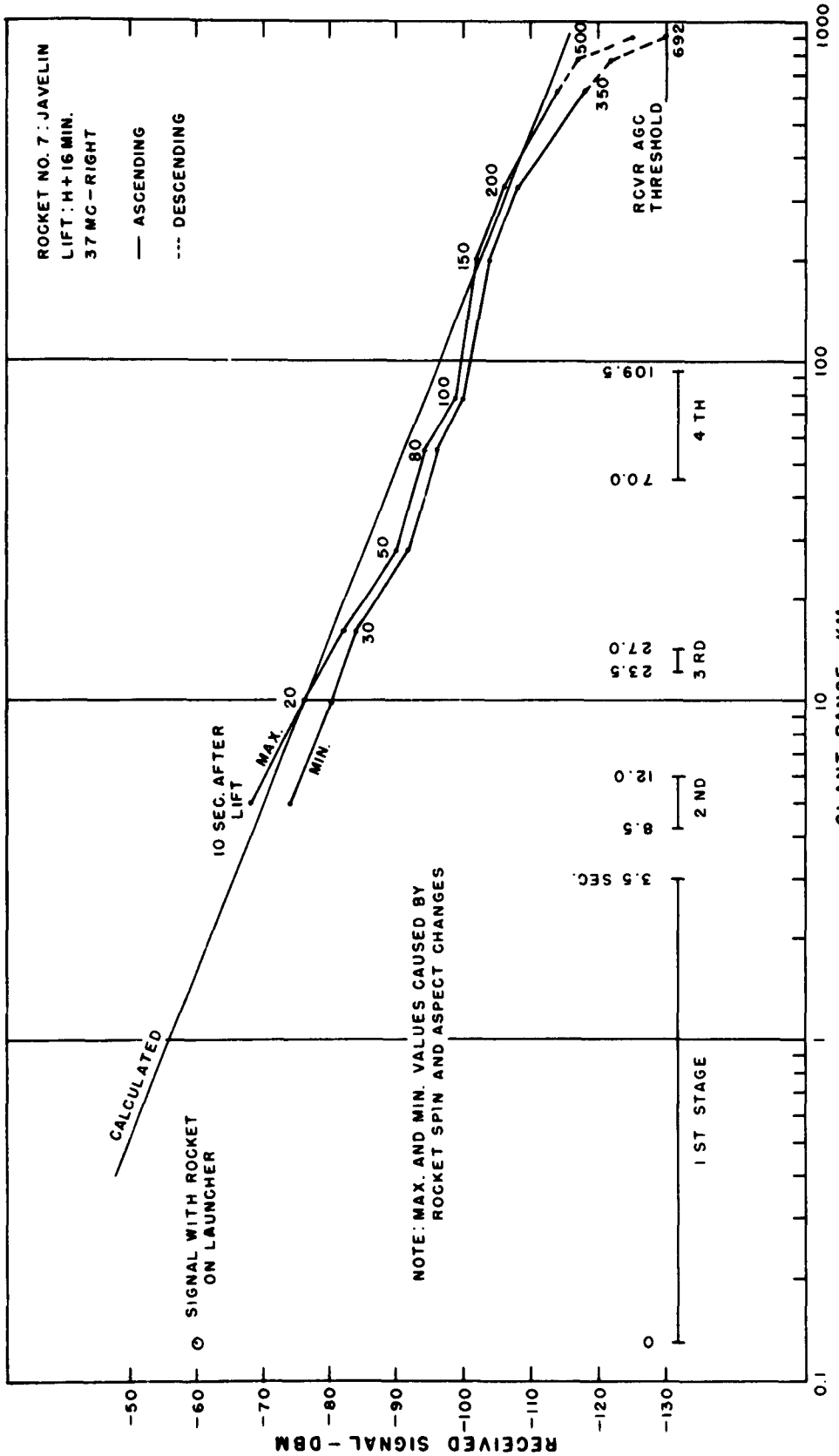

Figure C.115 Received signal strength versus slant range for 3-frequency beacon, 37 Mc right, Rocket 7, Star Fish.

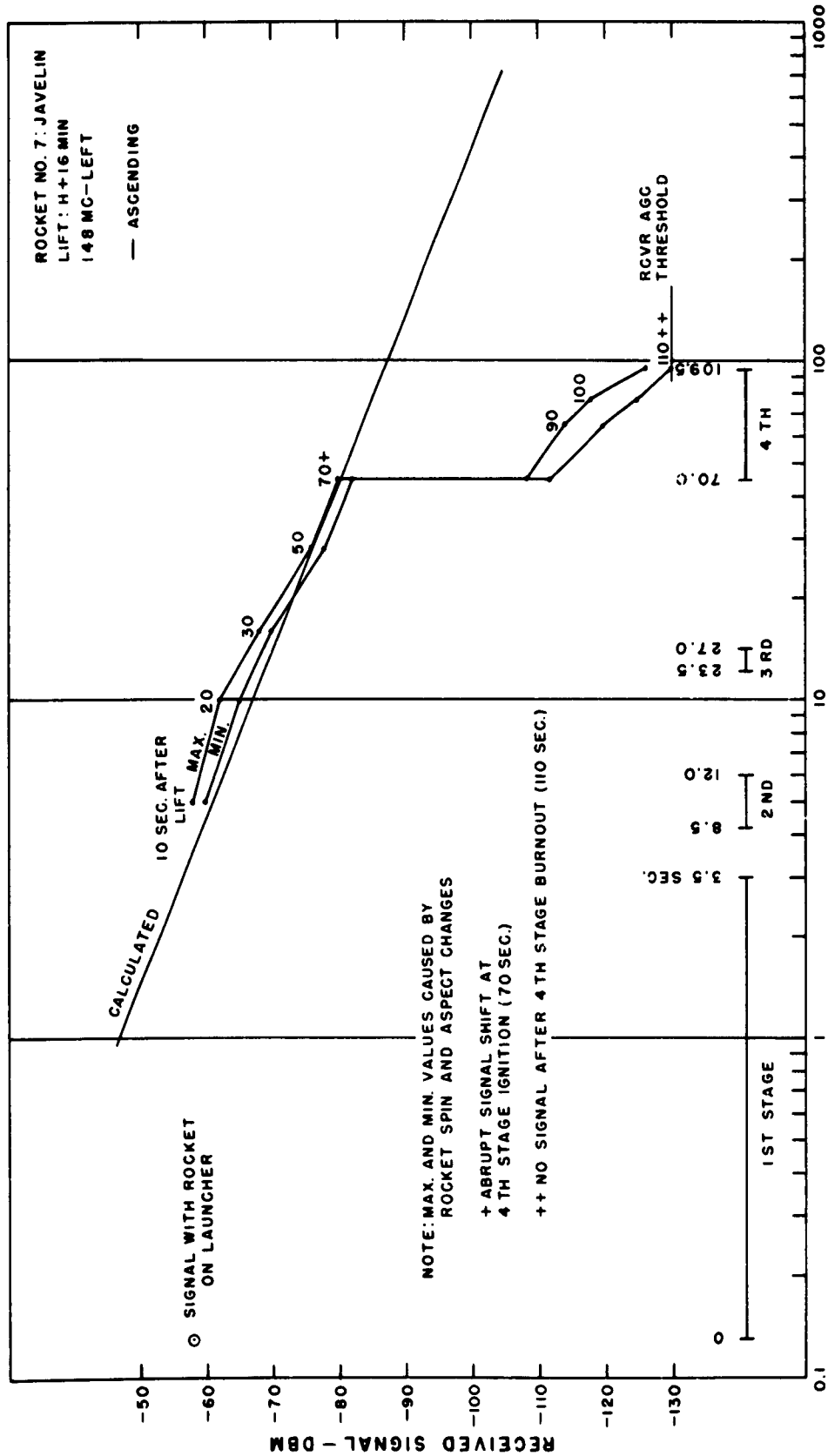

Figure C.116 Received signal strength versus slant range for 3-frequency beacon, 148 Mc left, Rocket 7, Star Fish.

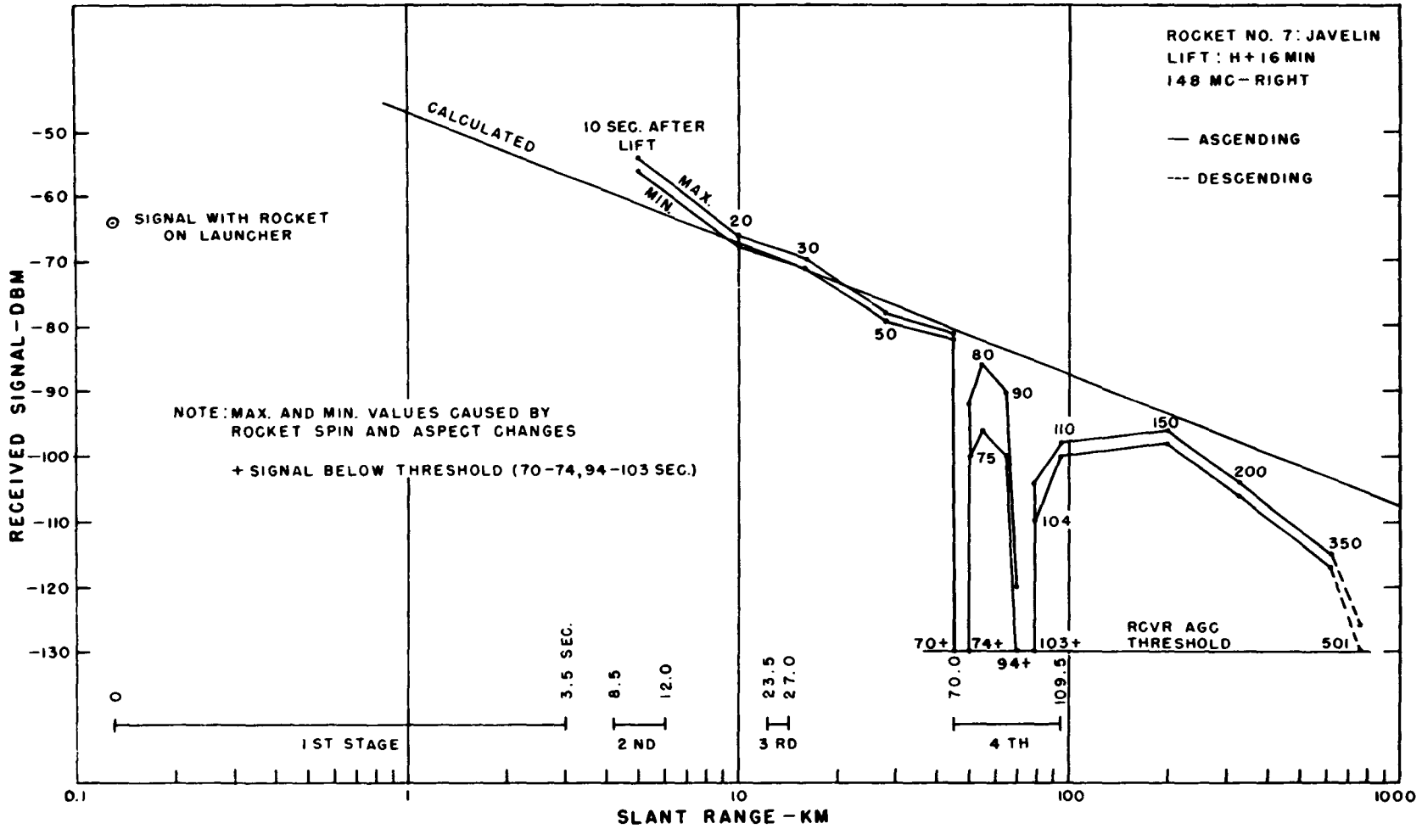

Figure C.117 Received signal strength versus slant range for 3-frequency beacon, 148 Mc right, Rocket 7, Star Fish.

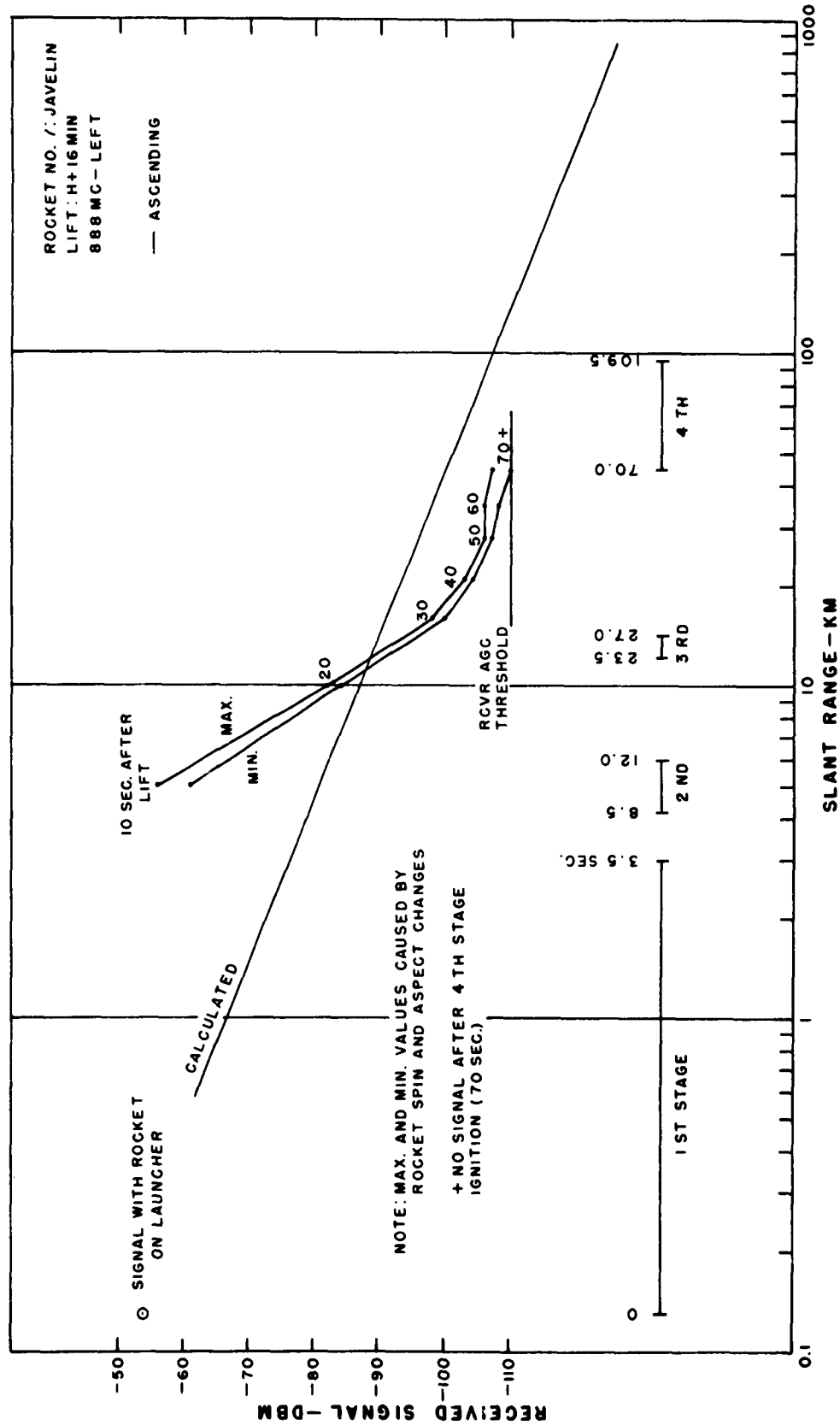

Figure C.118 Received signal strength versus slant range for 3-frequency beacon, 888 Mc left, Rocket 7, Star Fish.

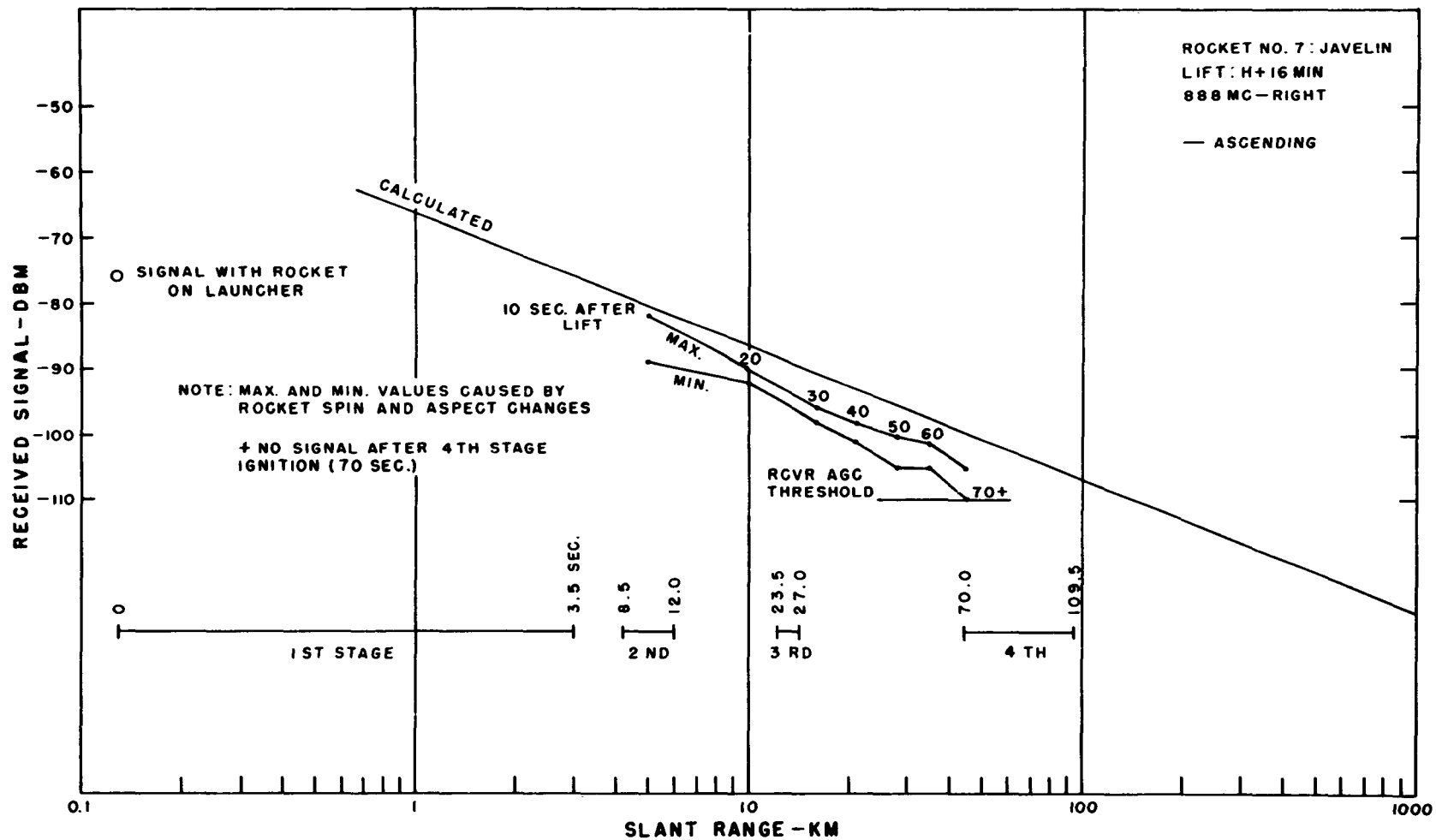

Figure C.119 Received signal strength versus slant range for 3-frequency beacon, 888 Mc right, Rocket 7, Star Fish.

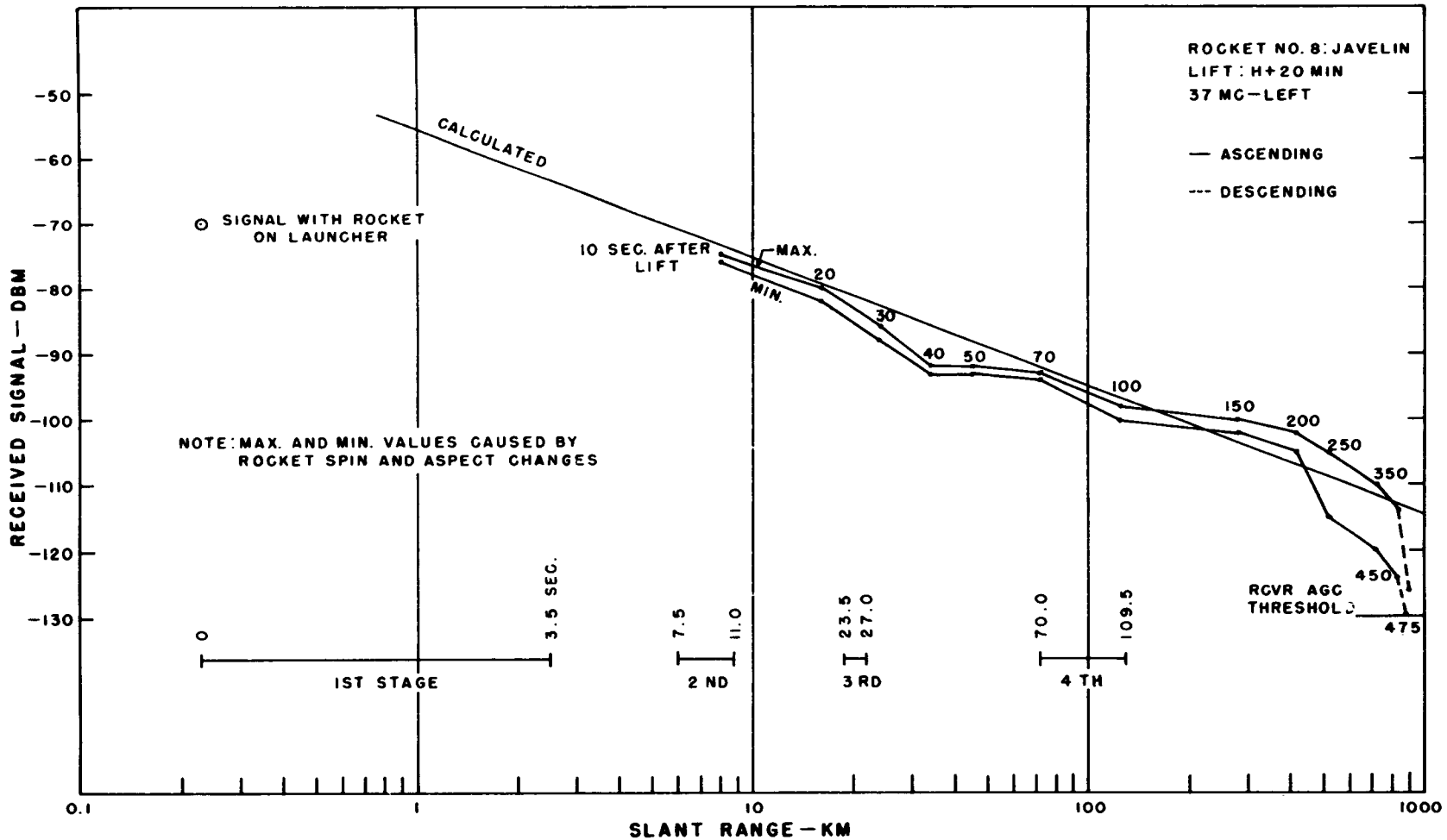

Figure C.120 Received signal strength versus slant range for 3-frequency beacon, 37 Mc left, Rocket 8, Star Fish.

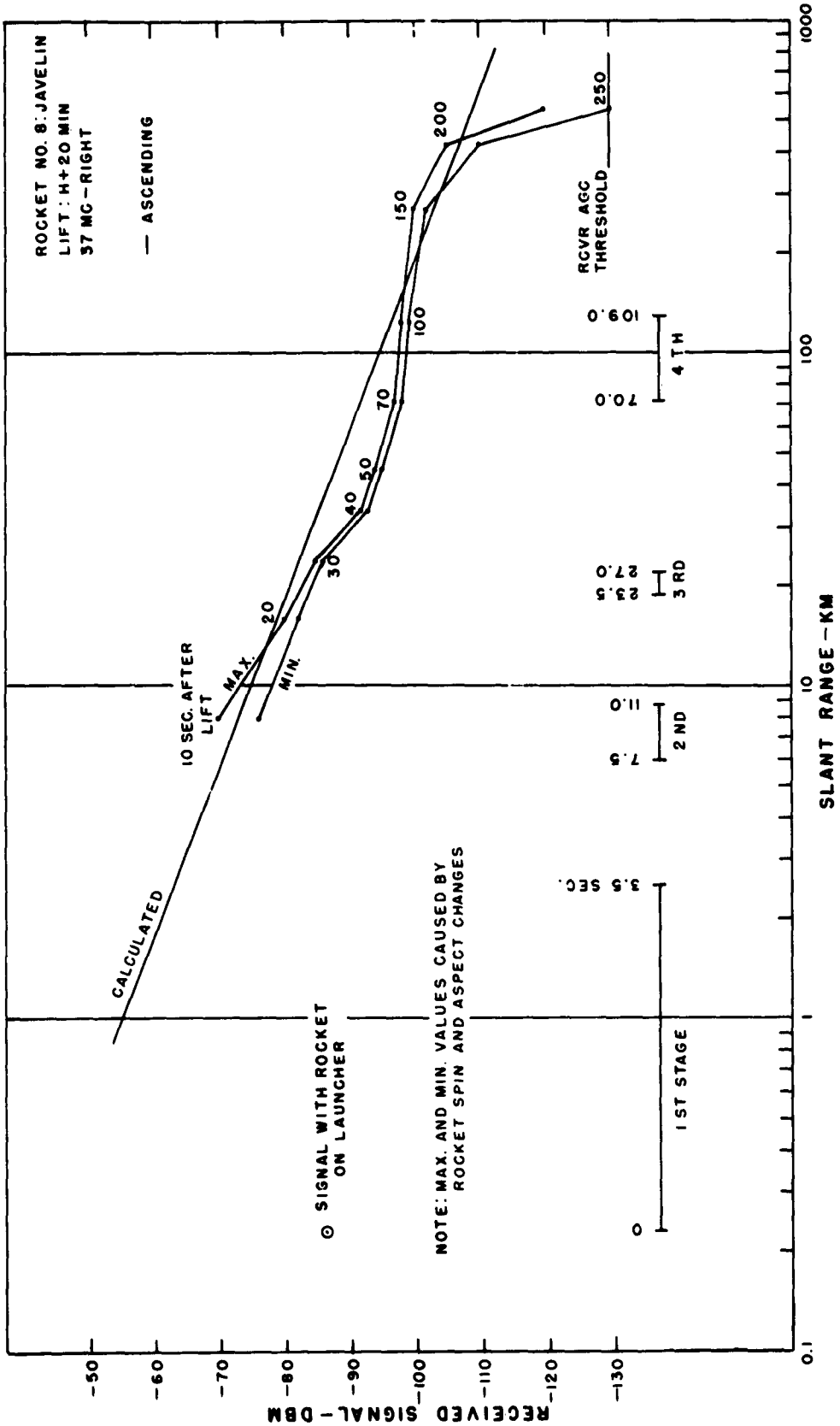

Figure C.121 Received signal strength versus slant range for 3-frequency beacon, 37 Mc right, Rocket 8, Star Fish.

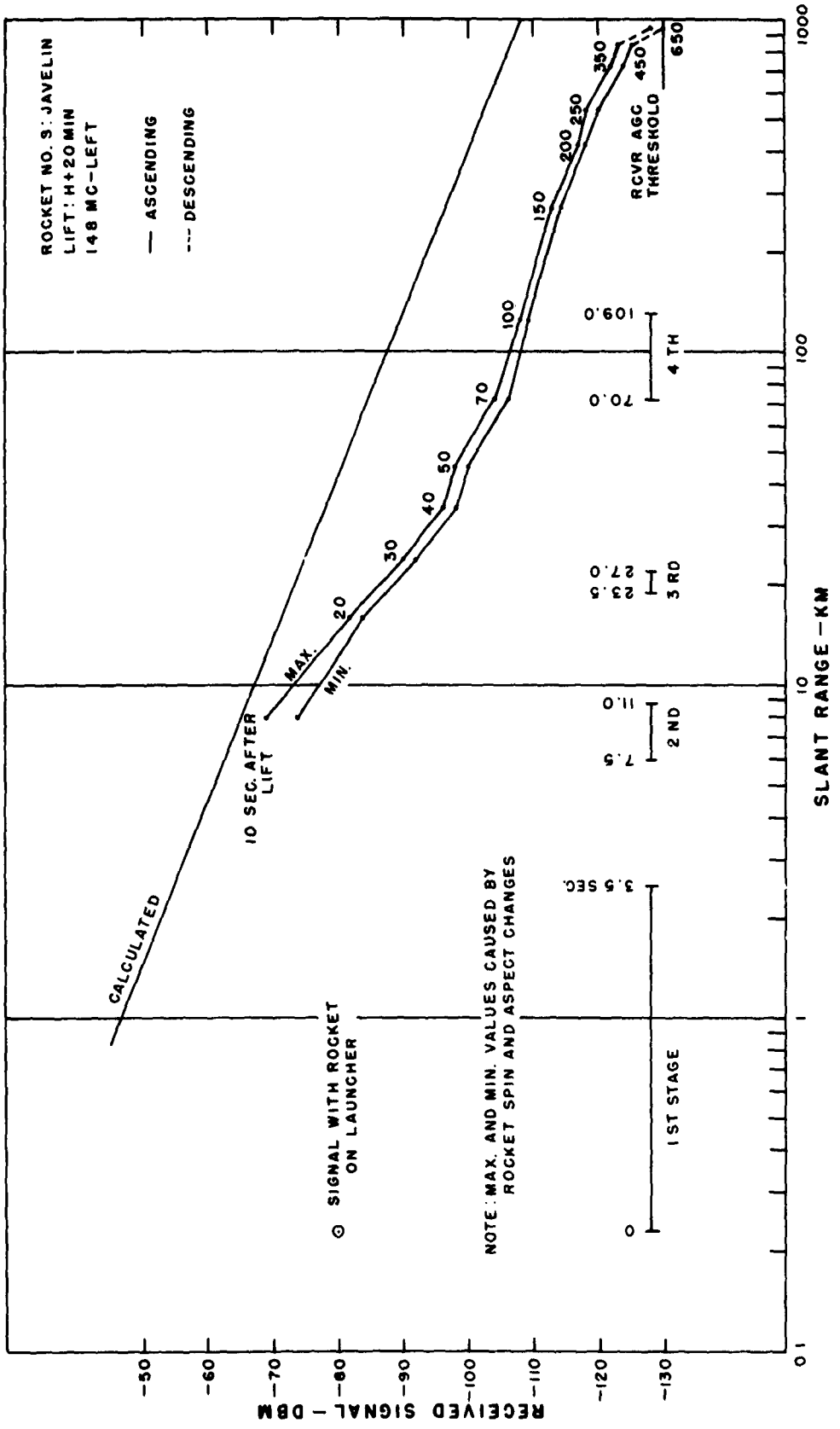

Figure C.122 Received signal strength versus slant range for 3-frequency beacon, 148 Mc left, Rocket 8, Star Fish.

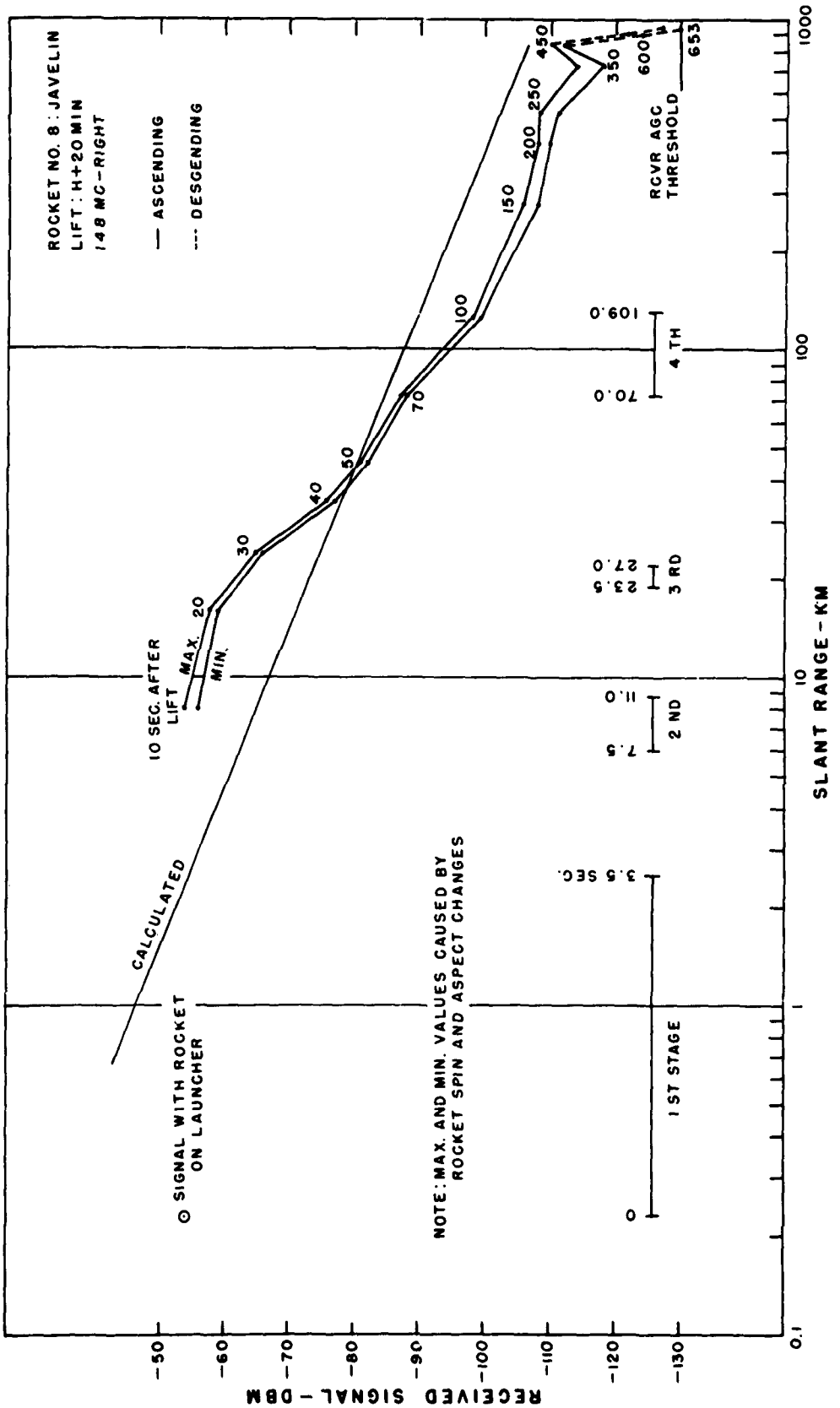

Figure C.123 Received signal strength versus slant range for 3-frequency beacon, 148 Mc right, Rocket 8, Star Fish.

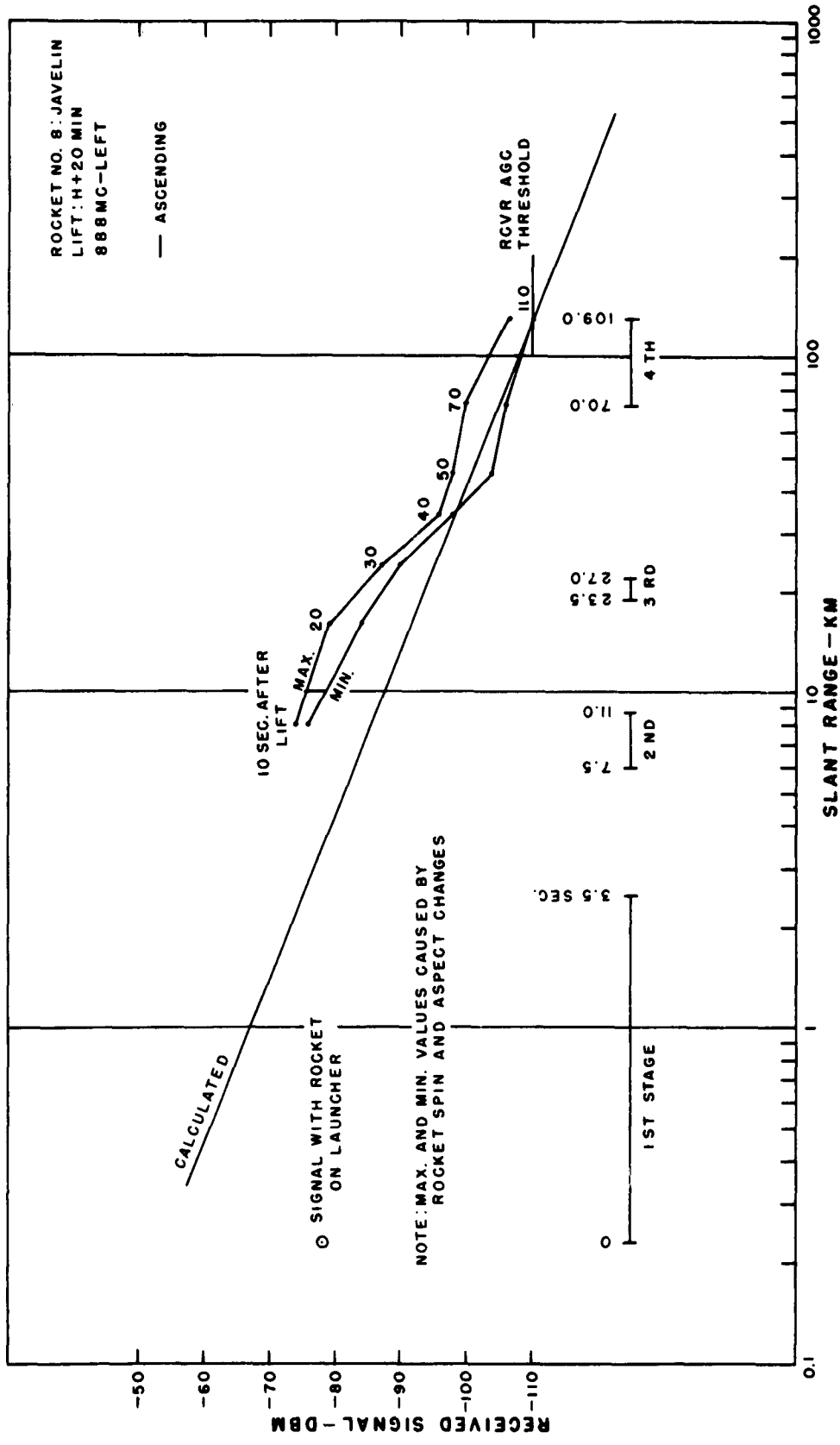

Figure C.124 Received signal strength versus slant range for 3-frequency beacon, 888 Mc left, Rocket 8,Star Fish.

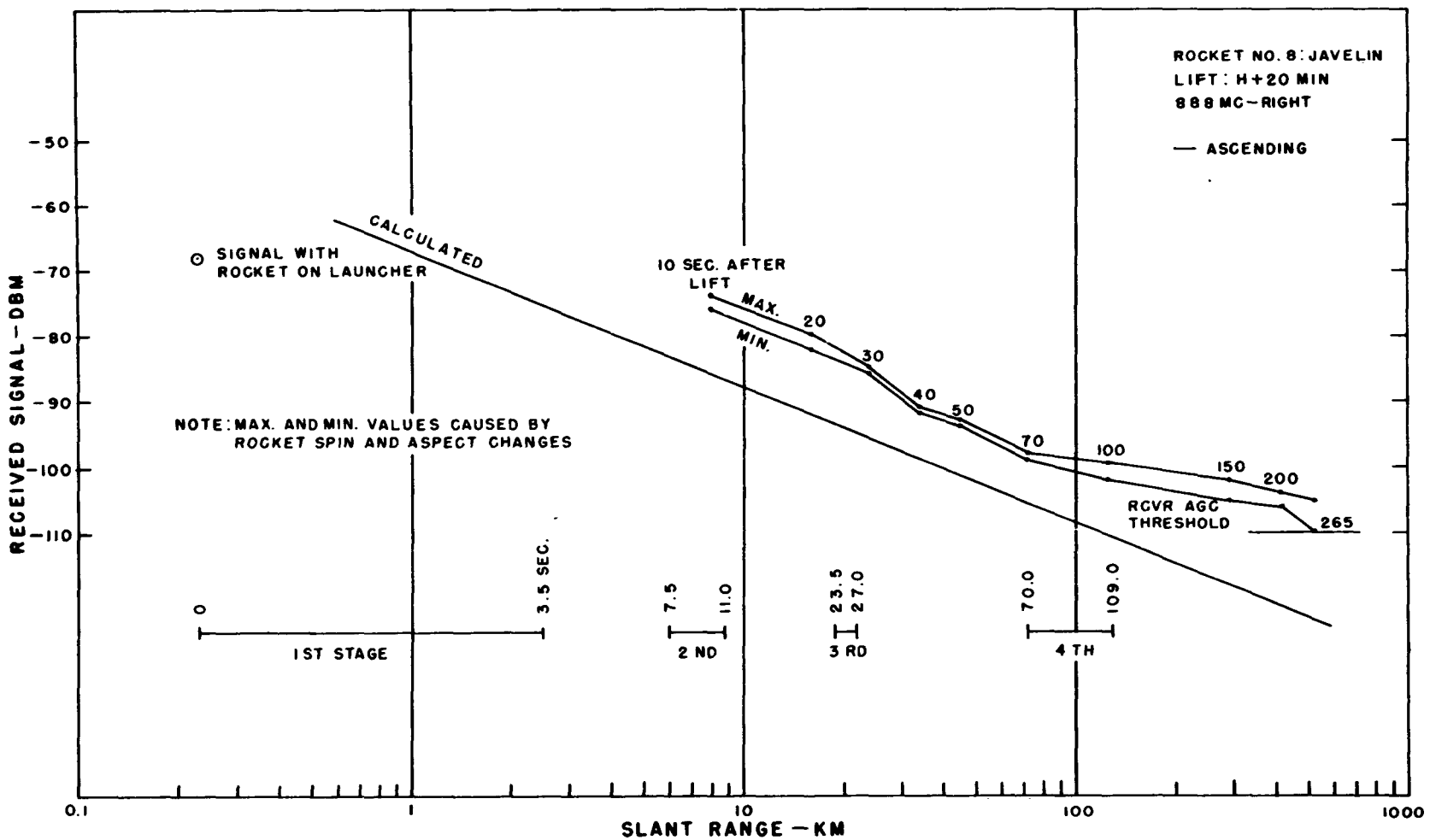

Figure C.125 Received signal strength versus slant range for 3-frequency beacon, 888 Mc right, Rocket 8, Star Fish.

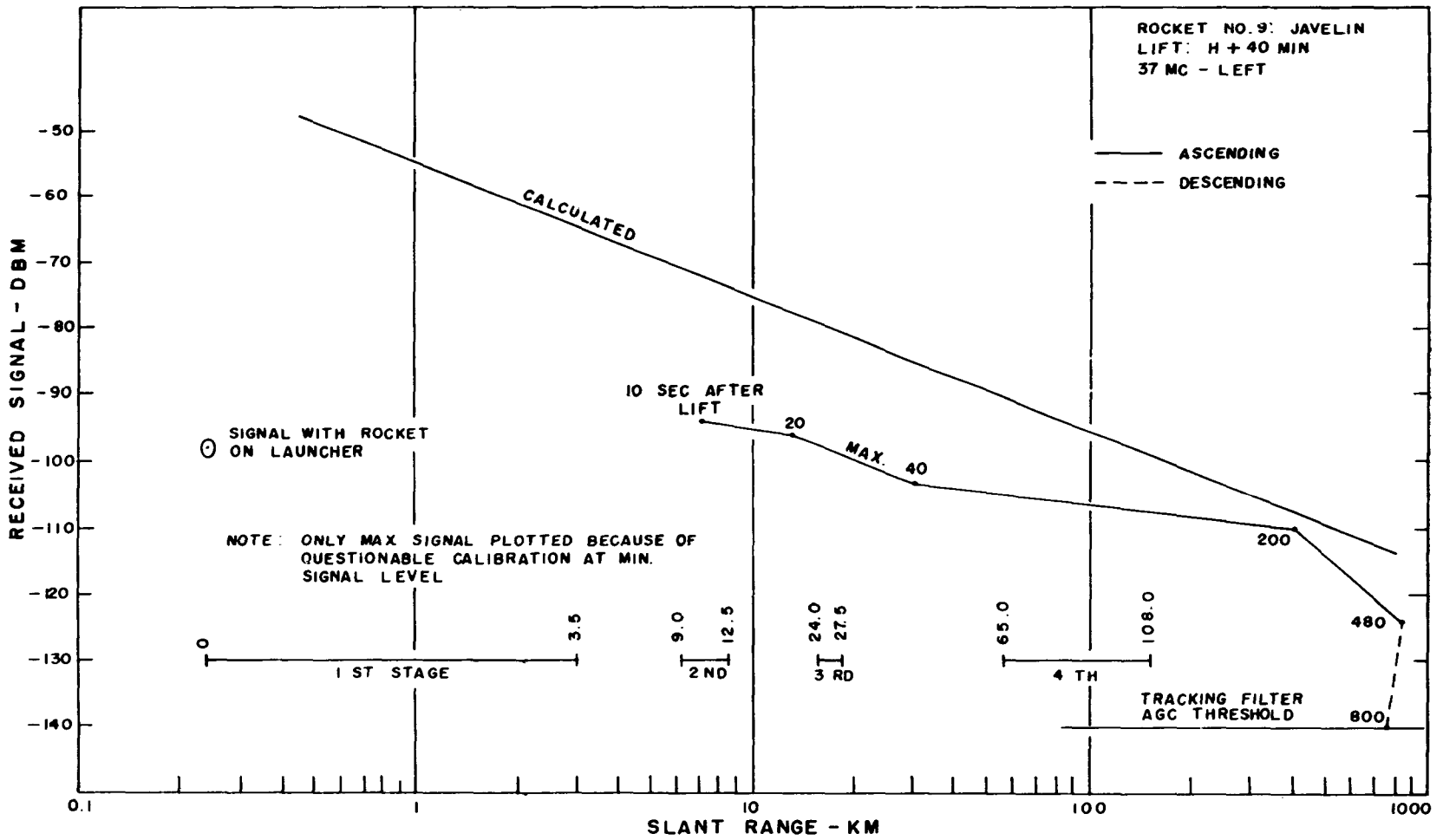

Figure C.126 Received signal strength versus slant range for 3-frequency beacon, 37 Mc left, Rocket 9, Star Fish.

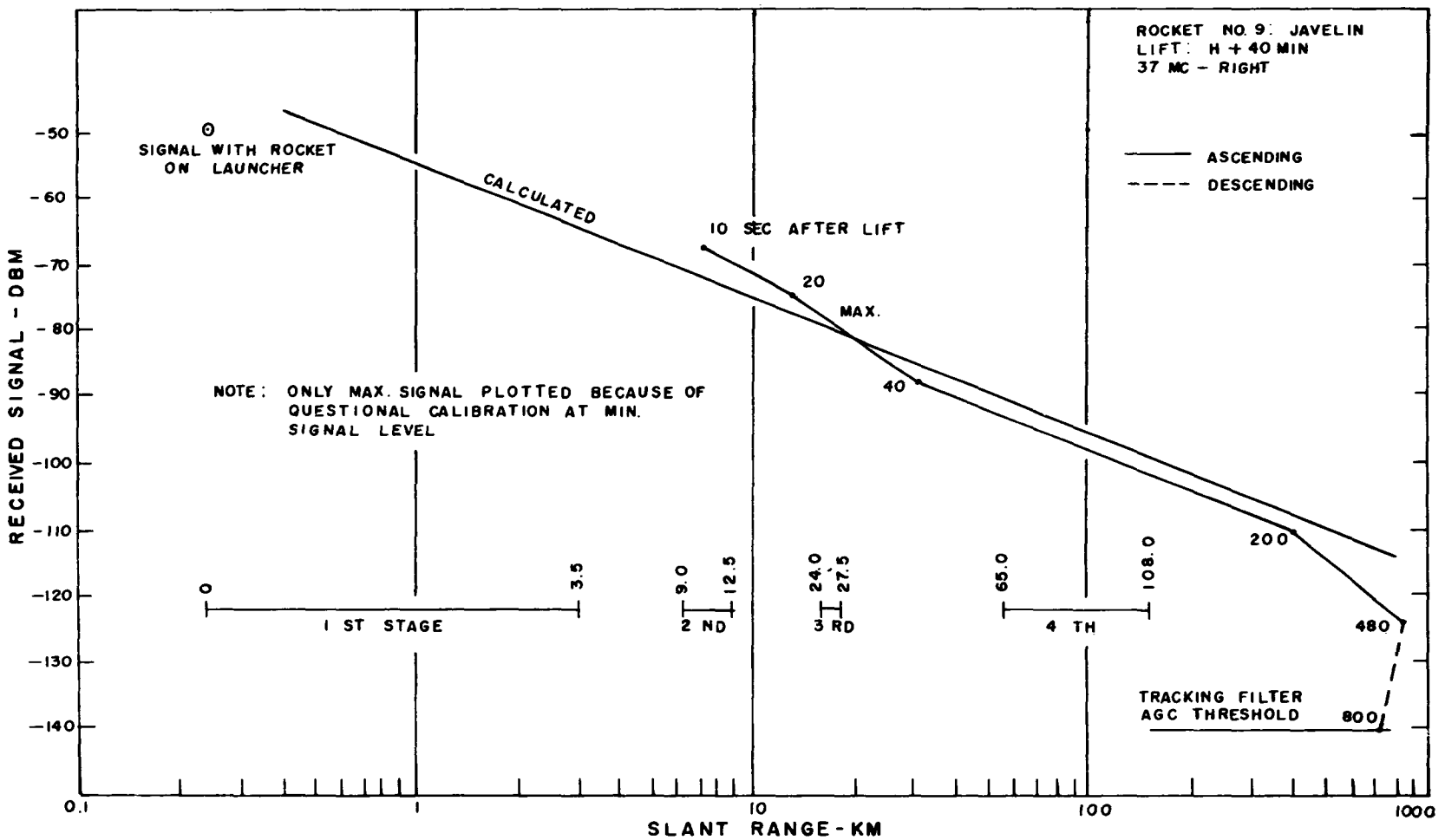

Figure C.127 Received signal strength versus slant range for 3-frequency beacon, 37 Mc right, Rocket 9, Star Fish.

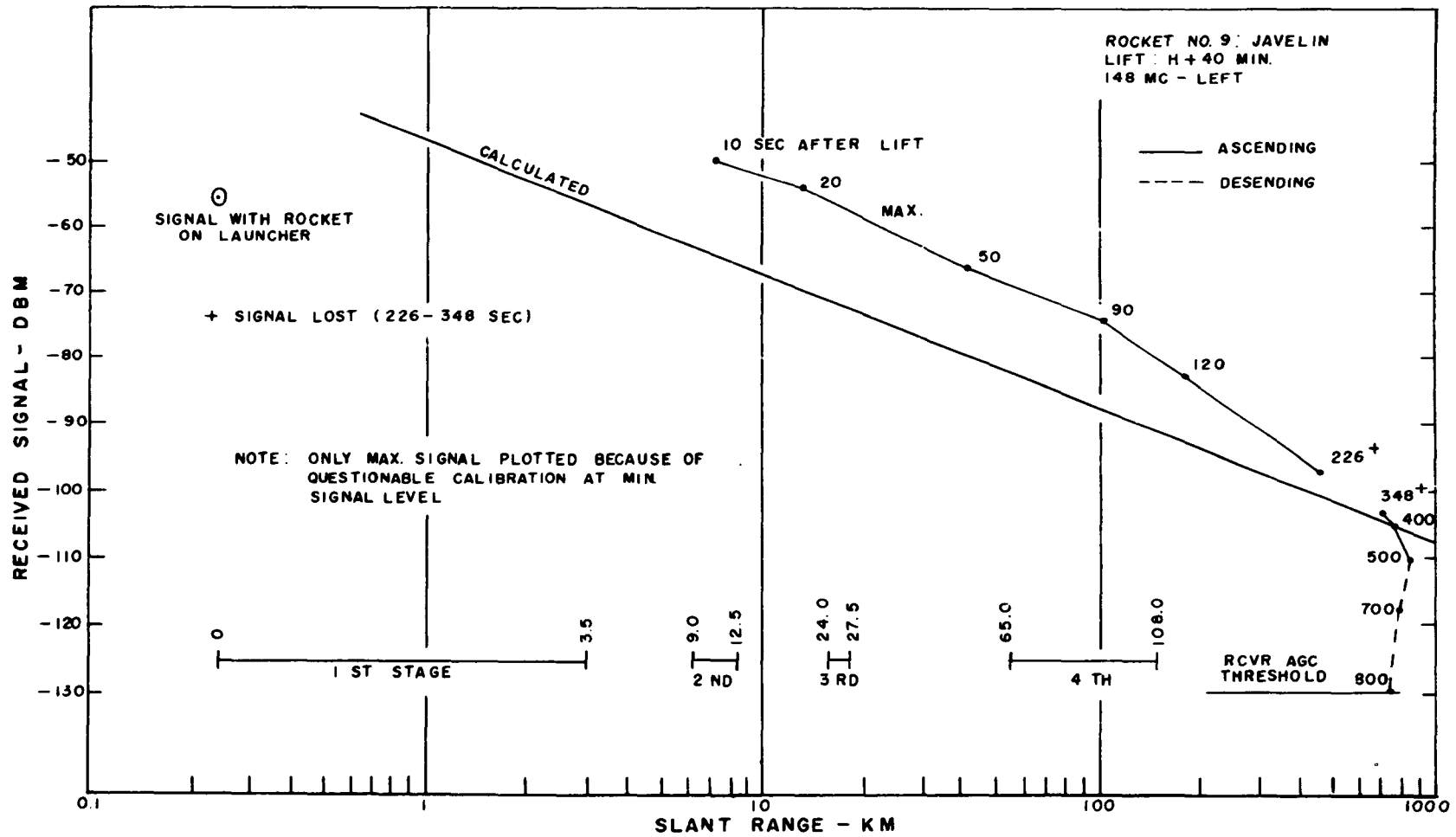

Figure C.128 Received signal strength versus slant range for 3-frequency beacon, 148 Mc left, Rocket 9, Star Fish.

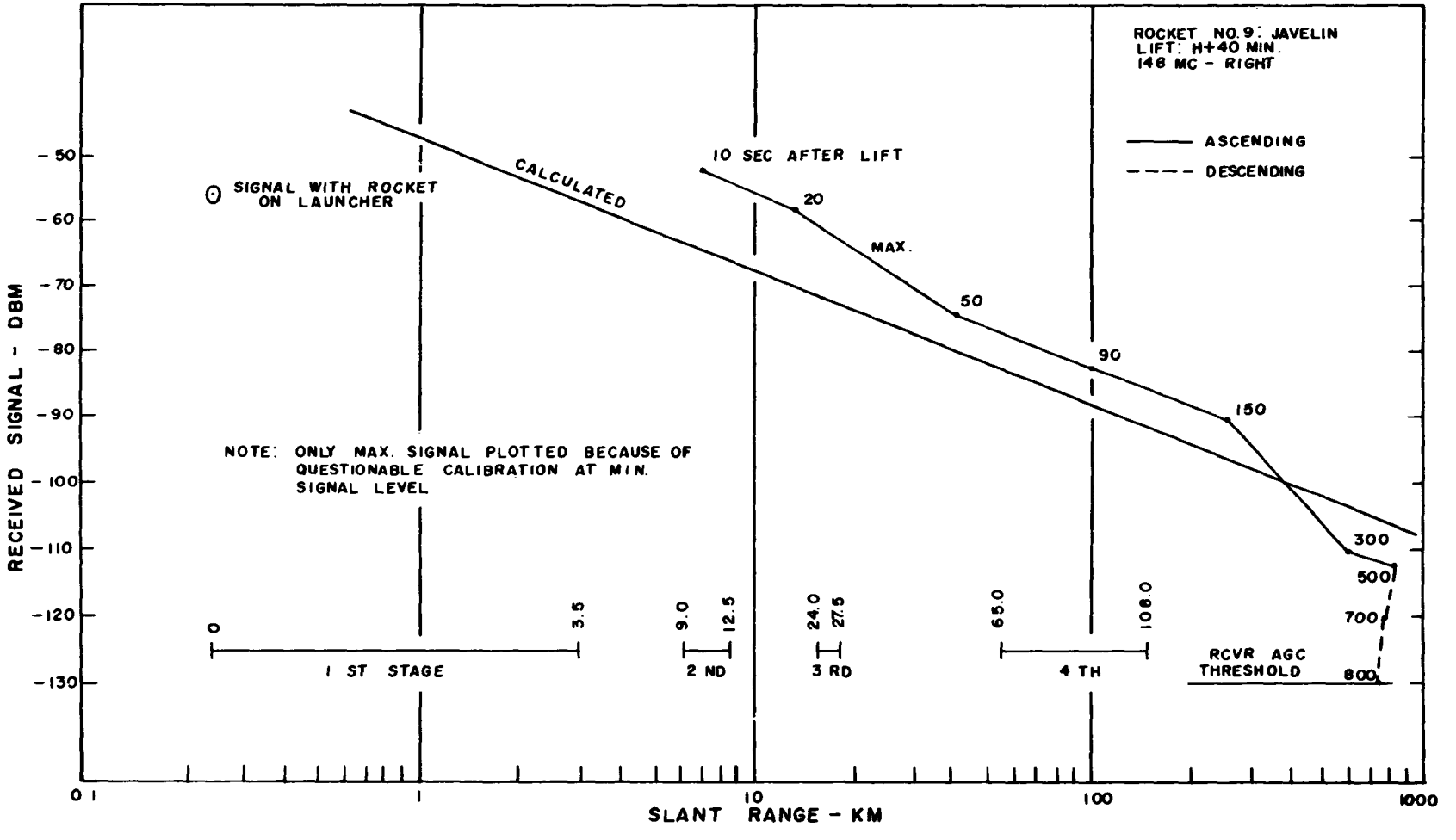

Figure C.129 Received signal strength versus slant range for 3-frequency beacon, 148 Mc right, Rocket 9, Star Fish.

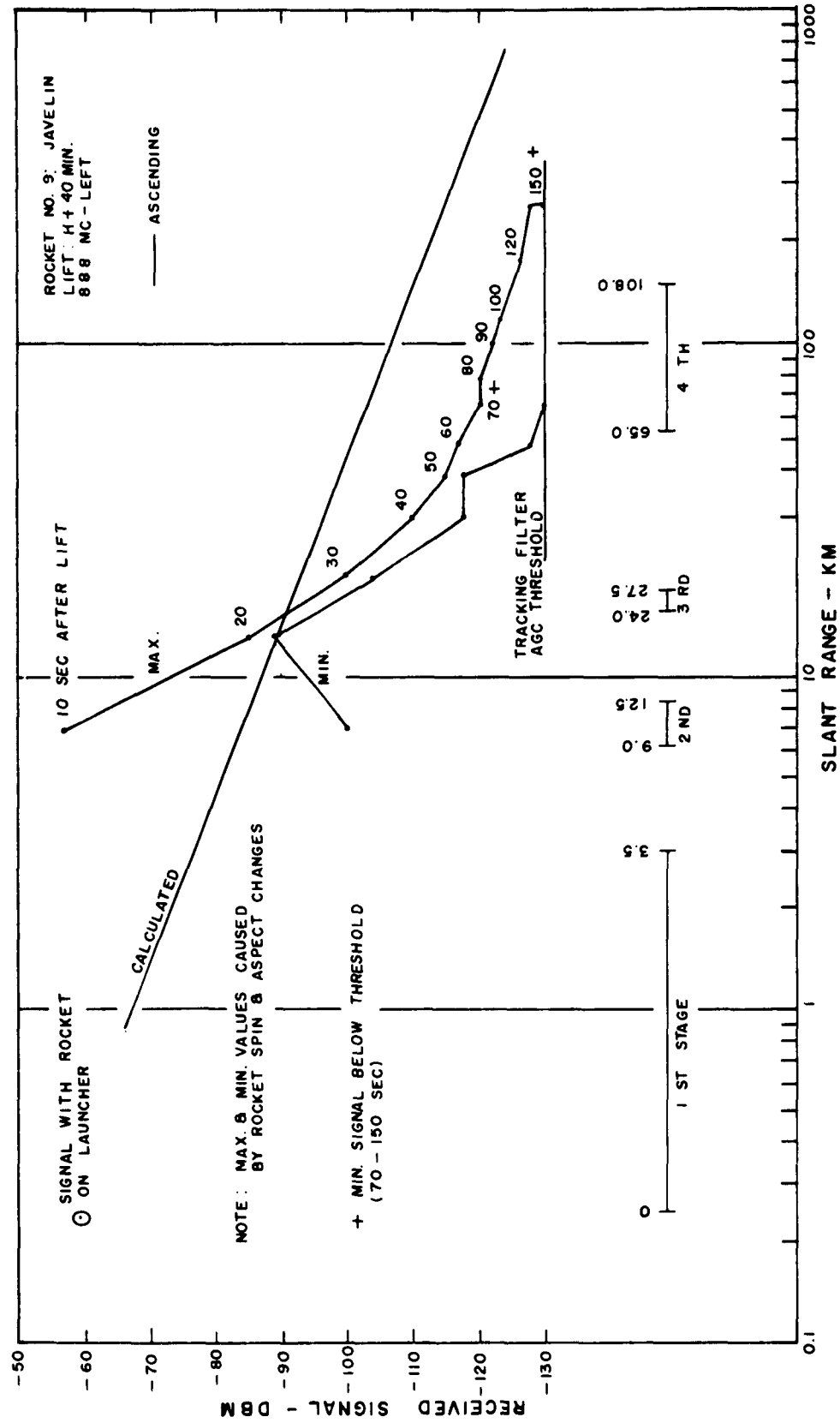

Figure C.130 Received signal strength versus slant range for 3-frequency beacon, 888 Mc left, Rocket 9, Star Fish.

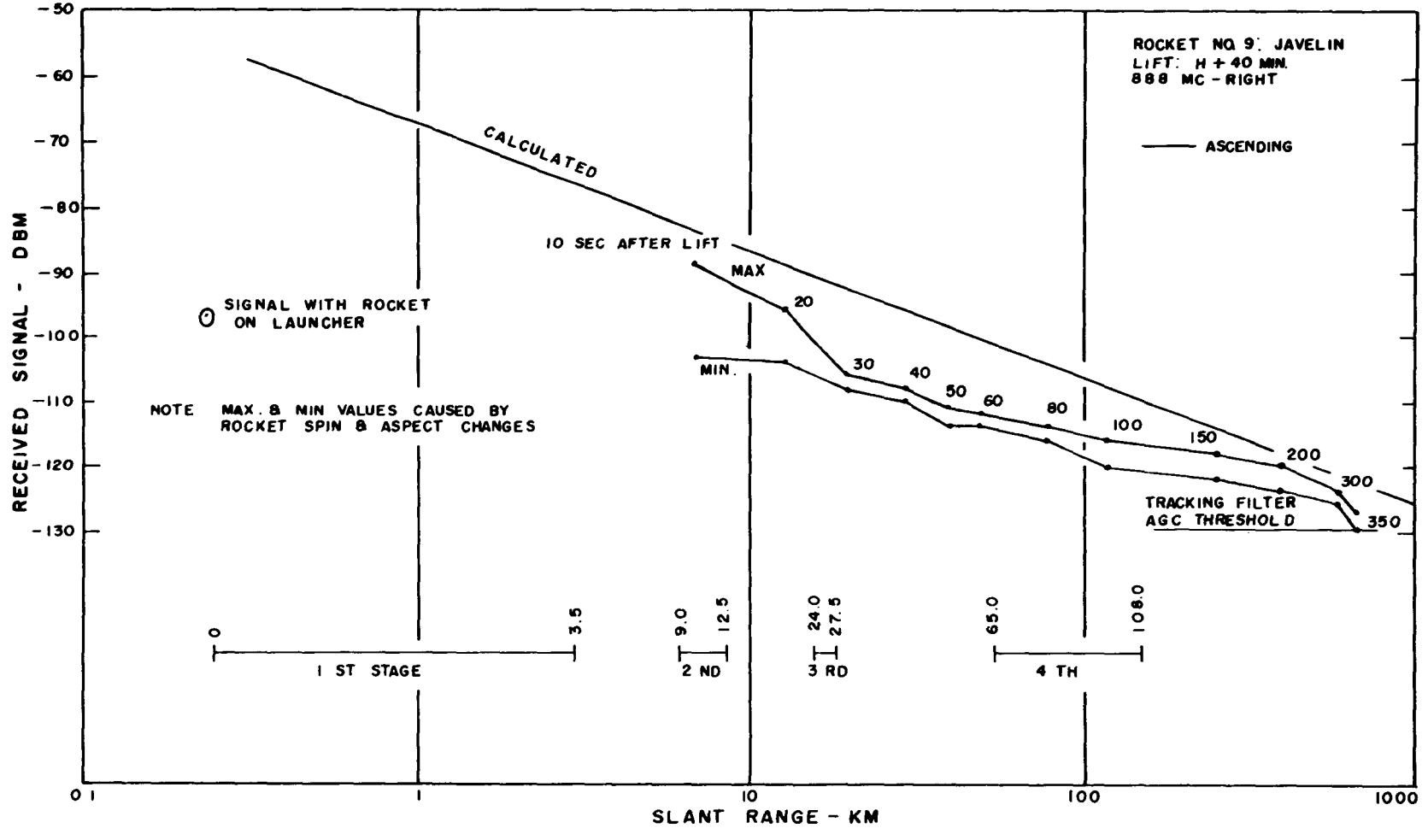

Figure C.131 Received signal strength versus slant range for 3-frequency beacon, 888 Mc right, Rocket 9, Star Fish.

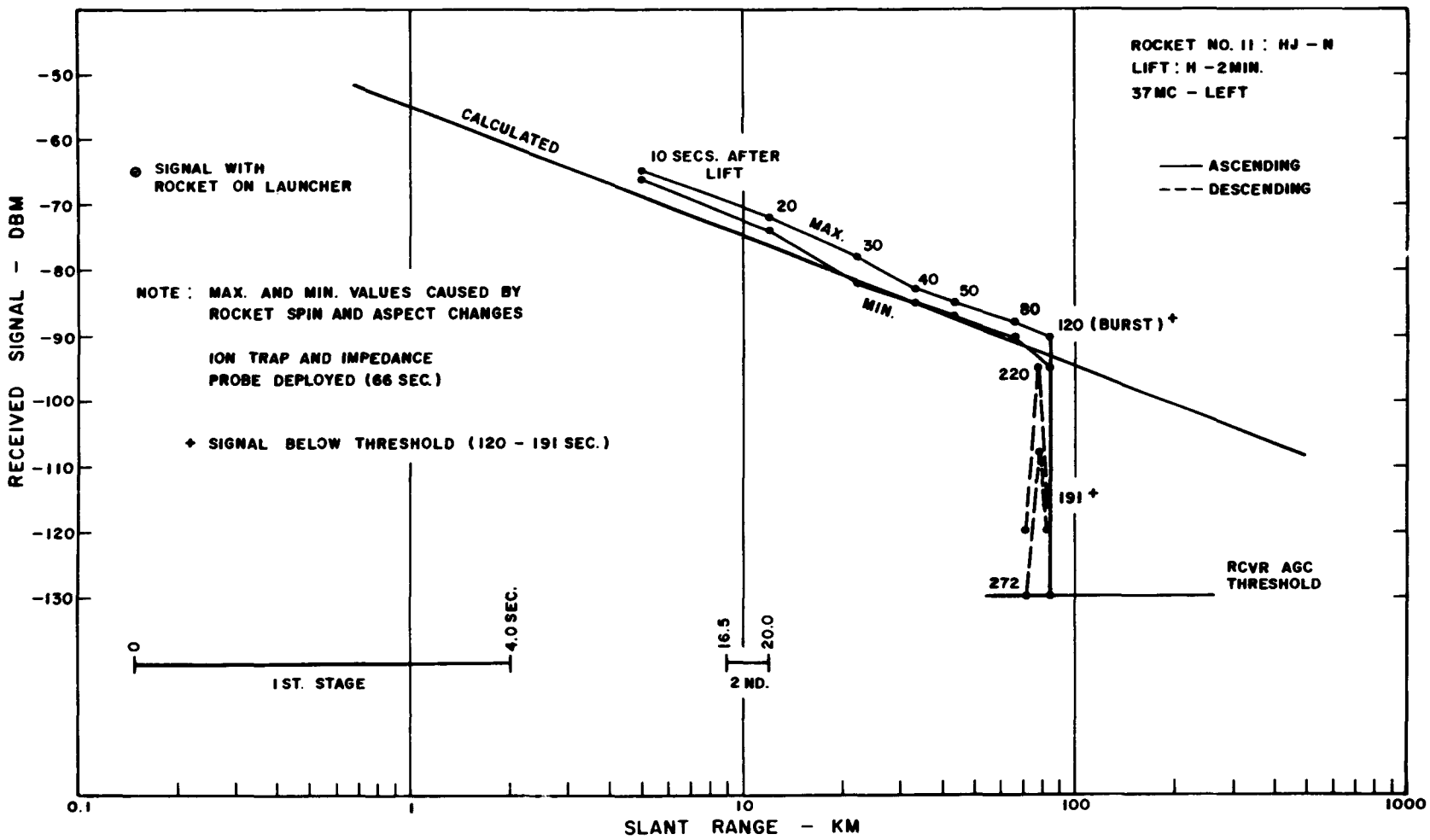

Figure C.132 Received signal strength versus slant range for 3-frequency beacon, 37 Mc left, Rocket 11, Blue Gill.

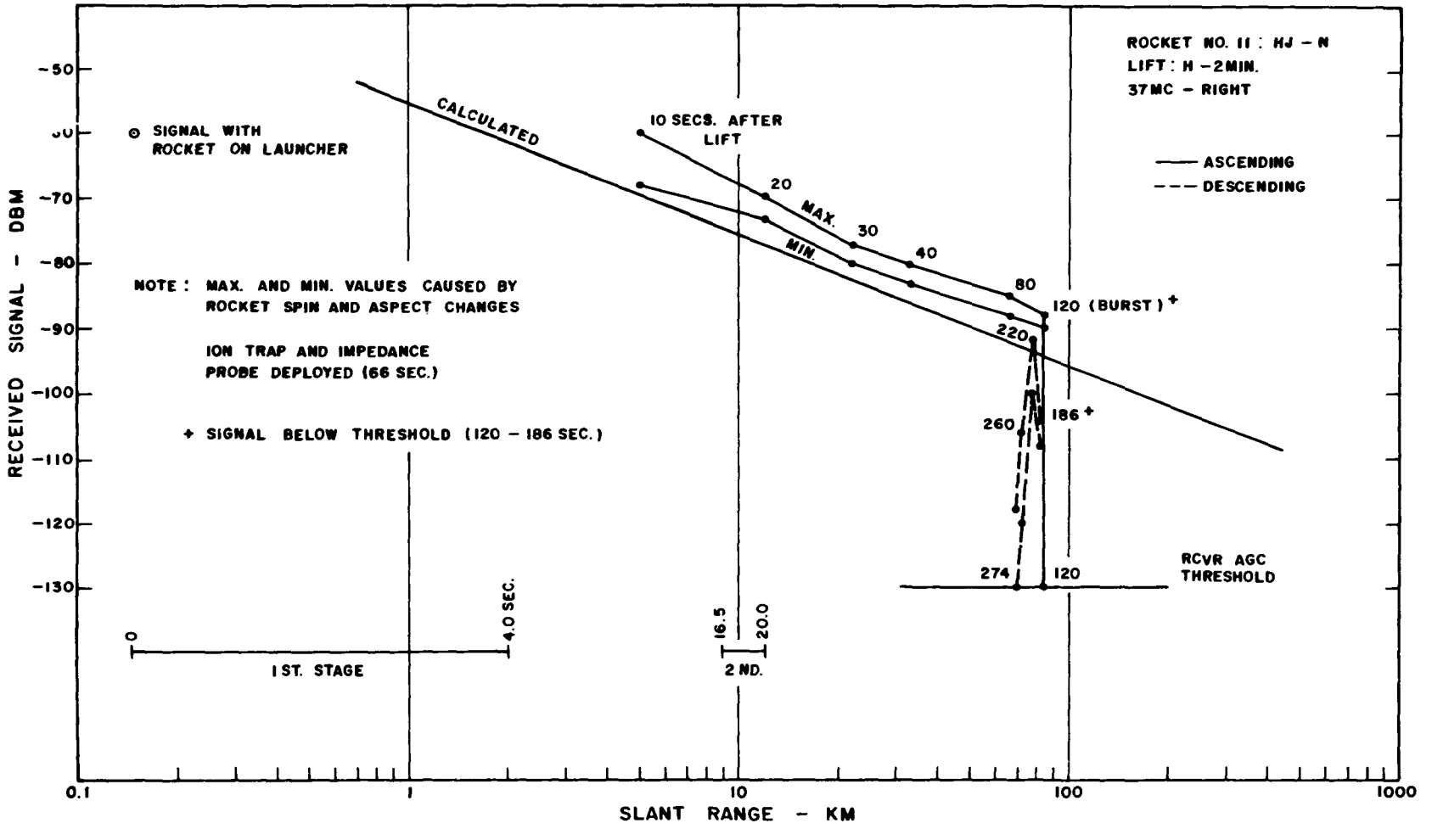

Figure C.133 Received signal strength versus slant range for 3-frequency beacon, 37 Mc right, Rocket 11, Blue Gill.

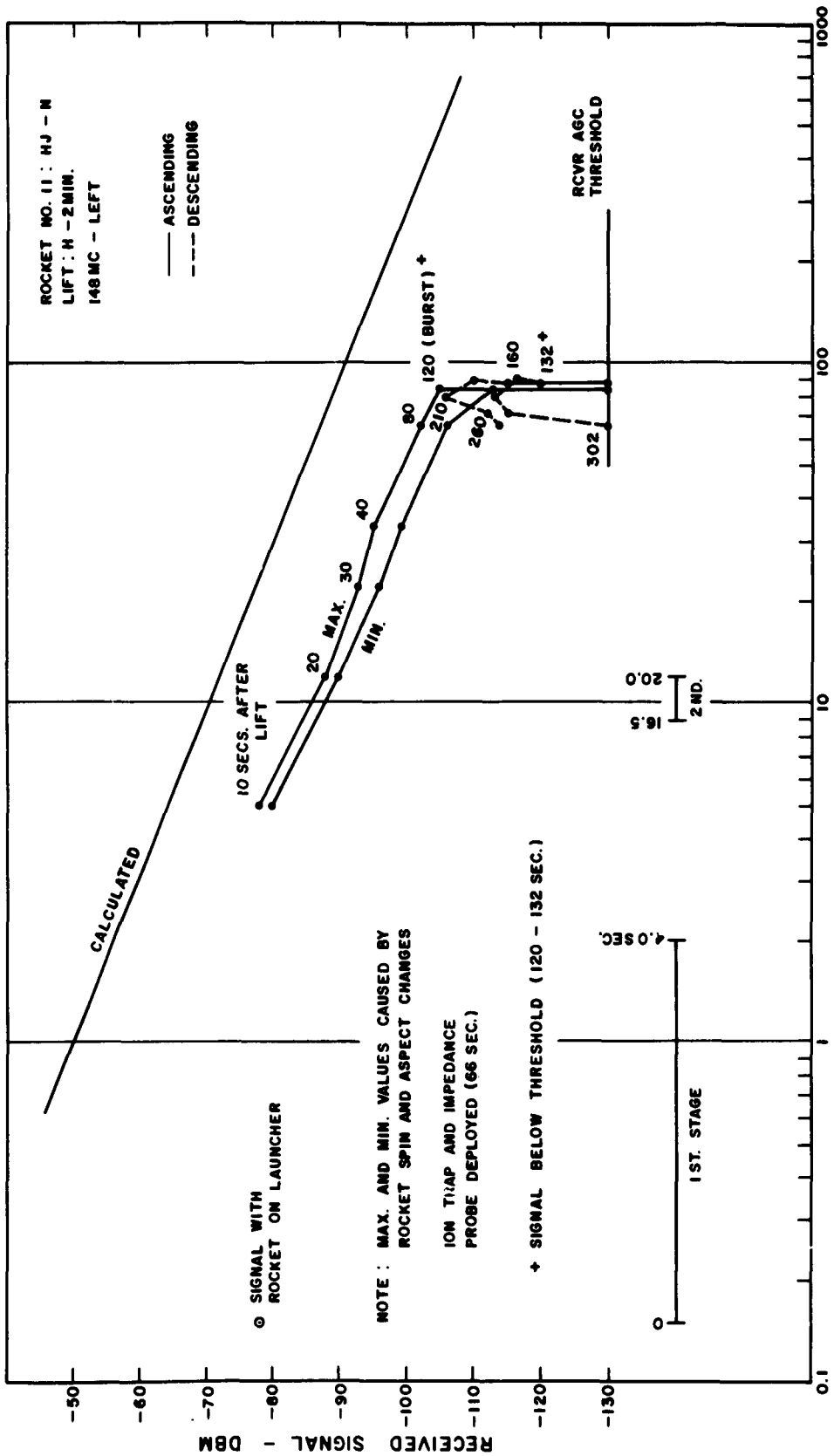

Figure C.134 Received signal strength versus slant range for 3-frequency beacon, 148 Mc left, Rocket 11, Blue Gill.

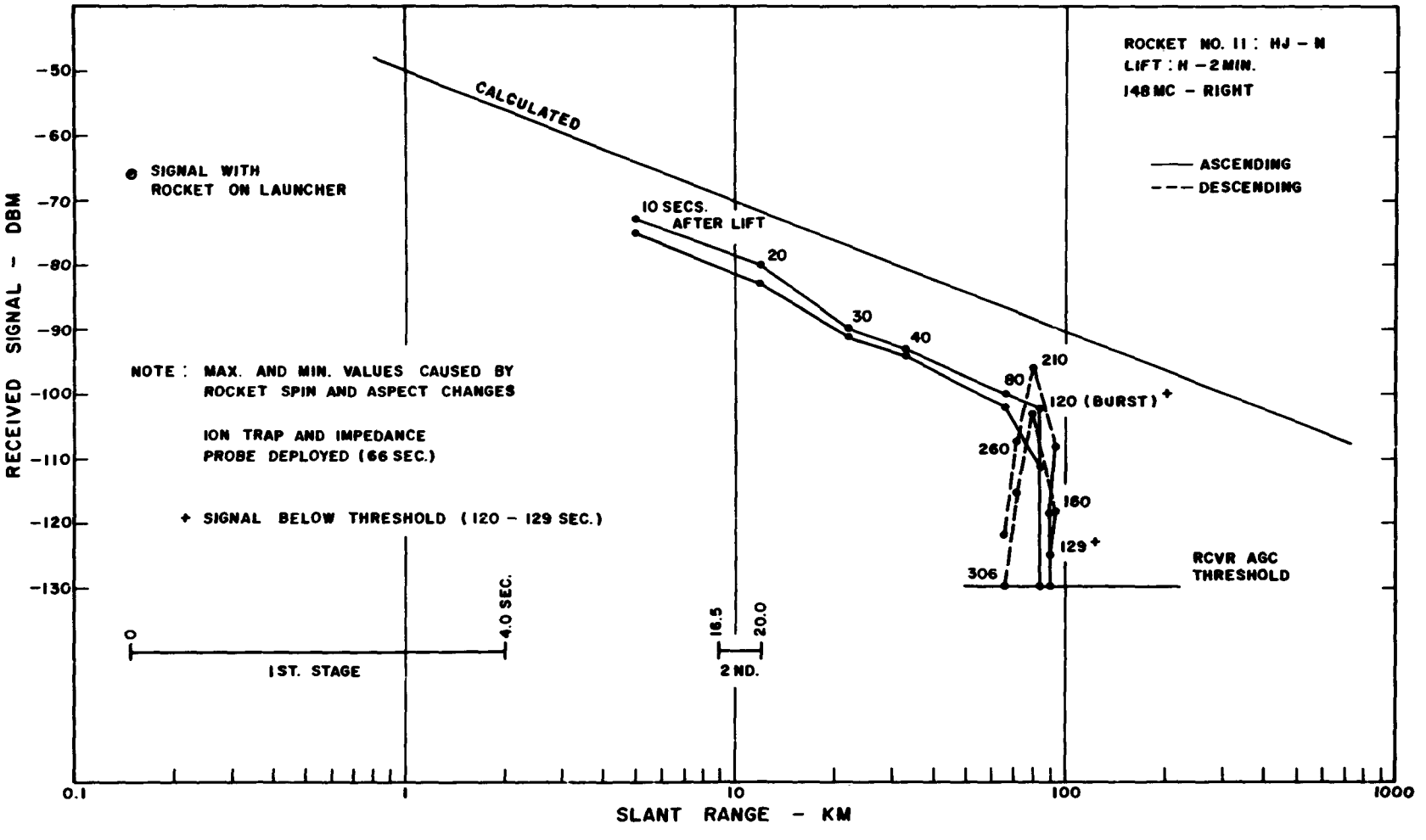

Figure C.135 Received signal strength versus slant range for 3-frequency beacon, 148 Mc right, Rocket 11, Blue Gill.

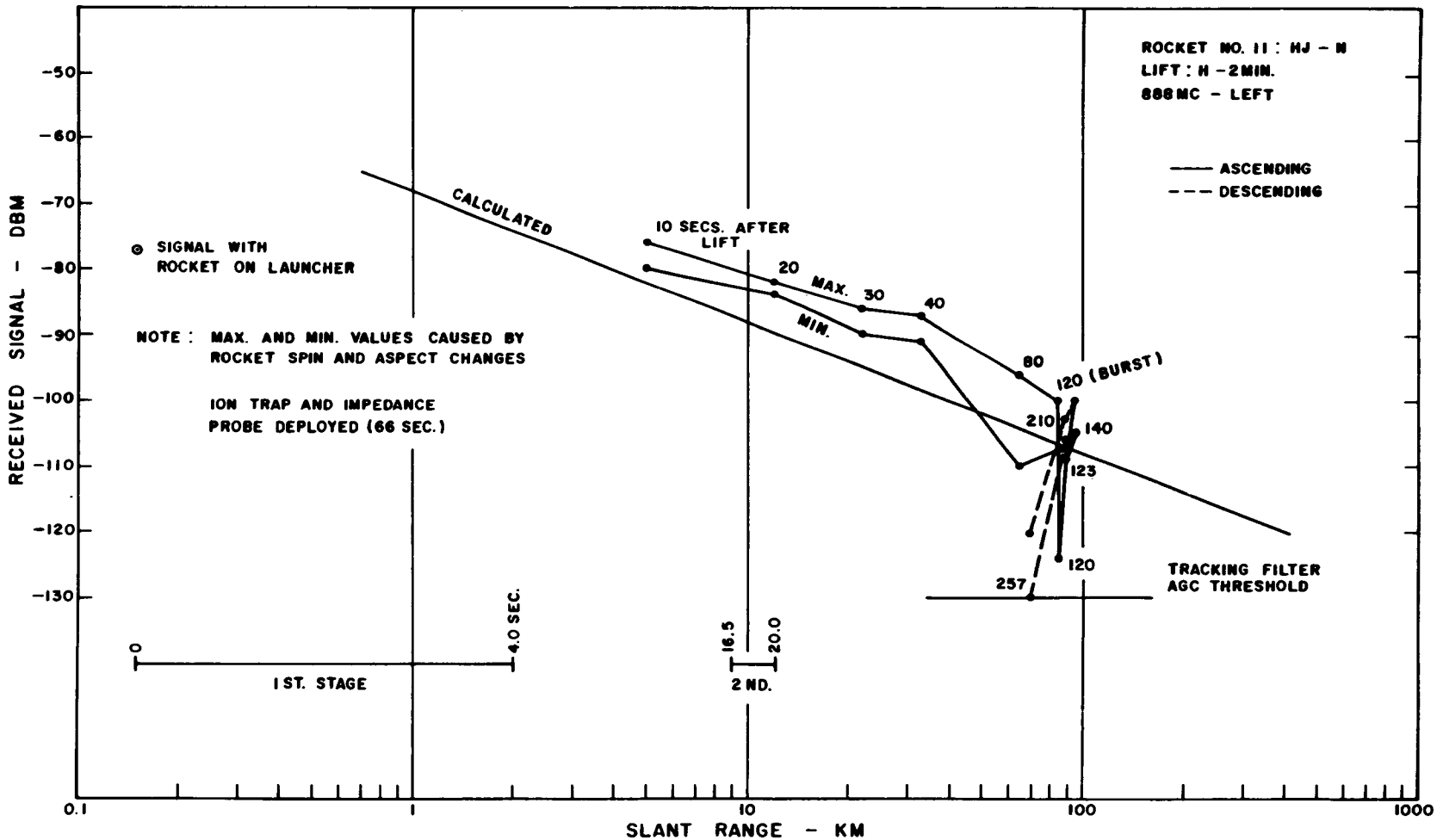

Figure C.136 Received signal strength versus slant range for 3-frequency beacon, 888 Mc left, Rocket 11, Blue Gill.

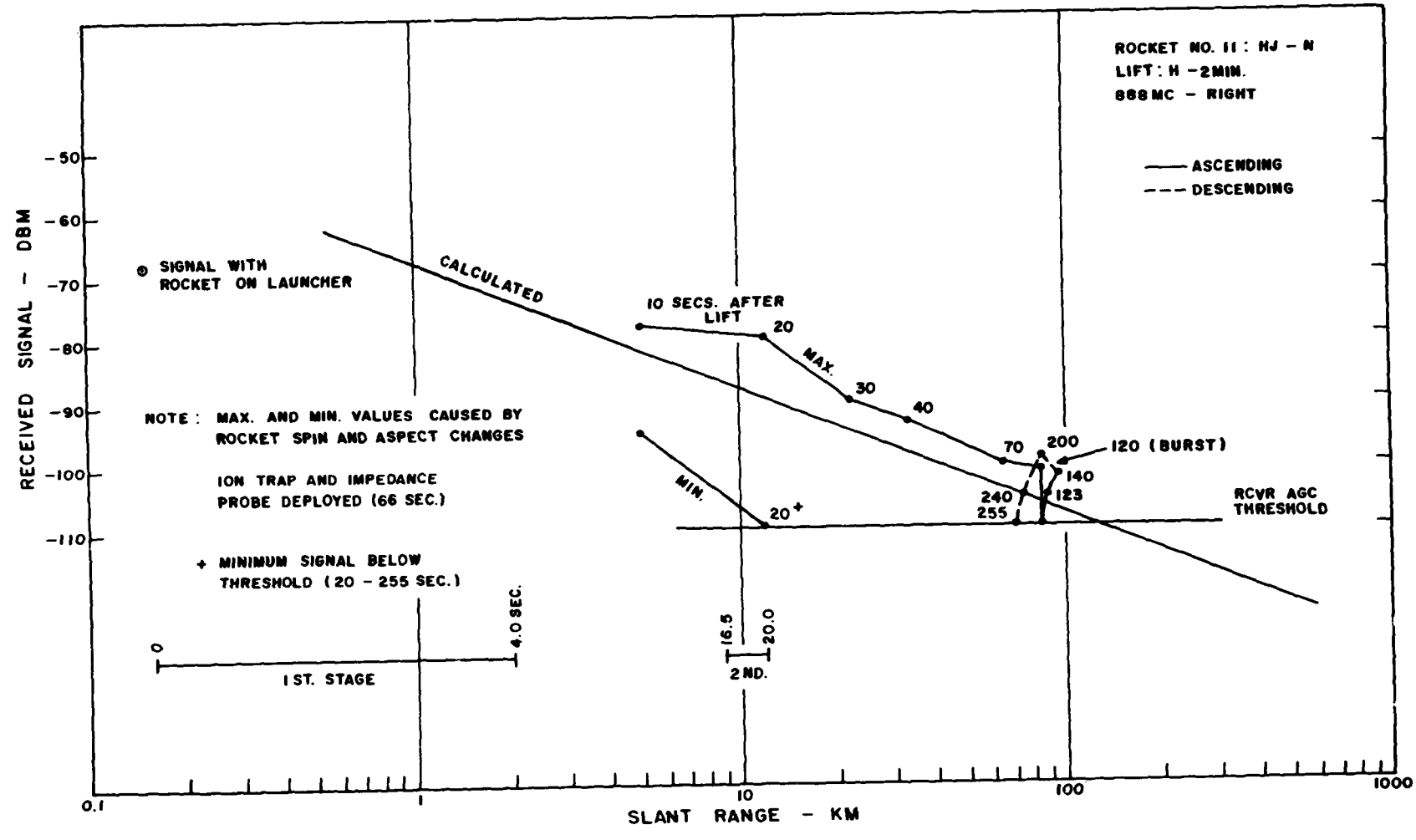

Figure C.137 Received signal strength versus slant range for 3-frequency beacon, 888 Mc right, Rocket 11, Blue Gill.

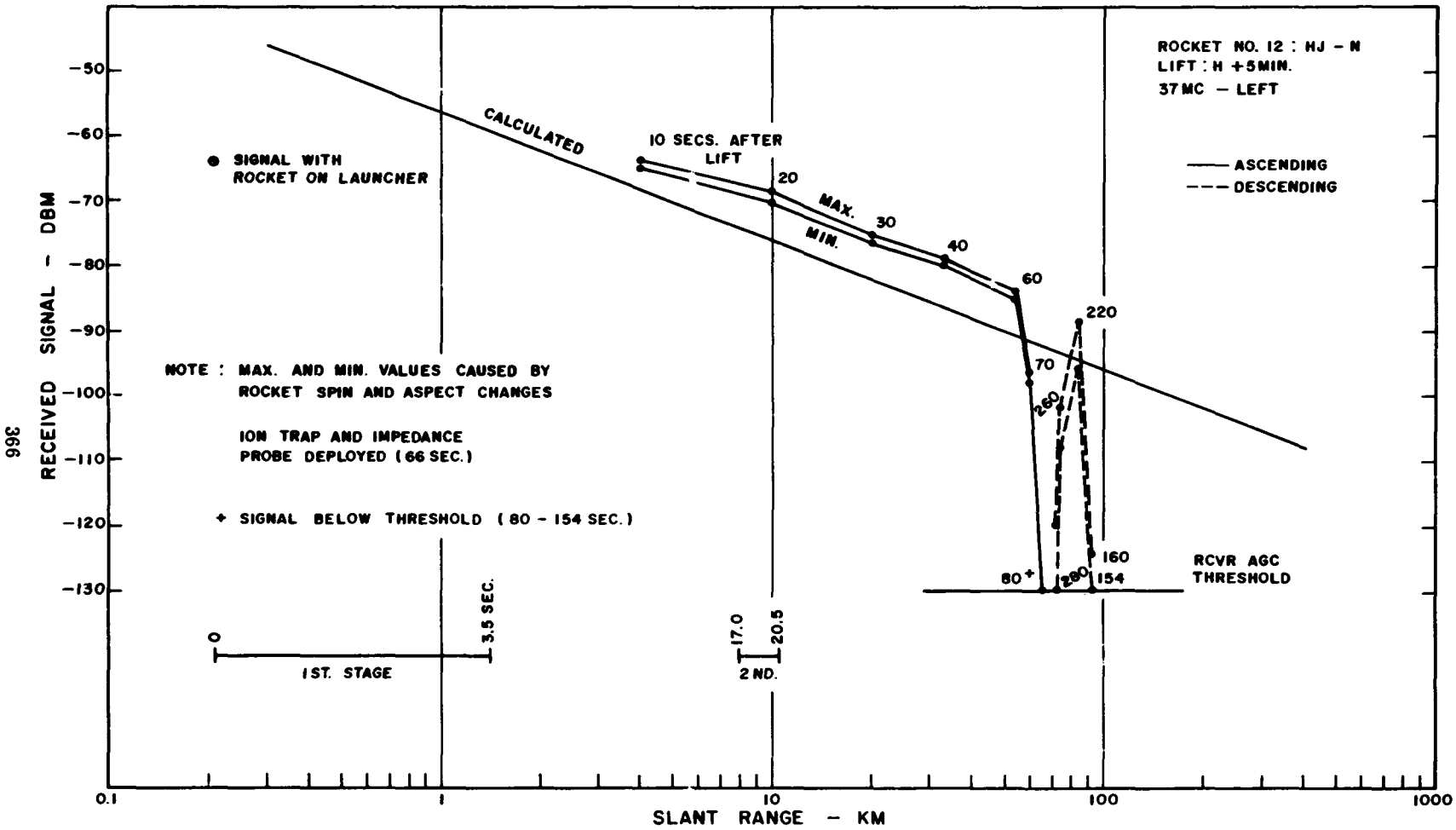

Figure C.138 Received signal strength versus slant range for 3-frequency beacon, 37 Mc left, Rocket 12, Blue Gill.

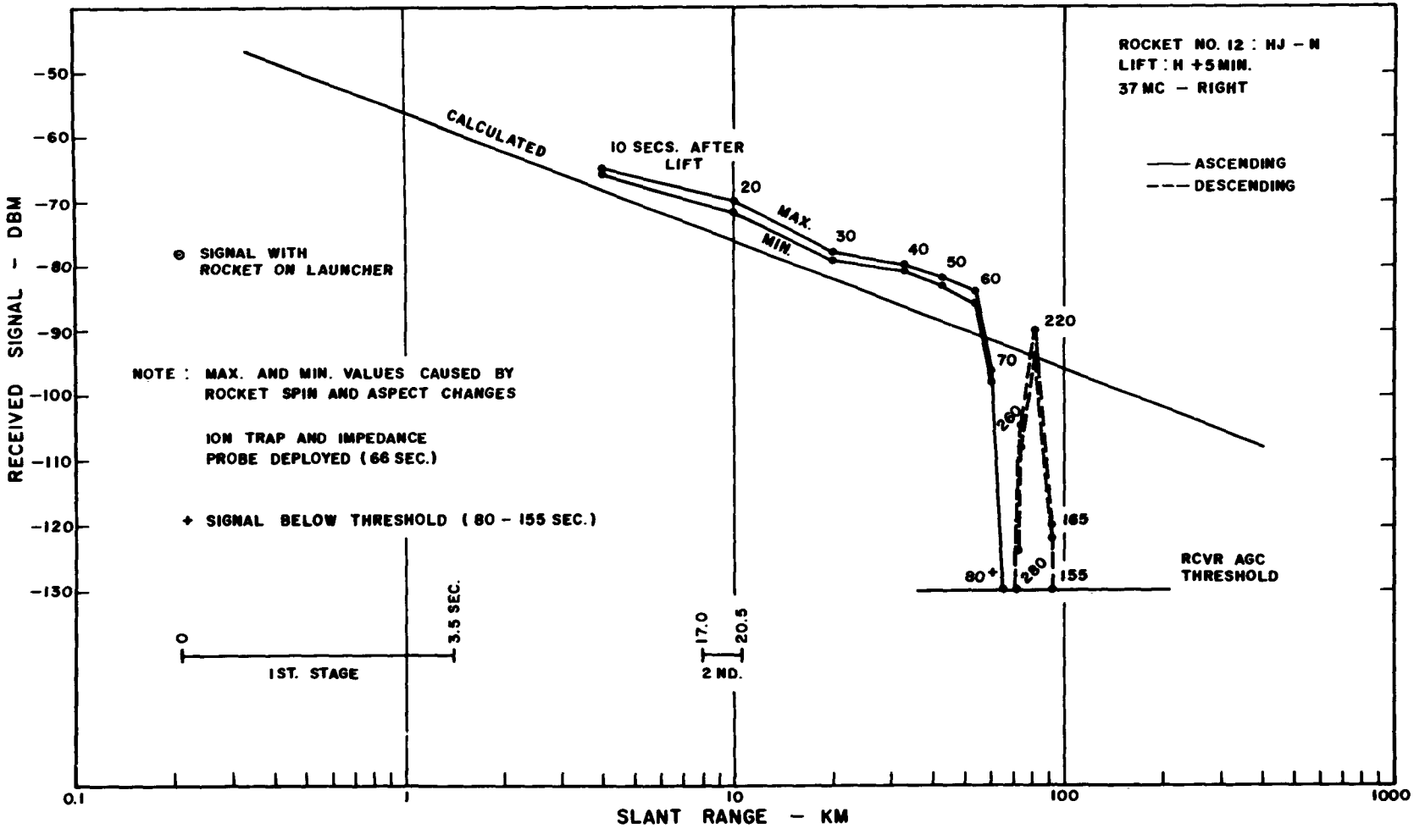

Figure C.139 Received signal strength versus slant range for 3-frequency beacon, 37 Mc right, Rocket 12, Blue Gill.

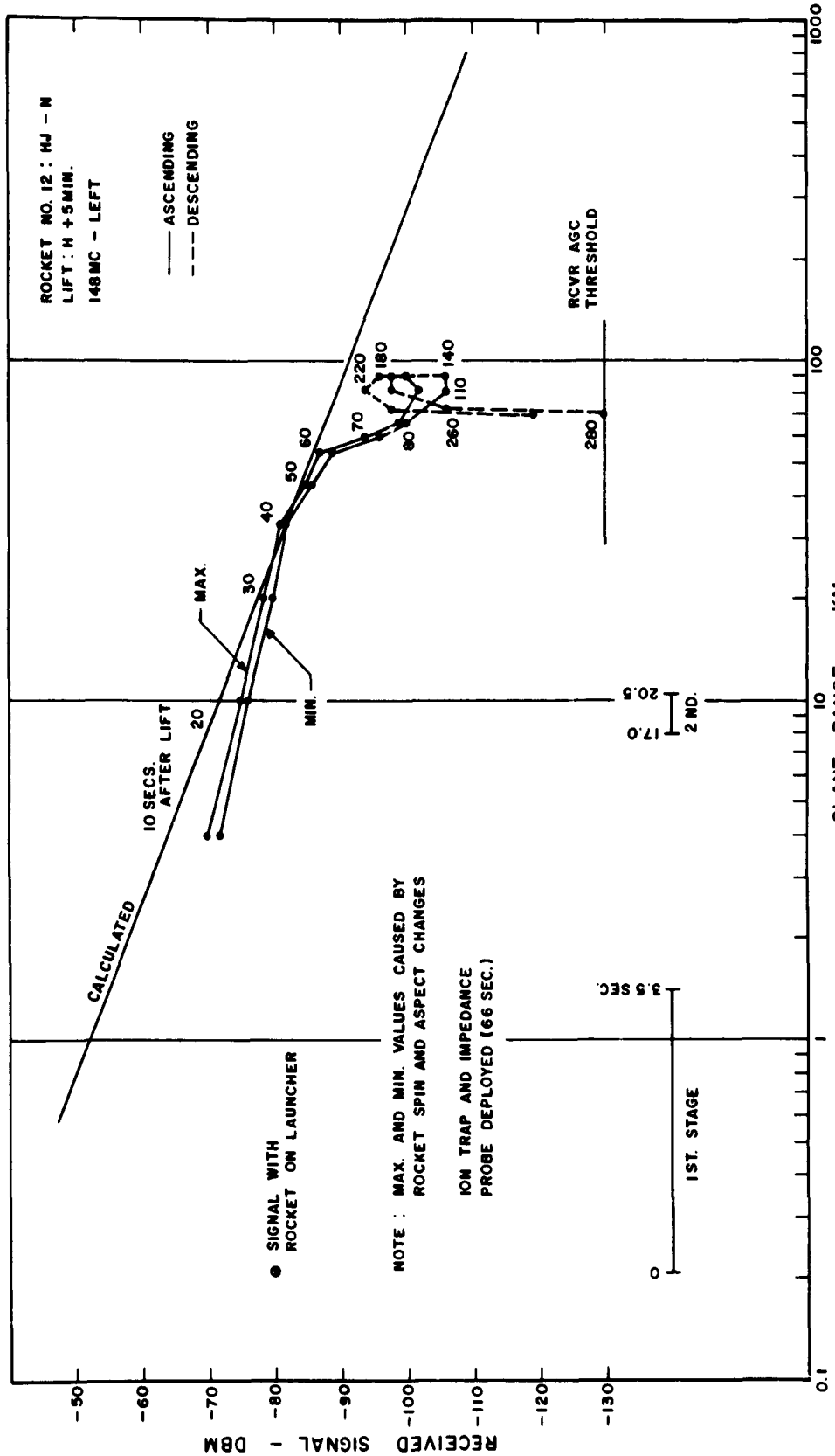

Figure C.140 Received signal strength versus slant range for 3-frequency beacon, 148 Mc left, Rocket 12, Blue Gill.

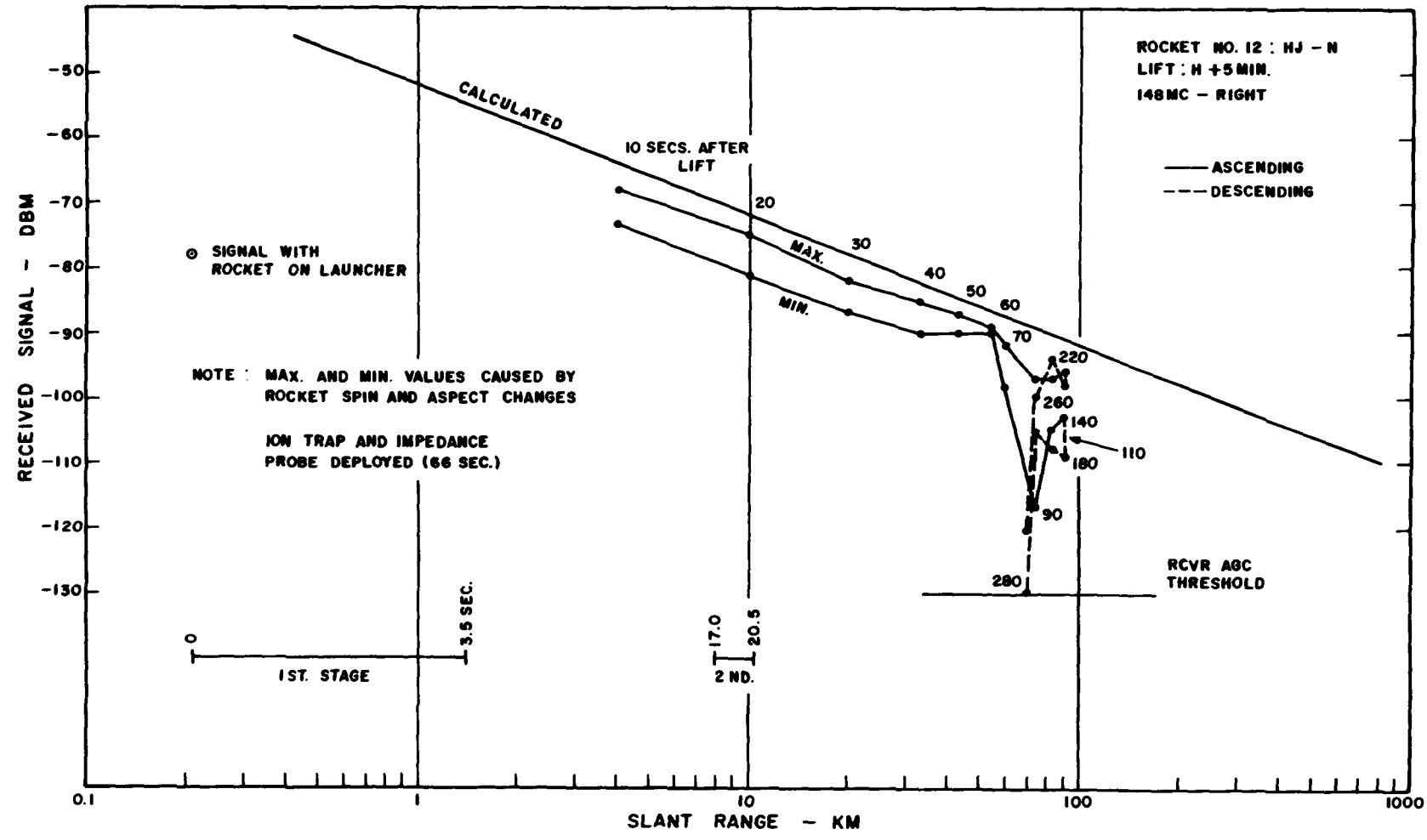

Figure C.141 Received signal strength versus slant range for 3-frequency beacon, 148 Mc right, Rocket 12, Blue Gill.

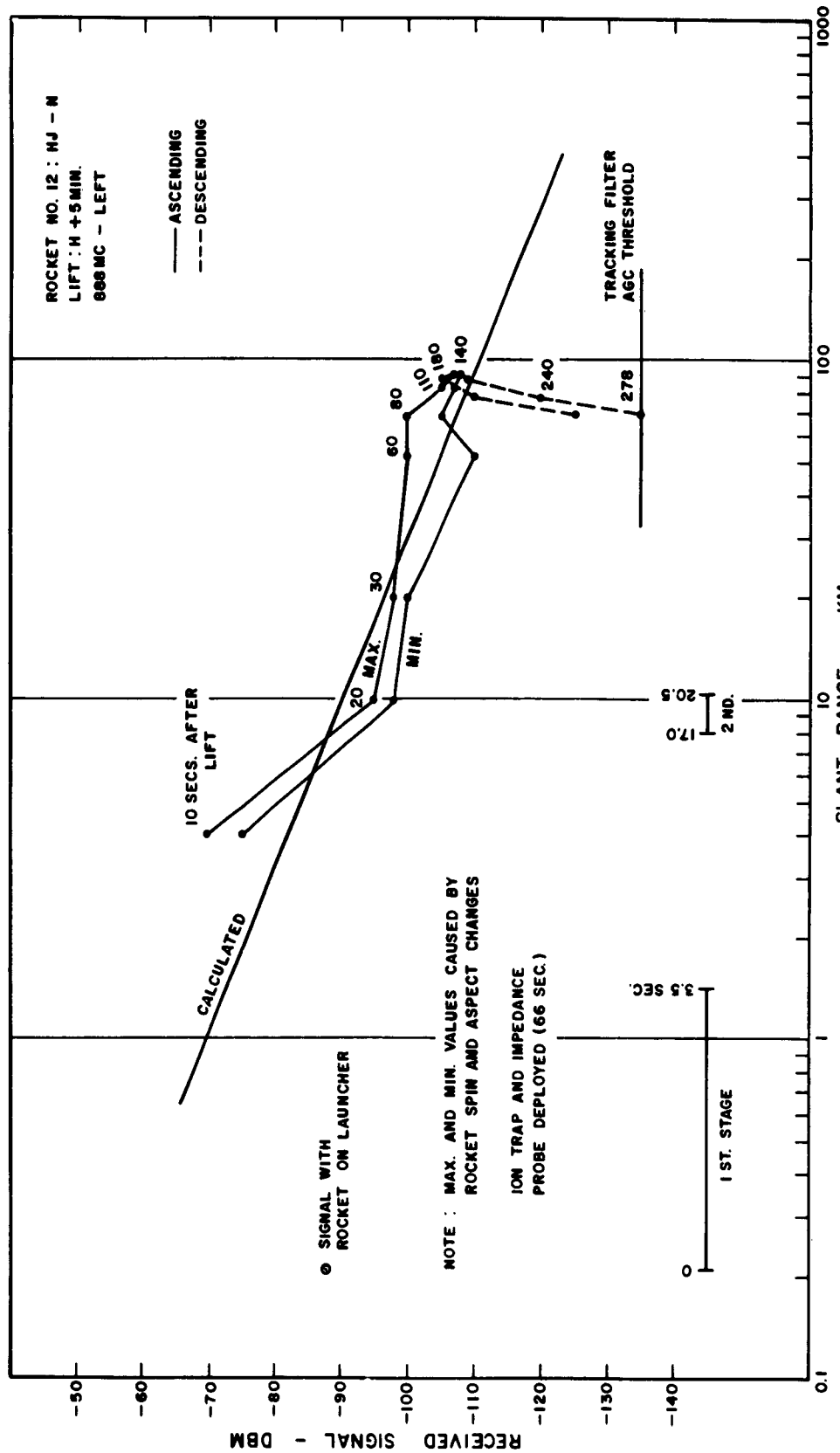

Figure C.142 Received signal strength versus slant range for 3-frequency beacon, 888 Mc left, Rocket 12, Blue Gill.

SECRET

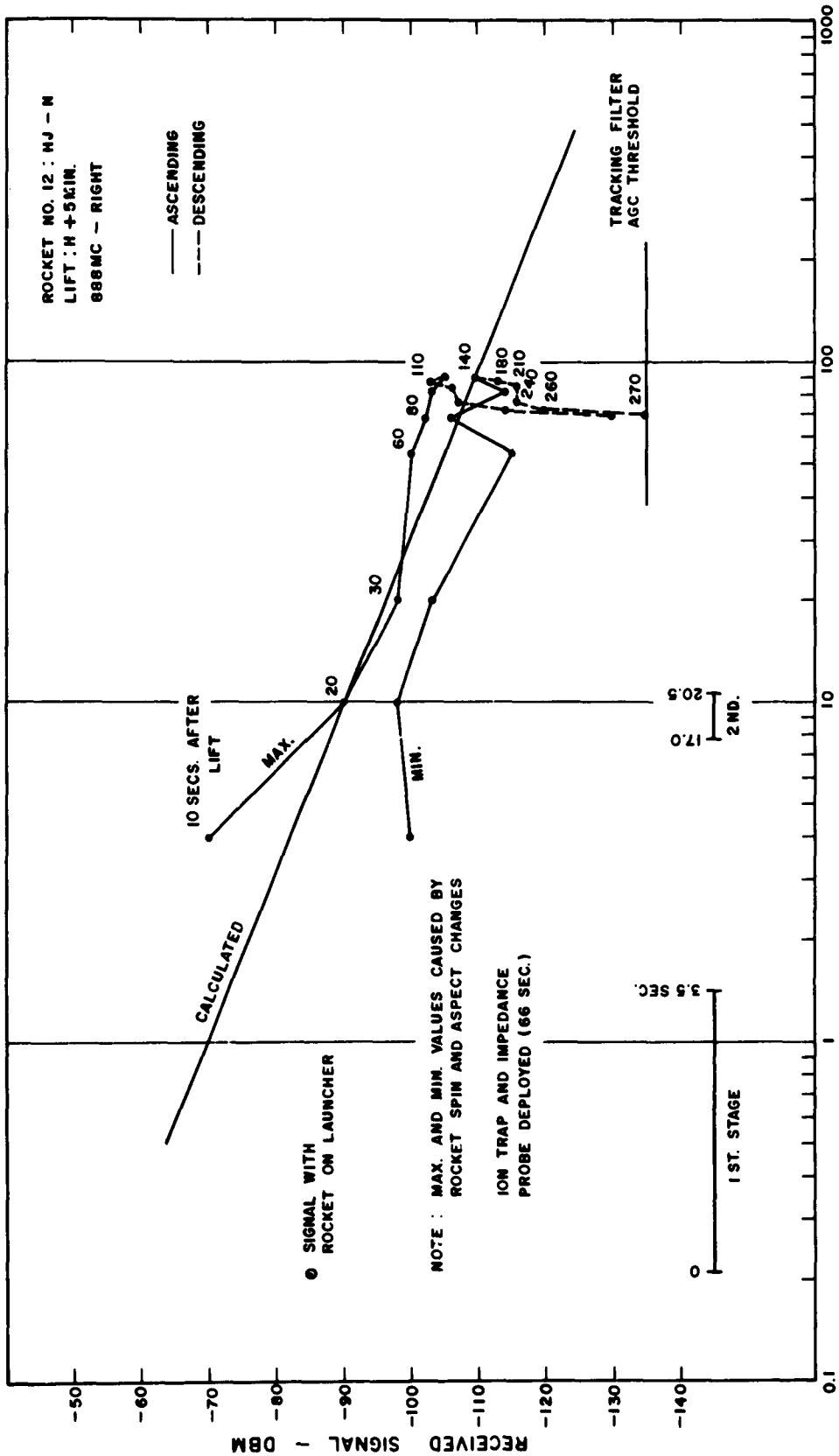

Figure C.143 Received signal strength versus slant range for 3-frequency beacon, 888 Mc right, Rocket 12, Blue Gill.

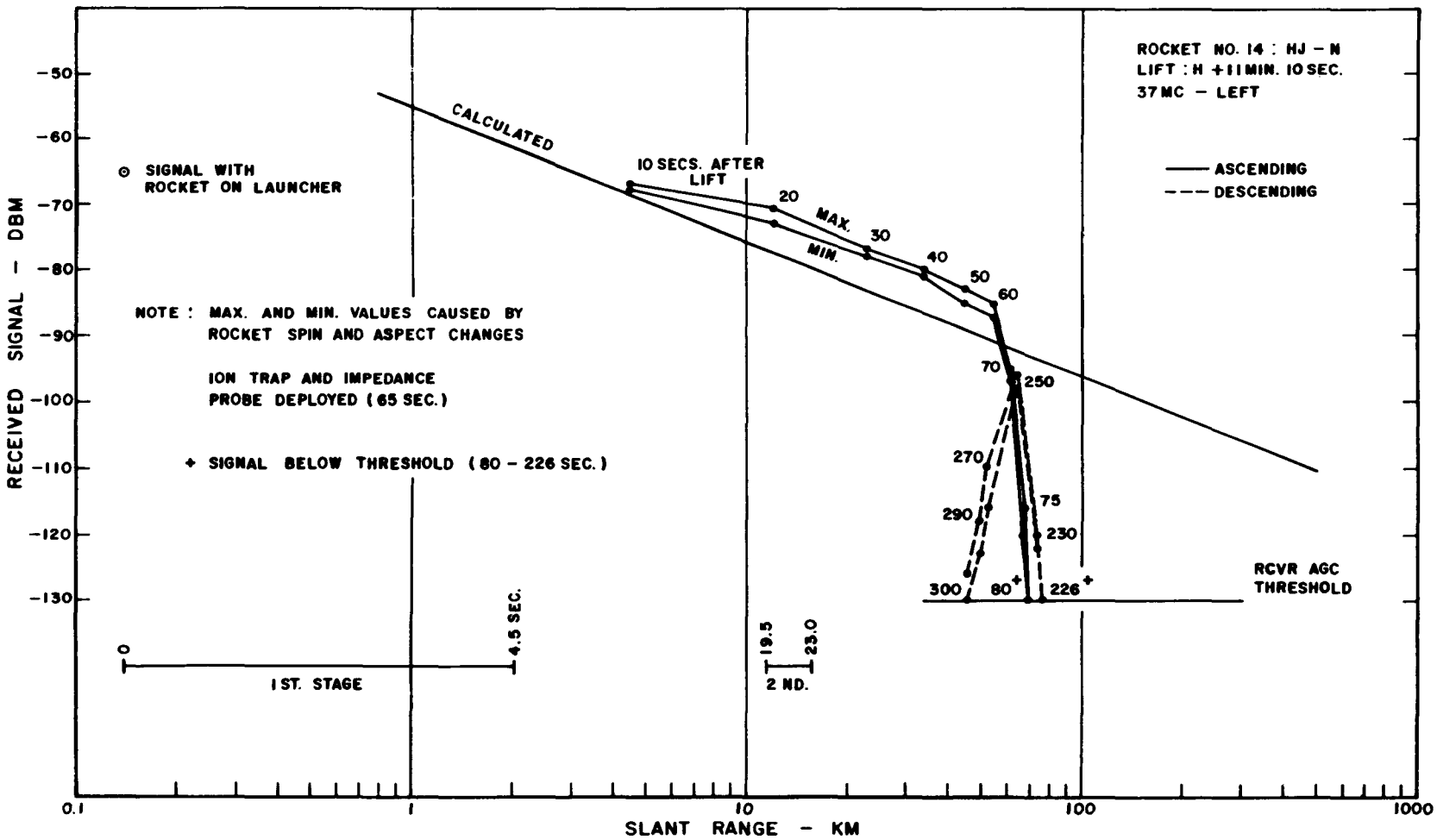

Figure C.144 Received signal strength versus slant range for 3-frequency beacon, 37 Mc left, Rocket 14, Blue Gill.

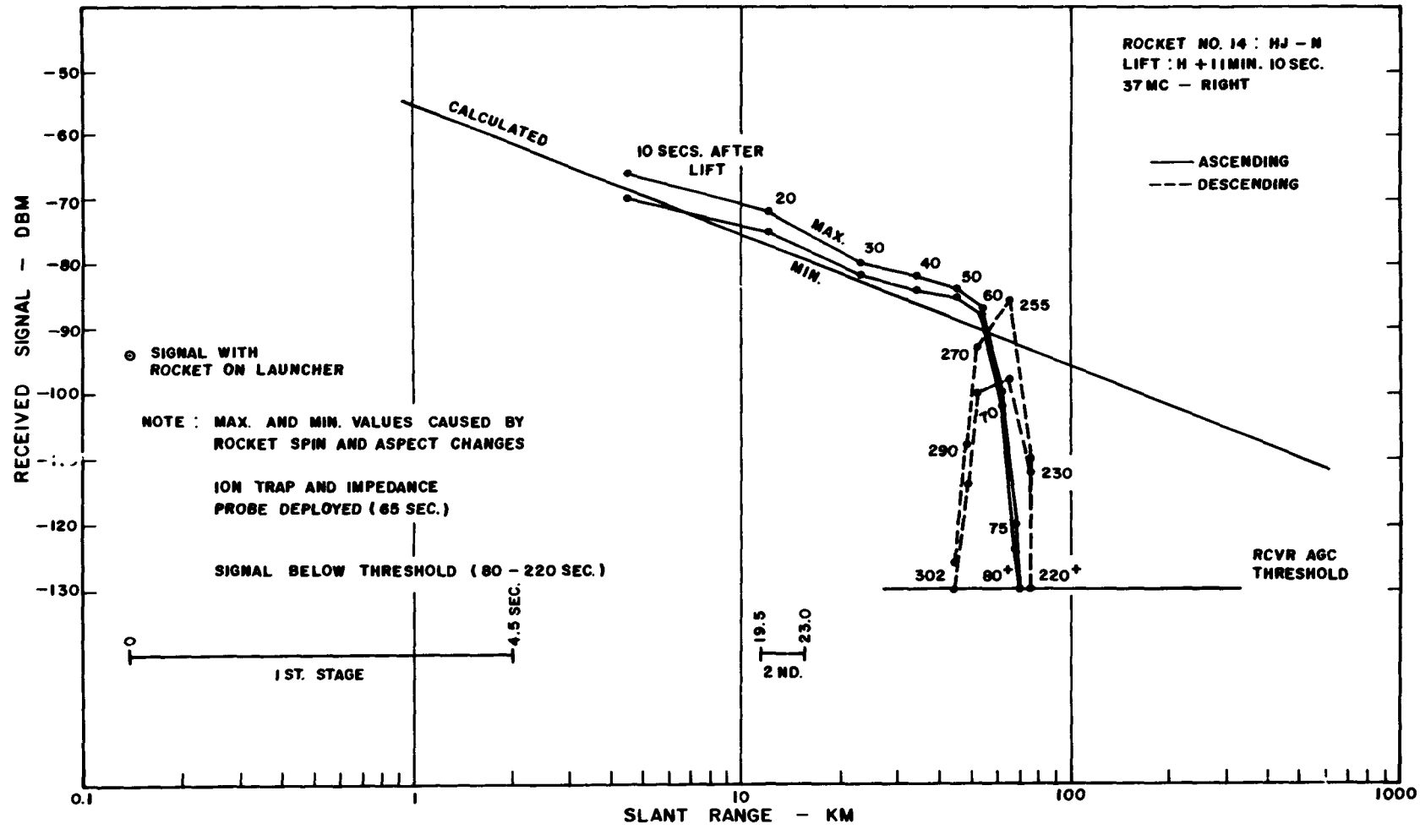

Figure C.145 Received signal strength versus slant range for 3-frequency beacon, 37 Mc right, Rocket 14, Blue Gill.

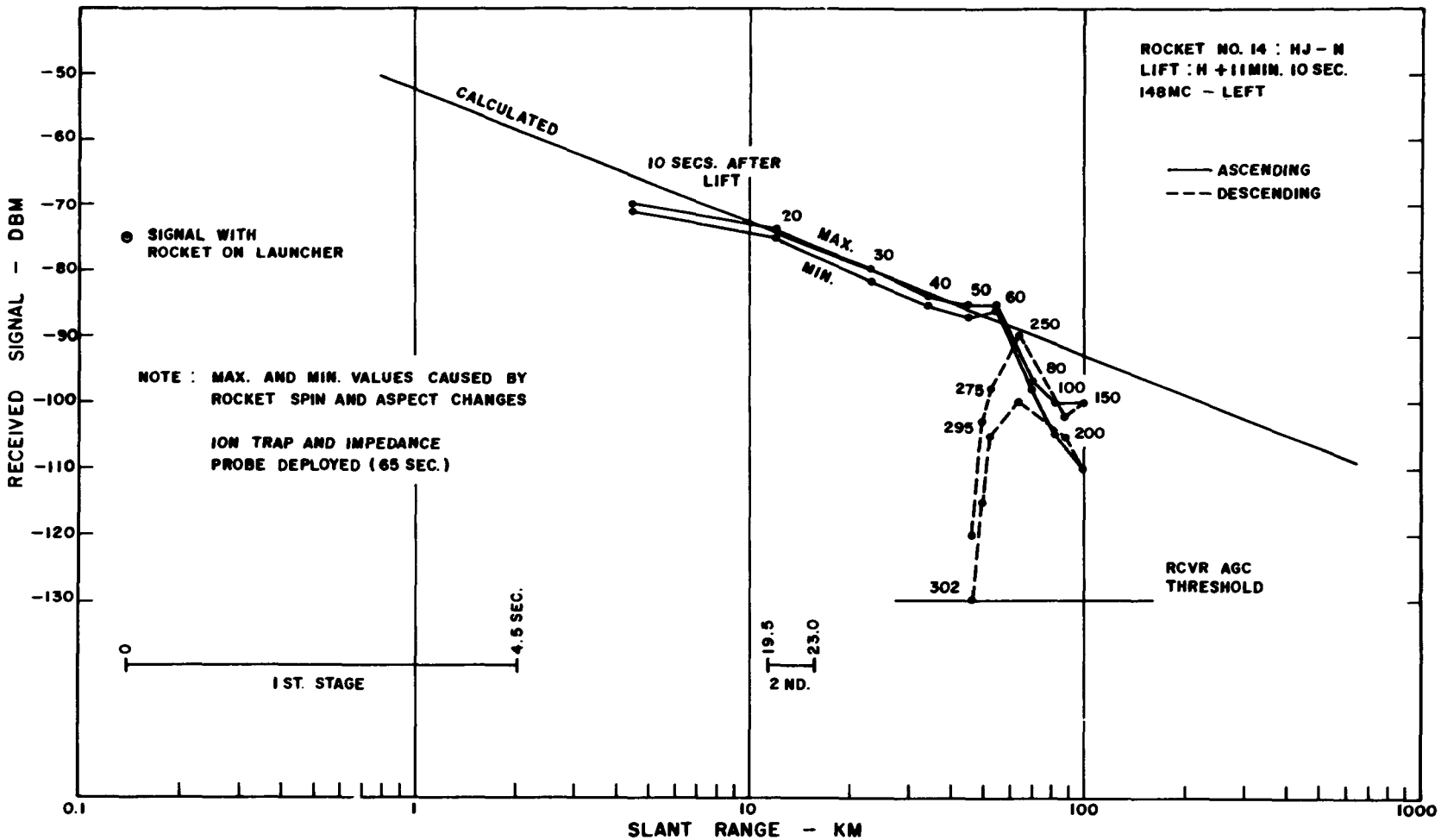

Figure C.146 Received signal strength versus slant range for 3-frequency beacon, 148 Mc left, Rocket 14, Blue Gill.

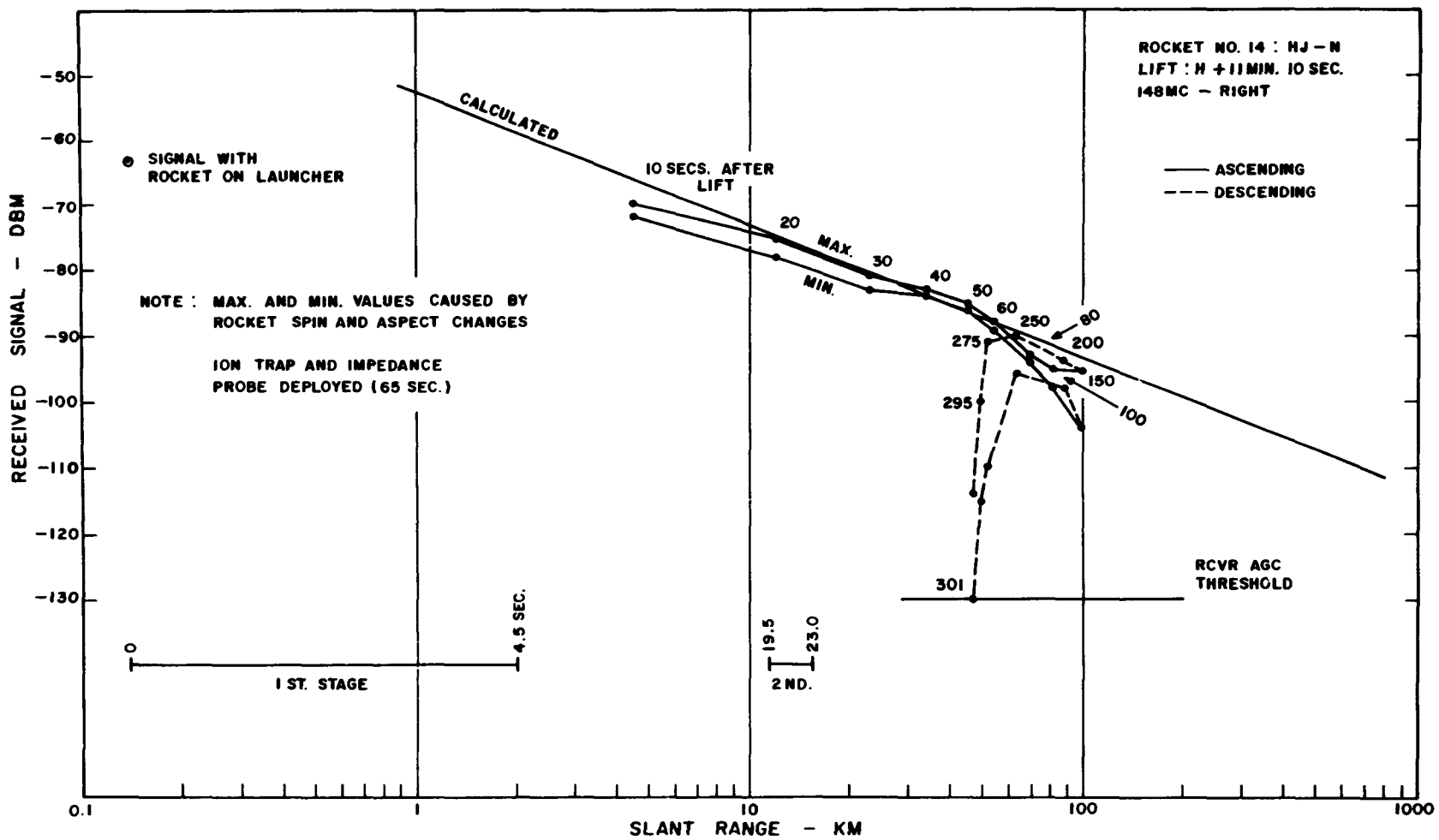

Figure C.147 Received signal strength versus slant range for 3-frequency beacon, 148 Mc right, Rocket 14, Blue Gill.

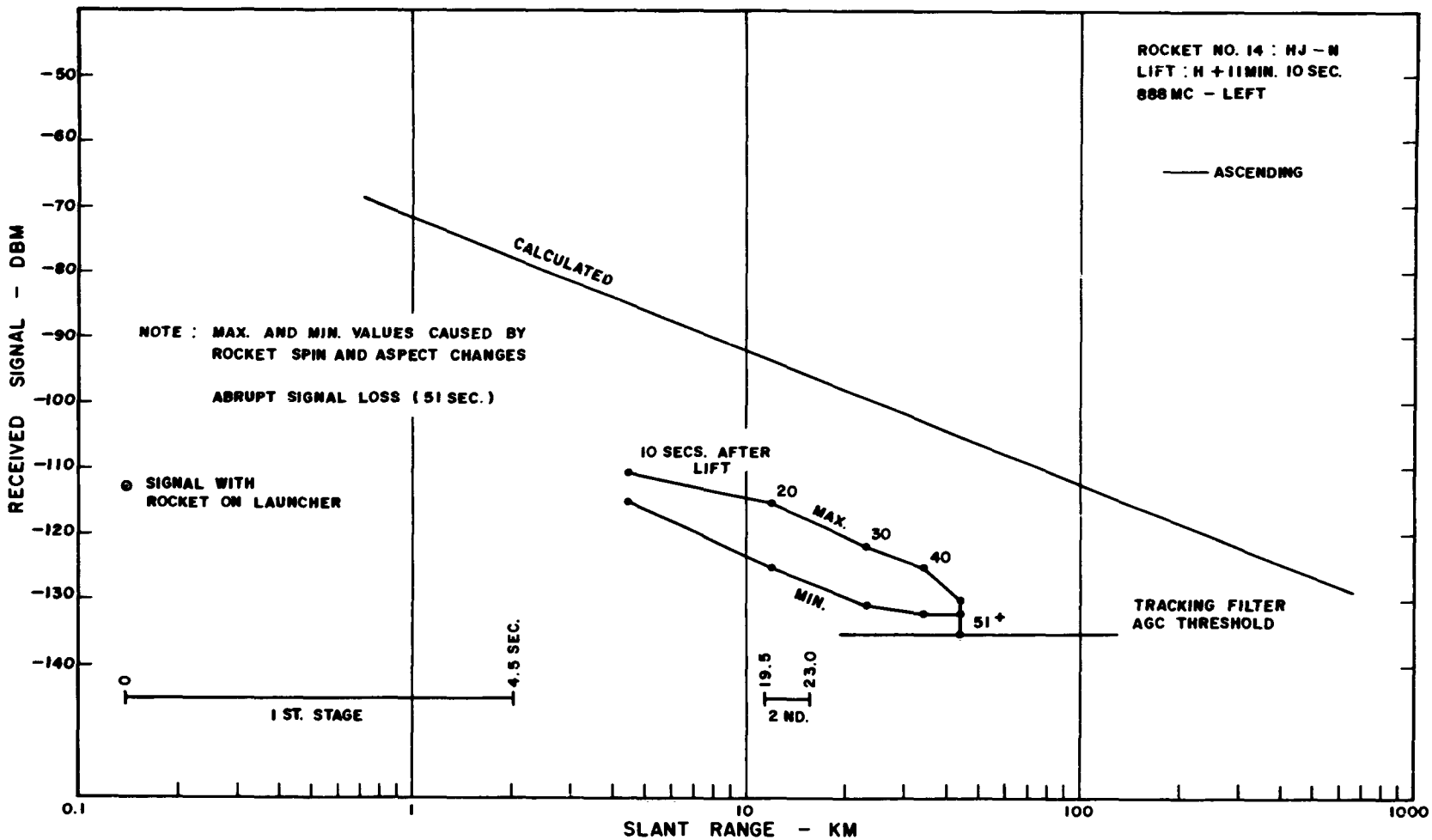

Figure C.148 Received signal strength versus slant range for 3-frequency beacon, 888 Mc left, Rocket 14, Blue Gill..

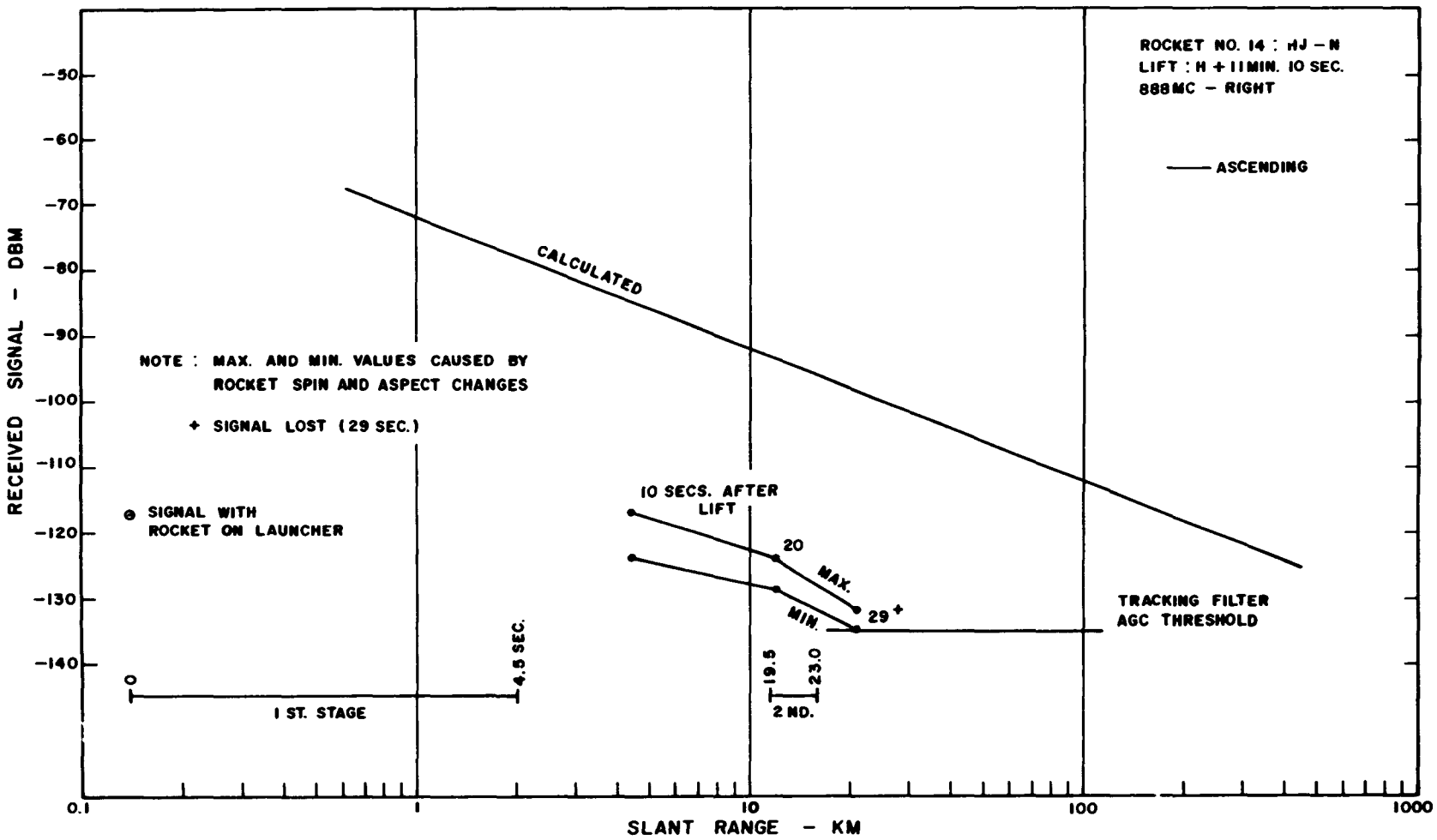

Figure C.149 Received signal strength versus slant range for 3-frequency beacon, 888 Mc right, Rocket 14, Blue Gill.

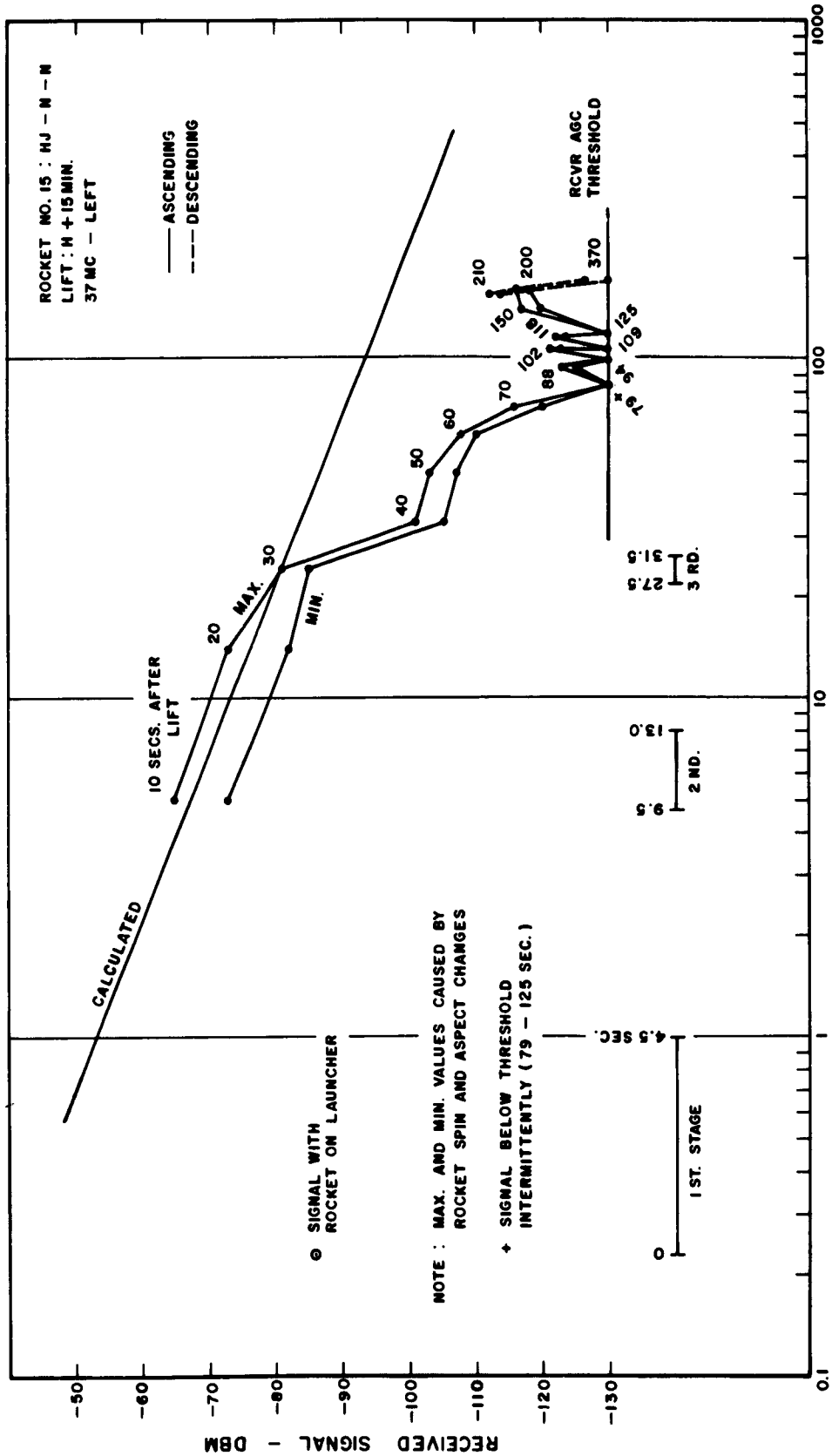

Figure C.150 Received signal strength versus slant range for 3-frequency beacon, 37 Mc left, Rocket 15, Blue Gill.

SECRET

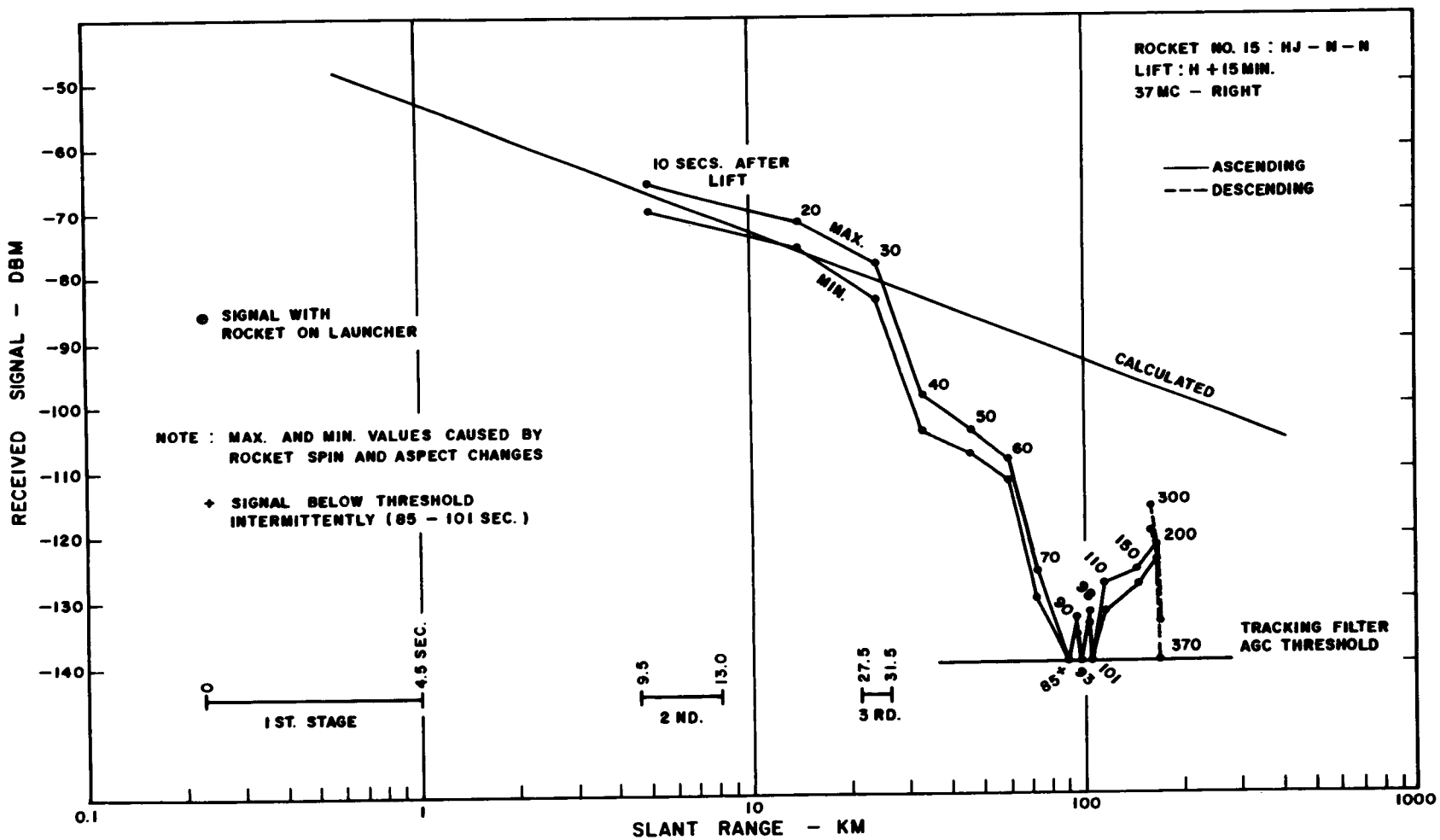

Figure C.151 Received signal strength versus slant range for 3-frequency beacon, 37 Mc right, Rocket 15, Blue Gill.

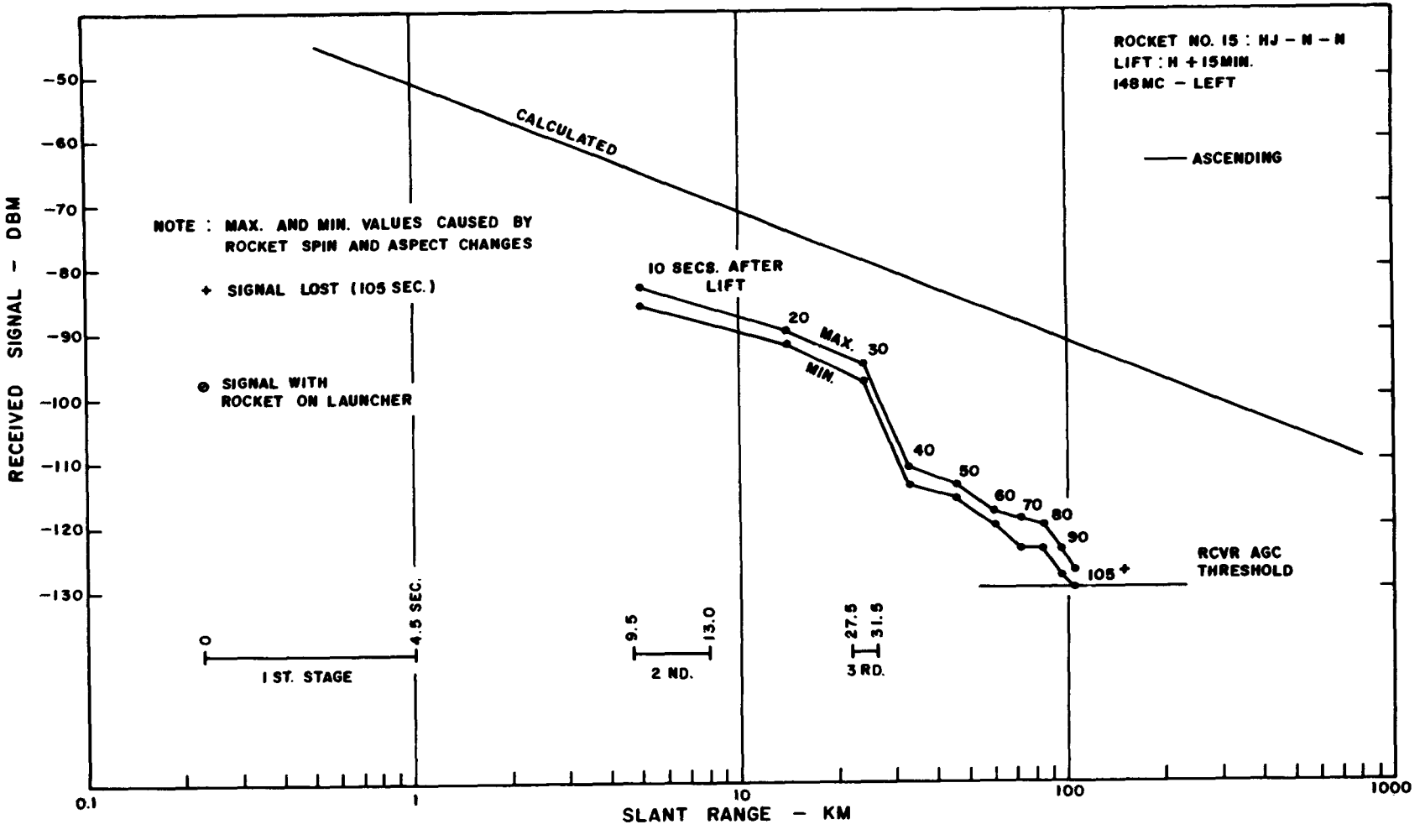

Figure C.152 Received signal strength versus slant range for 3-frequency beacon, 148 Mc left, Rocket 15, Blue Gill.

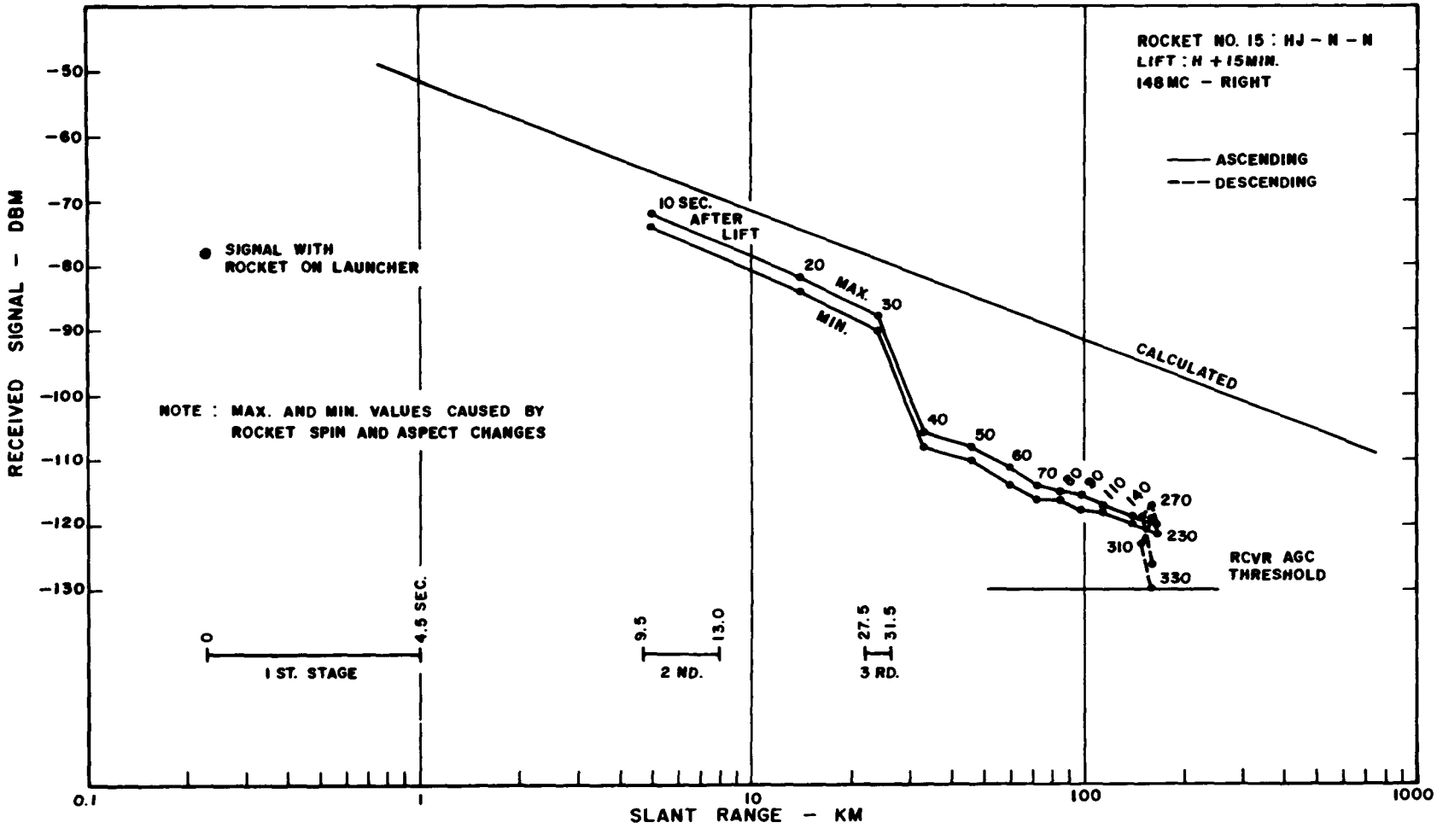

Figure C.153 Received signal strength versus slant range for 3-frequency beacon, 148 Mc right, Rocket 15, Blue Gill.

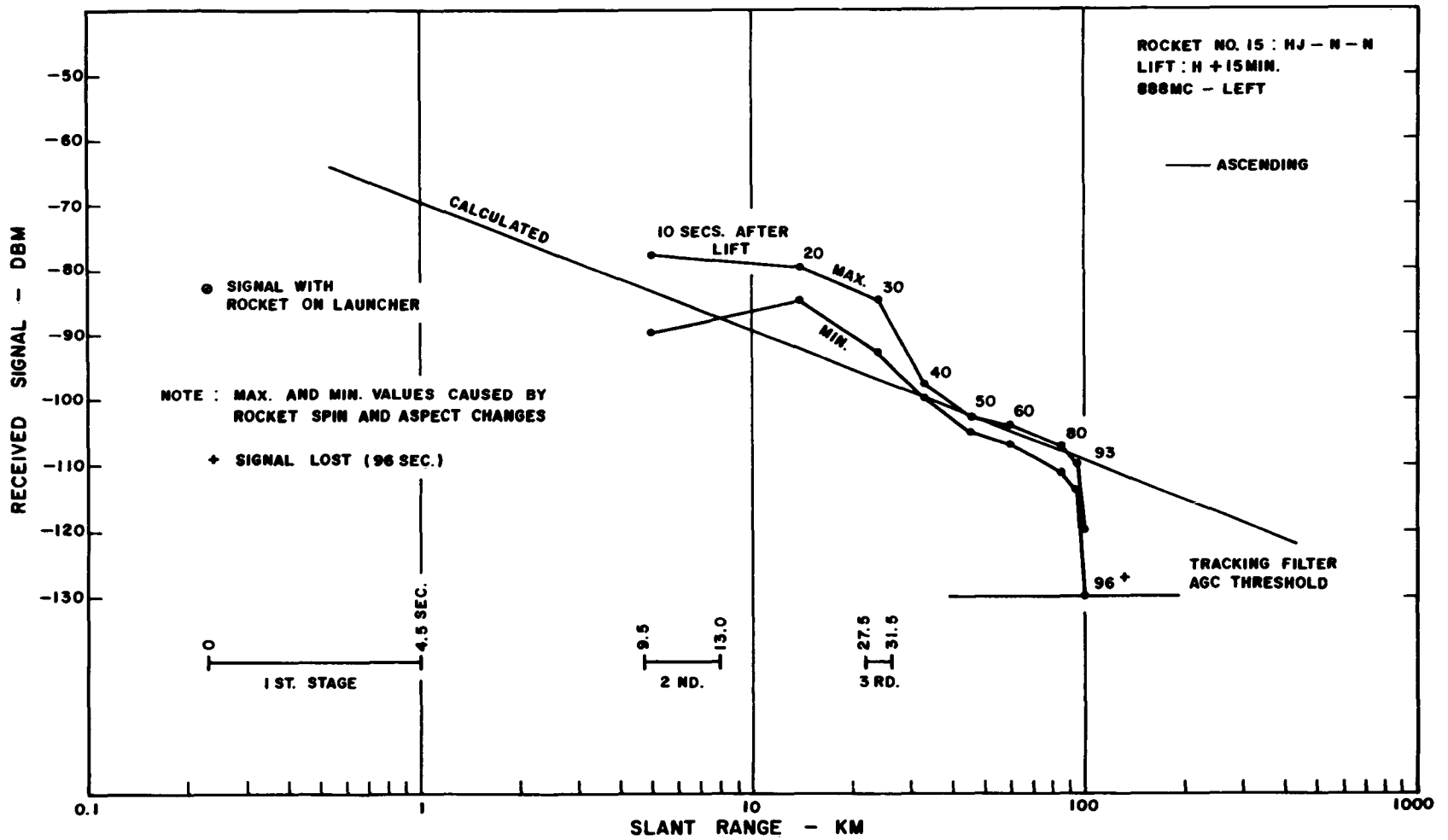

Figure C.154 Received signal strength versus slant range for 3-frequency beacon, 888 Mc left, Rocket 15, Blue Gill.

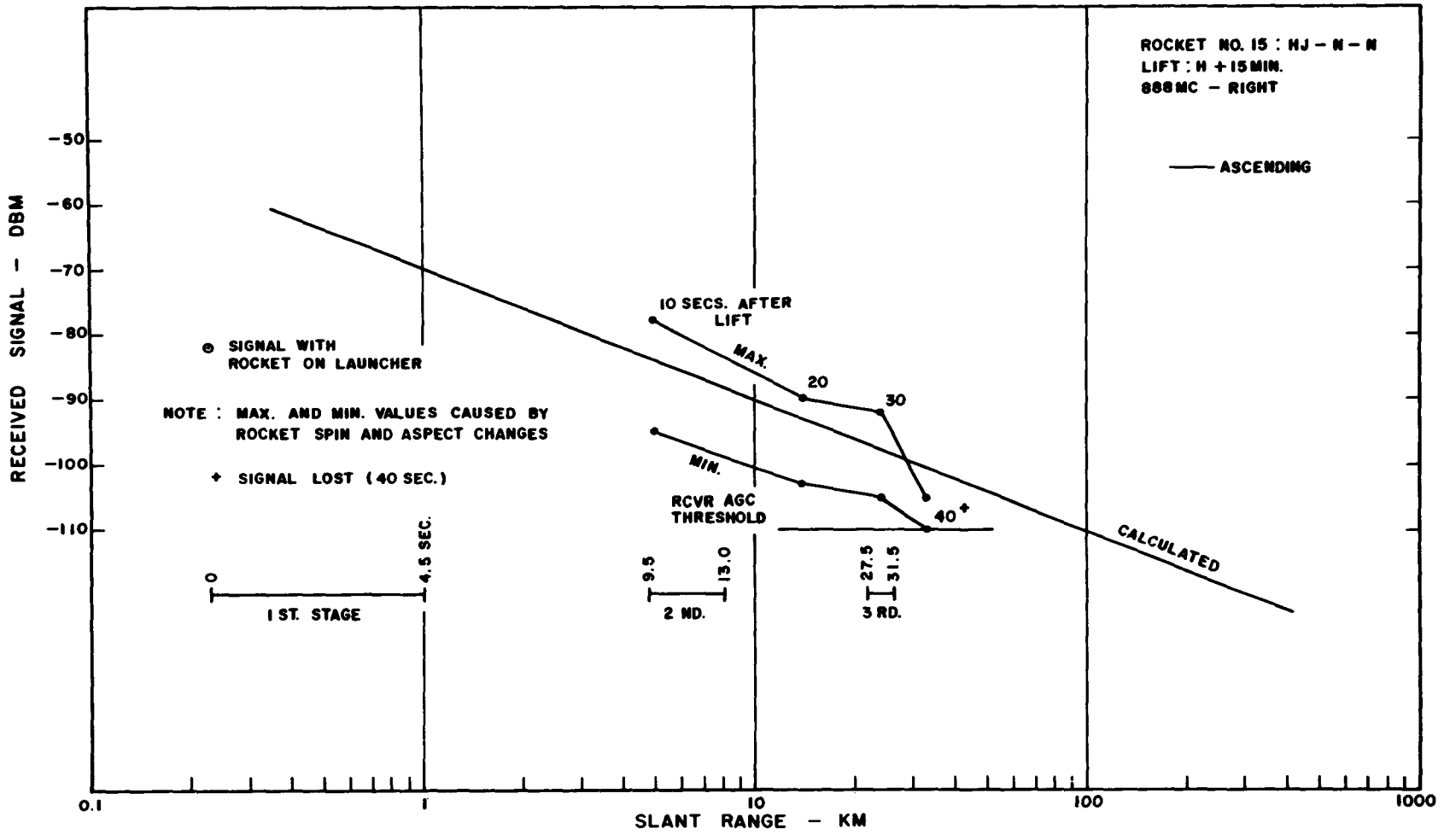

Figure C.155 Received signal strength versus slant range for 3-frequency beacon, 888 Mc right, Rocket 15, Blue Gill.

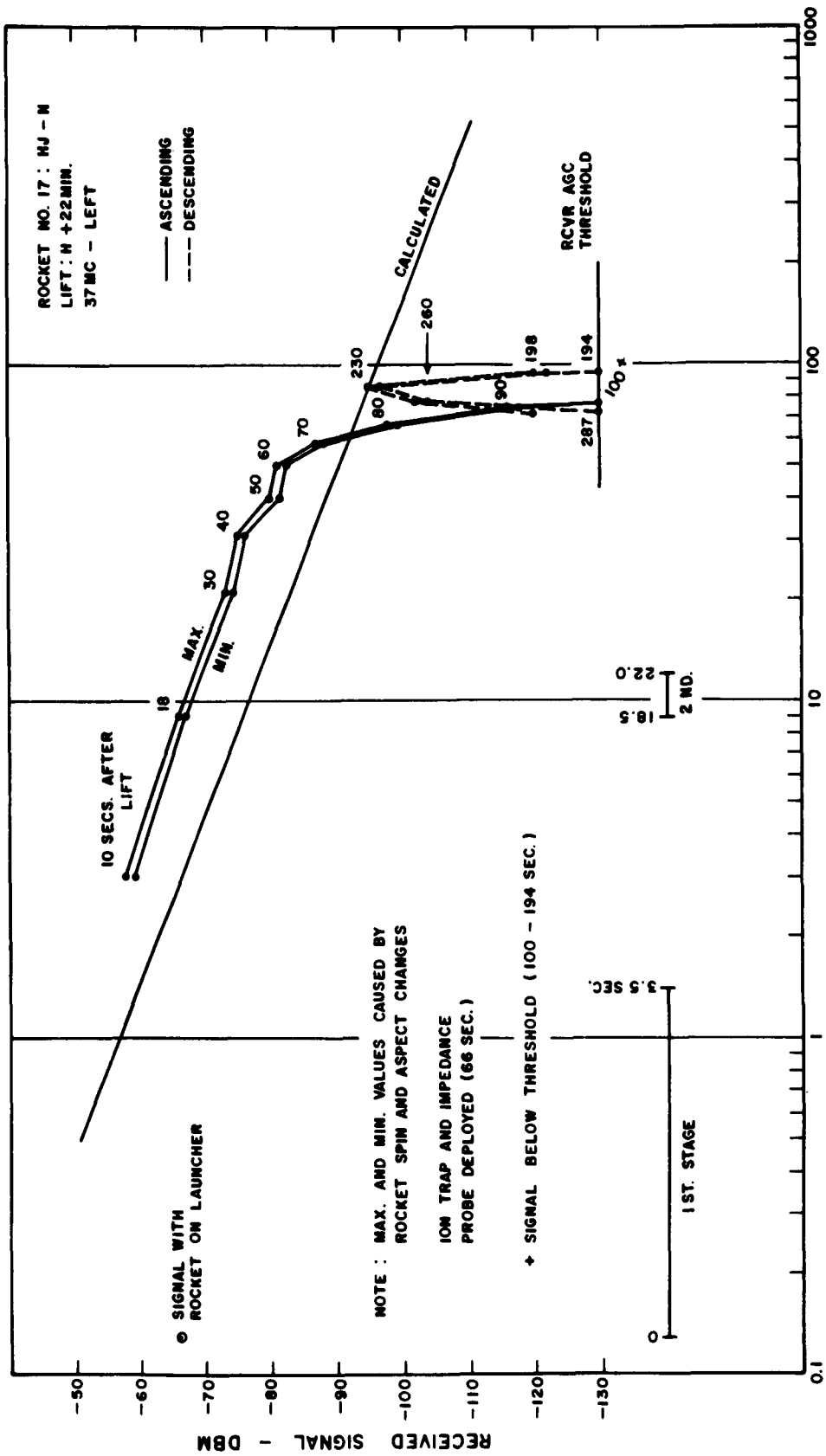

Figure C.156 Received signal strength versus slant range for 3-frequency beacon, 37 Mc left, Rocket 17, Blue Gill.

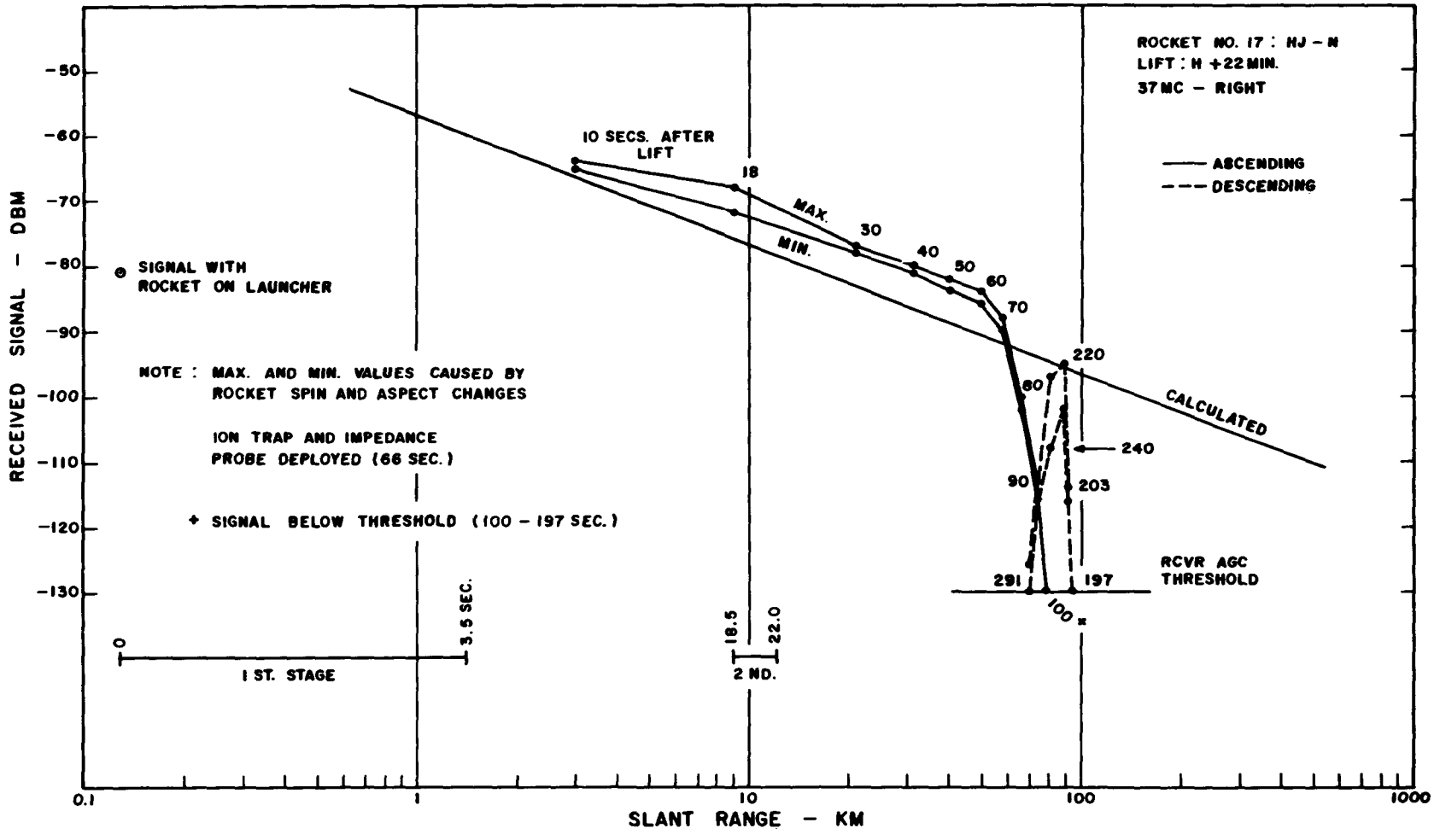

Figure C.157 Received signal strength versus slant range for 3-frequency beacon, 37 Mc right, Rocket 17, Blue Gill.

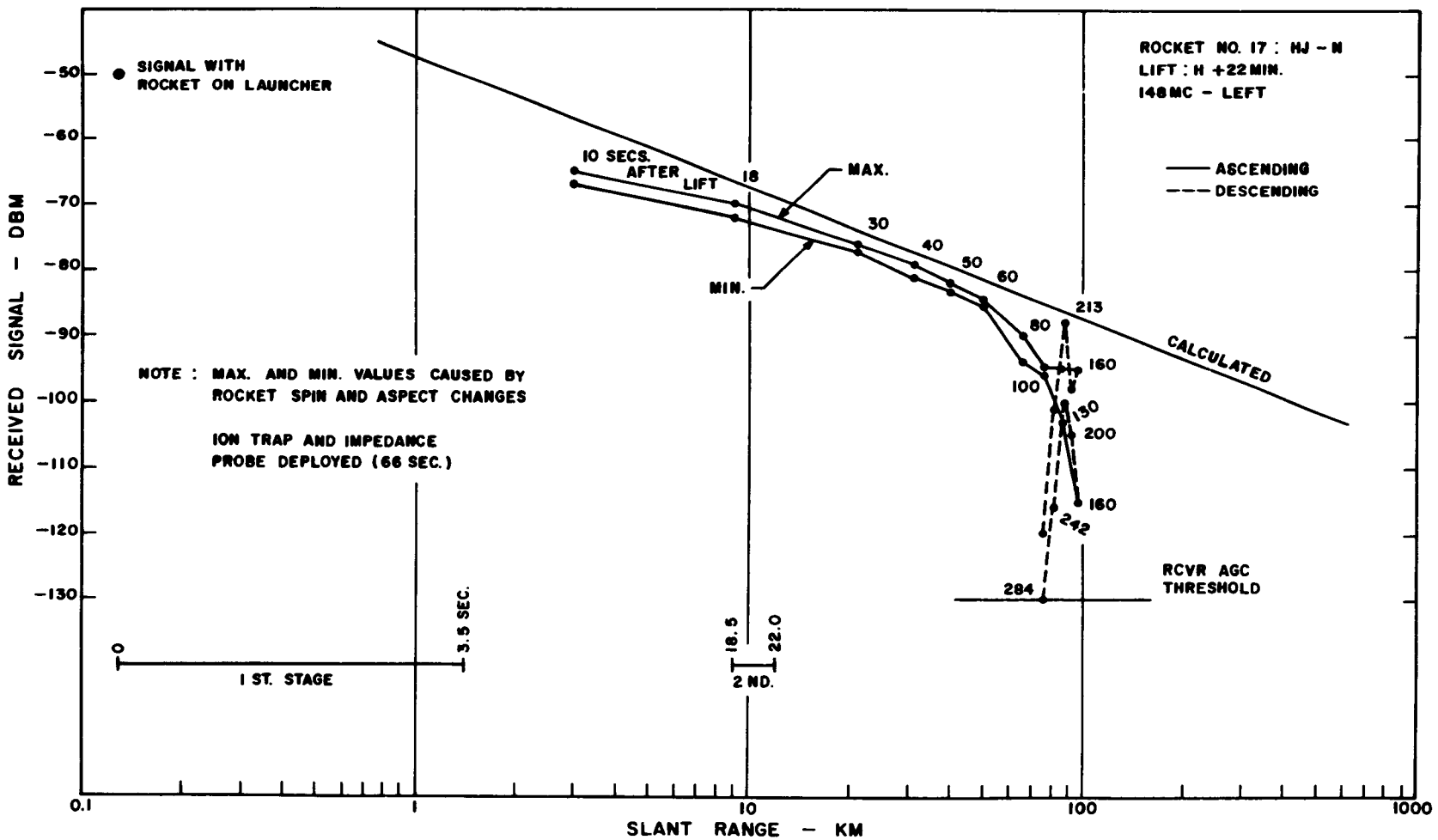

Figure C.158 Received signal strength versus slant range for 3-frequency beacon, 148 Mc left, Rocket 17, Blue Gill.

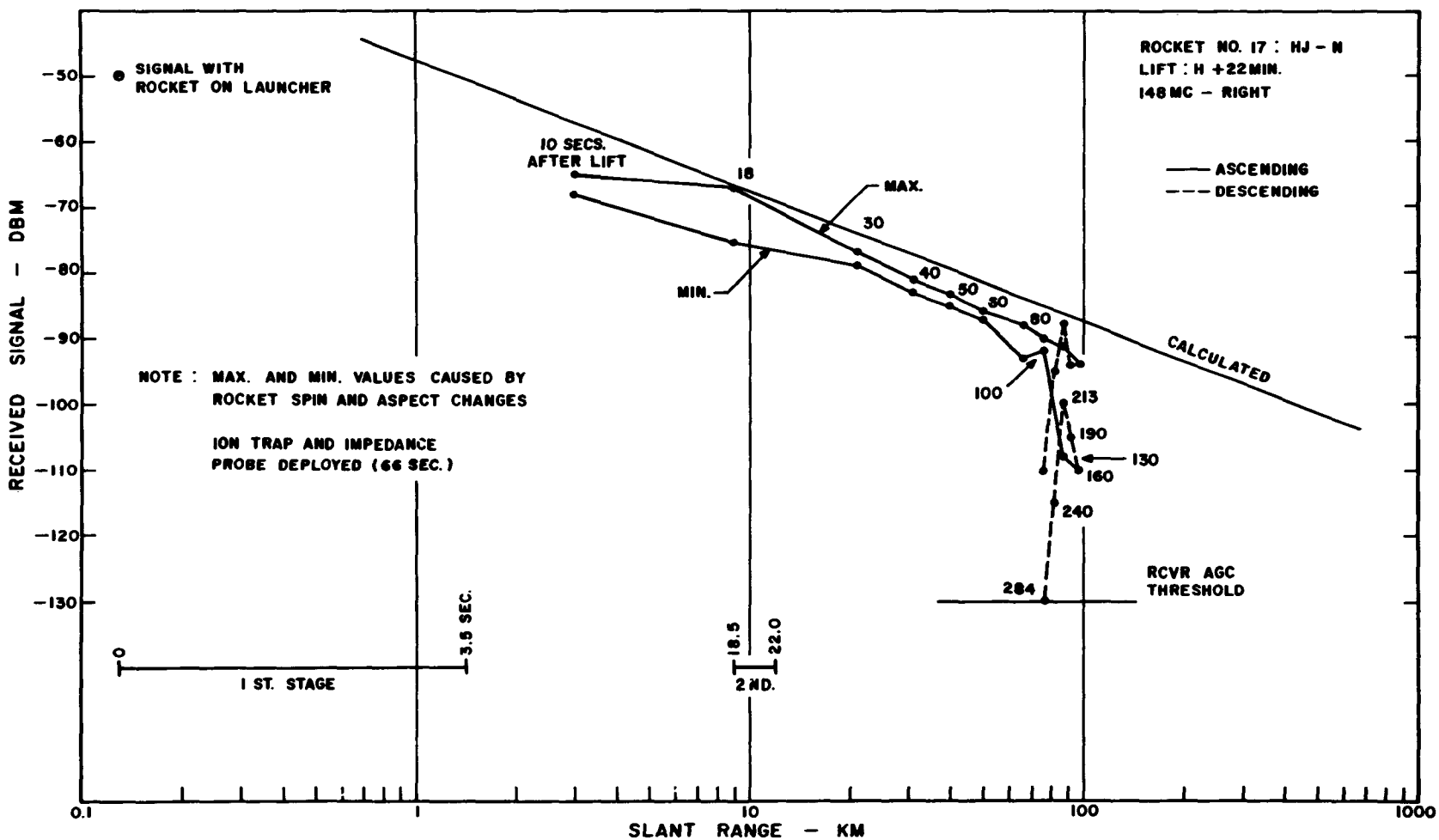

Figure C.159 Received signal strength versus slant range for 3-frequency beacon, 148 Mc right, Rocket 17, Blue Gill.

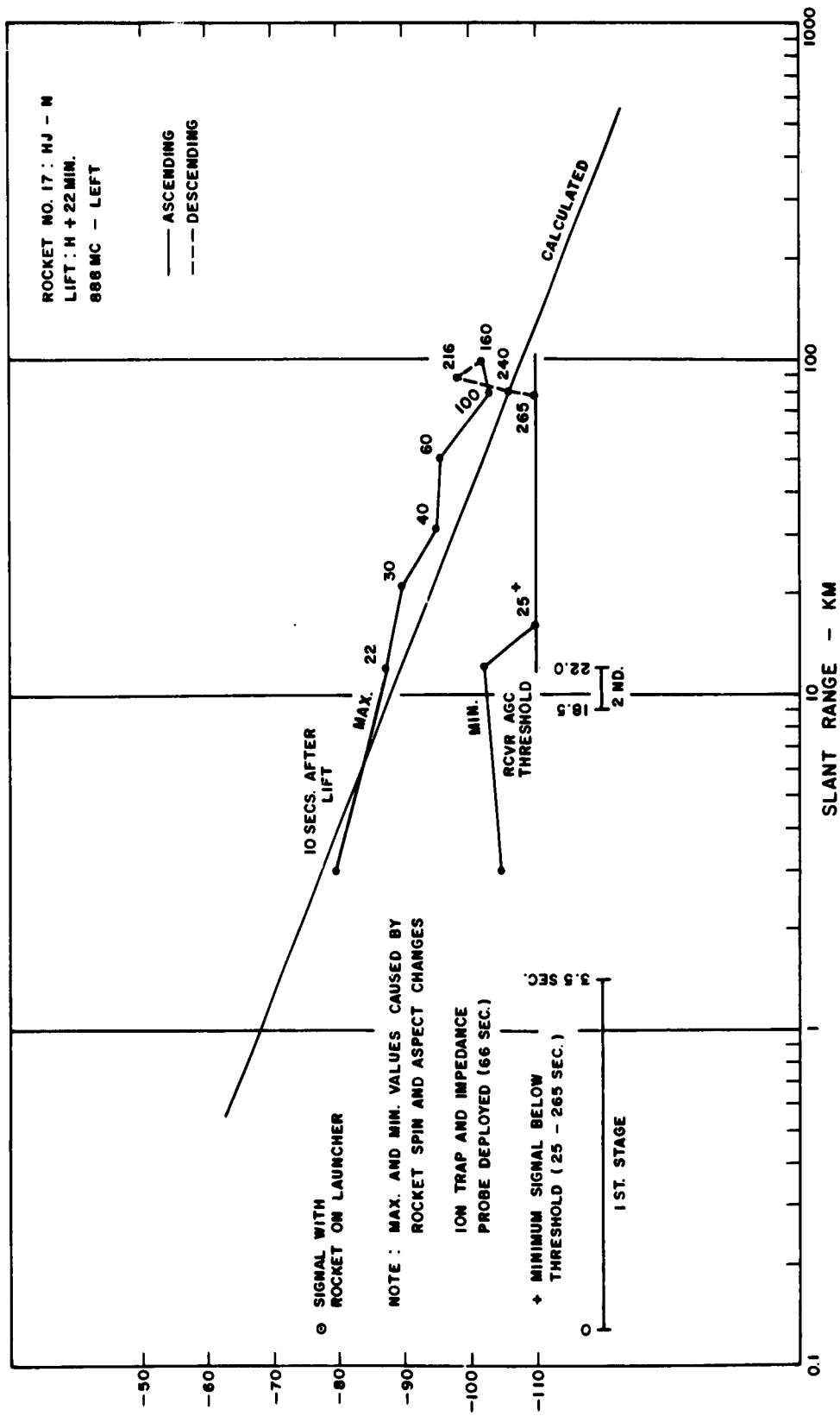

Figure C.160 Received signal strength versus slant range for 3-frequency beacon, 888 Mc left, Rocket 17, Blue Gill.

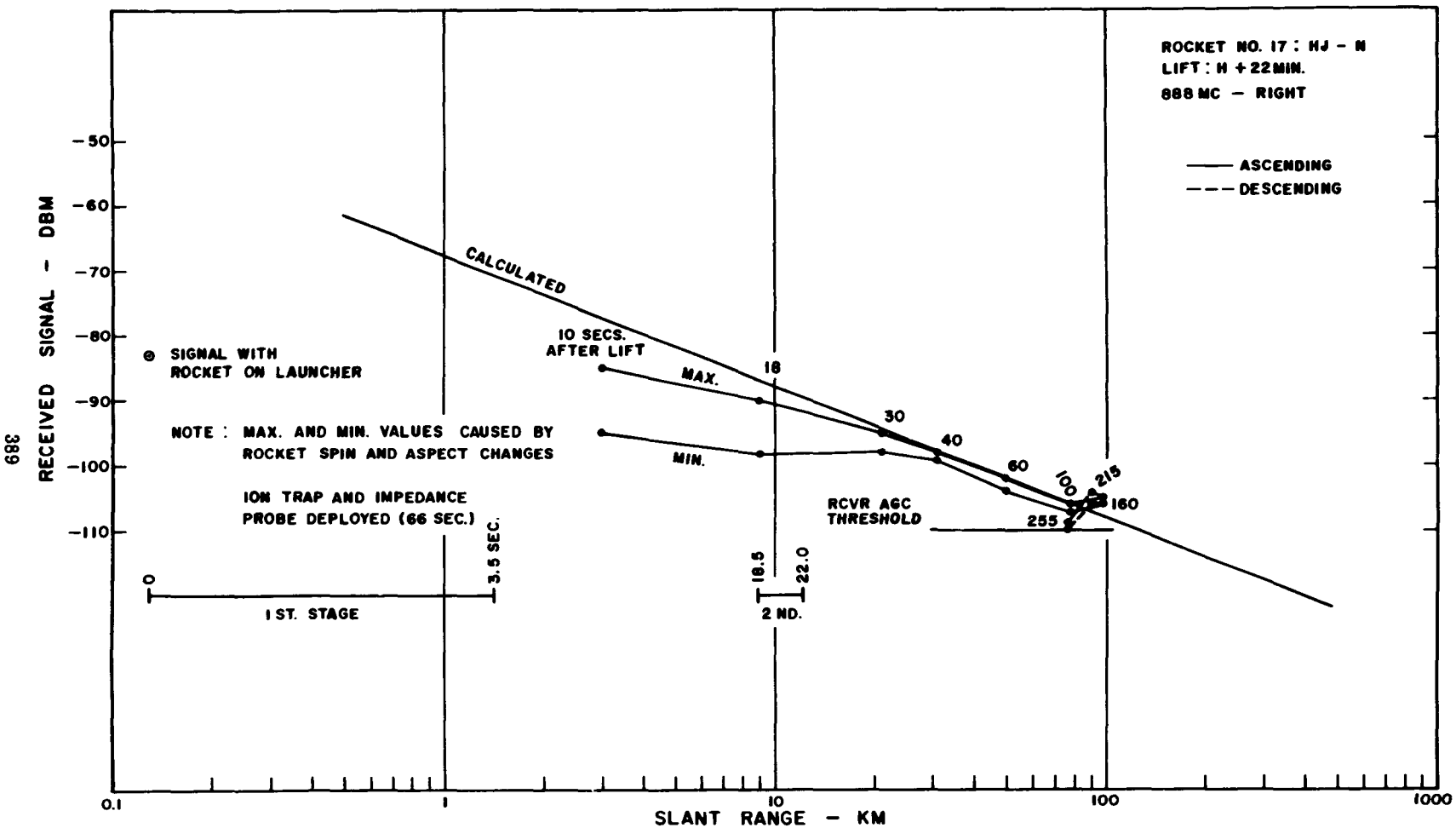

Figure C.161 Received signal strength versus slant range for 3-frequency beacon, 888 Mc right, Rocket 17, Blue Gill.

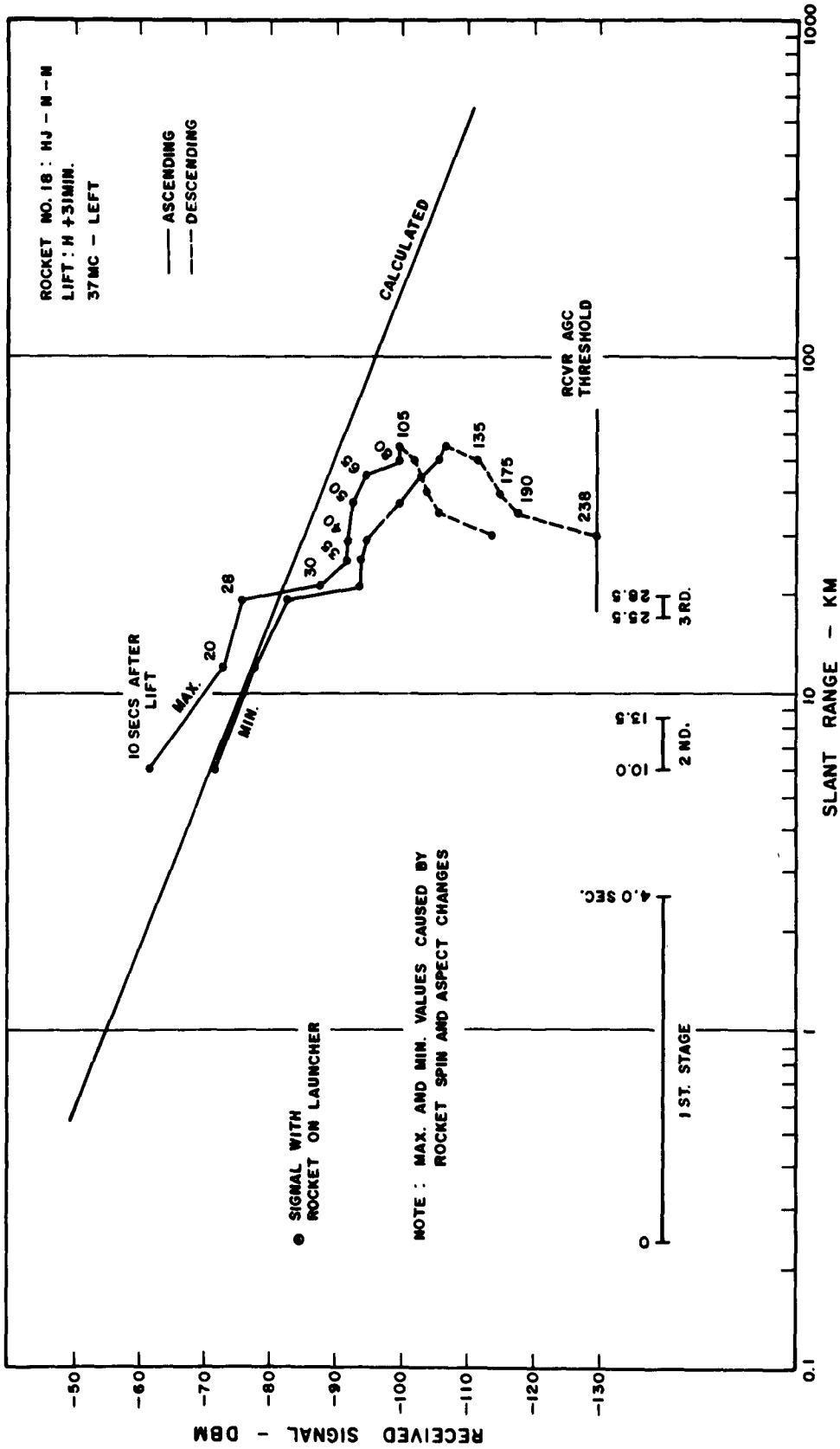

Figure C.162 Received signal strength versus slant range for 3-frequency beacon, 37 Mc left, Rocket 18, Blue Gill.

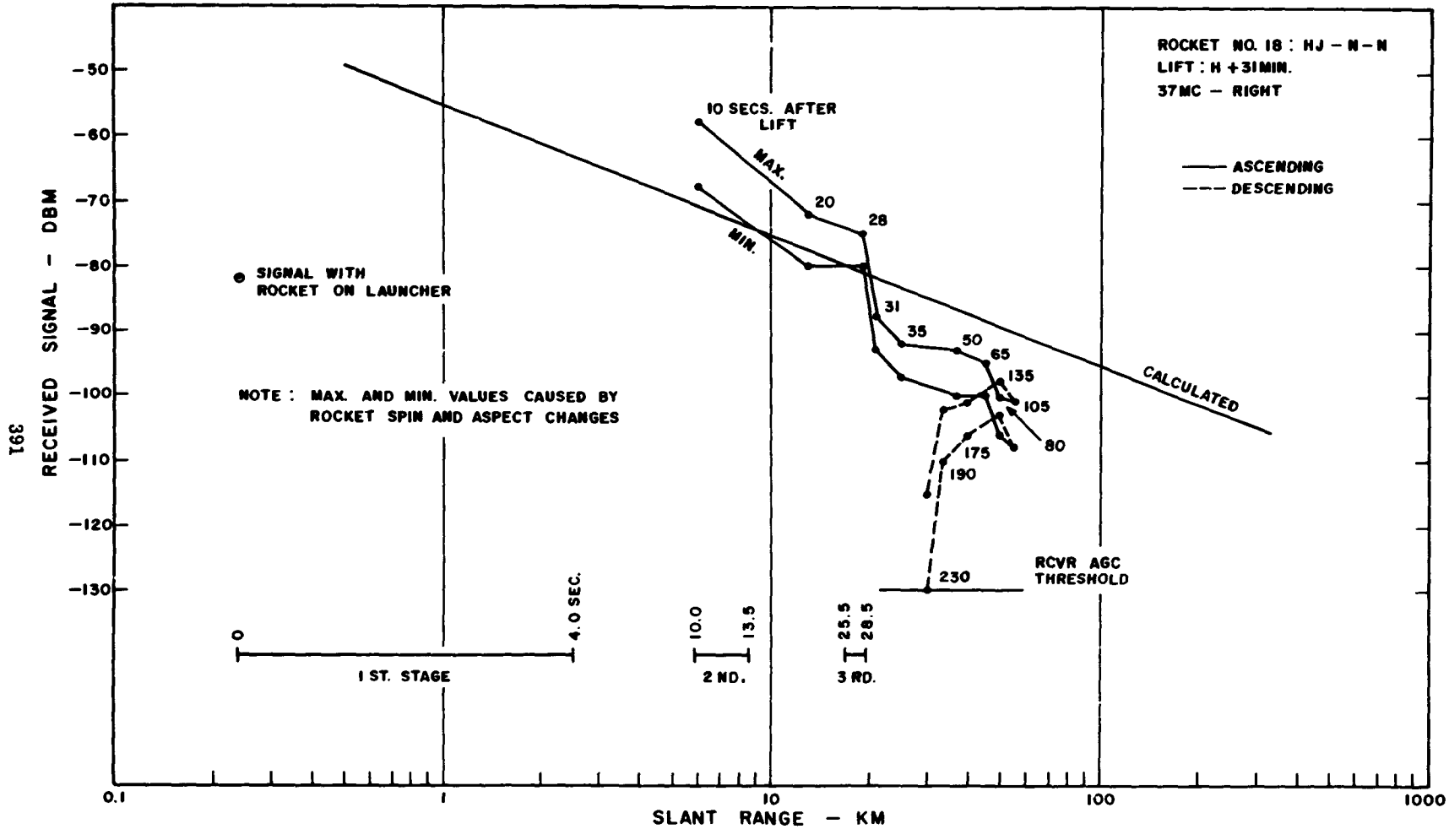

Figure C.163 Received signal strength versus slant range for 3-frequency beacon, 37 Mc right, Rocket 18, Blue Gill.

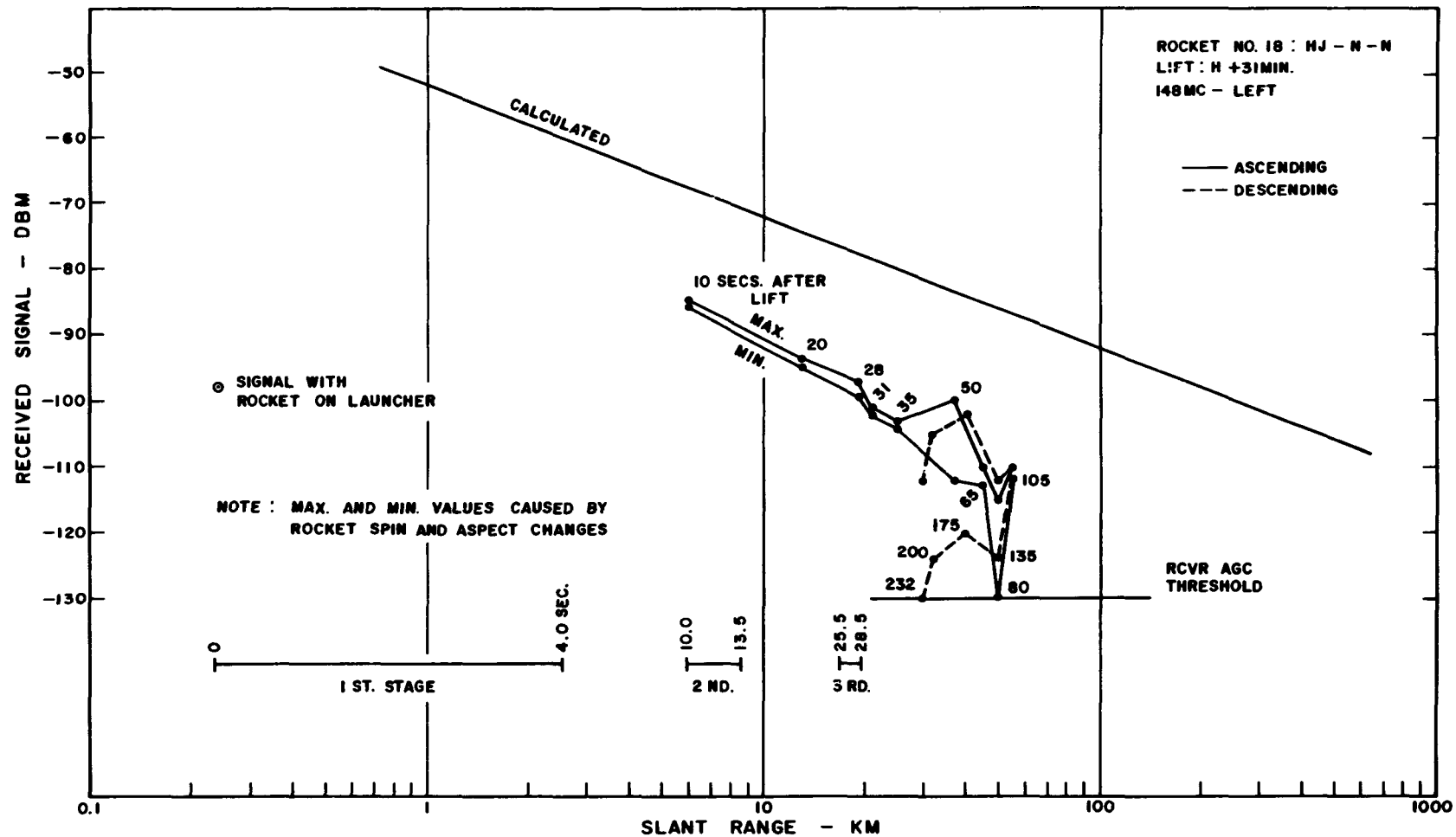

Figure C.164 Received signal strength versus slant range for 3-frequency beacon, 148 Mc left, Rocket 18, Blue Gill.

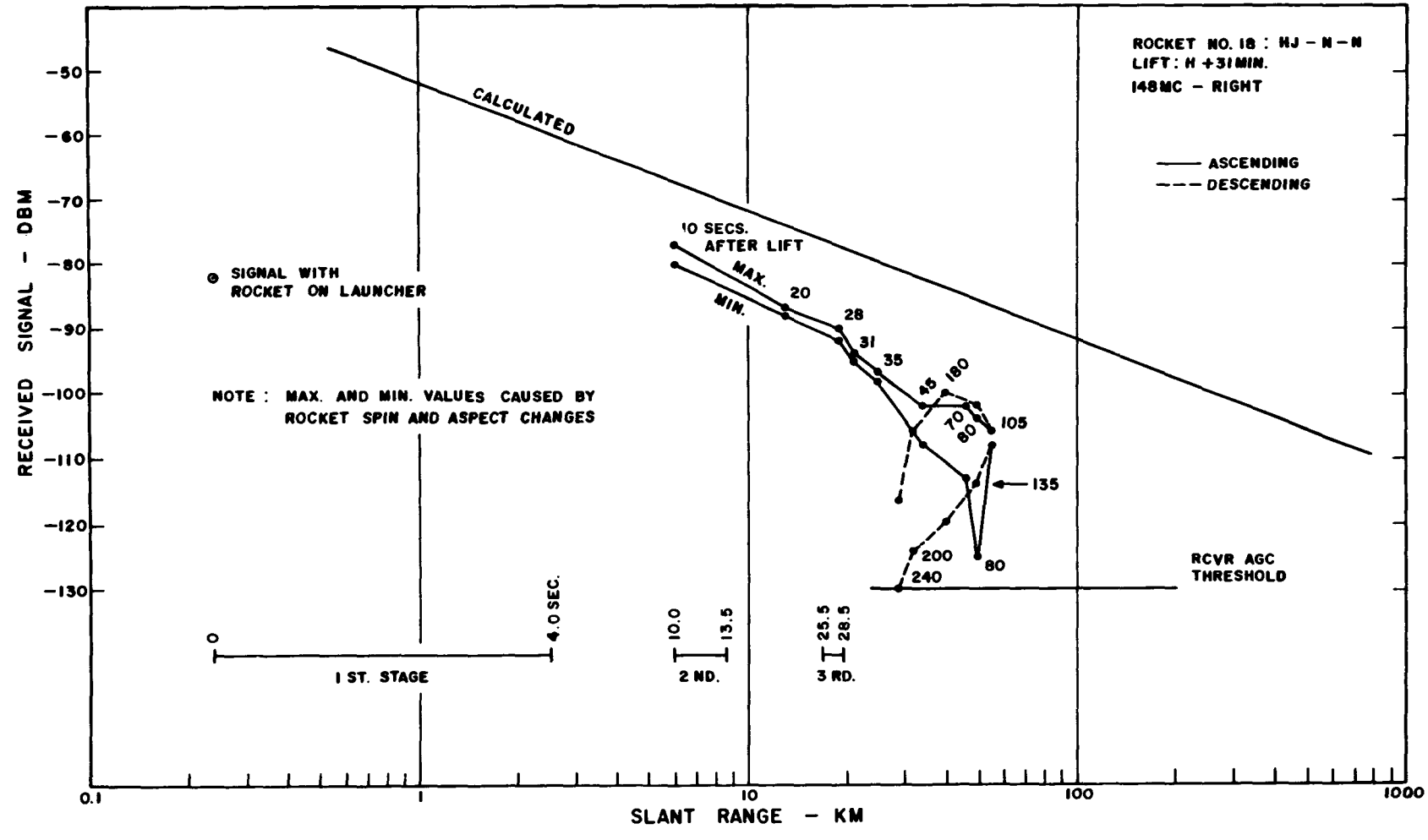

Figure C.165 Received signal strength versus slant range for 3-frequency beacon, 148 Mc right, Rocket 18, Blue Gill.

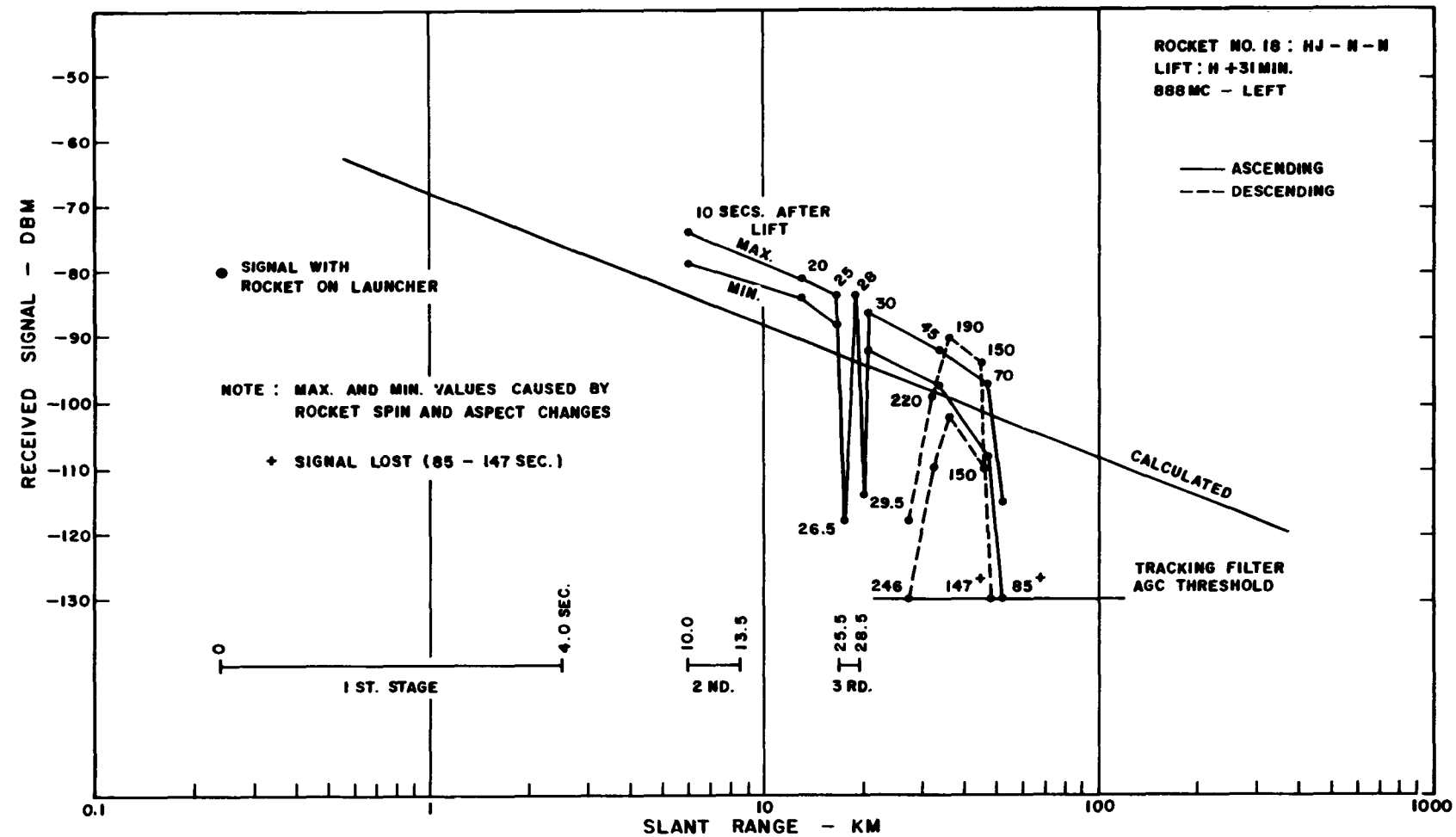

Figure C.166 Received signal strength versus slant range for 3-frequency beacon, 888 Mc left, Rocket 18, Blue Gill.

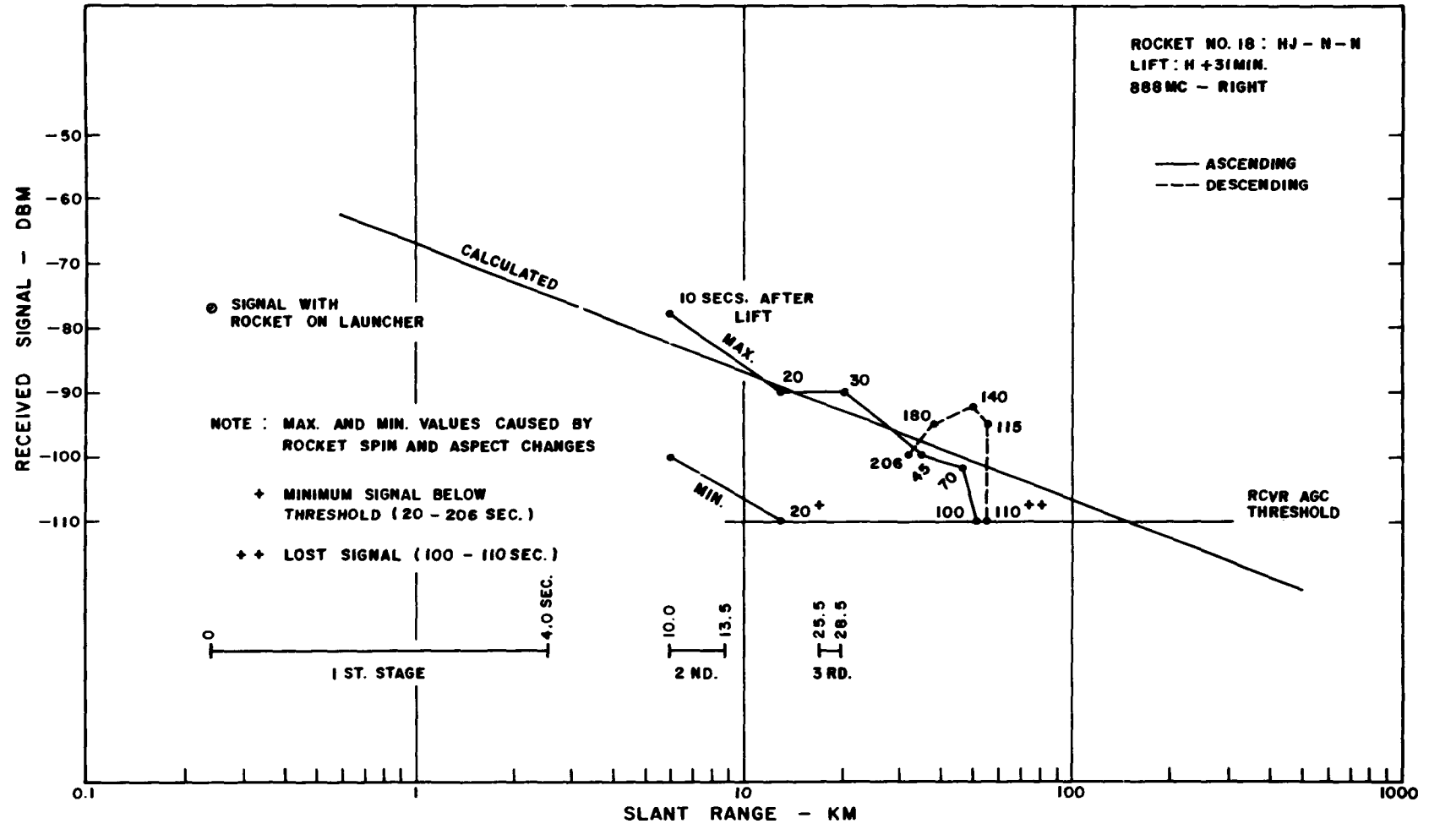

Figure C.167 Received signal strength versus slant range for 3-frequency beacon, 888 Mc right, Rocket 18, Blue Gill.

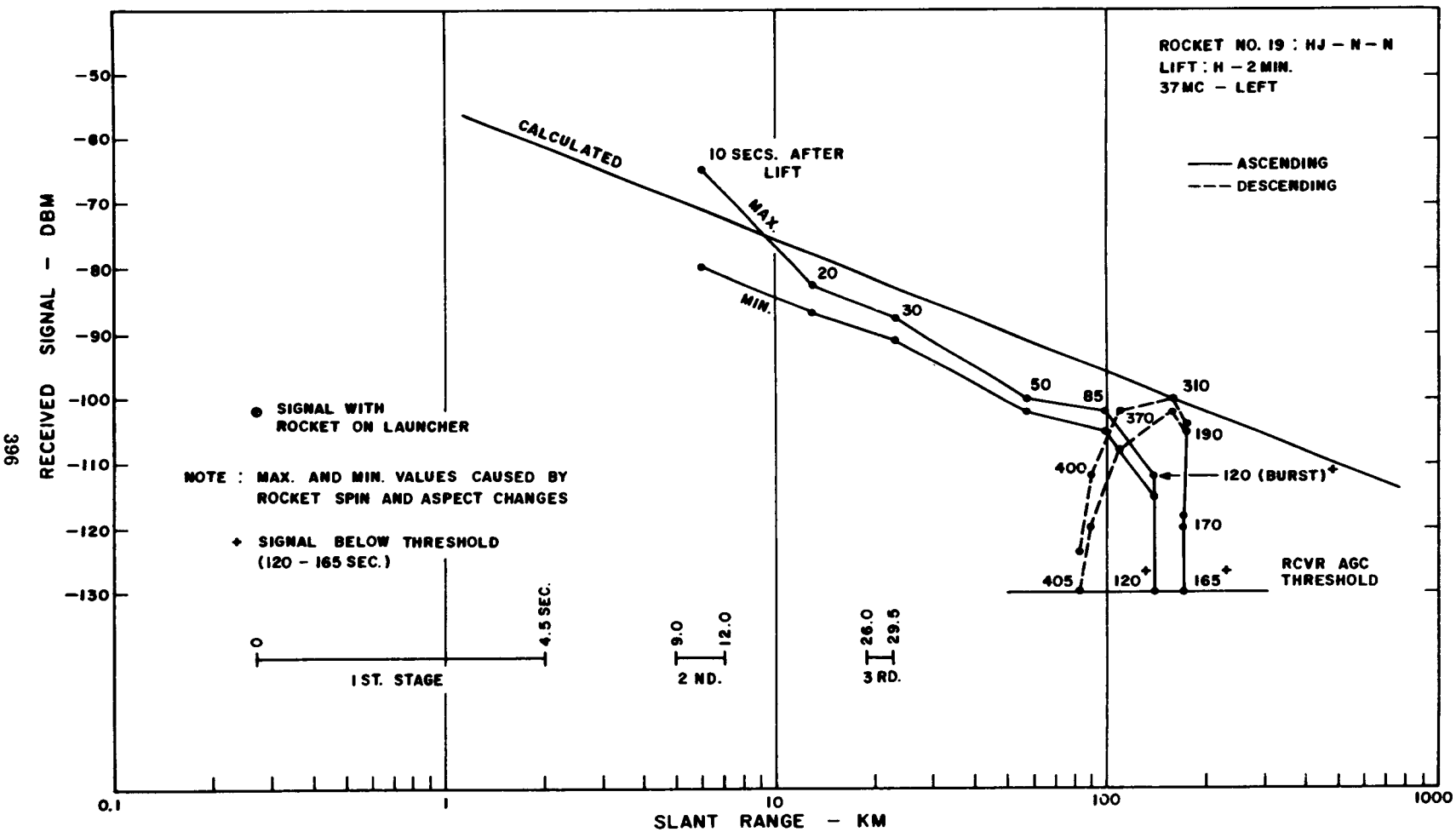

Figure C.168 Received signal strength versus slant range for 3-frequency beacon, 37 Mc left, Rocket 19, King Fish.

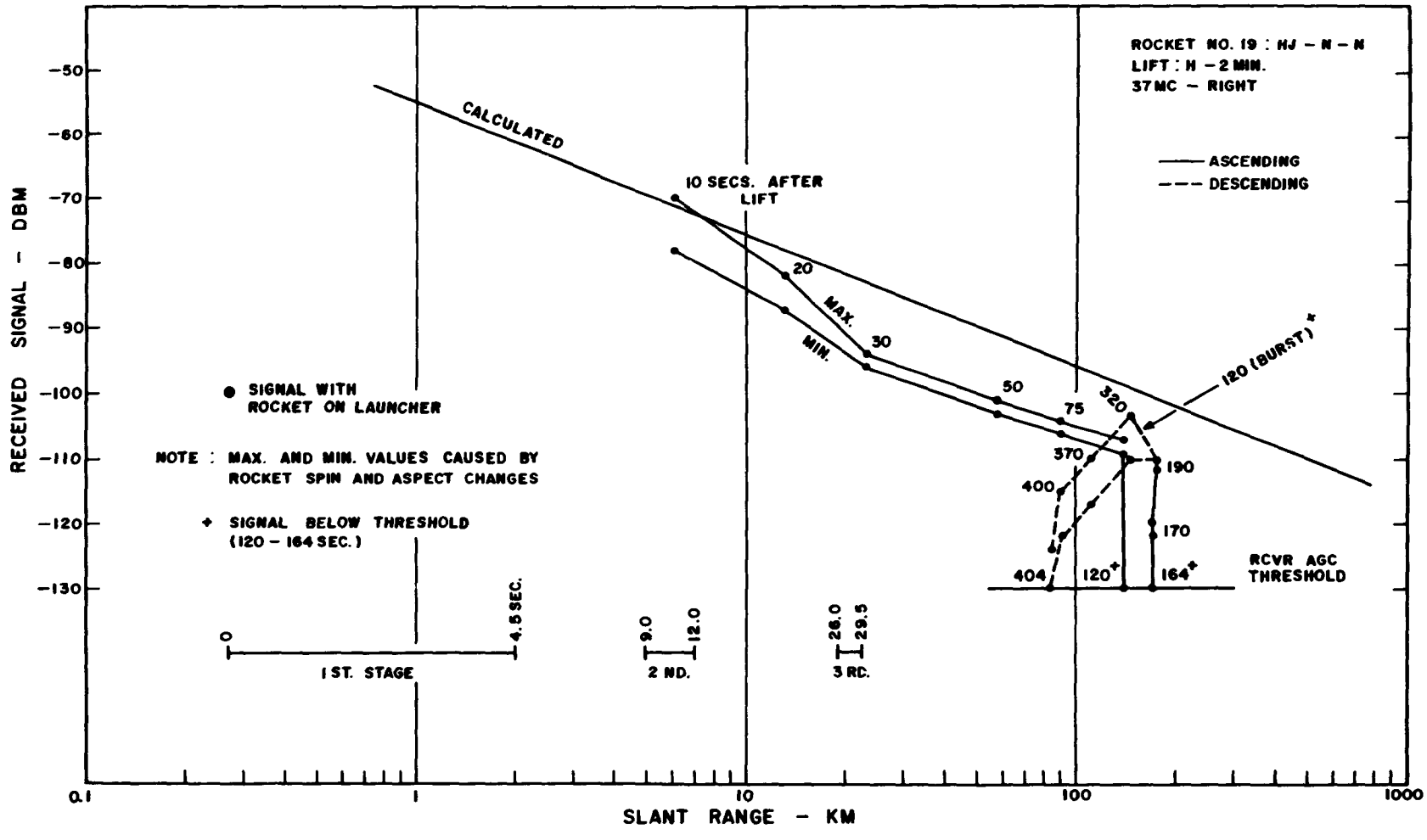

Figure C.169 Received signal strength versus slant range for 3-frequency beacon, 37 Mc right, Rocket 19, King Fish.

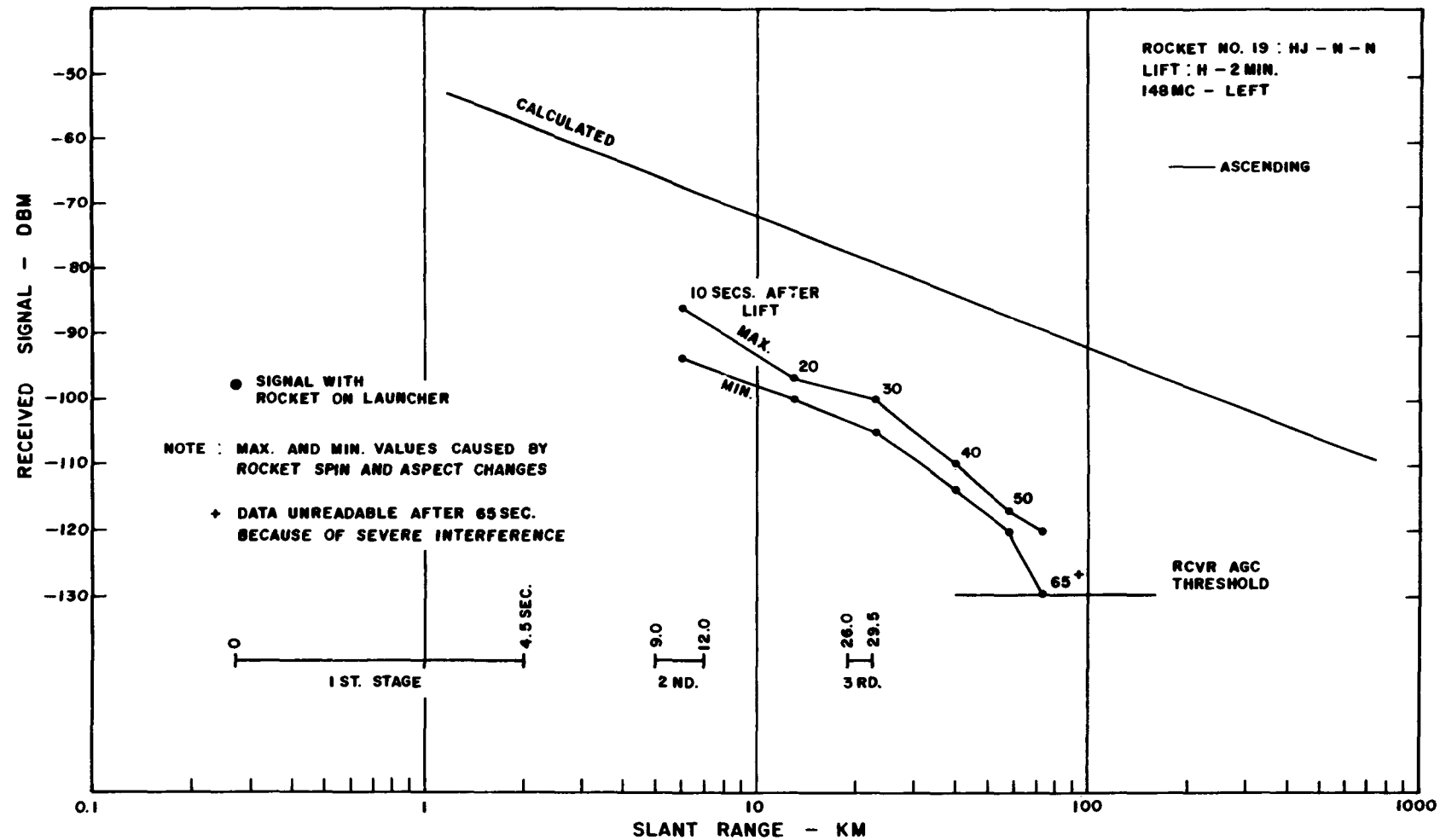

Figure C.170 Received signal strength versus slant range for 3-frequency beacon, 148 Mc left, Rocket 19, King Fish.

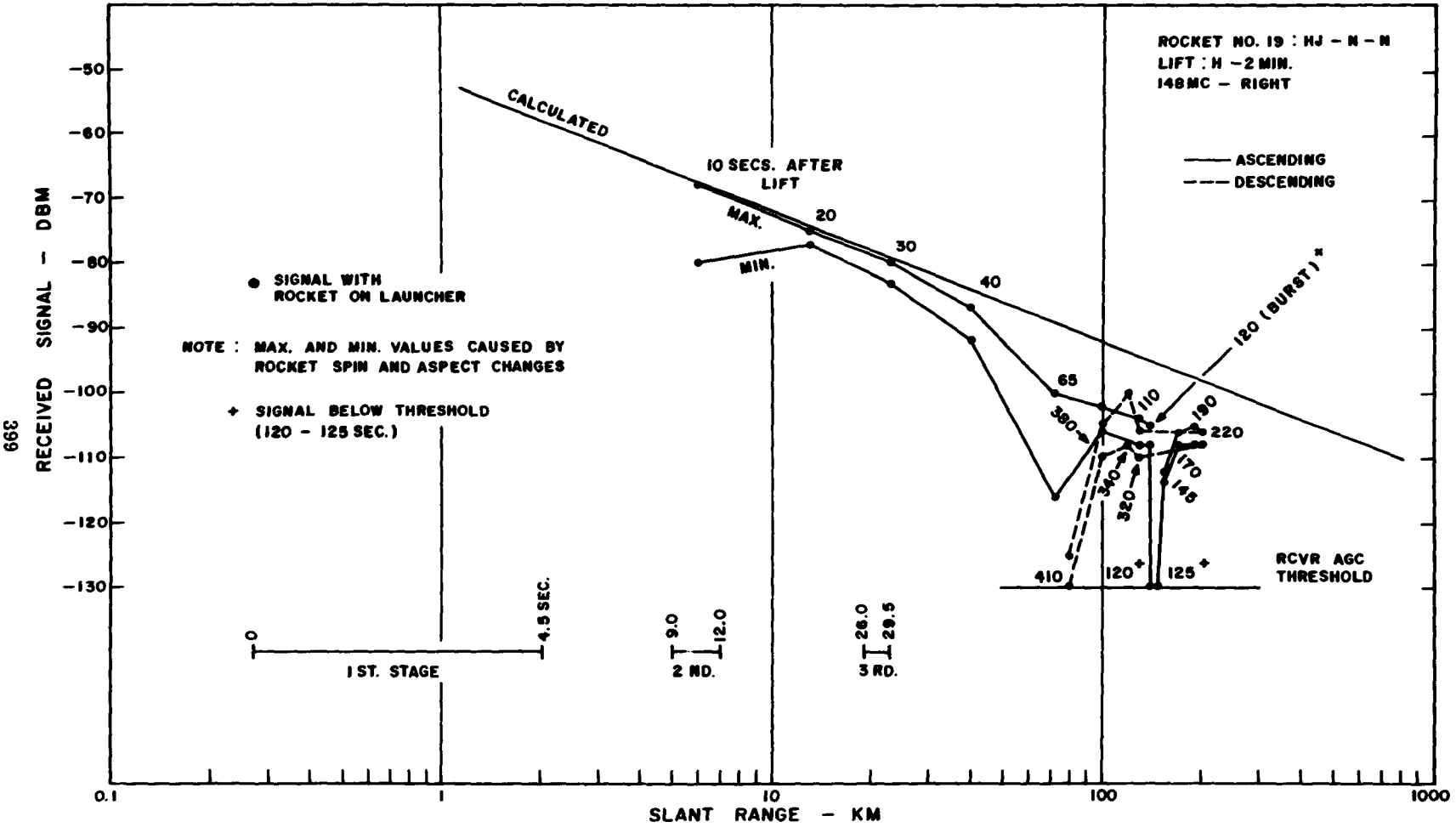

Figure C.171 Received signal strength versus slant range for 3-frequency beacon, 148 Mc right, Rocket 19, King Fish.

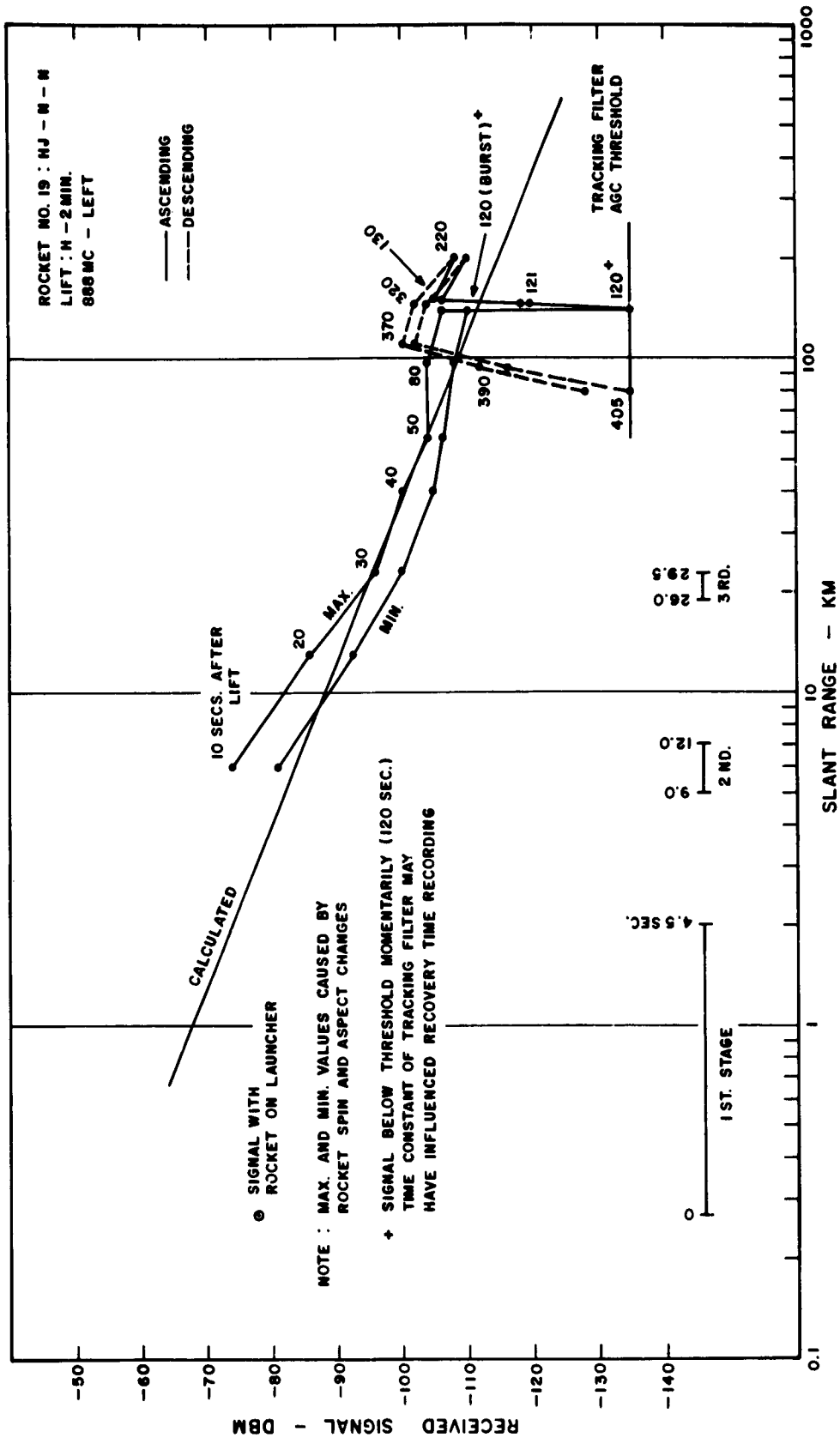

Figure C.172 Received signal strength versus slant range for 3-frequency beacon, 888 Mc left, Rocket 19, King Fish.

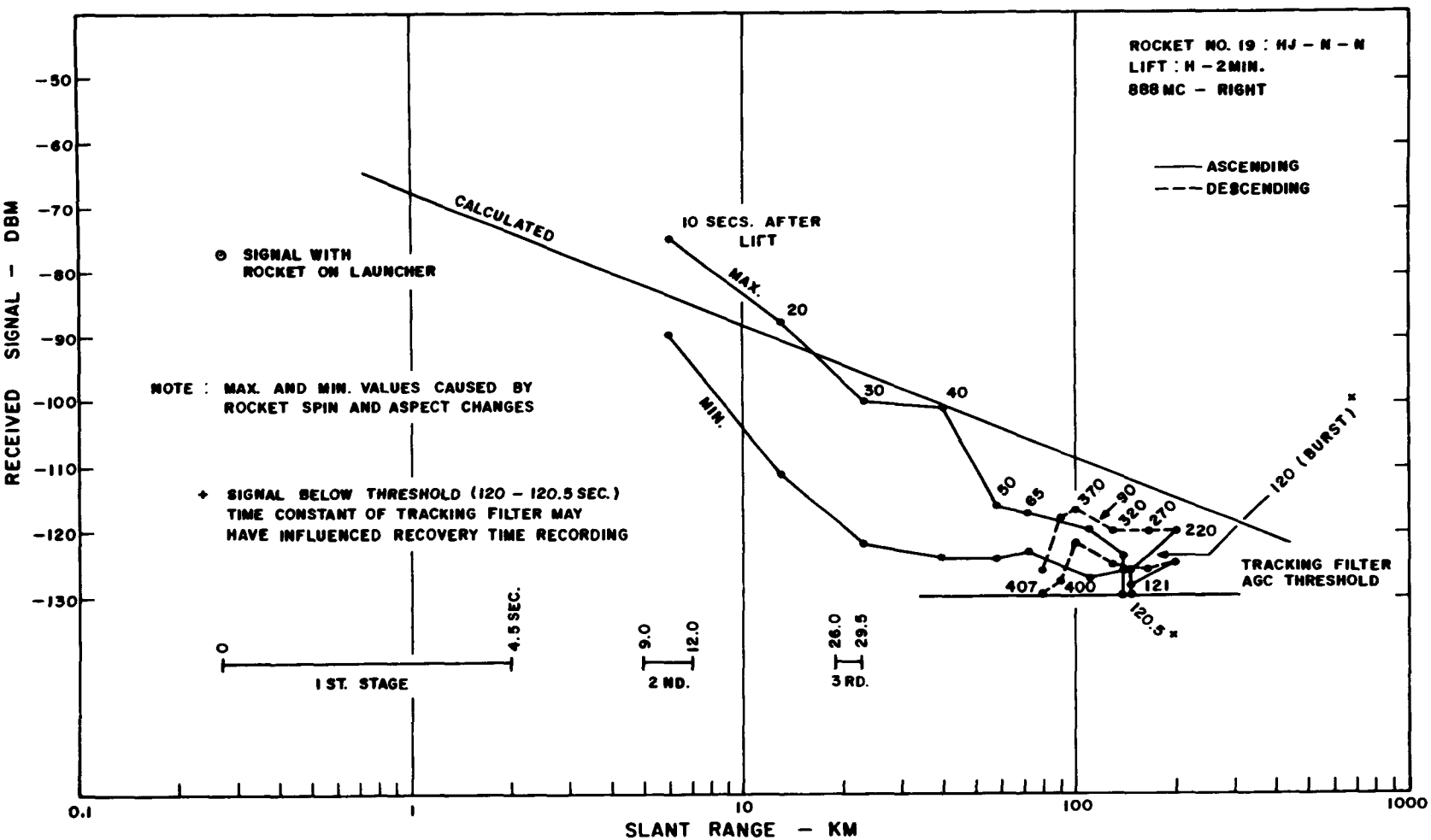

Figure C.173 Received signal strength versus slant range for 3-frequency beacon, 888 Mc right, Rocket 19, King Fish.

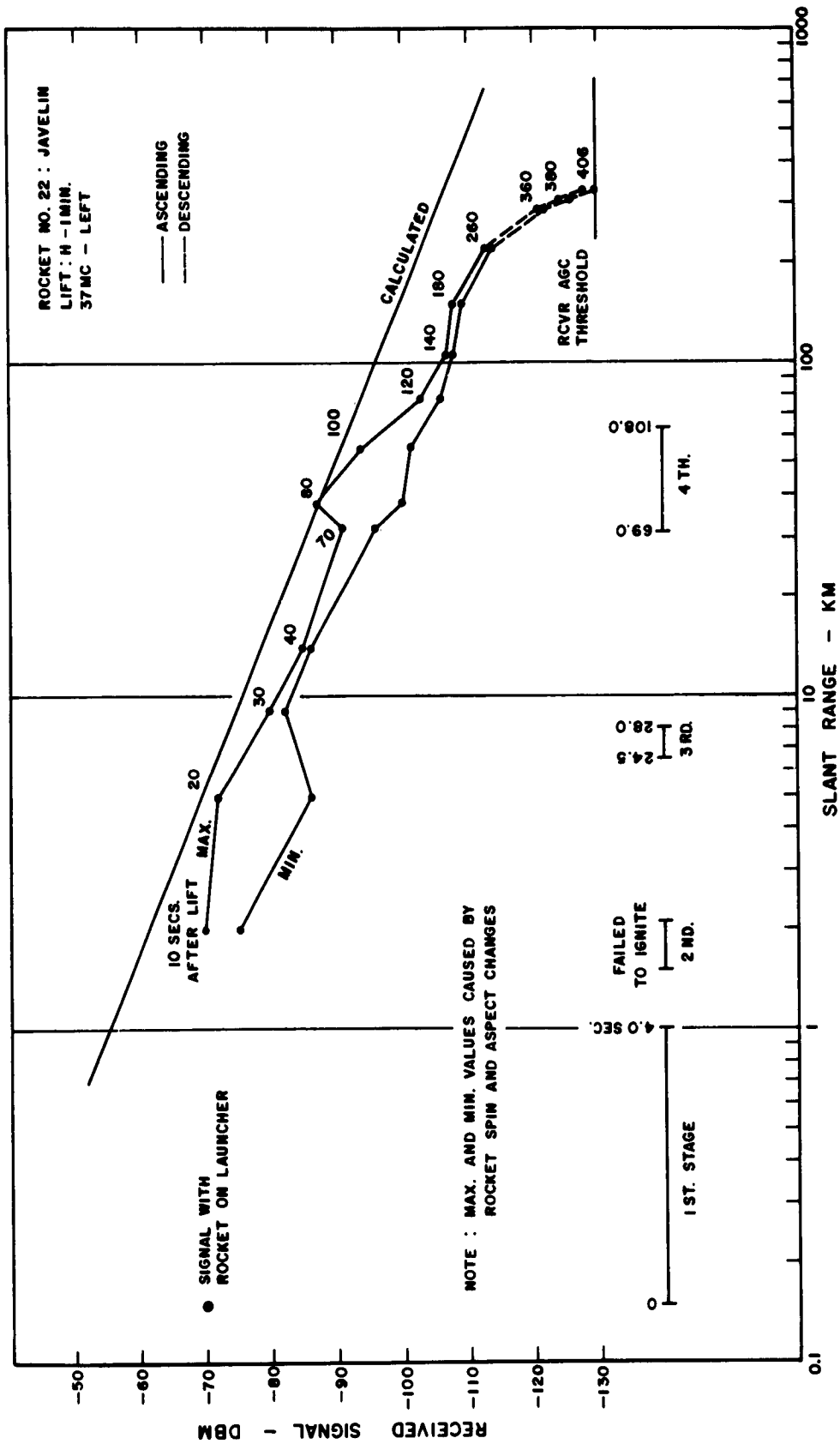

Figure C.174 Received signal strength versus slant range for 3-frequency beacon, 37 Mc left, Rocket 22, King Fish.

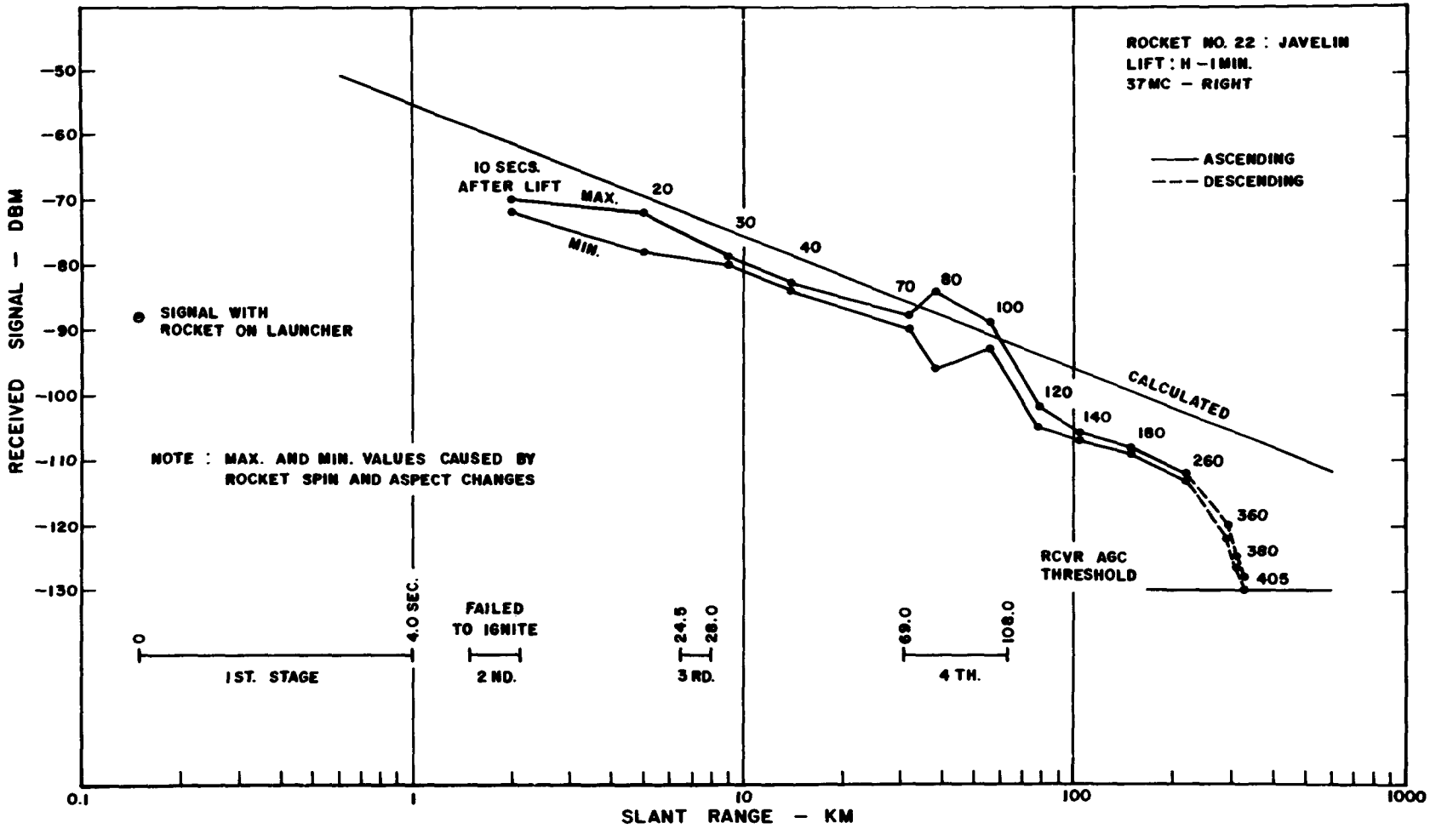

Figure C.175 Received signal strength versus slant range for 3-frequency beacon, 37 Mc right, Rocket 22, King Fish.

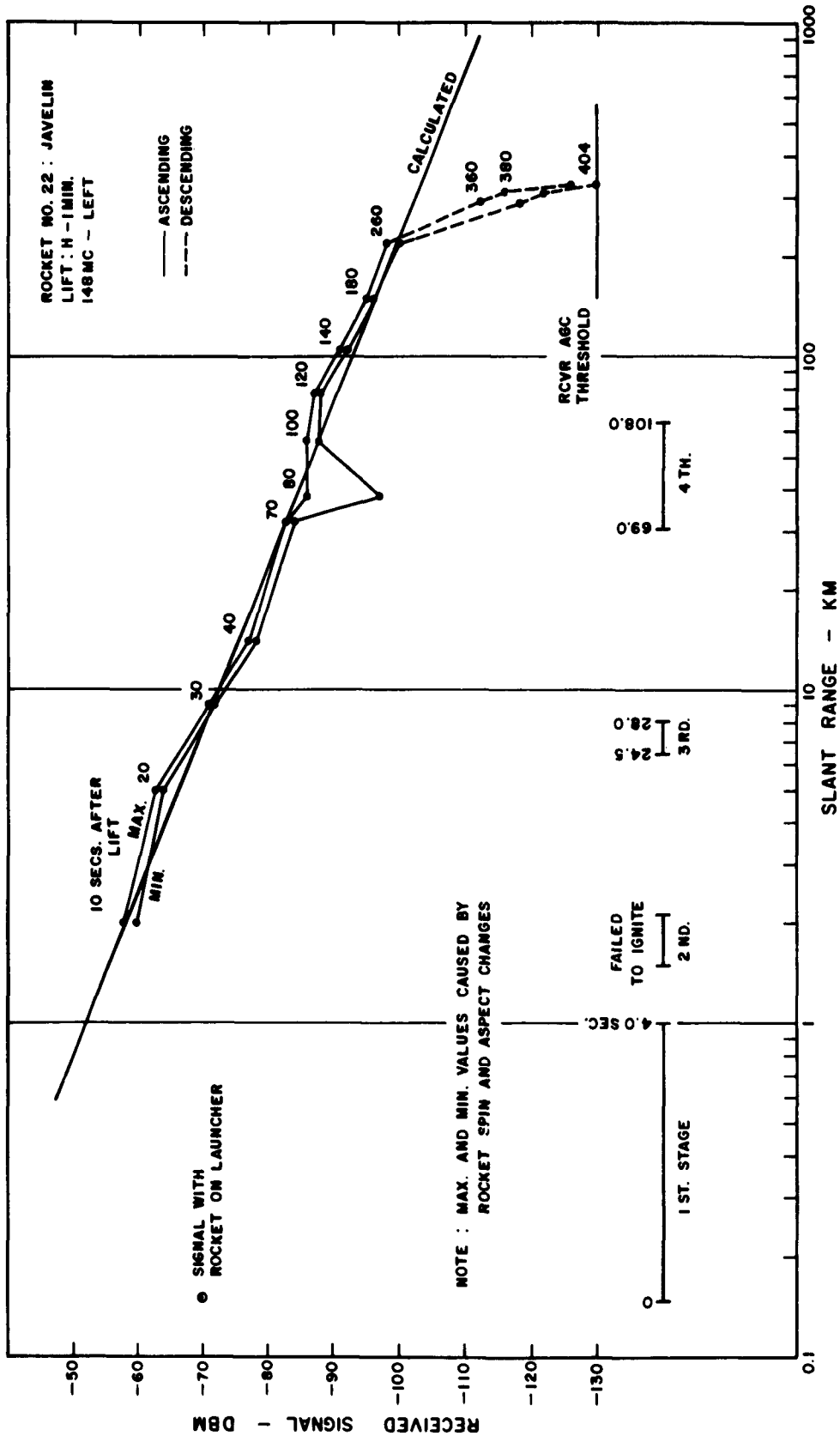

Figure C.176 Received signal strength versus slant range for 3-frequency beacon, 148 Mc left, Rocket 22, King Fish.

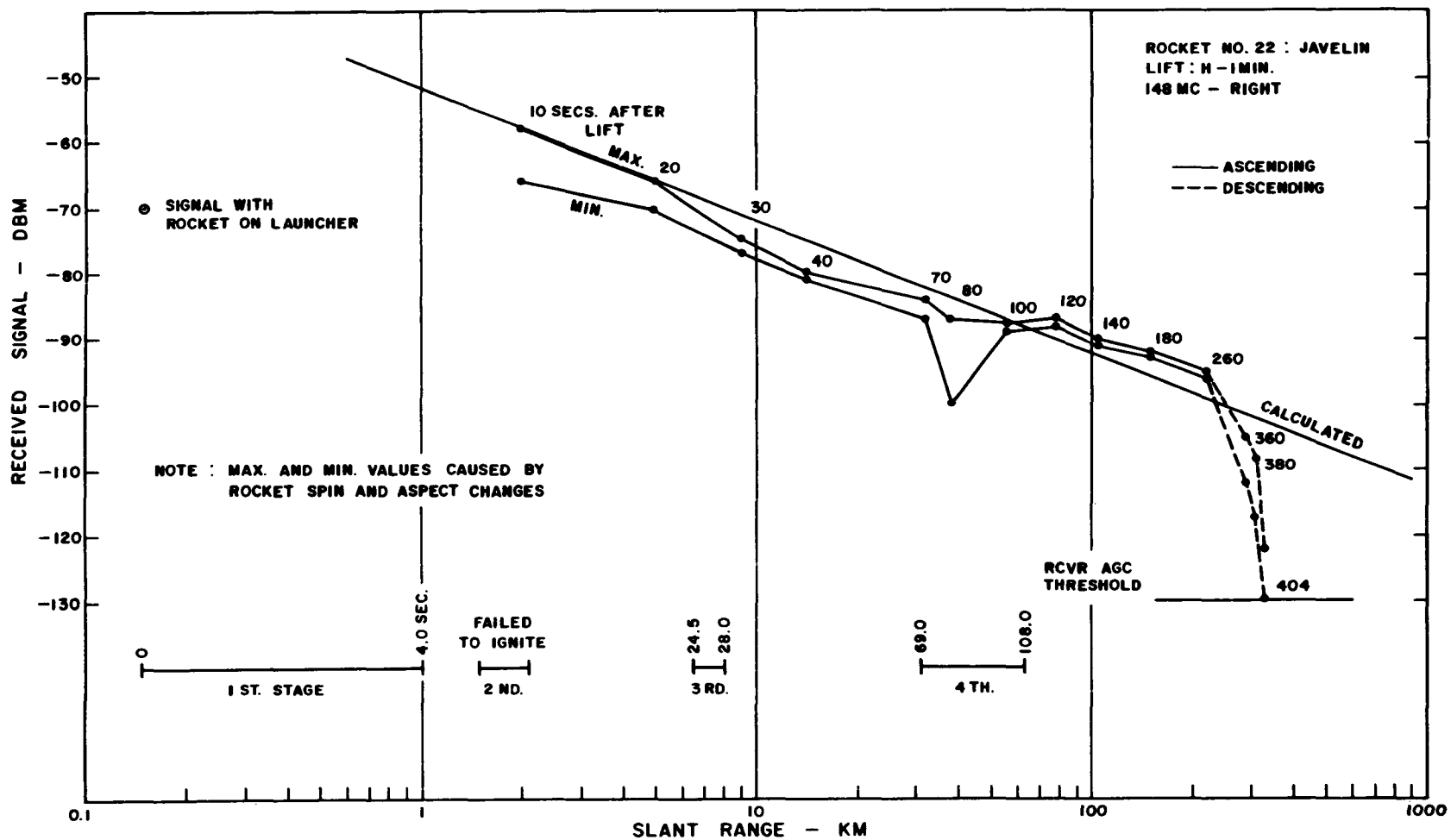

Figure C.177 Received signal strength versus slant range for 3-frequency beacon, 148 Mc right, Rocket 22, King Fish.

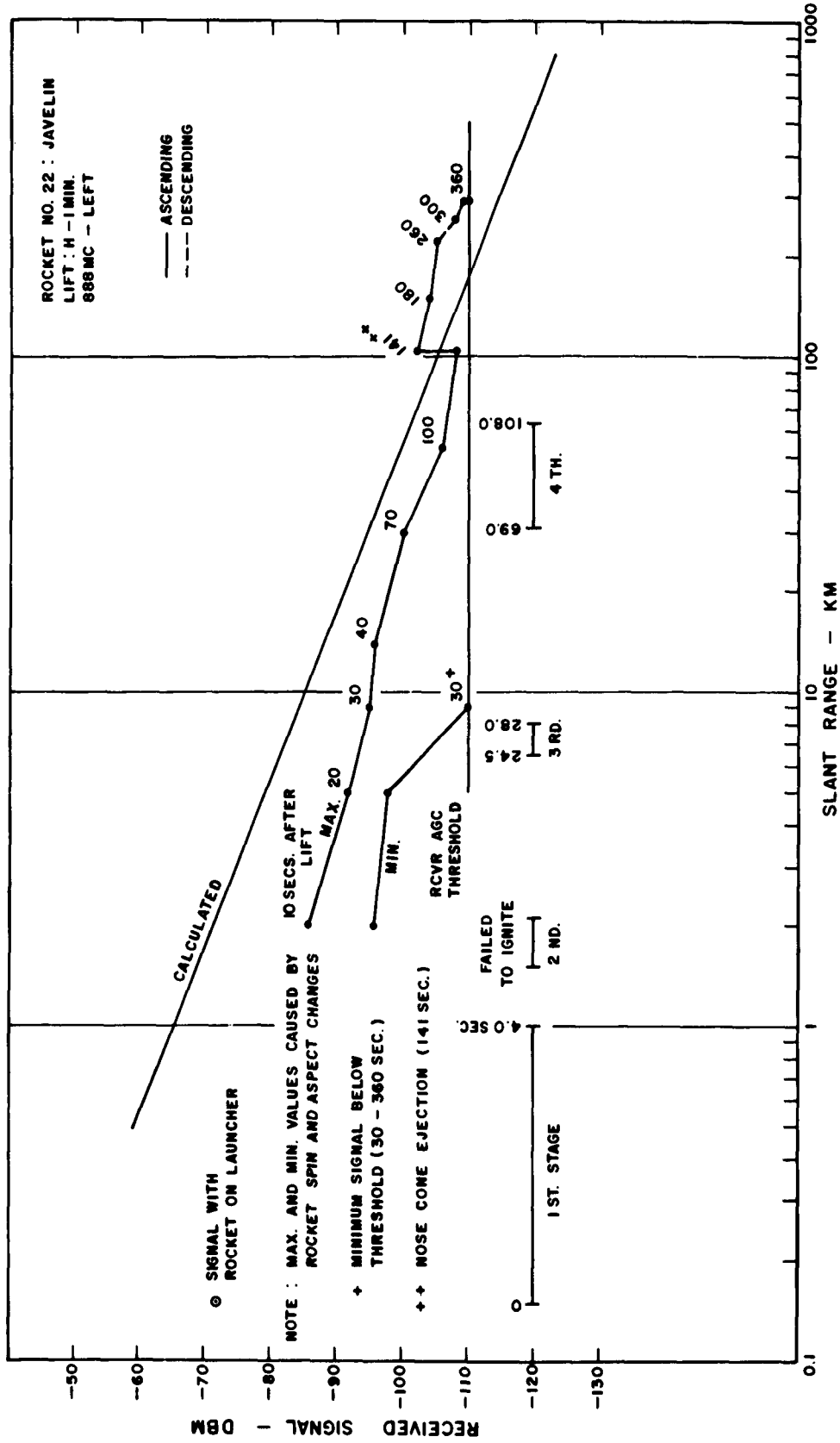

Figure C.178 Received signal strength versus slant range for 3-frequency beacon, 888 Mc left, Rocket 22, King Fish.

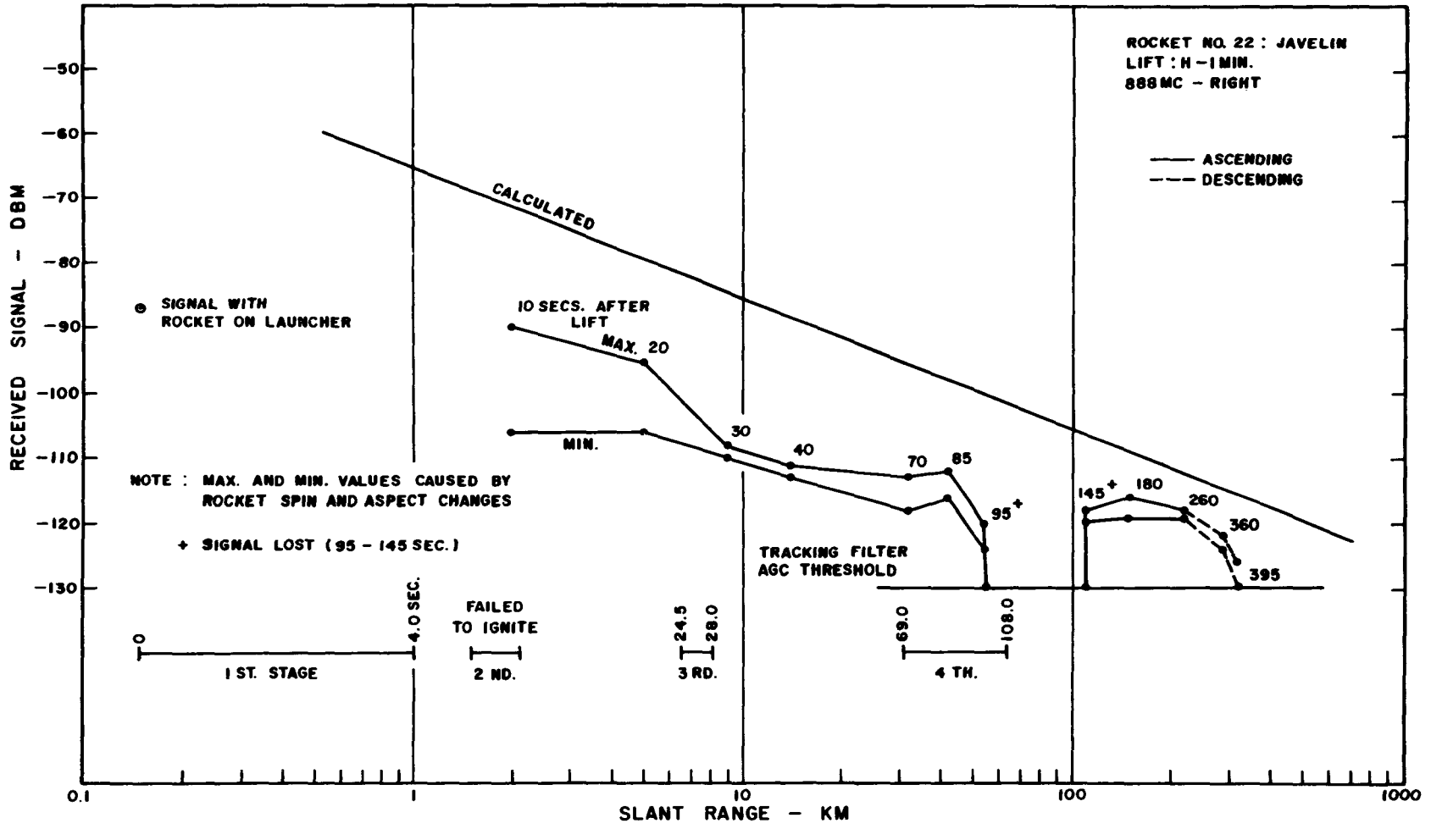

Figure C.179 Received signal strength versus slant range for 3-frequency beacon, 888 Mc right, Rocket 22, King Fish.

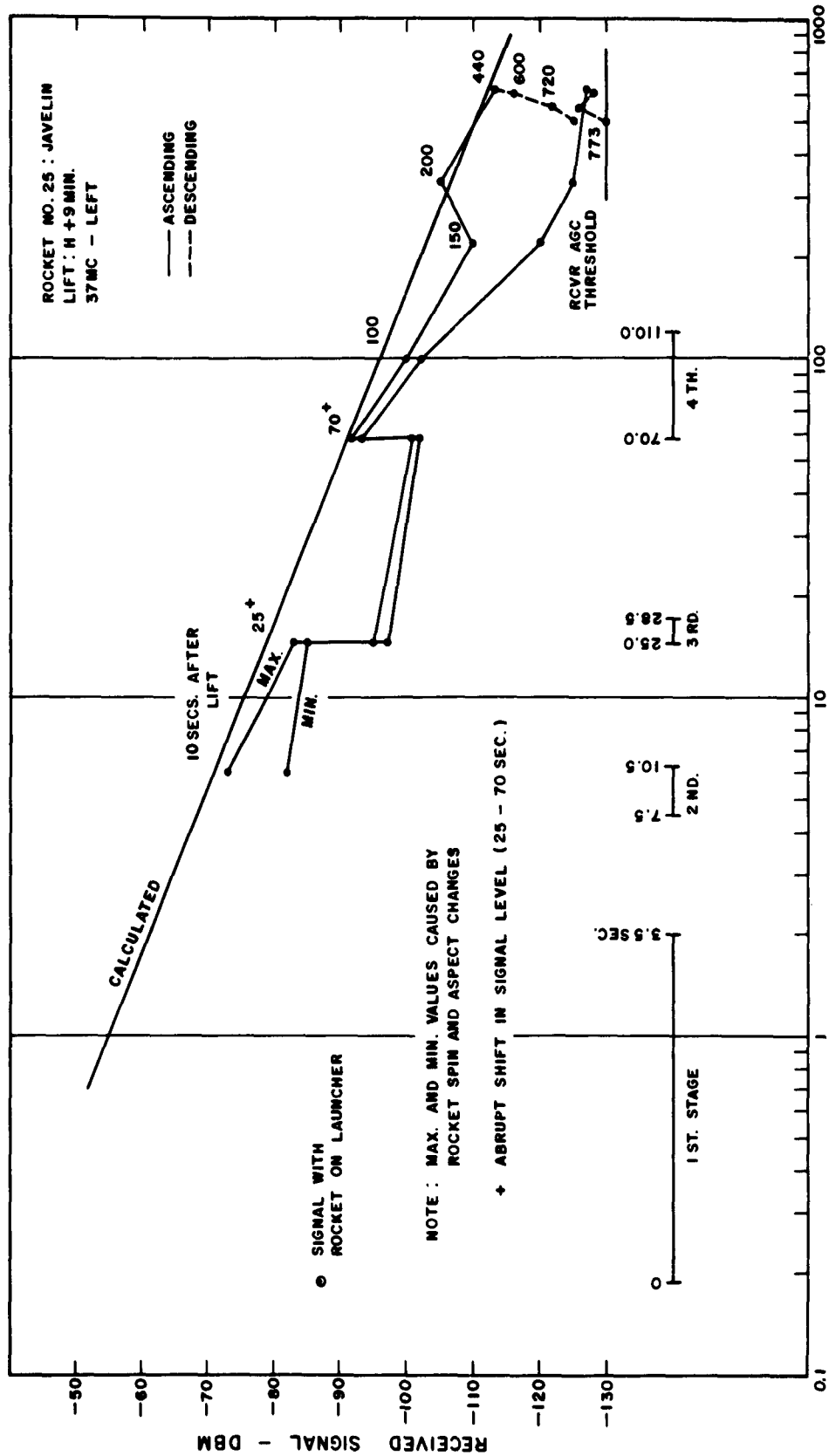

Figure C.180 Received signal strength versus slant range for 3-frequency beacon, 37 Mc left, Rocket 25, King Fish.

SECRET

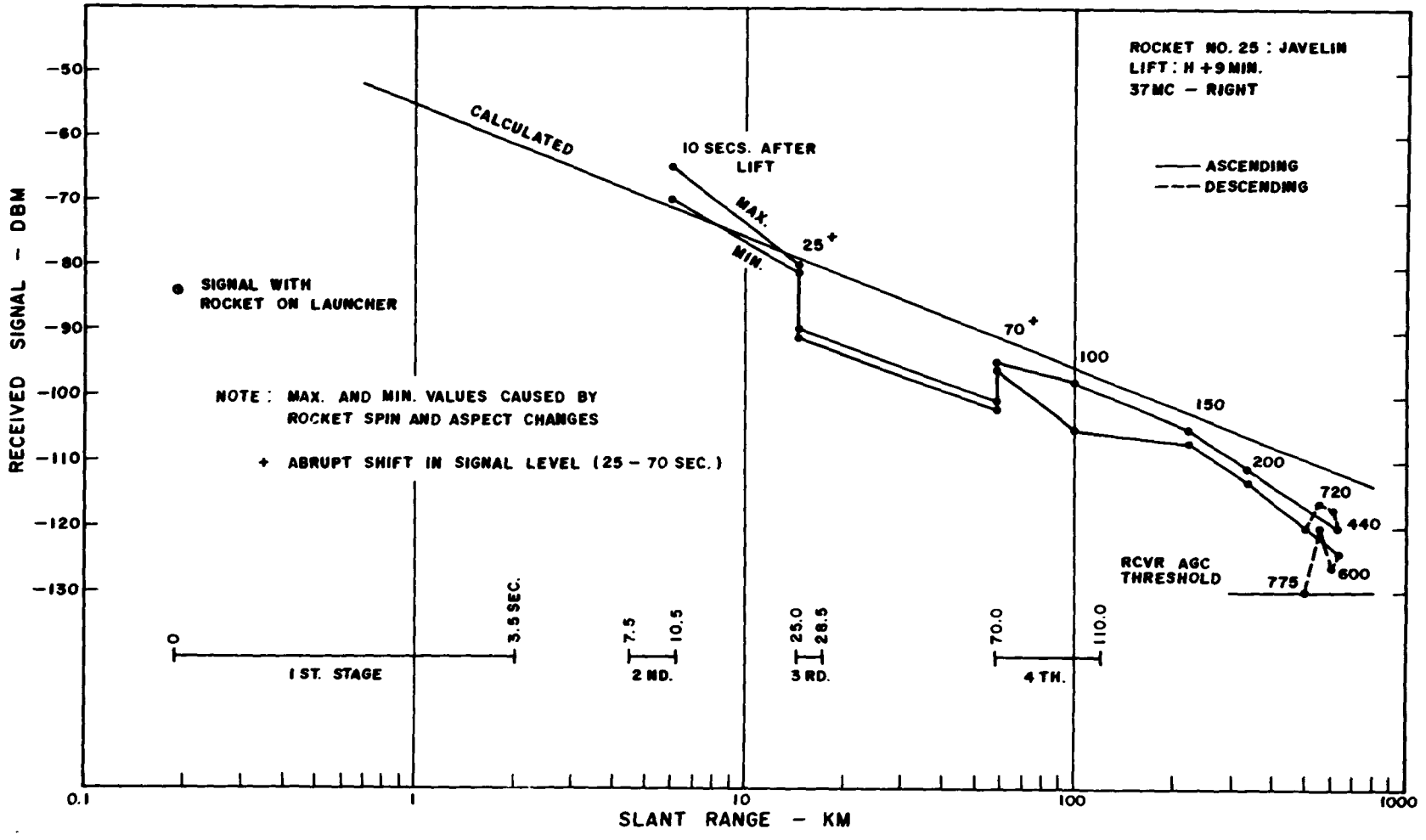

Figure C.181 Received signal strength versus slant range for 3-frequency beacon, 37 Mc right, Rocket 25, King Fish.

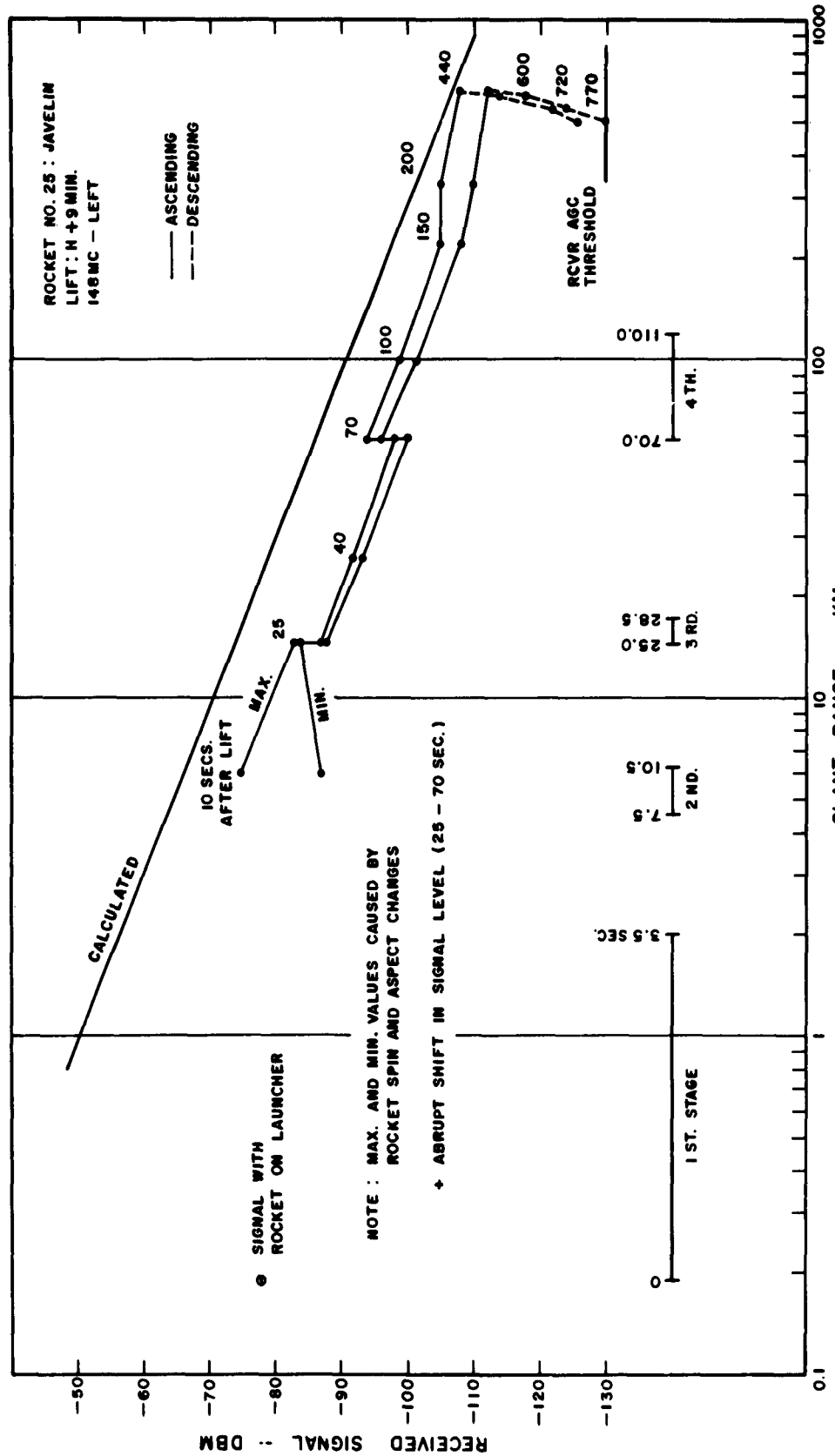

Figure C.182 Received signal strength versus slant range for 3-frequency beacon, 148 Mc left, Rocket 25, King Fish.

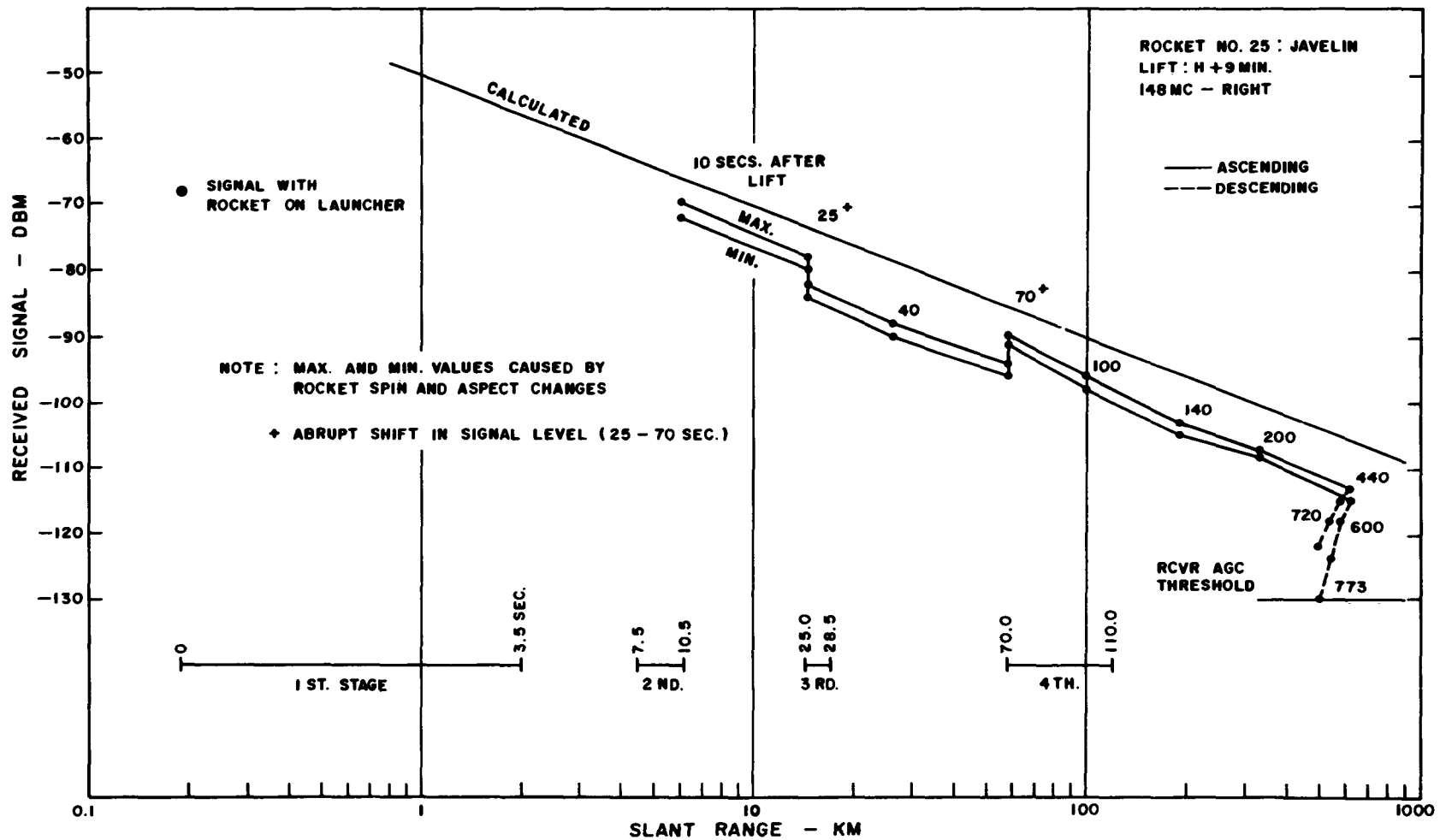

Figure C.183 Received signal strength versus slant range for 3-frequency beacon, 148 Mc right, Rocket 25, King Fish.

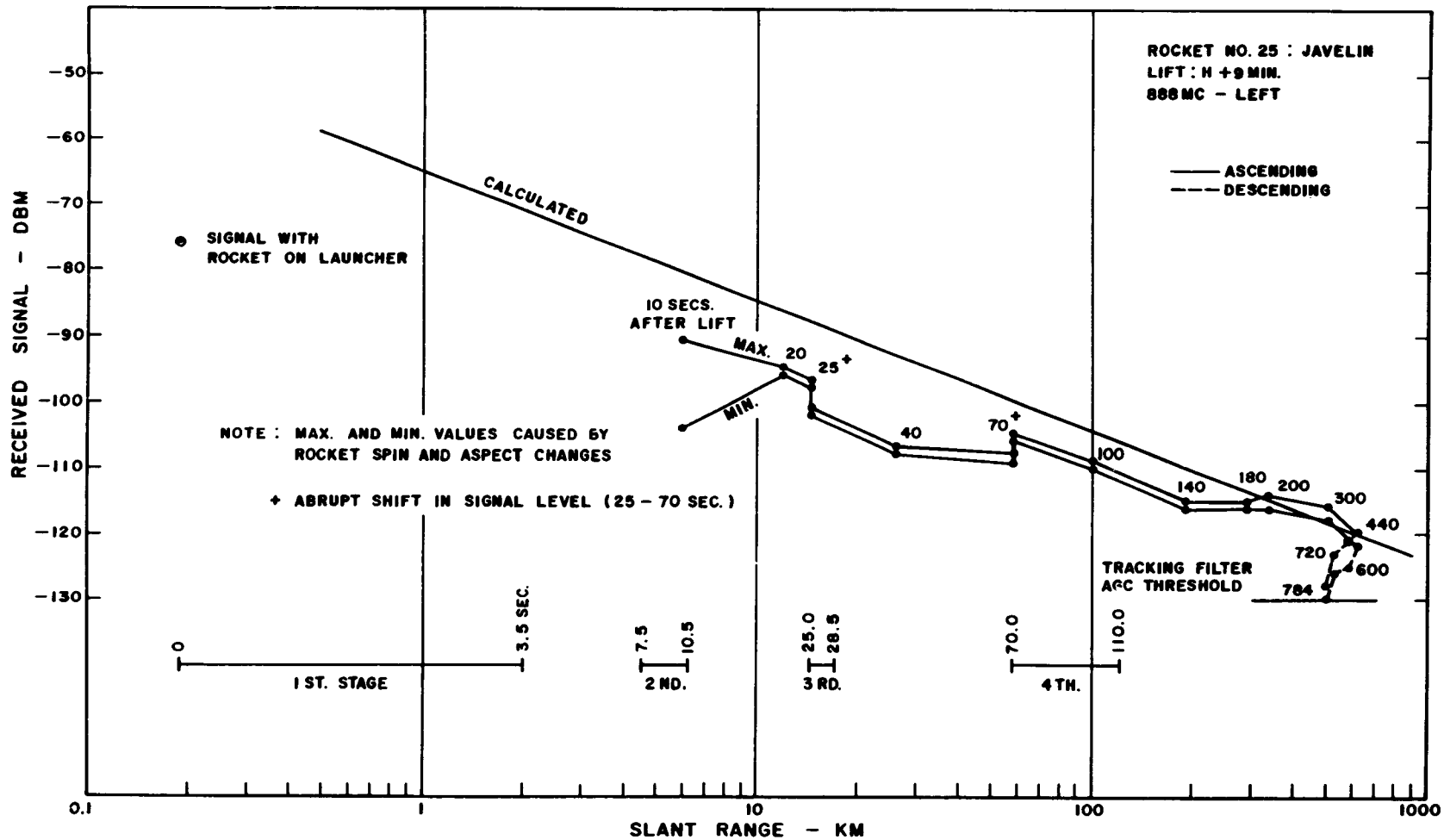

Figure C.184 Received signal strength versus slant range for 3-frequency beacon, 888 Mc left, Rocket 25, King Fish.

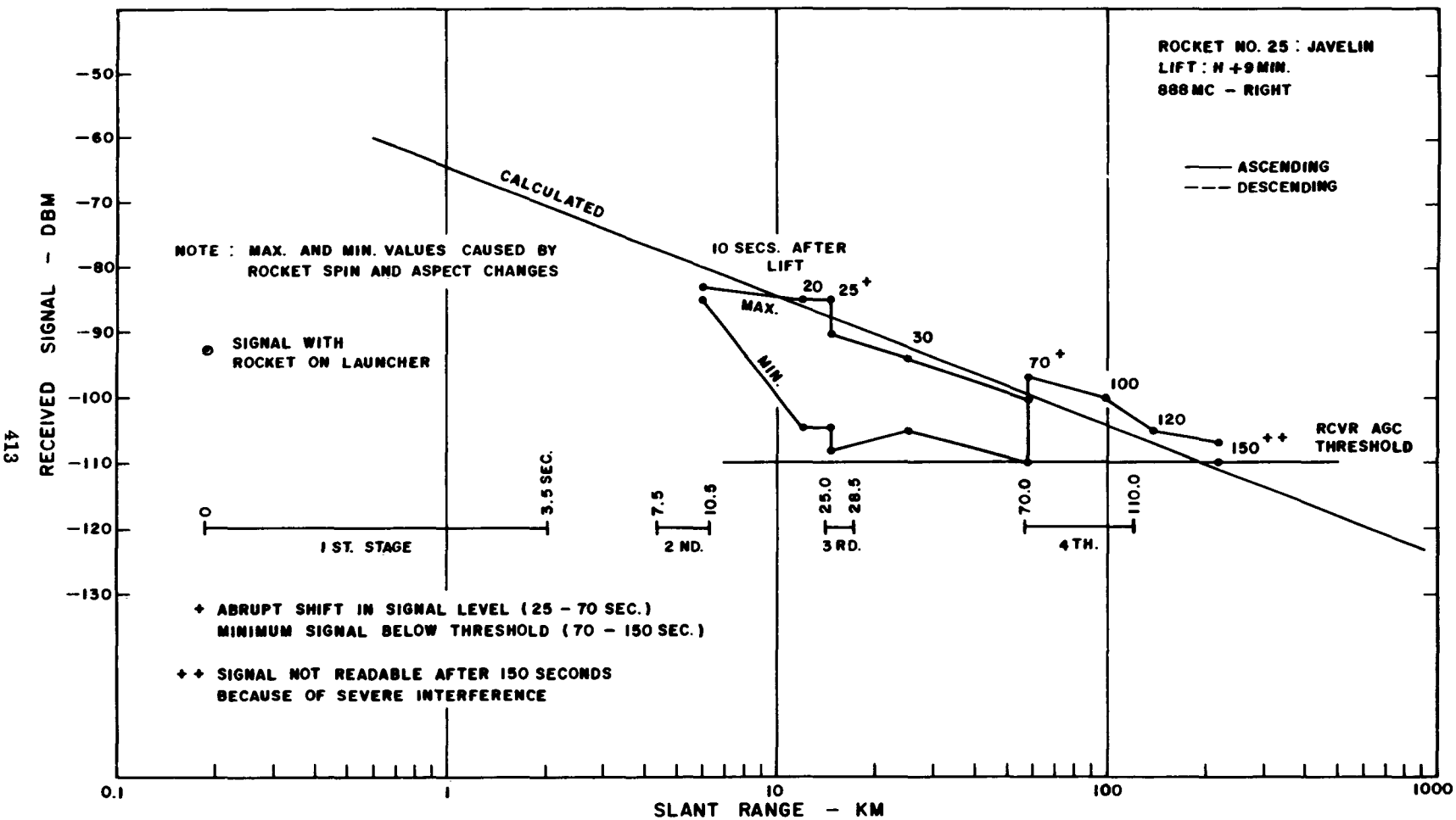

Figure C.185 Received signal strength versus slant range for 3-frequency beacon, 888 Mc right, Rocket 25, King Fish.

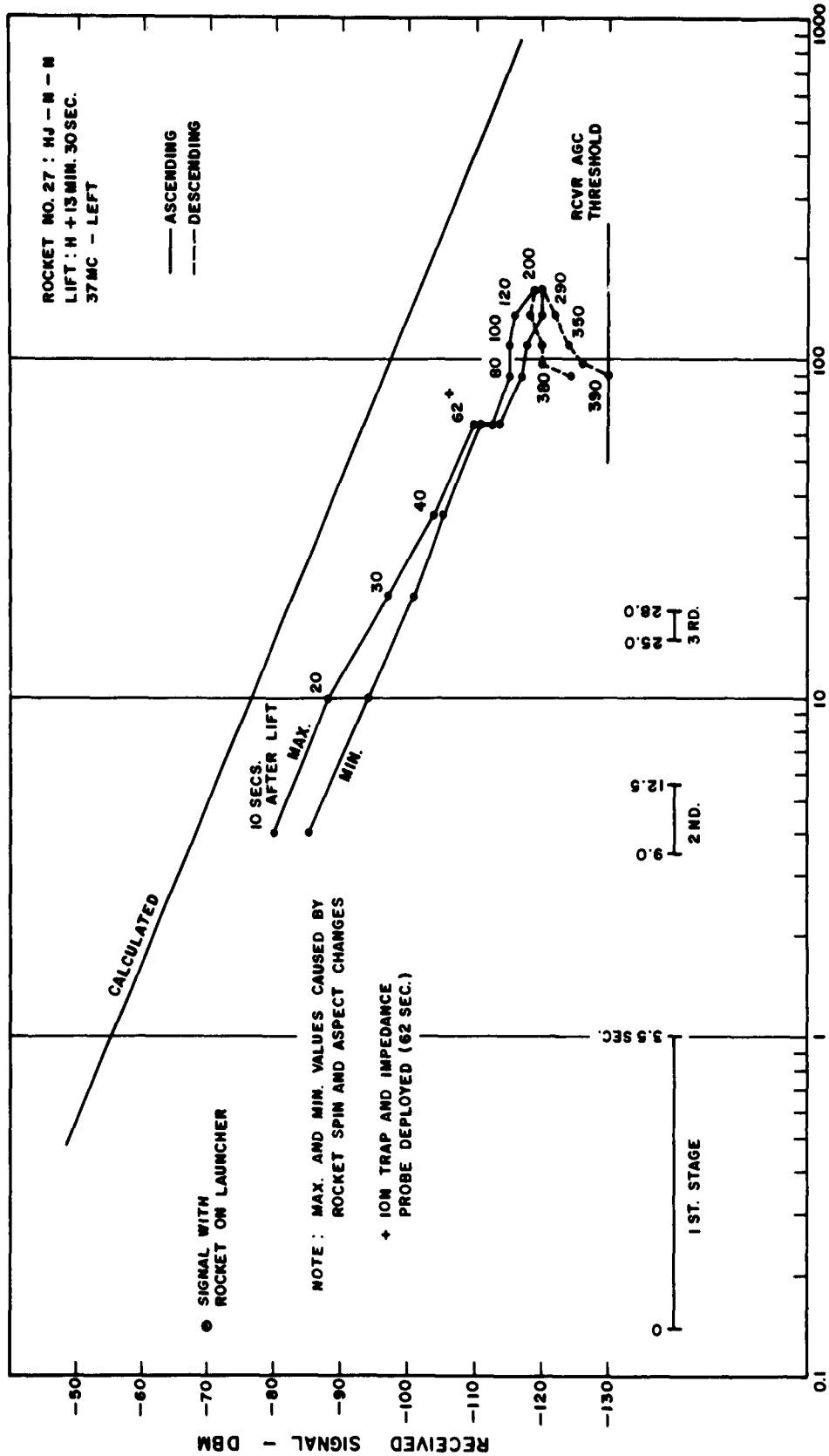

Figure C.186 Received signal strength versus slant range for 3-frequency beacon, 37 Mc left, Rocket 27, King Fish.

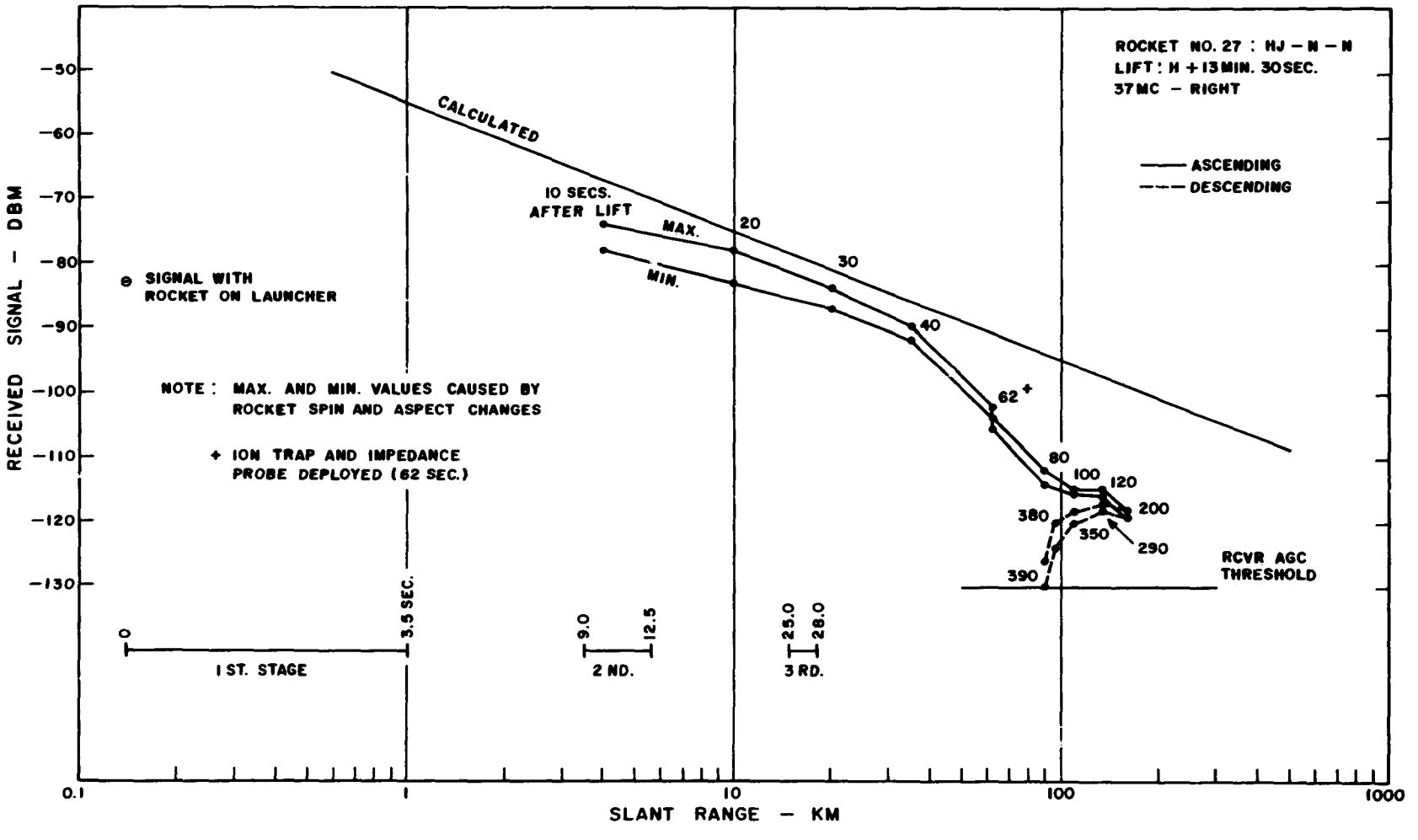

Figure C.187 Received signal strength versus slant range for 3-frequency beacon, 37 Mc right, Rocket 27, King Fish.

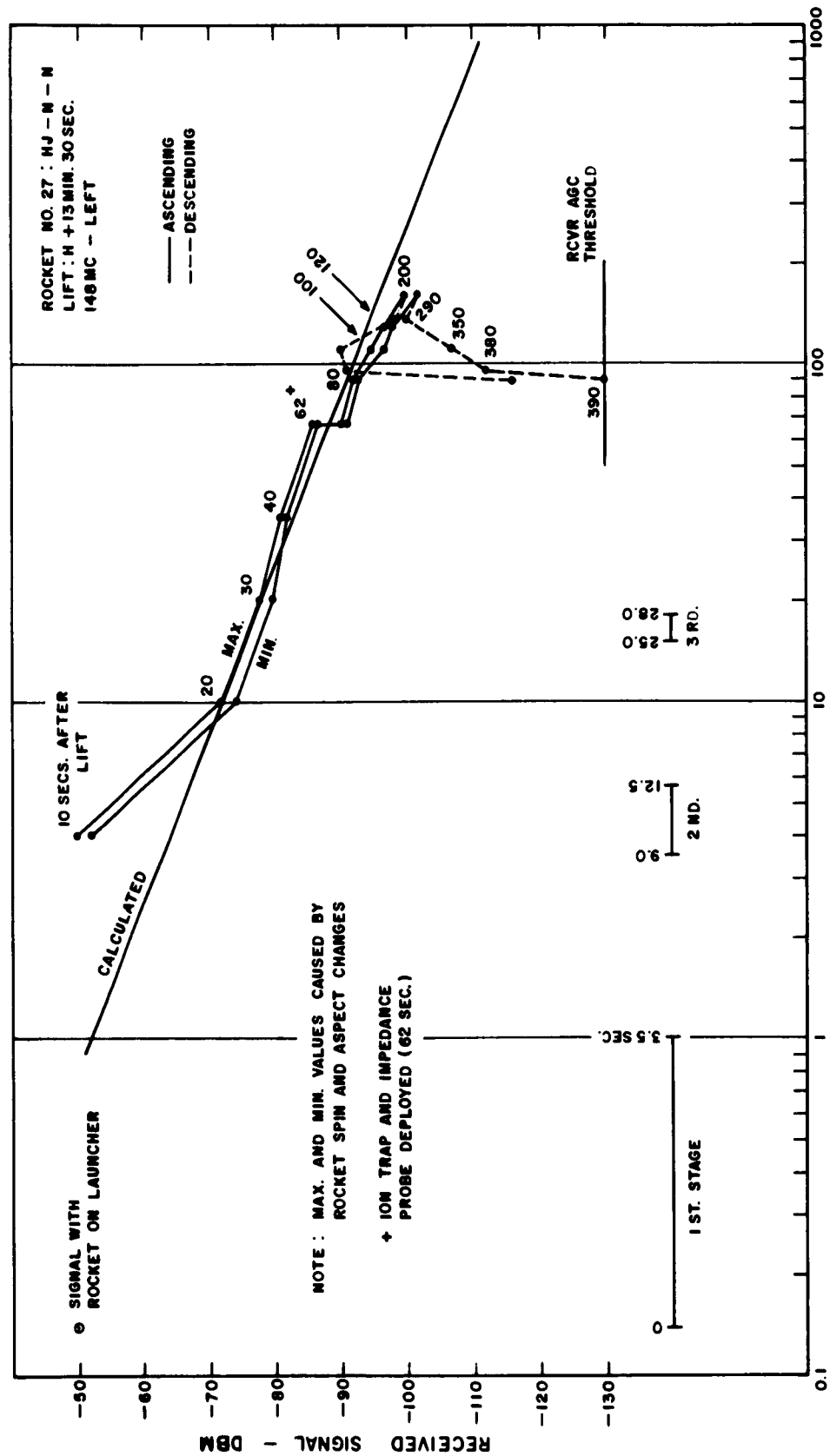

Figure C.188 Received signal strength versus slant range for 3-frequency beacon, 148 Mc left, Rocket 27, King Fish.

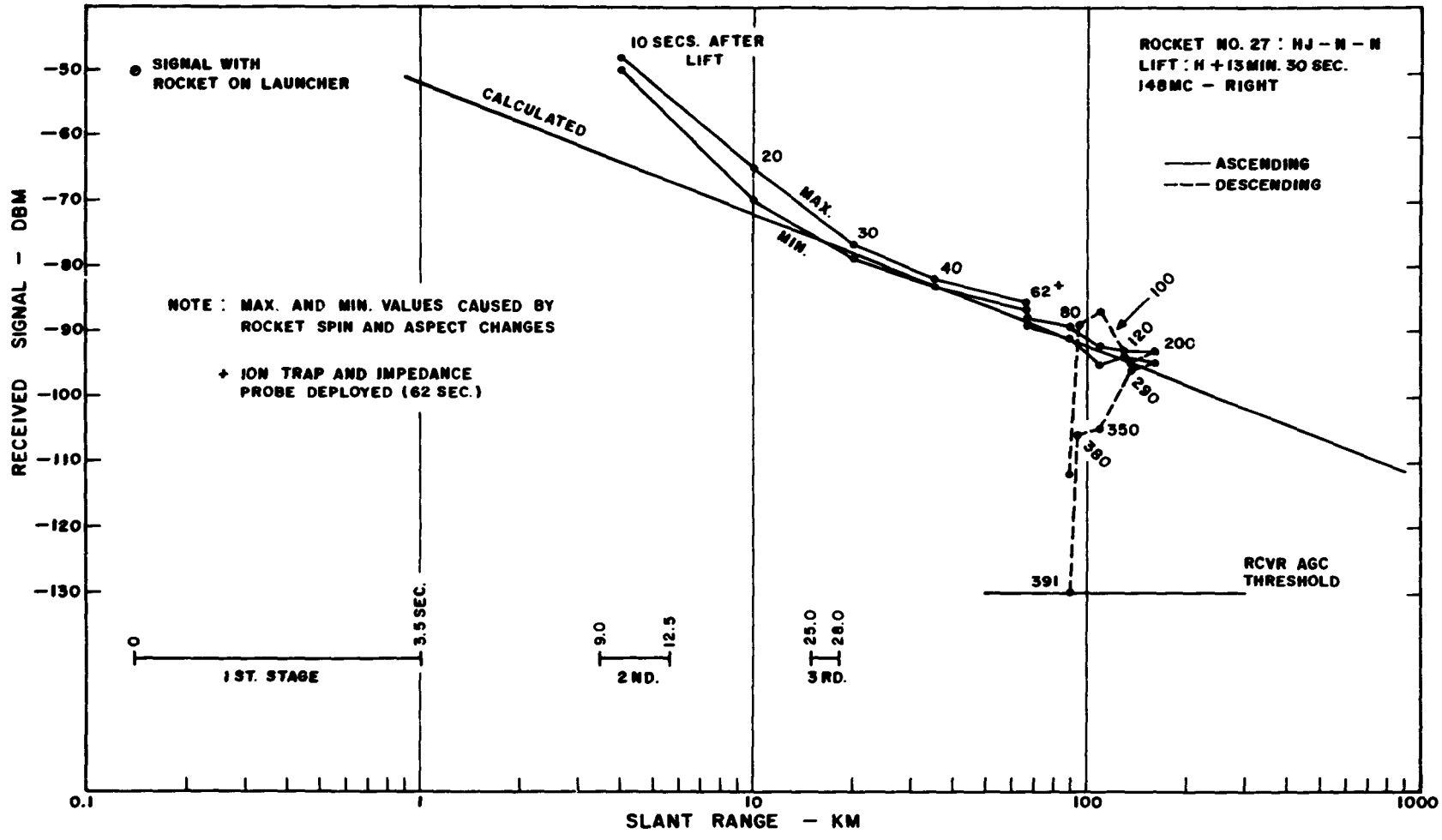

Figure C.189 Received signal strength versus slant range for 3-frequency beacon, 148 Mc right, Rocket 27, King Fish.

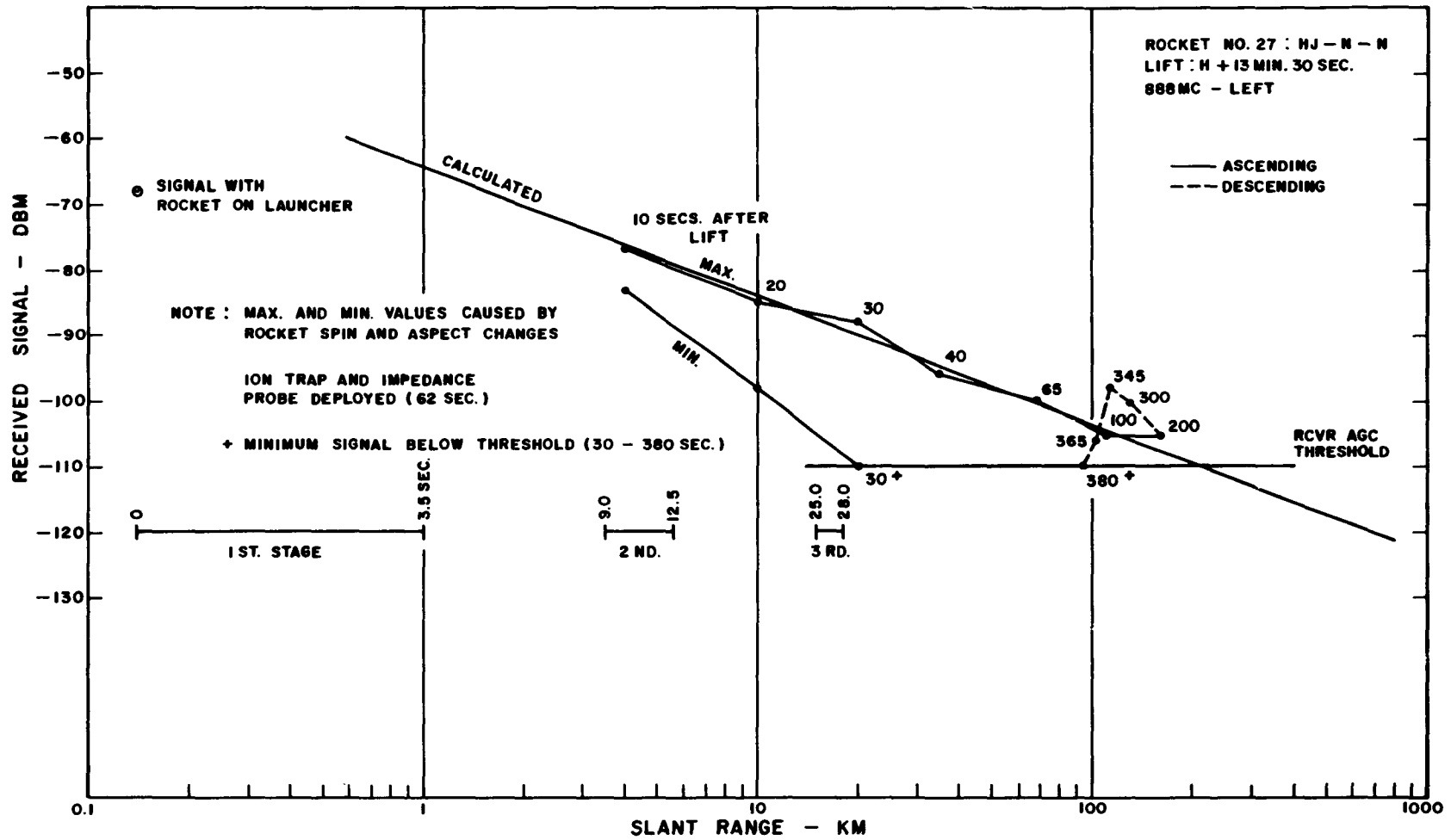

Figure C.190 Received signal strength versus slant range for 3-frequecny beacon, 888 Mc left, Rocket 27, King Fish.

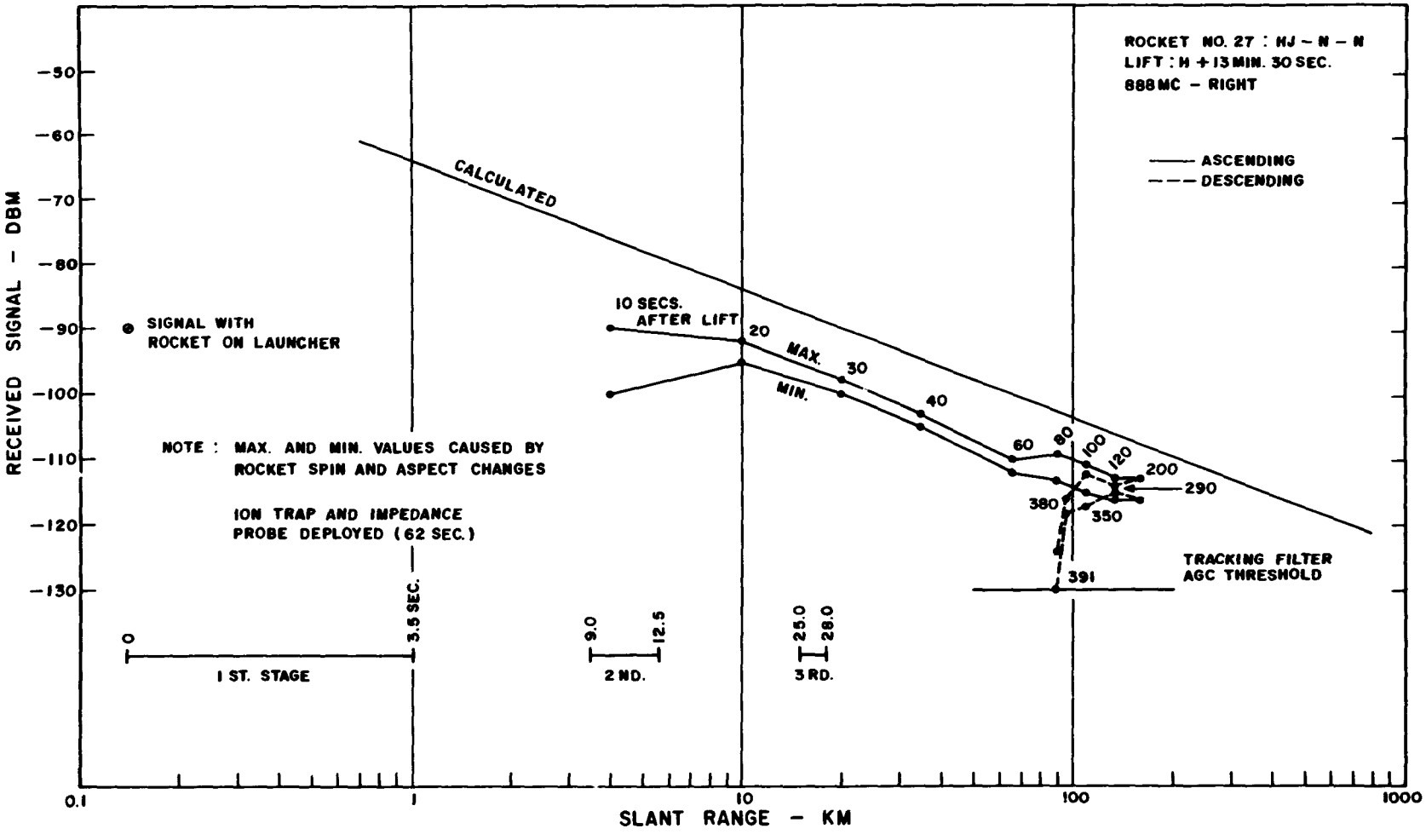

Figure C.191 Received signal strength versus slant range for 3-frequency beacon, 888 Mc right, Rocket 27, King Fish.

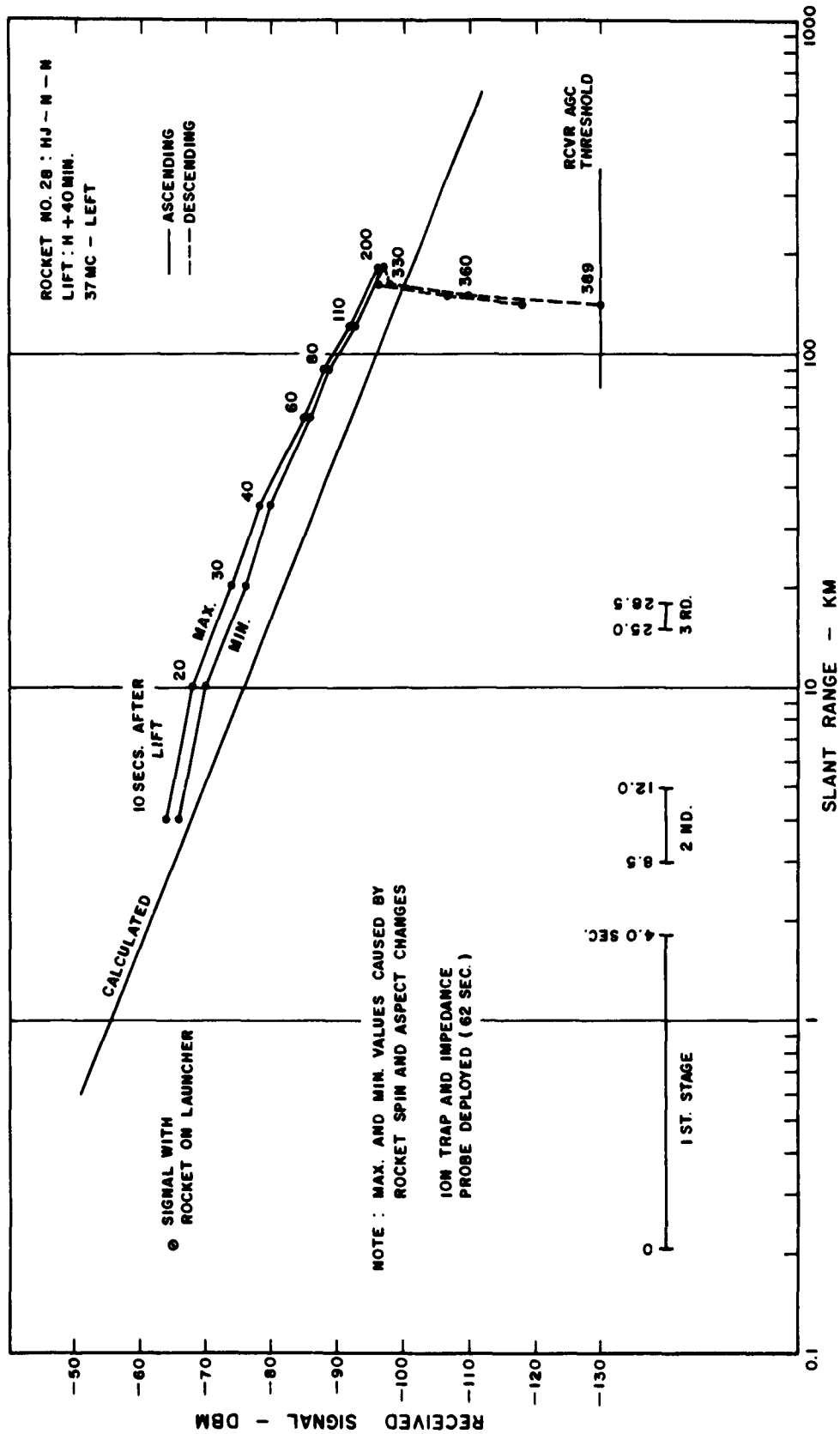

Figure C.192 Received signal strength versus slant range for 3-frequency beacon, 37 Mc left, Rocket 28, King Fish.

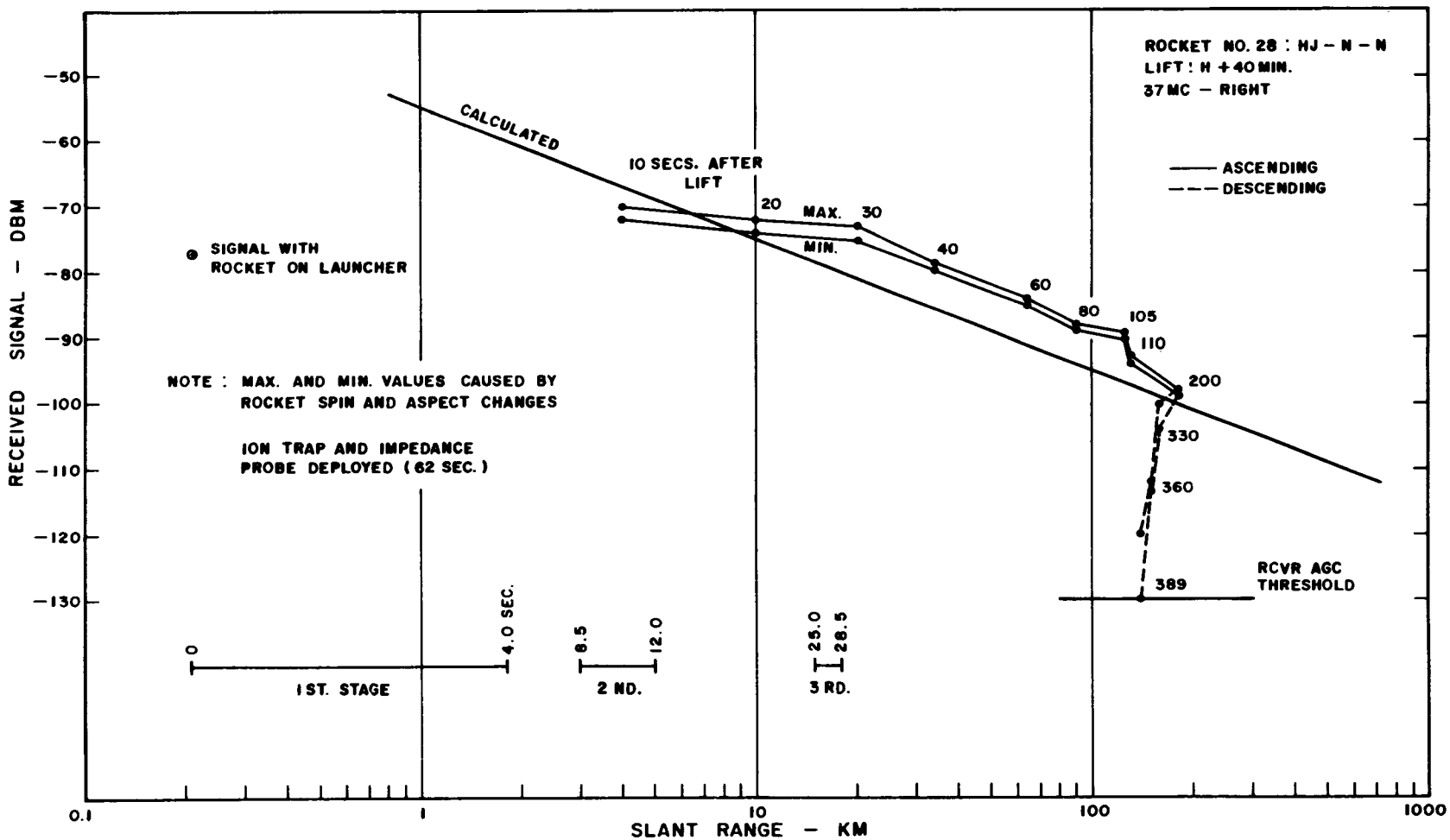

Figure C.193 Received signal strength versus slant range for 3-frequency beacon, 37 Mc right, Rocket 28, King Fish.

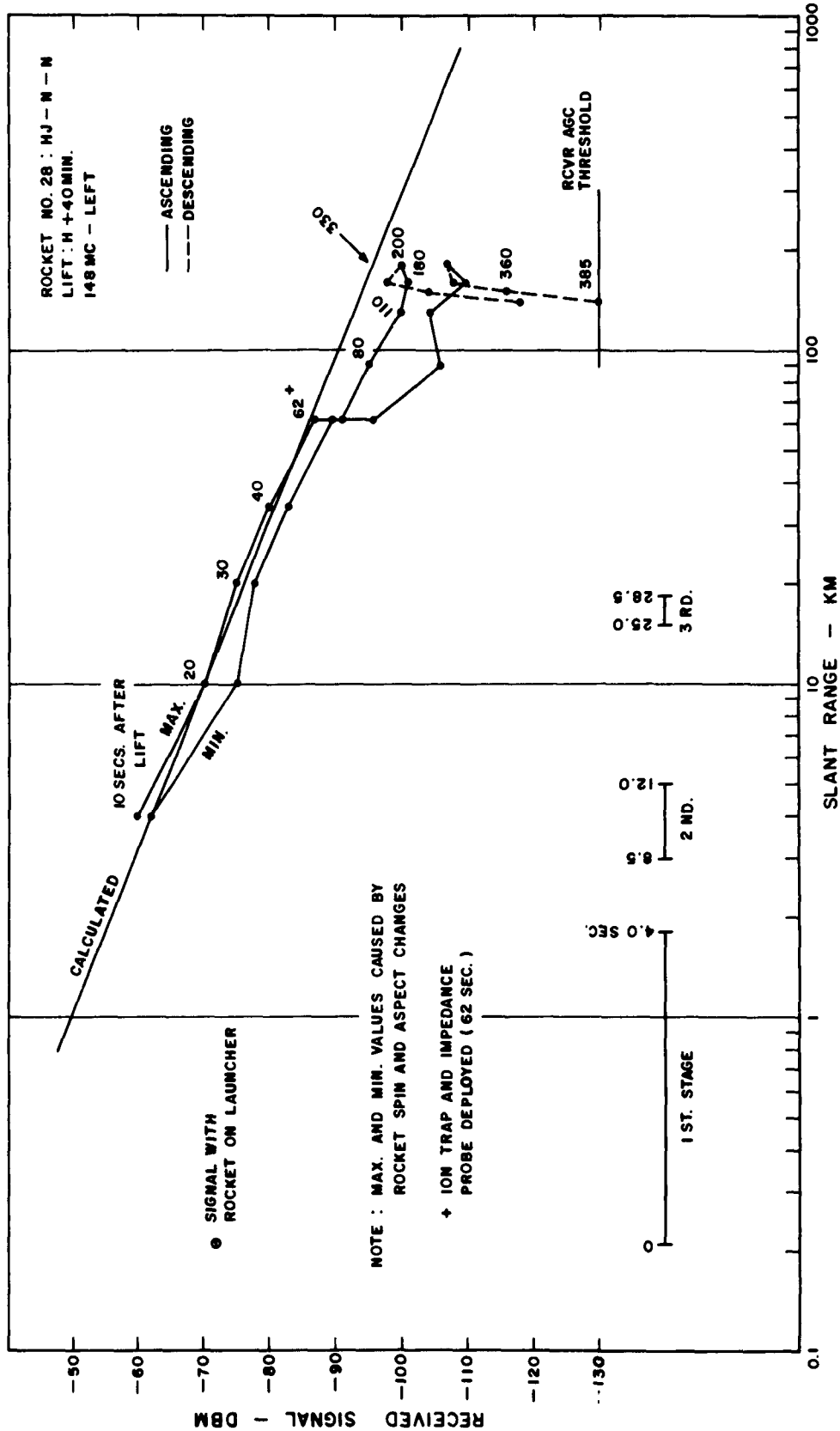

Figure C.194 Received signal strength versus slant range for 3-frequency beacon, 148 Mc left, Rocket 28, King Fish.

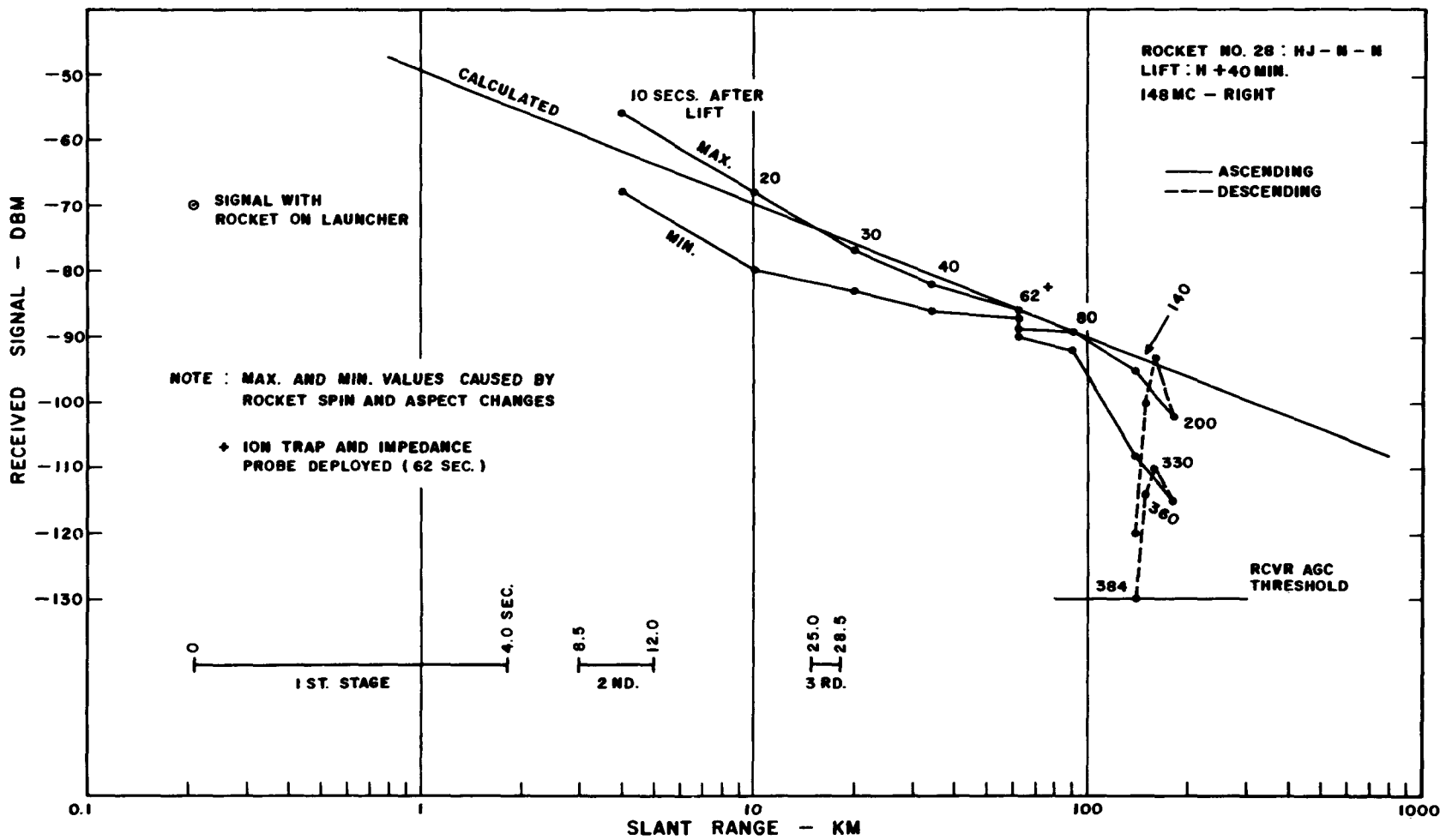

Figure C.195 Received signal strength versus slant range for 3-frequency beacon, 148 Mc right, Rocket 28, King Fish.

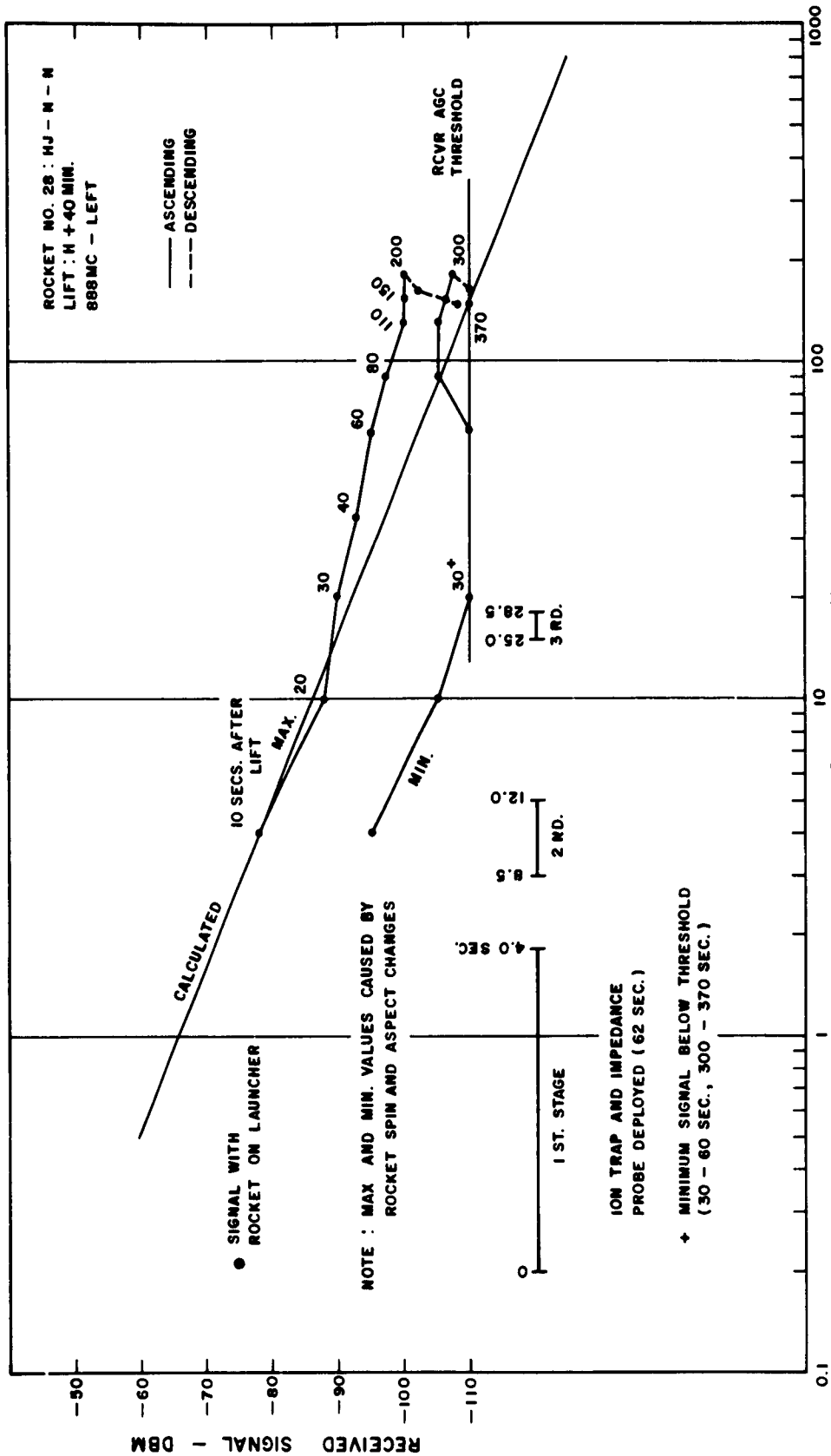

Figure C.196 Received signal strength versus slant range for 3-frequency beacon, 888 Mc left, Rocket 28, King Fish.

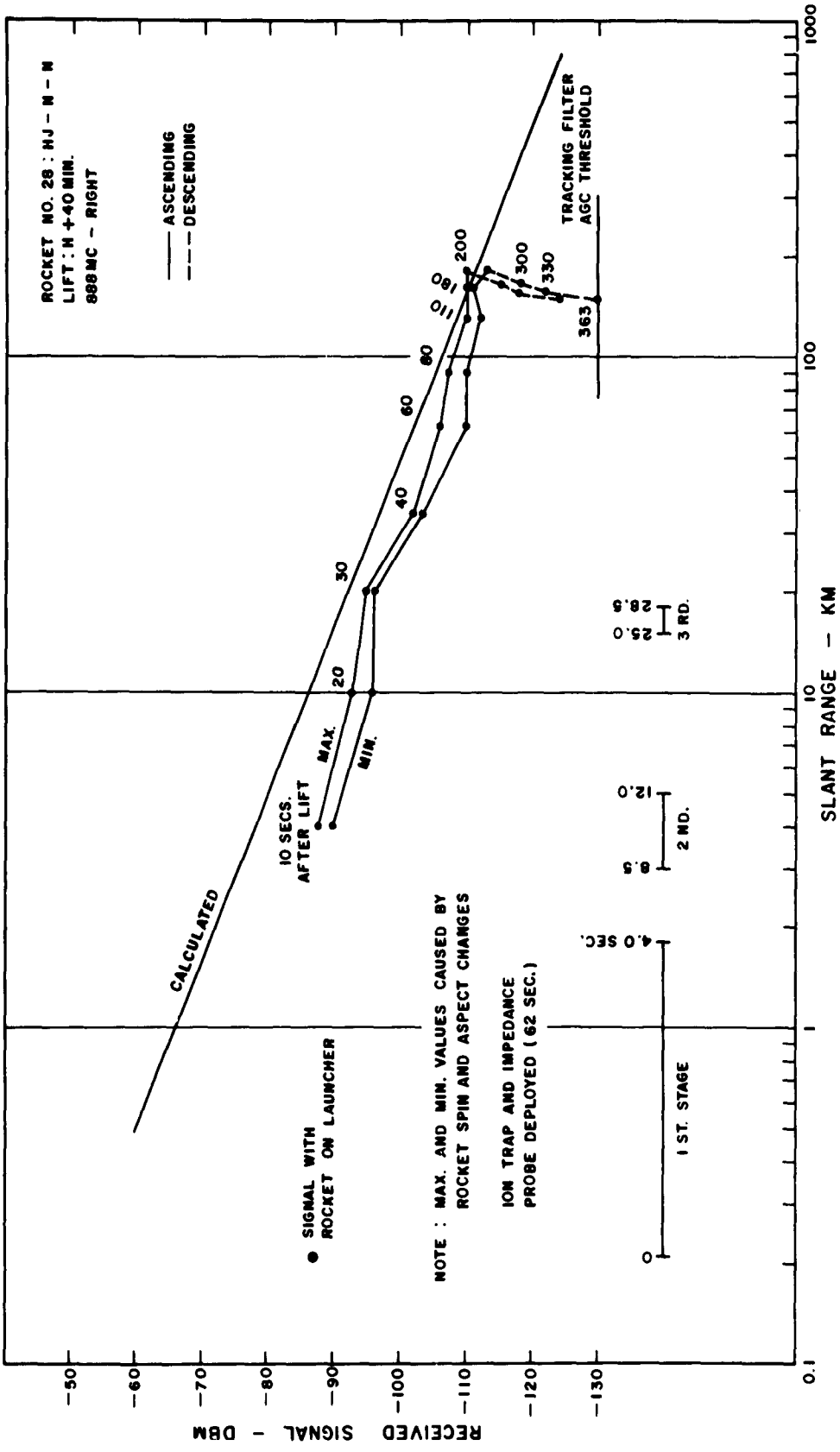

Figure C.197 Received signal strength versus slant range for 3-frequency beacon, 888 Mc right, Rocket 28, King Fish.

SECRET

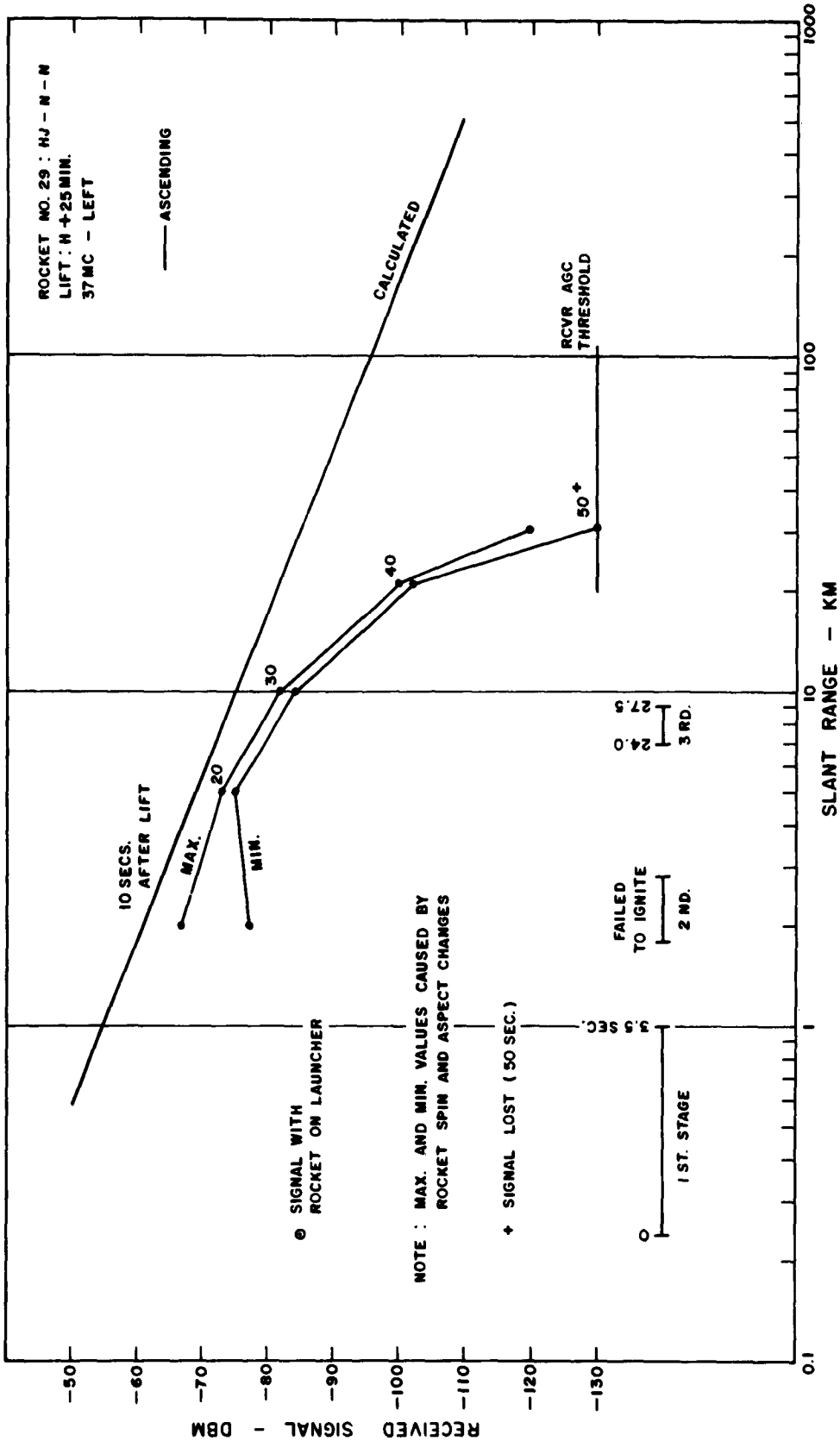

Figure C.198 Received signal strength versus slant range for 3-frequency beacon, 37 Mc left, Rocket 29, King Fish.

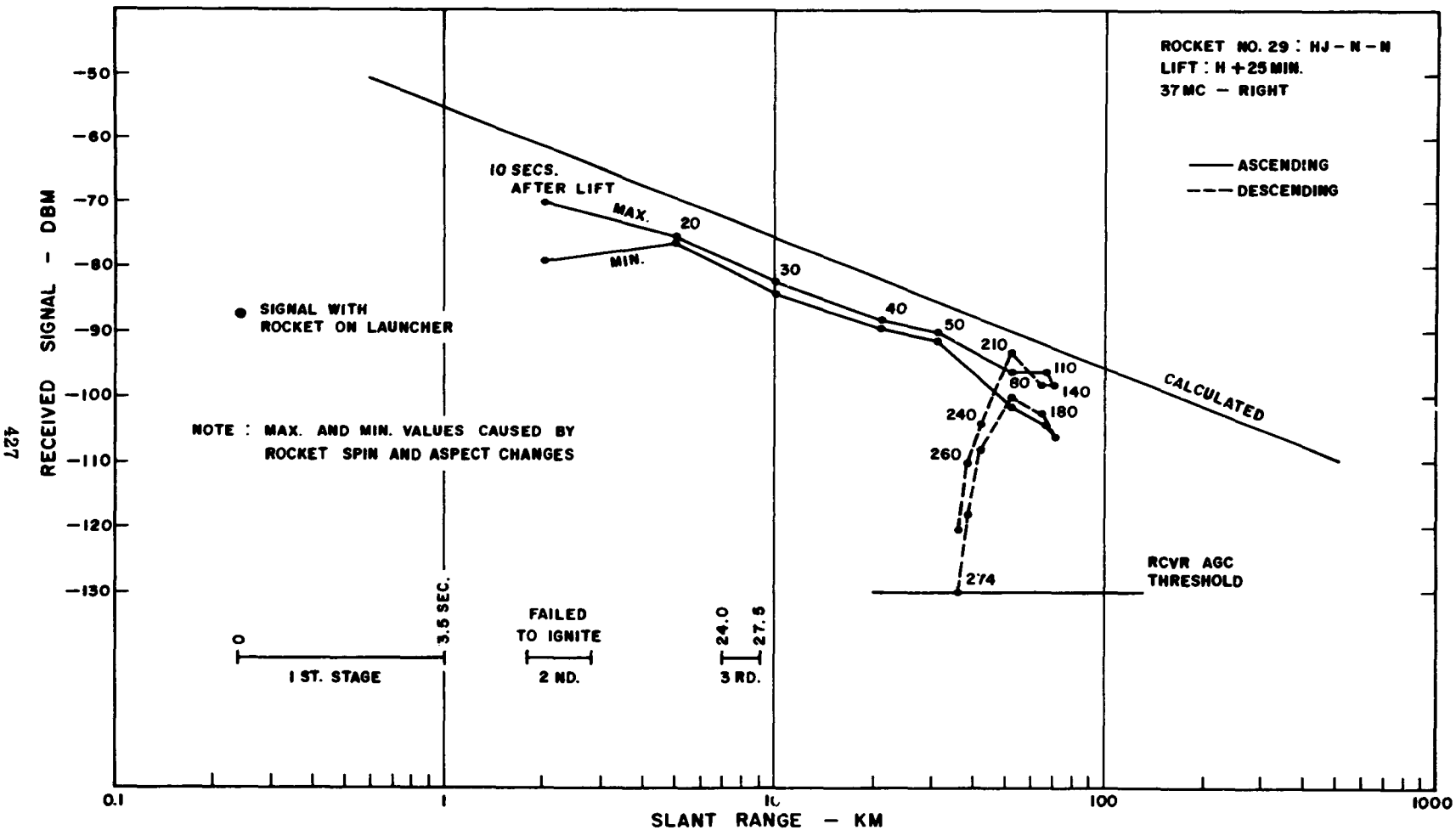

Figure C.199 Received signal strength versus slant range for 3-frequency beacon, 37 Mc right, Rocket 29, King Fish.

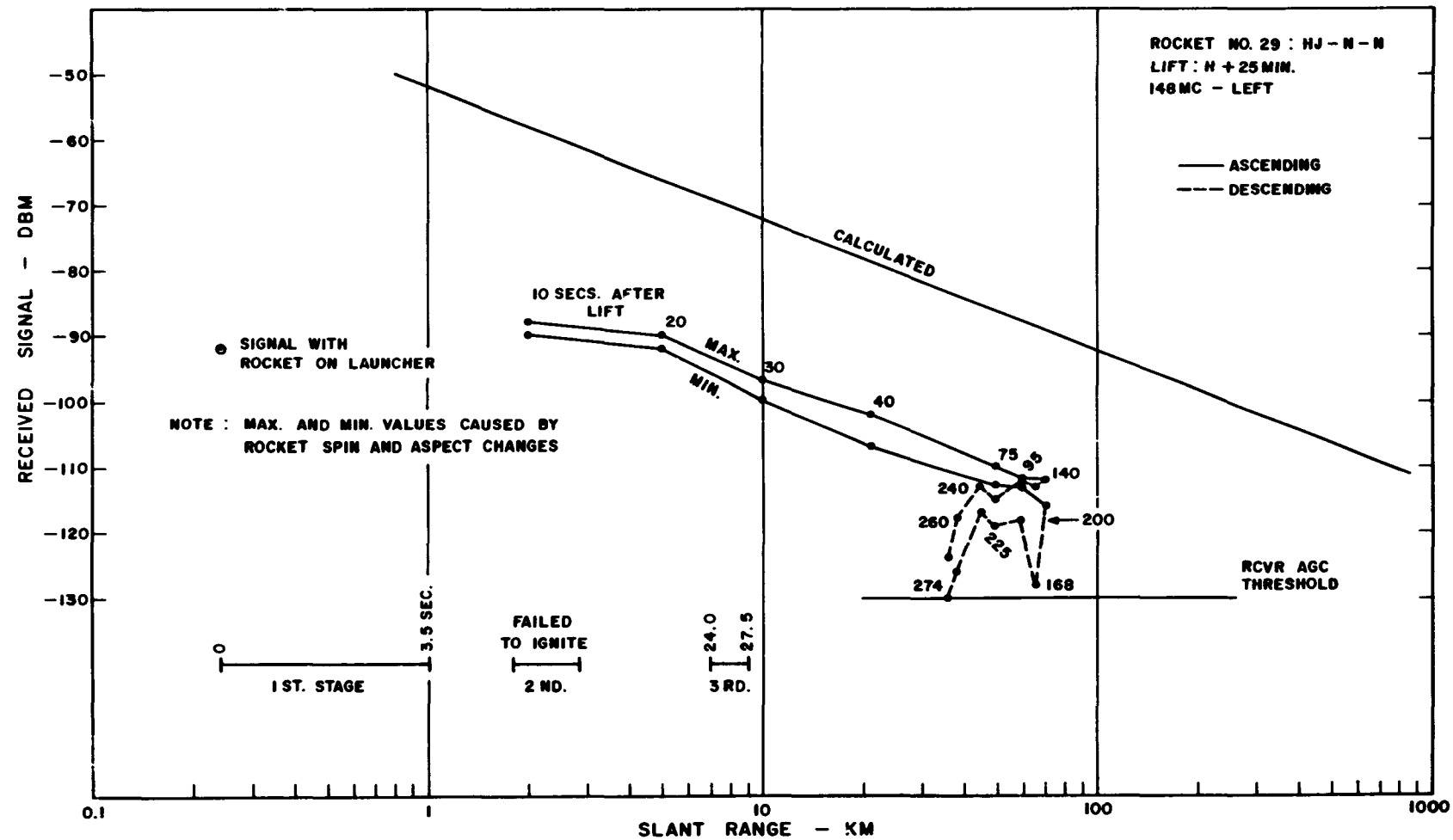

Figure C.200 Received signal strength versus slant range for 3-frequency beacon, 148 Mc left, Rocket 29, King Fish.

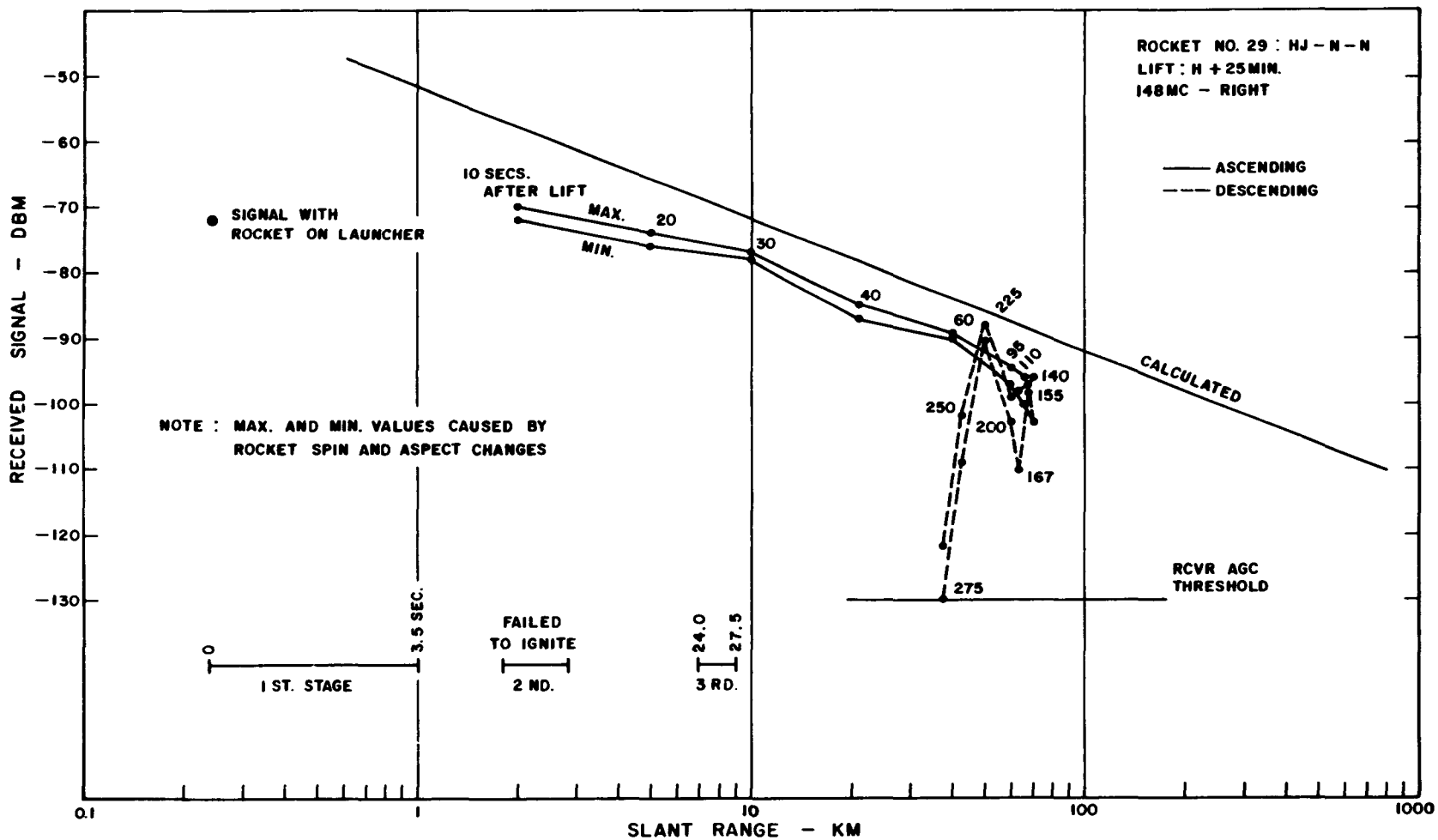

Figure C.201 Received signal strength versus slant range for 3-frequency beacon, 148 Mc right, Rocket 29, King Fish.

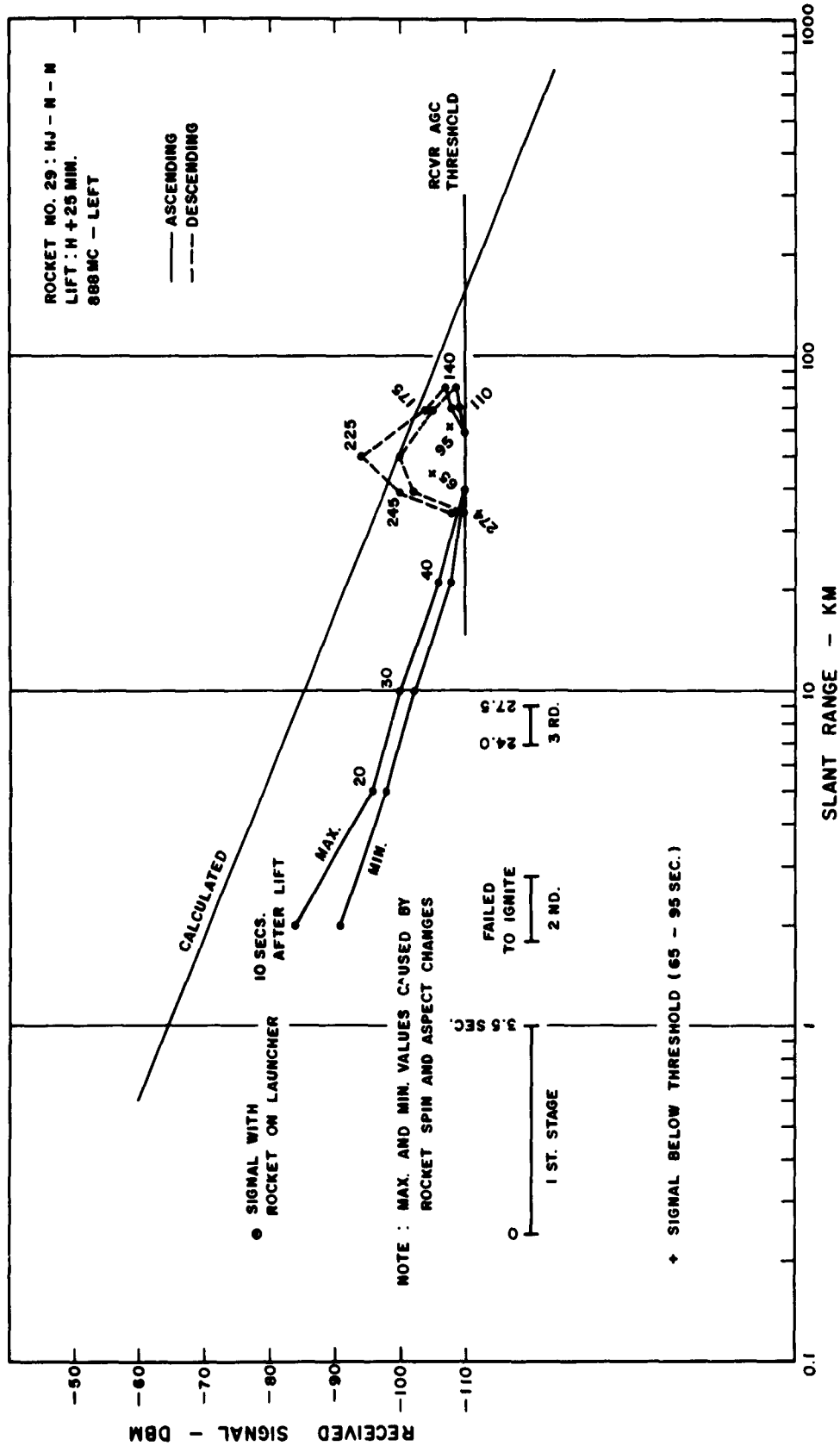

Figure C.202 Received signal strength versus slant range for 3-frequency beacon, 888 Mc left, Rocket 29, King Fish.

SECRET

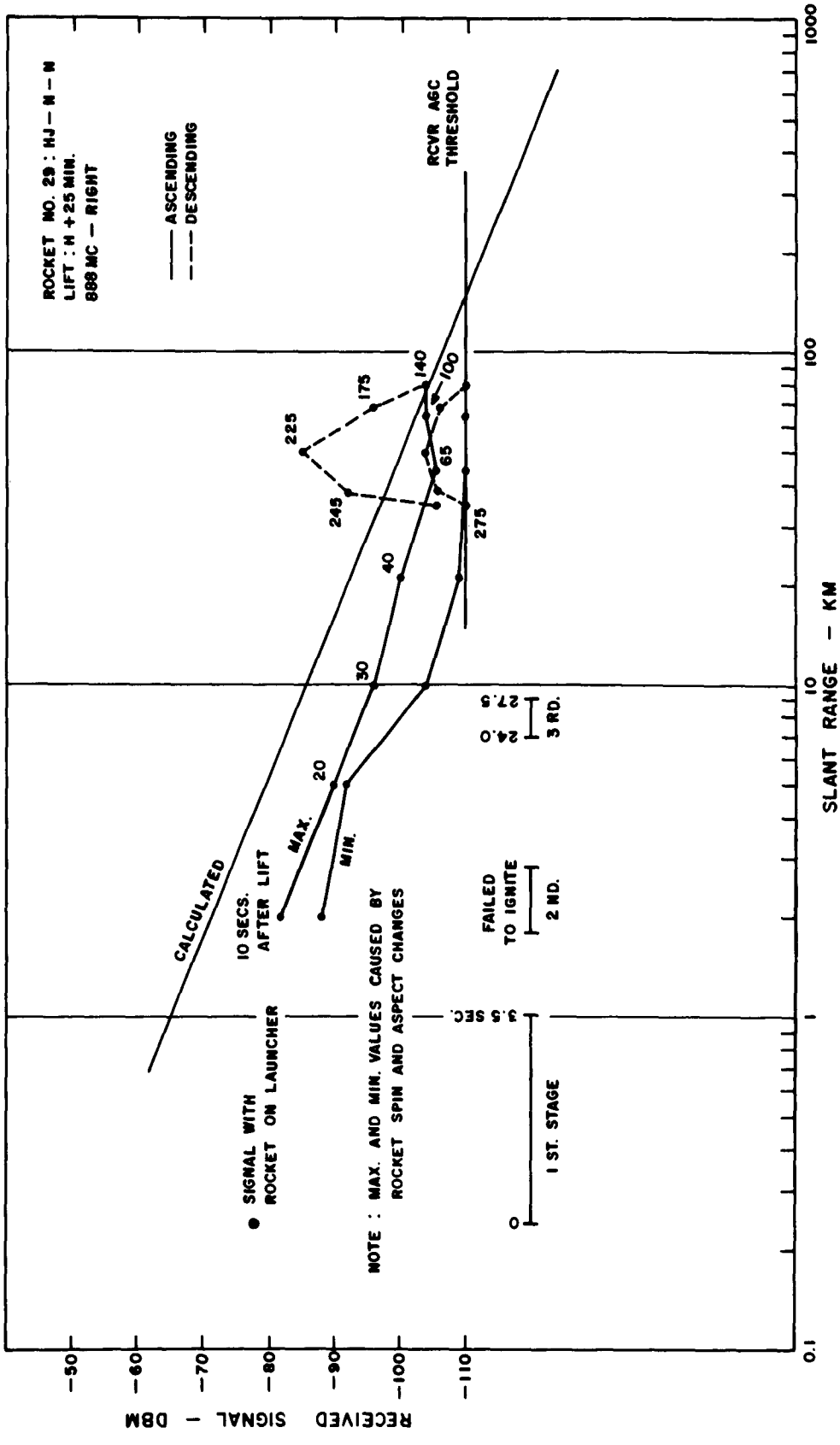

Figure C.203 Received signal strength versus slant range for 3-frequency beacon, 888 Mc right, Rocket 29, King Fish.

SECRET

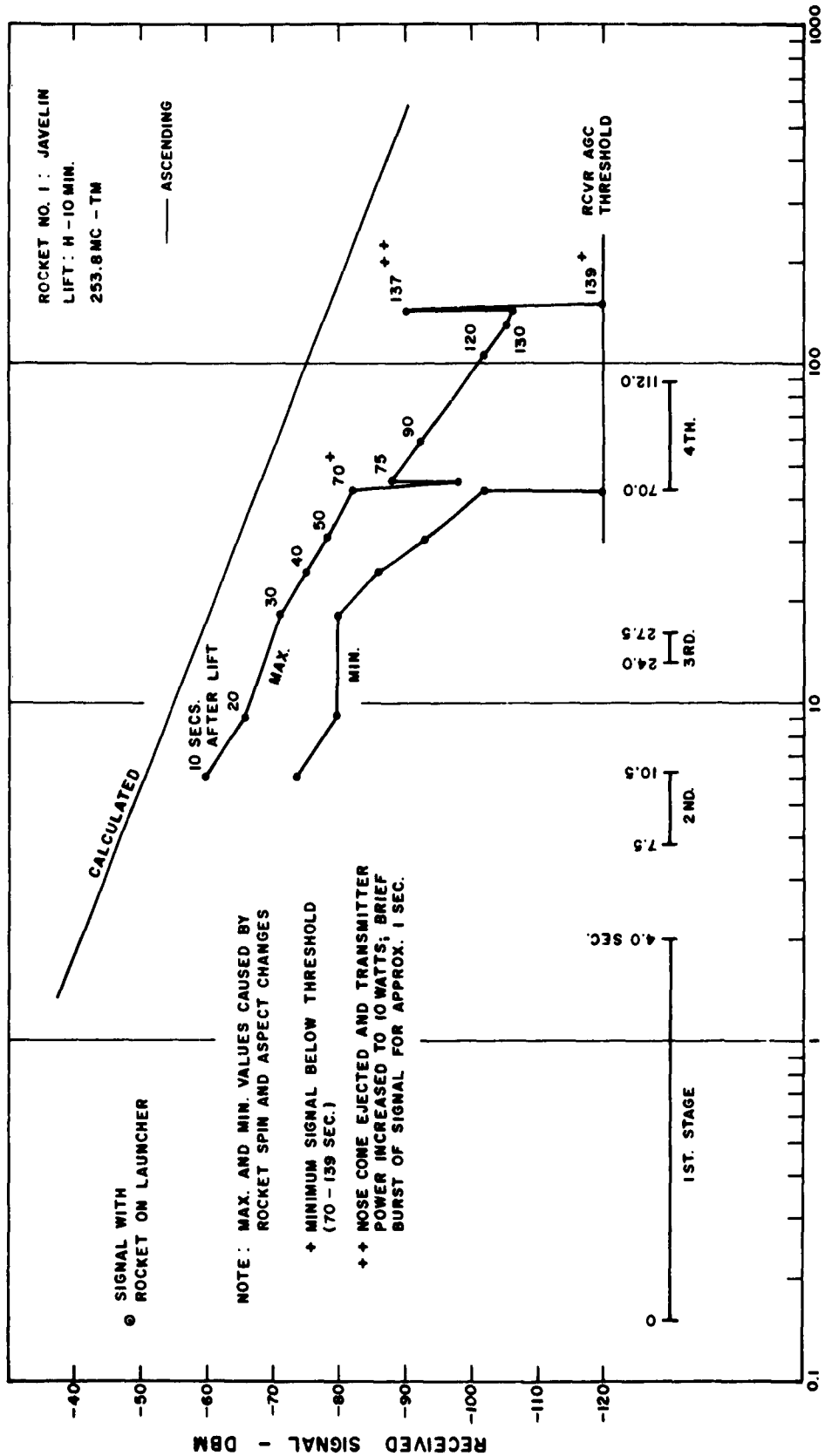

Figure C.204 Received signal strength versus slant range for VHF telemetry, Rocket 1, Star Fish.

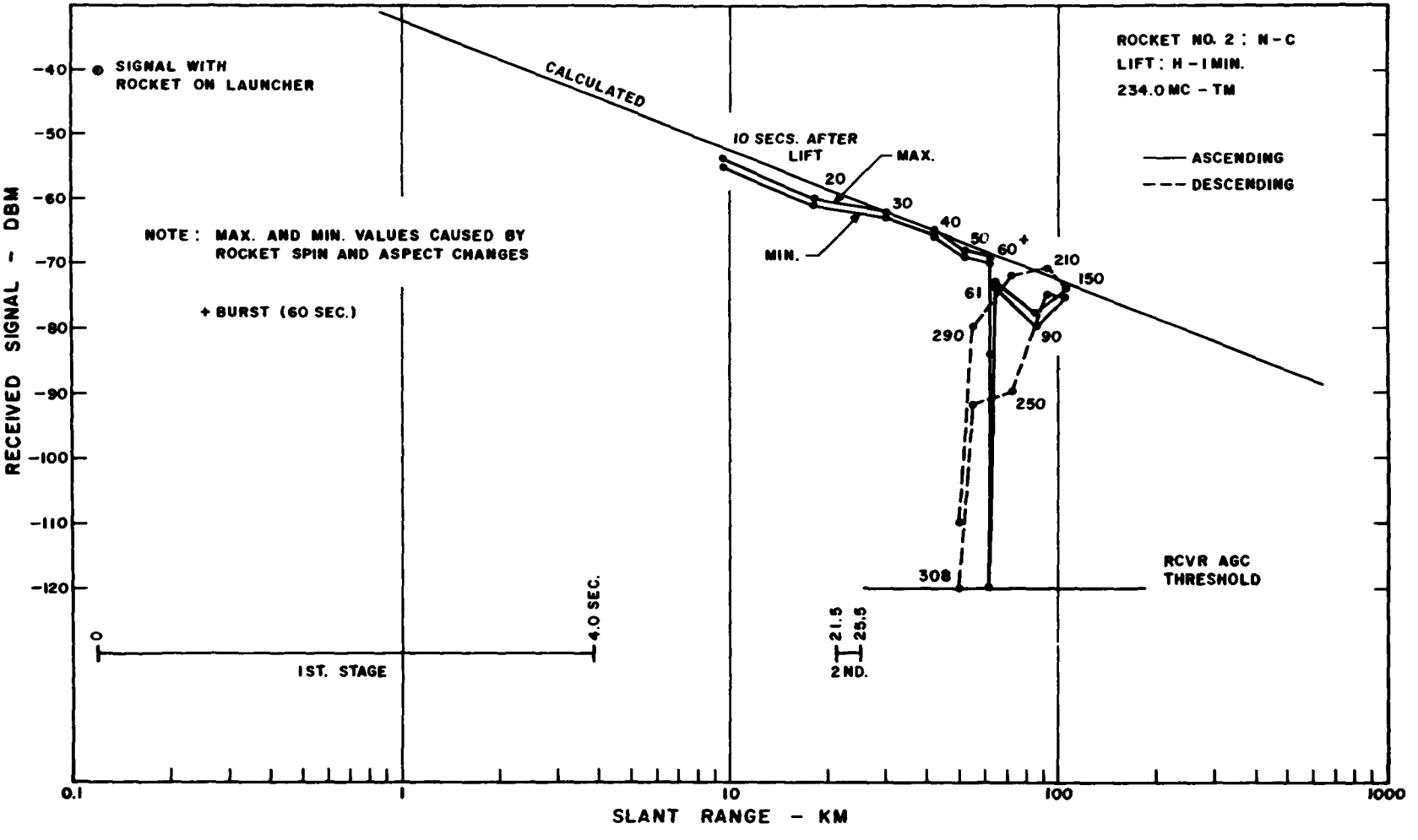

Figure C.205 Received signal strength versus slant range for VHF telemetry, Rocket 2, Star Fish.

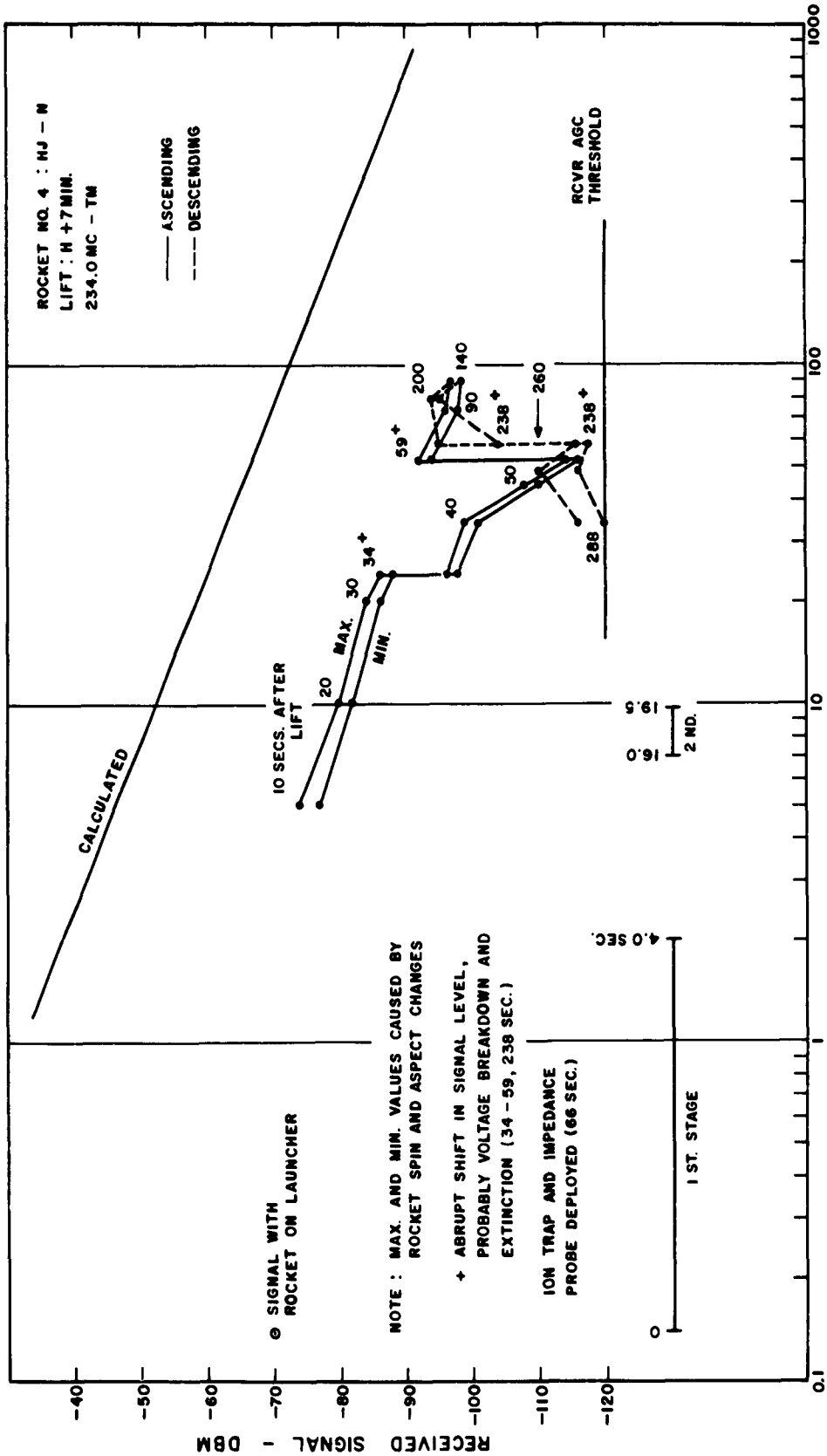

Figure C.206 Received signal strength versus slant range for VHF telemetry, Rocket 4, Star Fish.

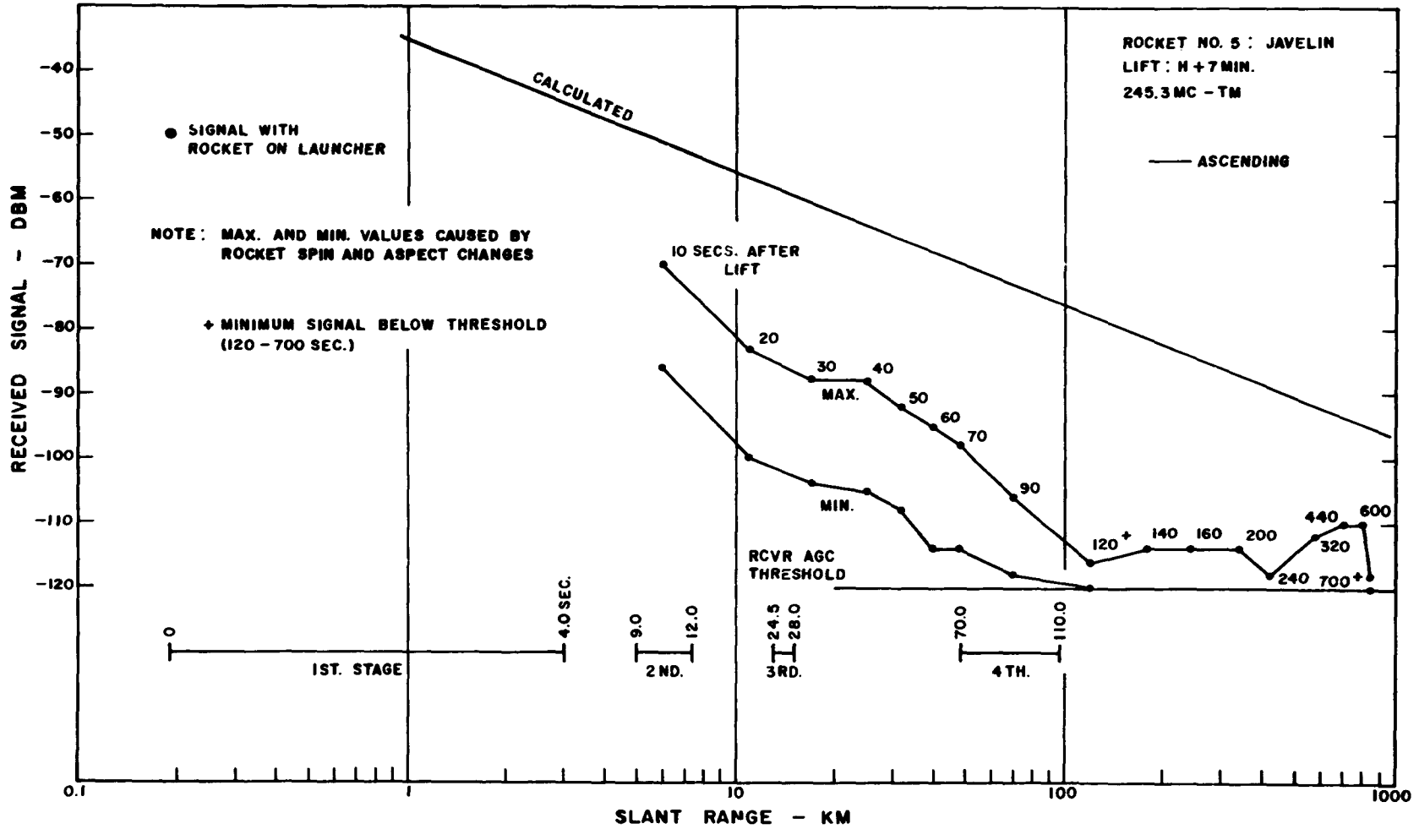

Figure C.207 Received signal strength versus slant range for VHF telemetry, Rocket 5, Star Fish.

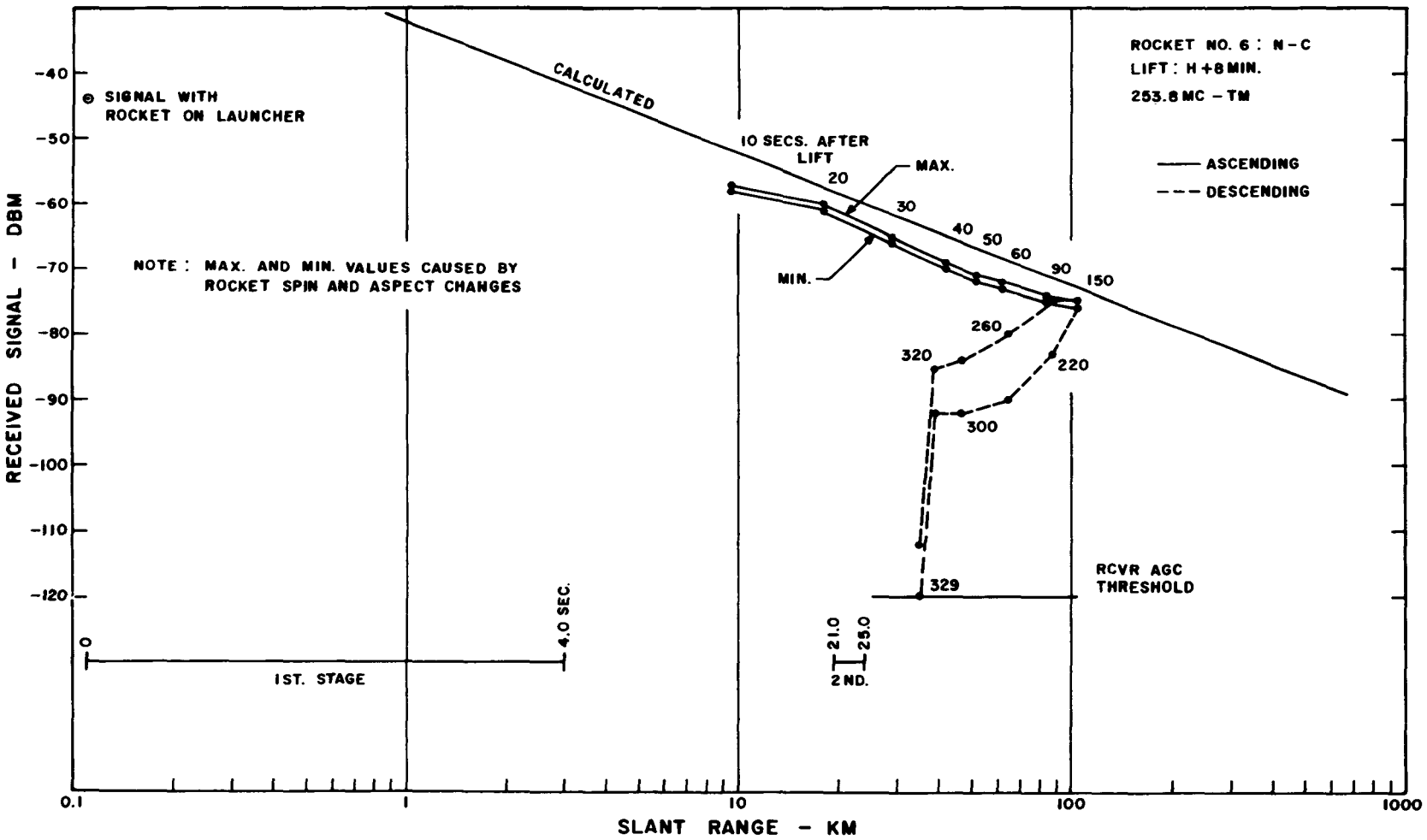

Figure C.208 Received signal strength versus slant range for VHF telemetry, Rocket 6, Star Fish.

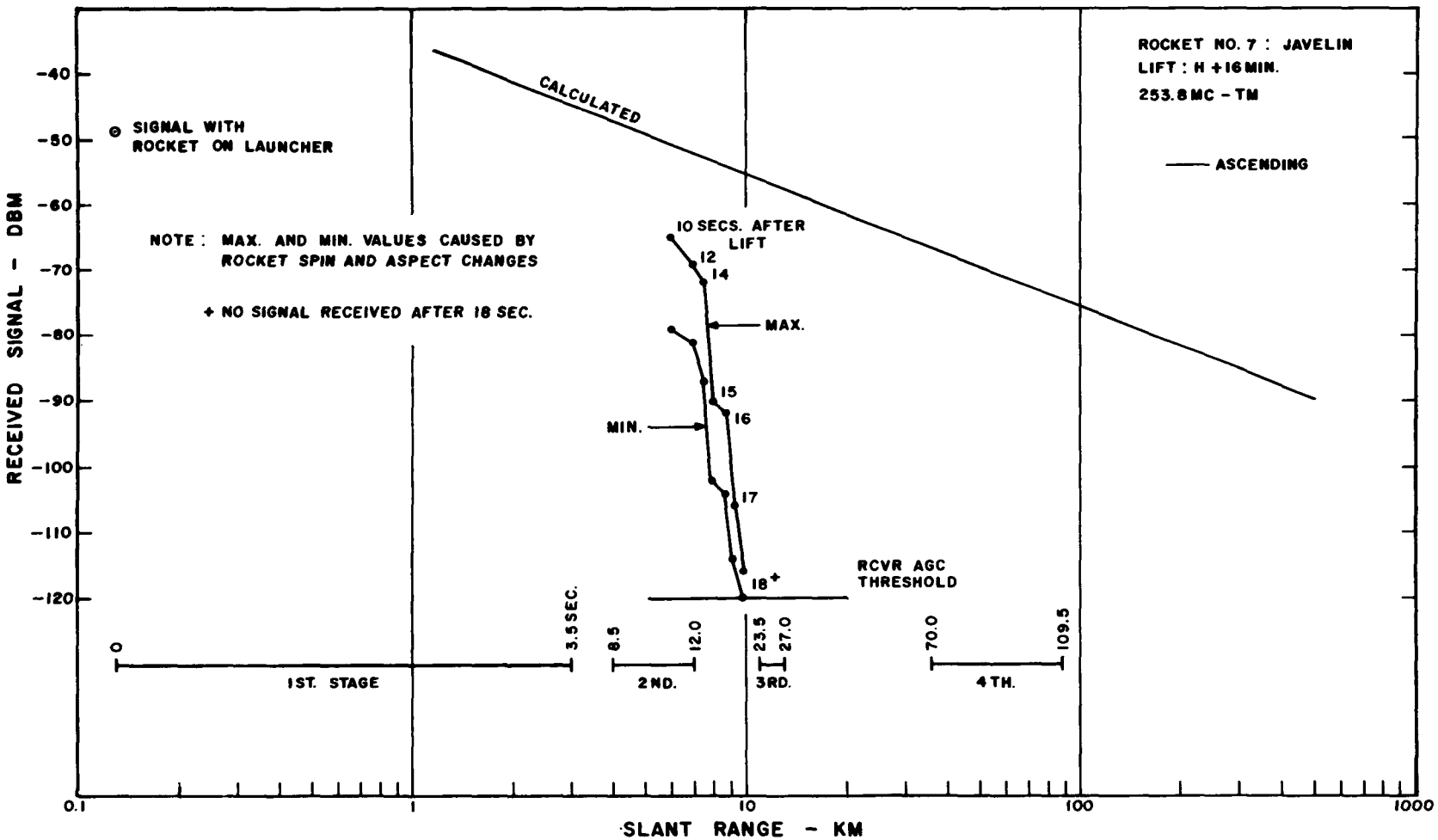

Figure C.209 Received signal strength versus slant range for VHF telemetry, Rocket 7, Star Fish.

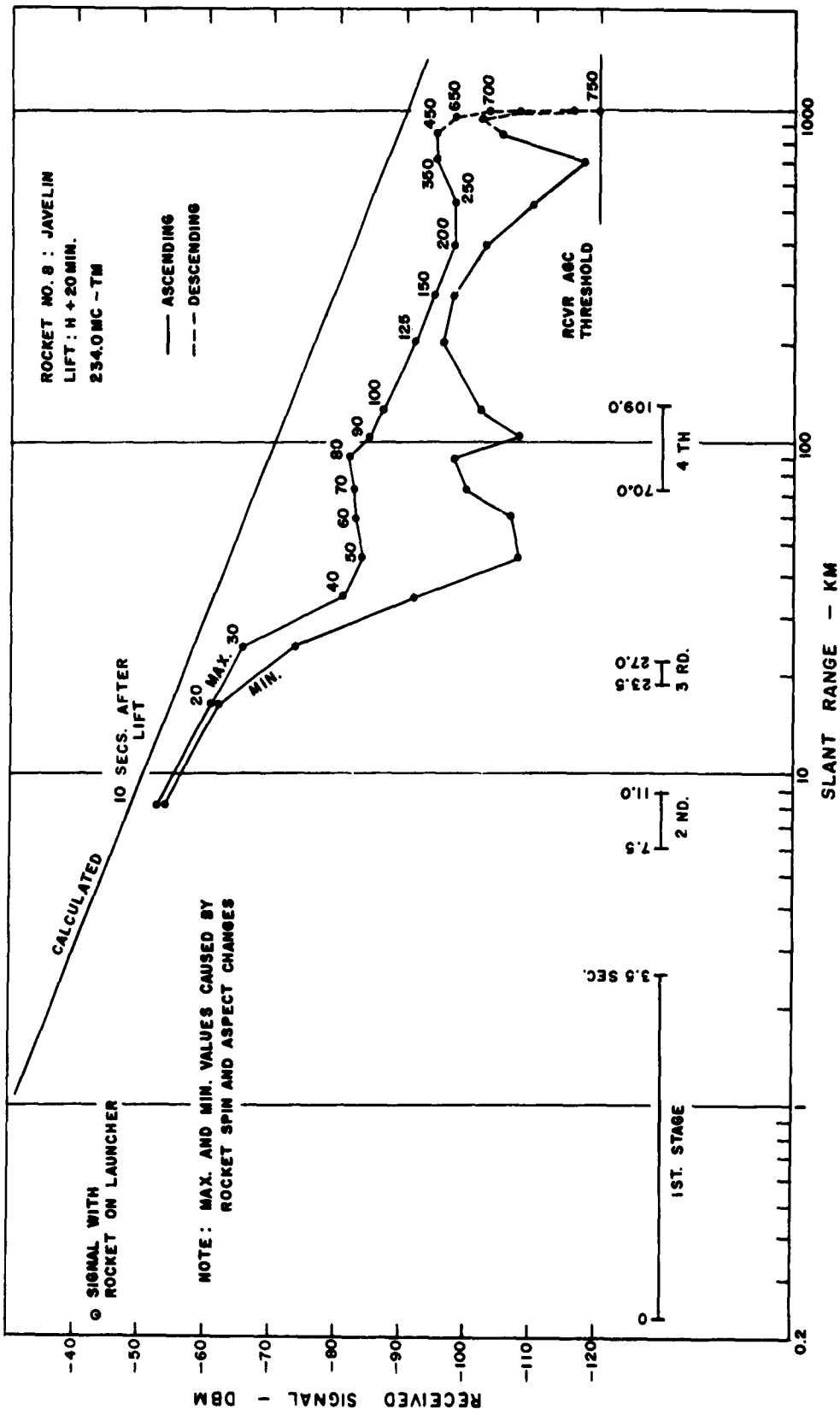

Figure C.210 Received signal strength versus slant range for VHF telemetry, Rocket 8, Star Fish.

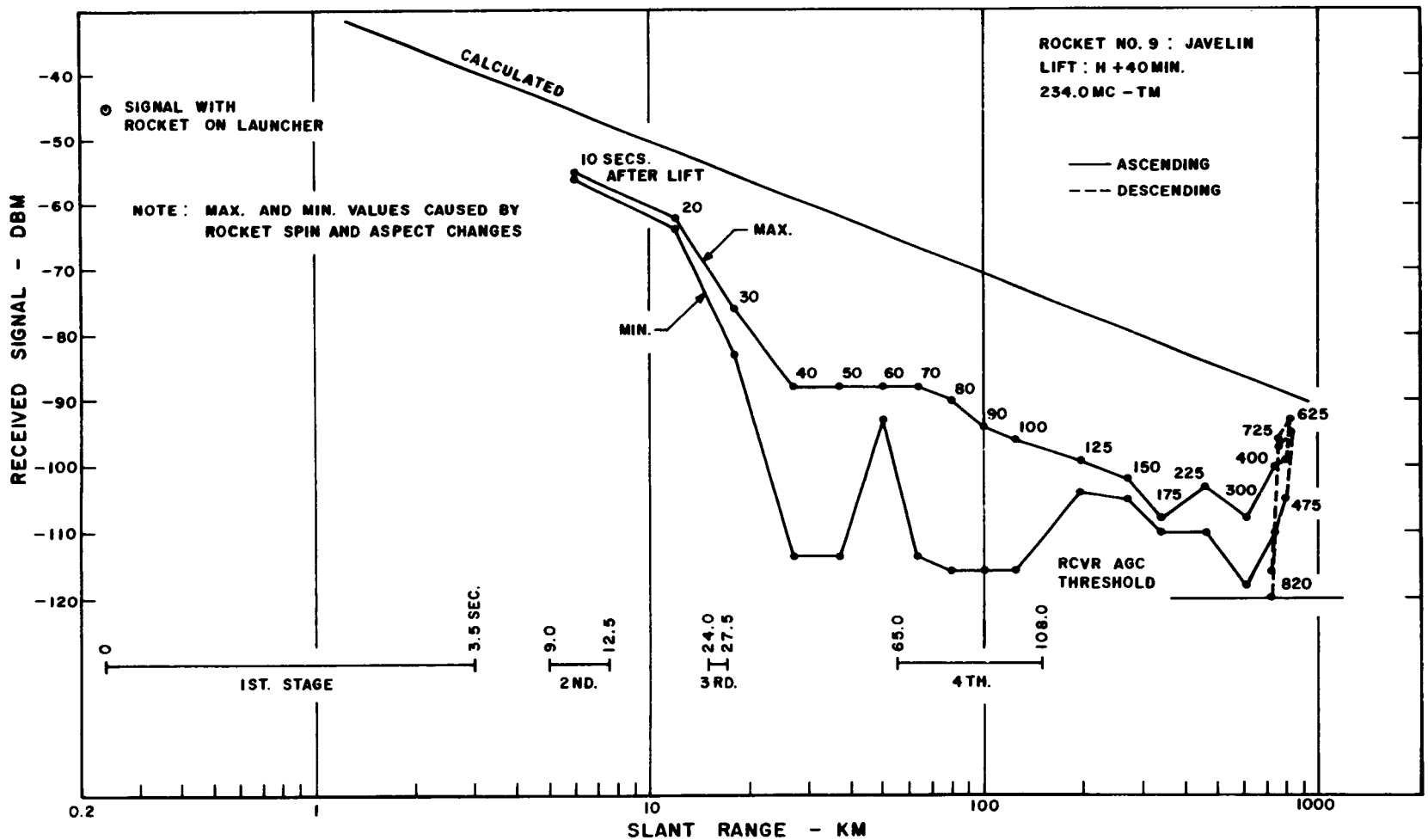

Figure C.211 Received signal strength versus slant range for VHF telemetry, Rocket 9, Star Fish.

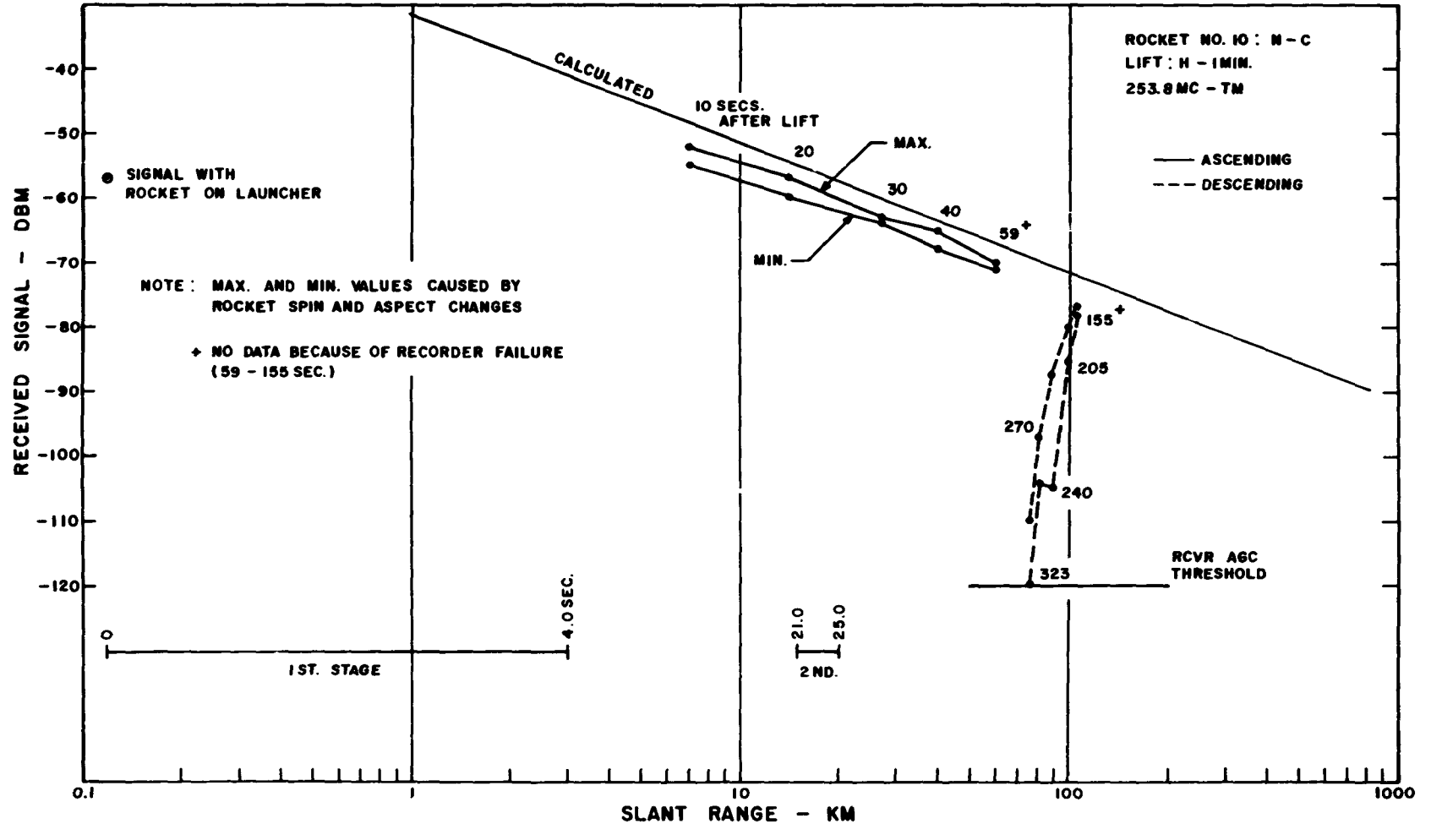

Figure C.212 Received signal strength versus slant range for VHF telemetry, Rocket 10, Blue Gill.

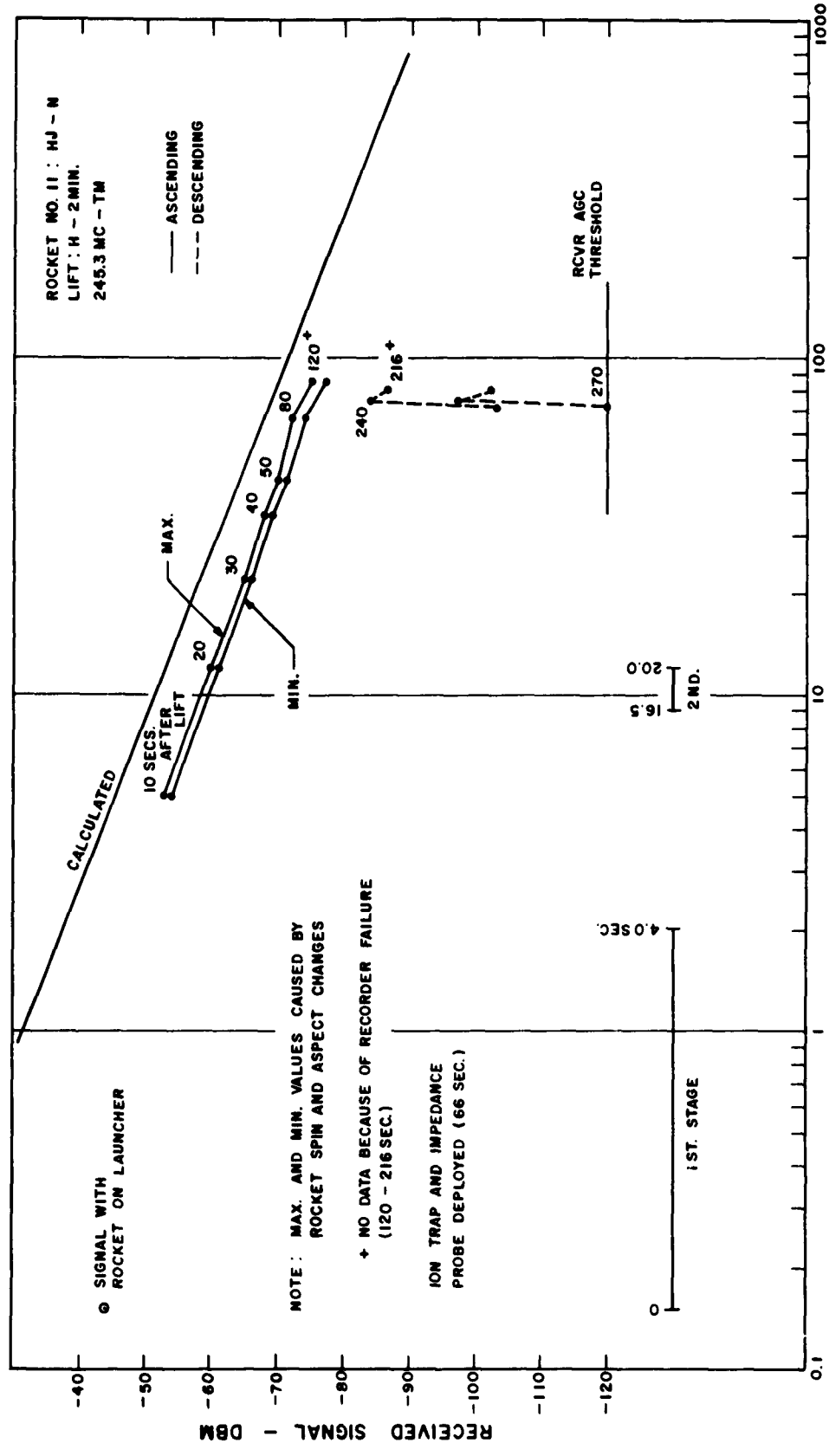

Figure C.213 Received signal strength versus slant range for VHF telemetry, Rocket 11, Blue Gill.

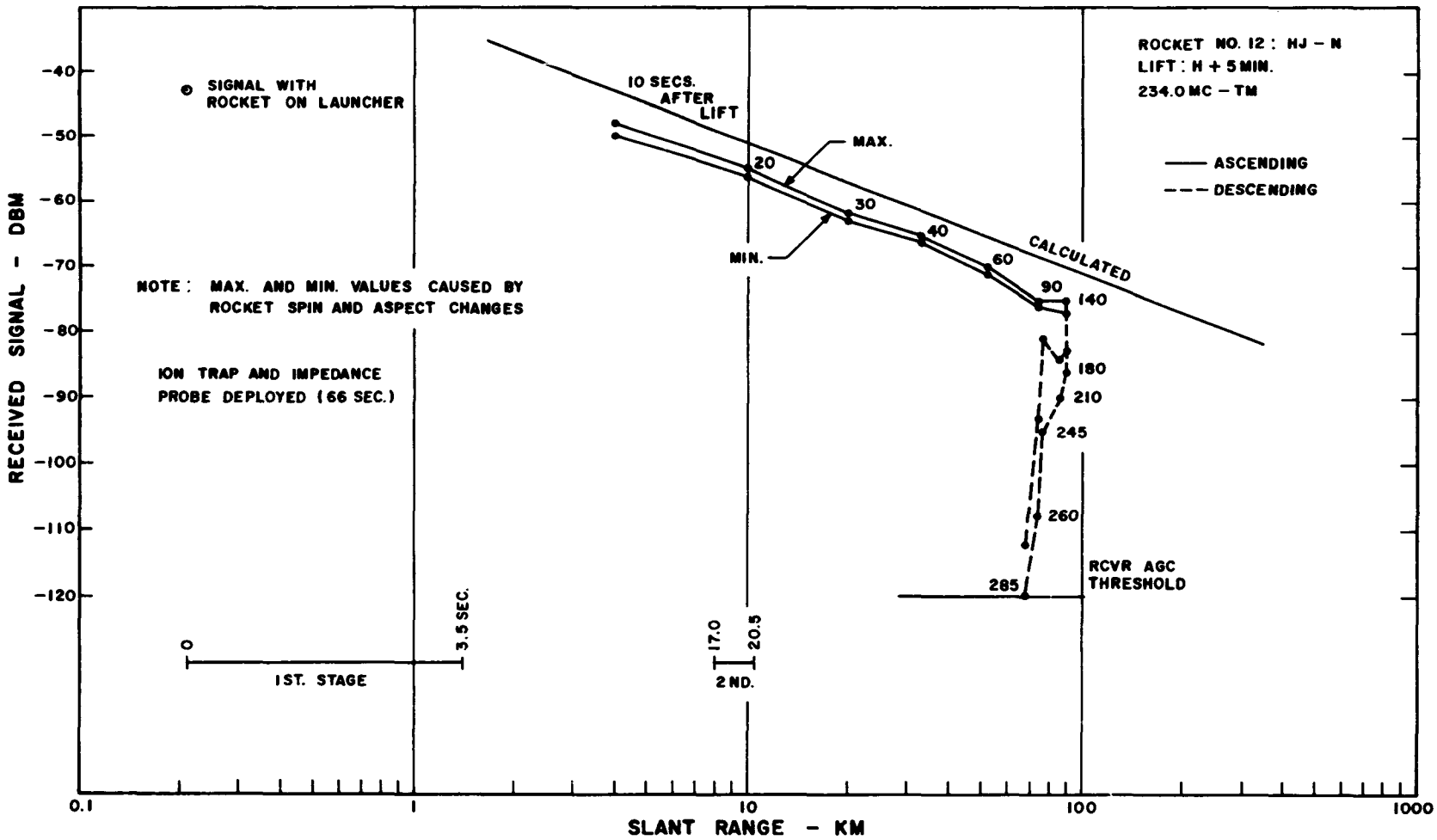

Figure C.214 Received signal strength versus slant range for VHF telemetry, Rocket 12, Blue Gill.

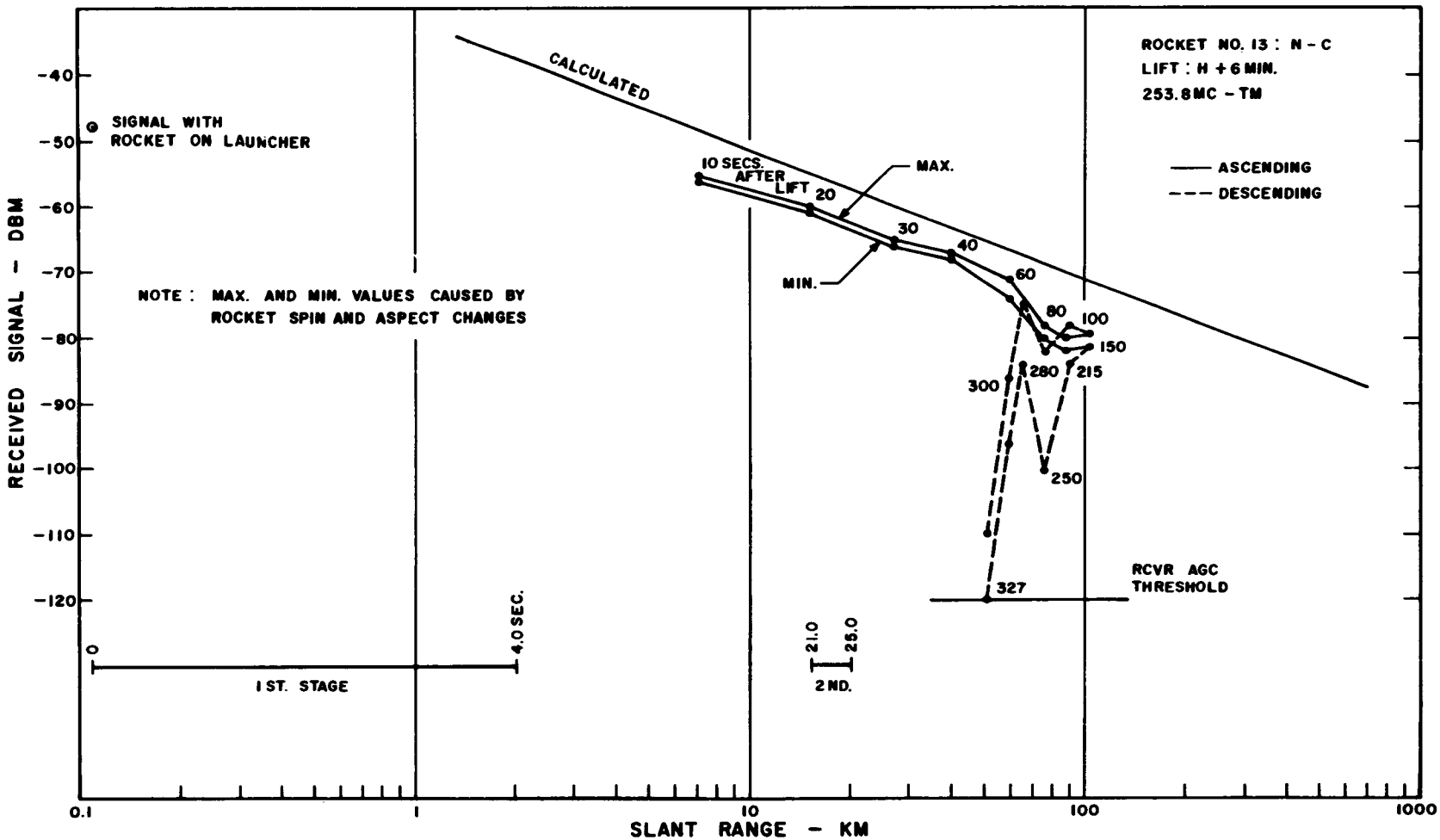

Figure C.215 Received signal strength versus slant range for VHF telemetry, Rocket 13, Blue Gill.

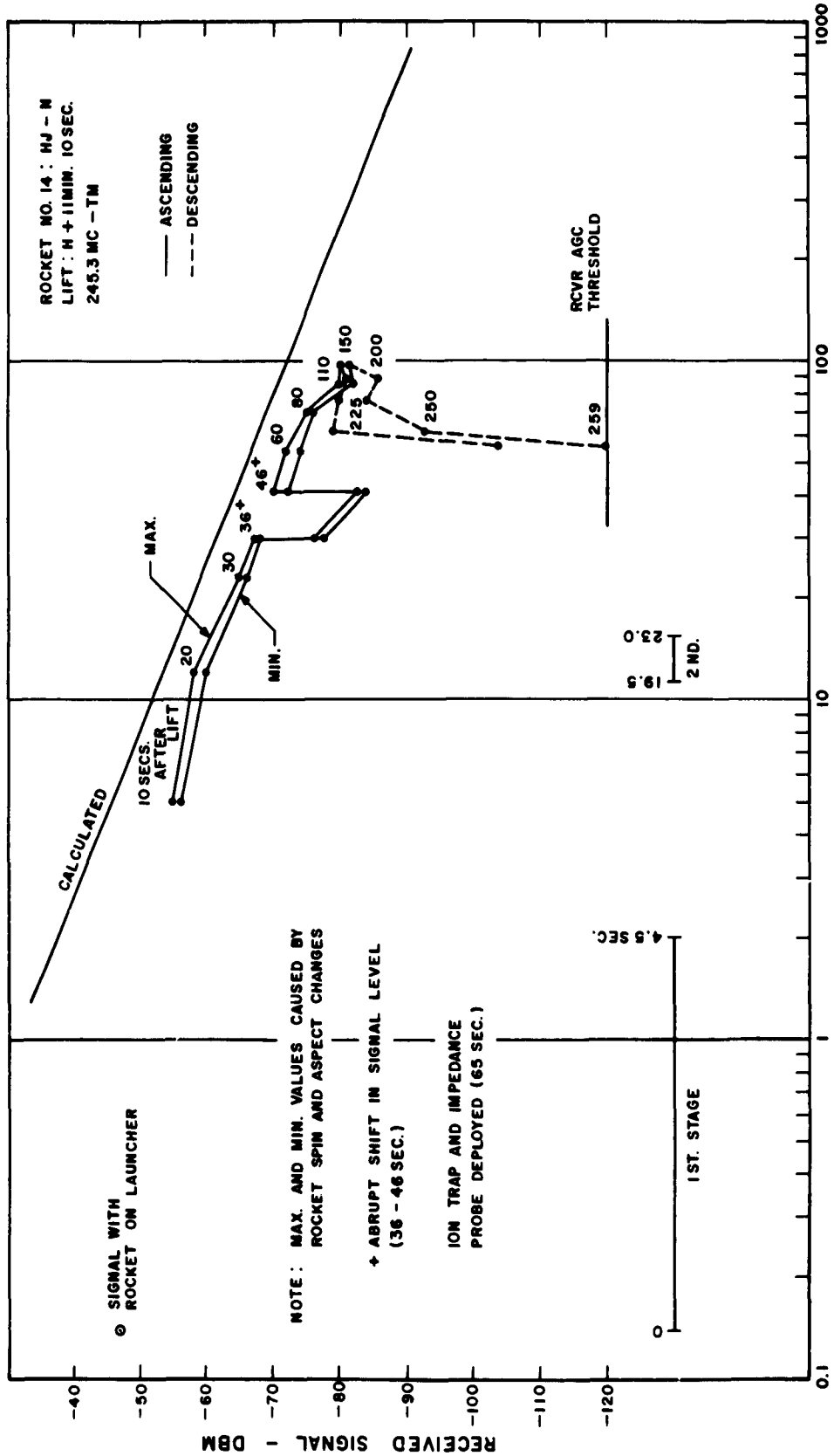

Figure C.216 Received signal strength versus slant range for VHF telemetry, Rocket 14, Blue Gill.

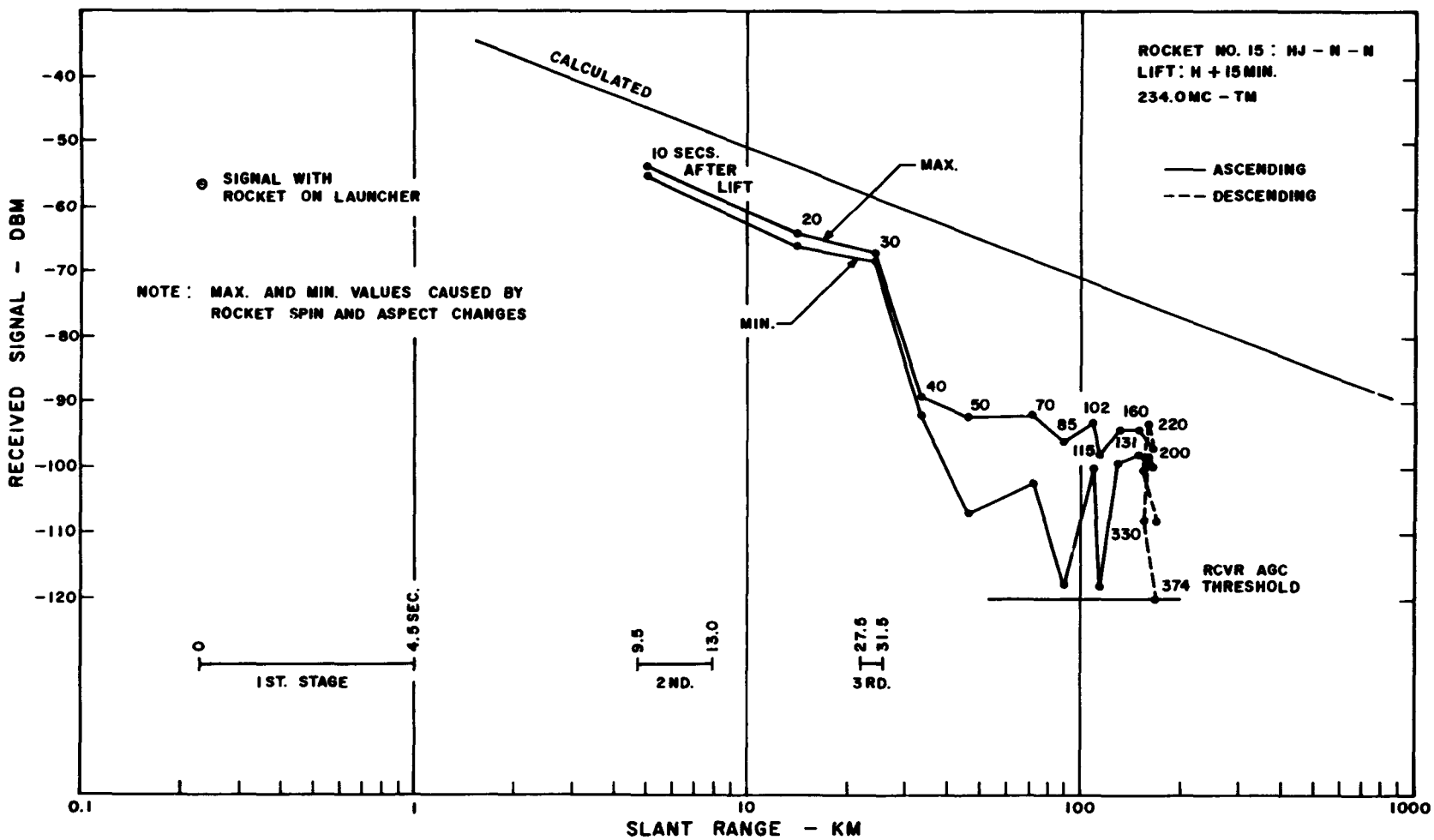

Figure C.217 Received signal strength versus slant range for VHF telemetry, Rocket 15, Blue Gill.

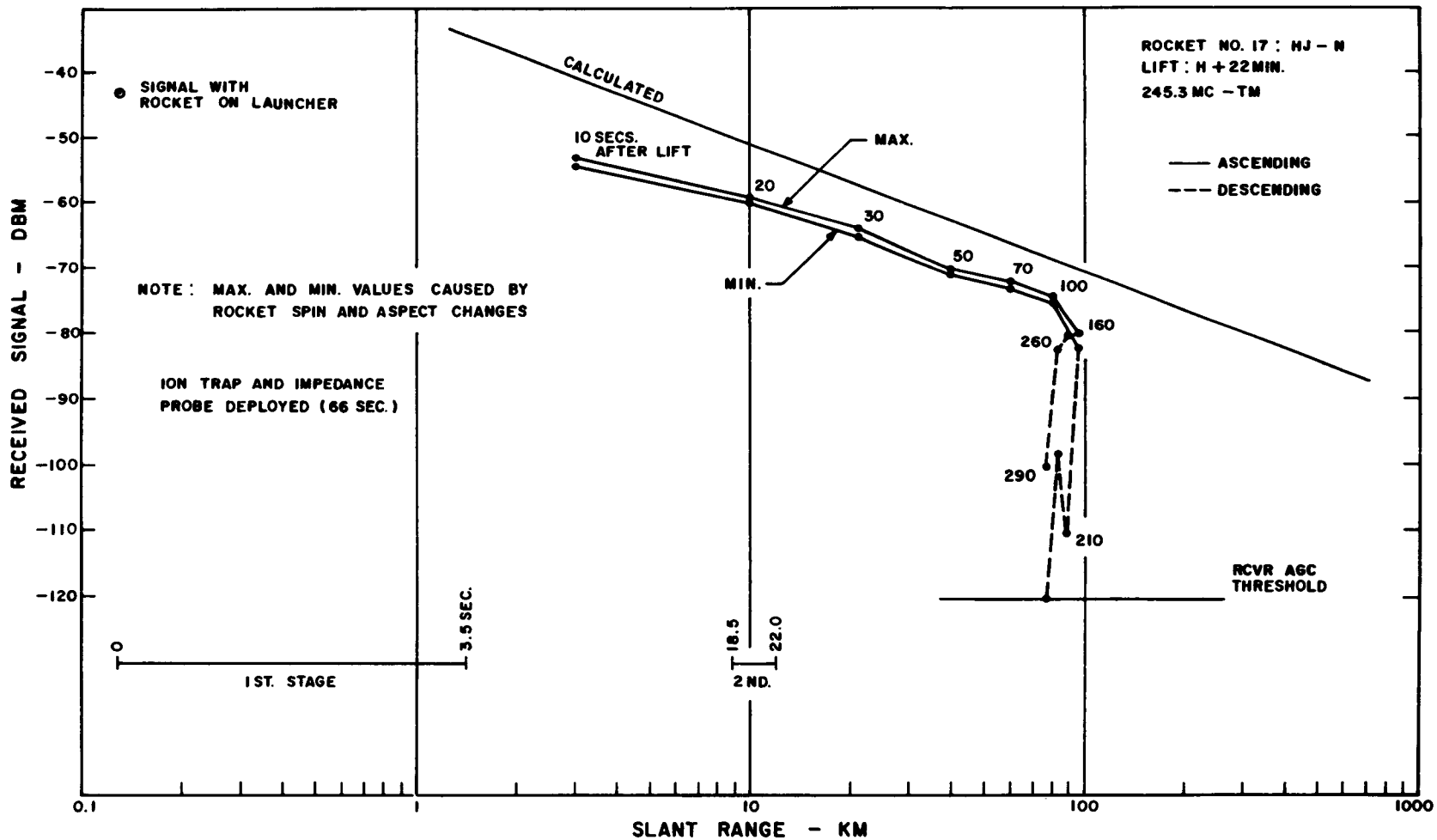

Figure C.218 Received signal strength versus slant range for VHF telemetry, Rocket 17, Blue Gill.

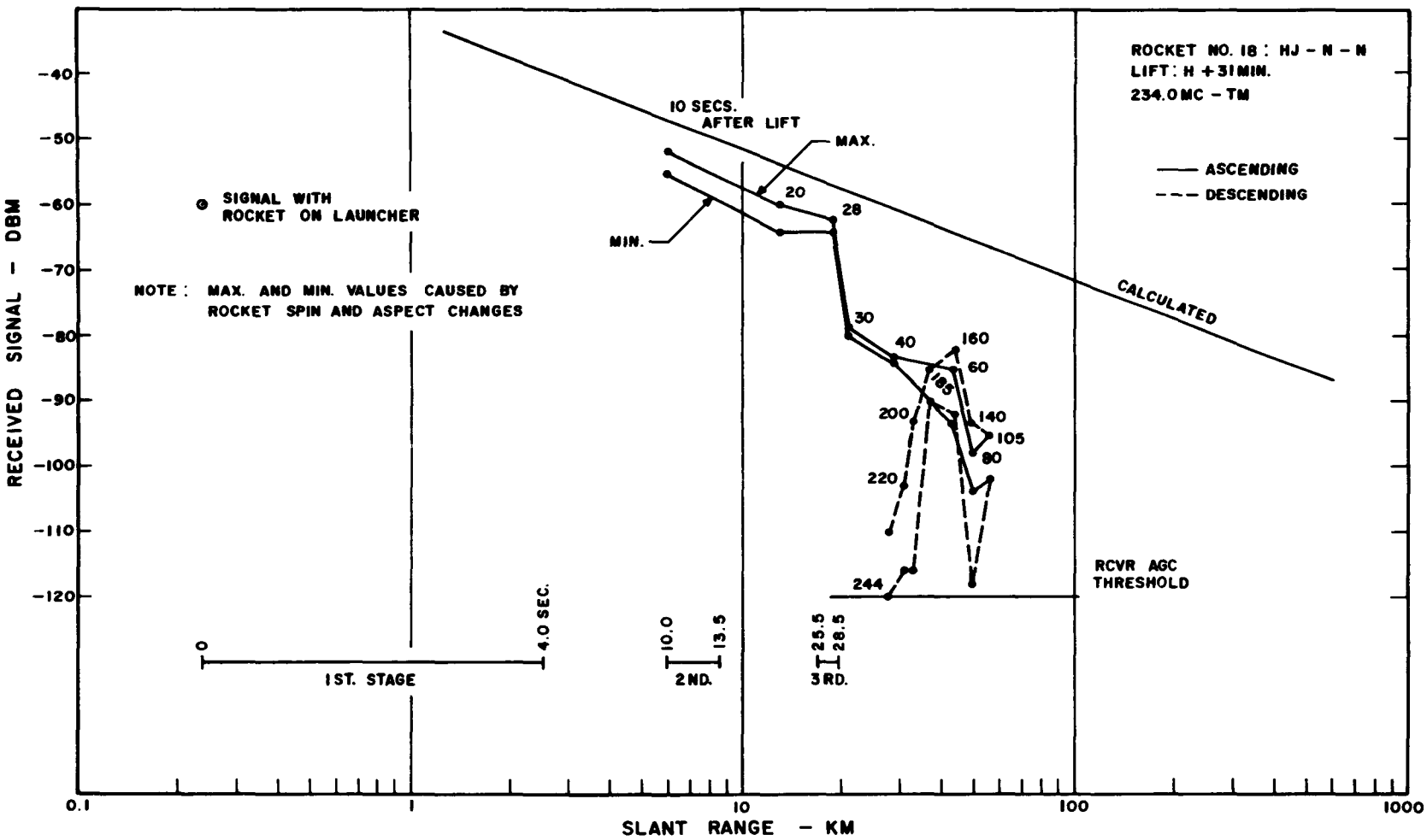

Figure C.219 Received signal strength versus slant range for VHF telemetry, Rocket 18, Blue Gill.

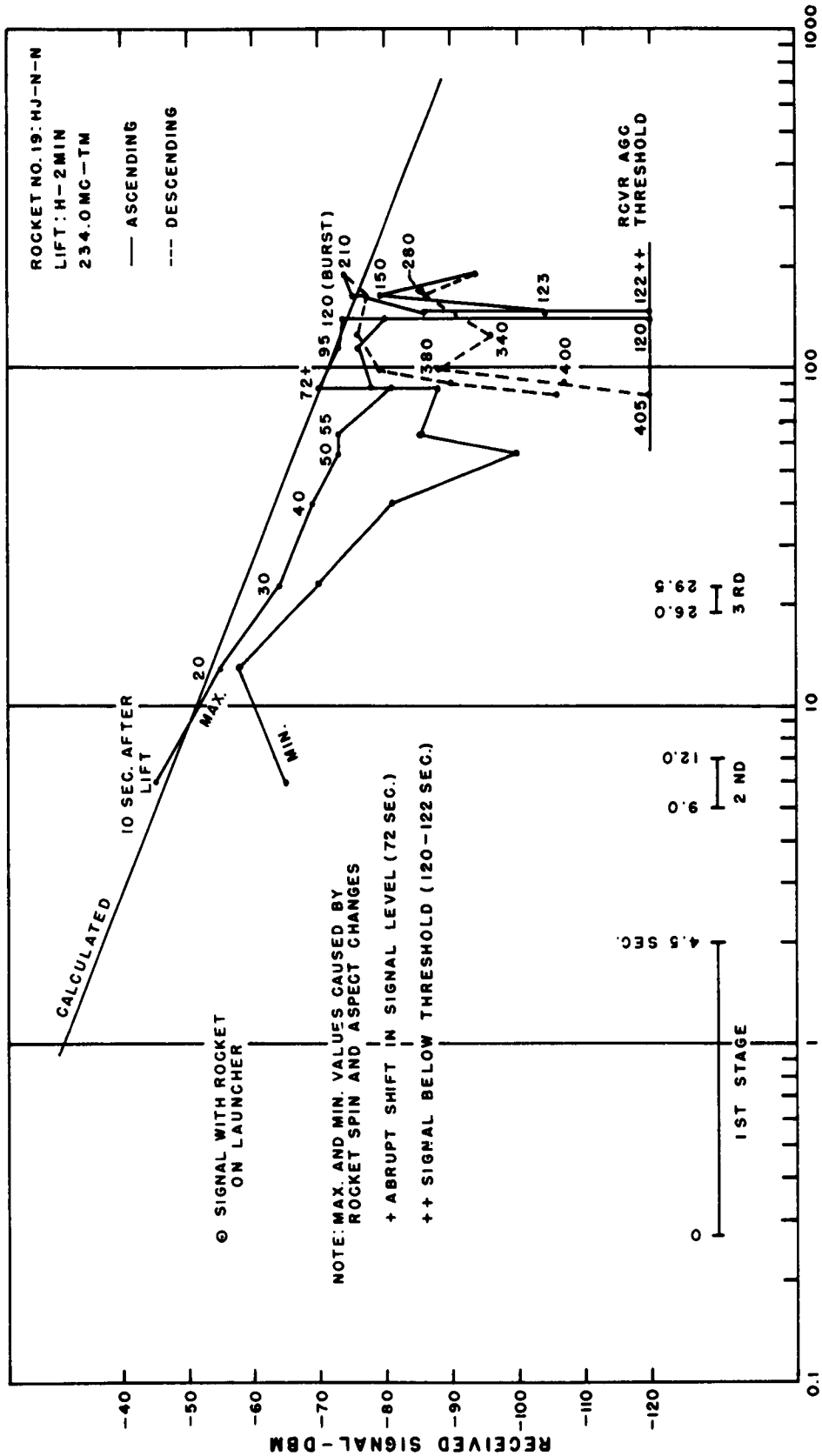

Figure C.220 Received signal strength versus slant range for VHF telemetry, Rocket 19, King Fish.

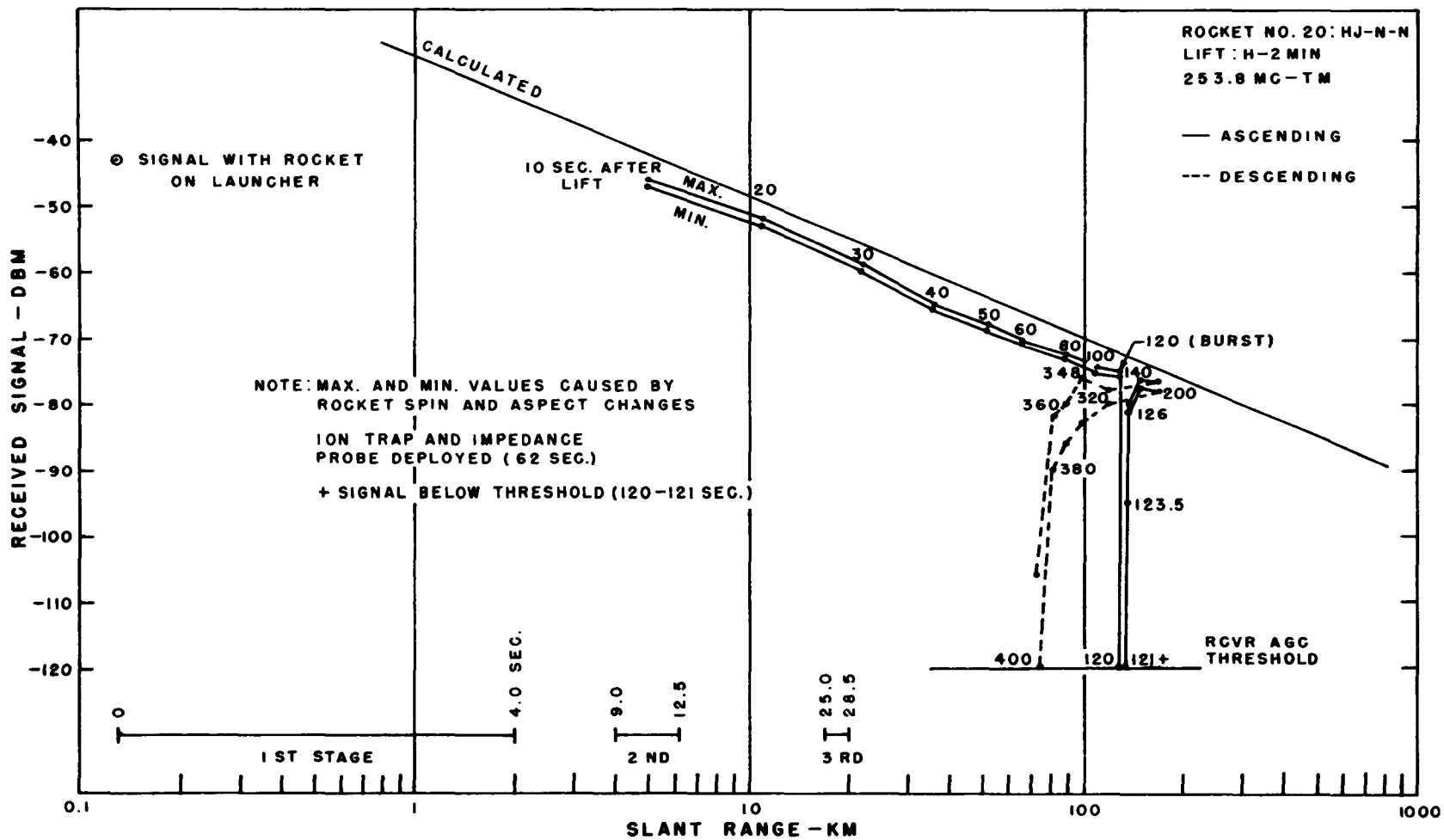

Figure C.221 Received signal strength versus slant range for VHF telemetry, Rocket 20, King Fish.

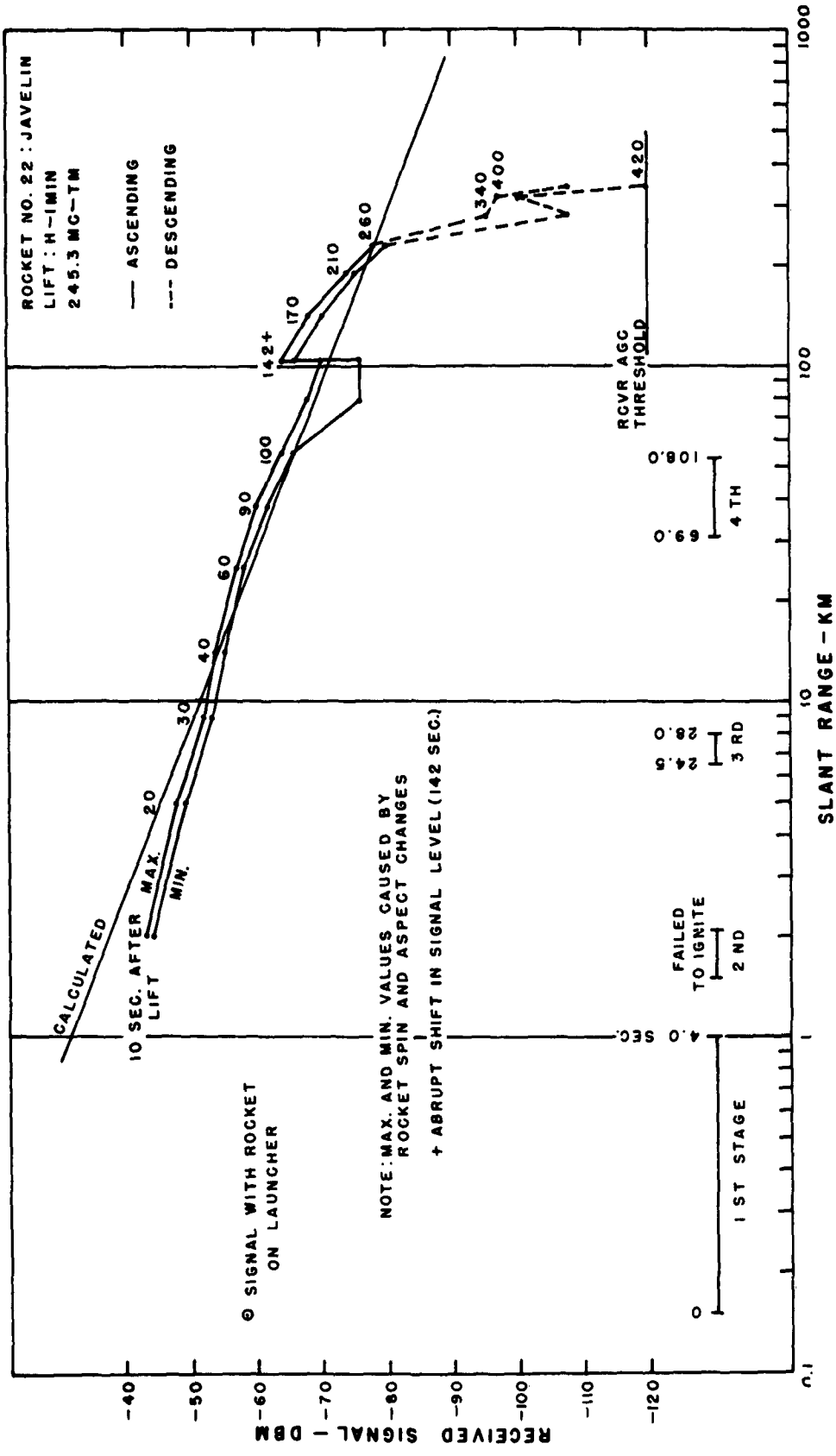

Figure C.222 Received signal strength versus slant range for VHF telemetry, Rocket 22, King Fish.

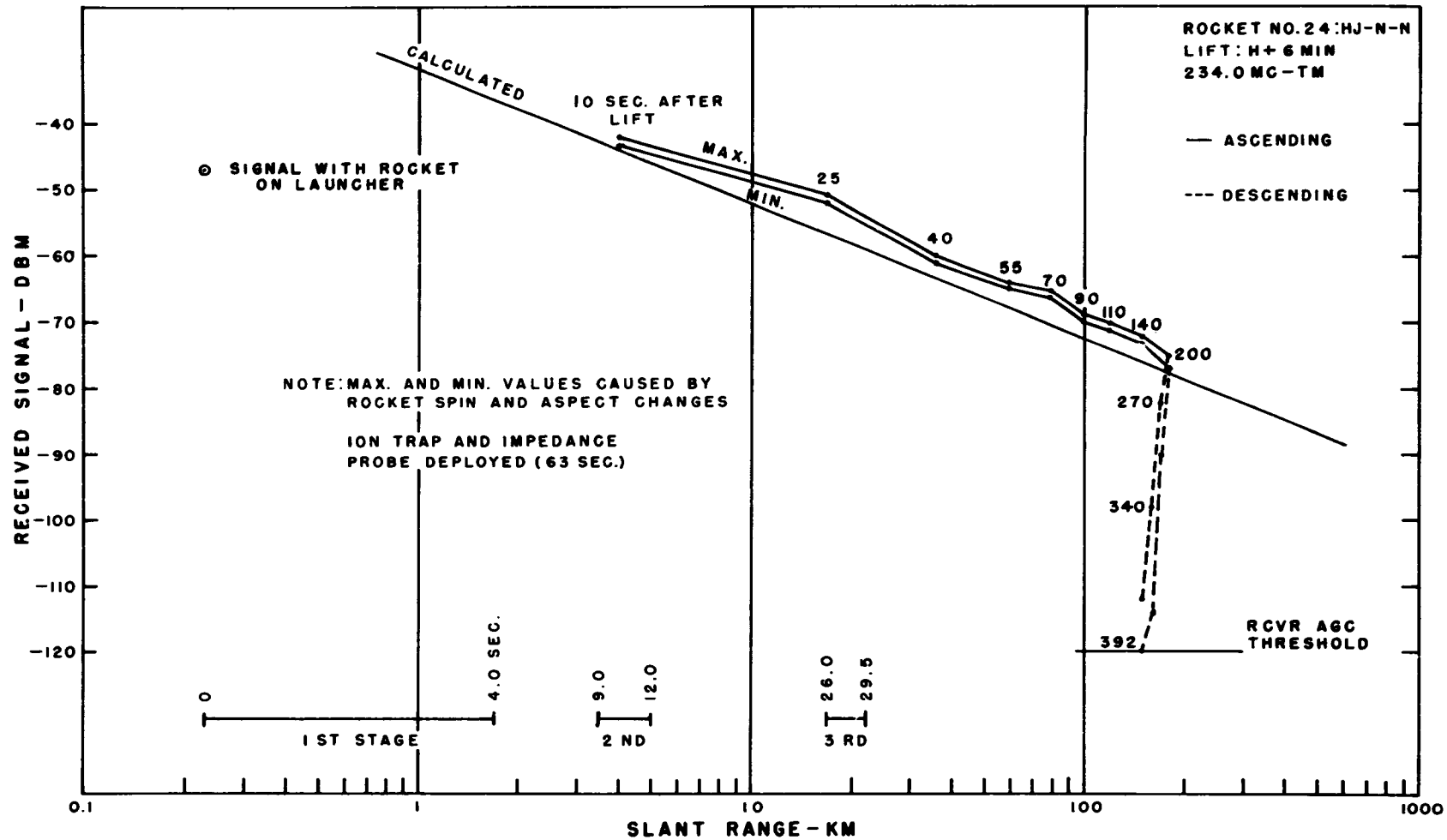

Figure C.223 Received signal strength versus slant range for VHF telemetry, Rocket 24, King Fish.

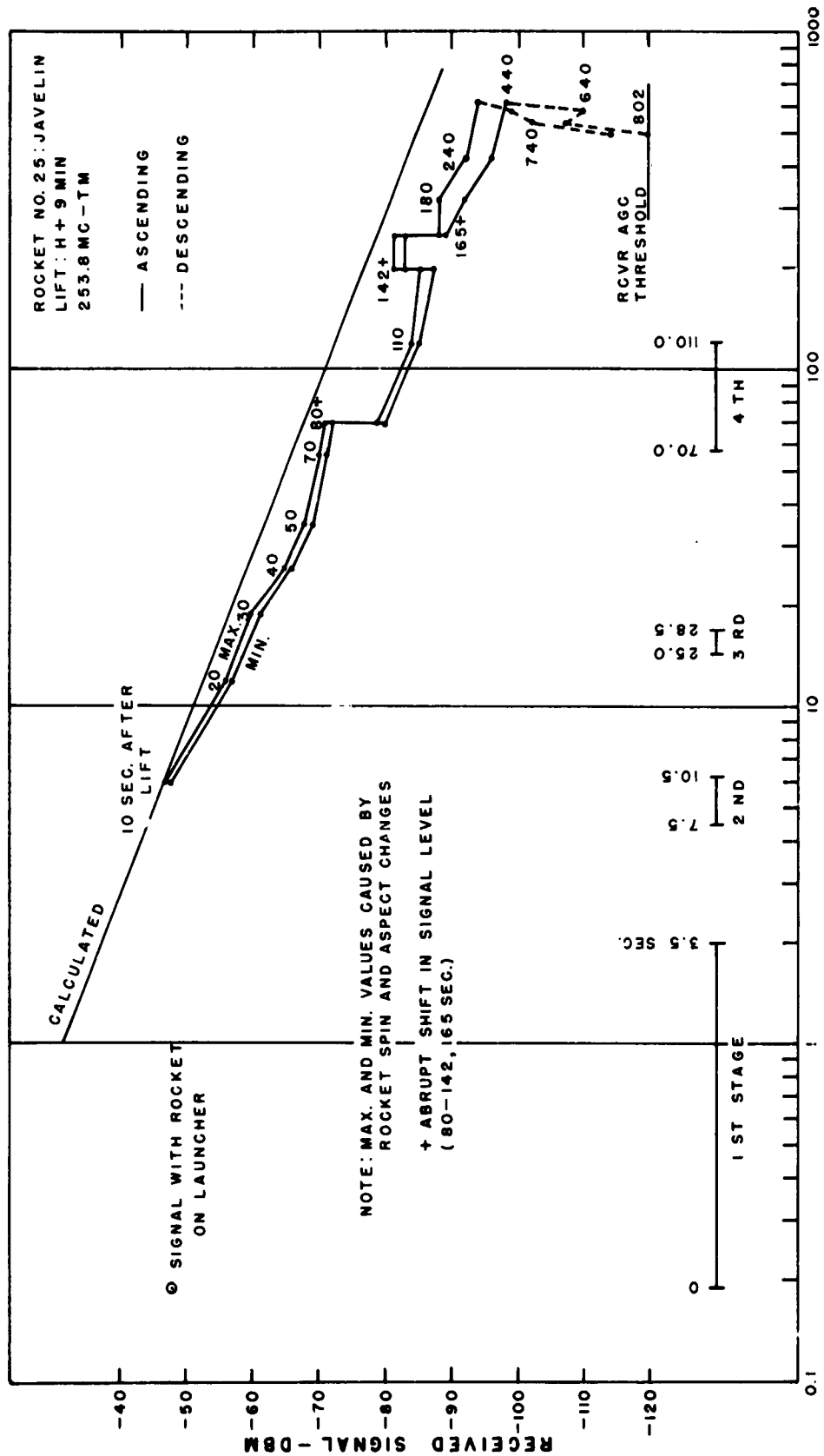

Figure C.224 Received signal strength versus slant range for VHF telemetry, Rocket 25, King Fish.

SECRET

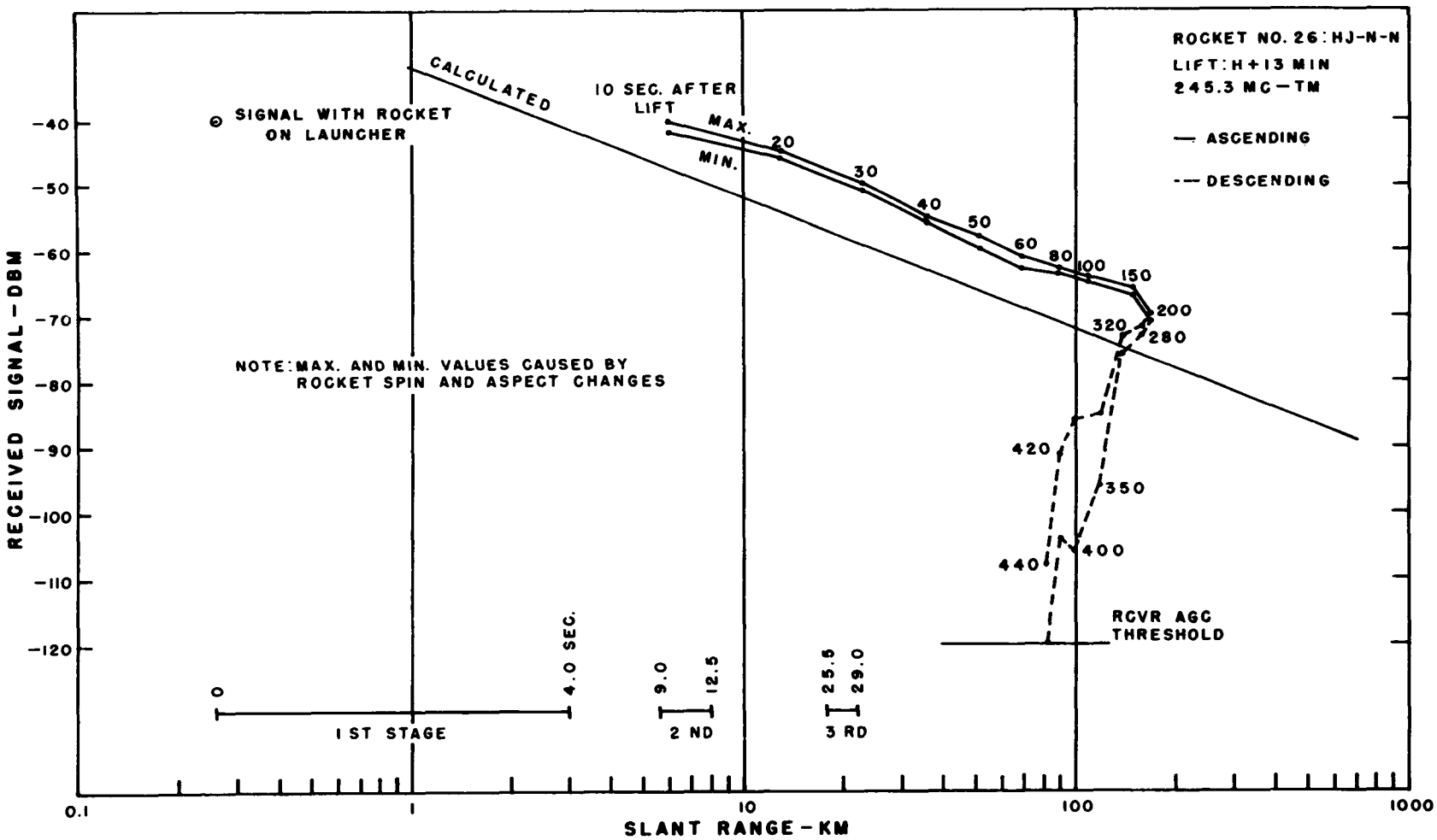

Figure C.225 Received signal strength versus slant range for VHF telemetry, Rocket 26, King Fish.

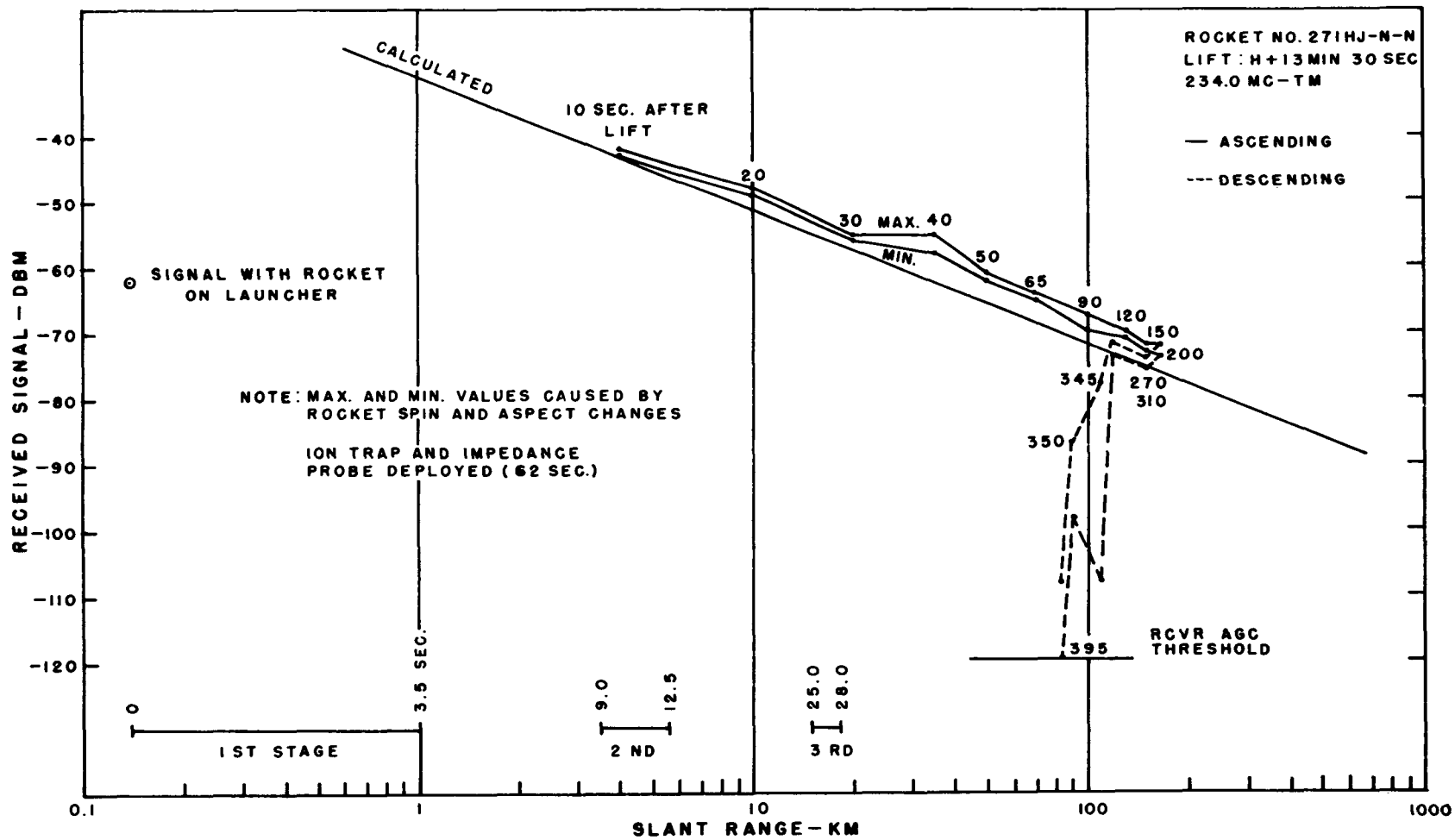

Figure C.226 Received signal strength versus slant range for VHF telemetry, Rocket 27, King Fish.

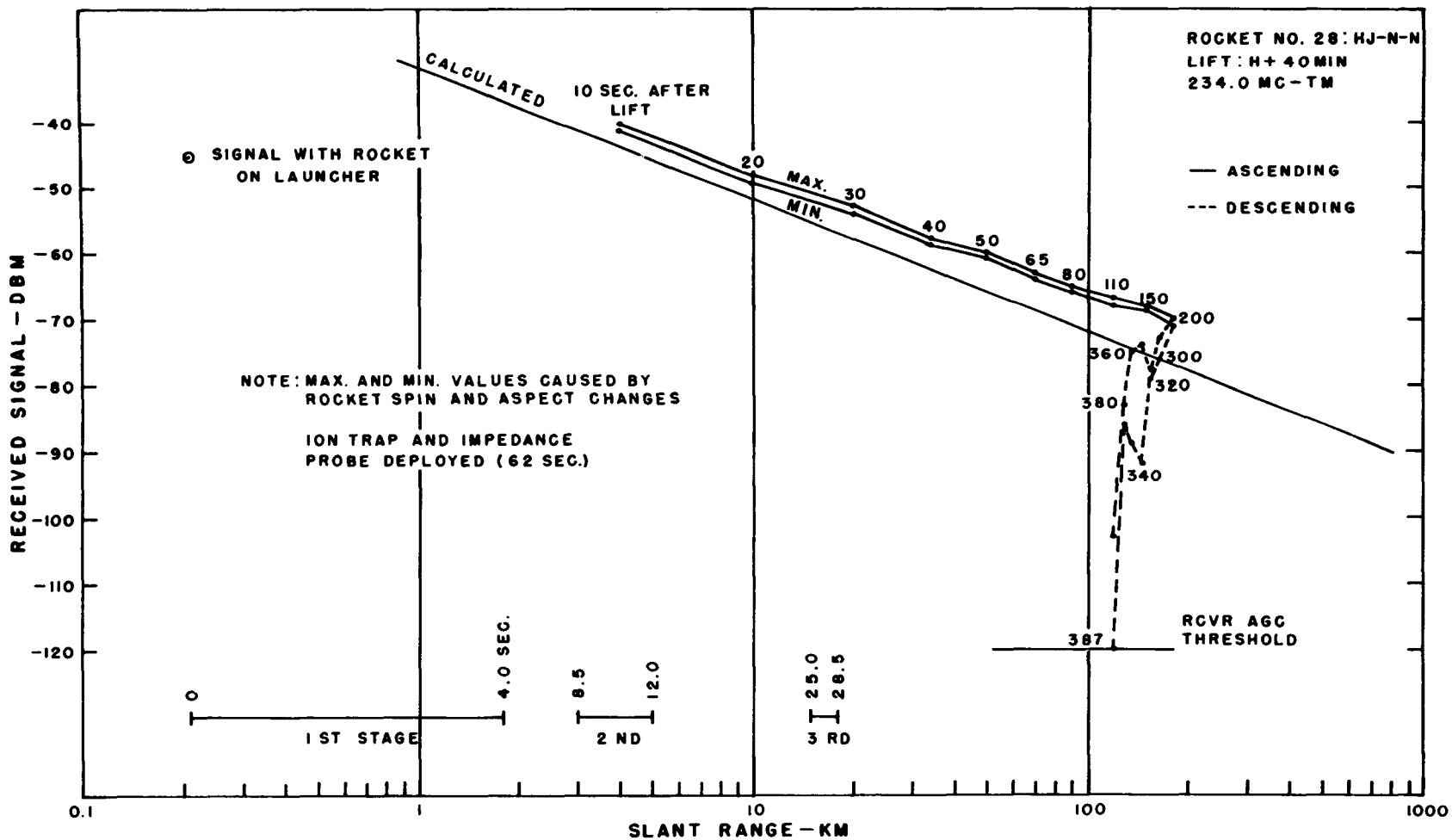

Figure C.227 Received signal strength versus slant range for VHF telemetry, Rocket 28, King Fish.

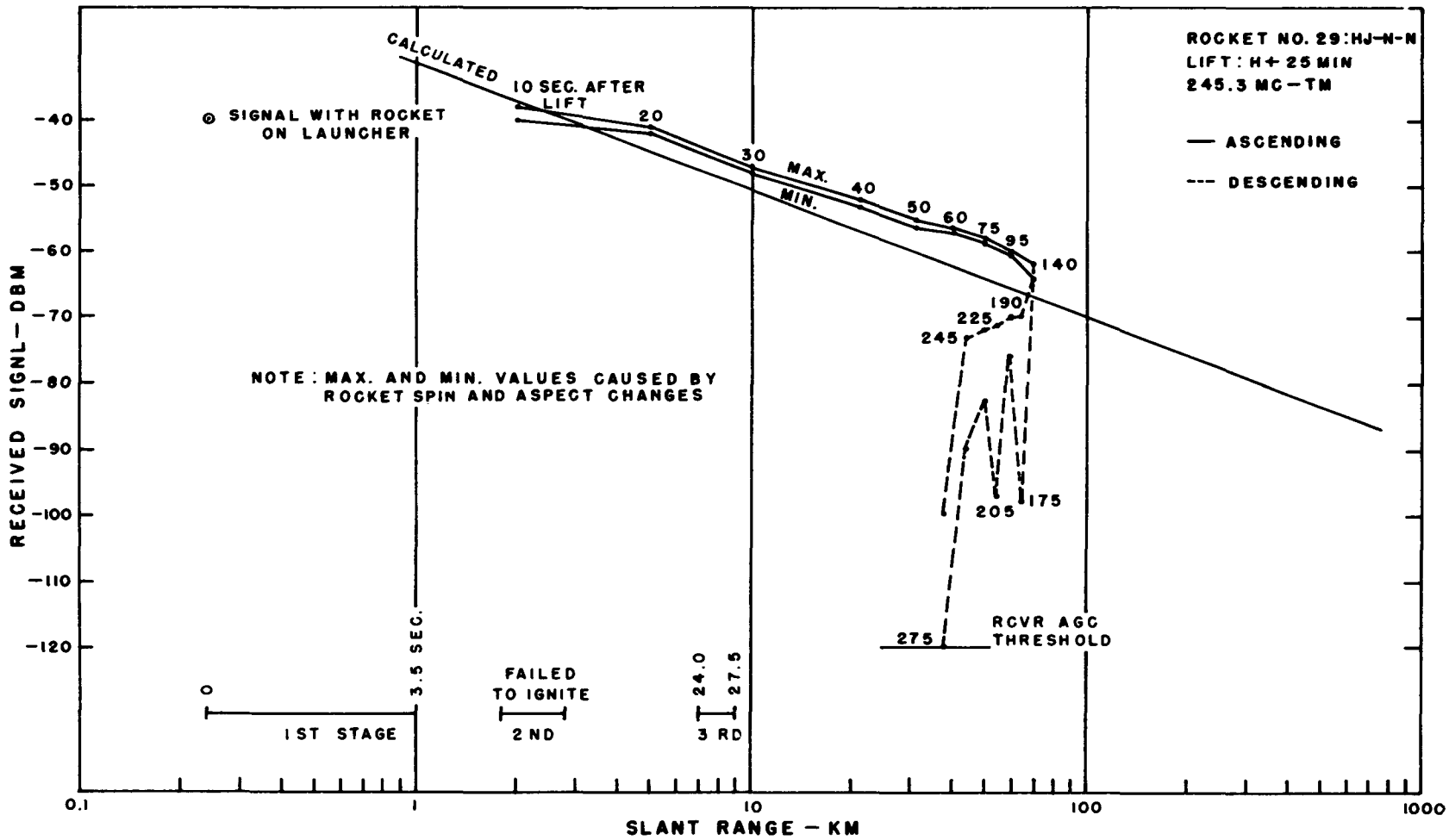

Figure C.228 Received signal strength versus slant range for VHF telemetry, Rocket 29, King Fish.

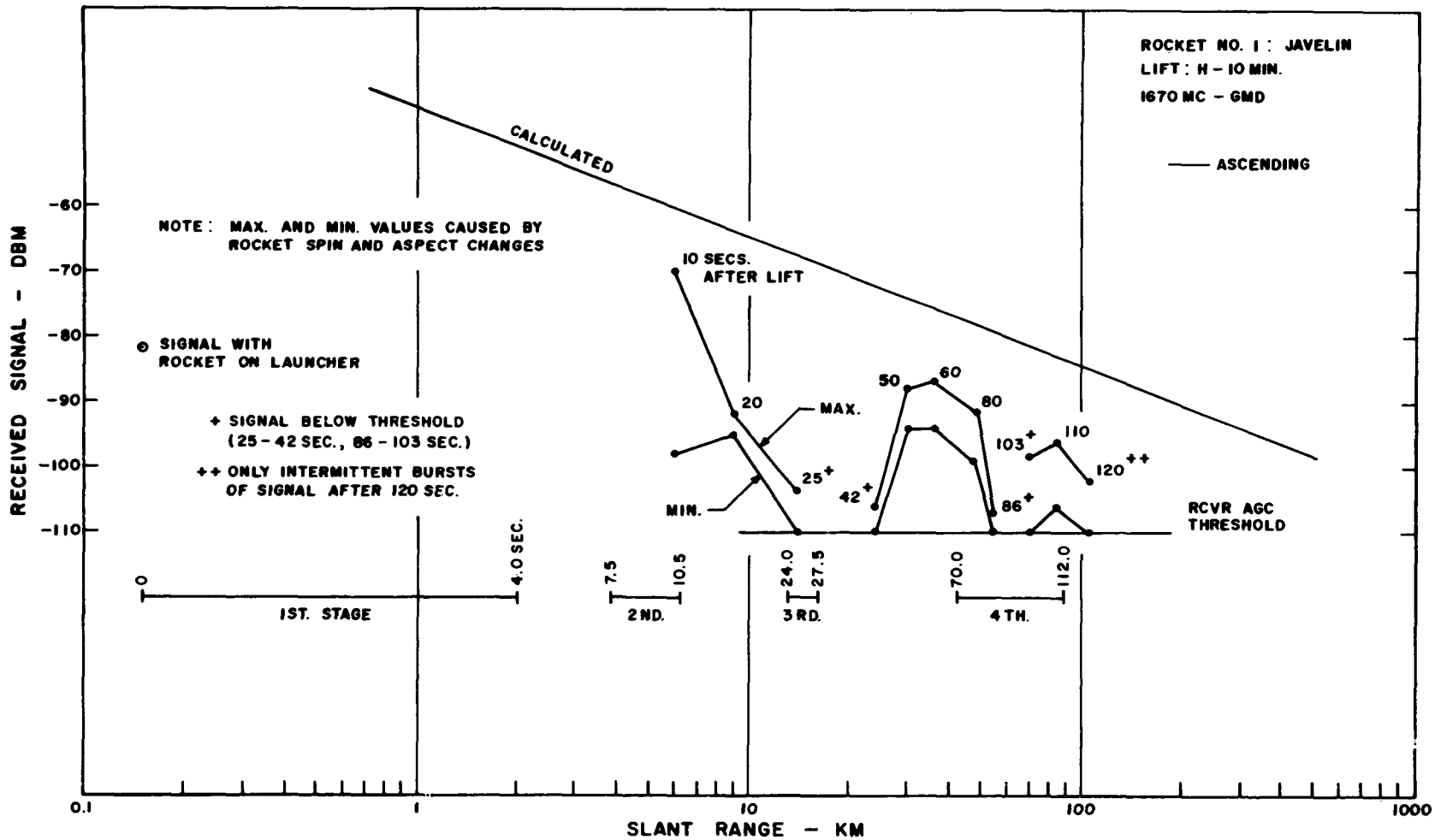

Figure C.229 Received signal strength versus slant range for GMD telemetry, Rocket 1, Star Fish.

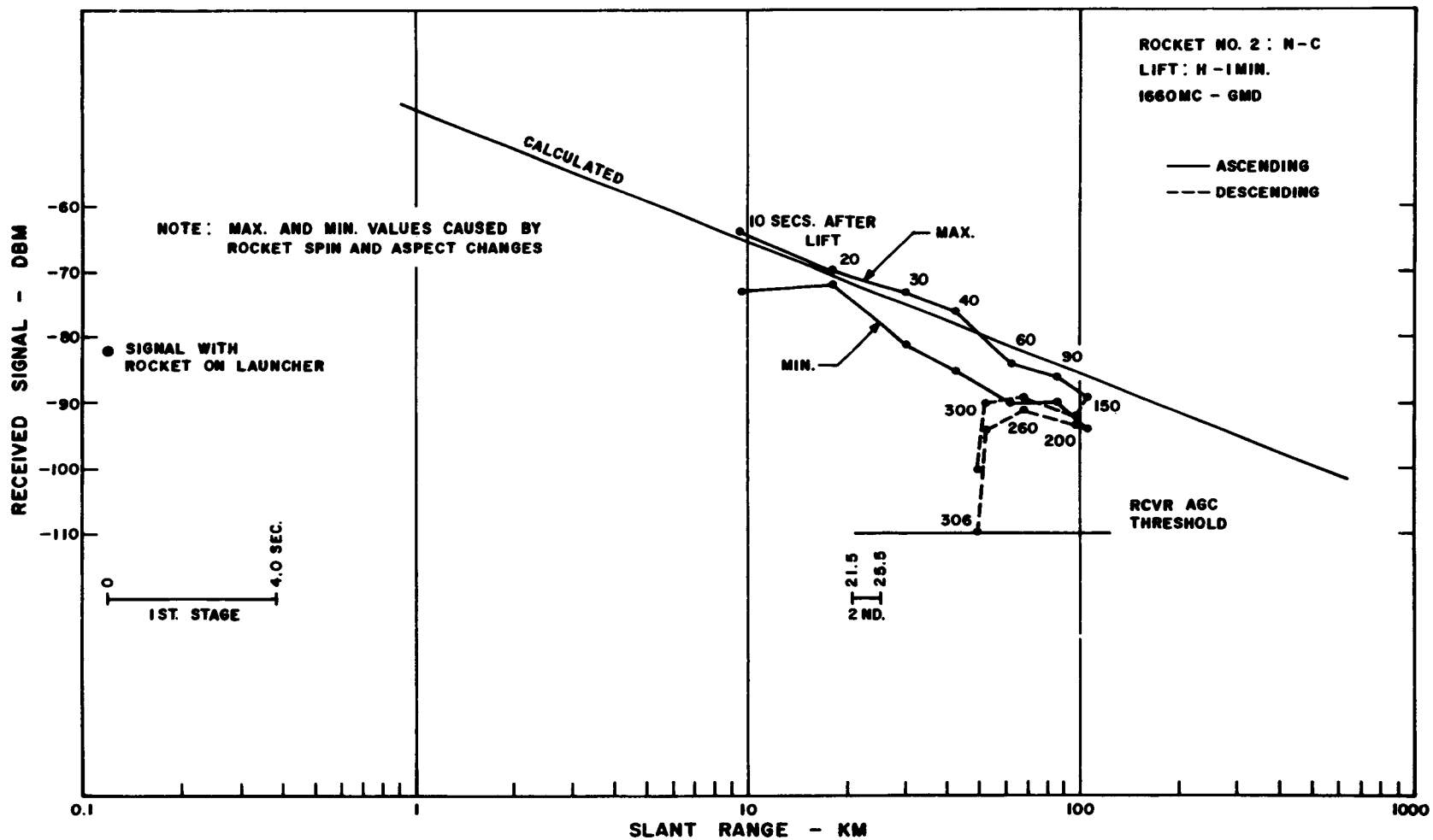

Figure C.230 Received signal strength versus slant range for GMD telemetry, Rocket 2, Star Fish.

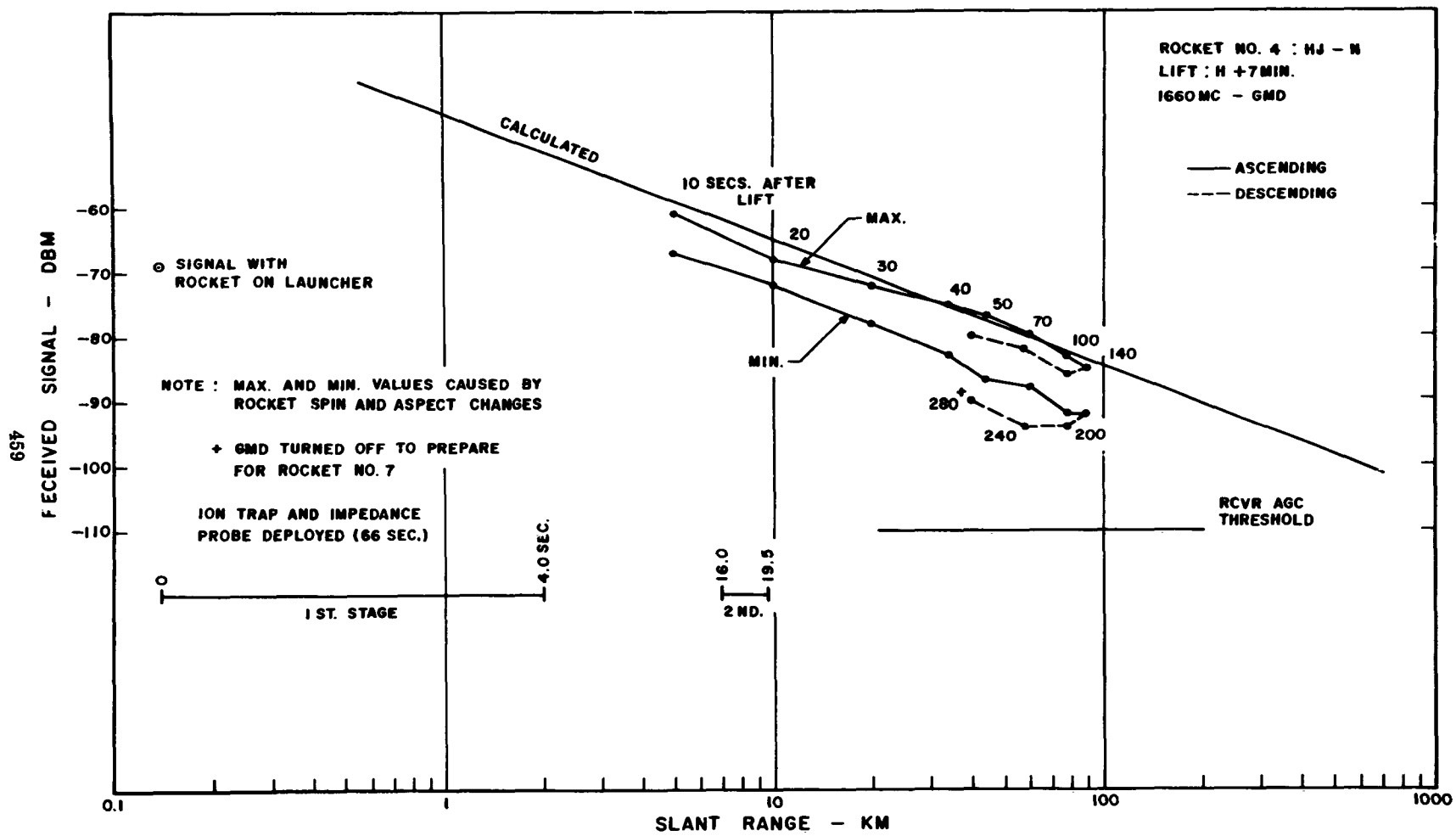

Figure C.231 Received signal strength versus slant range for GMD telemetry, Rocket 4, Star Fish.

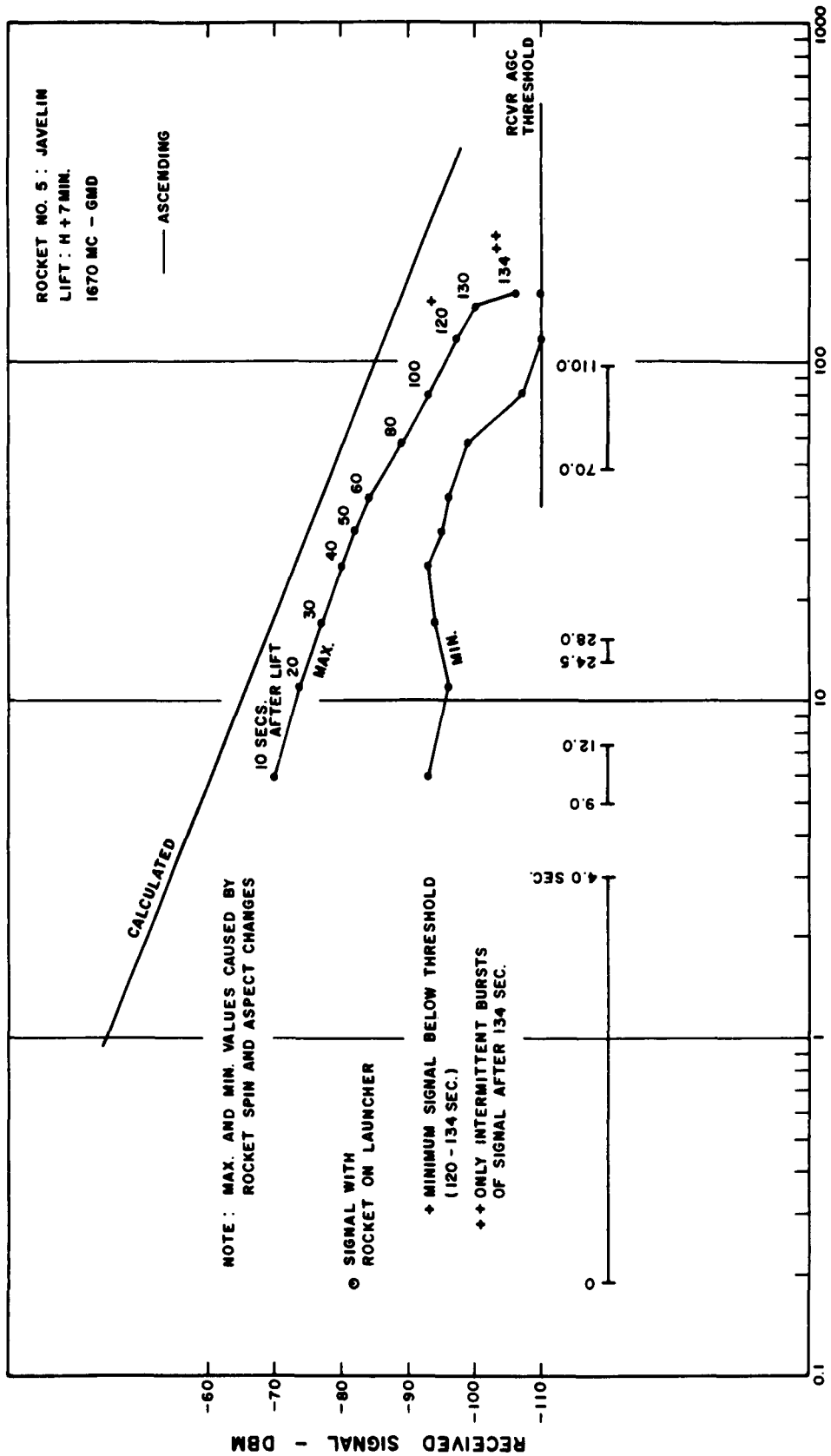

Figure C.232 Received signal strength versus slant range for GMD telemetry, Rocket 5, Star Fish.

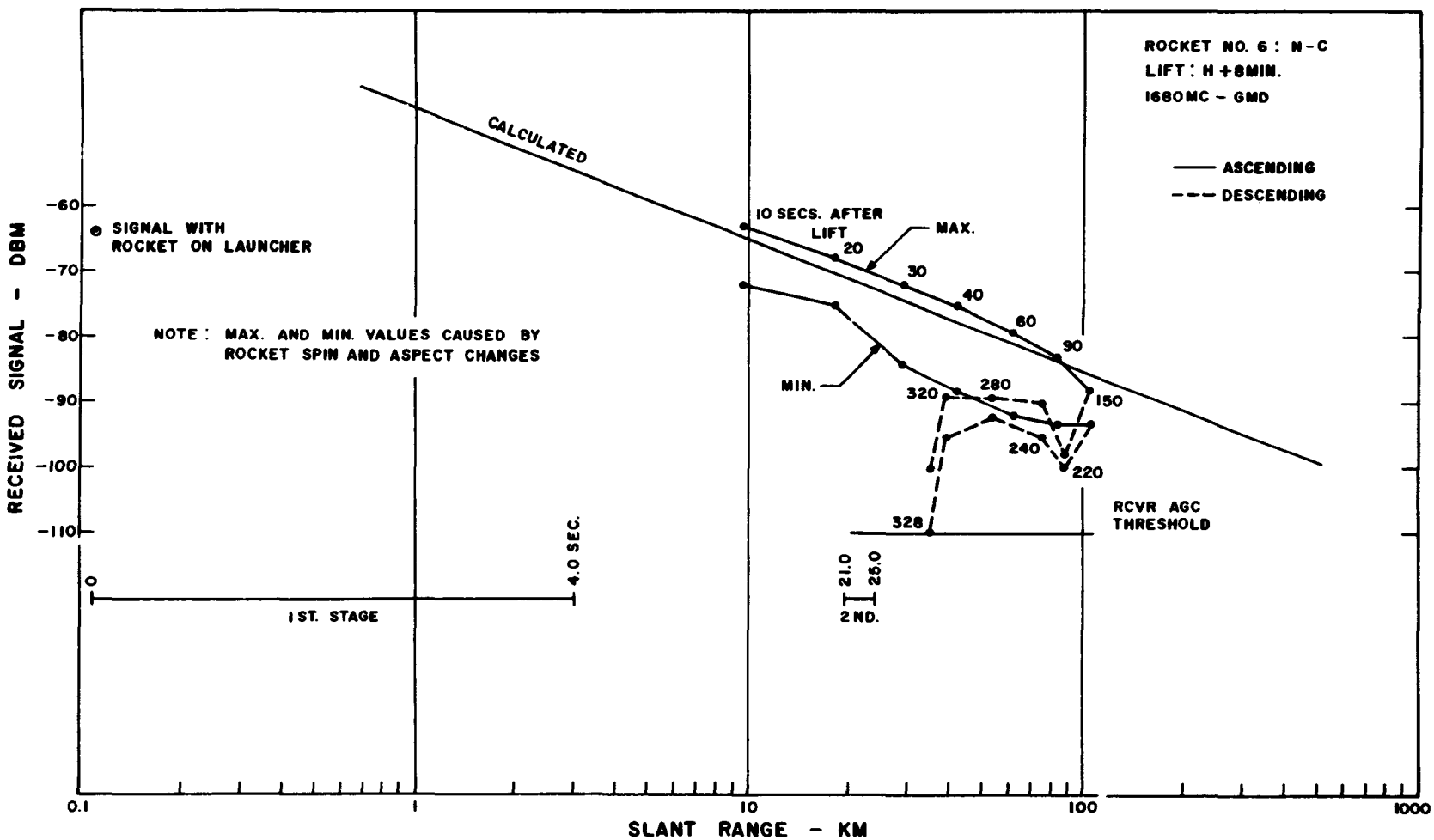

Figure C.233 Received signal strength versus slant range for GMD telemetry, Rocket 6, Star Fish.

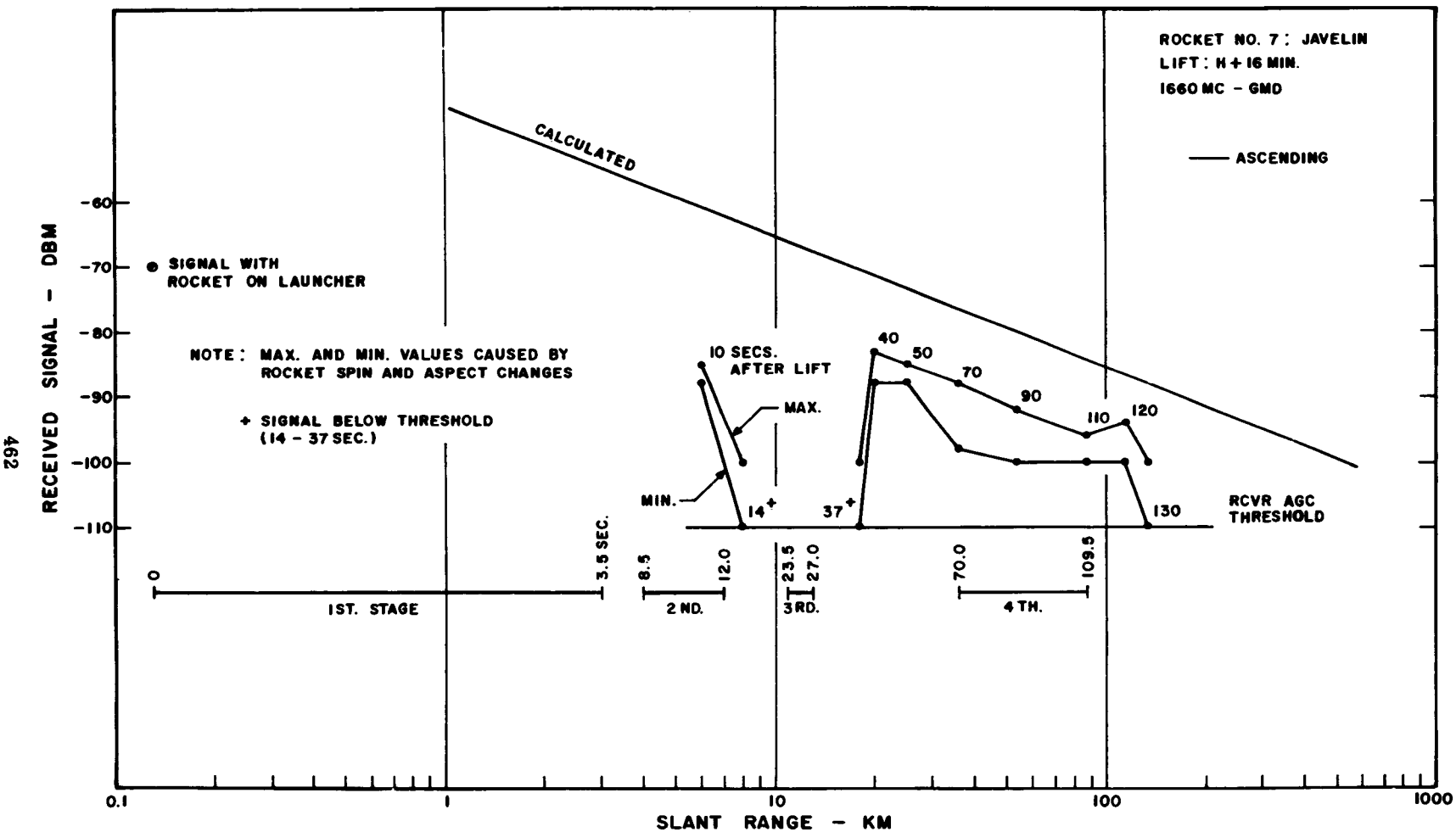

Figure C.234 Received signal strength versus slant range for GMD telemetry, Rocket 7, Star Fish.

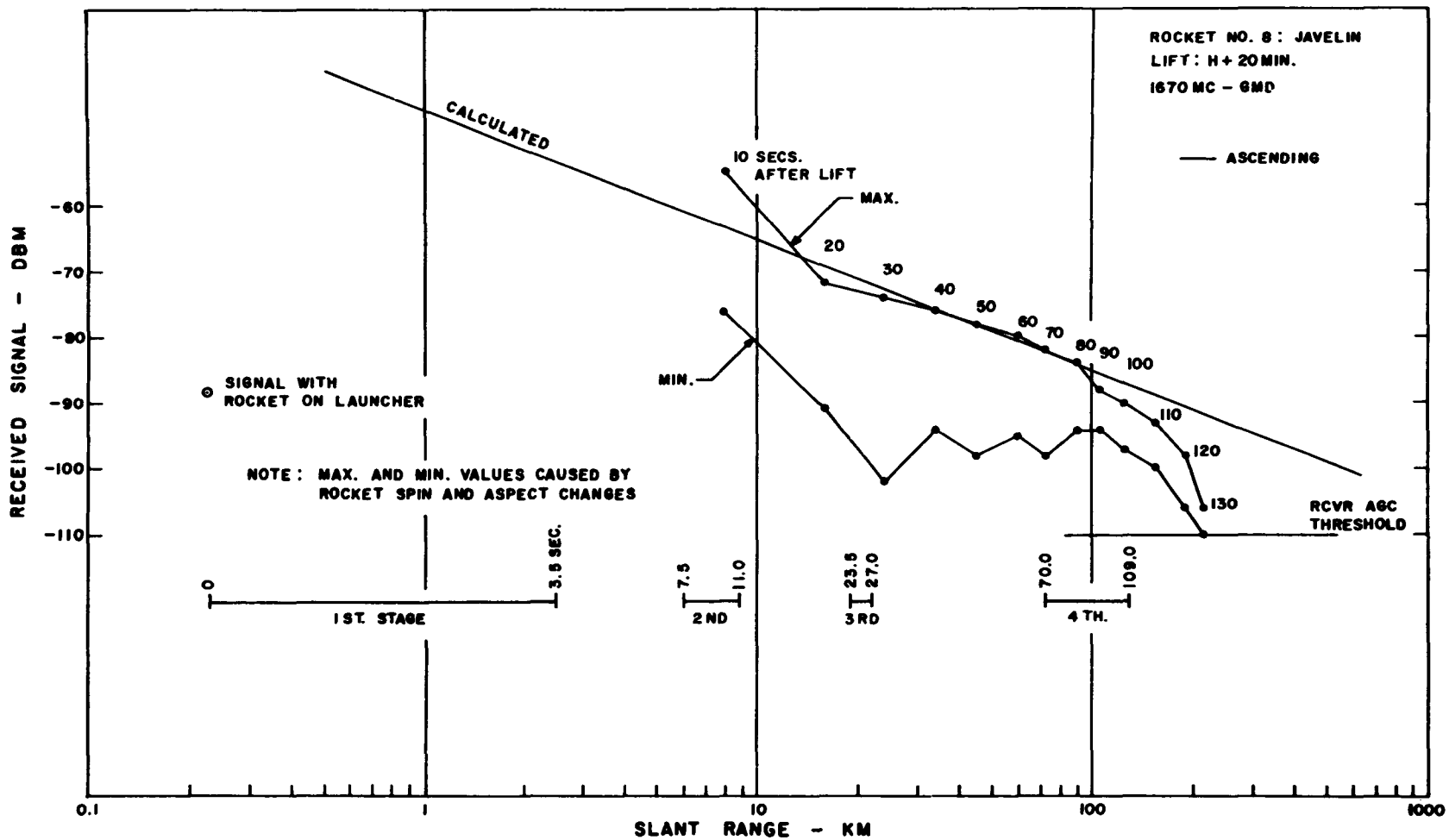

Figure C.235 Received signal strength versus slant range for GMD telemetry, Rocket 8, Star Fish.

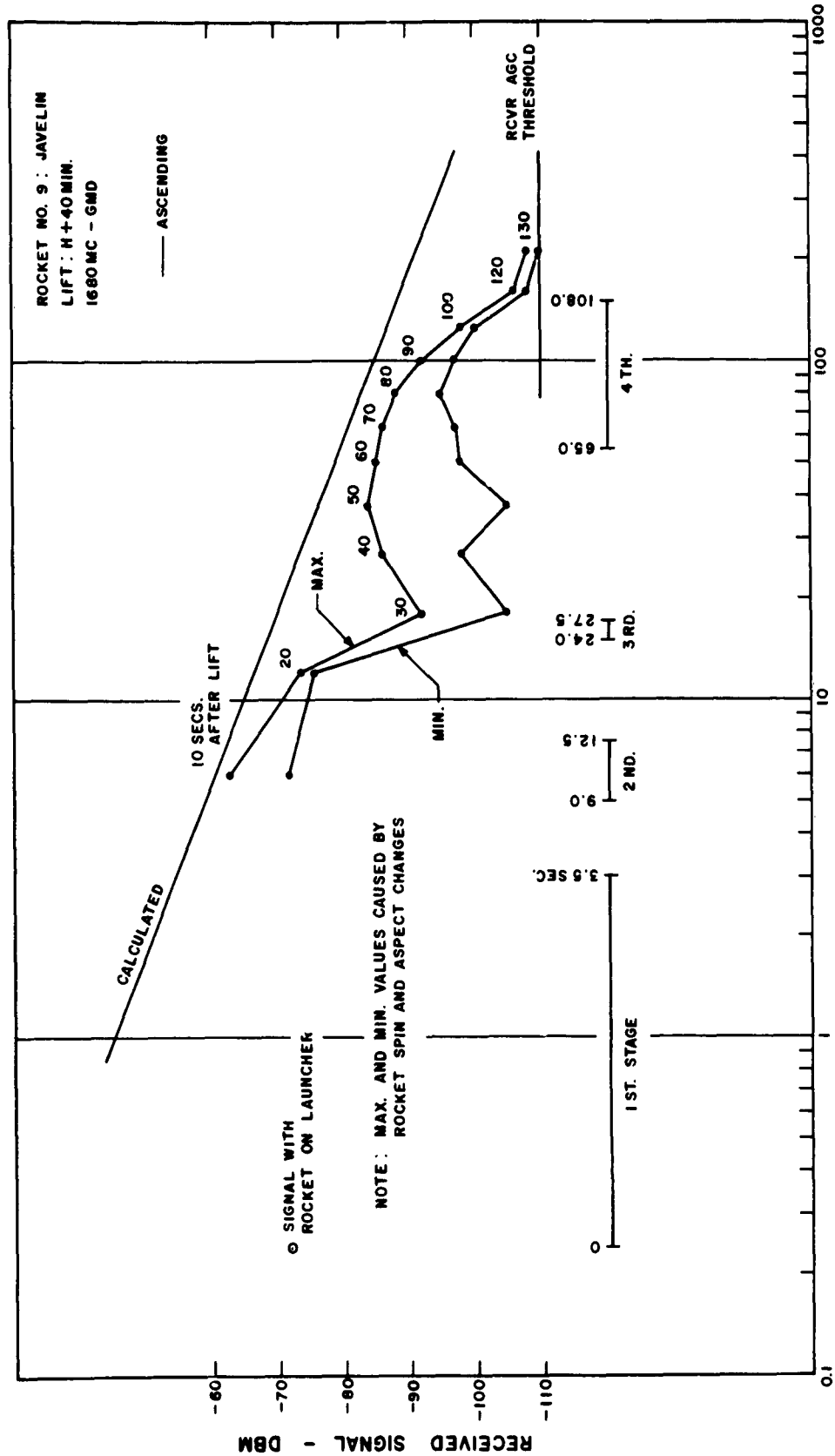

Figure C.236 Received signal strength versus slant range for GMD telemetry, Rocket 9, Star Fish.

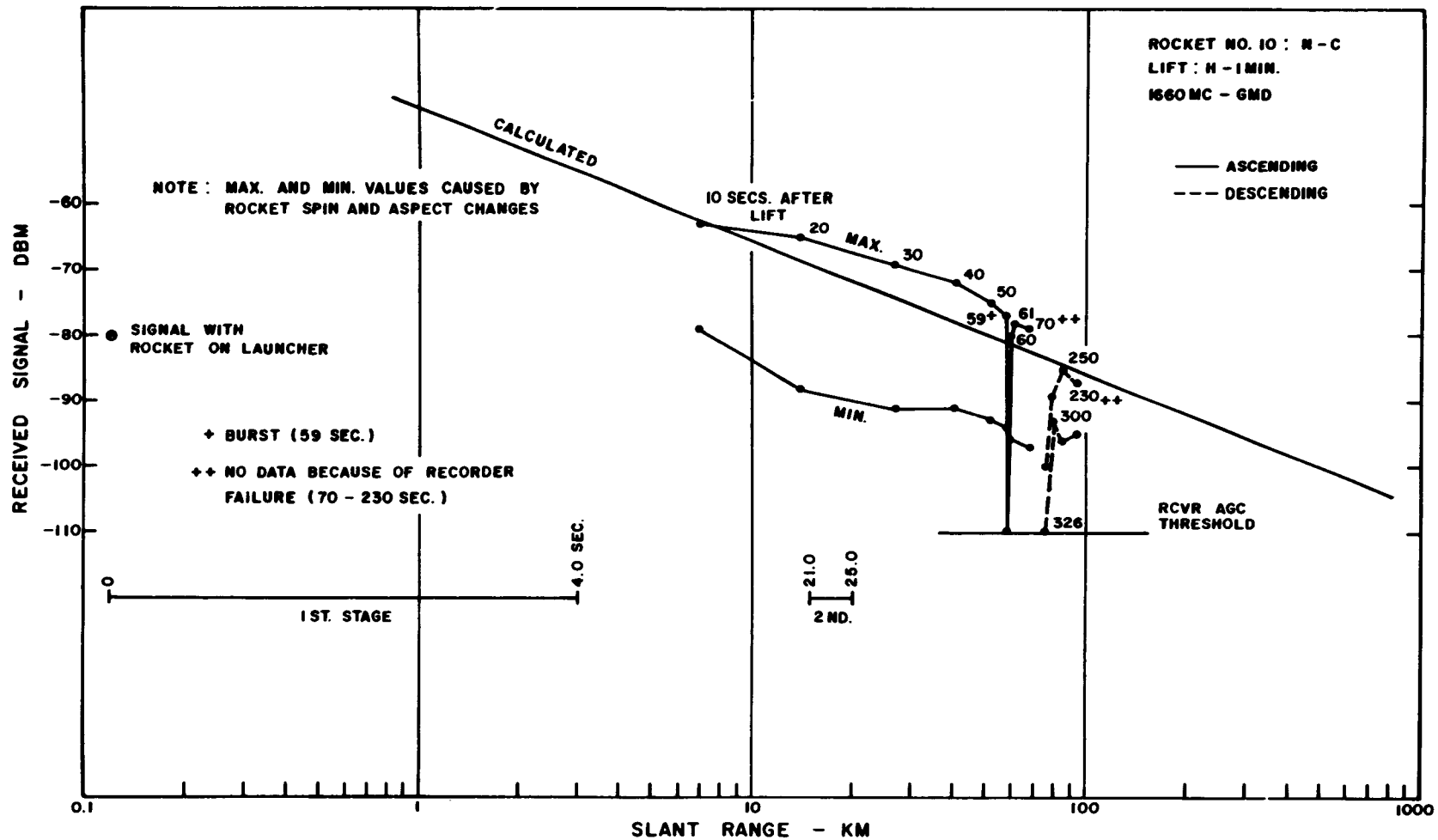

Figure C.237 Received signal strength versus slant range for GMD telemetry, Rocket 10, Blue Gill.

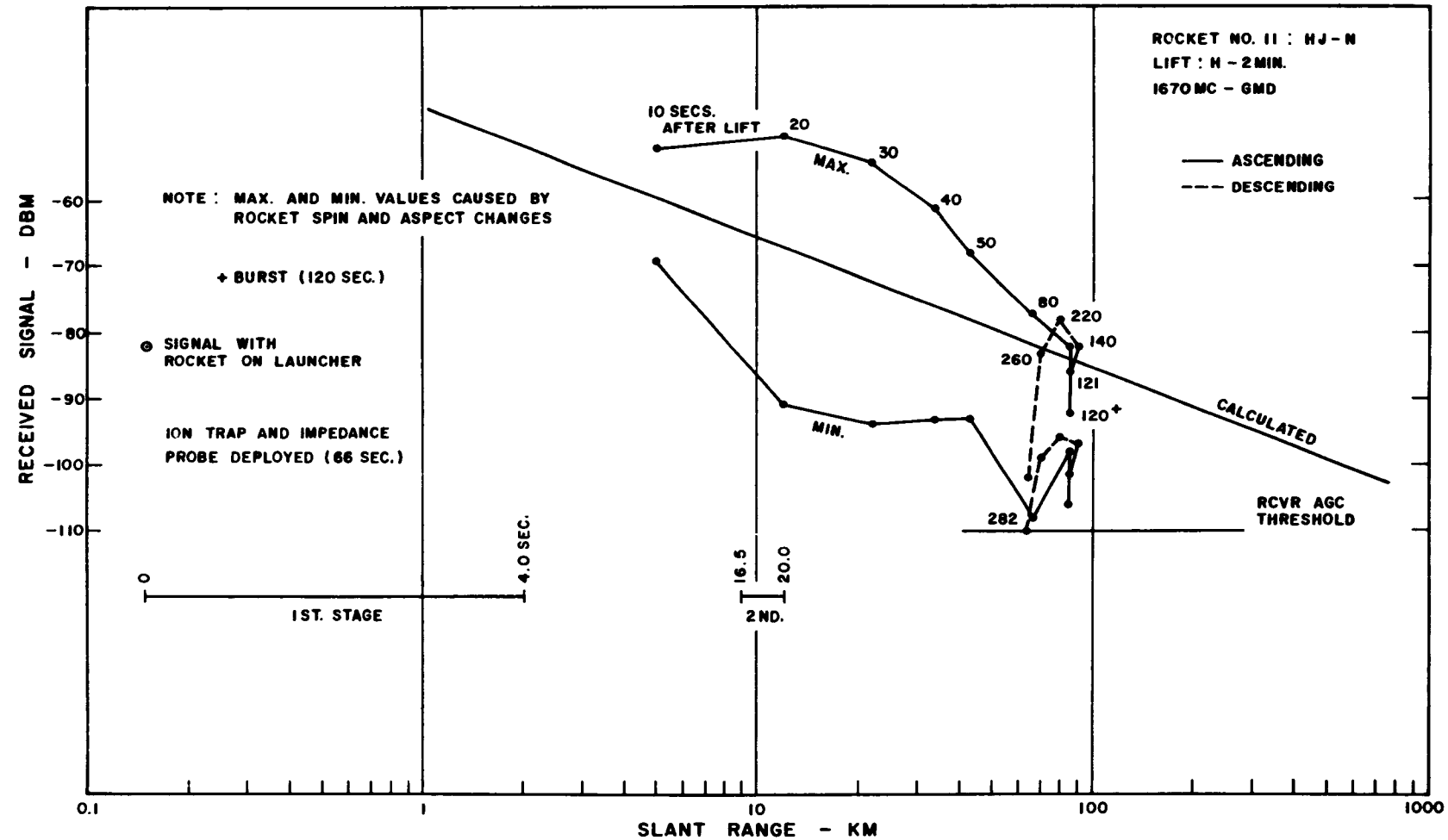

Figure C.238 Received signal strength versus slant range for GMD telemetry, Rocket 11, Blue Gill.

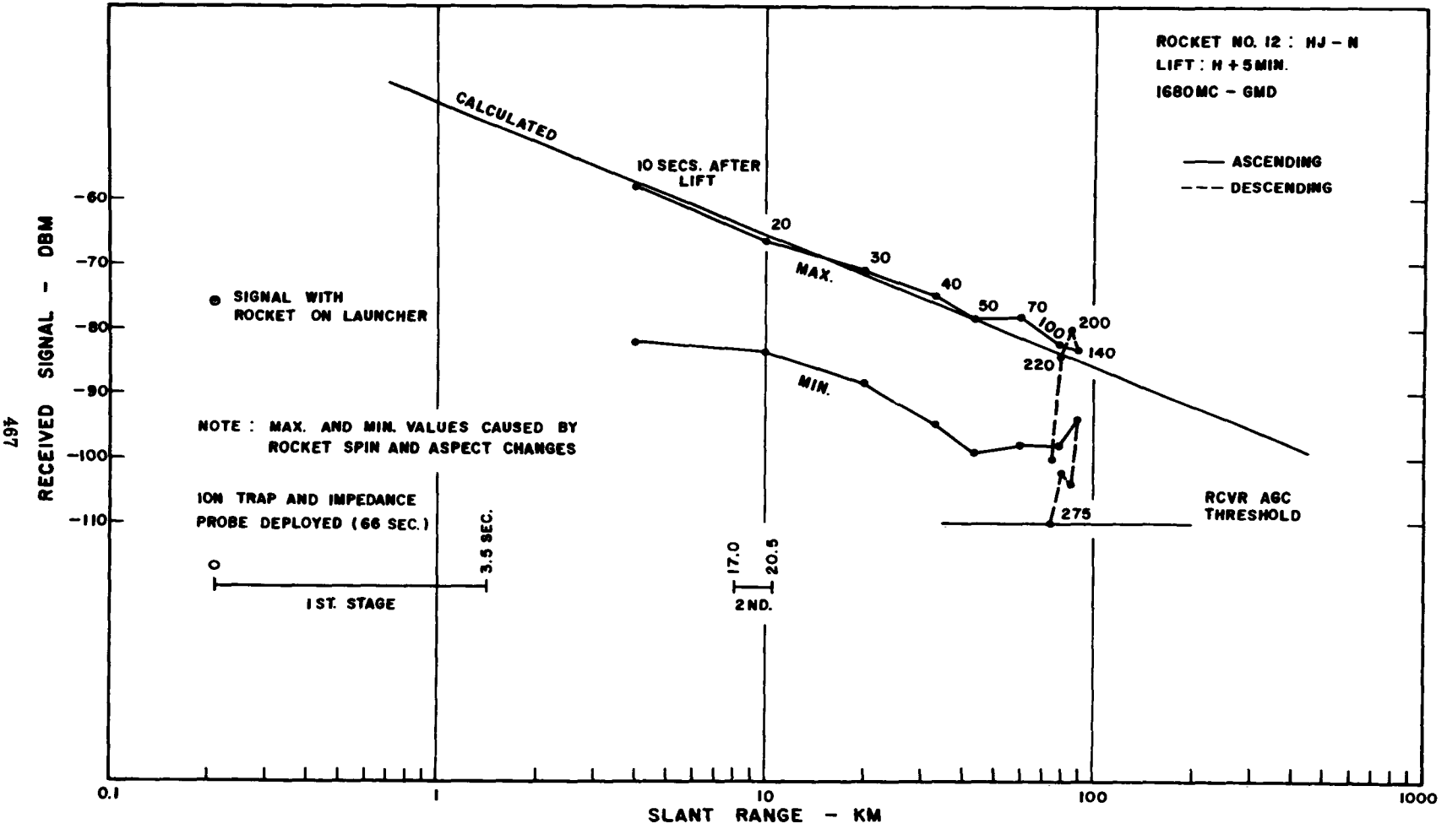

Figure C.239 Received signal strength versus slant range for GMD telemetry, Rocket 12, Blue Gill.

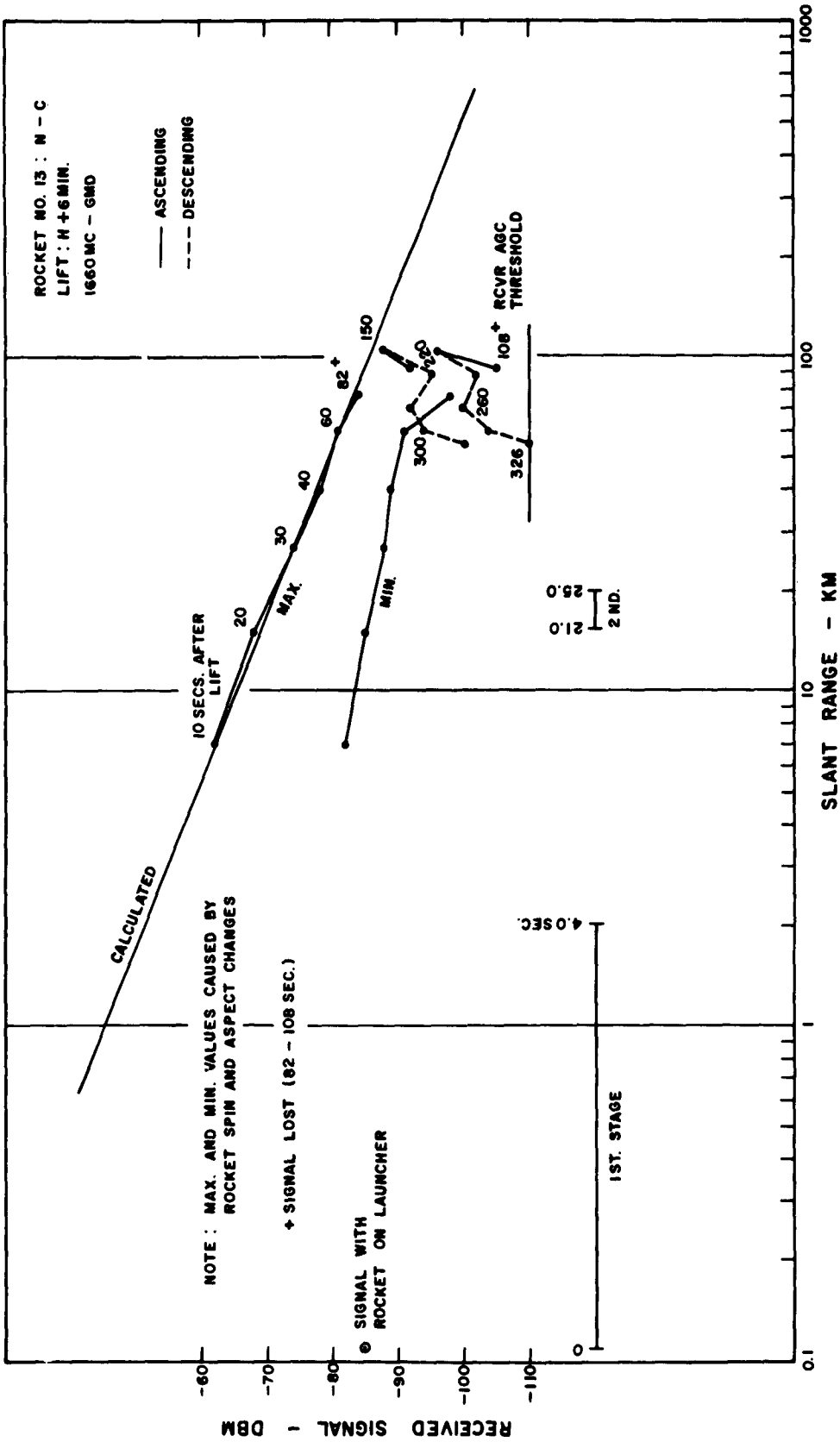

Figure C.240 Received signal strength versus slant range for GMD telemetry, Rocket 13, Blue Gill.

SECRET

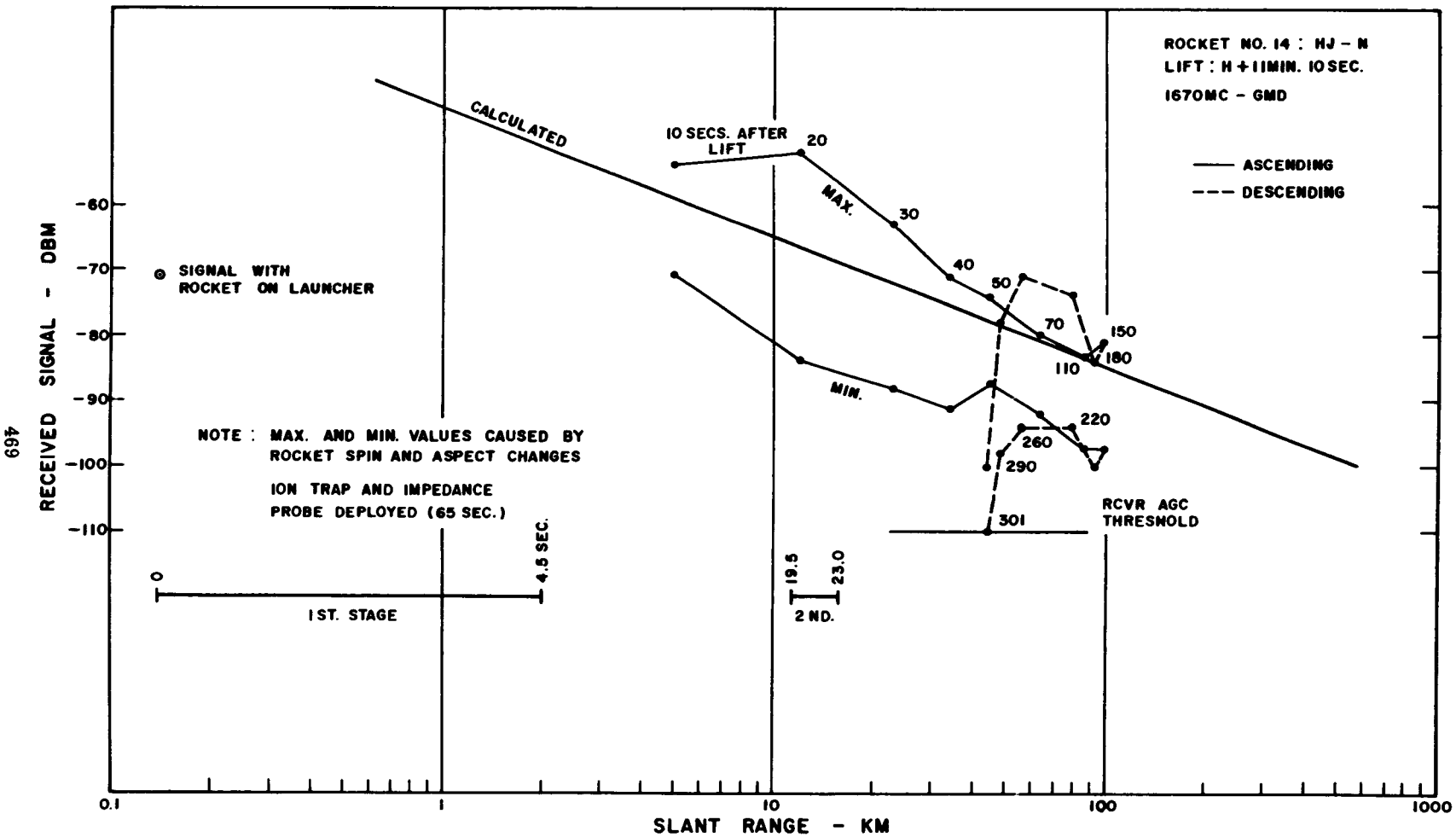

Figure C.241 Received signal strength versus slant range for GMD telemetry, Rocket 14, Blue Gill.

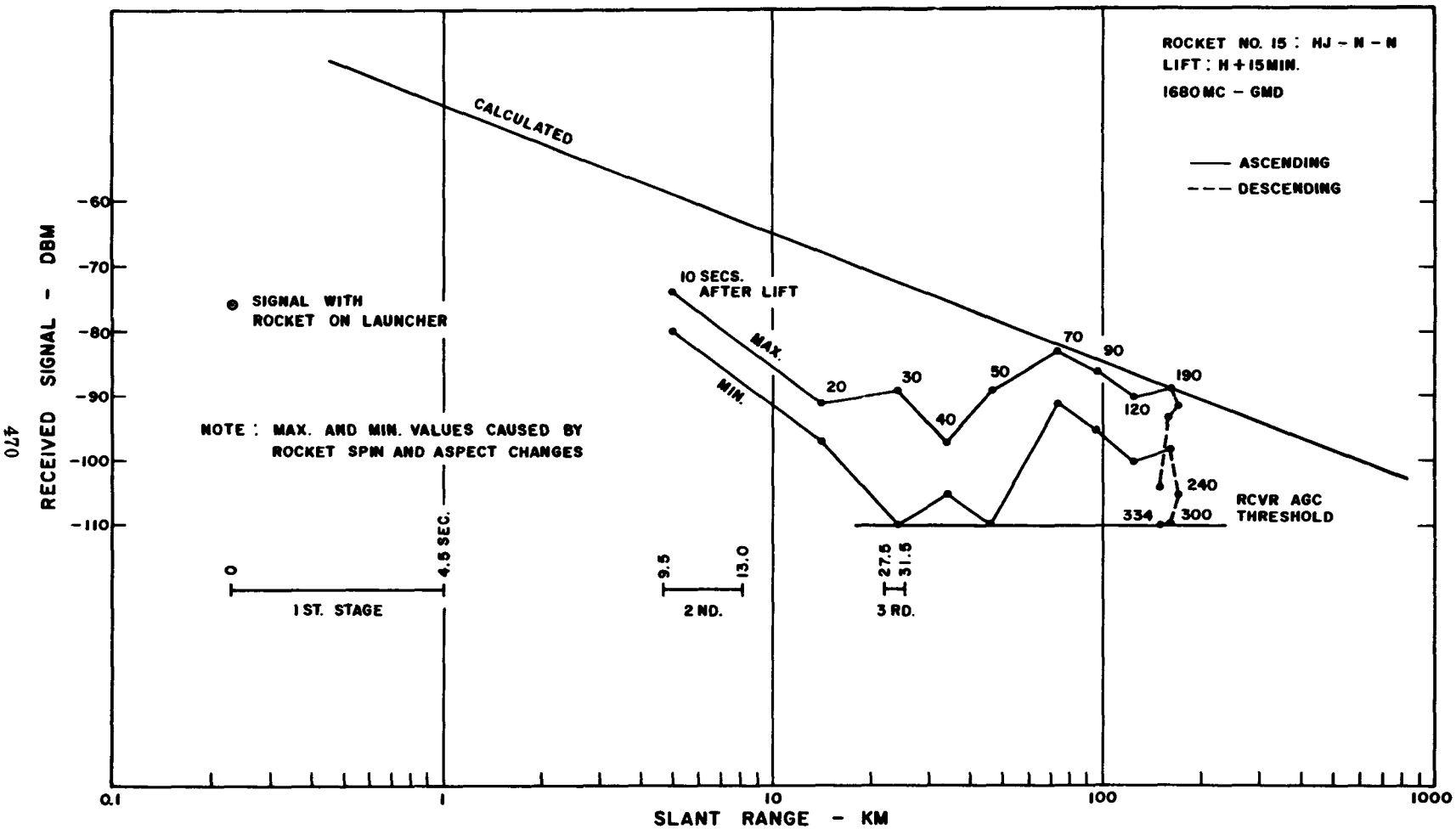

Figure C.242 Received signal strength versus slant range for GMD telemetry, Rocket 15, Blue Gill.

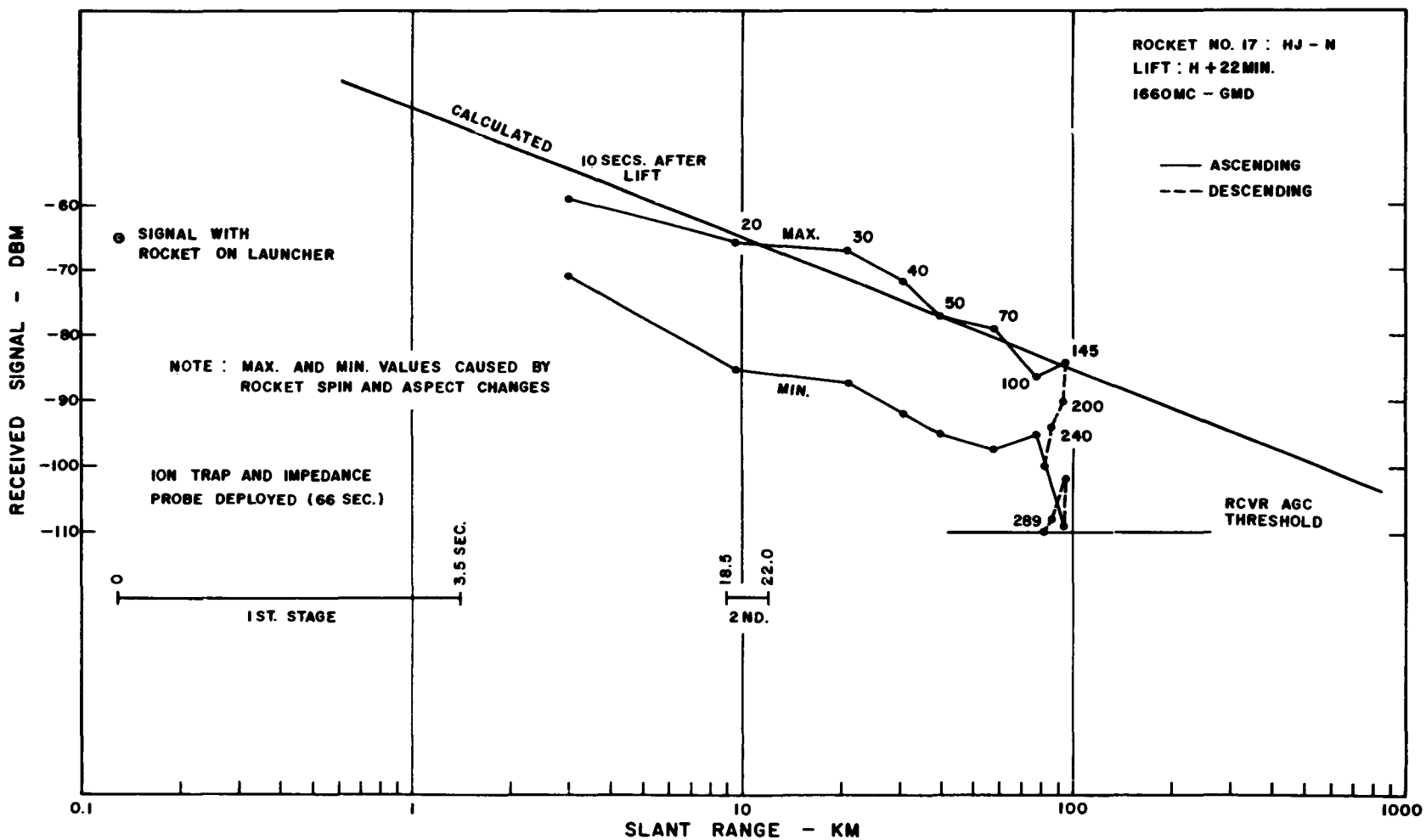

Figure C.243 Received signal strength versus slant range for GMD telemetry, Rocket 17, Blue Gill.

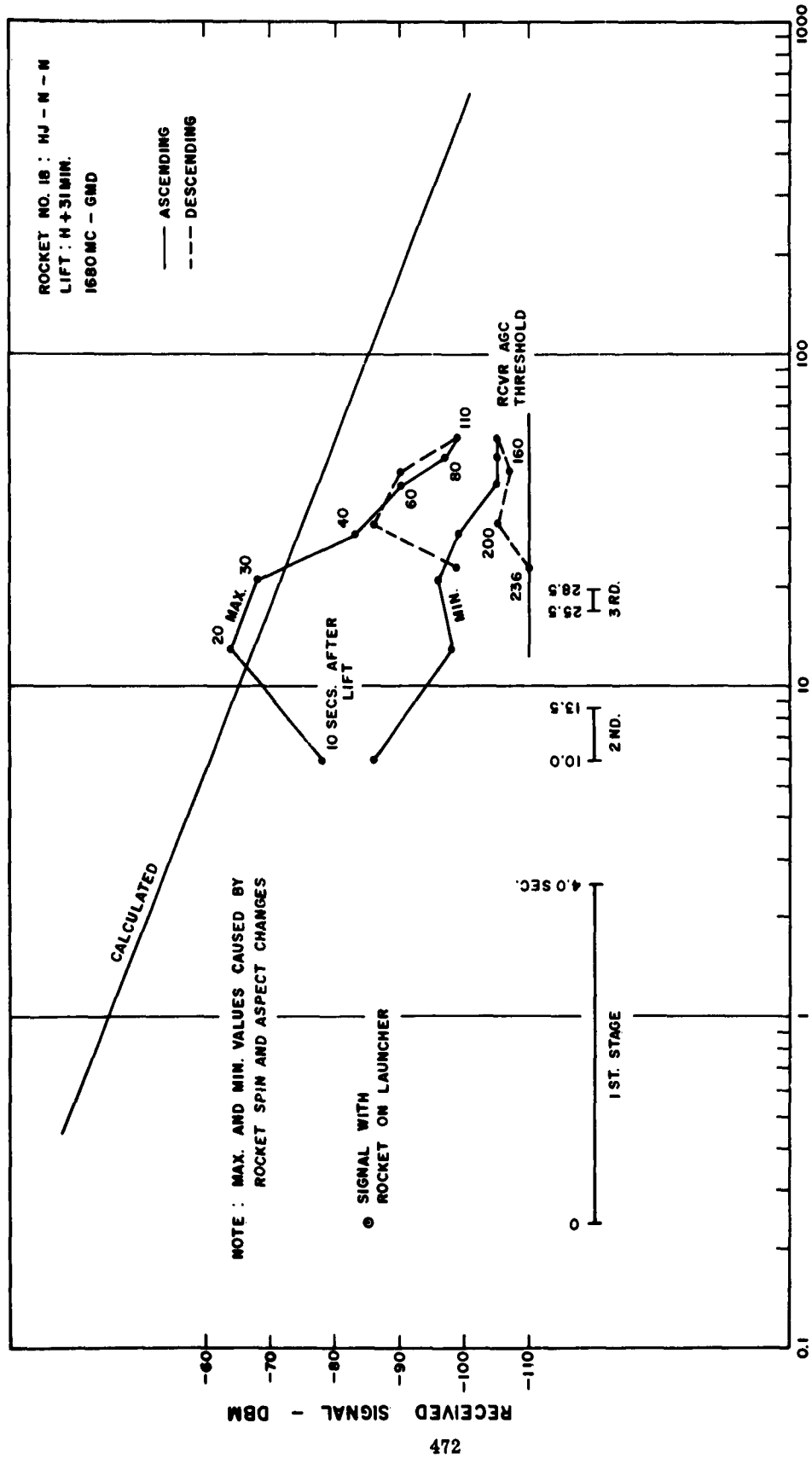

Figure C.244 Received signal strength versus slant range for GMD telemetry, Rocket 18, Blue Gill.

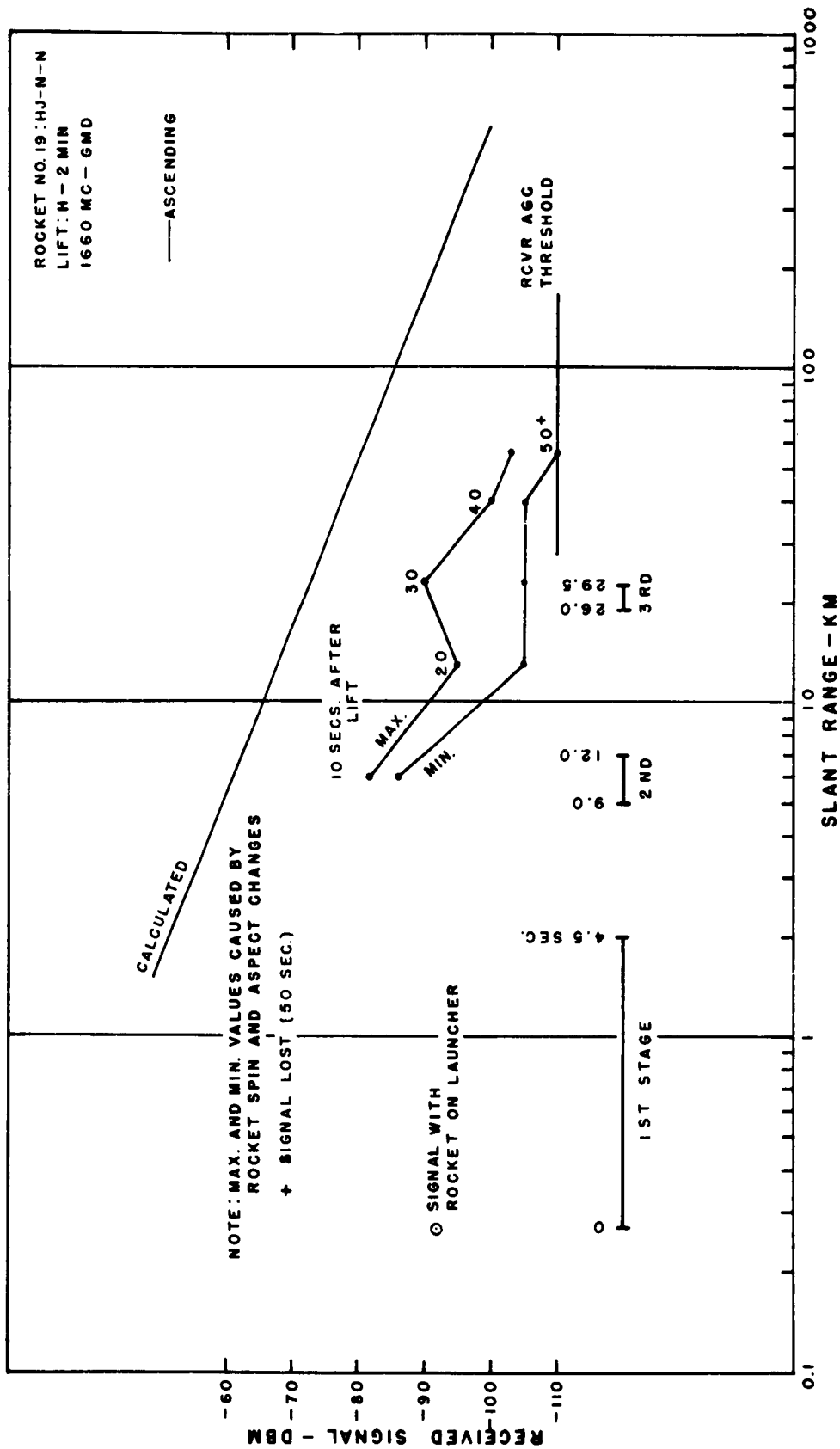

Figure C.245 Received signal strength versus slant range for GMD telemetry, Rocket 19, King Fish.

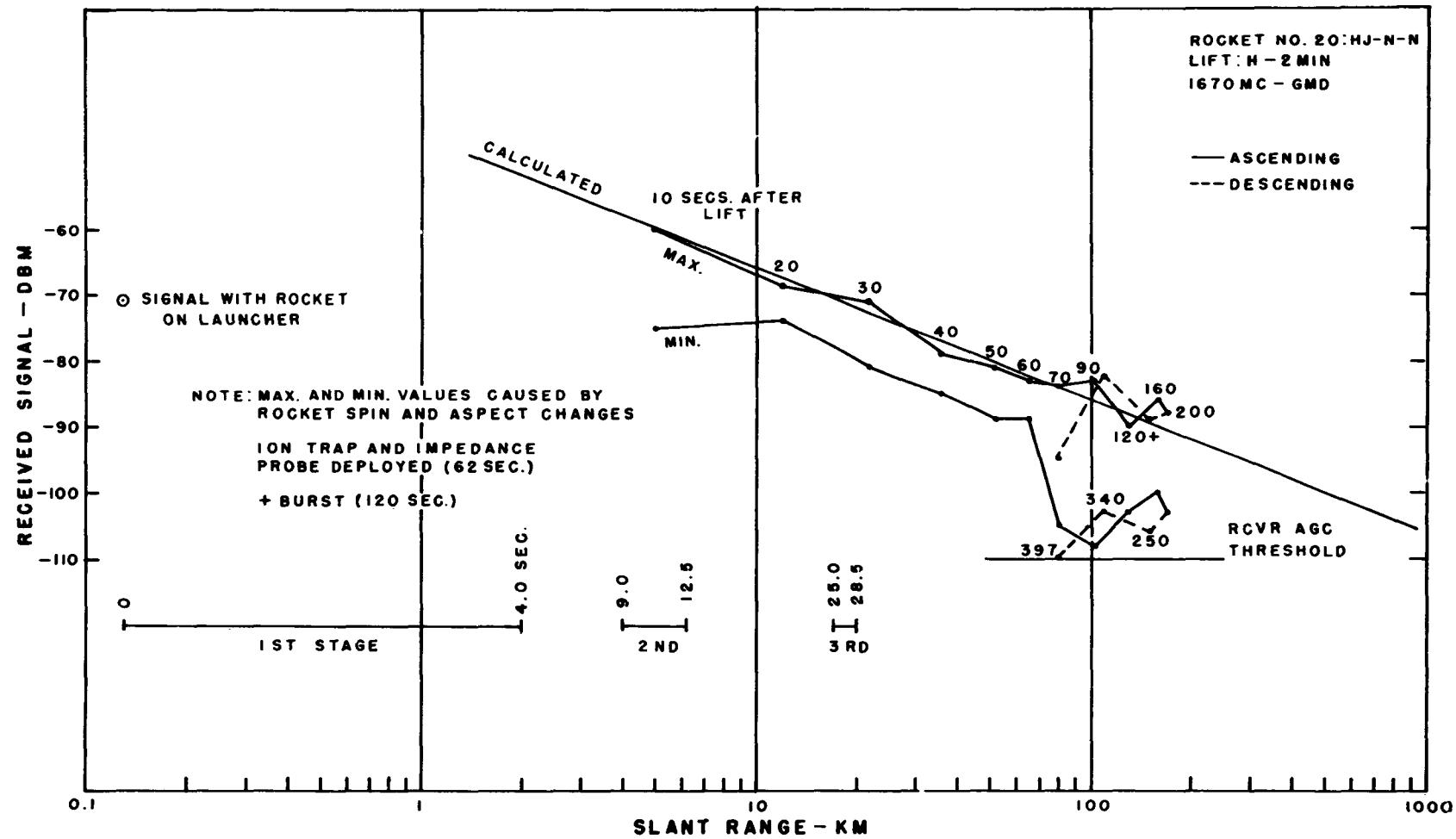

Figure C.246 Received signal strength versus slant range for GMD telemetry, Rocket 20, King Fish.

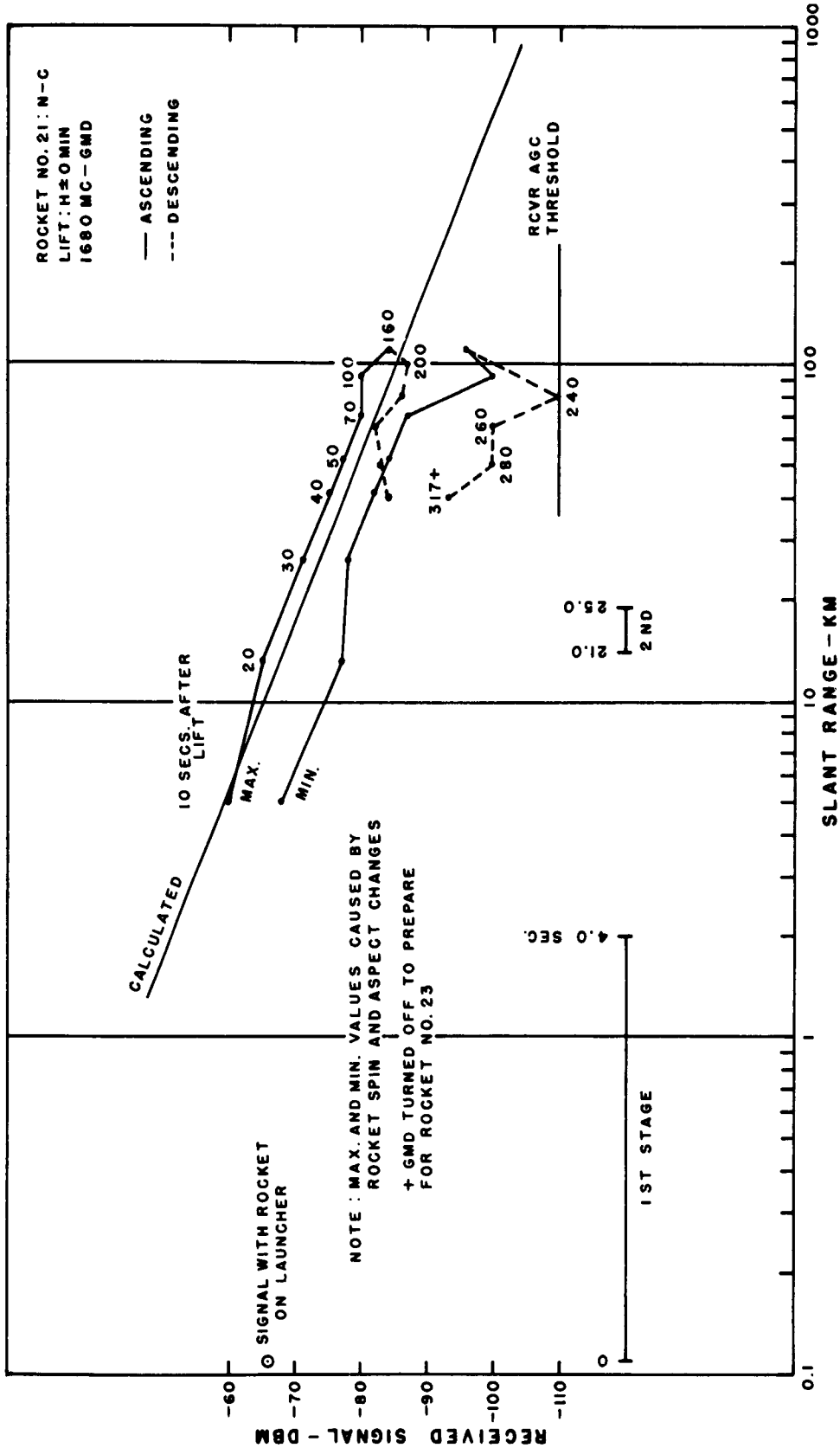

Figure C.247 Received signal strength versus slant range for GMD telemetry, Rocket 21, King Fish.

SECRET

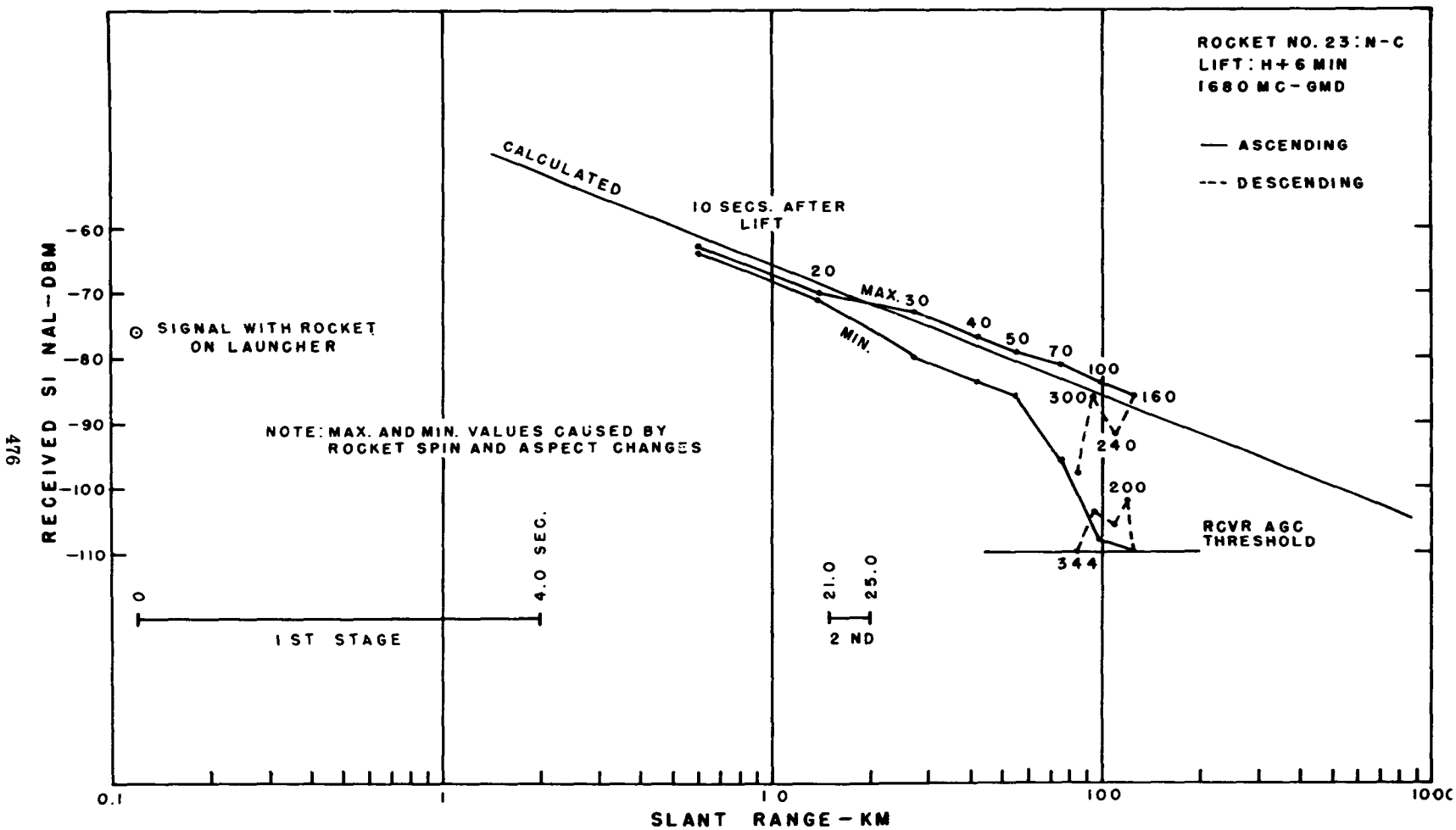

Figure C.248 Received signal strength versus slant range for GMD telemetry, Rocket 23, King Fish.

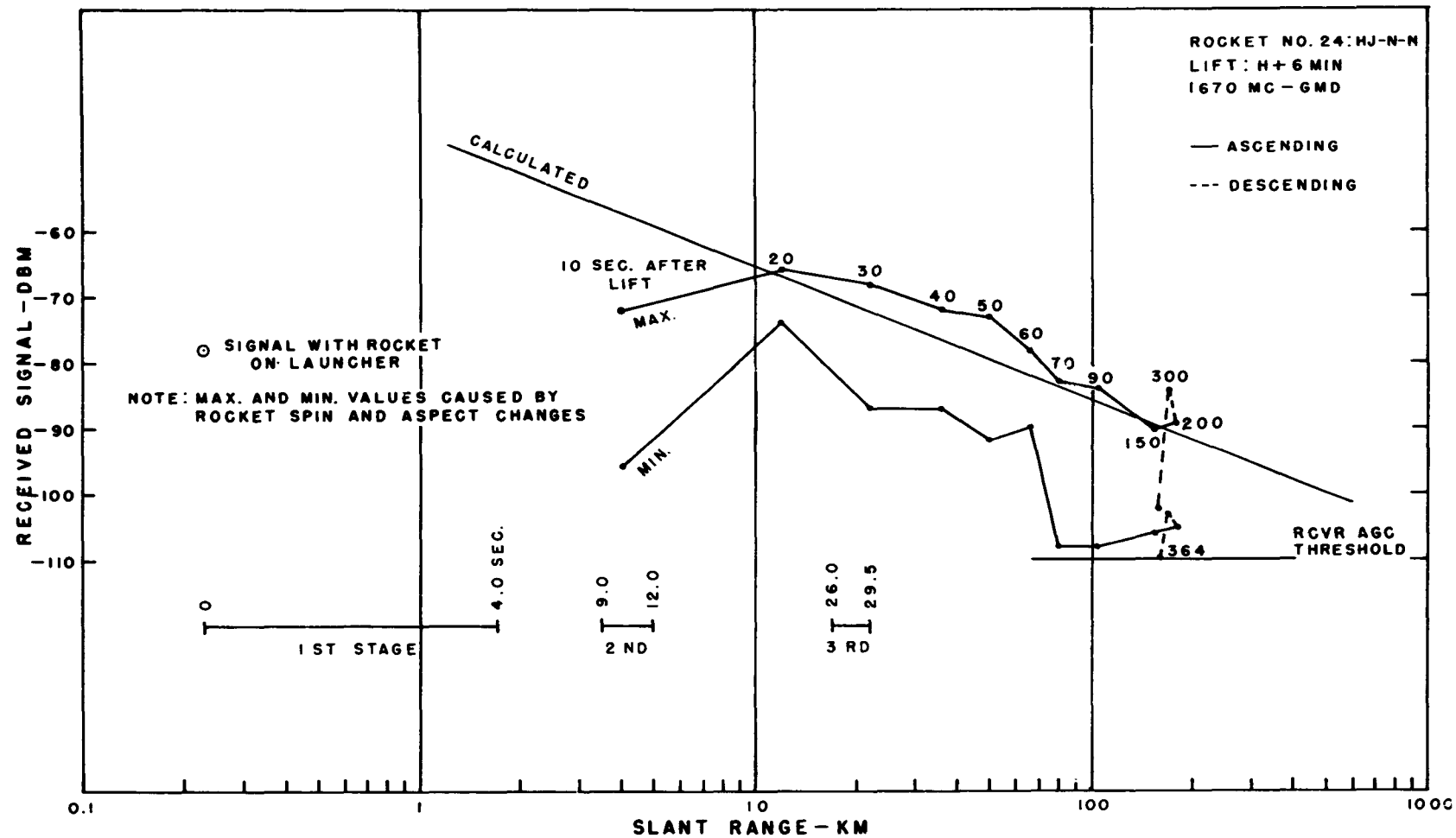

Figure C.249 Received signal strength versus slant range for GMD telemetry, Rocket 24, King Fish.

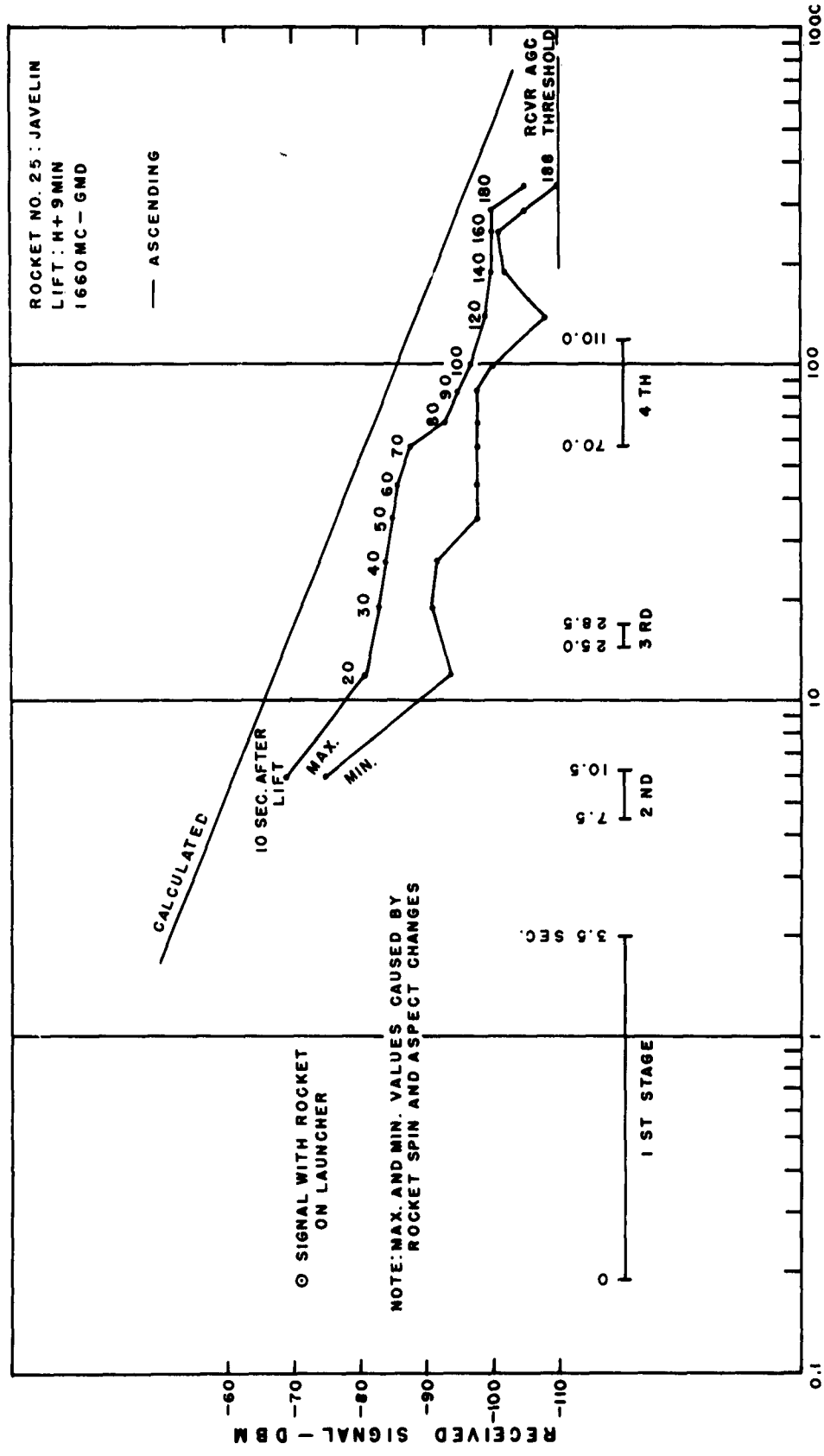

Figure C.250 Received signal strength versus slant range for GMD telemetry, Rocket 25, King Fish.

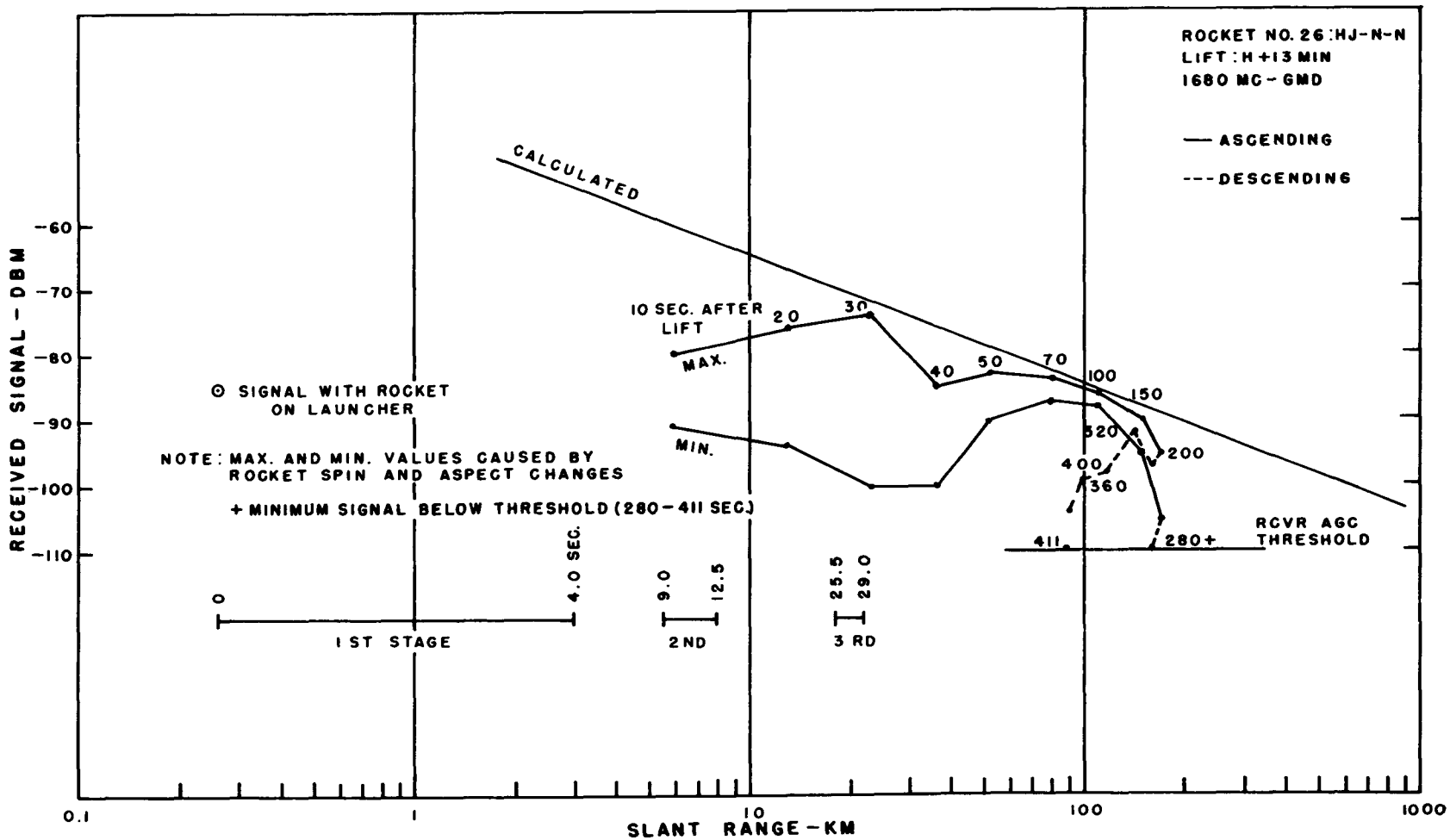

Figure C.251 Received signal strength versus slant range for GMD telemetry, Rocket 26, King Fish.

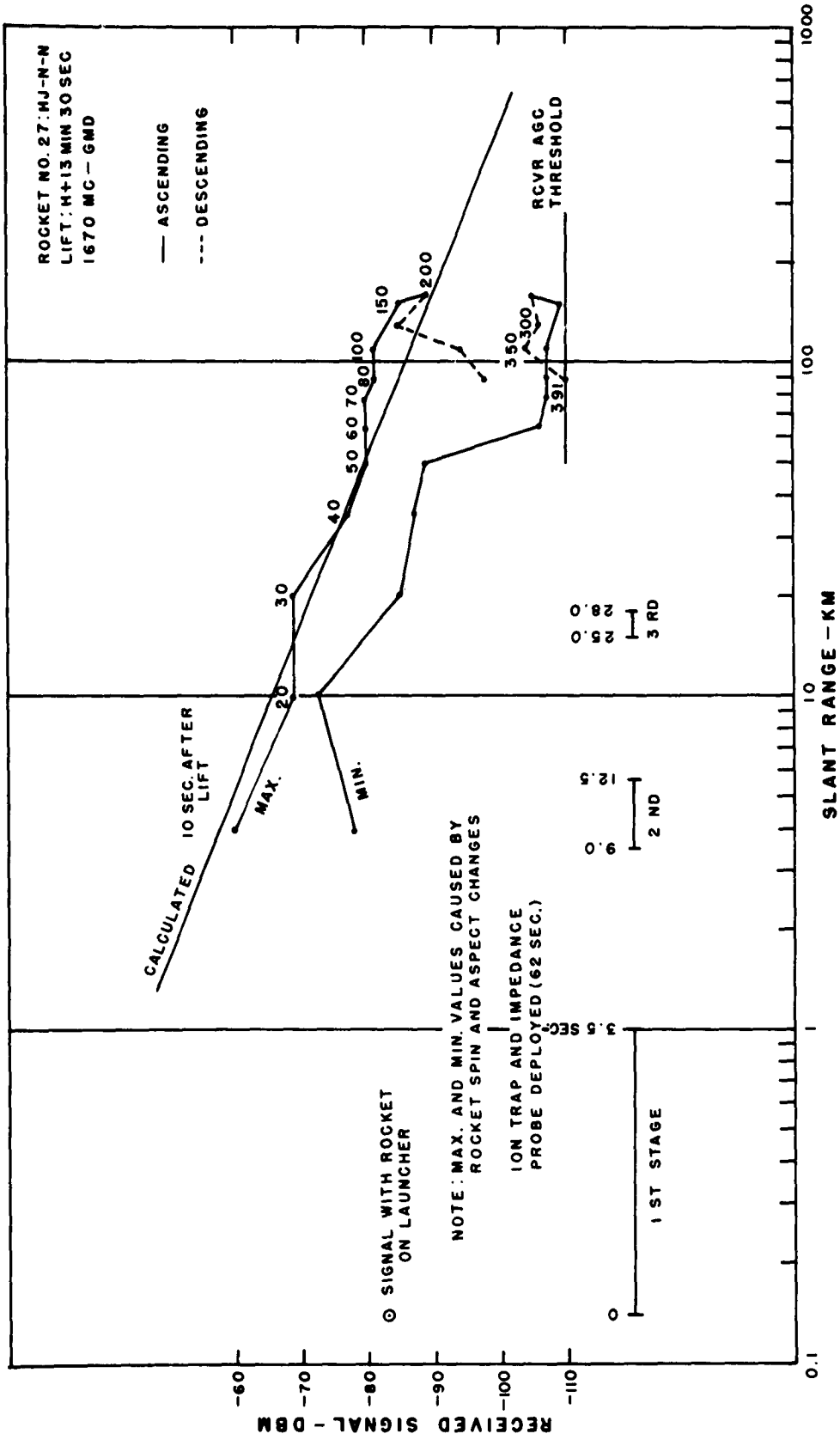

Figure C.252 Received signal strength versus slant range for GMD telemetry, Rocket 27, King Fish.

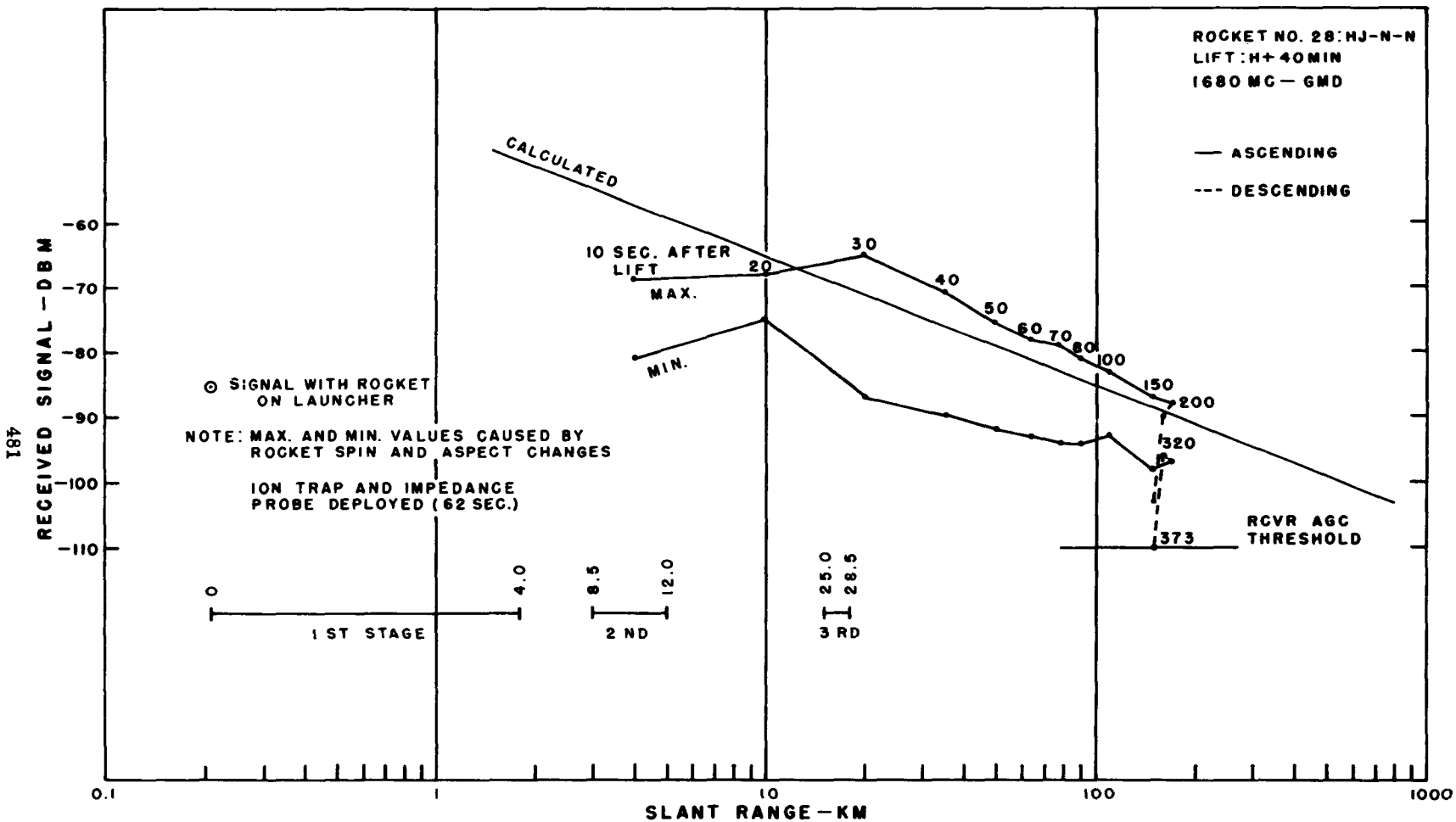

Figure C.253 Received signal strength versus slant range for GMD telemetry, Rocket 28, King Fish.

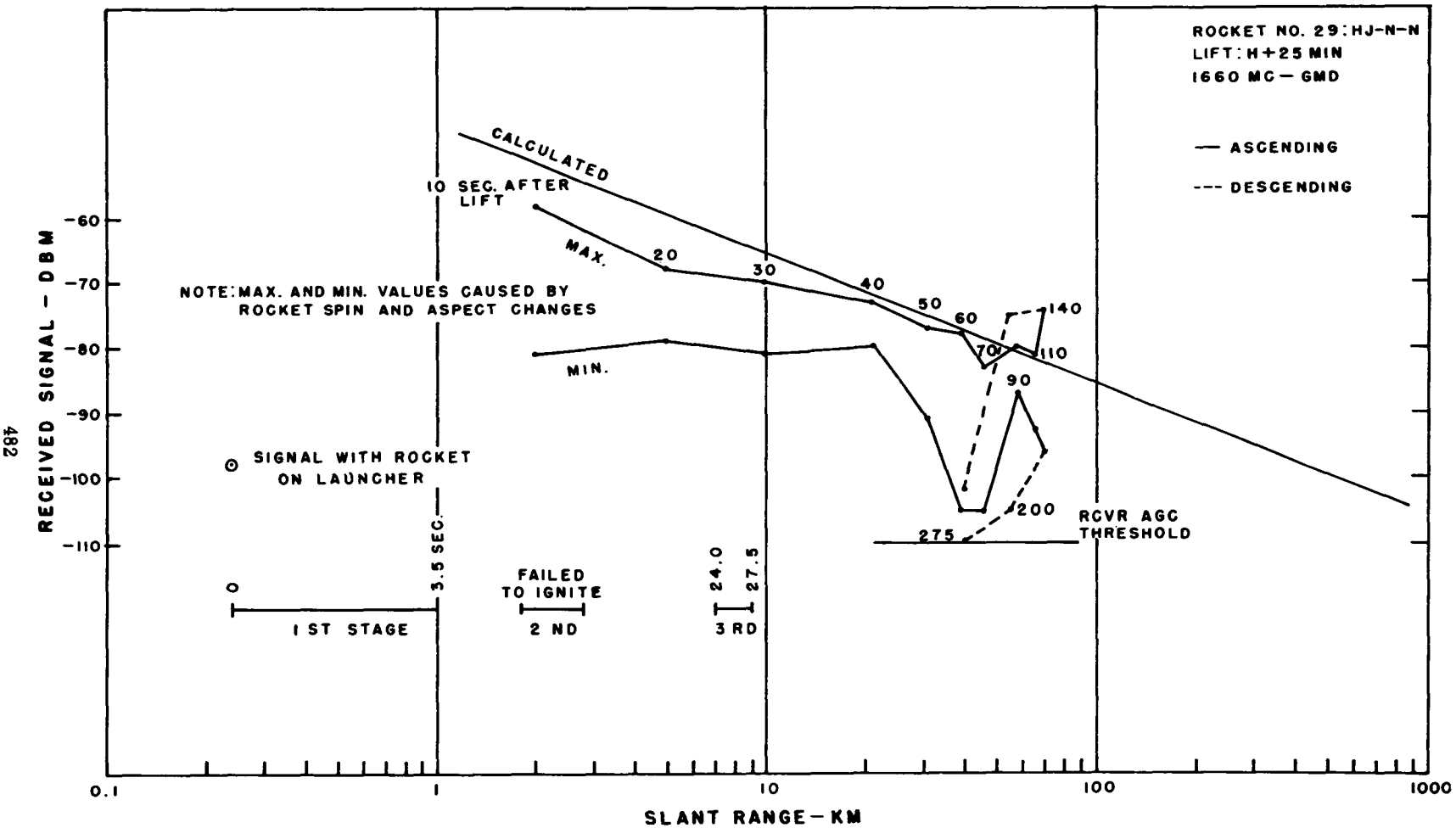

Figure C.254 Received signal strength versus slant range for GMD telemetry, Rocket 29, King Fish.

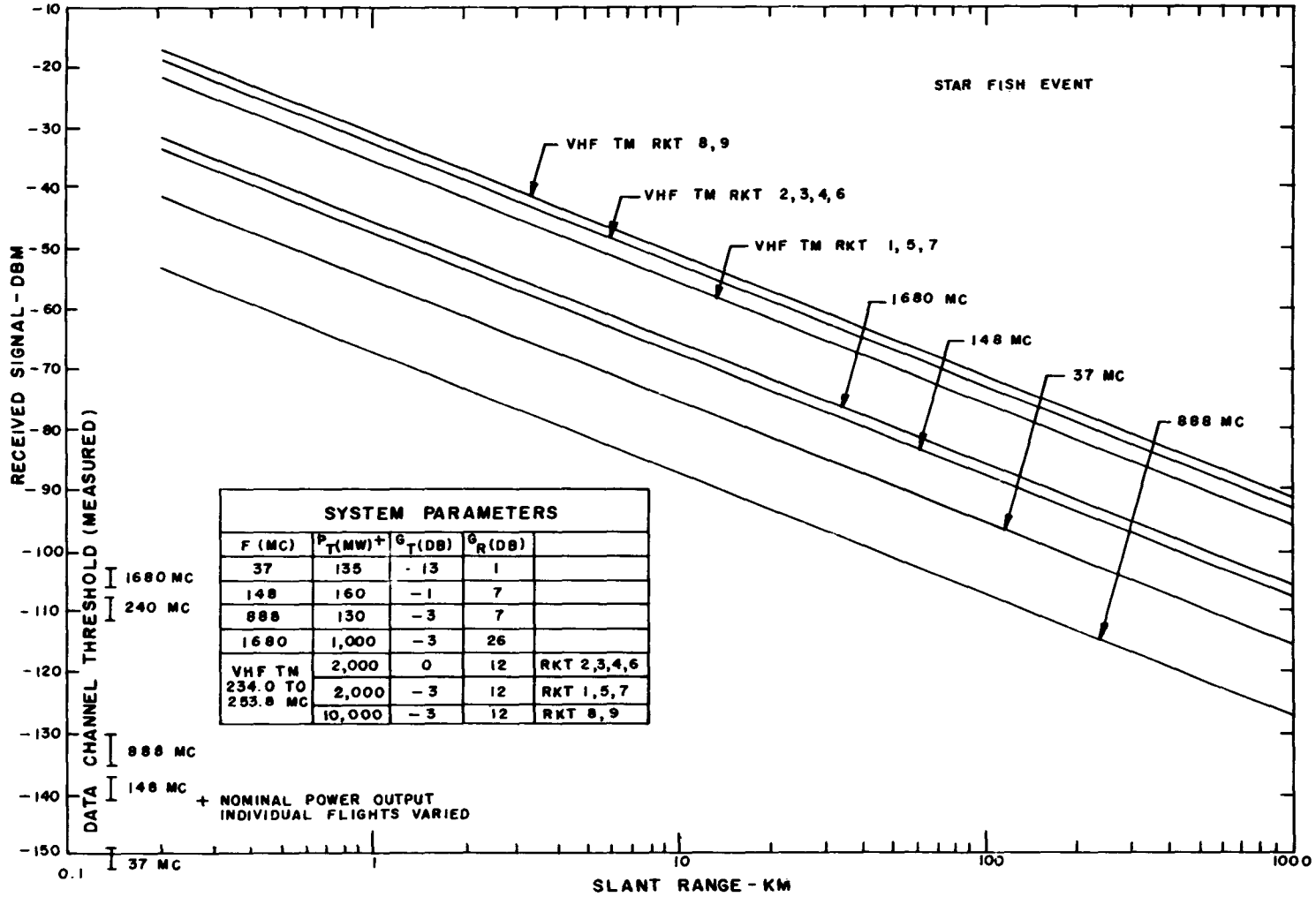

SYSTEM PARAMETERS

F (MC)	P_T(MW)+	G_T(DB)	G_R(DB)	
37	135	-13	1	
148	160	-1	7	
888	130	-3	7	
1680	1,000	-3	26	
VHF TM 234.0 TO 253.8 MC	2,000	0	12	RKT 2,3,4,6
	2,000	-3	12	RKT 1,5,7
	10,000	-3	12	RKT 8,9

Figure C.255 Calculated received signal strength versus slant range for the 3-frequency beacon, VHF telemetry and GMD, Star Fish.

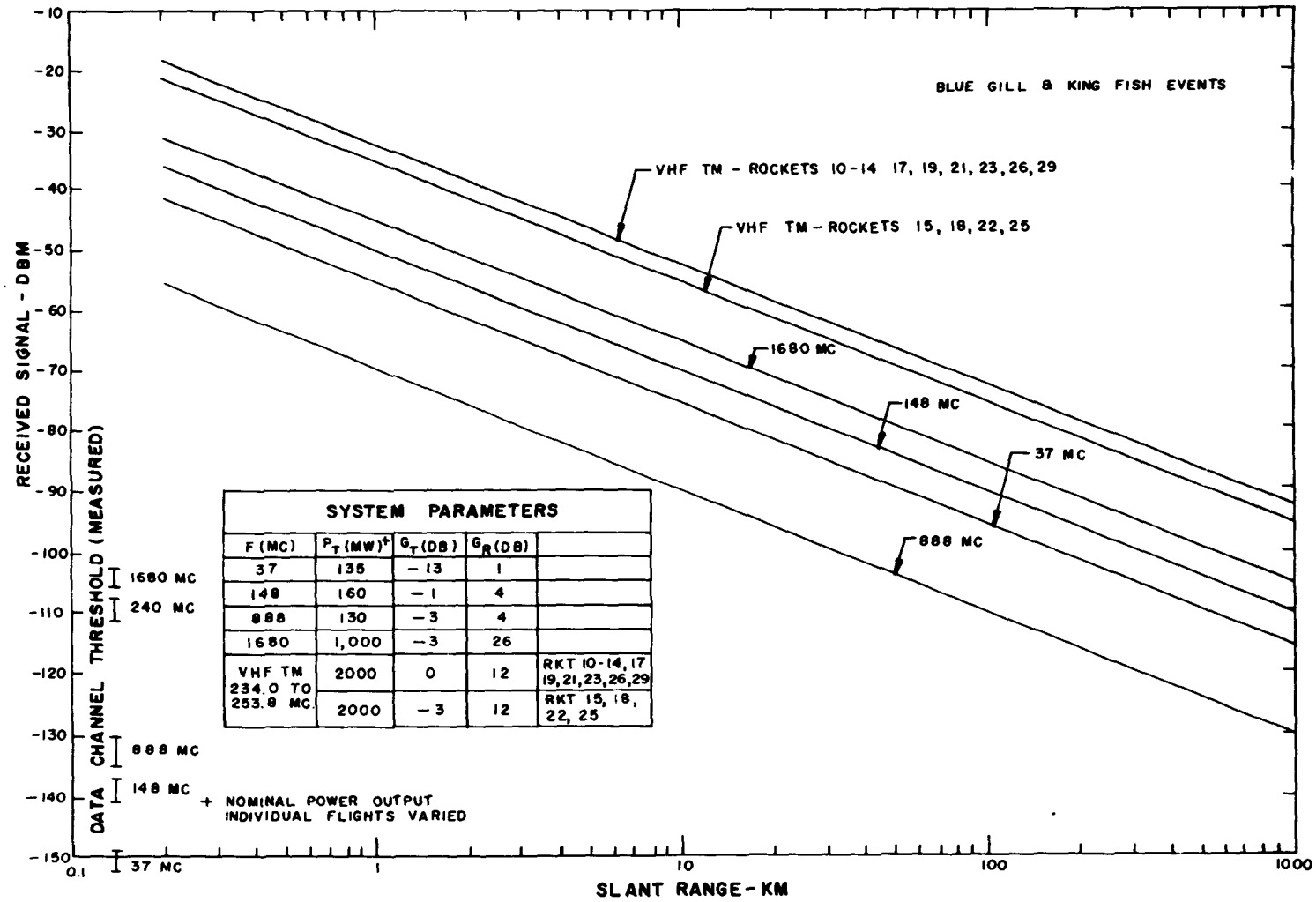

SYSTEM PARAMETERS

F (MC)	P_T (MW)+	G_T (DB)	G_R (DB)	
37	135	-13	1	
148	160	-1	4	
888	130	-3	4	
1680	1,000	-3	26	
VHF TM 234.0 TO 253.8 MC.	2000	0	12	RKT 10-14, 17 19, 21, 23, 26, 29
	2000	-3	12	RKT 15, 18, 22, 25

Figure C.256 Calculated received signal strength versus slant range for the 3-frequency beacon, VHF telemetry and GMD, Blue Gill and King Fish.

REFERENCES

1. "Electromagnetic Blackout Handbook", DASA 1280, Technical Military Planning Operation, Report No. RM62TMP-20, May 1962; General Electric Company, Santa Barbara, California; Secret-Restricted Data.

2. J. C. Seddon; "Propagation Measurements in the Ionosphere with the Aid of Rockets"; Journal of Geophysical Research, September 1953, Vol 58, No. 3, Pages 323-335; American Geophysical Union, Washington, D. C.; Unclassified.

3. W. W. Berning; "Charge Densities in the Ionosphere from Radio Doppler Data"; Journal of Meteorology, June 1951, Vol 8, No. 3, Pages 175-181; American Meteorology Society, Lancaster, Pa.; Unclassified.

4. R. E. Prenatt; "Ionospheric Structure Above Fort Churchill, Canada, from Faraday Rotation Measurements"; ARS Journal, August 1960, Pages 763-765; American Rocket Society, New York, N. Y.; Unclassified.

5. S. A. Bowhill; "The Faraday Rotation Rate of a Satellite Radio Signal"; Journal of Atmospheric and Terrestrial Physics, December 1958, Vol 13, No. 1, Pages 175-176; Pergamon Press, New York, N. Y.; Unclassified.

6. O. K. Garriott; "The Determination of Ionospheric Electron Content and Distribution from Satellite Observations; Part 1. Theory of the Analysis"; Journal of Geophysical Research, April 1960, Vol 65, No. 4, Pages 1139-1150; American Geophysical Union, Washington, D. C.; Unclassified.

7. O. K. Garriott; "The Determination of Ionospheric Electron Content and Distribution from Satellite Observations; Part 2. Results of the Analysis"; Journal of Geophysical Research, April 1960, Vol 65, No. 4, Pages 1151-1157; American Geophysical Union, Washington, D. C.; Unclassified.

8. C. G. Little and R. S. Lawrence; "The Use of Polarization Fading of Satellite Signals to Study the Electron Content and Irregularities in the Ionosphere"; National

Bureau of Standards Journal of Research, July-August 1960, Vol 64D, No. 4, Pages 335-345; National Bureau of Standards, Washington, D. C.; Unclassified.

9. J. M. Kelso; "Doppler Shifts and Faraday Rotation of Radio Signals in a Time Varying, Inhomogeneous Ionosphere. Part 1, Single Signal Case"; Journal of Geophysical Research, December 1960, Vol 65, No. 12, Pages 3909-3914; American Geophysical Union, Washington, D. C.; Unclassified.

10. J. M. Kelso; "Doppler Shifts and Faraday Rotation of Radio Signals in a Time Varying, Inhomogeneous Ionosphere. Part 2, Two Signal Case"; Journal of Geophysical Research, April 1961, Vol 66, No. 4, Pages 1107-1115; American Geophysical Union, Washington, D. C.; Unclassified.

11. W. J. Ross; "The Determination of Ionospheric Electron Content From Satellite Doppler Measurements; 1. Method of Analysis"; Journal of Geophysical Research, September 1960,

Vol 65, No. 9, Pages 2601-2606; American Geophysical Union, Washington, D. C.; Unclassified.

12. W. J. Ross; "The Determination of Ionospheric Electron Content from Satellite Doppler Measurements; 2. Experimental Results"; Journal of Geophysical Research, September 1960; Vol 65, No. 9, Pages 2607-2615; American Geophysical Union, Washington, D. C.; Unclassified.

13. F. de Mendonca; "Ionospheric Electron Content and Variations Measured by Doppler Shifts in Satellite Transmissions"; Technical Report No. 2, October 1961; Stanford Electronics Laboratory, Stanford University; Stanford, California; Unclassified.

14. G. A. Dulk and W. A. Dean; "Rocket and Satellite Ionosphere Studies Using a Digital Ray Tracing Procedure: Summary Report"; BRL Report No. 1163, December 1962; Ballistic Research Laboratories, Aberdeen Proving Ground, Md; Unclassified.

15. J. A. Ratcliffe; "The Magneto-Ionic Theory and Its Applications to the Ionosphere"; 1959, Page 171; Cambridge University Press, London, England; Unclassified.

16. H. K. Sen and A. A. Wyller; "On the Generalization of the Appleton-Hartree Magnetoionic Formulas"; Journal of Geophysical Research, December 1960, Vol. 65, No. 12, Pages 3931-3950; American Geophysical Union, Washington, D. C.; Unclassified.

17. H. A. Lorentz: "The Theory of Electrons"; 1952, Page 163; Dover Publications, Inc., New York, N. Y.; Unclassified.

18. B. Burgess; "Ionospheric Studies Using Satellite Radio Transmissions"; NATO Conference Series, 1962, Vol 2, Pages 224-227; The Macmillan Company, New York; Unclassified.

19. F. de Mendonca and O. K. Garriott; "Ionospheric Electron Content Calculated by a Hybrid Faraday—Doppler Technique"; Journal of Atmospheric and Terrestrial Physics, April 1962, Vol 24, Pages 317-324; Pergamon Press, New York; Unclassified.

20. E. Gotton; "A Method for the Analysis of Combined Faraday Differential Doppler Recordings in the Presence of Horizontal Gradients and Vertical Satellite Motion"; Journal of Atmospheric and Terrestrial Physics, June 1962, Vol 24, Pages 554-558; Pergamon Press, New York, N. Y.; Unclassified.

21. O. K. Garriott and F. de Mendonca; "A Comparison of Methods Used in the Reduction of Satellite Data Relating to the Ionosphere"; Paper presented at spring URSI Meeting sponsored by National Academy of Sciences, April-May 1963, Washington, D. C.; Unclassified.

22. I. L. Chidsey; "Electron Column Densities and Effective Ionosphere Heights in the Vicinity of Star Fish"; DASA Data Center Review, April 1963, Vol 63, No. 1, Pages 93-103; Defense Atomic Support Agency, Washington, D. C.; Secret, Restricted Data.

23. G. A. Dulk; "Faraday Rotation Near the Transverse Region of the Ionosphere"; BRL Report No. 1200, April 1963; Ballistic Research

Laboratories, Aberdeen Proving Ground, Md.; Unclassified.

24. K. C. Yeh and G. W. Swenson, Jr.; "Ionospheric Electron Content and Its Variations Deduced From Satellite Observations"; Journal of Geophysical Research, April 1961, Vol 66, No. 4, Pages 1061-1068; American Geophysical Union, Washington, D. C.; Unclassified.

25. D. C. Jensen and J. C. Cain; "An Interim Magnetic Field"; Journal of Geophysical Research, August 1962, Vol 67, No. 9, Pages 3568-3569; American Geophysical Union, Washington, D. C.; Unclassified.

26. W. F. Dudziak, D. D. Klernecke, and T. J. Kostigen; "Graphic Displays of Geomagnetic Geometry"; RM 63 TMP-2, DASA 1372, 1 April 1963, Contract DA 49-146-XZ-109, Technical Military Planning Operation, General Electric Company, Santa Barbara, California; Unclassified.

27. R. S. Leonard; "Magnetic Field Model Variations"; Paper presented at Trapped Radiation

Symposium, April 1963, Goddard Space Flight Center, Greenbelt, Maryland; Secret, Restricted Data.

28. K. H. Patterson; "A Broad-Band Frequency Multiplier and Mixer for Dispersive Doppler Measurements"; BRL Memorandum Report No. 1343, April 1961; Ballistic Research Laboratories, Aberdeen Proving Ground, Md.; Unclassified.

29. K. H. Patterson; "The Design for a Special Receiver for Satellite Ionosphere Experiments"; BRL Technical Note 1158, December 1957; Ballistic Research Laboratories, Aberdeen Proving Ground, Md.; Unclassified.

30. V. W. Richard; "DOPLOC Tracking Filter"; BRL Memorandum Report No. 1173, October 1958; Ballistic Research Laboratories, Aberdeen Proving Ground, Md.; Unclassified.

31. C. L. Adams; "The DOPLOC Instrumentation System for Satellite Tracking"; BRL Report No. 1123, January 1961; Ballistic Research Laboratories, Aberdeen Proving Ground,

Md.; Unclassified.

32. W. J. Cruickshank; "GMD Telemetry"; (BRL Memorandum Report in publication); Ballistic Research Laboratories, Aberdeen Proving Ground, Md.; Unclassified.

33. "Rawin Set, AN/GMD-1A"; TM 11-271A, August 1954; U. S. Department of Army, Washington, D. C.; Unclassified.

34. R. W. Hendrick, Jr., R. H. Christian and P. G. Fischer; "Operation Fish Bowl Theoretical Estimates of Expected Phenomena"; Technical Military Planning Operation, Report No. RM 62 TMP-36, May 1962; General Electric Company, Santa Barbara, California; Secret, Restricted Data.

35. S. T. Marks and others; "Summary Report on Strongarm Rocket Measurements of Electron Density to an Altitude of 1500 Kilometers"; BRL Report No. 1187, January 1963; Ballistic Research Laboratories, Aberdeen Proving Ground, Md.; Unclassified.

36. A. V. Phelps and J. L. Pack; "Electron Collision Frequencies in Nitrogen and in the Lower Ionosphere"; Physical Review Letters, October 1959, Vol 3, No. 4, Pages 340-342; American Physical Society, New York, N. Y.; Unclassified.

37. J. A. Kane; "Reevaluation of Ionospheric Electron Densities and Collision Frequencies Derived from Rocket Measurements of Refractive Index and Attenuation"; NASA Technical Note D-503, November 1960; National Aeronautics and Space Administration, Washington, D. C.; Unclassified.

38. D. L. Carpenter; "The Magnetosphere During Magnetic Storms; A Whistler Analysis"; Technical Report No. 12, June 1962, Contract AF 18(603)-126 and Grant NSF G-17037; Stanford Electronics Laboratories, Stanford, California; Unclassified.

39. J. W. Wright; "Vertical Cross Sections of the Ionosphere Across the Geomagnetic Equator"; Technical Note No. 138, PB 161639, U. S. Department of Commerce, National Bureau of Standards,

Washington, D. C.; Unclassified.

40. C. Blank; "1962 Soviet Nuclear Test Series"; DASA Data Center Review, April 1963, Vol 63, No. 1, Pages 75-77; Defense Atomic Support Agency, Washington, D. C.; Secret, Restricted Data.

41. "Third Report of the Fish Bowl Rapid Interpretation Group, Blue Gill"; DASA Data Center Special Report No. 8, 30 November 1962; Defense Atomic Support Agency, Albuquerque, New Mexico; Secret, Restricted Data.

42. "Second Report of the Fish Bowl Rapid Interpretation Group, Check Mate"; DASA Data Center Special Report No. 7, 30 November 1962; Defense Atomic Support Agency, Albuquerque, New Mexico; Secret, Restricted Data.

43. O. L. Johnson and R. A. Ladson; "Magnetic Field Lines in the Vicinity of Johnston Island"; DASA Data Center Review, April 1963, Vol 63, No. 1, Pages 87-91; Defense Atomic Support Agency, Washington, D. C.; Secret, Restricted Data.

44. W. Pfister, J. C. Ullwick and R. P. Vancour; "Some Results of Direct Probing in the Ionosphere"; Journal of Geophysical Research, April 1961, Vol 66, No. 4, Pages 289-296; American Geophysical Union, Washington, D. C.; Unclassified.

45. D. McGuire; Los Alamos Scientific Laboratory, Private Communications, 1961. Unclassified.

46. Institute for Defense Analysis; Report on Nuclear Interference, IDA ARPA TR 60-3, Secret-Restricted Data.

47. R. W. King and J. F. Perkins; Phys. Rev. 112 963 (1958).

48. Maienschein, Peele, Zobel and Love; Proceedings of the Second Geneva Conference, p. 670, 1958.

49. K. O. Nielsen; Electromagnetically Enriched Isotopes and Mass Spectrometry, Academic Press, New York 1956.

50. The Nuclear Radiation Handbook, AFSWP-1100, 1957, Defense Atomic Support Agency, Washington, D.C.; Secret-Restricted Data.

51. H. Kallman-Bijl, R. L. F. Boyd, H. Laglow, Sm. M. Poloskov and W. Priester; COSPAR International Reference Atmosphere, 1961.

52. W. Paul, H. P. Reinhard and U. vonZahn; "Das Elektrische Massenfilter als Massenspektrometer und Isotopentrenner"; Zeitschrift fur Physik, 1958, Vol 152, Pages 143-182; Springler-Verlag, Berlin, Germany; Unclassified.

53. K. I. Gringauz and M. Kh. Zelikman, "Measuring the Concentration of Positive Ions Along the Orbit of an Artificial Earth Satellite", USP. Fiz. Nauk, 63(1b) 239-252, 1957.

54. I. Langmuir and H. M. Mott-Smith, "The Theory of Collectors in Gaseous Discharges", Phys Rev., 28(4), 727-763, 1926.

55. R. C. Sagalyn, M. Smiddy and J. Wisnia, "Measurement and Interpretation of Ion Density Distributions in the Daytime F Region", 68(1)199-210, 1963.

56. K. S. W. Champion and R. Minzner, "Proposed Revision of the U. S. Standard Atmosphere", AFCRL-62-802, 1961, **Air Force Cambridge Research Laboratories, Bedford, Massachusetts.**

57. M. H. Bortner and C. W. Baulknight, "Deionization Kinetics, General Electric Missile and Space Vehicle Department Scientific Report," DASA No. 1244, July 1961; General Electric Company, Philadelphia, Pennsylvania; Unclassified.

58. C. M. Haaland, "Wave Propagation Under Anomalous Conditions", Part I, ARF 1176-9 (Final Report) Dec 19, 1961; Armour Research Foundation, Chicago, Illinois; Unclassified.

59. K. G. Budden; "Radio Waves in the Ionosphere"; 1961, Cambridge University Press, Bentley House, 200 Euston Road, London, England, and 32 E. 57th Street, New York, New York, and P. O. Box 33, Ibadan, Nigeria. Unclassified.

60. Lyman Spitzer, Jr.; "Physics of Fully Ionized Gases"; 1956, Interscience Publishers Inc., New York, and Interscience Publishers Ltd., London. Unclassified.

61. J. A. Stratton; "Electromagnetic Theory"; First Edition, 1941, McGraw-Hill Book Company, Inc., New York and London. Unclassified.

62. Technical Report 2013; U. S. Army Signal Research and Development Laboratory; 15 January 1959. Unclassified.

63. C. A. Syvertson and D. H. Dennis; "A Second Order Shock-Expansion Method Applicable to Bodies of Revolution Near Zero Lift"; National Advisory Committee for Aeronautics Report 1328, 1957. Unclassified.

64. Military Handbook-5; "Strength of Metal Aircraft Elements"; Armed Forces Supply Support Center, Washington 25, D. C., March 1959. Unclassified.

65. Millard V. Barton; "Fundamentals of Aircraft Structures"; First Edition, 1948; Prentice-Hall, Inc., New York, New York; Unclassified.

66. Bjorn Thorstensen; "Structural Analysis of Firefly Series Honest John-Nike Test Vehicle"; Special Report 1908 Contract AF19(604)-7235; Aerojet General Corp., Azusa, California; November 1960. Unclassified.

67. Raymond J. Roark; "Formulas for Stress and Strain"; Third Edition, 1954; McGraw-Hill Book Company, Inc., New York, Toronto, London. Unclassified.

68. Herbert J. Reich; "Very High Frequency Techniques"; First Edition, 1947, Volume 1 compiled by Staff of Radio Research Laboratory, Harvard University; McGraw-Hill Book Company, Inc., New York, New York. Unclassified.

69. K. H. Patterson; "A Preamplifier Design for Satellite Receivers"; BRL Memorandum Report No. 1154, July 1958; Ballistic Research Laboratories, Aberdeen Proving Ground, Maryland. Unclassified.

70. L. W. Orr, P. G. Cath and B. R. Darnall; "A Two-Frequency Beacon for High Altitude Ionosphere Rocket Research"; Final Report; December 1959; University of Michigan, College of Engineering, Ann Arbor, Michigan; Unclassified.

71. V. W. Richard; "The Shroud Antenna"; BRL Memorandum Report No. 1283, June 1960; Ballistic Research Laboratories, Aberdeen Proving Ground, Md. Unclassified.

72. Dr. K.S.W. Champion; "Ionospheric Wind and Diffusion Measurements"; POR-2051; Air Force Cambridge Research Laboratories, L.G. Hanscom Field, Bedford, Massachusetts; Secret Formerly Restricted Data.

73. W.W. Berning; "Gamma Ray Scanning of Debris Cloud"; POR-2017; Ballistic Research Laboratories, Aberdeen Proving Ground, Maryland; Secret Formerly Restricted Data.

74. R.H. Dowd; "E- and F-Region Physical Chemestry"; POR-2019; Air Force Cambridge Research Laboratories, Bedford, Massachusetts; Secret Formerly Restricted Data.

75. G.C. Tweed; "Tracking and Positioning"; POR-2042; Cubic Corporation, San Diego, California; Confidential.

DISTRIBUTION

Military Distribution Category 62

ARMY ACTIVITIES

1 CHIEF OF R & D DA
2 AC OF S INTELLIGENCE DA
3 CHIEF OF ENGINEERS DA
4- 7 ARMY MATERIAL COMMAND
8 CHIEF SIGNAL OFFICER DA
9- 10 U S ARMY COMBAT DEVELOPMENTS COMMAND
11 U S ARMY CDC NUCLEAR GROUP
12 U S ARMY ARTILLERY BOARD
13 U S ARMY AIR DEFENSE BOARD
14 U S ARMY AVIATION BOARD
15 U S ARMY COMMAND AND GENERAL STAFF COLLEGE
16 U S ARMY AIR DEFENSE SCHOOL
17 U S ARMY CDC ARMOR AGENCY
18 U S ARMY CDC ARTILLERY AGENCY
19 U S ARMY CDC INFANTRY AGENCY
20 U S ARMY CDC CBR AGENCY
21 U S ARMY SIGNAL SCHOOL
22 ARMY MEDICAL RESEARCH LAB
23- 24 ENGINEER RESEARCH & DEV LAB
25 WATERWAYS EXPERIMENT STATION
26 PICATINNY ARSENAL
27 DIAMOND ORDNANCE FUZE LABORATORY
28 BALLISTIC RESEARCH LABORATORY
29- 31 REDSTONE SCIENTIFIC INFORMATION CENTER
32- 33 WHITE SANDS MISSILE RANGE
34 U S ARMY MOBILITY COMMAND
35 U S ARMY AMMUNITION COMMAND
36 ELECTRONICS COMMAND
37 U S ARMY ELECTRONIC PROVING GROUND
38- 41 U S ARMY ELECTRONIC R & D LABORATORY
42- 43 U S ARMY CDC COMBAT SERVICE SUPPORT GROUP
44 THE RESEARCH & ANALYSIS CORP
45- 46 WHITE SANDS SIGNAL SUPPORT AGENCY
47 U S ARMY NUCLEAR DEFENSE LABORATORY
48 U S ARMY CDC AIR DEFENSE AGENCY
49 UNITED STATES CONTINENTAL ARMY COMMAND
50 U S ARMY CDC COMBINED ARMS GROUP
51 US ARMY ENGINEER R&D LABS SMOFB-EP
52- 55 US ARMY MATERIAL COMMAND,SANDIA
56- 57 US ARMY ENGR.RES. & ENGR.LABS.

NAVY ACTIVITIES

58- 59 CHIEF OF NAVAL OPERATIONS OP03EG
60 CHIEF OF NAVAL OPERATIONS OP-096
61 CHIEF OF NAVAL OPERATIONS OP-75
62 CHIEF OF NAVAL OPERATIONS OP-922G1
63 CHIEF OF NAVAL OPERATIONS OP-94
64 CHIEF OF NAVAL OPERATIONS OP-922F2
65- 67 CHIEF BUREAU OF NAVAL WEAPONS DLI-3
68 CHIEF BUREAU OF SHIPS CODE 423
69 CHIEF BUREAU OF YARDS & DOCKS CODE 74
70 DIR. US NAVAL RESEARCH LAB.
71- 72 U S NAVAL ORDNANCE LABORATORY
73 NAVY ELECTRONICS LABORATORY
74 U S NAVAL RADIOLOGICAL DEFENSE LAB
75 U S NAVAL CIVIL ENGINEERING LABORATORY
76 U S NAVAL SCHOOLS COMMAND U S NAVAL STATION
77 U S NAVAL POSTGRADUATE SCHOOL
78 AIR DEVELOPMENT SQUADRON 5 VX-5
79 U S NAVAL AIR DEVELOPMENT CENTER
80 U S NAVAL WEAPONS EVALUATION FACILITY
81 U S NAVAL MEDICAL RESEARCH INSTITUTE
82 DAVID W TAYLOR MODEL BASIN
83- 86 U S MARINE CORPS CODE A03H

AIR FORCE ACTIVITIES

87- 89 HQ USAF AFTAC-TD
90 HQ USAF AFRDPF
91 HQ USAF AFXPDG
92 HQ USAF AFOCEKA
93 HQ USAF AFGOA
94- 98 HQ USAF AFNINDE
99 RESEARCH & TECHNOLOGY DIV BOLLING AFB
100 BALLISTIC SYSTEMS DIVISION
101 SPACE SYSTEMS DIVISION SSTDS
102 TACTICAL AIR COMMAND
103 AIR DEFENSE COMMAND
104 AIR FORCE SYSTEMS COMMAND
105 AF COMMUNICATIONS SERVICE
106 RADC-RAALD,GRIFFISS AFB
107 SECOND AIR FORCE
108-109 AF CAMBRIDGE RESEARCH CENTER
110-112 AFWL WLL-3 KIRTLAND AFB
113 SCHOOL OF AVIATION MEDICINE
114-116 AERONAUTICAL SYSTEMS DIVISION
117-118 USAF PROJECT RAND
119 ELECTRONIC SYSTEMS DIV ESAT
120 AIR TECHNICAL INTELLIGENCE CENTER
121 HQ USAF AFORQ
122 HQ USAF AFXPDK

OTHER DEPARTMENT OF DEFENSE ACTIVITIES

123 DIRECTOR OF DEFENSE RESEARCH AND ENGINEERING
124 ASST TO THE SECRETARY OF DEFENSE ATOMIC ENERGY
125-126 ADVANCE RESEARCH PROJECT AGENCY
127 WEAPONS SYSTEM EVALUATION GROUP
128-131 DEFENSE ATOMIC SUPPORT AGENCY
132 FIELD COMMAND DASA
133 FIELD COMMAND DASA FCTG
134-135 FIELD COMMAND DASA FCWT
136-137 DEFENSE INTELLIGENCE AGENCY
138 DEFENSE COMMUNICATIONS AGENCY
139 JOINT TASK FORCE-8
140 COMMANDER-IN-CHIEF PACIFIC
141 COMMANDER-IN-CHIEF ATLANTIC FLEET
142 STRATEGIC AIR COMMAND
143 CINCONAD
144 DIR.DEFENSE INTELLIGENCE AGENCY
145-164 DEFENSE DOCUMENTATION CENTER

POR CIVILIAN DISTR CAT. B 1

165 AEROSPACE CORPORATION ATTN DR.I.F.WEEKS
166 AEROJET GENERAL NUCLEONICS SAN RAMON CALIF
167 FORD MOTOR CO NEWPORT BEACH CALIF ATTN TECH LIBRARY
168 AEROSPACE CORP EL SEGUNDO CALIF
169 ALLIED RESEARCH ASSOC.INC CNCORD MASS
170 AMER.SCIENCE &ENG CO CAMBRIDGE MASS
171 IIT RESEARCH INSTITUTE CHICAGO ILL.
172 AVCO CORP EVERETT MASS
173 AVCO CORP WILMINGTON MASS ATTN TECH.LIBRARY
174 BMI COLUMBUS OHIO ATTN DEFENDER INFO CENTER
175 BELL TEL LAB.WHIPPANY NEW JERSEY
176 BENDIX CORP. SOUTHFIELD,MICH.
177 BOEING COMPANY SEATTLE WASHINGTON ATTN TECH LIBRARY
178 COLLINS RADIO CO.CEDAR RAPIDS IOWA
179 COLUMBIA UNIV ELEC RESEARCH LAB NEW YORK
180 CORNELL AERONAUTICAL LAB INC BUFFALO NY
181 DEFENSE RESEARCH CORP SANTA BARBARA ATTN WEITZ
182 DOUGLAS AIRCRAFT CORP SANTA MONICA CALIF
183 EDGERTON GERMESHAUSEN & GRIER INC BOSTON
184 E H PLESSET ASSOC INC LOS ANGELES ATTN TECH.LIBRARY
185 ELECTRO-OPTICAL SYSTEMS PASADENA CALIF
186 SPERRY RAND CORP LONG ISLAND N Y
187 GEN DYNAMICS ASTRO DIV SAN DIEGO ATTN HAMLIN
188 GEN DYNAMICS GEN ATOMIC DIV SAN DIEGO ATTN T I S
189 GEN DYNAMICS CORP FT WORTH TEXAS
190 GEN ELEC CO ADVANCED ELEC CENTER ITHACA N Y
191 GEC TECH MIL PLANNING OPER SANTA BARBARA ATTN DASA
192 SYLVANIA DIV ELEC DEF LAB MT VIEW CALIF
193 GEOPHYSICS CORP OF AMER BEDFORD MASS
194 H R B SINGER INC STATE COLLEGE PA
195 GEC,RE-ENTRY SYSTEMS DEPT ATTN TECH.INFO.CENTER

196 HUGHES AIRCRAFT CO CULVER CITY CALIF ATTN HANSCOME
197 INST FOR DEFENSE ANALYSIS WASHINGTON
198 INTER TEL & TELGR CORP NUTLEY N J
199 J HOPKINS UNIV APPL PHYSICS LAB SILVER SPRINGS
200 KAMAN NUCLEAR COLORADO SPRINGS ATTN SHELTON
201 LOCKHEED AIRCRAFT CORP PALO ALTO CALIF ATTN MEYROTT
202 MARTIN MARIETTA CO DENVER,COLORADO
203 LINCOLN LABORATORY ATTN.TECH.LIBR. PANNELL
204 MITRE CORP BEDFORD MASS ATTN TECH LIBRARY
205 MT.AUBURN RESEARCH ASSOC.,INC.
206 N AMERICAN AVIATION DOWNEY CALIF
207 NORTHROP AIRCRAFT INC HAWTHORNE CALIF
208 RCA DEFENSE ELCE PRODUCTS MOORESTOWN ATTN ENGR. LIB
209 RCA DAVID SARNOFF RES CENTER PRINCETON NJ
210 THOMPSON RAMO-WOOLDRIDGE CALIF.ATTN TECH.LIBRARY
211 RAND CORP SANTA MONICA CALIF
212 RAYTHEON CO MISSILE & SPACE DIV BEDFORD MASS
213 REPUBLIC AVIATION FARMINGDALE,L.I. NY
214 SPACE GEN CORP EL MONTE CALIF
215 SPCE TECH LAB LOS ANGELES CALIF
216 STANFORD RESEARCH INST.,ATTN TECH.LIBR.
217 STANFORD RESEARCH INST.ATTN RADIO PHYSICS LAB
218 TECH OPER.INC BURLINGTON MASS ATTN RICHARDS
219 UNIV OF MICHIGAN ANN ARBOR MICH ATTN BAMIRAC LIBR
220 VITRO CORP OF AMERICA WEST ORANGE N J
221 WESTINGHOUSE RESEARCH LAB PITTSBURGH PA
222 WESTINGHOUSE ELEC.CORP. WASH.ATTN PRYTULA
223 NATIONAL BUREAU OF STANDARDS BOULDER LABS UTLAUT
224 GENERAL ELCTRIC CO DEF.ELEC.DIV.

ATOMIC ENERGY COMMISSION ACTIVITIES

225-227 AEC WASHINGTON TECH LIBRARY
228-229 LOS ALAMOS SCIENTIFIC LAB
230-234 SANDIA CORPORATION
235-244 LAWRENCE RADIATION LAB LIVERMORE
245 NEVADA OPERATIONS OFFICE,LAS VEGAS
246 DTIE OAK RIDGE,MASTER
247-276 DTIE OAK RIDGE SURPLUS